Oscar De Feo

MODELING DIVERSITY BY STRANGE ATTRACTORS

With Applications to Temporal Pattern Recognition

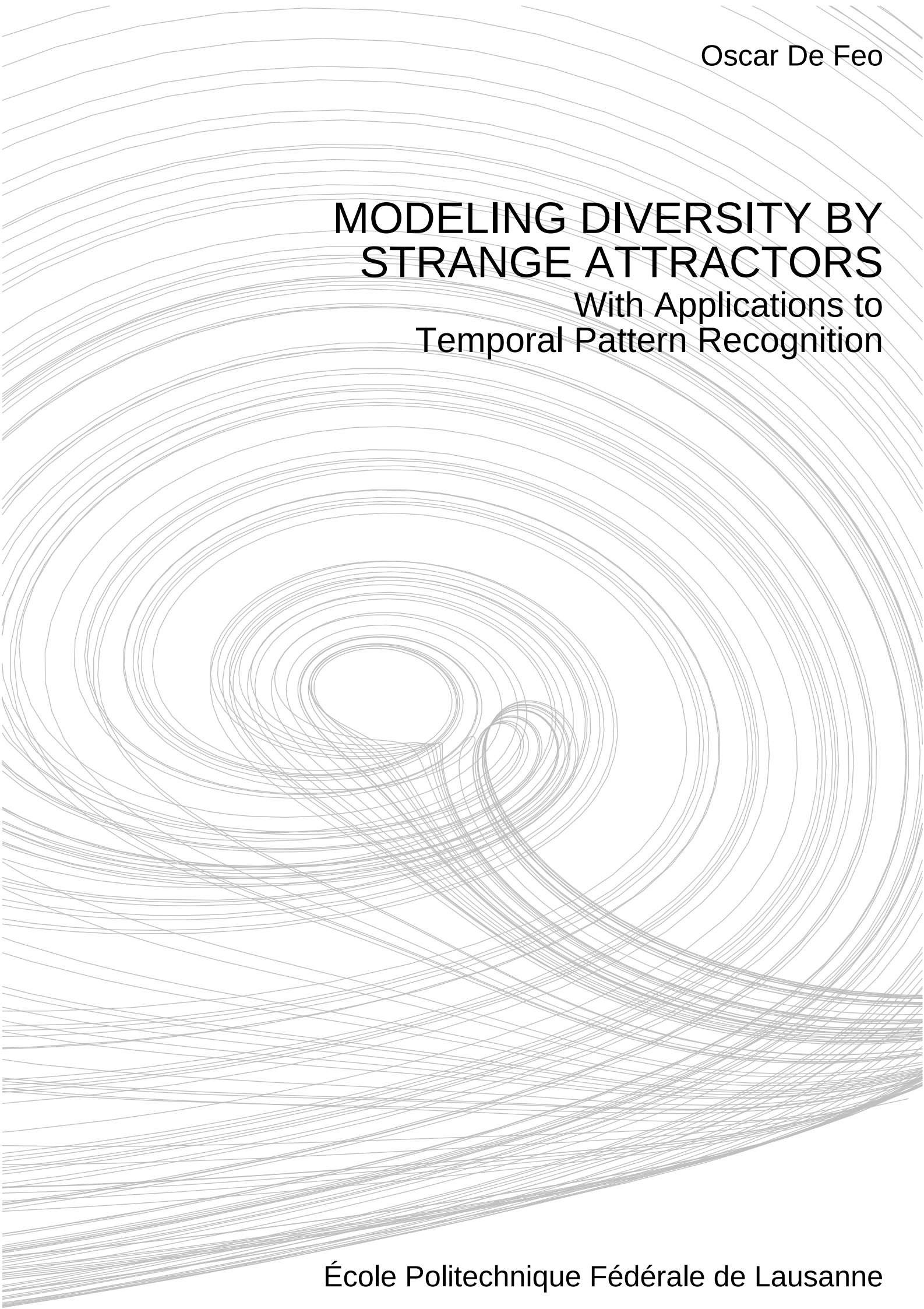

École Politechnique Fédérale de Lausanne

MODELING DIVERSITY BY STRANGE ATTRACTORS WITH APPLICATION TO TEMPORAL PATTERN RECOGNITION

THÈSE N^{O} 2344 (2001)

PRÉSENTÉE AU DÉPARTEMENT DE SYSTÈMES DE COMMUNICATION

ÉCOLE POLYTECHNIQUE FÉDÉRALE DE LAUSANNE

POUR L'OBTENTION DU GRADE DE DOCTEUR ÈS SCIENCES TECHNIQUES

PAR

Oscar DE FEO

laurea in ingegneria informatica, Politecnico di Milano, Italie
de nationalité italienne

acceptée sur proposition du jury:

Prof. M. Hasler, directeur de thèse
Prof. M. Colombetti, rapporteur
Prof. R. Ferrière, rapporteur
Dr B. Schoelkopf, rapporteur
Prof. G. Setti, rapporteur
Prof. M. Vetterli, rapporteur

Lausanne, EPFL
2001

A Lara, Martina e Natasha,
inconscie prove viventi
dell'esistenza e tangibilitá
del caos in Natura

ABSTRACT

This thesis belongs to the general discipline of establishing black-box models from real-word data, more precisely, from measured time-series. This is an old subject and a large amount of papers and books has been written about it. The main difficulty is to express the diversity of data that has essentially the same origin without creating confusion with data that has a different origin.

Normally, the diversity of time-series is modeled by a stochastic process, such as filtered white noise. Often, it is reasonable to assume that the time series is generated by a deterministic dynamical system rather than a stochastic process. In this case, the diversity of the data is expressed by the variability of the parameters of the dynamical system. The parameter variability itself is then, once again, modeled by a stochastic process. In both cases the diversity is generated by some form of exogenous noise.

In this thesis a further step has been taken. A single chaotic dynamical system is used to model the data and their diversity. Indeed, a chaotic system produces a whole family of trajectories that are different but nonetheless very similar. It is believed that chaotic dynamics not only are a convenient means to represent diversity but that in many cases the origin of diversity stems actually from chaotic dynamic.

Since the approach of this thesis explores completely new grounds the most suitable kind of data is considered, namely approximately periodic signals. In nature such time-series are rather common, in particular the physiological signal of living beings, such as the electrocardiograms (ECG), parts of speech signals, electroencephalograms (EEG), etc. Since there are strong arguments in favor of the chaotic nature of these signals, they appear to be the best candidates for modeling diversity by chaos. It should be stressed however, that the modeling approach pursued in this thesis is thought to be quite general and not limited to signals produced by chaotic dynamics in nature.

The intended application of the modeling effort in this thesis is temporal signal classification. The reason for this is twofold. Firstly, classification is one of the basic building block of any cognitive system. Secondly, the recently studied phenomenon of synchronization of chaotic systems suggests a way to test a signal against its chaotic model.

The essential content of this work can now be formulated as follows.

Thesis:

The diversity of approximately periodic signals found in nature can be modeled by means of chaotic dynamics. This kind of modeling technique, together with selective properties of the synchronization of chaotic systems, can be exploited for pattern recognition purposes.

This Thesis is advocated by means of the following five points.

1. *Models of randomness* (Chapter 2)
   It is argued that the randomness observed in nature is not necessarily the result of exogenous noise, but it could be endogenally generated by deterministic chaotic dynamics. The diversity of real signals is compared with signals produced by the most common chaotic systems.

2. *Qualitative resonance* (Chapter 3)
   The behavior of chaotic systems forced by periodic or approximately periodic input signals is studied

theoretically and by numerical simulation. It is observed that the chaotic system "locks" approximately to an input signal that is related to its internal chaotic dynamic. In contrast to this, its chaotic behavior is reinforced when the input signal has nothing to do with its internal dynamics. This new phenomenon is called "qualitative resonance".

3. *Modeling and recognizing* (Chapter 4)
   In this chapter qualitative resonance is used for pattern recognition. The core of the method is a chaotic dynamical system that is able to reproduce the class of time-series that is to be recognized. This model is excited in a suitable way by an input signal such that qualitative resonance is realized. This means that if the input signal belongs to the modeled class of time-series, the system approximately "locks" into it. If not, the trajectory of the system and the input signal remain unrelated.

4. *Automated design of the recognizer* (Chapters 5 and 6)
   For the kind of signals considered in this thesis a systematic design method of the recognizer is presented. The model used is a system of Lur'e type, *i.e.* a model where the linear dynamic and nonlinear static part are separated. The identification of the model parameters from the given data proceed iteratively, adapting in turn the linear and the nonlinear part. Thus, the difficult nonlinear dynamical system identification task is decomposed into the easier problems of linear dynamical and nonlinear static system identification. The way to apply the approximately periodic input signal in order to realize qualitative resonance is chosen with the help of periodic control theory.

5. *Validation* (Chapter 7)
   The pattern recognition method has been validated on the following examples

   — A synthetic example
   — Laboratory measurement from Colpitts oscillator
   — ECG
   — EEG
   — Vowels of a speech signals

   In the first four cases a binary classification and in the last example a classification with five classes was performed.

To the best of the knowledge of the author the recognition method is original. Chaotic systems have been already used to produce pseudo-noise and to model signal diversity. Also, parameter identification of chaotic systems has been already carried out. However, the direct establishment of the model from the given data and its subsequent use for classification based on the phenomenon of qualitative resonance is entirely new.

RÉSUMÉ

Cette thèse se situe dans le cadre de la vaste discipline qui a comme but d'établir des modèles de type boîte-noire à partir de données réelles, plus précisément, à partir de séries temporelles mesurées. C'est un thème plutôt ancien et donc une grande quantité de papiers et livres existe à ce sujet. La difficulté principale est d'exprimer la diversité des données qui sont de la même origine sans créer de confusion avec les données qui ont essentiellement une origine différente.

Normalement, la diversité des séries temporelles est modélisée par un processus stochastique, comme, par exemple, le bruit blanc filtré. Souvent, il est raisonnable de supposer que la série temporelle est produite par un système dynamique déterministe plutôt qu'un processus stochastique. Dans ce cas, la diversité des données est exprimée par la variabilité des paramètres du système dynamique. La variabilité des paramètres elle-même est alors, encore une fois, modélisée par un processus stochastique. Dans les deux cas la diversité est supposée être produite par une forme de bruit exogène.

Dans cette thèse, un pas supplémentaire a été fait. Un seul système dynamique chaotique est utilisé pour modéliser à la fois les données et leur diversité. En effet, un système chaotique peut produire une famille entière de trajectoires qui sont différentes mais néanmoins semblables. A ce propos, il est admis non seulement que les dynamiques chaotiques sont un moyen convenable pour la modélisation de la diversité mais que, aussi, en beaucoup de cas, elles sont à l'origine même de celle-ci.

Puisque l'approche proposée dans cette thèse explore des territoires inexplorés, les signaux les plus prometteurs, dans la direction proposée, ont été considérés, soit les signaux approximativement périodiques. Ces types de signaux sont plutôt communs dans les phénomènes naturels, notamment les signaux physiologiques des êtres vivants tels que les électrocardiogrammes (ECG), les signaux de parole en partie, les électroencéphalogrammes, etc. Comme il y a des bonnes raisons pour supposer une nature chaotique de ces signaux, leur diversité apparaît comme une bonne candidate pour être modélisée de façon chaotique. Pourtant, il faut préciser que l'approche de modélisation poursuivie dans cette thèse est supposée être plutôt générale donc pas limitée à des signaux produits par des systèmes chaotiques par nature.

Le but ultime de l'effort de modélisation de cette thèse est la classification de signaux temporels. La raison en est double: premièrement, la classification est un des éléments de base de tous les systèmes cognitifs; deuxièmement, le phénomène de la synchronisation des systèmes chaotiques, récemment étudié, se prête comme une possibilité pratique de comparer un signal à son modèle chaotique.

L'essentiel du contenu de ce travail peut être formulé comme suit.

Thèse:

> La diversité des signaux approximativement périodiques qui s'observent dans la nature peut être modélisée au moyen de dynamiques chaotiques. Cette technique de modélisation, avec les propriétés sélectives de la synchronisation des systèmes chaotiques, peut être exploitée pour la reconnaissance de patterns.

Cette Thèse est soutenue par les cinq points suivants.

1. *Modèles des phénomènes aléatoires* (Chapitre 2)

On soutient que le caractère aléatoire observé dans la nature n'est pas nécessairement le résultat de perturbations bruyantes exogènes mais que, au contraire, il peut être engendré de manière endogène par des dynamiques chaotiques déterministes. La diversité caractéristique de signaux réels est comparée avec celle qui peut être produite par les systèmes chaotiques les plus simples.

2. *Résonance qualitative* (Chapitre 3)
   Le comportement de systèmes chaotiques forcés périodiquement, ou approximativement périodiquement, est étudié soit en théorie soit à l'aide de simulations numériques. On observe qu'un type particulier de systèmes chaotiques "s'accroche" approximativement aux signaux d'entrée quand ils sont corrélés avec leur propre dynamique chaotique interne. Au contraire, le comportement chaotique de ces systèmes est renforcé par des signaux d'entrée qui n'ont rien à faire avec leur dynamique interne. Ce nouveau phénomène dynamique a été appelé "résonance qualitative".

3. *Modéliser et reconnaître* (Chapitre 4)
   Dans ce chapitre la résonance qualitative est utilisée pour la reconnaissance de patterns. Le noyau de la méthode est un système dynamique chaotique qui peut reproduire la classe de séries temporelles à reconnaître. Un signal extérieur est appliqué au système de manière à réaliser un filtre à résonance qualitative. Donc, si le signal d'entrée appartient à la classe de séries temporelles modélisée alors le système "s'accroche" approximativement. Dans le cas contraire, la trajectoire du système et le signal d'entrée restent non corrélés.

4. *La conception automatisée du classificateur* (Chapitres 5 e 6)
   Il est présenté, spécifiquement pour le type de signaux considéré dans cette thèse, une méthode pour la réalisation systématique du classificateur. Le modèle de référence utilisée est un système de Lur'e, c'est-à-dire un système dynamique dans lequel il y a une séparation nette entre la partie linéaire, qui est dynamique, et la partie non linéaire, qui est statique. L'identification des paramètres du modèle à partir des données procède itérativement en adaptant alternativement la partie linéaire et la partie non linéaire. Donc, la tâche difficile de l'identification du système dynamique non linéaire est décomposée dans les taches plus faciles d'identification du système linéaire dynamique et d'identification du système non linéaire statique. Finalement, la manière avec laquelle l'entrée doit agir sur le système de façon que la résonance qualitative soit garantie est déterminée à l'aide de la théorie du contrôle périodique linéaire.

5. *Validation* (Chapitre 7)
   La méthode de la reconnaissance de patterns a été validée sur les exemples suivants

   — Un exemple synthétisé à l'ordinateur
   — Mesures de laboratoire d'un oscillateur de Colpitts
   — ECG
   — EEG
   — Voyelles de signaux de parole

   Dans les quatre premier cas il s'agit de classement binaire tandis que le dernier concerne un classement en cinq classes.

A connaissance de l'auteur, la méthode de reconnaissance proposée est originale. Les systèmes chaotiques ont déjà été utilisés pour produire des séquences pseudo-aléatoires et pour modéliser la diversité de quelques signaux. L'identification paramétrique de systèmes chaotiques n'est pas nouvelle non plus. Par contre, l'établissement direct du modèle à partir des données et son usage pour des problèmes de classement utilisant le phénomène de la résonance qualitative est complètement nouveau.

RIASSUNTO

Questa tesi si situa nell'ambito di quell'ampia disciplina che ha come scopo il determinare modelli a scatola nera partendo da dati reali, in particolare a partire da serie temporali. Il soggetto è piuttosto datato, di conseguenza una consistente letteratura esiste a proposito di questo argomento. Il problema principale è d'esprimere la diversità di quei dati che hanno sostanzialmente la stessa origine senza così generare confusione con altri dati la cui natura è essenzialmente diversa.

Di solito, la diversità delle serie temporali è modellizata a mezzo di processi stocastici come, ad esempio, rumore bianco filtrato. D'altro canto, è spesso ragionevole supporre un'origine deterministica per i dati, considerandoli di conseguenza generati da un sistema dinamico piuttosto che da un processo stocastico. In questi casi, la diversità dei dati è trasferita sui parametri del sistema dinamico la cui variabilità è poi, ancora una volta, modellizata per mezzo di processi stocastici. Comunque sia, in entrambi i casi la diversità tipica delle misure è ricondotta ad un'origine stocastica, vale a dire ad un rumore esogeno.

In questa tesi è stato compiuto un ulteriore passo. Un solo sistema dinamico caotico è utilizzato per modellizare ad un sol tempo sia i dati sia la loro diversità. In effetti, un sistema dinamico caotico è in grado di generare un'intera famiglia di traiettorie differenti ma comunque simili tra loro. A tal proposito, non solo si crede che le dinamiche caotiche siano un mezzo conveniente per la modellizzazione della diversità ma anche che, in molti casi, esse siano all'origine stessa di questa.

Poiché l'approccio proposto in questa tesi esplora territori inesplorati, sono stati considerati i segnali più promettenti nella direzione proposta, ovvero i segnali approssimativamente periodici. Questo tipo di segnali è piuttosto comune in natura, in particolare sono tali quei segnali fisiologici degli esseri viventi quali gli elettrocardiogrammi (ECG), porzioni dei segnali del parlato, gli elettroencefalogrammi, etc. Siccome vi sono buone ragioni che fanno supporre una natura caotica di questi segnali, la loro diversità appare come buona candidata al fine d'essere modellizata per via caotica. Ciononostante, è necessario far presente che l'approccio modellistico perseguito in questa tesi è supposto essere piuttosto generale e, di conseguenza, si ritiene che esuli dall'effettiva natura caotica dei segnali.

Il fine ultimo dello sforzo modellistico di questa tesi è la classificazione di segnali temporali. La ragione è duplice. In primo luogo, la classificazione è uno tra gli elementi di base di ogni sistema cognitivo. Secondariamente, il fenomeno della sincronizzazione dei sistemi caotici, recentemente studiato, si offre come possibile modalità pratica per confrontare un segnale al suo modello caotico.

L'essenza di questo lavoro può essere espressa come segue.

Tesi:

La diversità dei segnali approssimativamente periodici che si osservano in natura può essere modellizata da sistemi dinamici caotici. Questa tecnica di modellizzazione, insieme alle le proprietà selettive della sincronizzazione dei sistemi caotici, può essere sfruttata per il riconoscimento di patterns.

Questa Tesi è sostenuta a mezzo dei cinque punti seguenti.

1. *Modelli dei fenomeni aleatori* (Capitolo 2)
   Si sostiene che l'aleatorietá osservata in natura non è necessariamente il risultato di perturbazioni rumorose

esogene ma che, al contrario, può essere generata in maniera endogena da dinamiche caotiche deterministiche. La diversità caratteristica di segnali reali è confrontata con quella che può essere prodotta dai più comuni sistemi caotici.

2. *Risonanza qualitativa* (Capitolo 3)
   Il comportamento dei sistemi caotici sotto forzante periodica, o approssimativamente periodica, è studiato sia teoreticamente che con il supporto di simulazioni numeriche. Si osserva che un particolare tipo di sistemi caotici si "aggancia" approssimativamente ai segnali d'ingresso che sono correlati con la dinamica caotica interna di questi sistemi. Al contrario, il comportamento caotico di questi sistemi e rinforzato da segnali d'ingresso che non hanno nulla a che fare con la loro dinamica interna. Questo nuovo fenomeno dinamico è stato chiamato "risonanza qualitativa".

3. *Modellizare e riconoscere* (Capitolo 4)
   In questo capitolo la risonanza qualitativa è utilizzata per il riconoscimento di patterns. Il cuore del metodo è un sistema dinamico caotico che può riprodurre la classe di serie temporali che si vuole riconoscere. Un segnale esterno è applicato al sistema in modo tale da realizzare un filtro a risonanza qualitativa. Dunque, se il segnale d'ingresso appartiene alla classe di serie temporali modellizzate allora il sistema vi si "aggancia" approssimativamente. In caso contrario, la traiettoria del sistema ed il segnale d'ingresso rimangono incorrelati.

4. *Realizzazione automatica del classificatore* (Capitoli 5 e 6)
   É presentato, specificatamente per il tipo di segnali considerato in questa tesi, un metodo per la realizzazione sistematica del classificatore. Il modello di riferimento usato è un sistema di Lur'e, ovvero un sistema dinamico non lineare in cui vi è una netta separazione tra la parte lineare, che è dinamica, e la parte non lineare, che è statica. L'identificazione dei parametri del modello a partire dai dati avviene in maniera iterativa, adattando alternativamente la parte lineare e quella non lineare. Di conseguenza, il difficile compito di identificazione non lineare è decomposto nei due più semplici compiti di identificazione dinamica lineare e statica non lineare. Infine, la maniera in cui l'ingresso deve agire sul sistema cosicché la risonanza qualitativa sia garantita è determinata con l'aiuto della teoria del controllo periodico lineare.

5. *Validazione* (Capitolo 7)
   Il metodo di riconoscimento di patterns proposto è stato validato sui seguenti esempi

   — Un esempio sintetizzato al calcolatore

   — Misure di laboratorio di un oscillatore di Colpitts

   — ECG

   — EEG

   — Vocali del segnale parlato

   Nei primi quattro casi si tratta di classificazione binaria mentre l'ultimo riguarda una classificazione su cinque classi.

Sulla base di quanto noto all'autore il metodo di riconoscimento proposto è originale. I sistemi caotici sono già stati utilizzati per produrre sequenze pseudo aleatorie e per modellizare la diversità di alcuni segnali. Anche l'identificazione parametrica di sistemi caotici non è nuova. Ciononostante, la costituzione del modello a partire dai dati ed il suo conseguente utilizzo in problemi di classificazione per mezzo del fenomeno della risonanza qualitativa è completamente nuovo.

ZUSAMMENFASSUNG

Diese Dissertation gehört zur allgemeinen Disziplin der Black-Box-Modellierung basierend auf realen Daten, genauer gesagt, von gemessenen Zeit-Reihen. Dies ist ein altes Thema und eine große Menge von Artikeln und Büchern wurde schon darüber geschrieben. Die Hauptschwierigkeit liegt darin, die Vielfalt von Daten, die im Grunde den gleichen Ursprung haben, zu erfassen; ohne Verwirrung mit Daten zu schaffen, die einen anderen Ursprung haben.

Normalerweise wird die Vielfalt von Zeit-Reihen durch einen stochastischen Prozeß, wie gefiltertes weißes Rauschen, modelliert. Oft ist es vernünftig anzunehmen, daß die Zeitreihe statt durch einen stochastischen Prozeß von einem deterministischen dynamischen System erzeugt wird. In diesem Fall wird die Vielfalt der Daten durch die Variabilität der Parameter des dynamischen Systems ausgedrückt. Die Parameter-Variabilität wird dann, einmal mehr durch einen stochastischen Prozeß modelliert. In beiden Fällen wird die Vielfalt durch eine Art exogenen Rauschens erzeugt.

Diese Dissertation geht einen Schritt weiter. Ein einziges chaotisches dynamisches System wird benutzt, um die Daten und ihre Vielfalt zu modellieren. Ein chaotisches System produziert tatsächlich eine ganze Familie von Trajektorien, die sich voneinander unterscheiden, aber sich trotzdem sehr ähneln. Man nimmt an, daß chaotische Dynamik nicht nur ein zweckmäßiges Mittel ist, um Vielfalt darzustellen, sondern daß in vielen Fällen der Ursprung von Vielfalt tatsächlich von chaotischer Dynamik herrührt.

Da der Ansatz dieser Dissertation vollkommen neue Grundlagen erforscht, wird die geeigneteste Art von Daten betrachtet, nämlich ungefähr periodische Signale. In der Natur sind solche Zeitreihen relativ häufig anzutreffen, besonders bei physiologischen Signalen von Lebewesen, wie Elektrokardiogramme (EKG), Teile von Sprach-Signalen, Elektroenzephalogramme (EEG) etc. Dort gibt es starke Argumente zugunsten der chaotischen Natur dieser Signale; sie scheinen die besten Kandidaten für eine Modellieren von Vielfalt durch Chaos zu sein. Es sollte aber betont werden, daß der Modellierungsansatz, der in dieser Dissertation verfolgt wird, für ziemlich allgemein angesehen wird und wird nicht auf Signale beschränkt ist, die durch chaotische Dynamik in der Natur produziert werden.

Die vorgesehene Anwendung des Modellierungsansatzes in dieser Dissertation ist die Klassifikation von zeitlichen Signalen. Dafür gibt es zwei Gründe. Erstens ist Klassifikation ein wichtiger Baustein jedes kognitiven Systems. Zweitens schlägt das in der letzten Zeit studierte Phänomen der Synchronisation chaotischer Systeme einen Weg vor, ein Signal in Bezug zu seinem chaotischen Modell zu prüfen.

Der wesentliche Inhalt dieser Arbeit kann nunmehr wie folgt formuliert werden.

These:

Die Vielfalt in der Natur vorkommender annähernd periodischer Signale kann mittels chaotischer Dynamik modelliert werden. Diese Art von Modellierungs-Technik, zusammen mit der selektiven Eigenschaft der Synchronisation chaotischer Systeme, kann für Mustererkennungs-Zwecke genutzt werden.

Diese These wird mittels der folgenden fünf Punkte gerechtfertigt.

1. *Modell der Zufälligkeit* (Kapitel 2)
   Es wird argumentiert, daß der in der Natur beobachtete Zufall nicht notwendigerweise das Ergebnis

exogenen Rauschens ist, sondern endogen erzeugt worden sein könnte, durch deterministische chaotische Dynamik. Die Vielfalt realer Signale wird verglichen mit den Signalen, die von den bekanntesten chaotischen Systemen produziert werden.

2. *Qualitative Resonanz* (Kapitel 3)
   Das Verhalten chaotischer Systeme, getrieben durch annähernd periodische Eingangssignale, wird theoretisch und durch numerische Simulation studiert. Es wird beobachtet, daß das chaotische System annähernd auf einem Eingangssignal "einrastet", das mit seiner internen chaotischen Dynamik verwandt ist. Im Gegensatz dazu wird sein chaotisches Verhalten verstärkt, wenn das Eingangssignal nichts mit seiner internen Dynamik zu tun hat. Dieses neue Phänomen wird "qualitative Resonanz" genannt.

3. *Modellierung und Erkennung* (Chapter 4)
   In diesem Kapitel wird qualitative Resonanz zur Mustererkennung benutzt. Der Kern der Methode ist ein chaotisches dynamisches System, das fähig ist, die Klasse von Zeitreihen zu reproduzieren, die erkannt werden sollen. Dieses Modell wird auf eine geeignete Weise von einem Eingangssignal angeregt, damit qualitative Resonanz auftritt. Dies bedeutet, daß, wenn das Eingangssignal zur modellierten Klasse von Zeitreihen gehört, "rastet" das System annähernd darauf ein. Wenn nicht, bleiben die Trajektorie des Systems und das Eingangssignal ohne Beziehung.

4. *Automatisierter Entwurf des Erkenners* (Kapitel 5 und 6)
   Für die Art von Signalen, die in dieser Dissertation betrachtet werden, wird eine systematische Entwurfsmethode des Erkenners vorgestellt. Das benutzte Modell ist ein System vom Typ Lur'e, d.h. ein Modell, bei dem der lineare dynamische und nichtlineare statische Teil getrennt sind. Die Identifikationen der Modellparameter von den gegebenen Daten wird iterativ fortgesetzt, indem abwechselnd der lineare und der nichtlineare Teil verbessert wird. Dadurch wird das schwierige nichtlineare dynamische Systemidentifikationsproblem in die leichteren Probleme linearer dynamischer und nichtlinearer statischer Systemidentifikation aufgeteilt. Die Art und Weise, in der das ungefähr periodischen Eingangssignal eingespeist wird, um sicherzustellen, daß qualitative Resonanz auftritt, wird mit der Hilfe periodischen Steuerungstheorie gewählt.

5. *Validierung* (Kapitel 7)
   Die Mustererkennungsmethode ist für die folgenden Beispielen bestätigt worden

   — Ein synthetisches Beispiel

   — Labor-Messungen vom Colpitts-Oszillator

   — EKG

   — EEG

   — Vokale eines Sprachsignals

   In den ersten vier Fällen wurde eine binäre Einteilung getroffen. Im letzten Beispiel wurde eine Einteilung in fünf Klassen durchgeführt.

Nach bestem Wissen des Autors ist diese Erkennungsmethode neu. Chaotische Systeme wurden schon benutzt, um Pseudo-Rauschen zu produzieren und Signal-Vielfalt zu modellieren. Auch ist Parameter-Identifikation chaotischer Systeme schon ausgeführt worden. Aber die direkte Ableitung des Modells basierend auf den gegebenen Daten und seine nachfolgende Verwendung zur Klassifikation, basierend auf dem Phänomen der qualitativen Resonanz, ist völlig neu.

ACKNOWLEDGMENTS

It is always rather difficult to acknowledge the people who directly, but often indirectly, have contributed to the accomplishment of a task. This becomes even tougher when such sentiment of appreciation must be expressed in a foreign language; this is why I will be "strangely" brief.

In the first place, I am grateful to Professor Martin Hasler; firstly, for having proposed the research topic which finally results in this thesis and, in particular, for having chosen me for accomplishing his idea, giving me, in this way, the opportunity to come to work and live in Switzerland. Immediately thereafter, all the members of the referee committee deserve my best thanks; at first for having read, and corrected, with a lot of patience the first version of this manuscript, then for the wonderful and challenging discussions we had the day of the private defense.

From the private side, I wish to thank Rosario Pitarelli, Arnaud Robert, Thomas Schimming, and Joerg Schweizer who have been not simply colleagues but friends too. They substantially helped me on practical items when I just arrived in Switzerland; they have always endured all my idiosyncrasies, which is not always trivial; and, most important, they have been wonderful companions of everyday live as well as of tough discussion on any kind of topic, from epistemology to coarse engineering applications. In these discussions, I have found most of the inspirations that definitely influenced the development of this thesis. Together with them, I would like to thank all my non-engineers friends whose friendship and patience in explaining me their own interest has preserved me from becoming a narrow-minded engineer and kept alive my child curiosity in whatever happens around me. Actually, there are too many other persons deserving my thanks, but writing down their names explicitly would take another volume for this thesis. I am sure that they will forgive me for thanking them all together in this anonymous form: "Please, accept my best thanks for all that you have done".

Finally, I am grateful to the Swiss Confederation; in particular, to its Science National Found who sponsored me for four years.

Lausanne, March the 10th
Oscar De Feo

CONTENTS

CHAPTER 1

INTRODUCTION

Brief — This chapter gives an introductory view of the motivations that lead to begin this thesis project. The chapter gives as well a brief introduction about the two main topics that this thesis deals with, namely *nonlinear dynamics* and the *dynamical paradigm of cognitive sciences*, this should help the reader to understand what are the phenomena and the mathematical tools addressed in this thesis. A brief state of the art about the relevant topics is included too.

In the very recent years a new, strong, interest in nonlinear dynamics has been raised by the endeavor of engineers to bring the recent discoveries in nonlinear systems theory, like deterministic chaos and bifurcation theory, from a state of mathematical gadgets and amusing phenomena to a new state of application tools. This thesis, which belong to such attempts, would gives a new emphasis on the role played by chaotic dynamic in the process of learning and representing uncertainty.

1.1 Motivations of the Thesis

This thesis deals with the role of *chaotic dynamics* in *cognitive sciences*, more in particular it addresses the problem of *intelligent systems* dealing with, and representing, uncertainty. Questions about how intelligent systems deal with uncertainty arise in several fields, actually in all those fields that, in one way or another, are interested and clustered by the big topic of cognitive sciences as, for instance, psychology, philosophy, and engineering. Since these fields are so diverse, the very same problem can be addressed in several ways. In particular, the role of chaotic dynamics in cognitive sciences raises two main questions: one philosophical and the other one from engineering. The philosophical question asks whether or not, and if yes why, the brain, or better the living beings, are chaotic systems. The engineers, which are interested in more practical things, investigates the possibility of exploiting chaotic dynamics to emulate intelligent behavior. Naturally, this thesis addresses the second question but, nevertheless, the methodology and arguments used herein are helpful for some philosophical digression too.

Obviously, the problem of *machine intelligence* in engineering is a fairly large one and the role of chaos in it cannot be treated in its entirety in a single thesis. Here, the problem is addressed assuming the *pattern recognition* process as basic cognitive elaboration (refer, for instance, to [Alder, 1994; Newman, 1998; Russell and Norvig, 1999; Schalkoff, 1992]). Broadly speaking the pattern recognition is the process that concerns the description or classification, or recognition, of measurements and as such it is at the very base of those processes that should lead to an intelligent behavior. Indeed, at the base of an intelligent inferential process there is the collection and classification of data, *i.e.* measurements, from which to extract the information needed to infer the next intelligent action.

On the base of such hypothesis, the aim of this thesis is to propose new methods for pattern recognition based on nonlinear phenomena. The motivation of such a choice are in the strong results obtained in the field of Artificial Intelligence under the new *dynamical hypothesis*, which is described in the next sections, about mind and perception. To follow such new ideas is very advanced and exciting but, from the practical point

of view, choosing to exploit nonlinear dynamics is, on the other hand, quite a risk. Indeed, while the results obtained in several fields with new "nonlinear eyes" are definitely promising, they are typically not in a useful state for an engineering application. Commonly, these results are preliminary investigations aimed to confirm the chaotic nature of different "natural" phenomena or to probe the applicability of chaos theory in this or that application. Seldom these results are presented together with the design tools needed to master the engineering of an application. In fact, despite of the growing interest, and publications, about nonlinear phenomena in various fields, the role of the mathematical tools and theories related to nonlinear phenomena have difficulty in evolving from their state of mathematical curiosities to a more advanced and useful set of tools for engineering. This is mainly because of the *divide et impera* approach used by engineers which leads almost automatically to the use of the more easy and complete linear systems theory. Since among the aim of this thesis is the desire of bringing out the deterministic chaos from its state of mathematical amusement, particular attention has been given to avoid excessive mathematical complexity along the whole research path that has been conducted. Every choice has always been taken with the idea of an engineer-like final user in mind. An engineer that usually dislikes too complex or hardly tractable methods and algorithms.

With such an idea in mind, this thesis proposes a new way of designing pattern recognizers that exploit the nonlinear dynamical systems theory as well as to provide practical and theoretical confirmations about the role of chaos in cognitive sciences. In more detail, considering one-dimensional temporal patterns, namely real-time field measurements, the purpose of the thesis is to show how the new theoretical achievements obtained in nonlinear dynamical systems theory can be exploited for the design of general purpose pattern recognizers based on the synchronization properties of chaotic systems. In fact, rather than focusing on an entire specific application of temporal pattern recognition, the thesis focuses on general purpose recognizers that can be used as preprocessor for currently used, or eventually new, Artificial Intelligence applications. The main reason of such a choice are the new revolutionary ideas about the sensory system in living beings which are described, together with the justification of the choice of using of nonlinear dynamical systems, in the following paragraph.

1.1.1 Why Nonlinearity?

The question "Why nonlinear dynamical systems?" should immediately arise, indeed it is not a very common choice in engineering. Even if in the next two sections strong arguments are implicitly moved to justify such a choice, it is definitely worthwhile to report here those that should be considered the strongest.

Most of the engineering related to the modern Artificial Intelligence, in particular since the connectionist, *i.e.* neural, paradigm, is usually called *biologically inspired* to underline that the algorithms and methods proposed are, as a matter of fact, inspired by their biological counterpart; just an example are *artificial neural networks* and the *situated robotics*, known also as *behavioral robotics*. Actually, during the last decade big steps have been made in the classification of nonlinear systems that seem to be present in *Nature*, in particular systems that look like being chaotic. A parallel result of this work is a kind of principle saying that nature should be or should tend towards chaos. In other words, the "good behavior" of natural systems requires a chaotic dynamics, or, more in general, a behavior related with nonlinear dynamics. Such a principle has been advocated, with more or less convincing arguments, in various areas of biology and engineering[1]. At this point the conclusion should be quite automatic: "If Nature, namely biology, is chaotic, then biologically inspired engineering should be chaotic as well".

Supporting further such a hypothesis is the revolution in the understanding of the sensory system of living beings. Until not so long time ago, the sensory system was perceived as a simple transducing system, namely a simple system that transduces the external stimuli, light, odors, sound, pressure, etc., in an internal signal, like an electric current or a sequence of symbols. No intelligence was supposed at such level. Nowadays, it is clear that the sensory system itself is a more involved one, it processes the incoming stimuli providing to the higher levels of the cognitive agent, *i.e.* the brain or the intelligent machine, a highly formatted information which implies that a lot of intelligent behavior has been already involved at sensory level. The pattern recognizer presented in this thesis is an analogy of this sensory level, it does not suppose a high level, *i.e.* symbolic, but raw field signals, *i.e.* measurements, inputs and provide outputs to be treated by a higher level of the cognitive system.

[1] Examples in ecology are the heart beating [West and Goldberger, 1987], brain activity [Kelso, 1995; Rapp *et al.*, 1985], ecosystem [Abrams and Roth, 1994; De Feo and Rinaldi, 1997; Gragnani *et al.*, 1998], metapopulations [Rinaldi and De Feo, 1999] and natural selection [Ferrière and Gatto, 1993], just to cite few of them. Engineering is also full of examples such as self-organization [Kauffman, 1993; Thiran, 1996], fluid-dynamics [Bergé *et al.*, 1984], mechanics [Healey, 1992], automatic neural learning [Tani and Fukumura, 1995], autonomous mobile robot [Tani, 1996], and many others.

Since it is shown in several laboratory experiments, and in several models as well, that the preprocessing at sensory system level seems to be based on nonlinear properties and in particular on synchronization properties of oscillatory neurons, see for instance the overview in [Rabinovich *et al.*, 2000][2] and references therein, the choice of exploiting the very same properties for the artificial counterpart is straightforward.

1.2 Nonlinear Dynamical Systems and Chaos

Before introducing the *dynamical approach to cognition* it is better to introduce what is the *dynamical systems theory* and more in details what is meant here with *chaotic dynamics*.

The dynamical systems theory definitely finds its roots in the *differential calculus* formerly introduced by Newton and Leibniz in the fifteenth century. Newton's and Leibniz's invention of the differential calculus gave a new language with which to model natural phenomena. To the extent that the natural laws are objectively understood, they are written as *equations of motion*. These are procedures that, given a sufficient measurement of a system's configuration, specify how to compute its future behavior. Often articulated in the language of differential calculus, the equations of motion codify the interplay of the components of a system's configuration. They are, in fact, incremental rules, *i.e.* an *algorithm*, that determines the configuration at the next moment in terms of the one immediately preceding.

Albeit writing the equation of motions is usually a simple procedure that follows directly from the very basic laws of physics, or other fields, their implementation as a procedural description has only recently become feasible. Before this time, when sequential, compounded computation could only be performed by hand, even the simplest prediction problems demanded arduous and typically impractical efforts. Thus, mathematical techniques were developed to solve the equations of motion. In the limited settings for which this could be carried out, practically only linear equations, the analytic methods yielded *closed form solutions* which shortcut the direct incremental computation of future behavior. Closed form solutions has been the dominant criterion for understanding dynamical behavior since the time of Newton until very recently. Indeed, the research of closed form solutions for the natural laws, in order to forecast the evolution of the universe, has been one of the central themes in mathematics and physics until the turn of the last century. The belief that such solutions could be found in a closed form, and the assumption that it was easy to do so, was most succinctly expressed by Laplace more that two centuries ago:

> The present state of the system of nature is evidently a consequence of what it was in the preceding moment, and if we conceive of an intelligence which at a given instant comprehends all the relations of the entities of the universe, it could state the respective positions, motions, and general affects of all these entities at any time in the past or future.

Unfortunately, or maybe fortunately for the existence of this thesis, a vast number of phenomena cannot be described by equations of motions that allow for closed form solutions. The types of phenomena now demanding scientific attention, such as the fluid-dynamics and even substantially smaller systems, are explicitly nonlinear and do not, even in principle, allow for closed form solutions. That there was a fundamental limit to finding closed form solutions was appreciated by Poincaré at the turn of this century. Although he despaired of this, he was also the initiator of the alternative approach of describing complex behavior, qualitative dynamics, which later became dynamical systems theory.

1.2.1 Dynamical Systems Theory Primers[2]

A central abstraction in dynamical systems theory is that the instantaneous configuration of a process is represented as a point, or *state*, in a space of states, the *state space*. The *dimension* of the state space is the number of numbers required to specify uniquely the system's configuration at each instant. With this, the *temporal evolution* of the process becomes the motion from state to state along an *orbit* or *trajectory* in the state space. For a simple moving mass the state space is the two-dimensional plane. A state here consists of two numbers: one denoting the position, the other the velocity. The state space of a fluid in a pipe is the velocity field: the space of all possible instantaneous changes in fluid particle positions. If every particle moves independently, the dimension of the equivalent dynamical system is exceedingly large: proportional to the number of particles. Despite of the difficulty in picturing this representation directly, the temporal

[2]In this respect, these are very interesting references too [Basar, 1990; Elbert *et al.*, 1994; Freeman, 2000; Getting, 1989; Hopfield, 1991, 1995, 1996; Izhikevich, 2000].

[2] For those readers that would like to know more about systems theory, these references are suggested [Callier and Desoer, 1991; Katok and Hasselblatt, 1995; Ott, 1993; Strogatz, 1994].

evolution of the fluid is abstractly associated with a trajectory in this high-dimensional state space. In the fortunate case when there is strong coherence between components of a large system or when the system itself has only a few significant components, the trajectory can be visualized in a much lower-dimensional space.

If a temporal sequence of configurations is observed to be stable under perturbations and is approximately recurrent, then the trajectory is said to lie on an *attractor* in the state space. The attractor concept is a generalization of the classical notion of equilibrium. One of the main contributions of dissipative dynamical systems theory is the categorization of all long term behaviors into four attractor classes. A *fixed point*, *i.e.* an *equilibrium*, attractor is a single, isolated state toward which all neighboring states evolve. A *limit cycle* is a sequence of states that are repetitively visited, the minimal time interleaving the visit of the very same state is called the *period* of the cycle. A *torus* is the product of multiple limit cycles which have irrational ratio of their frequencies. These attractors describe predictable behavior: two orbits starting from nearby states on such an attractor stay close as they evolve. Unpredictable behavior, for which the latter property is not true, is described by chaotic attractors. In a crude approximation, these are often defined negatively as attractors that are neither fixed points, limit cycles, nor products of limit cycles. The next paragraph is entirely dedicated to such objects.

Aside from attractor classification, another significant contribution of dynamical systems theory is a geometric picture of transients: how states off an attractor relax onto it. An attractor's *basin of attraction* is the set of all initial states that evolve towards it. There can be multiple basins, so that radically different behavior may be seen depending on the initial configuration, namely *multiple attractors* can be observed. The complete catalogue of attractors and their basins for a given dynamical system is called its attractor—basin portrait.

Dynamical systems theory is also the study of how attractors and basin structures change with the variation of external control parameters. A *bifurcation* occurs when, with the smooth variation of a control parameter, the attractor—basin portrait changes qualitatively.

1.2.2 Deterministic Chaos[3]

Chaos is the deterministic production of behavior that is unpredictable over long times. Although there are a number of ways to express its defining properties, a simple example will serve to introduce the key considerations in deterministic chaos: the breakdown of predictability, observation of a complex process, and the mathematical effort required to forecast. These have their analogues in the dynamical systems theory of chaos, information theory of measurement, and computational theory of modeling.

The weather is often considered a prime example of unpredictable behavior. In fact, it is quite predictable. Over the period of one minute, one can surely predict it. With a glance out the nearest window to note the sky's disposition, one can immediately report back a forecast. To predict over one hour, one would search to the horizon, noting more of the sky's prevailing condition. Only then, and not without pause to consider how that might change during the hour, would one offer a tentative prediction. If asked to forecast two weeks in advance one would probably not even attempt the task since the necessary amount of information and the time to assimilate it would be overwhelming. Despite of the long term unpredictability, a meteorologist can write down the equations of motion for the forces controlling the weather dynamics in each case. In this sense, the weather's behavior is symbolically specified in its entirety. The short way of justifying how unpredictability arises in such a situation is that the governing natural laws, although expressible in a compact symbolic form, can implicitly prescribe arbitrarily complicated behavior.

There are several complementary descriptions of the basic properties of chaotic attractors. Analytically, they consist of highly convoluted orbits. An infinite number of unstable limit cycles and an infinite number of aperiodic orbits can be embedded in a chaotic attractor [Cvitanović, 1984; Devaney, 1995; Eckmann and Ruelle, 1985; Ott, 1993]. Topologically, chaotic attractors often display self-similar, or fractal, structure. Geometrically, although globally stable to perturbations off the attractor, they exhibit average local instability. Orbits starting at close initial states on a chaotic attractor separate exponentially fast. Physically, this local instability amplifies microscopic fluctuations to affect macroscopic scales. Although the resulting macroscopic behavior may be predictable over sufficiently short times, to an observer it is unpredictable over long times. Even in the absence of microscopic fluctuations, forecasting typical chaotic orbits requires maximal computational effort on the part of an observer who knows the governing equations

[3]For those readers that would like to know more about deterministic chaos these references are suggested [Abraham and Shaw, 1989; Devaney, 1989, 1992; Gleick, 1987; Ott, 1993; Ruelle, 1991; Strogatz, 1994].

of motion. The size of the minimal computer program to predict grows with the length of the forecast since the number of symbols used to represent the real numbers must grow to reflect the desired precision.

To the way of exploiting these properties for the purposes of this thesis is entirely dedicated the Chap. 2.

1.3 The Dynamical Approach to Cognition

Attempts to understand the mind and its operations go back at least to the Ancient Greeks, when philosophers such as Plato and Aristotle tried to explain the nature of human knowledge. The study of mind remained the province of philosophy until the nineteenth century, when experimental psychology developed. Within a few decades, however, experimental psychology became dominated by behaviorism, a view that virtually denied the existence of mind. According to behaviorists, psychology should restrict itself to examining the relation between observable stimuli and observable behavioral responses. Even though the behaviorism was dominating the scene, around 1956 the intellectual landscape began to change dramatically (refer to [Donald, 1991] for a more detailed historical view). George Miller [Miller, 1956], around 1956, summarized numerous studies which showed that the capacity of human thinking is limited, with short-term memory, for example, limited to around seven items. He proposed that memory limitations can be overcome by recoding information into chunks, mental representations that require mental procedures for encoding and decoding the information. At this same time, primitive computers had been around for only a few years, but pioneers such as John McCarthy, Marvin Minsky, Allen Newell, and Herbert Simon were founding the field of Artificial Intelligence [McCarthy, 1956; Minsky, 1954, 1956; Newell *et al.*, 1957]. In addition, Noam Chomsky [Chomsky, 1957] rejected behaviorist assumptions about language as a learned habit and proposed instead to explain language comprehension in terms of mental grammars consisting of rules. In these days the foundations of the *computational paradigm* of cognitive sciences were born and its central hypothesis was formulated: *thinking can best be understood in terms of representational structures in the mind and computational procedures that operate on those structures* (refer, for example, to [Churchland and Sejnowski, 1992]). While there is much disagreement about the nature of the representations and computations that constitute thinking, the central hypothesis is general enough to encompass the current range of thinking in cognitive sciences, including connectionist theories which model thinking using artificial neural networks.

Only recently, the nonlinear systems theory entered the domain of Artificial Intelligence, in particular, in the 1992, Globus [Globus, 1992] proposed a noncomputational approach to cognitive sciences. Nevertheless, even before the work of Globus the Artificial Intelligence community exploited the methods of dynamical systems theory to analyze their main product, namely the automatic learning algorithms (ALA), refer for instance to [Michalski *et al.*, 1983, 1986; Nilsson, 1990; Pollack, 1991]. Although at the beginning the motivation that lead to a dynamical interpretation of the *learning machines* was mainly of analysis purposes (the aim was to discover the stability of such machines/algorithms), soon it was putting in doubt the central hypothesis of cognitive sciences. The claim that human minds work by representation and computation is an empirical conjecture and might be wrong. Albeit the computational-representational approach to cognitive sciences has been successful in explaining many aspects of human problem solving, learning, and language use, some philosophical critics such as those of Hubert Dreyfus, Tim Van Gelder, and John Searle (refer, for instance, to [Dreyfus and Dreyfus, 1987; Thagard, 1996; van Gelder, 1998]) have claimed that this approach is fundamentally mistaken. In the very recent, philosophers, supported by the recent advance in chaos theory, have come to the belief that the mind is a dynamical system, not a computational one. This new hypothesis and the recent applications of nonlinear dynamics in the field of Artificial Intelligence have lead to what today is known as *dynamical paradigm of cognitive sciences*.

Although its formal formulation is quite recent, the dynamical approach is not a recent development. It is not a fad or a proposal or a vision. It's a framework for the study of cognition which has been under active exploration throughout the existence of cognitive sciences. It subsumes a great deal of connectionism, situated robotics, psychology and neuroscience. The most powerful accounts of a wide variety of aspects of cognition already take dynamical form. It is currently the most rapidly growing form of research in cognitive sciences. Perhaps the only new thing is the realization that the dynamical approach is a research paradigm: that, in other words, dynamics provides the deep organizing principles for a general approach to the study of cognition.

The main points of the classical *computational approach* and the modern *dynamical approach* are summarized in the next two paragraph. For more details please refer for instance to [Fodor, 1975; Johnso-Laird, 1988; Pylyshyn, 1984; Thelen and Smith, 1994; van Gelder, 1998; van Gelder and Port, 1995]. In particular a very nice, biased, review on the argument can be found in [Beer, 2000].

1.3.1 Computational Approach

The core of the computational approach is the idea that cognitive systems are a special kind of computer. For current purposes, a computer is a device which automatically manipulates symbol structures in ways that are accordance with a systematic interpretation of those symbols. Standardly, the symbol structures are taken to be static; that is, the symbols themselves don't change over time. Computational operations take the system from one configuration of static symbols to the next.

The computational approach places the computer inside the head. The result is a general picture of the nature of cognitive systems. This picture has a number of central structural elements. Cognitive systems are hypothesized to be internal to the body; representational: the medium of cognitive processing is the internal, static, symbolic representation; computational: cognitive processes are sequences of discrete transformations from one configuration of static symbols to the next; homuncular: the overall cognitive system has a hierarchical structure of components, each of which is computational in its own right, and which interact by passing representations; sequential: tasks are carried out in a discrete temporal order; and cyclic: the system operates on a sequential cycle of input—internal computation—output.

1.3.2 Dynamical Approach

The core of the dynamical conception is the idea that cognitive systems are a special kind of dynamical system. Around this core is constructed a broad picture of the nature of cognitive systems, a picture which is diametrically opposed to the computational one.

For current purposes, a dynamical system is a system which evolves over time in a dynamical fashion. A system is a self-contained complex of parts or aspects that can interact. What is it for a system to evolve dynamically? The term "dynamical" is derived from the Greek word $\Delta\gamma\nu\alpha\mu\omega\sigma$ meaning forceful or powerful. Thus, in a paradigmatic dynamical system, changes are the result of the forces operating within the system.

The dynamical hypothesis of cognition identifies cognitive phenomena with the behavior of a dynamical system. Consequently, the cognitive system is taken to be a complex of parts or aspects, each of which evolves over time in a way that simultaneously influences and is influenced by the evolution of others. Since activity in the nervous system, in the body, and in the environment are all simultaneously affecting each other, none is self-contained; hence the true unit of cognitive performance spans all three. However, since it is impossible in practice to model the whole system at once, dynamicists in cognitive sciences focus on particular cognitive phenomena and demonstrate that they can be modeled as the evolution of smaller component systems.

In the resulting overall picture, cognitive systems are not internal, but span brain, body and environment; not inherently representational; not computational, but rather a matter of continuous real-time evolution; not homuncular, since subsystems of a dynamical system interact by shaping each other's dynamics, not passing representations; not sequential, since all parts or aspects of the system are continuously and simultaneously co-evolving; and not cyclic, since there is no sequence and hence no possibility of an input—internal activity—output cycle.

It could be thought that, since dynamical systems are commonly *simulated* on digital computer, the two paradigms are essentially the same. It is just a matter of saying. Actually, this is not the case; the crucial point of the central hypothesis of computationalism is not the "computer" but its "internal" symbolic representation of reality which, in a computational[5], *i.e.* symbolic, paradigm is supposed to be *grounded* [Harnad, 1990] to the reality that it represents. On the contrary, in the dynamical approach, the "internal" symbolic representation is not supposed to be a straightforward representation of any of the "outside" reality. Hence, in the computationalism, the intelligent behavior is the result of the manipulation, by means of a high level computer, of a grounded symbolic representation of reality. On the contrary, in the dynamicism, the intelligent behaviour could emerge without the consciousness of the self [Tani, 1998] necessary to ground the symbolic "internal" representation to the outside reality.

1.3.3 Why the Dynamical Approach?

Nonetheless the fact that the computational and dynamical hypotheses are thus very different, there are no *a priori* reasons to claim that one is better than the other. Very recently, a lot of arguments have been moved to support one or the other party, see for instance [Beer, 2000; Fodor and Pylyshyn, 1988; Mitchell,

[5]The computational paradigm is also known as *symbolic paradigm* of cognitive science. Actually, this term reflect better the main hypothesis of the computational paradigm.

2000; Pinker and Prince, 1988]. In the following those reasons pro dynamicism that mainly lead to consider the dynamicist approach for this thesis are reported.

From a practical point of view, it should be considered that, even if the total quantity of research under the dynamical assumption is currently smaller than the counterpart under the computational paradigm, its scope is more broad. Its explanatory principles operate as effectively in describing neural activity and the behavior of the body as they do for "central" or "higher" cognitive processes. Indeed, the research under the dynamical assumption spans such diverse aspects of cognition as visual, auditory and haptic perception, decision making, syntax, phonology, speech production, coordination, and development. Furthermore, the cognitive processes always unfold in real time. Where "real time" means more than "fast enough to follow the environment"; it means that time is a continuous index, and there's a changing state of the cognitive system at every point in this continuum. An adequate model of cognitive processes will specify these states and how they change. It is of the essence of dynamical models to describe how processes unfold in real time. Computational models, with their sequence of operations in an abstract time that is simply the index of in the operation sequence (usually called *ersatz*), are inherently incapable of doing this. The sum of these two considerations lead to conclude that the dynamical approach is the only one that could cope with the new vision of cognitive agents in which sensory and decisional subsystem are both "intelligent" and tightly connected.

From a more speculative[6] point of view, it should be considered that dynamical systems theory is the single most powerful and successful explanatory framework science has ever known. It can be used to describe countless aspects of the natural world, ranging from subatomic behavior to planetary motion, from neurons to ecosystems. Computation theory, by contrast, is known to apply to only one thing in the universe: digital computers; and these, of course, were artificially constructed by humans according to the computational blueprint.

1.4 Current State of the Art

The main topics engaged by this thesis project are *pattern recognition*, *nonlinear systems theory*, and *cognitive sciences*. In these rapidly advancing fields, especially in the last ten years, it has become quite difficult to have a real overview of all the latest results in each of the specific fields. Nevertheless, it is possible to restrict the field of interest substantially since the thesis project is focused on pattern recognition methods based on nonlinear dynamics.

There are several works and reference books aimed to show the importance of a dynamical approach to cognitive sciences. Refer, for instance, to [Beer, 2000; Holyoak and Thagard, 1995; Robertson *et al.*, 1993; Thagard, 1992; Thelen and Smith, 1994; van Gelder, 1998]. Two of the most methodological analyses in this direction are presented in the two Ph.D theses of Chris Elias [Elias, 1995] and of David Newman [Newman, 1995], whose contents are well summarized in [Newman, 1996, 2001]. There, the dynamic hypothesis for cognitive sciences has been evaluated from a purely abstract, almost philosophical, point of view, reaching the conclusion that : "It is undeniable that brains are dynamical systems".

Staying in speculative environments the works of [Barton, 1994; Globus, 1992; Miller, 1988; Morton, 1988; Skarda and Freeman, 1987] are notable. There, the needs of complexity for resolving different problems, among which there are those of symbolization necessary for the language and number concept, are presented in terms of chaotic dynamical systems. Less directly but anyway related are the works collected in [Kauffman, 1993] regarding the capabilities of self organization spanned by chaotic dynamical systems.

From a more practical point of view, some of the best results in the same direction are those obtained at the Sony labs [Tani, 1996, 1998; Tani and Fukumura, 1995] and at the Nec research institute [Giles *et al.*,

[6] The philosophical reasoning is restricted to this note since it is surely not essential in an engineering thesis. The computational conception of cognition is essentially just the seventeenth century vision of the nature of mind as implemented by twentieth-century computer science. In particular, it span Descartes' idea that mind is an inner representational entity that is causally responsible for our sophisticated behaviors; Hobbes' idea that the mind is identical with the brain, and that thought is the manipulation of neural symbols; and Leibniz's idea that all the knowledge necessary for intelligent behavior can be made explicit in theoretical form. The obviousness of the computational approach for many cognitive scientists can be explained in terms of their prior, and usually unwitting, acceptance of this worldview. The seventeenth century picture has been attended by a wide variety of metaphysical and epistemological difficulties. One of the most important ongoing achievements of philosophy of mind this century has been to diagnose these difficulties as flowing directly from the basic ontological structure of the picture itself. Philosophers such as Ryle and Heidegger have replaced the generically Cartesian conception of mind as the inner computer with an understanding of mind as essentially situated activity. This activity is directed and evolves in the same time frame as the physical and social contexts in which it is situated; as Heidegger put it in Being and Time, the essence of Dasein is temporality. In studying temporal phenomena, science has always turned to dynamics. Hence the dynamical conception of cognition is the scientific realization of the post-Cartesian ontology of mind.

1994; Giles and Omlin, 1993].

The works at the Sony labs have been dedicated mainly to showing how complex behaviors, *i.e.* bifurcations and chaos, can arise in *agents* that learn in a unknown and noisy environment. More precisely, these works successfully move towards demonstrating the natural tendency of behavioral based artificial agents to build a symbolic representation of the grammars hidden in the geometry of the workspace by means of multi-wing chaotic attractors. Furthermore, the artificial agents are able to build different action plans to reach an arbitrary goal exploiting the self organization of the symbolic process embedded into the strange attractor.

The works from Nec have mainly addressed two issues: to determine the computational power of dynamical learning models and how they scale with the problem size. The results are definitively encouraging showing that both the issues are well handled by the dynamical learning models. On one hand the possible complex dynamics of a dynamic learning model allows to span, *i.e.* learn, complex grammars, both deterministic and stochastic ones, emulating the underlying stochastic processes by means of chaotic dynamics with similar statistical properties. On the other hand, results show that simple dynamical learning models can handle rather large grammatical inference problems encoding finite memory machine strings in temporal patterns.

In a similar direction are the works dealing with the human language understanding and production. In particular, [Browman and Goldstein, 1995; Port *et al.*, 1995], whose aim is to give dynamical foundations to models of the temporal structure of speech perception and production, and [Petitot, 1995; Pollack, 1991; Seigelmann, 1999] which, on the other hand, deal with the more abstract models of the grammatical structure.

On the side of pure pattern recognition theory, it is quite difficult to establish the current state of the art with respect to our aim. With respect to this thesis, pattern recognition is taken as one of the fundamental cognitive elaborations [Alder, 1994] and not as stand-alone signal processing as done in several single purpose applications such as handwriting and speech recognition. In the context of dynamical learning models the three fundamental approaches to pattern recognition [Schalkoff, 1992]: statistical, syntactic, and neural, *i.e.* connectionist, approaches mix up. In fact, it has been shown (refer, for example, to [Omlin *et al.*, 1999]) that dynamical learning models can imitate/emulate one of these approaches depending upon the context. In such a sense the amazing results obtained nowadays for handwriting, speech, heart pathologies, etc. recognition (refer, for instance, to [Cole *et al.*, 1997; Lecun *et al.*, 1998]) cannot be taken as reference because of their structure that is tied to the specific problem.

From a "dynamicist" approach to pattern recognition the latest and strongest results are in a symbolic context. Namely, most of the proposed pattern recognizers, or *associative memories*, based on chaotic dynamics until nowadays, see for instance [Andreyev *et al.*, 1996, 1999] and the references therein, are based on a symbolic representation of the patterns. More in detail, this kind of approaches usually map an alphabet of symbols on the state space of a low-dimensional discrete time system associating patterns to the unstable limit cycles that compose chaotic attractors. Even if very similar to the method proposed herein it is diagonally opposite with respect to the context of the approach. The proposed methods discussed above receive as input a sequence of symbols or, alternatively, a probability density over an alphabet of symbols, therefore these systems suppose the existence of a further external system that will treat the field signals, namely a system that will transform external inputs into symbolic sequence, or in a probability density over an alphabet of symbols. On the contrary, what is proposed in this thesis are exactly this kind of system, namely the sensory system of intelligent machines.

In this respect, the latest and strongest result in an approach similar to that presented herein are those of Nec and Sony [Giles and Omlin, 1993; Tani, 1996]. Even if these works are not explicitly dedicated to pattern recognition problems, the pattern recognition is a key process in the problems they deal with, namely, complex grammatical inference and autonomous mobile robotics. Furthermore, the systems considered there are complete system, from sensors to "brain", and the architectures presented in such works do not imply a division from "sensing" and "thinking" therefore they are very close to the methods presented here.

1.5 Organization of the Thesis

This thesis is divided into eight Chapters. To assist the reader, each one of the chapter begin with a very brief description of what is its content and end with a brief discussion of the results presented. Here the topics treated in each Chapter follows.

Chp. 1. Here the context in which the thesis has been developed is introduced as well as the *dynamical systems theory* and the *cognitive approach to cognitive sciences*.

Chp. 2. In this Chapter the relationship between chaotic dynamics, class of strange attractors, and randomness is given.

Chp. 3. In this chapter the main nonlinear phenomena exploited through this thesis is presented.

Chp. 4. Here the overall picture to exploit strange attractors to build pattern recognizers as well as the *Thesis* of this research work is introduced.

Chp. 5. This Chapter is dedicated to the modeling of the diversity of approximately periodic temporal patterns by means of strange attractors.

Chp. 6. This Chapter is dedicated to the test of a pattern inside a strange attractor, namely the pattern matching procedure.

Chp. 7. Here very simple and quite academic examples are described to show the capabilities of the presented method.

Chp. 8. In this final Chapter a discussion of the results is summarized together with some more philosophical conclusion. Proposal for future research are given too.

Bibliography

Abraham, R. and C. Shaw (1989). *Dynamics: The Geometry of Behavior*. Aerial Press, Santa Cruz, CA, fourth edition.

Abrams, P. and J. Roth (1994). The responses of unstable food chains to enrichment. *Evolutionary Ecology*, 8, pp. 150–171.

Alder, M. (1994). *Principles of Pattern Classification: Statistical, Neural Net and Syntactic Methods of Getting Robots to See and Hear*. Not published. Freely available on the world wide web: ftp://ciips.ee.uwa.edu.au/pub/syntactic/book,http://ciips.ee.uwa.edu.au/ mike/PatRec/.

Andreyev, Y., Y. Belsky, A. Dmitriev, and D. Kuminov (1996). Information processing using dynamical chaos. *IEEE Transactions on Neural Networks*, 7, pp. 290–299.

Andreyev, Y., A. Dmitriev, and A. Ovsyannikov (1999). Chaotic processors and content-based search of information in unstructured data bases. *Interdisciplinary Journal of Nonlinear Phenomena in Complex Systems*, 2, pp. 48–53.

Barton, S. (1994). Chaos, self-organization, and psychology. *American Psychologist*, 49, pp. 5–14.

Basar, E. (1990). *Chaotic Dynamics and Resonance Phenomena in Brain Function: Progress, Perspectives, and Thoughts*, pp. 1–30. Springer-Verlag, Berlin, Germany.

Beer, R. (2000). Dynamical approaches to cognitive science. *Trends in Cognitive Science*, 4, pp. 91–99.

Bergé, P., Y. Pomeau, and C. Vidal (1984). *L'Ordre dans le Chaos: Vers une Approache Déterministe de la Turbolance*. Hermann, Paris, France. In French.

Browman, C. and L. Goldstein (1995). *Dynamics and articulatory phonology*, pp. 175–193. MIT Press, Cambridge, MA.

Callier, F. and C. Desoer (1991). *Linear System Theory*. Springer-Verlag, New York, NY.

Chomsky, N. (1957). *Syntactic Structures*. Mouton, The Hague, The Netherlands.

Churchland, P. and T. Sejnowski (1992). *The Computational Brain*. MIT Press, Cambridge, MA.

Cole, R., J. Mariani, H. Uszkoreit, A. Zaenen, and V. Zue, editors (1997). *Survey of the State of the Art in Human Language Technology*. Cambridge University Press, Cambridge, UK.

Cvitanović, P., editor (1984). *Universality in Chaos*. Adam Hilter, Bristol, UK.

De Feo, O. and S. Rinaldi (1997). Yield and dynamics in tritrophic food chains. *The American Naturalist*, 150, pp. 328–345.

Devaney, R. (1989). *An Introduction to Chaotic Dynamical Systems*. Addison-Wesley, New York, NY.

Devaney, R. (1992). *A First Course in Chaotic Dynamical Systems: Theory and Experiment*. Addison-Wesley, New York, NY.

Devaney, R. (1995). *Chaotic Dynamical Systems*. Addison-Wesley, New York, NY.

Donald, M. (1991). *Origins of the Modern Mind: Three Stages in the Evolution of Culture and Cognition*. Harvard University Press, Cambridge, MA.

Dreyfus, H. and S. Dreyfus (1987). *From Socrates to Expert Systems: The Limits of Calculative Rationality*, pp. 327–350. University of California Press, Berkeley, CA.

Eckmann, J. and D. Ruelle (1985). Ergodic theory of chaos and strange attractors. *Review of Modern Physics*, 57, pp. 617–656.

Elbert, T., W. Ray, Z. Kowalik, J. Skinner, K. Graf, and N. Birbaumer (1994). Chaos and physiology: Deterministic chaos in excitable cell assemblies. *Physiological Reviews*, 74, pp. 1–47.

Elias, C. (1995). *Mynd as Dynamical System*. Ph.D. thesis, University of Waterloo, Waterloo, Ontario, Canada.

Ferrière, R. and M. Gatto (1993). Chaotic population dynamics can result from natural selection. *Proceedings of the Royal Society of London B*, 251, pp. 33–38.

Fodor, J. (1975). *The Language of Thought*. Harvard University Press, Cambridge, MA.

Fodor, J. and Z. Pylyshyn (1988). Connectionism and cognitive architecture: A critical analysis. *Cognition*, 28, pp. 3–71.

Freeman, W. (2000). Characteristics of the synchronization of brain activity imposed by finite conduction velocities of axons. *International Journal of Bifurcation and Chaos*, 10, pp. 2307–2322.

Getting, P. (1989). Emerging principles governing the operation of neural network. *Annual Review of Neuroscience*, 12, pp. 185–204.

Giles, C., G. Kuhn, and R. Williams (1994). Dynamic recurrent neural networks: Theory and applications. *IEEE Transactions on Neural Networks*, 5. Special issue.

Giles, C. and C. Omlin (1993). Extraction, insertion and refinement of symbolic rules in dynamically driven recurrent neural networks. *Connection Science*, 5, pp. 307–337.

Gleick, J. (1987). *Chaos: Making a New Science*. Viking, New York, NY.

Globus, G. (1992). Toward a noncomputational cognitive neuroscience. *Journal of Cognitive Neuroscience*, 4, pp. 299–310.

Gragnani, A., O. De Feo, and S. Rinaldi (1998). Food chains in the chemostat: Relationships between mean yield and complex dynamics. *Bulletin of Mathematical Biology*, 60, pp. 703–719.

Harnad, S. (1990). The symbol grounding problem. *Physica D*, 42, pp. 335–346.

Healey, T. (1992). Large rotary oscillations of nonlinearly elastic rods: Spatio-temporal symmetry-breaking bifurcation. *SIAM Journal of Applied Mathematics*, 52, pp. 1120–1135.

Holyoak, K. and P. Thagard (1995). *Mental Leaps: Analogy in Creative Thought*. MIT Press, Cambridge, MA.

Hopfield, J. (1991). Olfactory computation and object perception. *Proceedings of the National Academy of Science USA*, 88, pp. 6462–6466.

Hopfield, J. (1995). Pattern recognition computation using action potential timing for stimulus representation. *Nature*, 376, pp. 33–36.

HOPFIELD, J. (1996). Transforming neural computations and representing time. *Proceedings of the National Academy of Science USA*, 93, pp. 15440–15444.

IZHIKEVICH, E. (2000). Neural excitability, spiking and bursting. *International Journal of Bifurcation and Chaos*, 10, pp. 1171–1266.

JOHNSO-LAIRD, P. (1988). *The Computer and the Mind: An Introduction to Cognitive Science*. Harvard University Press, Cambridge, MA.

KATOK, A. AND B. HASSELBLATT (1995). *Introduction to the Modern Theory of Dynamical Systems*. Cambridge University Press, Cambridge, UK.

KAUFFMAN, S. (1993). *The Origins of Order: Self-Organization and Selection in Evolution*. Oxford University Press, Oxford, UK.

KELSO, J. (1995). *Dynamic Patterns: The Self-Organization of Brain and Behavior*. MIT Press, Cambridge, MA.

LECUN, Y., L. BOTTOU, Y. BENGIO, AND P. HAFFNER (1998). Gradient-based learning applied to document recognition. *Proceedings of the IEEE*, 86, pp. 2278–2324.

MCCARTHY, J. (1956). *The Inversion of Functions Defined by Turing Machines*, volume 34, pp. 177–181. Princeton University Press, Princeton, NJ.

MICHALSKI, R., J. CARBONELL, AND T. MITCHELL, editors (1983). *Machine learning: An Artificial Intelligence Approach volume I*. Tioga, Palo Alto, CA.

MICHALSKI, R., J. CARBONELL, AND T. MITCHELL, editors (1986). *Machine learning: An Artificial Intelligence Approach Volume II*. Morgan Kaufmann, Los Altos, CA.

MILLER, G. (1956). The magical number seven, plus or minus two: Some limits on our capacity for processing information. *The Psychological Review*, 63, pp. 81–97.

MILLER, J. (1988). Discrete and continuous models of human information processing: Theoretical distincitons and empirical results. *Acta Psychologica*, 67, pp. 191–257.

MINSKY, M. (1954). *Neural Nets and the Brain Model Problem*. Ph.D. thesis, Princeton University, Princeton, NJ.

MINSKY, M. (1956). Heuristic aspects of the artificial intellegence problem. *Lincoln Laboratory Report*, pp. 34–55.

MITCHELL, M. (2000). Theories of structure versus theories of change (Commentary on T. van Gelder, "The dynamical hypothesis in cognitive science)". *Behavioral and Brain Sciences*. Submitted.

MORTON, A. (1988). The chaology of mind. *Analysis*, 48, pp. 135–142.

NEWELL, A., J. SHAW, AND H. SIMON (1957). Empirical explorations of the logic theory machine. A case study in heuristic. In *Proceedings of the Western Joint Computer Conference*, pp. 218–230. Institute of Radio Engineers, New York, NY.

NEWMAN, D. (1995). *Chaos and Consciousness*. Ph.D. thesis, University of Texas, Austin, TX.

NEWMAN, D. (1996). Emergence and strange attractors. *Philosophy of Science*, 63, pp. 244–260.

NEWMAN, D. (1998). Chaos, classification, and intelligence. In COLUMBO, R., editor, *Origine Della Vita Intelligente Nell'Universo: Atti del Convegno Internazionale*, pp. 93–106. New Press, Como, Italy.

NEWMAN, D. (2001). Chaos, emergence, and the mind-body problem. *Australasian Journal of Philosophy*. To Appear.

NILSSON, N. (1990). *The Mathematical Foundationd of Learning Machines*. Morgan Kaufmann, San Mateo, CA.

Omlin, C., C. Giles, and K. Thornber (1999). Equivalence in knowledge representetion: Automata, recurrent neural networks, and dynamical fuzzy systems. *Proceedings of IEEE*. To appear.

Ott, E. (1993). *Chaos in Dynamical Systems*. Cambridge University Press, New York, NY.

Petitot, J. (1995). *Morphodynamics and attractor syntax: Constituency in visual perception and cognitive grammar*, pp. 339–371. MIT Press, Cambridge, MA.

Pinker, S. and A. Prince (1988). On language and connectionism: Analysis of parallel distributed processing model of language acquisition. *Cognition*, 28, pp. 73–193.

Pollack, J. (1991). The induction of dynamical recognizers. *Machine Learning*, 7, pp. 227–252.

Port, R., F. Cummins, and J. McAuley (1995). *Naive time, temporal patterns and human audition*, pp. 339–371. MIT Press, Cambridge, MA.

Pylyshyn, Z. (1984). *Computation and Cognition*. MIT Press, Cambridge, MA.

Rabinovich, M., P. Varona, and H. Abarbanel (2000). Nonlinear cooperative dynamics of living neurons. *International Journal of Bifurcation and Chaos*, 10, pp. 913–933.

Rapp, P., I. Zimmerman, A. Albano, G. de Guzman, and N. Greenbaum (1985). Dynamics of sponataneous neural activity in the simian motor cortex: The dimension of chaotic neurons. *Physics Letter*, 110A, pp. 335–338.

Rinaldi, S. and O. De Feo (1999). Top-predator abundance and chaos in tritrophic food chains. *Ecology Letters*, 2, pp. 6–10.

Robertson, S., A. Cohen, and G. Mayer-Kress (1993). *Behavioural Chaos: Beyond the Metaphor. A Dynamic Systems Approach to Development: Applications*. MIT Press, Cambridge, MA.

Ruelle, D. (1991). *Hasard et Chaos*. Odile Jacob, Paris, France.

Russell, S. and P. Norvig (1999). *Artificial Intelligence: A Modern Approach*. Prentice-Hall, New York, NY.

Schalkoff, R. (1992). *Pattern Recognition: Statistical, Structural and Neural Approaches*. John Wiley & Sons, New York, NY.

Seigelmann, H. (1999). *Neural Networks and Analog Computation: Beyond the Turing Limit*. Springer-Verlag, New York, NY.

Skarda, C. and W. Freeman (1987). Does the brain make chaos in order to make sense of the world? *Behavioral and Brain Sciences*, 10, pp. 161–165.

Strogatz, S. (1994). *Nonlinear Dynamics and Chaos: With Applications in Physics, Biology, Chemistry, and Engineering*. Addison-Wesley, New York, NY.

Tani, J. (1996). Model-based learning for mobile robot navigation from the dynamical systems perspective. *IEEE Transacions on System, Man and Cybernetics Part B*, 26, pp. 421–436. Special issue on learning autonomous robots.

Tani, J. (1998). An interpretation of the "Self" from the dynamical systems perspective: A constructivist approach. *Journal of Consciousness Studies*, 5.

Tani, J. and N. Fukumura (1995). Embedding a grammatical description in deterministic chaos: An experiment in recurrent neural learning. *Biological Cybernetics*, 72, pp. 365–370.

Thagard, P. (1992). *Conceptual Revolutions*. Princeton University Press, Princeton, NJ.

Thagard, P. (1996). *Mind: Introduction to Cognitive Science*. MIT Press, Cambridge, MA.

Thelen, E. and L. Smith (1994). *A Dynamic Systems Approach to the Development of Cognition and Action*. MIT Press, Cambridge, MA.

THIRAN, P. (1996). *Dynamics and Self-Organization of Locally Coupled Neural Networks*. Ph.D. thesis, Swiss Federal Institute of Technology Lausanne, Lausanne, Switzerland.

VAN GELDER, T. (1998). The dynamical hypothesis in cognitive science. *Behavior and Brain Sciences*, 21, pp. 615–665.

VAN GELDER, T. AND R. PORT, editors (1995). *Mind as Motion: Explorations in the Dynamics of Cognition*. MIT Press, Cambridge, MA.

WEST, B. AND A. GOLDBERGER (1987). Physiology in fractal dimension. *American Scientist*, 75, pp. 354–365.

CHAPTER 2

MODELS OF RANDOMNESS

Brief — In this chapter it is argued that the randomness that is usually observed in nature is not necessarily the result of exogenous noise perturbations. This is a counterflow with respect to the usual approach of scientists and engineers who, usually, assume very simple models for their signals, collecting all the fluctuations of such signals in an exogenous *evil demon* called *noise*. It is shown that the cause of such fluctuations is not necessarily an *exogenous* external influence but, on the contrary, such fluctuations could be part, an *endogenous* part, of the signals themselves. If this is the case, a lot of information about the signals is usually disregarded, dumped in the evil demon of noise, while, for a good approach, this knowledge should be exploited in problems of pattern recognition and signal processing in general.

Personal Contribution — Almost all the material here presented is known. Nevertheless, the way, adopted here, to present this material is rather new. In particular, the decomposition of the Shil'nikov-like strange attractors into its three part has never been officially presented, as far as known by the author, albeit it is surely known to the specialists. Finally, the nonlinear analysis, as conducted here, of the considered field signals, *i.e.* ECG, EEG, and Vowels, can be considered as original.

As described in the introductory chapter, the main topic of this thesis is one-dimensional temporal pattern recognition. More in particular, the main interest is in *approximately periodic* temporal patterns. These signals approximately repeat themselves after a time interval, that is contextually almost always the same, called *pseudo-period*. Examples of such a kind of signals can be found in several fields. In bioengineering examples are the electrocardiogram (ECG) [de Luna, 1998], the electroencephalogram (EEG) [Nunez, 1995], the neural spikes [Johnston and Wu, 1995], the olfactory stimuli [Laurent *et al.*, 1996] and the voice signals [Riley, 1989]. In geophysics there are the seismic waves, *i.e.* telluric oscillations, [Doyle, 1996], the sea tide [Knauss, 1997], and the weather temperature oscillations, both over the day and over the seasons [Holton, 1992]. In biology there are the time series of the population densities of certain types of populations: a given species in an ecosystem [Murray, 1993], the densities of infected children in a given town [Drepper *et al.*, 1994; Renshaw, 1993], or the mutant of a given species [De Feo and Ferrière, 2000; Sigmund, 1998]. In engineering there are the oscillations of a bridge when stimulated by the passage of cars and trucks [Waller and Schmidt, 1989], the heat waves in a media [Kondepudi and Prigogine, 1998], the flame waves [Lewis and von Elbe, 1961], the laser pulses [Hübner *et al.*, 1993] and the oscillation of the concentrations of chemical reactants [Scott, 1994]. Such a list could continue for several pages, the point is that pseudo-periodic signals are common signals in several fields of science and engineering. Their recognition and classification often represents a key point in modern application of engineering as decision support systems [Turban, 1998], expert systems [Weiss, 1991], or speech processing [Laface, 1992], just as examples.

As already said, the main property of these signals is their *approximate* periodicity, *i.e.* they look like periodic but they are not in a strict mathematical sense. Two main distortions from perfect periodicity can be identified. Firstly, their pseudo-period could vary from cycle to cycle, for instance in a ECG the

heart beating rate is not always the same [de Luna, 1998]. This does not refer to the fact that the heart can accelerate or decelerate according to the oxygen demand, since, as said before, the interest is in the contextual phenomena, *e.g.* no change in the oxygen demand. But even in a contextual case the elapsed time between two hearts beats may vary from beat to beat. The second possible distortion is about the amplitude, still referring to the ECG case, it is rare that the amplitudes from one beat to the next are equal, usually there are slight, some times not so slight, variations in the intensity of two successive beats. These variations of the signals are one of, if not the main, problem in recognizing and classifying such patterns. In fact, the recognizers must keep account of all kinds of possible variations.

The problem of recognizing one-dimensional approximately periodic temporal patterns is surely not a new topic, in fact the amount of literature about such a topic is definitely impressive. Despite of such an impressive amount of work, almost all the methods proposed always rely on a standard hypothesis: the signals are perfectly periodic indeed and their fluctuations are due to *external noise*. The rest of this chapter is dedicated to show that this is not the only possible approach.

2.1 Noise and Reality

As already mentioned before, in science and engineering there are many examples of periodic or approximately periodic signals. With respect to the aim of this thesis, especially for the case of engineering applications, this kind of signals should be divided into two big classes. The classes of *artificial* and *natural* periodic or approximately periodic signals.

The artificial (approximately) periodic signals are those kind of signals that engineers have invented in order to solve their problems, an example are the modulated sinusoidal carriers used in telecommunication. This kind of signals usually comes with a strong mathematical toolbox for their analysis and synthesis, their recognition is therefore a well defined mathematical problem with a precise solution, *e.g.* the demodulation of a sinusoidal signal modulated, in frequency or in amplitude, by another sinusoidal signal. More precisely, this kind of signals is often defined as the *optimal* solution of their recognition problem, namely they are the answer of a question like: "What is the best signal to use in order to recognize it as precisely as possible after that it propagates along this or that medium?". In their conception, these signals are perfectly mathematically defined and all their possible fluctuations are taken into account in the design of their recognizers. Thus, whatever is measured from the recognizers that is not inherent in their definition should indeed be treated as external noise.

The natural (approximately) periodic signals are those kind of signals with which scientists and engineers have to deal with whether they like it or not. They come from several problems and fields, for instance all those enumerated in the introduction of this chapter are natural approximately periodic signals. This kind of signals it not the result of human design, it is therefore rare that engineers have the mathematical framework that corresponds to the exact definition of such signals. In fact, the description of such signals is commonly done within a very simple mathematical framework treating whatever exceeds such a framework as exogenous noise. The typical engineers/scientists approach is to suppose the nature as simple as possible, mainly because of Newtonian and Laplacian influences, the random fluctuations of this signals are therefore regarded as unnatural, induced by some external force. Doing that, engineers could disregard a lot of information in the case that the signals' fluctuations would be an intrinsic component of the signal itself.

The methods and the argument used in this thesis are definitely not designed for the artificial kind of signals since all possible information about them is usually exploited, no simplification about their nature is made when their recognizers or classifiers are designed. On the contrary, it will be shown in the next sections that the apparent randomness of natural (approximately) periodic signals finds a suitable mathematical framework in chaotic dynamics. The randomness of these fluctuations can be described by means of chaotic dynamics and this thesis intends to show how to exploit the chaotic dynamics for pattern recognition.

Since the natural (approximately) periodic signals are those of interest for this thesis, from now on every reference to the term signal will implicitly assume that they are of natural origin and approximately periodic unless differently specified.

2.1.1 Dealing with Randomness

All the approaches for dealing with natural signals, proposed in several fields of science, can be seen within a single generic framework. The signals, that need to be recognized, classified, transformed or somehow treated, are projected into a suitable mathematical space used to model their *deterministic* endogenous cause. Whatever exceeds this space is considered, and therefore modeled, as the effect of an exogenous

cause, namely *noise*. Projecting, modeling, a signal in a given mathematical space for its treatment means to assign a *stereotype* to the signal under analysis and to deal, thereafter, with the part of the signal that is represented by this given stereotype.

There are several stereotypes, *i.e.* mathematical frameworks, used to describe signals. For instance, approximately periodic signals can be described by means of their Fourier series coefficients [Amerio, 1977b], by the ARMA coefficients of a linear filter that transforms a pulse train into a signal very close[1] to the given one [Deller *et al.*, 1993], or by an approximation of the signal in the time domain [Amerio, 1977b]. Another framework, usually implemented by neural networks, could extract the most meaningful parts of the time series of the signal. Often these methods are classified as frequency or temporal methods, depending on the mathematical space on which the modeling framework is based. Whatever the particular method is, the general approach consists in taking a mathematical framework that can describe a parametric family, *i.e.* class, of signals, then the observed signals are projected, namely approximated, into this class. The differences from the original observed signals and their representative in the mathematical framework is thus modeled, by means of a suitable stochastic framework, as effects of external noise.

Such a general framework is not restrictive at all and, indeed, the method that is proposed in this thesis can be considered as a special case of this general method. The limits of the methods proposed until now do not come from the general approach itself but from the particular mathematical frameworks usually considered for modeling the signals. These frameworks, albeit these may involve quite complex mathematics, are usually restricted to simple[2], namely linear or almost linear, signal generating processes. Due to this restriction, the stereotypes representing the observed signals are quite static, namely they represent strictly periodic signals and do not account for any possibility of very complex dynamics. In other words, the standard approaches do not consider the possibility that the fluctuations of approximately periodic signals could be of endogenous, deterministic, nature rather than of exogenous nature.

The modeling of the noise effects is, as well, usually very simple, it is modeled most of the time as colored, namely linearly filtered, white Gaussian noise [Johansson, 1993]. This is due to two main reasons, the first one is to keep the modeling of the noise effects coherent with the framework used to model the causes of the signal, namely linear or almost linear. The second reason is the well-known central limit theorem of statistics [Walpone, 1993] stating that the sum of independent sources of randomness is equivalent to a single Gaussian source of randomness. With such an approach, the fluctuations of approximately periodic signals are collected in an unstructured stochastic description which does not allow for any structure in these variations by linking them to a source of *randomness*, namely to a not predictable external source. The main problem in this modeling approach is hidden in the possibility that such fluctuations are deterministic. If this is the case all the signal processing techniques based on such models would waste most of their power dealing with a randomness that is not there.

As examples, in the next paragraph some of these modeling techniques are illustrated applying them for the modeling of some typical approximately periodic signals.

2.1.2 Examples of Stereotypes in Science

The modeling stereotypes and noise models of some of the most frequent modeling techniques are determined for seven approximately periodic signals of physiological nature.

The Electrocardiogram and the Electroencephalogram

In Figure 2.1 a typical normal lead II[3] electrocardiogram (ECG) [Bronzino, 1995] for a healthy human being *at rest* is shown. This is a very simple example of a natural approximately periodic signal. As can be easily noticed, the intensity of successive peaks and the time interval between them are not always the same. There are several ways of modeling the stereotype of this kind of signal. In Fig. 2.2 the typical stereotype considered by physicians [de Luna, 1998] is depicted. It consists of a temporal geometric stereotype where five peculiar parts of the signal, the P, Q, R, S and T-wave, are highlighted. For this stereotype there is not an explicit model of the noise effects, the model of the random fluctuations is left to the implicit knowledge, *i.e.* the

[1] With respect to a given measure, for instance the L^2 difference of their power spectral densities (PSD).

[2] Here the simplicity of the generating processes does not refer to the dimension of the systems used to model the source of the signals, as common in the ancient approaches [Katok and Hasselblatt, 1995], but to the completeness of the analysis tools available for a given type of model. In other words, linear models are very simple since they have a closed theory; slight variations of linear models ("nonlinear but not too much"), like systems that can be described by Volterra series or similar [Rugh, 1990], are of intermediate complexity; generic nonlinear models that admit multiple attractors and chaos are complex models [Ott, 1993; Strogatz, 1994].

[3] It is the ECG obtained measuring the voltage difference from the left foot and the right arm.

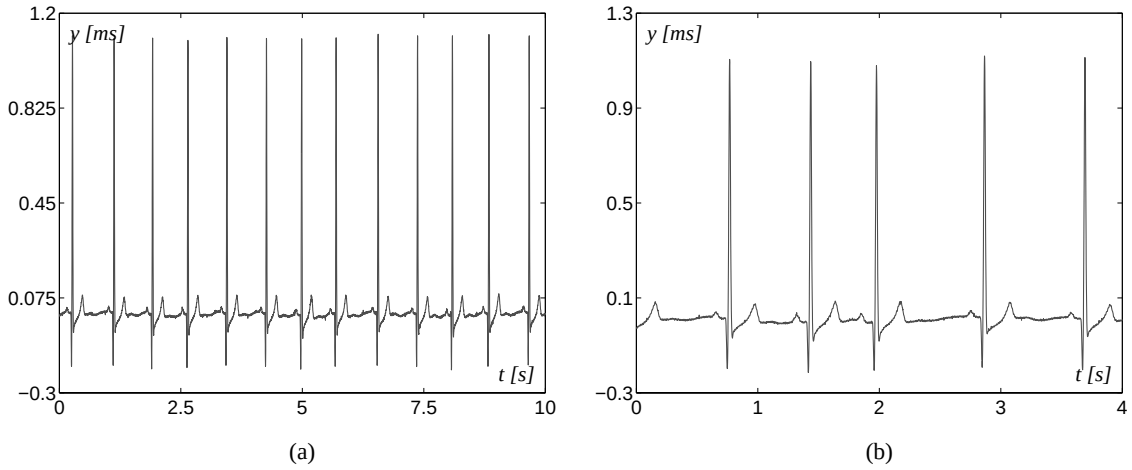

Figure 2.1: *Example of time series of a normal lead II ECG for a healthy human being at rest: (a) – ten seconds time series; (b) – zoom at five consecutive beats.*

model, that physicians build in their mind during their experiences. In Figure 2.3 a more engineering-like

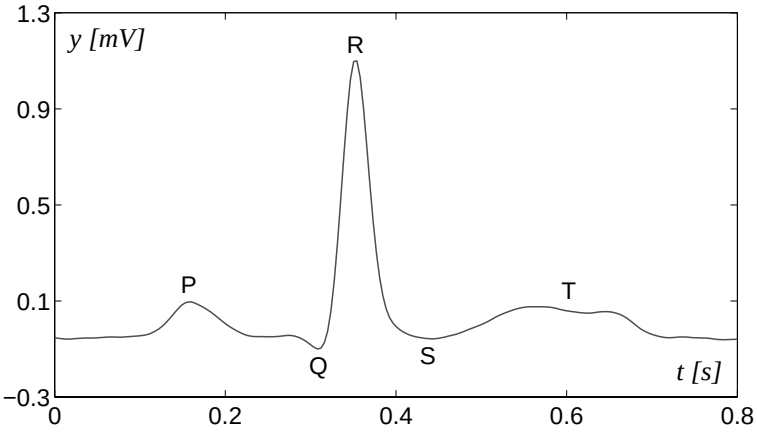

Figure 2.2: *The temporal stereotype of a normal lead II ECG typically considered by physicians.*

model for such a signal is represented. There the coefficients of the Fourier series of a perfect periodic signal, of angular frequency $\omega_0 = 2\pi/T_0$, for the temporal stereotype shown in Fig. 2.2, are reported. In Figure 2.4 the histograms of the Fourier series parameters for the entire ECG shown in Fig. 2.1 are represented, a set of parameters is computed for each pseudo-period. The picture shows, overimposed to the histograms, the approximating Gaussian distributions. Figure 2.4(a) and (b) report the distribution for amplitudes and phases, respectively, while Fig. 2.4(c) shows the histogram and the approximating Gaussian distribution of the pseudo-period. As can be easily observed neither the Gaussian approximation of the Fourier coefficients nor that of the pseudo-period is good. This is further confirmed in Fig. 2.5 where an inconsistent realization of the described Gaussian stochastic model (*cfr.* Fig. 2.4) is given, as can be seen the realization does not look like an ECG in the time domain.

Figure 2.6 shows another typical approximately periodic physiological signal, namely a δ-state electroencephalogram (EEG) of a healthy human being sleeping *at rest* [Nunez, 1995]. As for the ECG case, the EEG signal can be modeled is several ways. The following figures describe the models of such a signal that are analogous to the models presented before for the ECG signal. In Figure 2.7 the typical stereotype considered by physicians [Nunez, 1995] is shown. Figure 2.8 reports the coefficients of the Fourier series of a perfectly periodic signal, of angular frequency $\omega_0 = 2\pi/T_0$, for the temporal stereotype shown in Fig. 2.7. In Figure 2.9 the histograms and the approximating Gaussian distributions of the Fourier series parameters for the entire EEG shown in Fig. 2.6 are reported. In analogy with Fig. 2.5, Fig. 2.10 shows an inconsistent

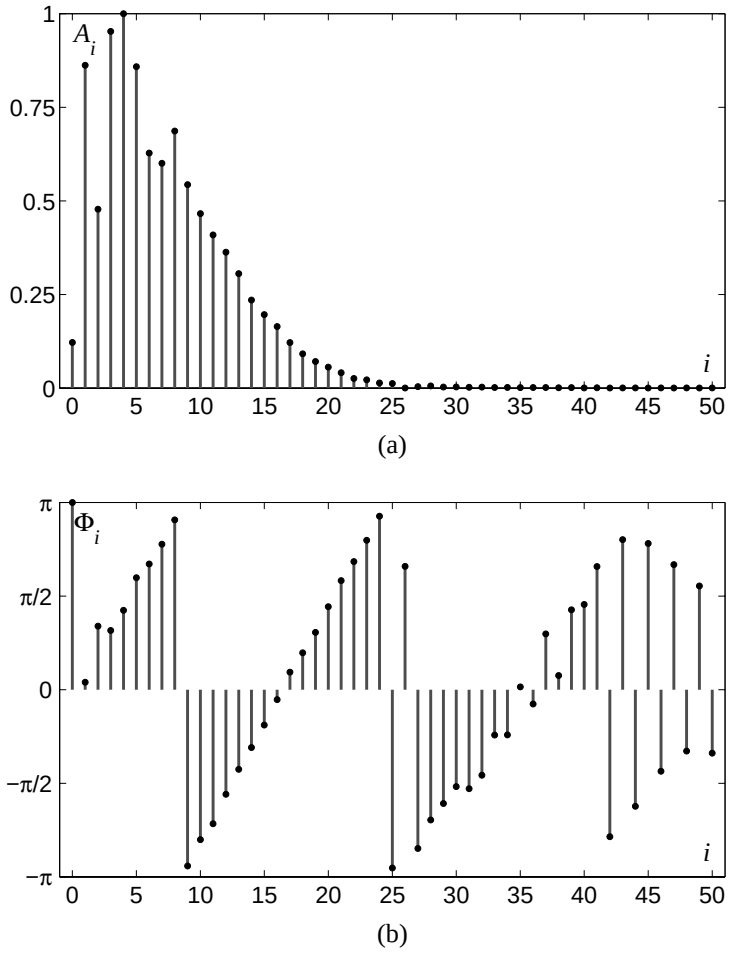

Figure 2.3: *Normalized coefficient of the Fourier series for the signal shown in Fig. 2.2: (a) – amplitude coefficients; (b) – phases.*

realization of the Gaussian stochastic model given in Fig. 2.9, as can be seen the realization does not look like an EEG in the time domain.

The Vowels in Speech

Figure 2.11 shows the time series of sustained pronunciation (by the author) of the five *Italian*[4] vowels. These five signal are another example of natural approximately periodic signal. As can be easily noticed, once again the intensity of successive peaks is not always the same as well as the time intervals between them. As the previous two signals, these five signals can be modeled in several ways. Figure 2.12 reports the temporal stereotype for the five vowels. These stereotypes are reported just for analogy to the stereotypes used by the physicians for the cases of the ECG and EEG but in reality they are not used very often.

The standard model of voiced signal [Deller *et al.*, 1993] is a linear autoregressive (AR) filter, from the eighth to the twelfth order, excited by an impulse train with period equal to the mean of the pseudo-periods of the observed signal. Since AR filters can uniquely be parameterized by their pole locations, Fig. 2.13 shows the poles of the eighth order AR models for the temporal stereotypes of the five vowels shown in Fig. 2.12. Figures 2.14-2.18 show the histograms and the approximating Gaussian distributions of the parameters of the AR models for the entire sustained pronunciation of the vowels shown in Fig. 2.11, an AR model is computed for each pseudo-period. In analogy with the previous cases, Fig. 2.19 shows the inconsistent realizations of the Gaussian stochastic models of Figs. 2.14-2.18, as can be seen the realizations do not look like as their corresponding vowels.

[4]The author apologizes but he cannot correctly pronounce the other six vowel sounds classified by the International Phonetics Association (IPA).

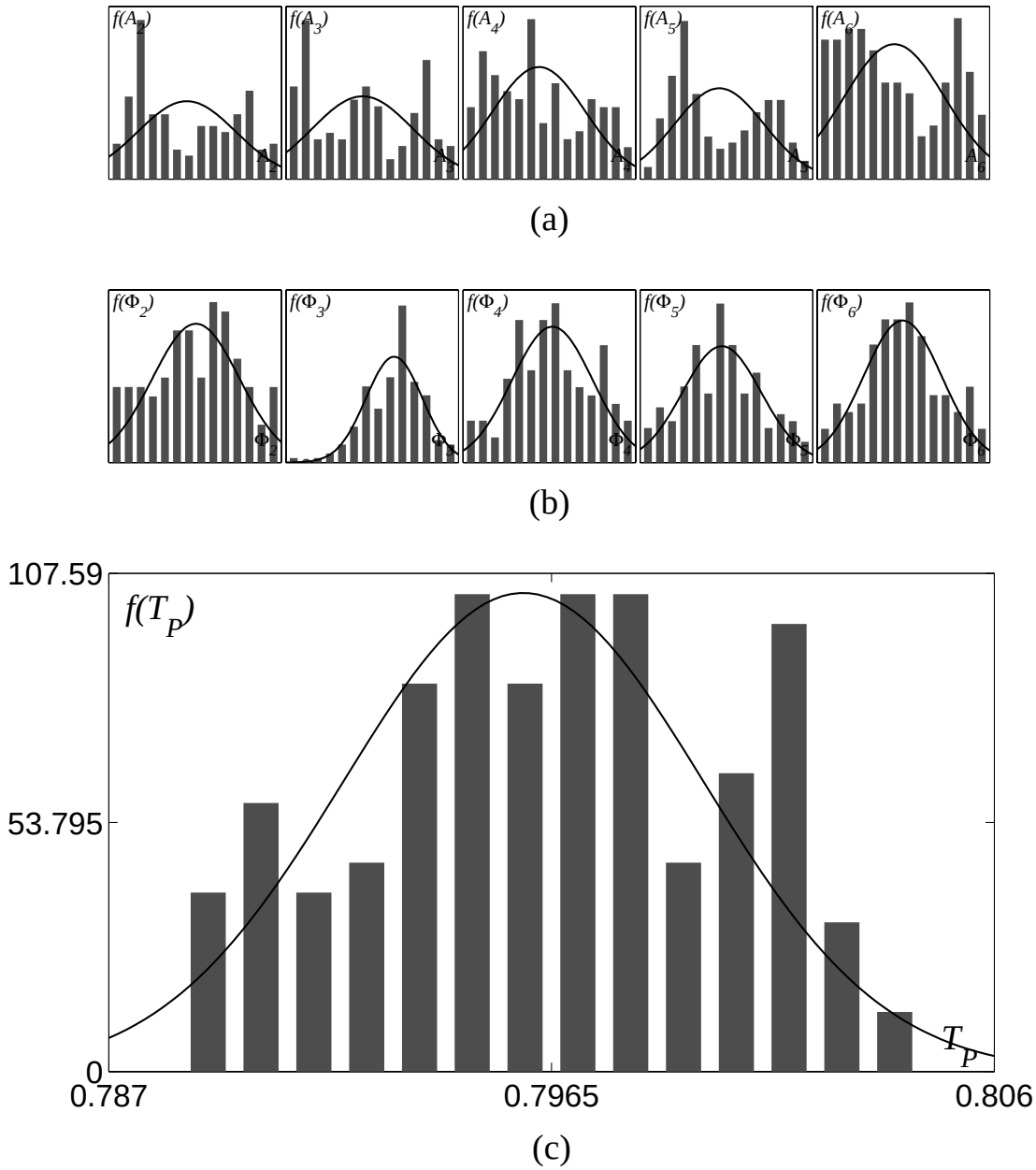

Figure 2.4: *Noise model for the parameters of the Fourier series of the signal shown in Fig. 2.1, histograms and approximating Gaussian distributions of: (a) – the amplitude coefficients; (b) – the phases; (c) – the pseudo-period.*

A final comment on the relationships between all the modeling methods considered here. Since most of these methods, actually all those shown, are based on a linear modeling of the signal generation, they are linked by some kind of transformation. For instance there is a simple algebraic relationship between the parameters of the AR modeling and the parameters of the Fourier series.

2.2 Exogenous Noise *vs* Endogenous Chaos

From the previous examples it emerges that the stochastic models of the apparently random fluctuations of the signals could result in too weak models, in other words, in a too large class of signals. In fact, there are

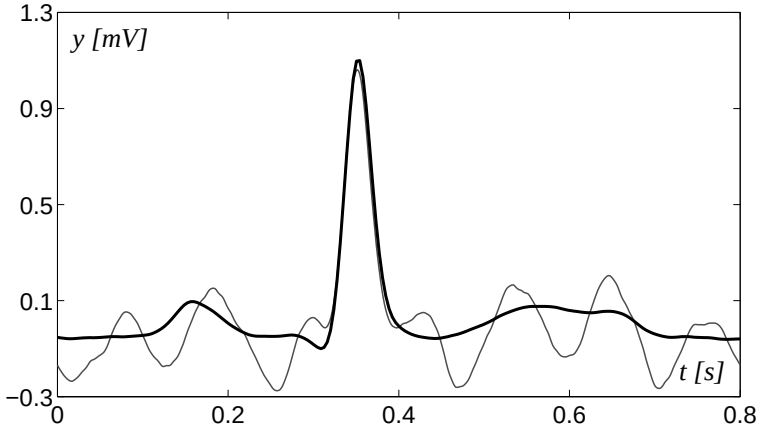

Figure 2.5: *Inconsistent realization, in the time domain, of the Gaussian noise model for the parameters of the Fourier series, it does not look like an ECG.*

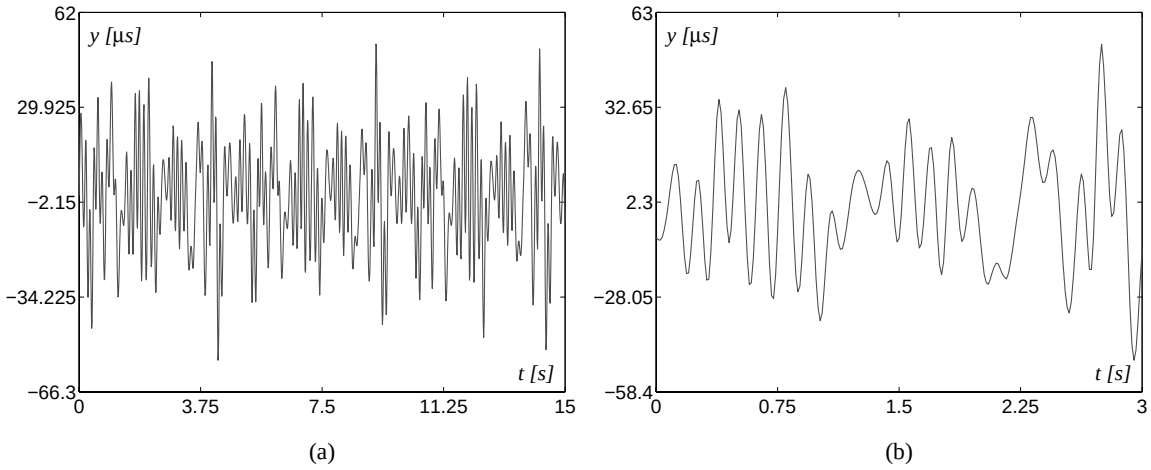

Figure 2.6: *Example of time series of a δ-state EEG for a healthy human being sleeping at rest: (a) – three seconds time series; (b) – zoom at twenty consecutive oscillations.*

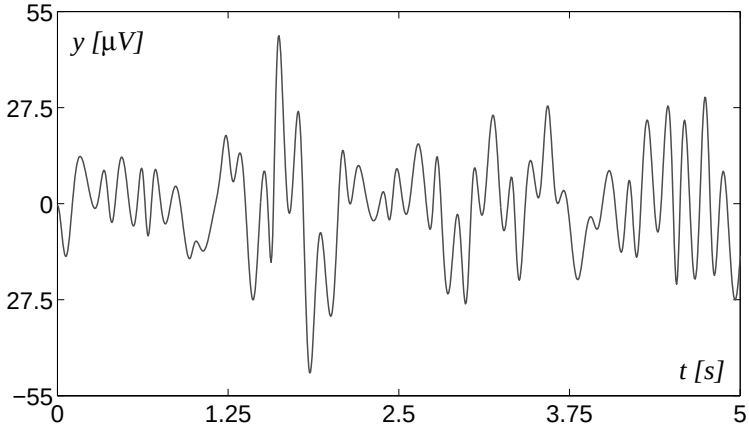

Figure 2.7: *The temporal stereotype of a δ-state EEG typically considered by physicians.*

signal realizations which are compatible with the stochastic model that do not belong to the signals that are

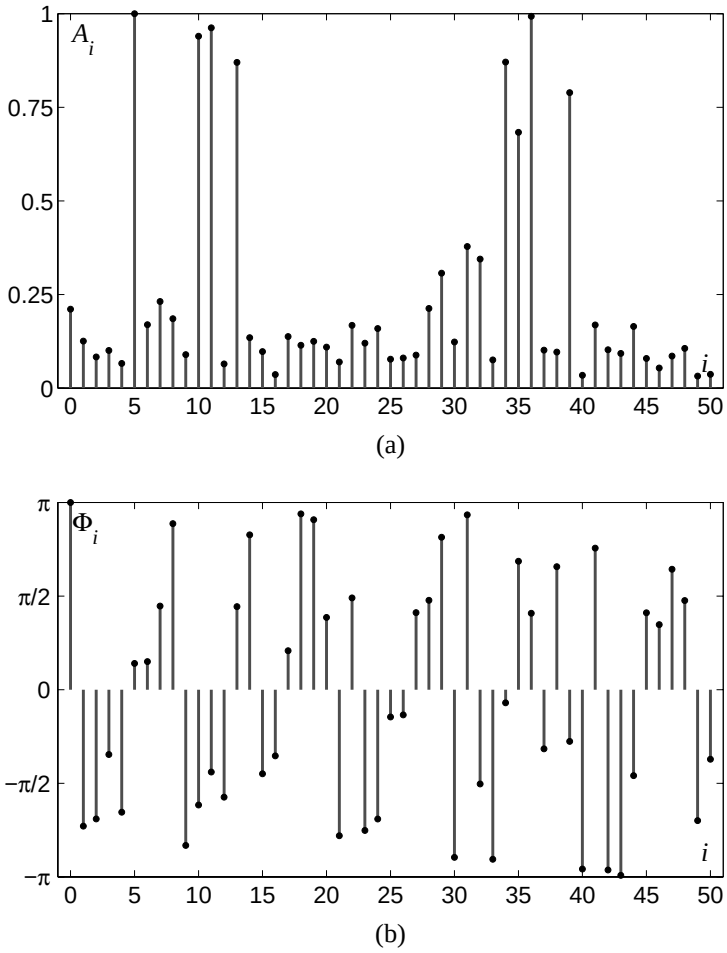

Figure 2.8: *Normalized coefficient of the Fourier series for the signal shown in Fig. 2.7: (a) – amplitude coefficients; (b) – phases.*

to be modeled.

Several reasons for such a weakness of the model can be found. A first one could be the Gaussian approximation used for the distributions of the model's parameters, but this cannot be the main problem since any unbounded probability distribution would admit, even if with a different probability, the same realizations of the Gaussian approximation. Given that, the main error could be the unboundedness of the probability density used for approximating the measured histograms that, on the contrary, are bounded. Unfortunately, the mathematical tools for bounded distributions are not so well defined and developed as those for unbounded, in particular Gaussian, distributions. Therefore, using bounded probability densities would result in models that cannot be easily treated. In reality, the stronger reason for the model's weakness is found in the fact that the distributions of the model's parameters are not independent as supposed in the previous examples. The computation of the higher order, self and cross, moments for the model's parameters of the previous examples shows a strong correlation among them. A strong correlation between the model's parameter values is a symptom of unexploited information about the modeled signal [Johansson, 1993; Ljung, 1999].

At this point there are mainly two possibilities to explain such strong correlation among the model's parameter distributions. The first hypothesis is that there are only few noise sources that determine the fluctuations of the signals, the parameters are thus necessarily correlated among them. As second hypothesis, the fluctuations around the stereotypes are not necessarily exogenous, they result from the same dynamical system that generate the main signal. Whatever the reason is, there is a large amount of information about the signals that is unexploited, it is not included in the models shown in the previous examples. Since there are two hypotheses about the cause of the correlation among the model's parameter values, there would be

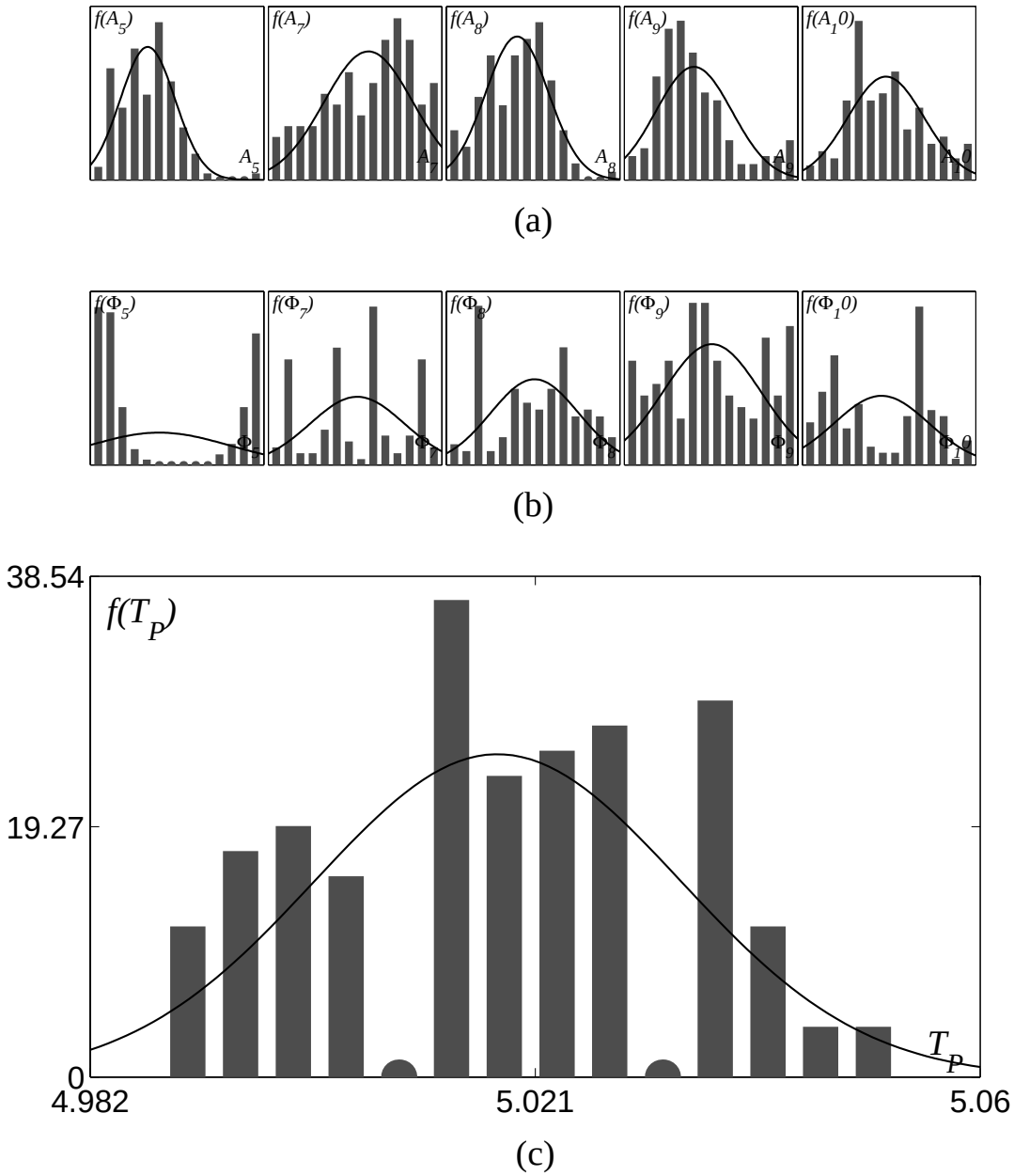

Figure 2.9: *Noise model for the parameters of the Fourier series of the signal shown in Fig. 2.6, histograms and approximating Gaussian distributions of: (a) – the amplitude coefficients; (b) – the phases; (c) – the pseudo-period.*

two main approaches to recover such information.

The first approach is the stochastic one, where the fluctuations are still considered of exogenous nature. This approach would try to describe up to the higher orders the joint distributions of the model parameters. *A priori*, nothing is wrong with that if it were not that in standard stochastic approaches it is rare to consider moments of higher order than the first and second order moments, namely means, variances, and cross-correlations. Thus, the mathematical tools for dealing with such an approach would miss or would be quite difficult to handle. A second argument against this approach[5] is that considering higher and higher correlation moments in a stochastic approach is equivalent to tending towards a deterministic approach, therefore a deterministic approach should be considered instead.

[5]Obviously, the main argument is the fact that this thesis is dedicated to nonlinear modeling of signals.

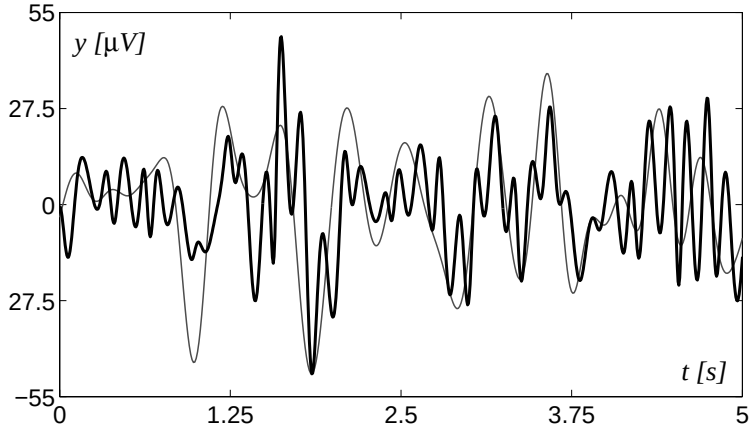

Figure 2.10: *Inconsistent realization, in the time domain, of the Gaussian noise model for the parameters of the Fourier series, it does not look like an EEG.*

In a deterministic approach the fluctuations of the signals are considered as an endogenous result. In this approach a model that would try to fit the signal exactly[6] is looked for, since the purpose is to fit all the apparently *random* fluctuation of the signals it is clear that linear or almost linear model cannot accomplish such a task. But nonlinear models, that admit multiple attractors and chaotic behavior, are good candidate to accomplish the task.

The random capabilities of chaotic dynamical systems are discussed in the next sections but before, in the next paragraph, it is shown why the apparently random fluctuation of approximately periodic signals should be expected to be of deterministic and endogenous nature rather than the effect of exogenous noise.

2.2.1 Reconstruction of Deterministic Signals

The seven signals considered in the examples described in Sect. 2.1 are herein analyzed with the standard technique of state space embedding [Packard *et al.*, 1980]. The aim is to show that their apparently random fluctuation are structured indeed, such fluctuations could therefore be the fingerprint of an endogenous chaotic dynamic.

The technique used here for the state space reconstruction is not the standard one of the successive lags as formerly proposed by Takens in [Takens, 1981]. The technique described in Appendix B, called *nonminimal phase reconstruction* is used instead. Such a technique is preferred to the standard one since it provides better three-dimensional pictures. Furthermore, the tuning of the filters used for the reconstruction is done automatically starting from the spectral analysis of the reconstructing signal. On the contrary, determining the optimal, for a good picture, lag for the space embedding of signals with the standard technique could be quite cumbersome [Ellner and Turchin, 1993; Smith, 1992].

The Electrocardiogram and the Electroencephalogram

Figure 2.20 shows the spectrum of the ECG signal shown in Fig. 2.1. The figure shows also the two frequencies used for the nonminimal phase reconstruction, as described in Appendix B they coincide with the first two uncorrelated resonance peaks. In Figure 2.21 the three-dimensional nonminimal phase reconstruction of the signal shown in Fig. 2.1 is reported.

Analogously, Figs. 2.22 and 2.23 show the spectrum and the three-dimensional nonminimal phase reconstruction of the EEG shown in Fig. 2.6, respectively.

The Vowels in Speech

In analogy to what is shown above for the ECG and EEG signals, here the spectral analysis, in Fig. 2.24, and the three-dimensional nonminimal phase reconstruction, in Fig. 2.25, of the entire sustained pronunciation of the five vowels shown in Fig. 2.11 are shown.

[6] Obviously, there will still be some noise over the signal, the measurements noise, but it is supposed in this thesis that this noise is very small with respect to the useful signal.

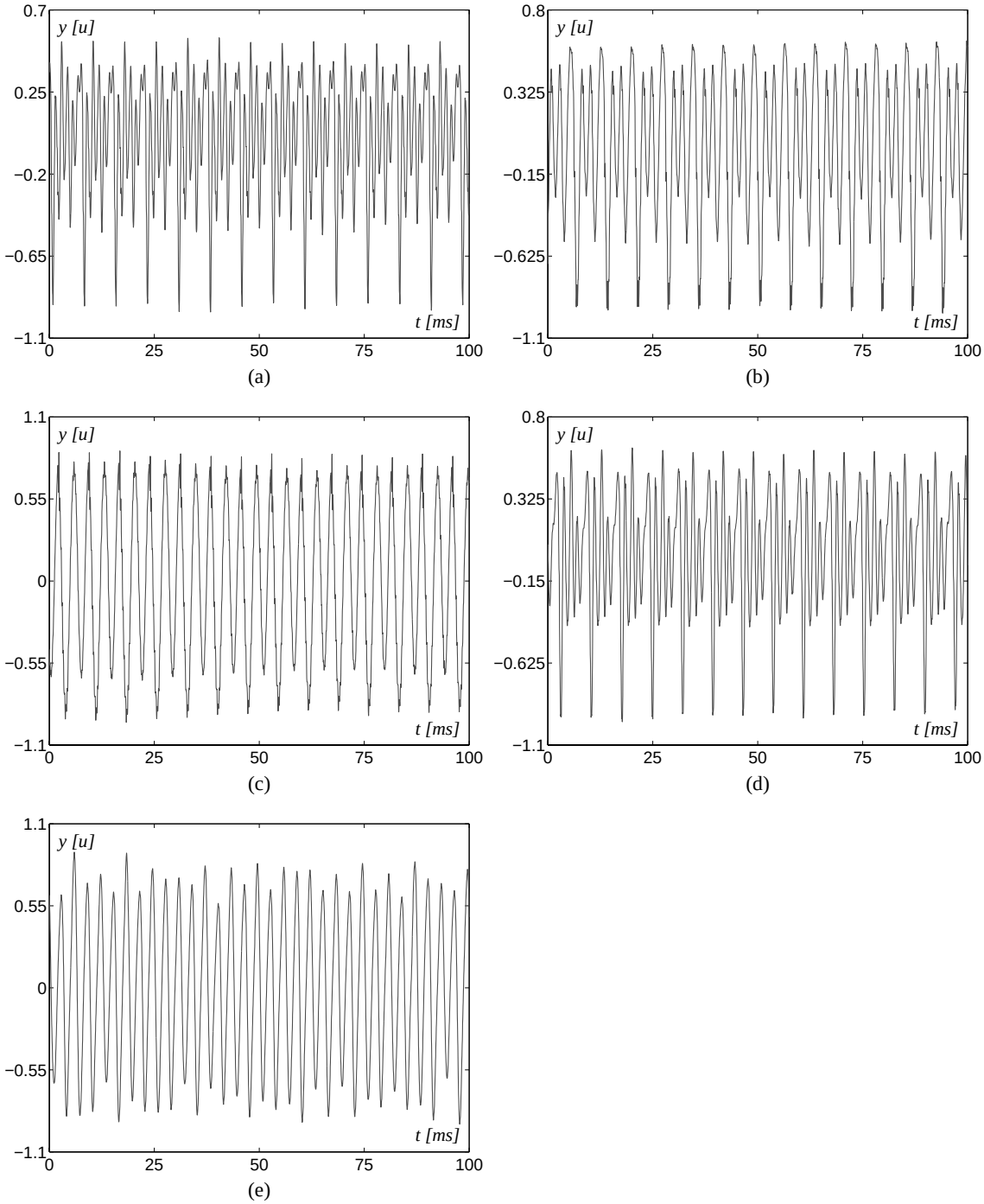

Figure 2.11: *Example of the time series of a sustained execution of two seconds, shown only hundred milliseconds, of the five Italian vowels: (a) – the [a:] vowel, as in* car*; (b) – the [e] vowel, as in* yes*; (c) – the [i] vowel, as in* pin*; (d) – the [ɔ] vowel, as in* clock*; (e) – the [u] vowel, as in* book*.*

From the emerging structures shown in Figs. 2.21, 2.23, and 2.25, it is evident that the fluctuations of the considered signals are not random indeed but definitely structured, hence deterministic.

2.3 Deterministic Sources of Randomness

It emerges from the previous discussions that the apparent randomness of natural approximately periodic signals should be related with some nonlinear phenomena in the dynamic process that generates them. In

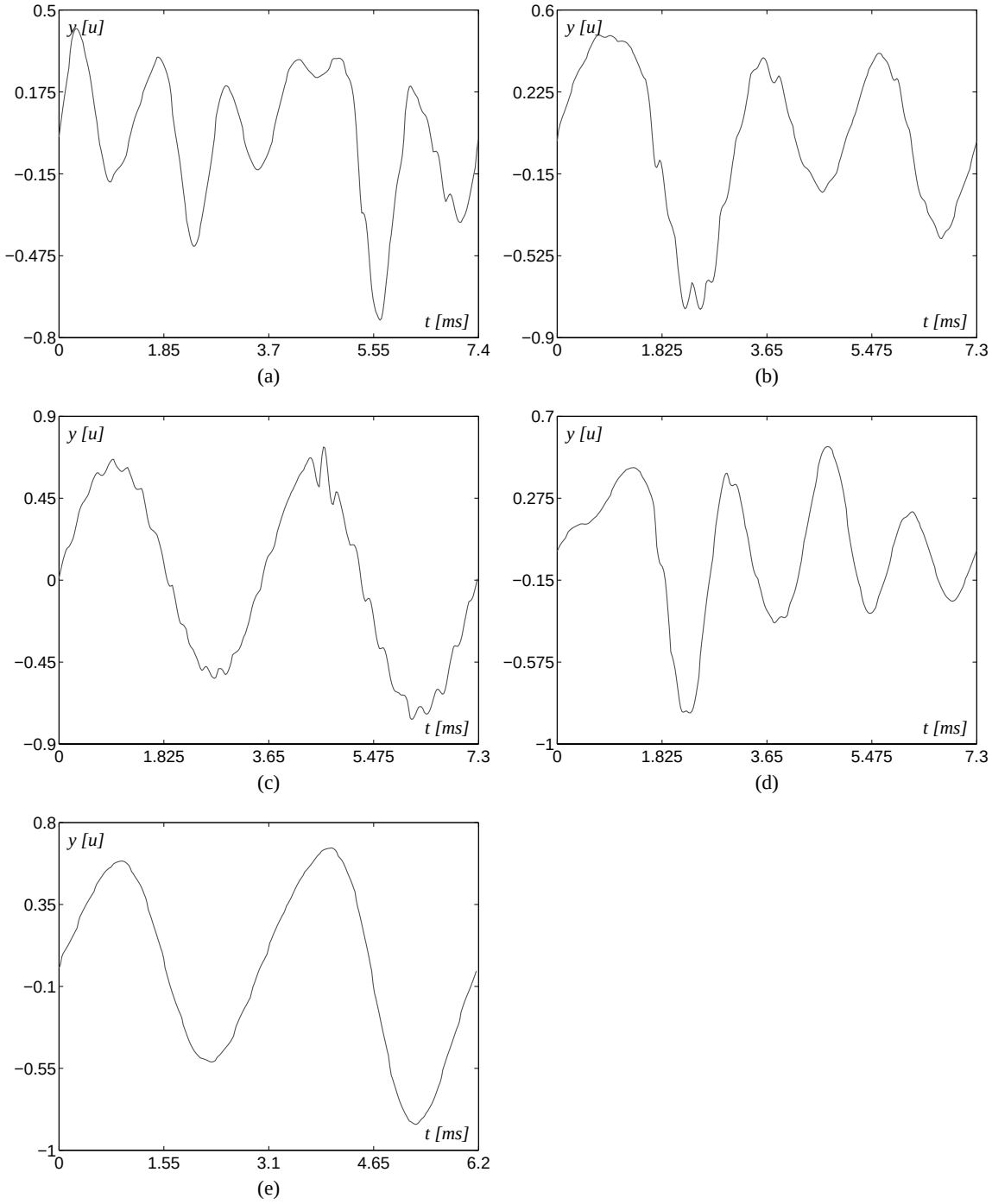

Figure 2.12: *The temporal stereotypes of the five Italian vowels: (a) – [a:]; (b) – [e]; (c) – [i]; (d) – [ɔ]; (e) – [u].*

dynamical systems theory three sources of unpredictability or effective randomness due to nonlinearities can be identified.

1. *Complex structure of the basin of attraction*: the borders between basins can be highly convoluted, so that completely different attractors can be seen with very small changes in initial conditions, *e.g.* the toss of a coin.

2. *Deterministic chaos*: this is the unpredictability of long-term behavior due to local instability on the attractor, *e.g.* the weather behavior.

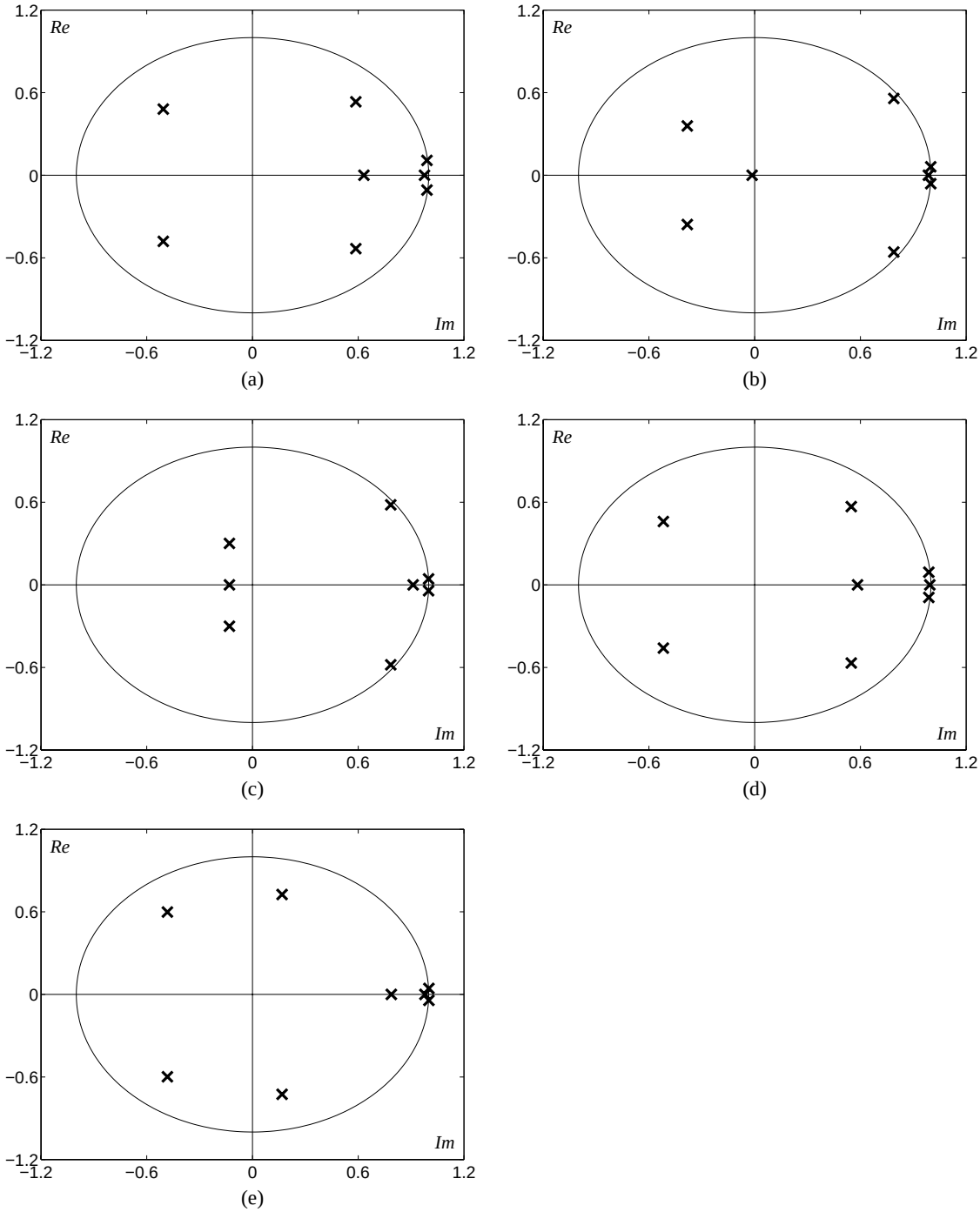

Figure 2.13: *Poles of the eighth order AR models for the signals shown in Fig. 2.12: (a) – [a:]; (b) – [e]; (c) – [i]; (d) – [ɔ]; (e) – [u].*

3. *Sensitive dependence on control parameter*: the attractor—basin portrait can be arbitrarily sensitive to changes in control parameters, *e.g.* the hysteretic phenomena.

The emergence of randomness from such sensitivities in systems governed by known laws was already noticed at the turn of the century by Poincaré [Poincaré, 1892].

> But even if it were the case that the natural laws had no longer any secret for us, we could still only know the initial situation approximately. If that enabled us to predict the succeeding situation with the same approximation, that is all we require, then we should say that the phenomenon had been predicted, that it is governed by laws. But it is not always so; it may happen that small

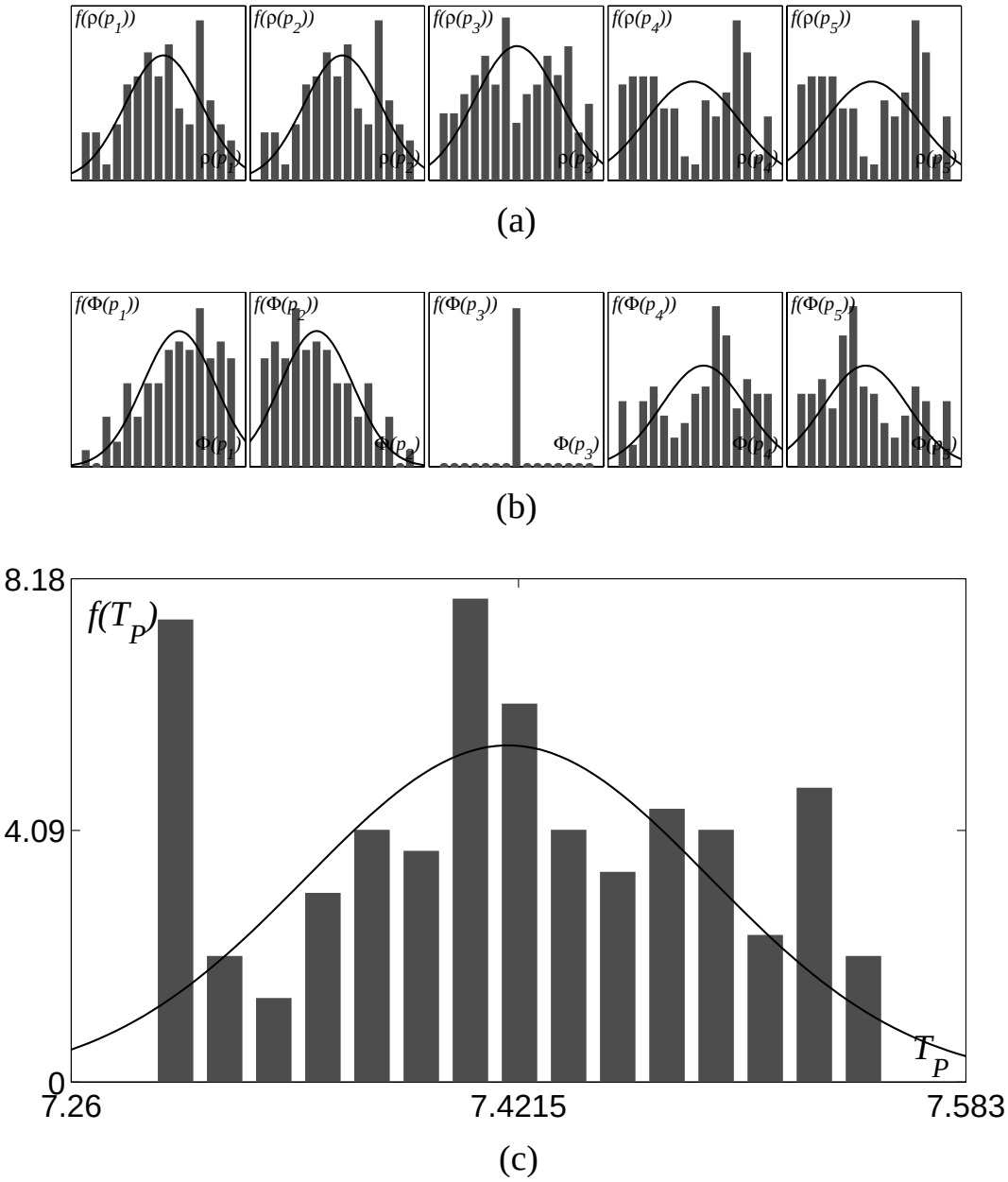

Figure 2.14: *Noise model for the parameters of the AR modeling of the signal shown in Fig. 2.11(a) [a:], histograms and approximating Gaussian distributions of: (a) – the amplitude of the poles; (b) – the phase of the poles; (c) – the pseudo-period.*

> differences in the initial conditions produce very great ones in the final phenomena. A small error in the former will produce an enormous error in the latter. Prediction becomes impossible, and we have the fortuitous phenomenon.

The Poincaré's remark closes with an implicit operational definition of randomness as a phenomenon which appears fortuitous due to ignorance. This and similar notions of uncertainty play an important role in probabilistic descriptions of unpredictable behavior.

For the particular case considered in this work, the form of randomness that is of most interest is definitely the one related with the deterministic chaos. Despite of the apparent complexity of deterministic chaos due to its long term unpredictability, the geometrical structure of chaotic attractors is highly regular and very similar to the geometrical structures shown in the previous reconstructions, *cfr.* Sect. 2.2.1.

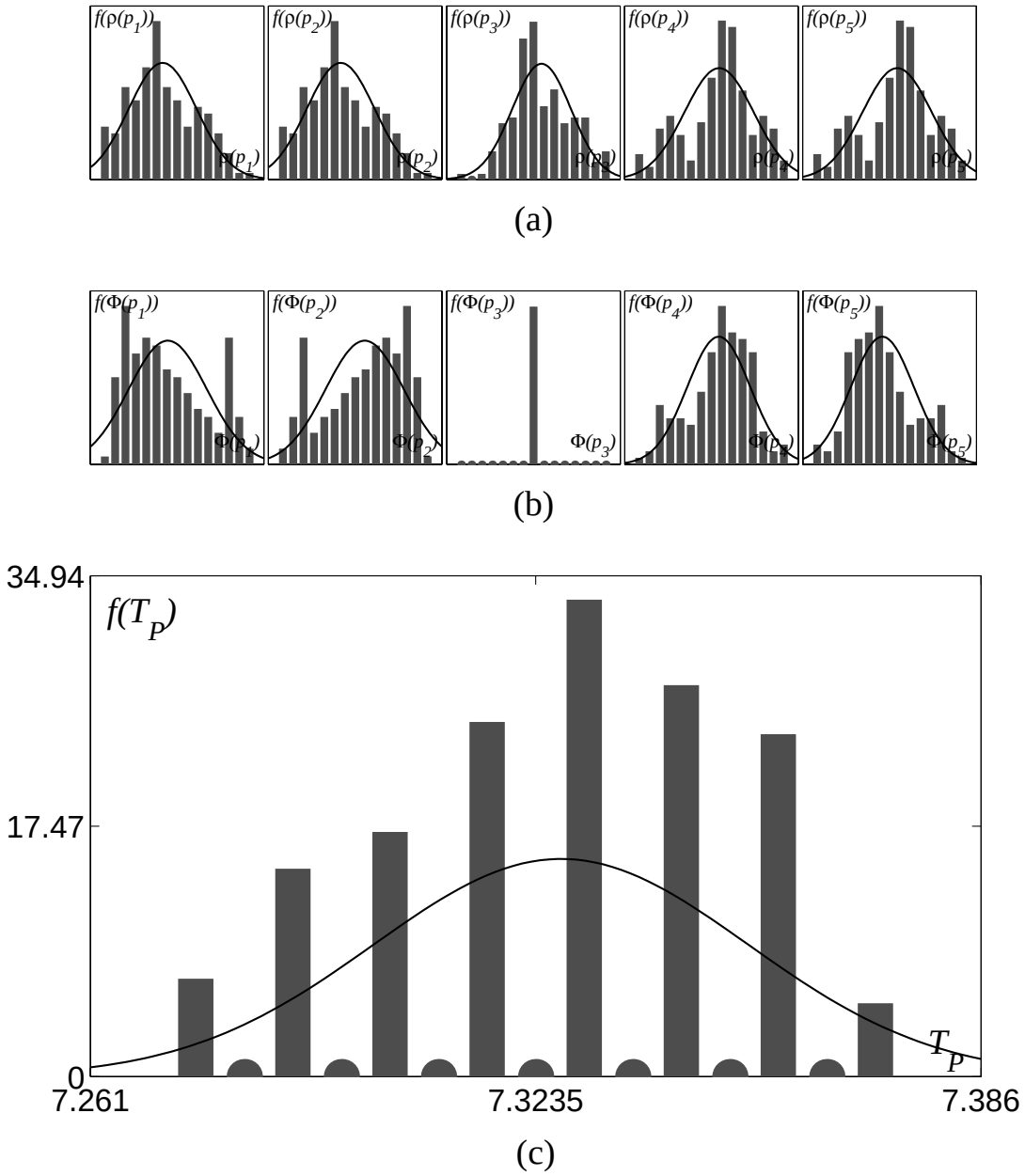

Figure 2.15: *Noise model for the parameters of the AR modeling of the signal shown in Fig. 2.11(b) [e], histograms and approximating Gaussian distributions of: (a) – the amplitude of the poles; (b) – the phase of the poles; (c) – the pseudo-period.*

2.3.1 Information and Geometry

In chaotic systems uncertainty and approximation are rapidly amplified. This precludes not only the long-term prediction of their behavior, but also the closed form solutions of their equations of motion. While the barring of long-term prediction leads, even in the classical setting of dynamical systems, to the complete accounting of the measurement process, the inexistence of closed form solutions for the equation of motions lead to the design of a computational theory for inferring models from measurements. The first problem for such an inferring theory is to determine how much information about the underlying dynamical system is hidden in a single measurement of an observed signal [Bittanti and Picci, 1996; Callier and Desoer, 1991].

Before quantifying the information about the underlying system contained in a measurement, the concept

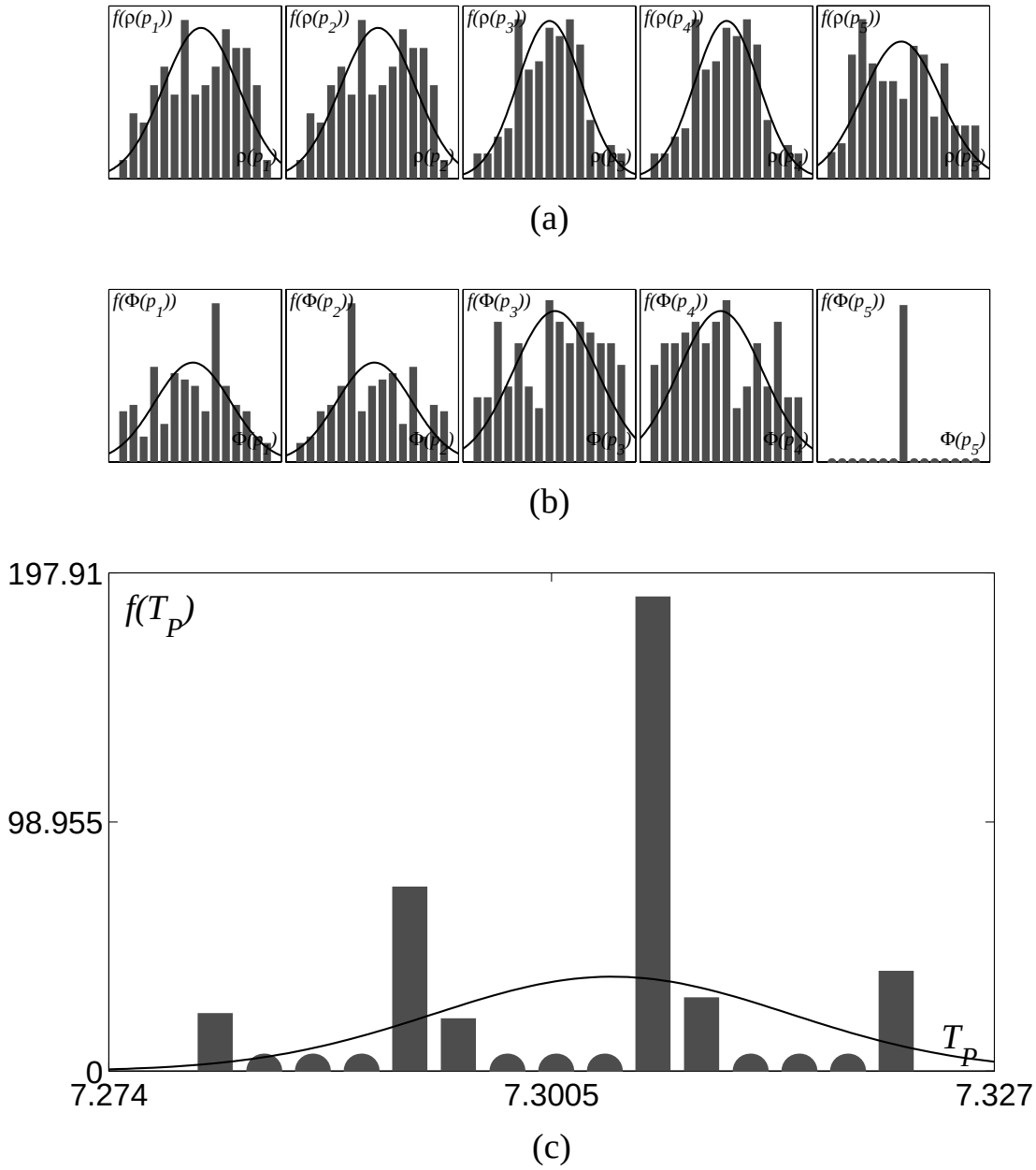

Figure 2.16: *Noise model for the parameters of the AR modeling of the signal shown in Fig. 2.11(c) [i], histograms and approximating Gaussian distributions of: (a) – the amplitude of the poles; (b) – the phase of the poles; (c) – the pseudo-period.*

of information itself should be quantified. The observation of a natural process entails measurement of its state, the act of measurement is a codification of the physical configuration of the underlying system. But how much do observations tell one about the process? Information theory [MacKay, 1999] measures the amount of information in an observation as the negative logarithm of the probability of occurrence of the observation. From such a definition it can be already noted that information itself is never rigorously defined, it is only quantified. The most concise attempt to define information is due to Bateson [Bateson, 1972]: "... information is a difference that makes a difference ...". This expresses the origin of information in the unanticipation of an event and also its essential relativity.

In dynamical system theory the average information contained in isolated measurements is called the dimension of the underlying process: it is the minimum amount of information necessary to uniquely identify

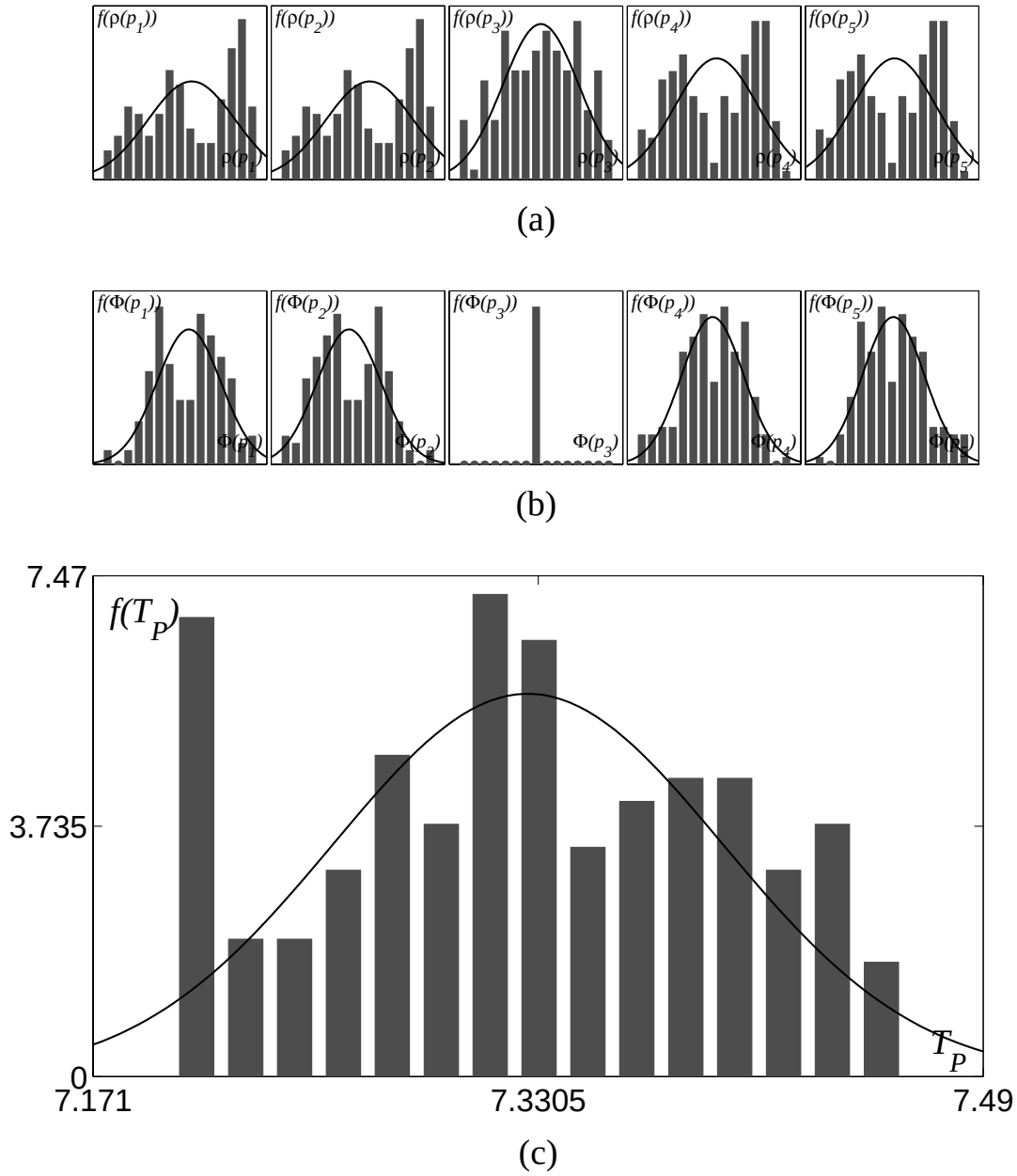

Figure 2.17: *Noise model for the parameters of the AR modeling of the signal shown in Fig. 2.11(d) [ɔ], histograms and approximating Gaussian distributions of: (a) – the amplitude of the poles; (b) – the phase of the poles; (c) – the pseudo-period.*

the state of the system [Katok and Hasselblatt, 1995]. In a complementary way, the dynamical entropy [Eckmann and Ruelle, 1985; Sinai, 1993; Walters, 1982] can be defined. It quantifies how much can be predicted about the next measurement given that one knows the entire history up to that point. The dynamical entropy measures the average temporal rate of information loss once a measurement is made. If a process is chaotic a new measurement must be made after a short time since the information about its previous state is rapidly lost. From the observer's point of view, the dynamical entropy is the rate at which a process produces new information. Since new information can be produced only by an unexpected event, the dynamical entropy gives a measure of the randomness of a measured process.

The complexity, both from dynamical system and information theory point of view, of deterministic chaos could lead to rough simplifications like a probabilistic description of its apparent random behavior. That

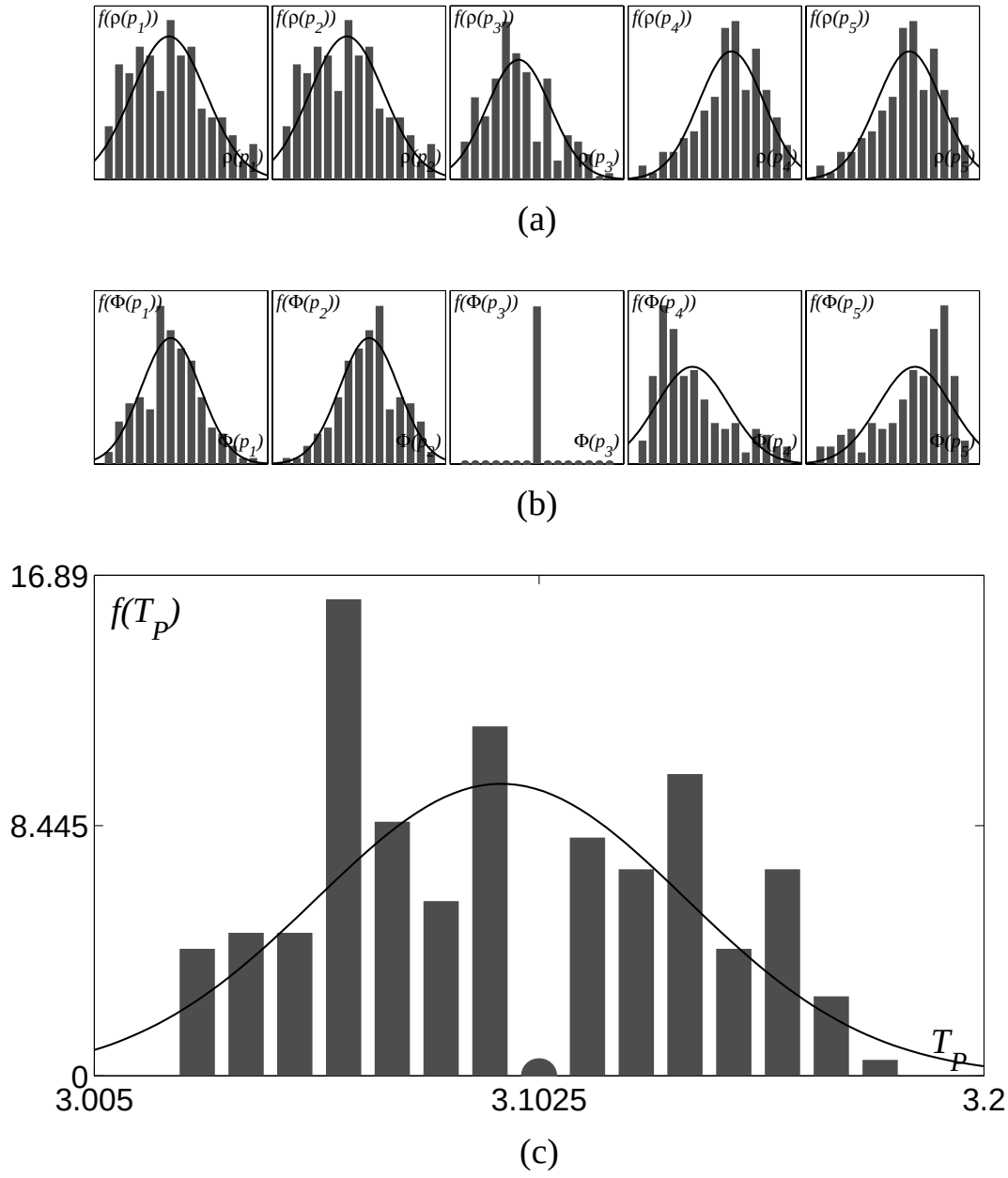

Figure 2.18: *Noise model for the parameters of the AR modeling of the signal shown in Fig. 2.11(e) [u], histograms and approximating Gaussian distributions of: (a) – the amplitude of the poles; (b) – the phase of the poles; (c) – the pseudo-period.*

would ignore the tremendous structure in deterministic behavior, such as the short-term predictability and the shape of a chaotic attractor. On the contrary, qualitative analysis of dynamical systems [Arnold, 1988; Poincaré, 1892; Strogatz, 1994] represents a powerful technique for dealing with deterministic chaos, it is a geometric approach intermediate between exact solution and probabilistic methods. In fact, information theory does not give a direct indication of a process's underlying geometric structure, since it is a probabilistic description of the behavior. However, as shown in Sect. 2.2.1, the geometry of the underlying attractor can be recovered, even from a single component time series produced by a multi-dimensional process. Reconstruction methods produce an equivalent state space representation from a time series of observations. They provide a direct connection between experimental data and the geometric tools of qualitative dynamical systems theory.

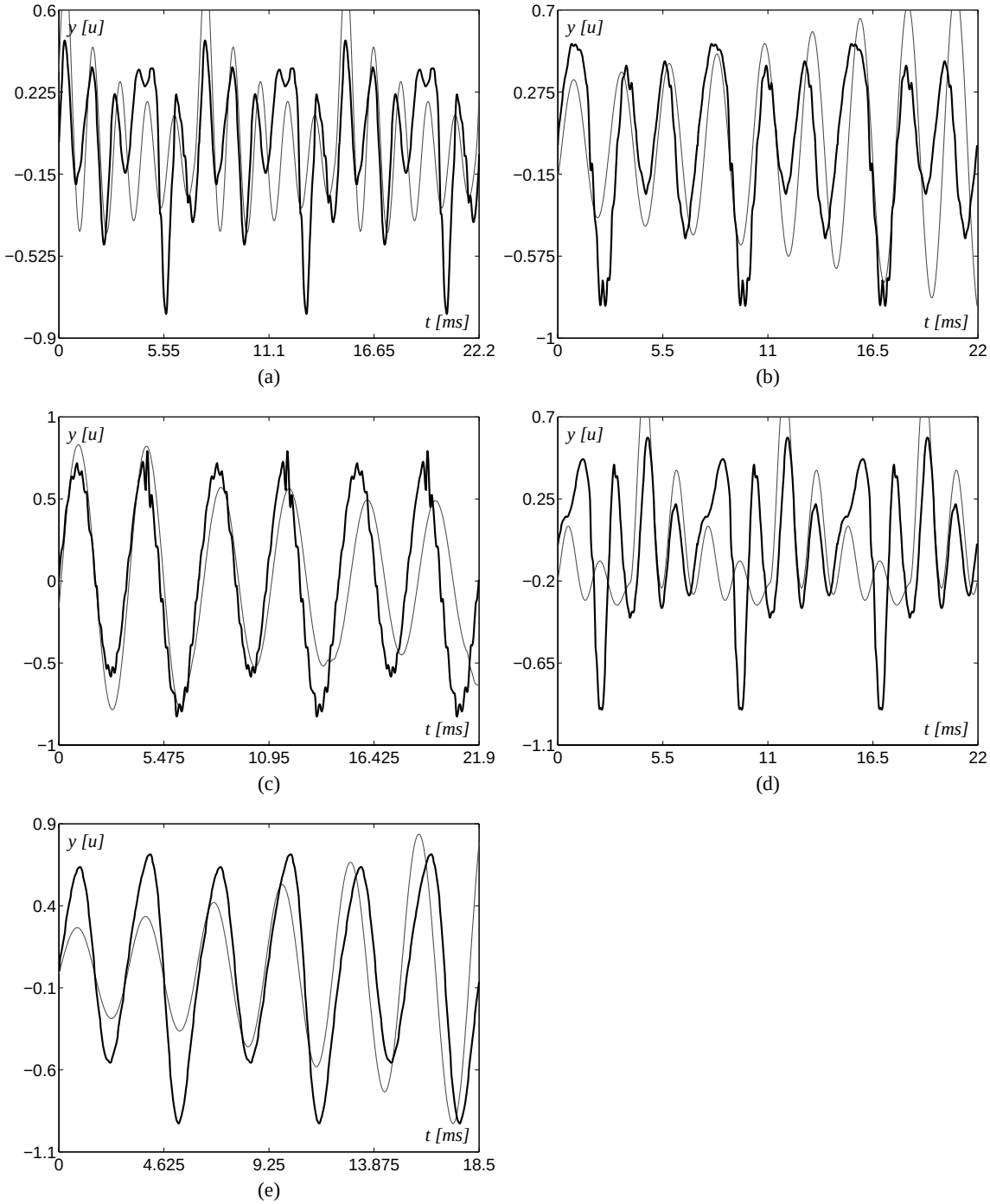

Figure 2.19: *Inconsistent realizations for the Gaussian noise model of the parameters of the AR modeling of the vowels: (a) – [a:]; (b) – [e]; (c) – [i]; (d) – [ɔ]; (e) – [u].*

Qualitative analysis of dynamical system is assumed in this thesis as one of the main tools for dealing with complex dynamics and in particular with deterministic chaos. Typical examples of application of qualitative analysis can be found in [De Feo and Ferrière, 2000; De Feo and Rinaldi, 1997; Maggio *et al.*, 1999b] as well as in the next paragraphs.

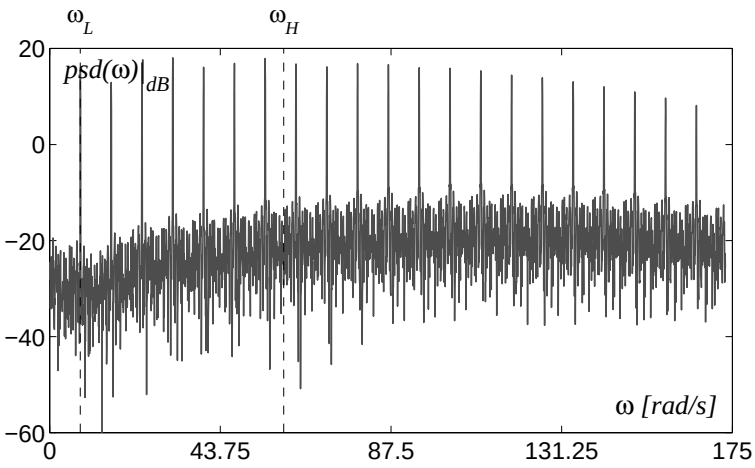

Figure 2.20: *Spectrum of the ECG signal shown in Fig. 2.1. The dashed lines at the angular frequencies ω_L and ω_H corresponds to the tuning of the two filters used for the nonminimal phase reconstruction shown in Fig. 2.21.*

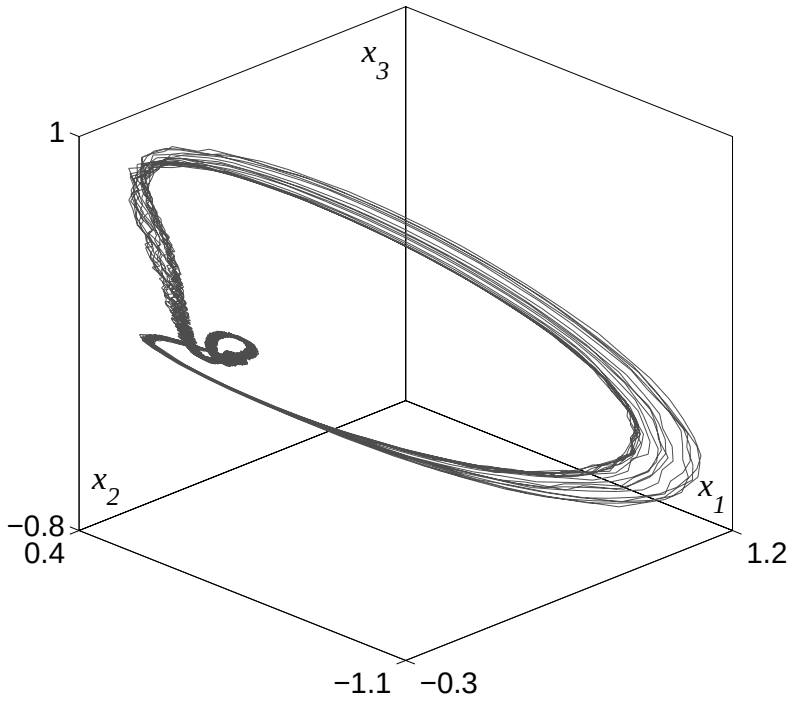

Figure 2.21: *Three-dimensional nonminimal phase reconstruction of the ECG signal shown in Fig. 2.1. The nonminimal phase filters used for the reconstruction are tuned at the angular frequencies ω_L and ω_H shown in Fig. 2.20.*

2.4 Analysis of Strange Attractors

Since the main interest of this work is on temporal patterns, the mathematical framework chosen for modeling the causes of these signals are the ordinary differential and difference equation (ODE). The attention will be restricted to the ordinary differential equations but most of what will be shown is valid for difference equations too. The analysis of chaos shown herein is conducted by means of the *qualitative analysis* [Arnold, 1988; Strogatz, 1994], namely rather than analyzing the chaos itself it is analyzed how the chaotic behavior emerges, because of parameter drift, from more regular behaviors like periodic or quasi-periodic, *i.e.* torus,

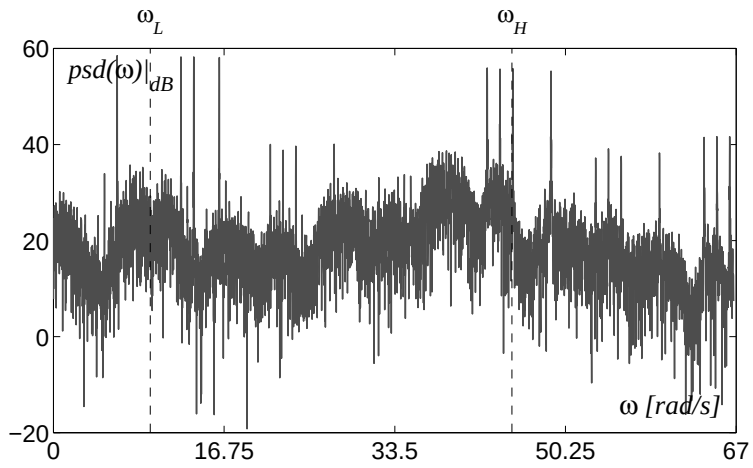

Figure 2.22: *Spectrum of the EEG signal shown in Fig. 2.6. The dashed lines at the angular frequencies ω_L and ω_H corresponds to the tuning of the two filters used for the nonminimal phase reconstruction shown in Fig. 2.23.*

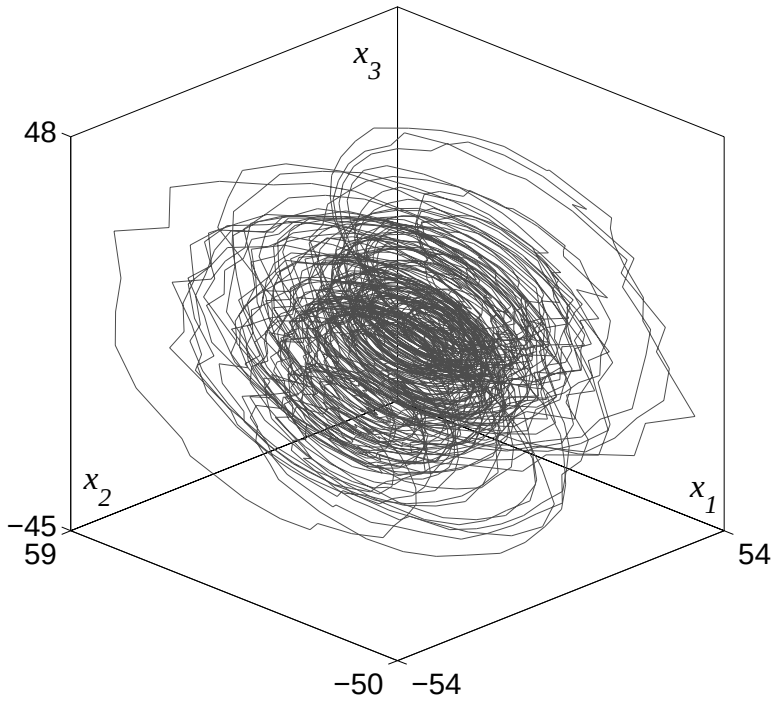

Figure 2.23: *Three-dimensional nonminimal phase reconstruction of the EEG signal shown in Fig. 2.6. The nonminimal phase filters used for the reconstruction are tuned at the angular frequencies ω_L and ω_H shown in Fig. 2.22.*

behavior. To summarize, the mathematical framework considered here are the parametric families of ODE which can always be described in the form

$$dotx = F(x,p); \qquad x \in \mathbb{R}^n,\ p \in \mathbb{R}^m,\ F : \mathbb{R}^n \mapsto \mathbb{R}^n \tag{2.1}$$

where $\dot{x}$ is synonymous of $\dfrac{dx}{dt}$; x is the state vector and n is the dimension of the state space; p is the parameter vector and m is the dimension of the parameter space and, finally, F is the function that describes the local variation of the state per unit of time.

As mentioned afore, in qualitative analysis rather than analyzing the chaos itself it is analyzed how

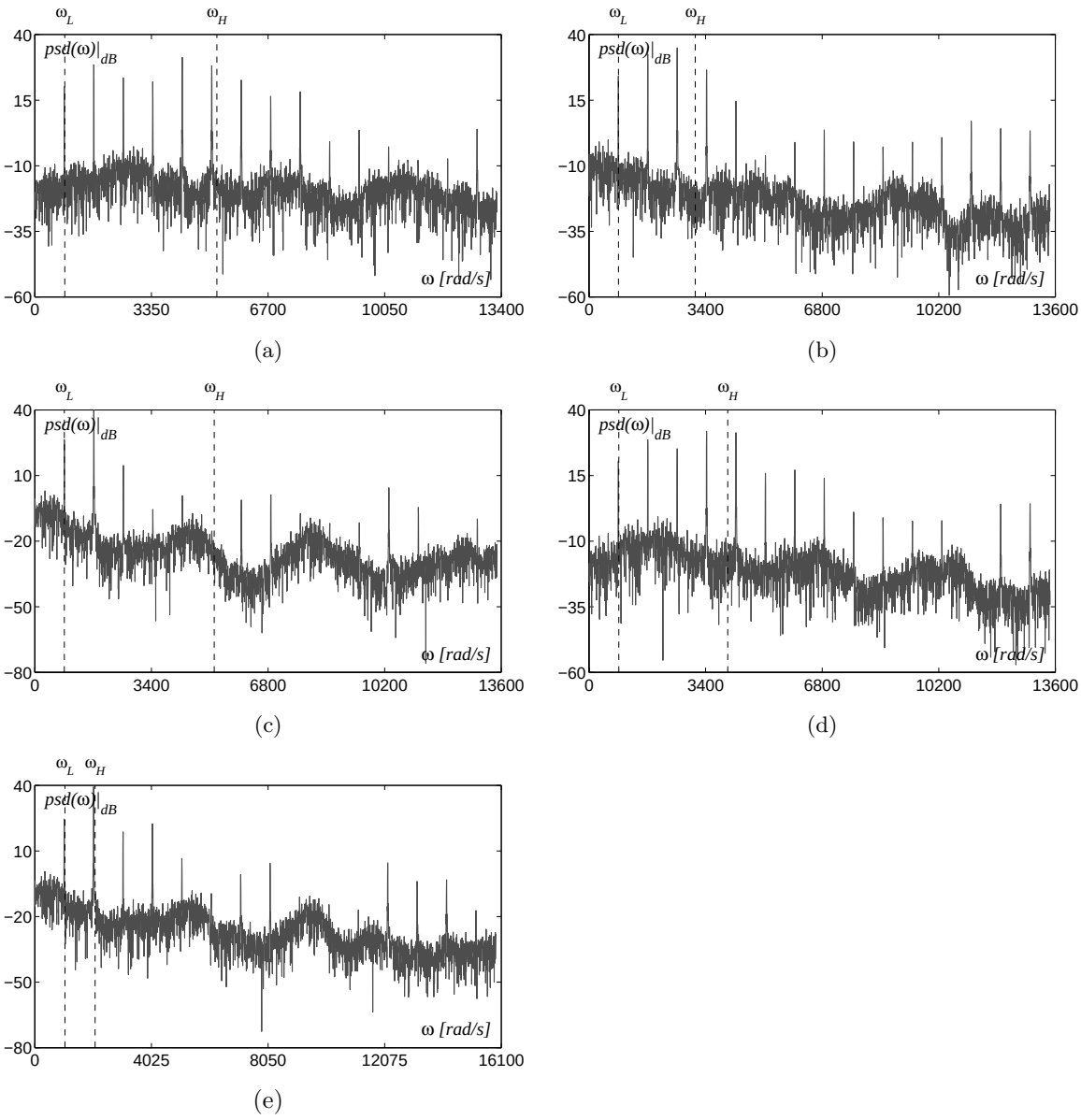

Figure 2.24: *Spectrum of the vowels signals shown in Fig. 2.11: (a) – [a:]; (b) – [e]; (c) – [i]; (d) – [ɔ]; (e) – [u]. The dashed lines at the angular frequencies ω_L and ω_H correspond to the tuning of the two filters used for the nonminimal phase reconstructions shown in Fig. 2.25.*

chaos emerges from more regular behavior when the parameter p changes. In particular, the interest is in the relationships between the chaotic behavior and the regular behavior from which the chaos emerges. This kind of analysis, namely what are and how change the attractors, or more in general the invariants, of Eq. (2.1) varying the parameters p is the argument of the *bifurcation theory* of dynamical systems [Kuznetsov, 1998].

2.4.1 Classifying Chaos

Despite of the large number of examples of physical, biological, economical, etc. systems that admit chaotic behavior, the ways in which this complex behavior appears and its mathematical properties can be commonly conducted to few theories known as *possible routes to chaos* [Wang, 1993]. These theories, that are described in more detail in the next section, show how chaos emerges from a more regular behavior. Three main routes to chaos can be listed [Alligood *et al.*, 1993; Ott, 1993; Strogatz, 1994].

1. *Feigenbaum's or period doubling route*: varying the parameters a sequence of subharmonic resonances lead the system to the aperiodicity, *i.e.* chaos.

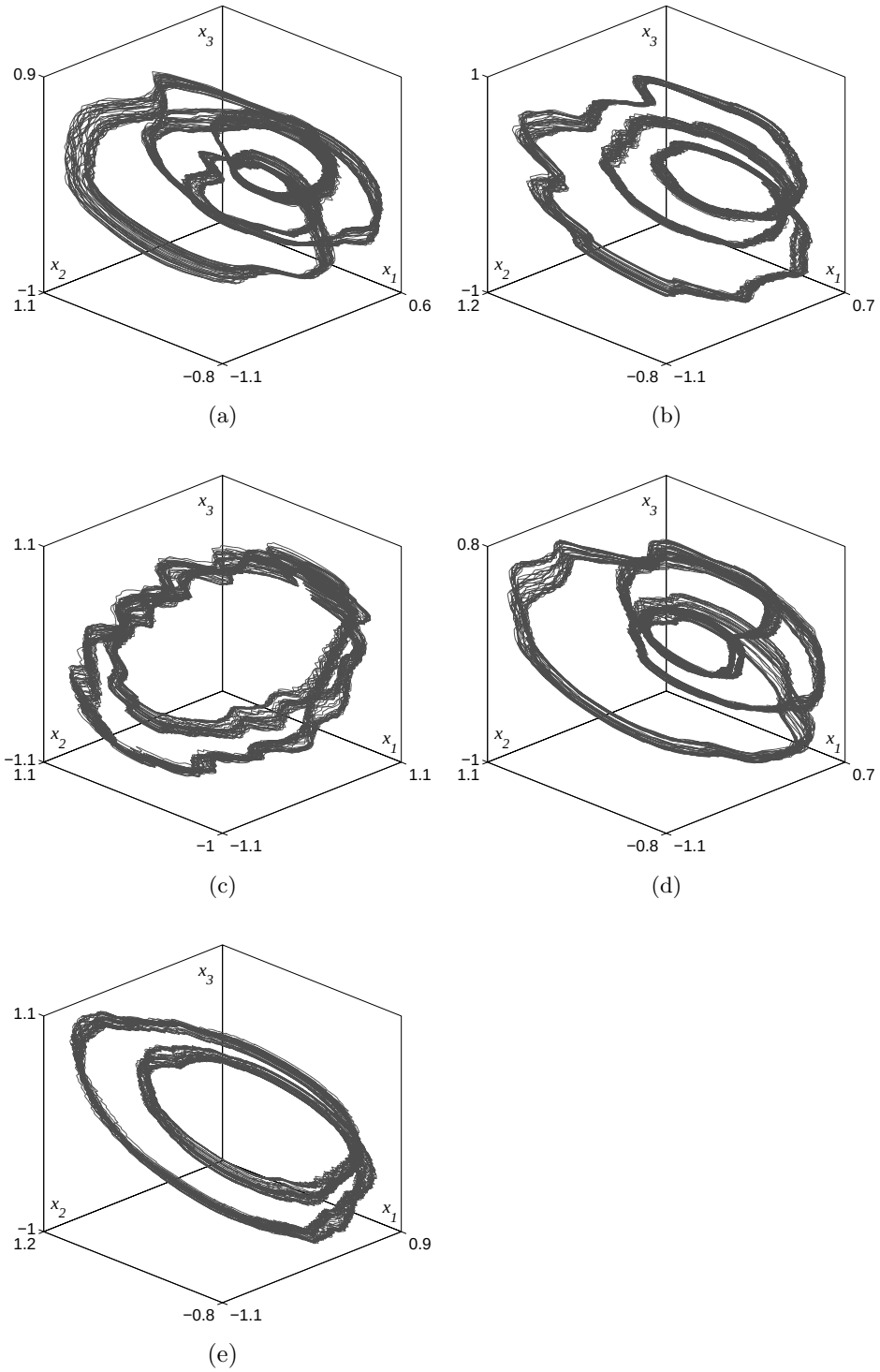

Figure 2.25: *Three-dimensional nonminimal phase reconstructions of the vowels signals shown in Fig. 2.6: (a) – [a:]; (b) – [e]; (c) – [i]; (d) – [ɔ]; (e) – [u]. The nonminimal phase filters used for the reconstructions are tuned at the angular frequencies ω_L and ω_H shown in Fig. 2.24.*

2. *Shil'nikov's or homoclinic route*: the collision between a cycle with a saddle focus equilibrium[7] lead to the existence of aperiodic invariant trajectories.

[7] In dynamical system theory there is a standard nomenclature for hyperbolic equilibria, see for instance [Kuznetsov, 1998].

3. *Torus destruction or strong resonance route*: the collision between a torus with a saddle cycle[8] leads to the existence of aperiodic invariant trajectories.

In all these three route to chaos the aperiodic trajectories[9] share common properties with the cycle or torus from which they emerge. Furthermore, all the bifurcations involved in the route to chaos mentioned afore can be linked to a single limit cycle [De Feo *et al.*, 2000; Glendinning and Sparrow, 1984] from which the bifurcation process that will lead to chaos initiates. Thus, such a periodic solution can be considered as the *generating cycle* of the strange attractor. In the following it will be useful to describe the fluctuations, namely the randomness, of strange attractors with respect to the regular behavior of the generating cycle.

2.4.2 Stochastic Analysis of Chaos

In the rest of the thesis it will be often necessary to compute some statistics of strange attractors. Stochastic properties of strange attractors or, more in general, of dynamical systems are the subject of the *ergodic theory of dynamical systems* [Eckmann and Ruelle, 1985; Sinai, 1993; Walters, 1982]. Ergodic theory is a branch of dynamical systems theory dealing with questions of averages. In particular, ergodic theory is the study of dynamical systems with an invariant probability measure, *i.e.* with a measure over the state space that is left unchanged by the evolution of the system.

Even though ergodic theory is quite developed and provides several tools for the stochastic description of chaotic system, the information that it provides is not easily connected with the stochastic description of interest in the applications discussed herein. The information needed here is definitely simpler than that provided by ergodic theory. The chaotic systems of interest for this thesis are those that can describe approximately periodic signals, *i.e.* with a strong leading periodic component. Consequently, this kind of systems are those that in ergodic theory are classified as *weakly mixing* [Pollicott and Michiko, 1998]. In other words the chaotic system considered herein are those that look approximately like a cycle, their property of interest is the fact that they generate some sort of randomness rather than their temporal unpredictability.

Ergodic theory, is usually more interested in average measures that describe how much unpredictable a chaotic system is, in fact typical results of ergodic theory are the *Lyapunov exponent*, the *entropy*, and the *mixing number* [Eckmann and Ruelle, 1985; Pollicott and Michiko, 1998; Sinai, 1993]. These quantities, that can be computed directly from the time series under the ergodic assumption, are statistical, namely averages, indexes of how much chaotic, namely unpredictable, the dynamical system is.

For what concerns the thesis, on the contrary, the interest is in describing the randomness of an approximately periodic signals with respect to the periodic stereotype. The typical statistical description consists of two distributions[10]. The first is the distribution of the pseudo-period with respect to the nominal period, *i.e.* the period of the stereotype[11]. The second is the distribution of the differences in amplitudes between each pseudo-period[12] of the measured signal and the stereotype. For this purpose, the temporal length of each pseudo-period needs to be normalized to the temporal length of the stereotype in such a way that only the amplitude fluctuations are considered.

Assuming as *standard* stereotype the generating cycle from which strange attractors emerge[13], the stochastic descriptions of the strange attractors considered herein are the two distribution mentioned afore with respect to such stereotype. In the next section that will be exemplified by means of several figures.

2.5 Description Capabilities of Strange Attractors

In order to verify the conjecture that the fluctuations of approximately periodic signals are the results of internal dynamics, the randomness of chaotic systems should be compared with that of measured signals. For this purpose it is necessary to know which kind of fluctuations a strange attractor can realize. More in detail, it should be known which kind of strange attractors can induce which kind of fluctuations. This section is exactly dedicated to the analysis of the randomness spanned by different kinds of strange attractors.

[8] In dynamical system theory there is a standard nomenclature for hyperbolic cycle too, still refer to [Kuznetsov, 1998].

[9] There is no proof that the existence of aperiodic trajectories corresponds to the existence of a strange attractor, even if that is commonly accepted there are counterexamples.

[10] Several examples will follow in the next section.

[11] Often, but not necessarily, chosen as the mean value of the pseudo-period.

[12] Abusing the terminology with the term pseudo-period it is referred not only the time interval but also the fragment of time series over it.

[13] This assumption is quite arbitrary but remove any ambiguity in defining the stereotype of a strange attractor.

In the sequel it will be often necessary to refer to true approximately periodic signals and to true chaotic systems. From now on a generalization of the well-known Colpitts oscillator [Sedra and Smith, 1998], described in Appendix A, will be assumed as paradigm for the generation of simple and complex oscillations. There are multiple reasons for such a choice: first, its behavioral classification with respect to parameter changes is known [De Feo *et al.*, 2000; Maggio *et al.*, 1999b]; second, the "stereotype" of this oscillator is a sinusoid that is a very simple signal that enjoy several properties useful for analysis purpose; third, it is a "relative" of the famous Chua's circuit [Madan, 1993] that is often assumed as standard paradigm for chaotic oscillations; fourth, the generalization considered in Appendix A make this dynamical system suitable for all the tests that will be shown; as last, but surely not least, it is very well-known to the author [De Feo and Maggio, 2000, 2001; De Feo *et al.*, 2000; Maggio *et al.*, 1998, 1999a,b].

2.5.1 Feigenbaum's Chaos

The discovery of the first and easiest route to chaos is due to the consequent researches of Walter Ricker and Mitchell Feigenbaum. In 1954, Walter Ricker has discovered that parameter drift can lead to a sequence of subharmonic resonances and could result in chaos [Ricker, 1954]. Later, in 1978, Mitchell Feigenbaum [Feigenbaum, 1979] gave an universal explanation for such a phenomena. Because the universality discovered by Feigenbaum, the complex behavior appearing from a subharmonic resonance phenomena is known nowadays as *Feigenbaum-like chaos*.

One of the simplest examples of such a route to chaos is given by the family of maps F defined over the unit interval given by

$$F: \; x(n+1) = \lambda x(n)\,(1 - x(n))\,; \quad F : [0,1] \mapsto [0,1] \;\; \forall \; 0 < \lambda \leq 4 \tag{2.2}$$

This is the family of *logistic maps* which in turn is part of the more general family of *unimodal maps* considered by Feigenbaum in his work [Feigenbaum, 1979].

For $1 < \lambda < 3$ the map has a stable equilibrium[14] at $\overline{x} = 1 - 1/\lambda$, increasing λ over the value $\overline{\lambda}_0 = 3$ the equilibrium $\overline{x}$ looses its stability and a stable period-two cycle[15] appears around it. Increasing further λ over the value $\overline{\lambda}_1 = 1+\sqrt{6}$, the period-two cycle looses in turn its stability and a period-four cycle appears around it. For an external observer, the switch from a period-one cycle to a period-two cycle, and analogously from a period-two cycle to a period-four cycle, appears as a sub-harmonic resonance. Indeed, it is as if the system would resonate with a frequency that is one-half of its original one. This phenomena is called *period doubling* or *Flip* bifurcation [Kuznetsov, 1998].

Increasing λ further and further this bifurcation phenomenon is repeated until the value $\overline{\lambda}_\infty = 3.57\ldots$ is passed, then the attractor becomes aperiodic, namely chaotic. This kind of chaotic attractor is known as Feigenbaum's attractor[16] and the sequence of subharmonic resonances that lead to it is known as Feigenbaum's cascade of bifurcations. There is an universal scaling law and several other properties for such sequences of *bifurcations* that lead to chaos [Cvitanović, 1984].

It should be noted that after each bifurcation the previously attracting period-2^n cycle does not disappear but simply becomes unstable, therefore when $\overline{\lambda}_\infty$ is reached there are infinitely many unstable periodic orbits embedded in the Feigenbaum's attractor [Ott, 1993].

A further increase of λ would show sudden appearance of periodic attractors followed by new Feigenbaum's cascades [Ott, 1993]. This is shown in Fig. 2.26 where the attractors of the logistic map (2.2) with respect to the parameter λ are reported. For a given value of λ, the color in the different points of the attractor gives an indirect measure of the *natural invariant density* [Eckmann and Ruelle, 1985; Ott, 1993] of the attractor, namely it codes how often the different parts of the attractor are visited. As can be seen, the trajectories mainly concentrate (dark regions) around some unstable periodic orbits of low period [Eckmann and Ruelle, 1985; Ott, 1993].

The described phenomenon is not only possible for discrete time systems but, it is possible in continuous time ODEs as well. In order to admit flip bifurcations and in particular chaos, a continuous time system must be at least of third order[17] [Ott, 1993; Strogatz, 1994]. Consider the following instance of the generalized

[14] The origin is an equilibrium too but it is always unstable for any $\lambda > 1$.

[15] A period-n cycle of a map F is an equilibria of the n^{th} iterate of the map. Thus, a period-two cycle is an equilibria of $x(n+2) = F\,(F\,(x(n)))$.

[16] The Feigenbaum's attractor is that observed exactly for $\lambda = \overline{\lambda}_\infty$.

[17] Since the trajectories cannot intersect in continuous time system described by ODEs.

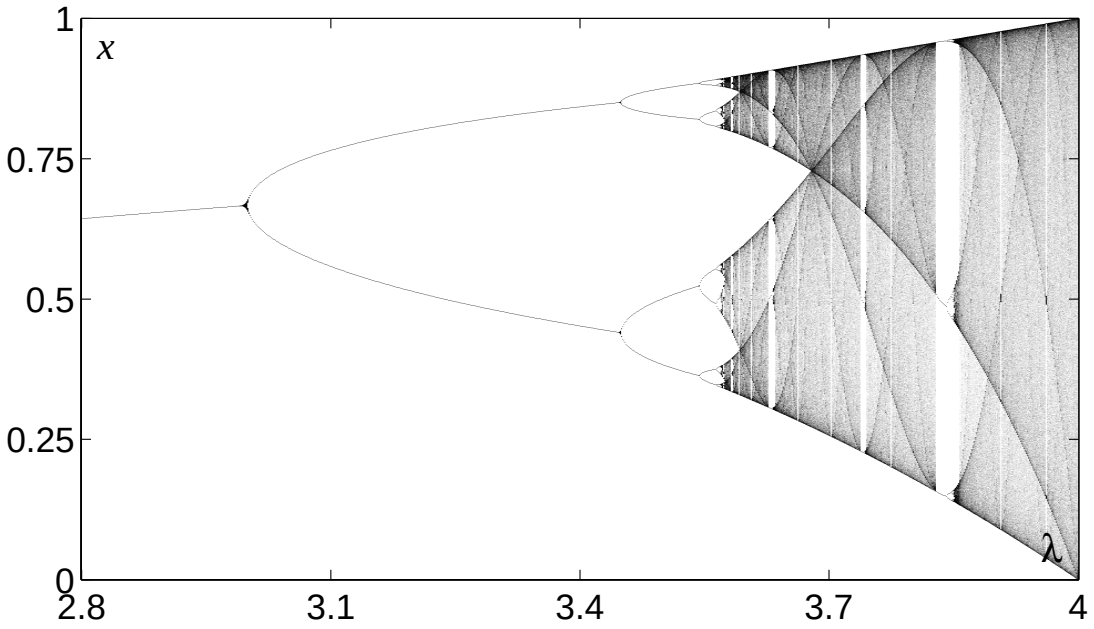

Figure 2.26: *The Feigenbaum-like bifurcation scenario for the logistic map (2.2).*

Colpitts oscillator (*cfr.* Appendix A):

$$\begin{aligned} \dot{x}_1 &= \frac{g}{Q\,(1-k)}\left[-\alpha_F n\,(x_2)+x_3\right] \\ \dot{x}_2 &= \frac{g}{Qk}\left[(1-\alpha_F)\,n\,(x_2)+x_3\right] \\ \dot{x}_2 &= -\frac{Qk\,(1-k)}{g}\left[x_1+x_2\right]-\frac{1}{Q}x_3 \end{aligned} \tag{2.3}$$

where

$$n\,(x)=e^{-x}-1$$

Let fix all the parameter but g: $k=0.5$, $\alpha=0.996$, and $Log_{10}\,(Q)=0.2480$. Moving g from the value of almost 1.96 towards 2.8 will drive the system through a series of period doubling bifurcations that will end in the appearance of aperiodic, namely chaotic, behavior as shown in Fig. 2.27.

In a system of ODEs, the periodic solutions that are born by period doubling bifurcation lie on a Möbius strip [Kuznetsov, 1998], namely on a nonorientable strip. Thus, the Feigenbaum-like strange attractors, whose skeletons are composed of these orbits, lie as well on such a kind of strip. This can be easily observed in Fig. 2.28 where a Feigenbaum-like attractor A_F for Eqs. (2.3) is shown.

There is a strong relationship between one-dimensional maps that admit a Feigenbaum's cascade, like the logistic map afore described, and three-dimensional continuous time systems that admit Feigenbaum-like attractors. Consider the Poincaré section[18] Π of Fig. 2.28, since A_F lies on a two-dimensional surface, the intersection between the strange attractor A_F and Π, called Γ_F, is almost a thin line segment, as shown in Fig. 2.29(a). A point on a one-dimensional line segment can be uniquely identified by its normalized curvilinear coordinate $s\in[0,1]$ [Amerio, 1977a,b], thus the restriction on Γ_F, *i.e.* to the attractor A_F, of the two-dimensional Poincaré map $P:\ \Pi\mapsto\Pi$ can uniquely be described by a one-dimensional map $P_1:\ \Gamma_F\mapsto\Gamma_F$ or, referring to the curvilinear coordinate, by $P_s:\ [0,1]\mapsto[0,1]$. Such a map for the attractor A_F is shown in Fig. 2.29(b), as can be noted it is a unimodal map as those considered by Feigenbaum for his theorem. It happens that many chaotic systems, not only the Feigenbaum-like ones, can be described by a one-dimensional map, as illustrated in [Candaten and Rinaldi, 2000].

The time series associated with the Feigenbaum-like attractor A_F are approximately periodic signals, it is then possible to compute the distributions of the pseudo-period and of the amplitudes as afore mentioned.

[18] The Poincaré section and the Poincaré map are two standard tools of nonlinear system analysis [Kuznetsov, 1998; Ott, 1993; Strogatz, 1994].

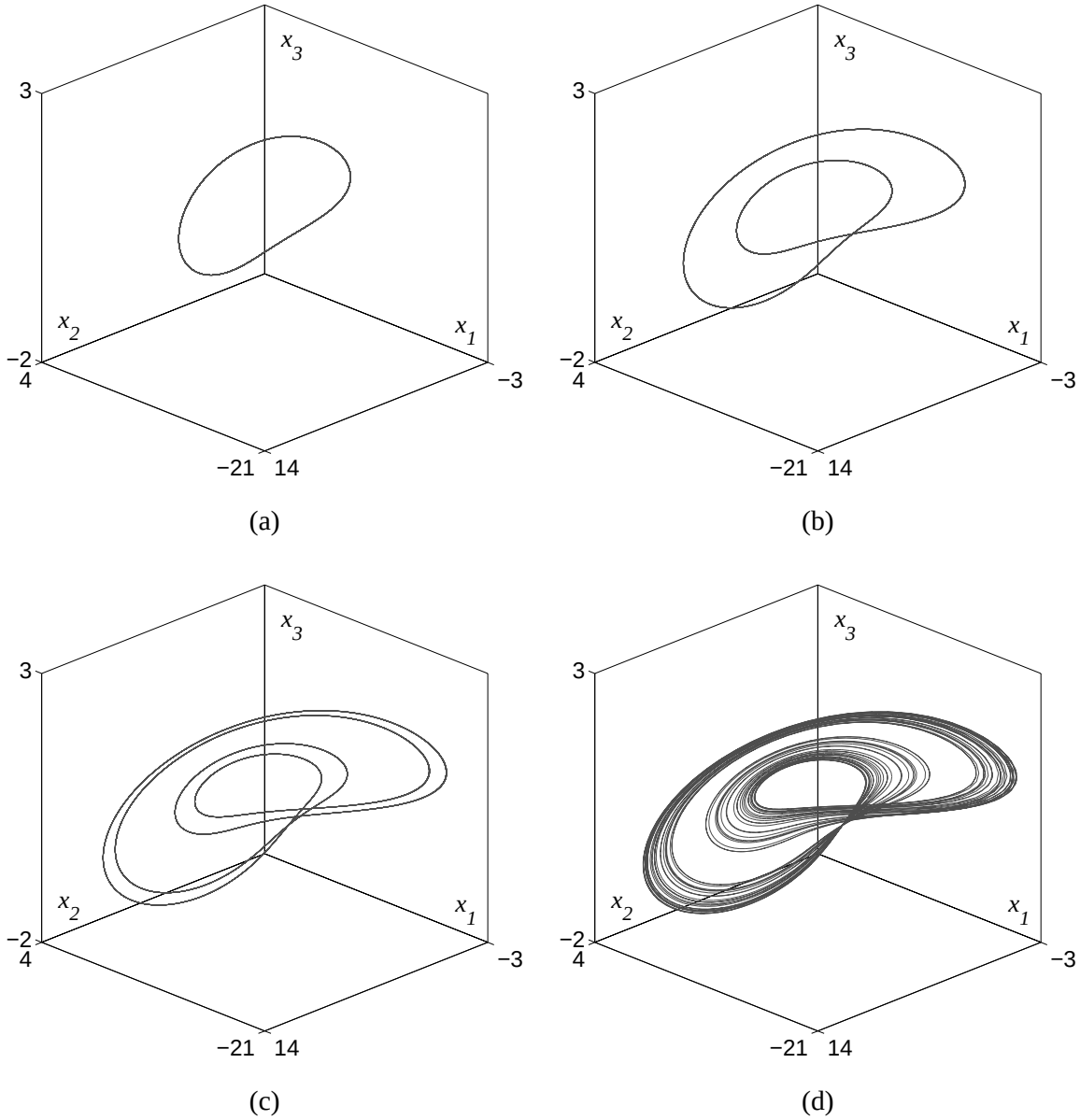

Figure 2.27: *Sequence of subharmonic resonances, Feigenbaum's cascade, that lead to aperiodic motion in the third order continuous time system given by Eqs. (2.3), $k = 0.5$, $\alpha = 0.996$, $Log_{10}(Q) = 0.2480$: (a) – $1:1$ resonance, period-one attractor, $Log_{10}(g) = 0.2939$; (b) – $1:1/2$ resonance, period-two attractor, $Log_{10}(g) = 0.3857$; (c) – $1:1/4$ resonance, period-four attractor, $Log_{10}(g) = 0.4290$; (d) – aperiodic, chaotic, attractor, $Log_{10}(g) = 0.4472$.*

Each pseudo-period of the attractor A_F is the trajectory segment that goes from Π back to Π, thus the pseudo-period is the time elapsed between two successive intersection, in the same direction, of the trajectory on A_F with Π. In other words, the pseudo-period is the time interval that corresponds to one iteration of the Poincaré map. As described before, the restriction to the attractor A_F of the Poincaré map leads to a one-dimensional map. In the same way, the map of the return time to Π can be described by a one-dimensional map that links the current curvilinear coordinate $s(n)$ with the next pseudo-period $T_P(n+1)$, *i.e.* with the elapsed time before the trajectory will hit again Π in $s(n+1)$. Such a map for the attractor A_F is shown in Fig. 2.30(a), as can be noted the return time is practically always 2π. Hence, the pseudo-period distribution is almost a δ centered in 2π. Such a strong determinism in the pseudo-period is not generic for Feigenbaum-like attractors but it is a peculiarity of the particular model herein considered. Anyway, even for other Feigenbaum-like attractors [Ott, 1993; Strogatz, 1994], the pseudo-period is almost

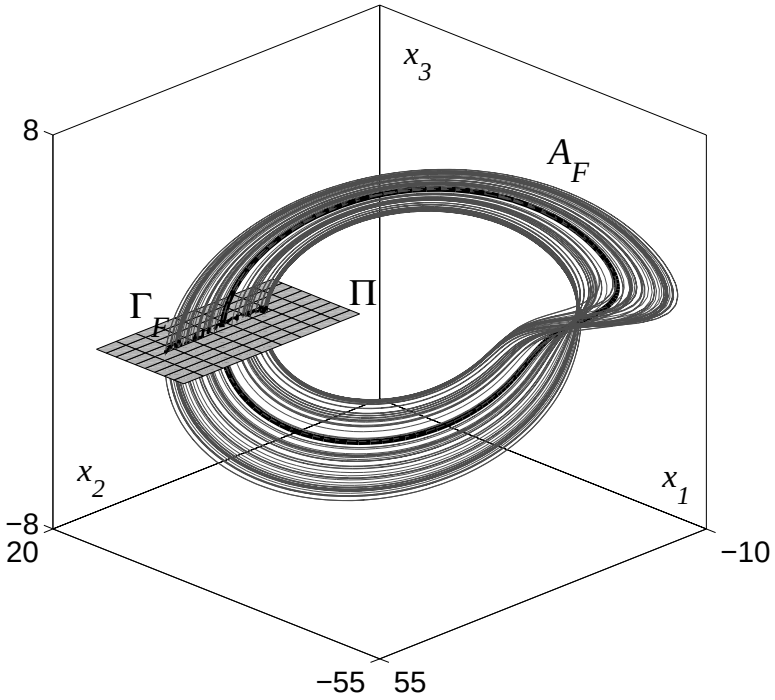

Figure 2.28: *Feigenbaum-like attractor for Eqs. (2.3), $k = 0.5$, $\alpha = 0.996$, $Log_{10}(Q) = 0.75$ and $Log_{10}(g) = 1$. The bold line is the embedded unstable generating cycle.*

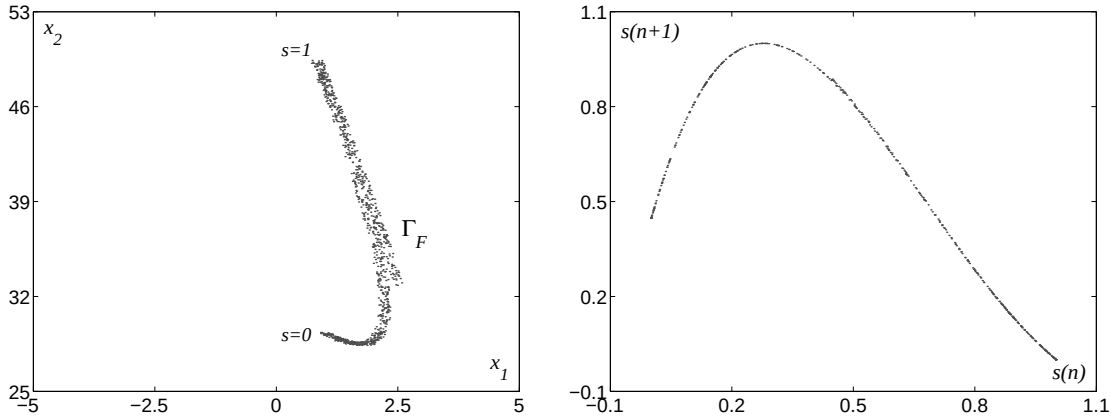

Figure 2.29: *The Poincaré maps of a continuous time Feigenbaum-like attractor: (a) – intersection (Γ_F) of the Feigenbaum-like attractor A_F with the Poincaré section Π, as shown in Fig. 2.28, it is almost a thin line; (b) – one-dimensional Poincaré map of the curvilinear coordinate s on Γ_F.*

concentrated around a single value, thus the δ shown in Fig. 2.30(b) will be in general a distribution with a distinct peak.

The distribution of the amplitudes over each pseudo-period can be easily shown by means of the so-called stroboscopic plot. Consider the time series of a scalar measurement of the internal state of the system given by an output function $y = h(x)$, for instance the time series of $y = x_2$ [19]. Let one start from a point on Γ_F and plot the evolution of y until the section Π is hit again, then let reset the time and repeat the procedure[20].

[19] Please refer to the Appendix A for the justification of such a choice.

[20] In a generic case it could be necessary to normalize the pseudo-period to the nominal period, here it is not the case since the pseudo-period is always the same.

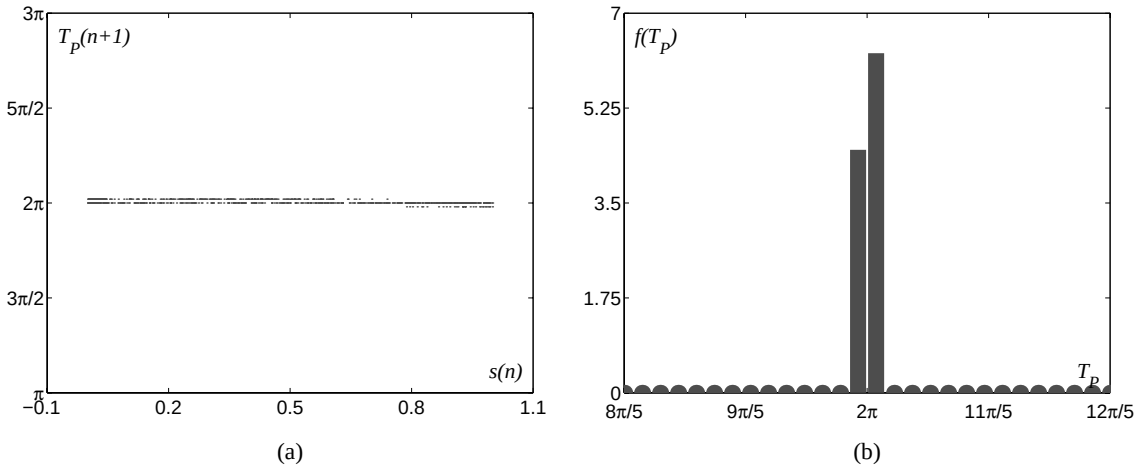

Figure 2.30: *Distribution of the pseudo-period of the Feigenbaum-like attractor A_F* (cfr. *Fig. 2.28*)*: (a) – Poincaré map of the pseudo-period $T_P(n+1)$* vs *the curvilinear coordinate $s(n)$; (b) – the distribution of the pseudo-period, it is almost a δ centered at 2π.*

The result of the stroboscopic plot of the Feigenbaum-like attractor A_F, together with the x_2 time series (bold) while behaving on the generating cycle, is reported in Fig. 2.31. It should be noticed that the torsion of the Möbius strip leads to have a time interval along which the distribution of the trajectories is fairly concentrated. This concentration of the trajectories does not happen necessarily, it depends on the particular output function $y = h(x)$ chosen. It always happens for linear output functions $y = Cx$, $C = [a\ b\ c]$, where a, b, and c are three real numbers. The time interval in which the concentration happens depends on the particular linear combination, specifically it happens in the time interval where the output assumes the values to which the linear transformation projects the torsion of the Möbius strip.

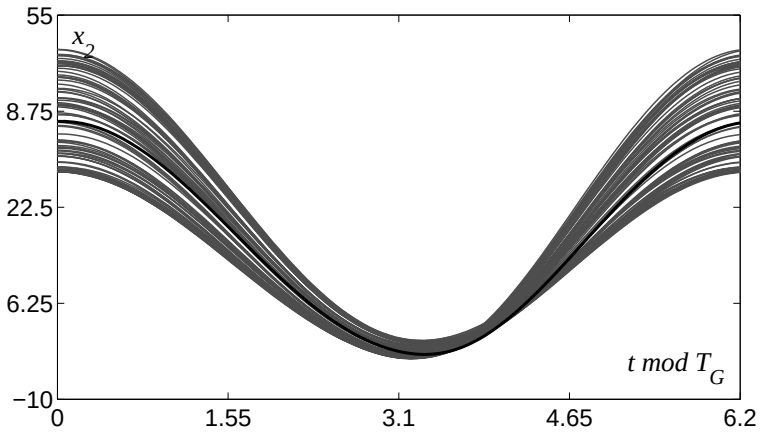

Figure 2.31: *Stroboscopic plot of the x_2 time series while behaving on the Feigenbaum-like attractor A_F* (cfr. *Fig. 2.28*)*. Each plot corresponds to the time series of an orbit starting from and coming back to Γ_F. The bold line is the time series while behaving on the generating cycle.*

The probability distribution of the amplitudes in the different points of the pseudo-period is shown in Fig. 2.32, as for the case of the one-dimensional map the trajectories in A_F mainly concentrate (dark peaks) around some unstable periodic orbits of low period. Such a distribution is not representative in general since it depends on the parameter values (see Fig. 2.26), varying the parameters it can be concentrated around a few unstable orbits or spread to reach an almost uniform distribution over an interval.

To summarize, Feigenbaum-like chaotic systems can describe approximately periodic signals with randomness mainly on the amplitude and with little or no randomness of the pseudo-period. For a given approximately periodic signal, the concentration of the amplitude distribution in a particular time interval of the pseudo-period can be a strong clue of a Feigenbaum-like chaotic source.

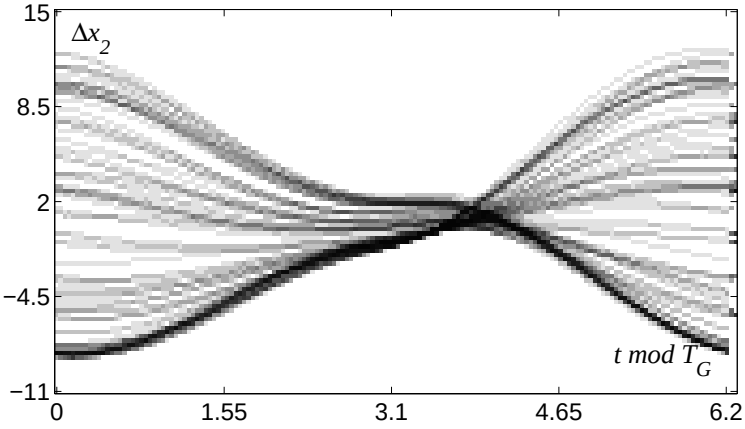

Figure 2.32: *Distributions, along the pseudo-period, of the discrepancies of x_2 while behaving on the Feigenbaum-like attractor A_F (*cfr. *Fig. 2.28) from x_2 while behaving on the generating cycle.*

2.5.2 Shil'nikov's Chaos

The discovery of the second, and, in some sense, more complex route to chaos is more recent. In 1968, Leonid Shil'nikov [Tresser, 1984] related the possibility of complex behavior to a particular trajectory which is starting from and coming back to an equilibrium with particular properties of the eigenvalues (*cfr.* Fig. 2.33). Subsequently, in 1983, Pierre Gaspard [Gaspard, 1983; Gaspard *et al.*, 1984; Gaspard and Nicolis, 1983] shows in which sense this kind of chaos, known as *Shil'nikov-like*, is more complex than the Feigenbaum chaos. As trajectories that are bi-asymptotic to an equilibrium point, or another invariant, are called homoclinic trajectories to this point, or invariant, this kind of chaos is also known as homoclinic chaos.

Simplifying, the Shil'nikov's condition for complex behavior [Kuznetsov, 1998; Silva, 1993; Tresser, 1984] can be summarized as follow.

Theorem 1 (Shil'nikov, case IV) *Let a third order system of ODEs depending on a parameter vector p (*cfr. *Eq. (2.1)) admit, for a given value of the parameters $\overline{p}$, a homoclinic trajectory Ψ to a saddle-focus equilibrium E (*cfr. *Fig. 2.33(a)), namely to an equilibrium with a real eigenvalue*[21] *and a pair of complex conjugate eigenvalues. If the complex conjugate eigenvalues are dominant (*cfr. *Fig. 2.33(b)),* i.e. *closer to the Imaginary axes than the real one, then, for any parameter value in a small neighborhood of $\overline{p}$, the system admits a countable infinity of periodic solutions and a countable infinity of aperiodic solutions.*

Note that nothing is said about the stability of the complex solutions even if, commonly, when the saddle quantity of the equilibrium E, *i.e.* the sum of the real parts of its eigenvalues, is negative then a Shil'nikov-like strange attractor is observed (*cfr.* Fig. 2.35).

The one reported above is not the only Shil'nikov's theorem regarding homoclinic orbits to an equilibria in three-dimensional systems. Actually, there are four of them depending on the different possible configurations of the eigenvalues at the equilibria E [Kuznetsov, 1998; Silva, 1993; Tresser, 1984]. The four cases can be collected into two big classes, respectively called Shil'nikov's or tame case depending on the fact that the equilibrium E has or does not have complex conjugate eigenvalues. From a global point of view the two cases are not very different, they can be seen as the collision, varying a parameter, of a limit cycle with a saddle equilibrium, the differences between the two cases lie on how this collision happens with respect to the changing parameter.

When a limit cycle approaches an equilibrium, its period tends asymptotically to infinity as the trajectory spends more and more time near the equilibrium where the vector field is very slow. For the two cases mentioned afore, this is illustrated in Fig. 2.34 which shows a sketch of the dependence of the period T_0, for a periodic orbit approaching the homoclinic bifurcation, on a parameter μ, for the tame and Shil'nikov's cases, respectively.

A main property of homoclinic bifurcations can be evinced from Fig. 2.34, irrespective of whether they are of tame type or Shil'nikov's type. From a global point of view, homoclinic bifurcations organize the existence of just one cycle and, in the Shil'nikov's case, of a set of other invariant sets in a neighborhood of

[21] The eigenvalues of an equilibrium are those of the Jacobian of the system (2.1) evaluated at the equilibrium itself. In other words they are the eigenvalues associated with the linearization of the system around the equilibria E.

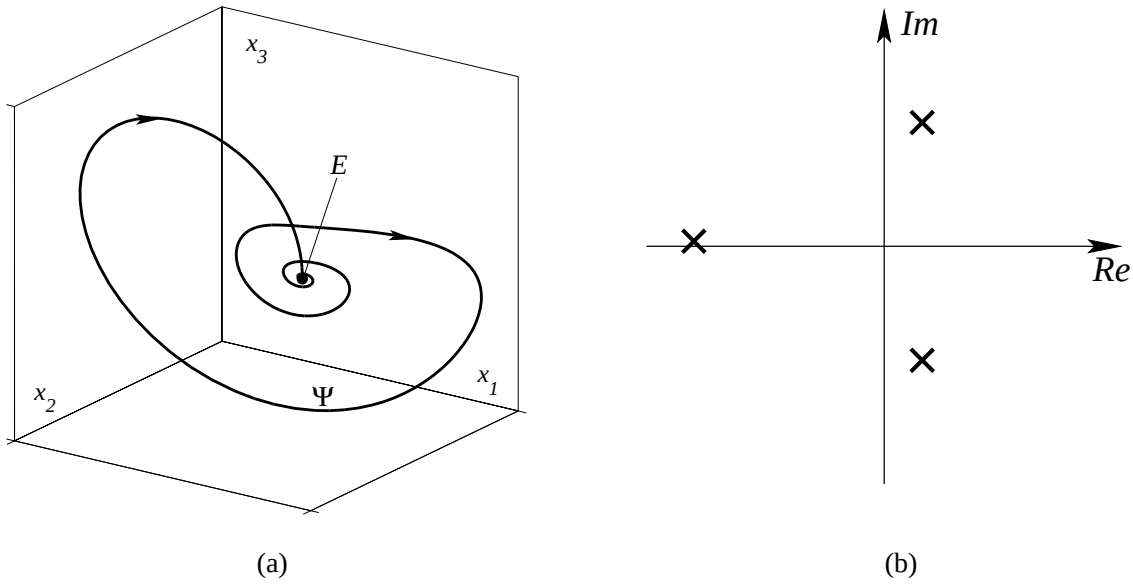

Figure 2.33: *Bifurcation condition that lead to Shil'nikov-like chaos: (a) – homoclinic connection to a saddle-focus equilibrium; (b) – the complex-conjugate eigenvalues of the equilibrium are dominant, closer than the real one to the imaginary axes.*

the homoclinic bifurcation. In fact, in both cases, from a global point of view, *i.e.* far from the bifurcation point, the homoclinic bifurcation at $\mu = 0$ divides the parameter space into roughly two parts: $\mu \ll 0$ where a periodic solution exists, and $\mu \gg 0$, where the periodic solution does not exist. Furthermore, it appears that, in some sense, all the periodic orbits in the neighborhood of a Shil'nikov's type homoclinic bifurcation are derived from the same cycle. These periodic orbits are some of those that compose the skeleton of the Shil'nikov-like strange invariant existing in a neighborhood of the homoclinic bifurcation [De Feo *et al.*, 2000; Glendinning and Sparrow, 1984]. Hence, summarizing, it can be said that in both cases, tame and Shil'nikov's, the periodic and aperiodic invariant sets involved in the bifurcation originate from only one cycle, namely the *generating cycle*.

The links between the skeleton of Shil'nikov-like strange attractors and their generating cycles are not restricted to their origin, in fact they share common geometric properties. Furthermore, there is a relationship between Shil'nikov-like and Feigenbaum-like strange sets. Indeed, as a corollary of Gaspard's works [Gaspard *et al.*, 1984; Gaspard and Nicolis, 1983] comes a geometrical interpretation of the unfolding of the Shil'nikov-like strange sets[22]. They can be imagined as a Russian doll, a matrioska, as shown in Fig. 2.35: the skeleton of a Shil'nikov-like attractor is composed of an infinite number of Feigenbaum-like sets, *i.e.* strange saddles, that in this sense is a simpler strange set than the Shil'nikov-like one. The skeleton of a Feigenbaum-like set is, in turn, composed of an infinite number of periodic saddle trajectories. All these sets, Shil'nikov-like attractor, Feigenbaum-like sets and the periodic orbits share common properties in terms of geometrical shapes and frequency components. In nonlinear jargon, they are said to be self-similar.

The typical trajectory in a Shil'nikov-like attractor spirals outwards from the neighborhoods of the equilibrium E, then after having moved far away it is reinjected again, by means of the homoclinic structure, into the neighborhoods of equilibrium E. In the theory about Shil'nikov-like attractors two kinds of strange attractors are identified depending upon the mechanism that reinjects the trajectories in proximity of the equilibrium E.

If the trajectories are reinjected always on one side[23] of E, the strange attractor is said to be of *spiral* type. This kind of strange attractor is nothing more than a rich (fat) Feigenbaum-like attractor [Gaspard and Nicolis, 1983], thus all the description previously given (*cfr.* Sect. 2.5.1) is still valid.

When the trajectories are reinjected on two sides of E, the strange attractor is said to be of *screw* type. This kind of strange attractor enjoys properties different from those of the Feigenbaum-like attractor. In the following analysis the attention is restricted to this kind of strange attractor.

[22] They do not need to be attractive.

[23] The two side of a saddle-focus equilibrium are defined in cylindrical coordinates with respect to the real eigenvector and a given phase [Gaspard, 1983].

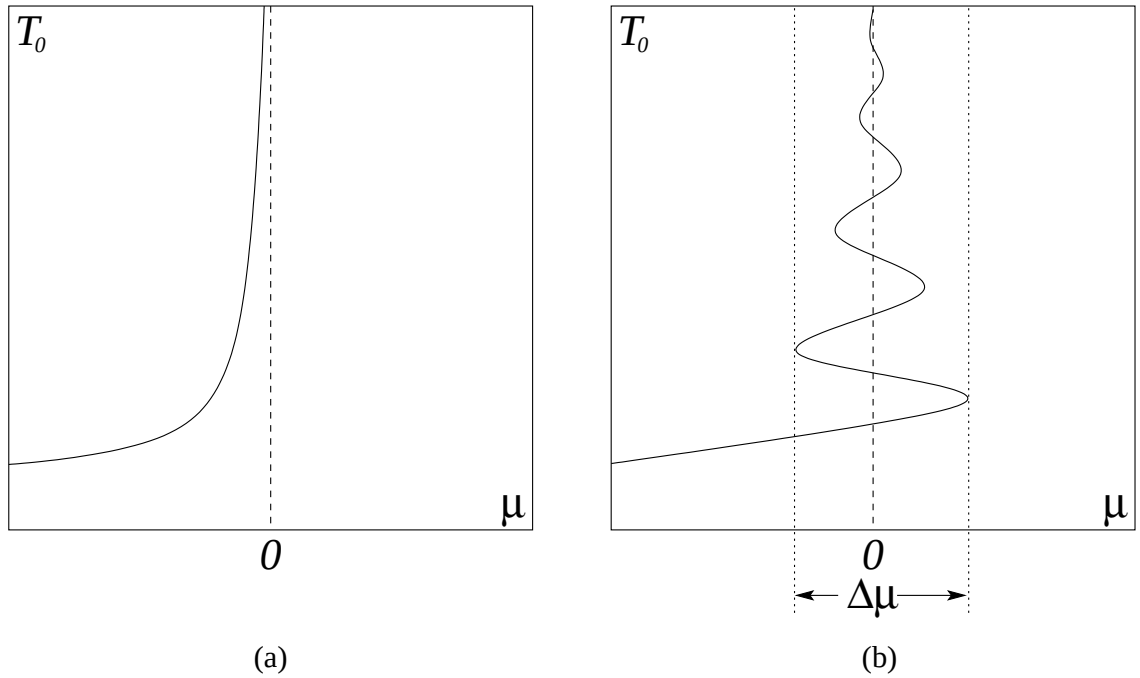

Figure 2.34: *Tame and Shil'nikov's homoclinic scenario with respect to a parameter: (a) – tame case, the periodic solution hit the equilibria monotonically; (b) – Shil'nikov's case, the periodic solution hit the equilibria with swings.*

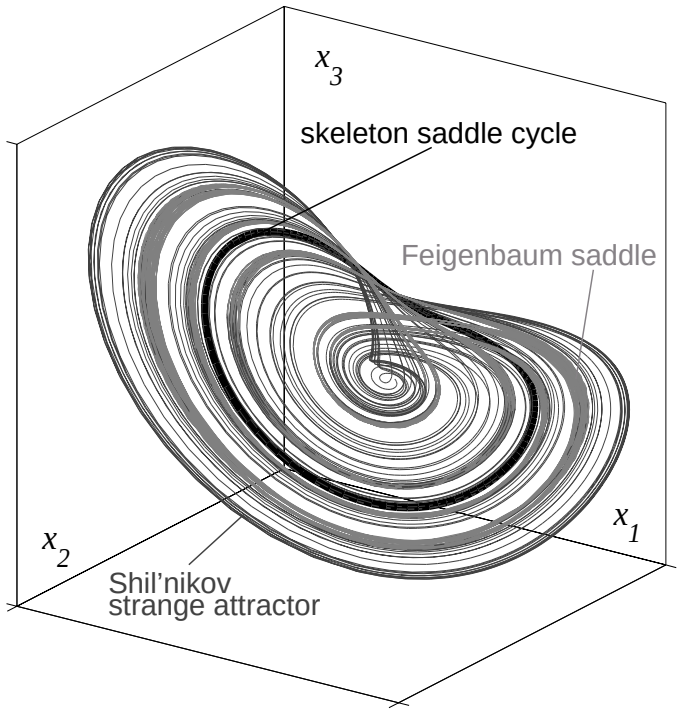

Figure 2.35: *Russian doll structure of a Shil'nikov-like attractor. The strange attractor is composed of infinite Feigenbaum-like strange saddles which in turns are composed of infinite saddle cycles.*

Equations (2.3) satisfies, for particular parameter values, the fourth case of the Shil'nikov's theorem [De Feo *et al.*, 2000] and, indeed, a screw-type Shil'nikov-like strange attractor can be observed in the neighborhood of such parameter values, as shown in Fig. 2.36(a).

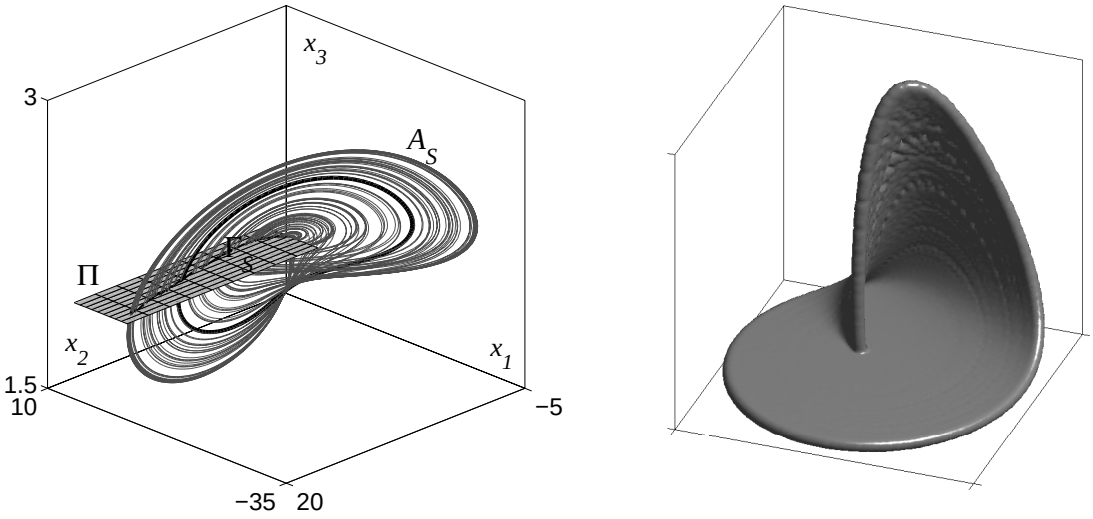

(a) (b)

Figure 2.36: *Shil'nikov-like attractor for Eqs. (2.3), $k = 0.5$, $\alpha = 0.996$, $Log_{10}(Q) = 0.75$ and $Log_{10}(g) = 1$: (a) – screw-type Shil'nikov-like attractor, the bold line is the embedded unstable generating cycle; (b) – the homoclinic reinjection manifold on which the Shil'nikov-like attractor lies.*

Figure 2.36(b) shows that the Shil'nikov-like attractor A_S lies on an almost two-dimensional surface [Gaspard *et al.*, 1984]. Hence, a suitably chosen Poincaré section Π will intersect A_S along a line segment Γ_S as for the case of the Feigenbaum-like chaos. By the same technique described in Sect. 2.5.1, two one-dimensional maps associated with Γ_S can be defined. The Poincaré map of the curvilinear coordinate s which map $s(n)$ in $s(n+1)$ and the map of the next return time to Γ_S which map $s(n)$ in $T_P(n+1)$, as shown in Fig. 2.37.

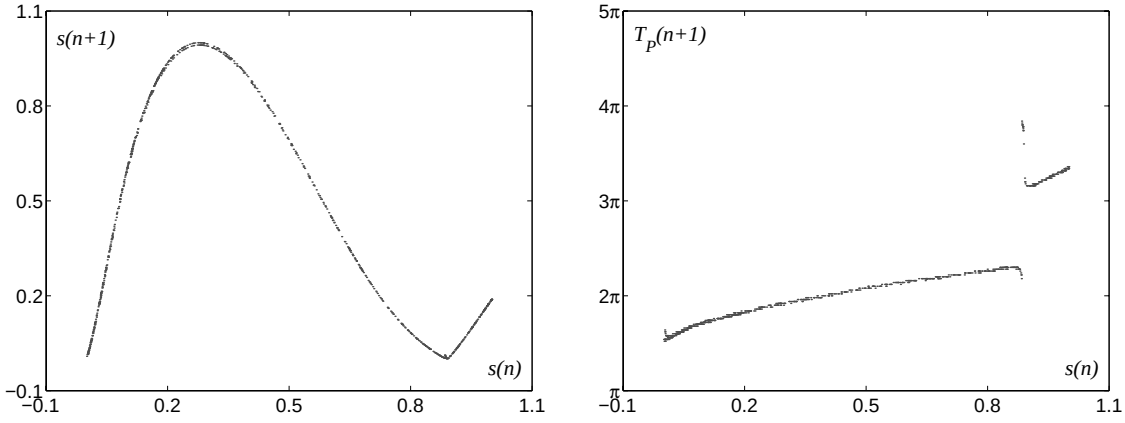

(a) (b)

Figure 2.37: *The Poincaré maps of a screw-type Shil'nikov-like attractor: (a) – one-dimensional Poincaré map of the curvilinear coordinate s on Γ_S; (b) – Poincaré map of the next return time $T_P(n+1)$ vs the curvilinear coordinate $s(n)$;*

An attentive look to Figs. 2.36 and 2.37 allows to realize quite easily that not all the trajectory segments that start from and come back to Π are of the same kind. Indeed, with the help of Fig. 2.37(b), at least three different kind of trajectory segments can be identified.

The first kind are the trajectory segments that emerges from points on Γ_S identified by a curvilinear coordinate $s(n) < 0.94$. These trajectory segments are reinjected quite far from the equilibrium E, thus their pseudo-period is always about 2π, furthermore they are geometrically very similar to the generating cycle, as shown in Figs. 2.38 and 2.39. Since this trajectory segments are very similar to the generating cycle, that is assumed to be the stereotype of the approximately periodic signals associated with the strange attractor, this segments are called *pattern trajectory segments*. The ensemble of these trajectory segments represent the Feigenbaum-like part of the Shil'nikov-like attractor, the part of the Poincaré map (*cfr.* Fig. 2.37(a)) associated with them is indeed a unimodal map as described in Sect. 2.5.1.

The second kind of trajectories are those that emerges from a point on Γ_S identified by a curvilinear coordinate $s(n) \approx 0.94$. These trajectory segments are reinjected fairly close to the equilibrium E. Hence, their pseudo-period strongly depends on the time spent to escape from the equilibria which, in turn, can vary tremendously with little changes in the reinjecting distance from the equilibrium[24]. This trajectory segments are geometrically very similar to the homoclinic trajectory[25] Ψ rather than to the generating cycle, as shown in Figs. 2.38 and 2.39. Since this trajectory segments are not very similar to the generating cycle and keeping in mind that they introduce a random delay, this segments are called *phase skip trajectory segments*. The ensemble of this segments determines the part of the Shil'nikov attractor which introduces a random phase shift in the approximately periodic signal associated to the attractor.

The third and last kind of trajectories are those that emerge from points on Γ_S identified by a curvilinear coordinate $s(n) > 0.94$. These trajectory segments are reinjected fairly far away from the equilibrium E but they are reinjected on the other side of E with respect to the pattern trajectory segments. Because of the continuity of the vector field, they must run half a turn more around the equilibrium than the pattern trajectory segments before escaping the equilibrium E. Therefore, their pseudo-period is fifty percent longer than that of the pattern trajectory segments, as can be easily noticed in Fig. 2.37(b) where $T_P(n+1) \approx 3\pi$ for $s(n) > 0.94$. These trajectory segments are more or less geometrically similar to the generating cycle depending upon how pronounced the half turn segment is. For the particular case herein considered, this trajectory segments are more similar to a phase skip trajectory segment rather than being similar to a pattern segment, but this is not general and depends on the particular model. These trajectory segments are called *reinjected trajectory segments* and from case to case they are considered as pattern or phase skip segments depending on how similar they are to the generating cycle. In particular, in the rest of the analysis they have been treated as phase skips.

Note that the threshold of $s(n)$ used to classify the trajectory segments depends upon the parameter values, the particular value $s(n) = 0.94$ is specific for the attractor A_S. In general, the threshold value for $s(n)$ coincides, by theory [Gaspard *et al.*, 1984], with the position of the minimum on the one-dimensional map. Actually, any screw-type Shil'nikov-like attractor has an associated one-dimensional map as shown in Fig. 2.37(a).

From the classification of the trajectory segments given above, it can be deduced that the time series associated with a Shil'nikov-like attractor do not appear like approximately periodic signal at all times as the time series from a Feigenbaum-like attractor. Indeed, they look like approximately periodic signals when pattern trajectory segments are involved. But, from time to time, when phase skip trajectory segments are followed, almost stationary intervals appear in the time series as the trajectory approaches the equilibrium. These stationary intervals introduce phase delays before starting with another series of approximately periodic cycles. In fact, from Fig. 2.37(a) it is clear that after a phase skip at least one pattern segment follows since all the points with $s(n) \geq 0.94$ are mapped to points with $s(n) < 0.94$.

Since the fact that not all the trajectory segments are of the same kind, it is necessary to specify with respect to which trajectory segments the pseudo-period and the amplitude distributions should be computed. Obviously, being interested in the stereotype-like signals, such distributions are computed with respect to the pattern trajectory segments only.

To describe the statistical properties of the phase lags two new distributions can be introduced. First, the distribution of the phase lags, namely the distribution of the time length of the phase skip trajectory segments. Second, the distribution of the frequency of the phase skips, namely the distribution of the pattern interval length between two phase skips. There are strong theoretical reasons [Anishchenko and Neiman, 1989; Brunsden and Holmes, 1987; Gaspard *et al.*, 1984] to suspect that these two distributions are not independent. That is why they are computed as a single joined distribution $p(N, \Delta T)$ which gives the

[24] Very close to the equilibria the linear approximation is valid, in linear systems there is a logarithmic relationship between the escape time and the distance from the equilibria, $T \propto -ln(\Delta)$ where Δ is the distance from the equilibria.

[25] Actually, Ψ is the trajectory corresponding to the minimum of the one-dimensional map in Fig. 2.37(a) for a parameter setting for which Ψ exists.

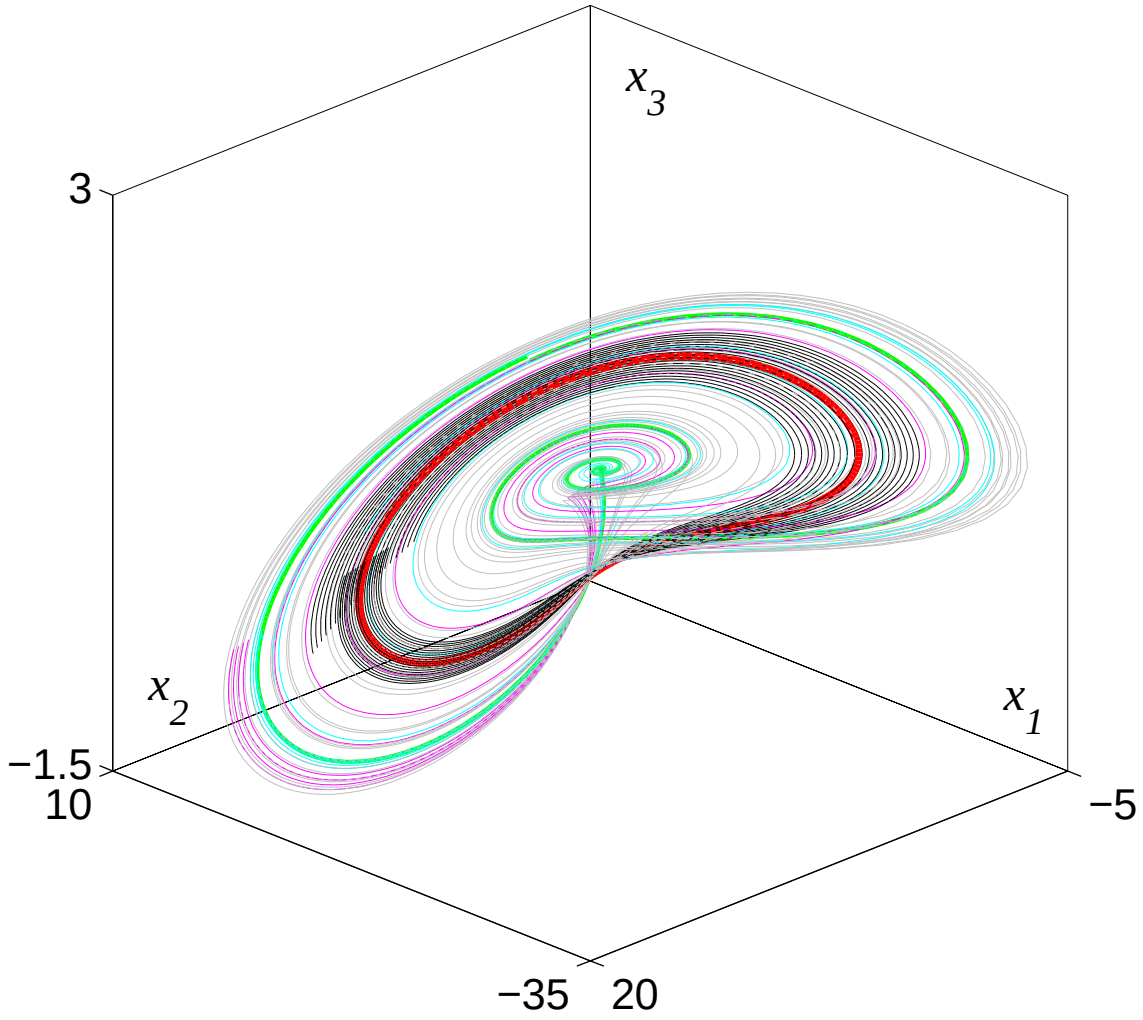

Figure 2.38: *Different kind of trajectories embedded in the Shil'nikov-like attractor A_S* (cfr. *Fig. 2.36*)*: green – the homoclinic trajectory; red – the generating cycle; black – pattern trajectory segment; cyan – phase skip trajectory segment; magenta – reinjected trajectory segment.*

probability of a phase skip of length ΔT after that N consecutive pattern trajectory segments have been run along.

Figure 2.40 shows the distribution of the pseudo-periods of pattern trajectory segments. As can be seen it is more smeared out than that shown in Fig. 2.30(b) (that anyway is a special case as mentioned afore) for the Feigenbaum's case but it is still quite concentrated about 2π.

In Figure 2.41 the stroboscopic plot of the x_2 time series while following the pattern trajectory segments of the Shil'nikov-like attractor A_S is depicted. The similarity with Fig. 2.31 is impressive.

In analogy with Fig. 2.32, the probability distribution of the amplitudes in the different point of the pseudo-period is shown in Fig. 2.42, again as for the Feigenbaum's case, such a distribution is not representative since it depends on the parameter values (*cfr.* Fig. 2.26), varying the parameters it can be concentrated around few unstable orbits or spread to reach an almost uniform distribution over an interval.

Finally, the joint probability distribution of phase skip lengths and pattern interval lengths is shown in Fig. 2.43. It is difficult to determine if the shape of this distribution is generic for all the Shil'nikov-like attractors or if it is specific for this case. Indeed, $p(N, \Delta T)$ looks like a χ^2 distribution [Walpone, 1993] with origin about 2π, and $N + 2$ degree of freedom. Although several other Shil'nikov-like attractor share such a shape, any attempt from the author to prove that $P(N, \Delta T) = \chi^2_{N+n}(\Delta T - T_0)$, where n and T_0 depend on the model, failed, *cfr.* Appendix E.

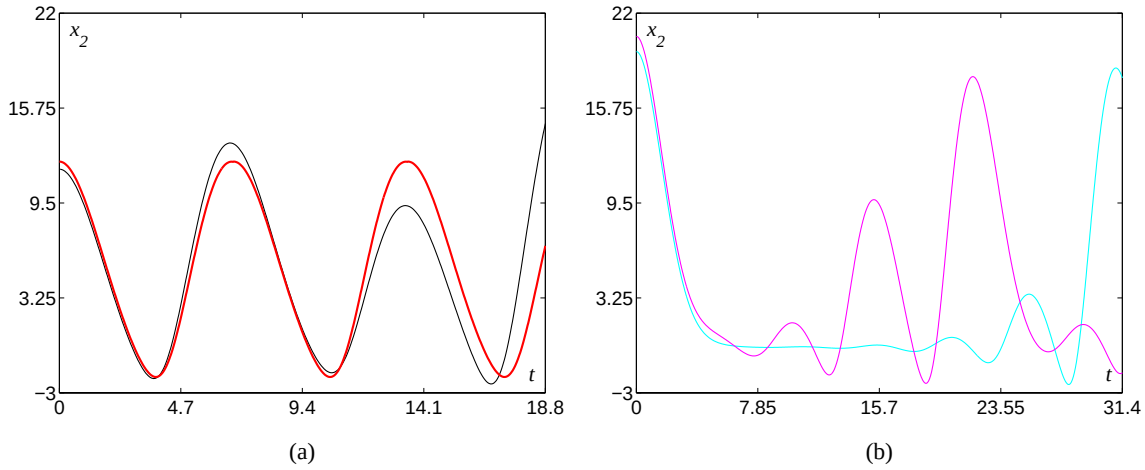

Figure 2.39: *x_2 time series while behaving on the different kind of trajectory segments embedded in the Shil'nikov-like attractor A_S* (cfr. *Fig. 2.36*)*: (a) – pattern trajectory segment (black) and the generating cycle (red); (b) – phase skip trajectory segment (cyan) and reinjected trajectory segment (magenta).*

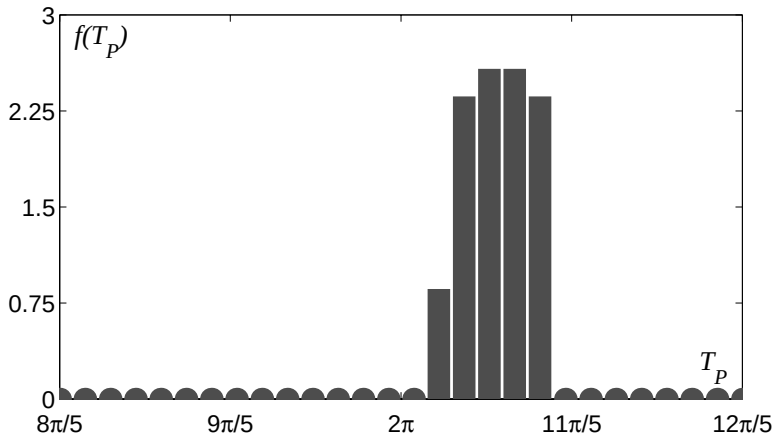

Figure 2.40: *Distribution of the pseudo-period of pattern trajectory segments embedded in the Shil'nikov-like attractor A_S* (cfr. *Fig. 2.36*)*.*

To summarize, Shil'nikov-like chaotic system can describe approximately periodic signals with randomness on the amplitude and with some randomness on the phase too. It will be shown in the next chapter that this kind of chaotic attractor is a good "box" where a Feigenbaum-like signal can be stored. Indeed, this kind of a chaotic attractor looks like a Feigenbaum-like attractor with random phase lags. To conclude, for a given approximately periodic signal, the presence of random phase lags can be a strong clue of a Shil'nikov-like chaotic source.

2.5.3 Torus Destruction Chaos

The third route to chaos represents one of the most complex phenomena known in modern system theory. It is related to the existence of a *quasi periodic* invariant, *i.e.* a torus. A torus is an invariant generated by the intermodulation of two or more periodic components with mutually irrational frequencies. For instance $y(t) = sin(\omega_1 t)\, cos(\omega_2 t)$ could be the time series observation of a torus for any ω_1 and ω_2 such that their ratio is irrational ($\omega_1, \omega_2 : \omega_1/\omega_2 \notin \mathbb{Q}$). In a three-dimensional system a two-dimensional, *i.e.* composed of two frequencies, torus would looks like a "donut".

When a dynamical system admits an invariant torus, a parameter drift can lead an external periodic invariant[26] to shrink on the torus and to collide with it. When this happens, aperiodic invariants can

[26] There are several periodic solutions lying on the torus itself [Alligood *et al.*, 1993; Ott, 1993].

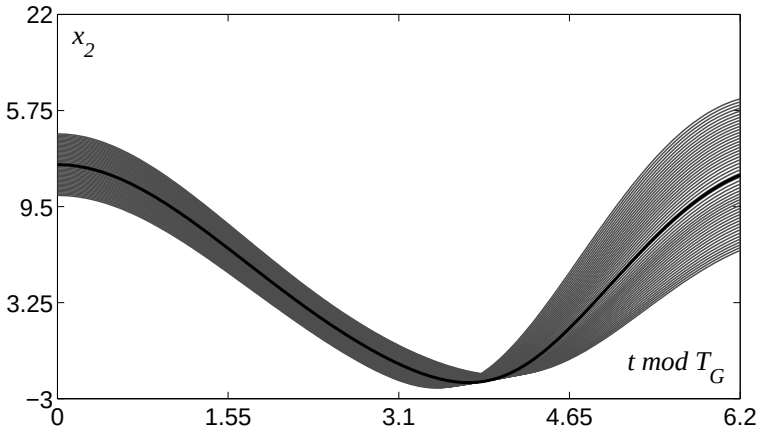

Figure 2.41: *Stroboscopic plot of the x_2 time series while behaving on the pattern trajectory segments of the Shil'nikov-like attractor A_S (*cfr. *Fig. 2.36). Each plot corresponds to the time series of a pattern trajectory segment. The bold line is the time series while behaving on the generating cycle.*

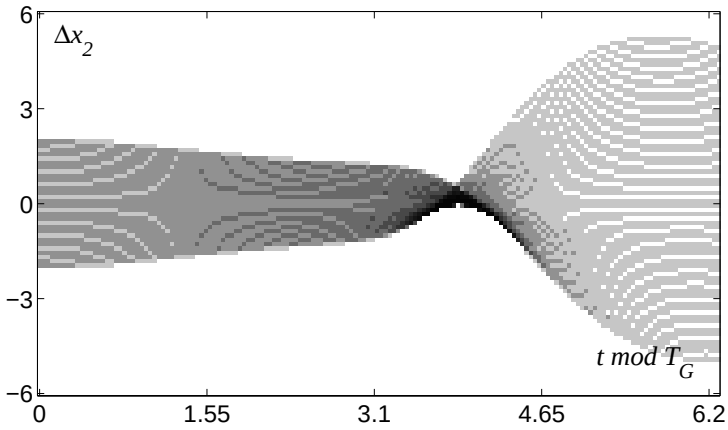

Figure 2.42: *Distributions, along the pseudo-period, of the discrepancies of x_2 while behaving on the pattern trajectory segments of the Shil'nikov-like attractor A_S (*cfr. *Fig. 2.36) from x_2 while following the generating cycle.*

exist. These phenomenon is known under the name of *strong resonance* and is related to the homoclinic or heteroclinic connection of one or more period-n periodic solutions surrounding a torus, Fig. 2.44. In a given sense it can be considered the discrete time analogy of the Shil'nikov-like chaos. In fact, on the n^{th} iterate of the Poincaré map a torus looks like a closed line while the surrounding period-n cycle is a fixed point, *i.e.* an equilibrium. The collision of the period-n cycle with the torus is equivalent to the homoclinic bifurcation of a fixed point of the n^{th} iterate of the Poincaré map.

The theory for strong resonances has been developed formerly for the case of Hamiltonian[27] systems around the 1968 by Kolmogorov, Arnold, and Moser [Ott, 1993] and is known as the theory of the KAM tori. The studies for the more complex case of torus destruction in dissipative systems are due to Chenciner, Melnikov, Sacker and Arnold [Kuznetsov, 1998]. In particular they have studied in detail the cases when a period-n cycle, with $n = 1, 2, 3, 4$, shrinks onto the torus. These cases are known as $1:1$, $1:2$, $1:3$ and $1:4$ resonances. This resonances phenomena can be classified as simple or complex depending on the local behavior of the period-n cycles, namely depending upon their multipliers[28]. When the periodic solution that touches the torus has a negative multiplier smaller than -1, infinite countable periodic and aperiodic

[27] Conservative systems, namely systems where the energy is preserved.

[28] The multipliers of a cycle are the eigenvalues of the corresponding fixed point on the Poincaré map. They determine the behavior of the trajectories in the neighborhood of the periodic solutions.

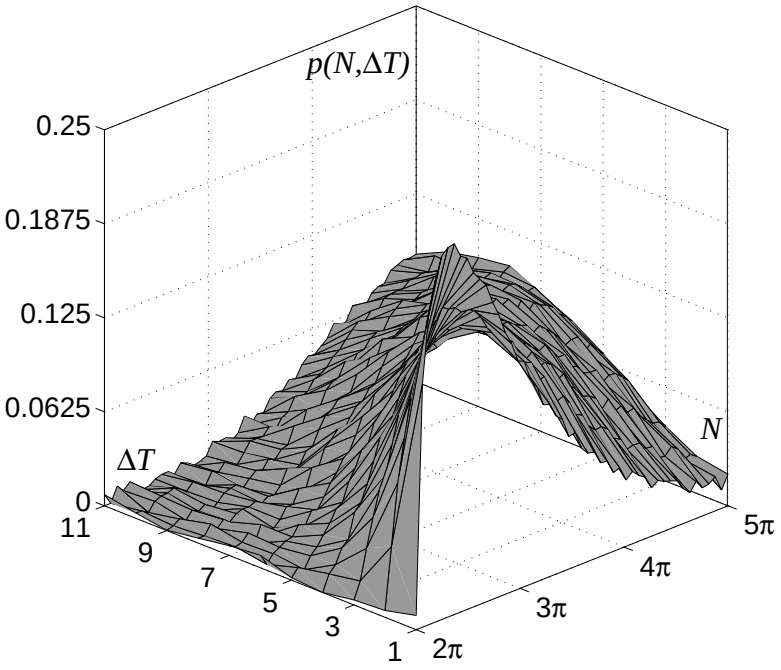

Figure 2.43: *Joint probability distribution of phase skip lengths and pattern interval lengths for the Shil'nikov-like attractor* A_S (cfr. *Fig. 2.36*).

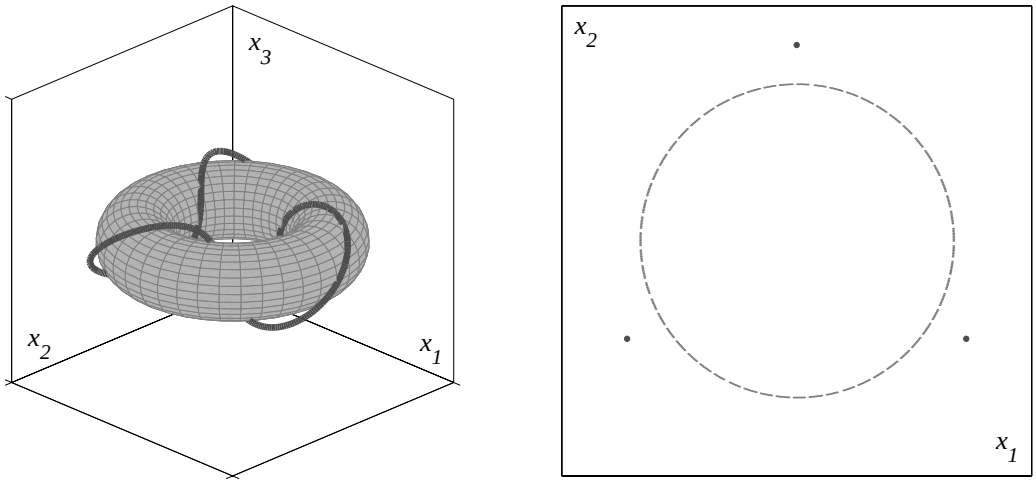

Figure 2.44: *A period-three cycle surrounding a torus: (a) – in the state space; (b) – on the Poincaré map.*

invariants exist; this is the analogous of the Shil'nikov's theorem discussed above[29].

The similarities between the Shil'nikov's theorems and strong resonances can be pushed further. In fact, from a global point of view, the bifurcations linked to a strong resonance organize the existence of just one cycle or torus and, in same case, of a set of other invariant sets in a neighborhood of the resonance bifurcation [Kuznetsov, 1998]. Once again, as for the homoclinic bifurcations, all the periodic orbits in the neighborhood

[29]Note that once again nothing is said about the stability of the aperiodic invariants, even if a strange attractor is commonly observed when the saddle quantity of the resonant saddle cycle is smaller than one, namely when the product of the modulus of the cycle's multipliers is smaller than one.

of strong resonance bifurcations are "relatives" of the same cycle. Actually, the typical bifurcation path that lead to torus destruction can be summarized as follow (*cfr.* Fig. 2.45). Changing the parameter values a period-one cycle undergoes a *Neimark—Sacker* bifurcation [Kuznetsov, 1998], it looses its stability while a torus of small amplitude is born around it, it is as if the period-one cycle became fat. A further change in parameter values leads the torus to resonate with a period-n cycle, namely the torus becomes the homoclinic trajectory, *i.e.* bi-asymptotic, to the period-n cycle. The contact with the period-n cycle destroys the torus and complex behavior can be observed. The initial period-one cycle never disappears, it simply looses its stability. In analogy with the Feigenbaum-like and Shil'nikov-like chaos, it can be considered as the *generating cycle*.

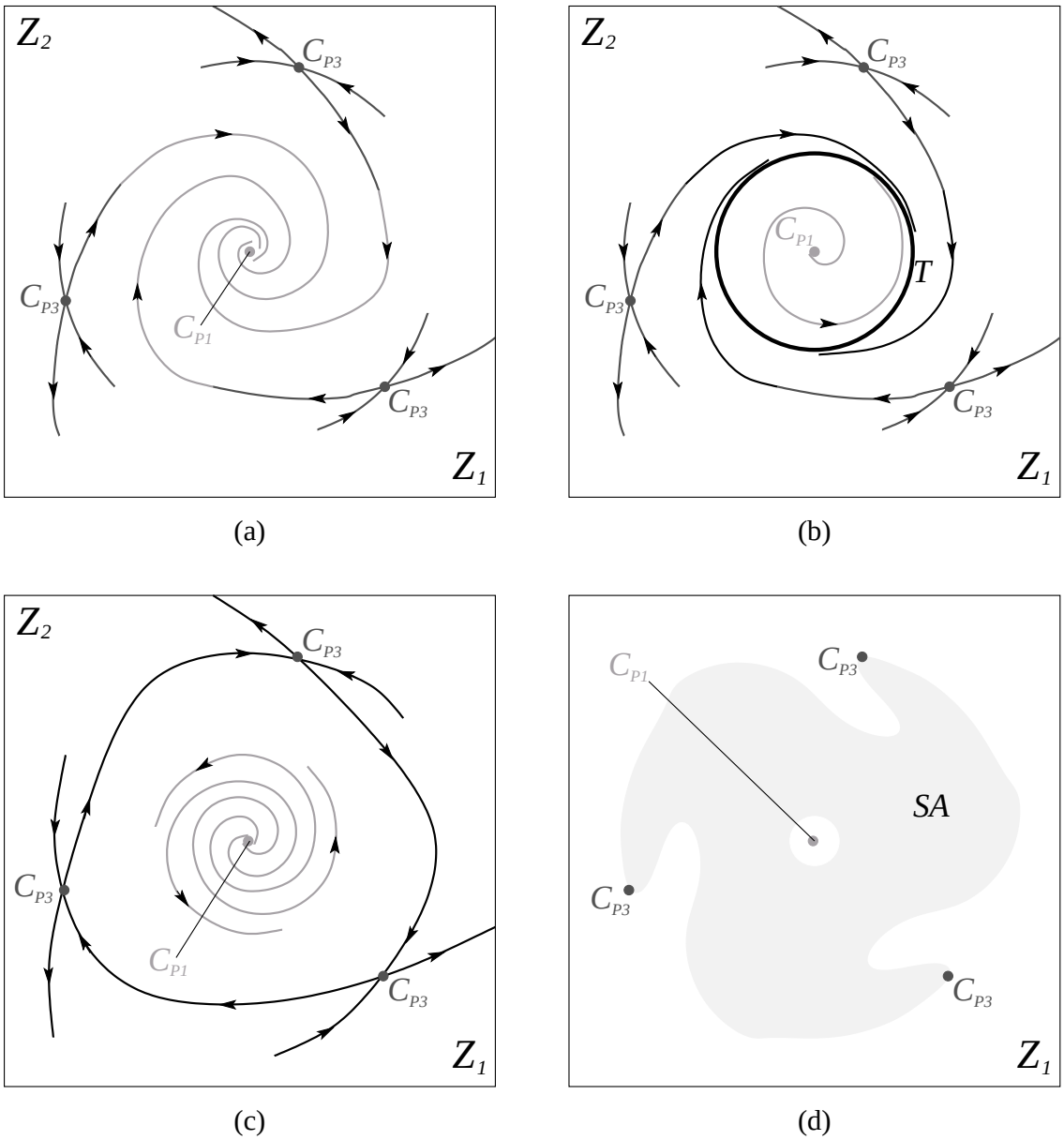

Figure 2.45: *View on the Poincaré section of the sequence of bifurcations that lead to the torus destruction: (a) – a period-one attractive cycle and a period-three saddle cycle coexists; (b) – the period-one cycle undergoes a Neimark—Sacker bifurcation and looses its stability, a torus is born around it; (c) – the torus and the period-three saddle cycle resonate; (d) – the torus is destroyed and a strange attractor is observed.*

In the previous two cases, Feigenbaum and Shil'nikov, a one-dimensional map has been used to describe the main properties of the strange attractors. For destroyed-torus-like chaos this is not possible, indeed the

intersection of the Poincaré section with a destroyed-torus-like chaos is not almost a line, on the contrary it can be a very complex fat fractal. Therefore, the restriction of the Poincaré map to the attractor does not decrease the order of the map.

When a period-n cycle pinches and destroys a torus the profile of the resulting strange attractor, namely its image on the Poincaré section, can be mainly of three types.

1. *Simple*: the generating cycle is dominant in the resonance. The destroyed torus gets filled after the destruction but its profile is still a more or less smooth looking closed curve, as shown in Fig. 2.46(a). The edges induced by the pinch of the torus by the period-n cycle and its relatives are not visible.

2. *n-point star*: the period-n cycle is dominant. Thus, only the edges induced by the pinching of the period-n cycle are visible. The filled destroyed torus looks like an n-point star as shown in Fig. 2.46(b).

3. *Complex*: neither the generating cycle nor the period-n cycle is dominant. All the cycles, the period-n cycle and its relatives, concur in determining the shape of the profile of the strange attractor that becomes very complex as shown in Fig. 2.46(c).

Note that, albeit it is not possible to define a simple one-dimensional map for the Poincaré section, this section remains a very useful tool for dividing the pseudo-periods from each other.

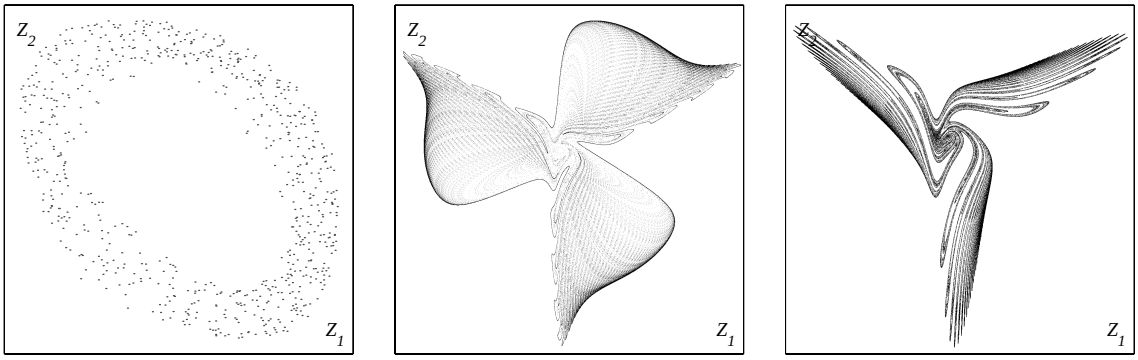

(a) (b) (c)

Figure 2.46: *Possible shapes of torus-destroyed-like strange attractors on the Poincaré section: (a) – simple shape; (b) – n-point star shape; (c) – complex shape.*

Equations (2.3) does not admit a torus invariant for any parameter values. The following variation of it must be considered instead.

$$\begin{aligned} \dot{x}_1 &= \frac{g}{Q(1-k)}\left[-\alpha_F n(x_2) + x_3\right] + \lambda x_1 + \omega x_2 \\ \dot{x}_2 &= \frac{g}{Qk}\left[(1-\alpha_F) n(x_2) + x_3\right] - \omega x_1 + \lambda x_2 \\ \dot{x}_2 &= -\frac{Qk(1-k)}{g}\left[x_1 + x_2\right] - \frac{1}{Q} x_3 \end{aligned} \tag{2.4}$$

where

$$n(x) = \frac{1}{2}\left(|x-1| - x - 1\right)$$

If the following condition are satisfied

$$\begin{cases} \omega = \pm\sqrt{\lambda(Q-\lambda)} + \varepsilon \\ \dfrac{1}{2}\left(Q - \dfrac{1}{Q} - \sqrt{Q^2+2}\right) < \lambda < \dfrac{1}{2}\left(Q - \dfrac{1}{Q} + \sqrt{Q^2+2}\right) \\ \lambda < \dfrac{1}{2Q} \end{cases}$$

where ε is a very small number, then Eqs. (2.4) can be regarded as a perturbation of a Hamiltonian system, as such it can admit torus-like invariants and, more in particular, destroyed-torus-like chaos.

Fixing all the parameters at the values reported in the caption of Fig. 2.47 but g, a torus destruction route to chaos can be observed. In particular, a $1:3$ resonance can be observed while varying $Log_{10}(g)$ from 0.6 to 0.75. The resulting strange attractor A_T and its intersection with a suitable Poincaré section Π are shown in Fig. 2.47. The strange attractor appearing from the destroyed torus has simple shape as can be

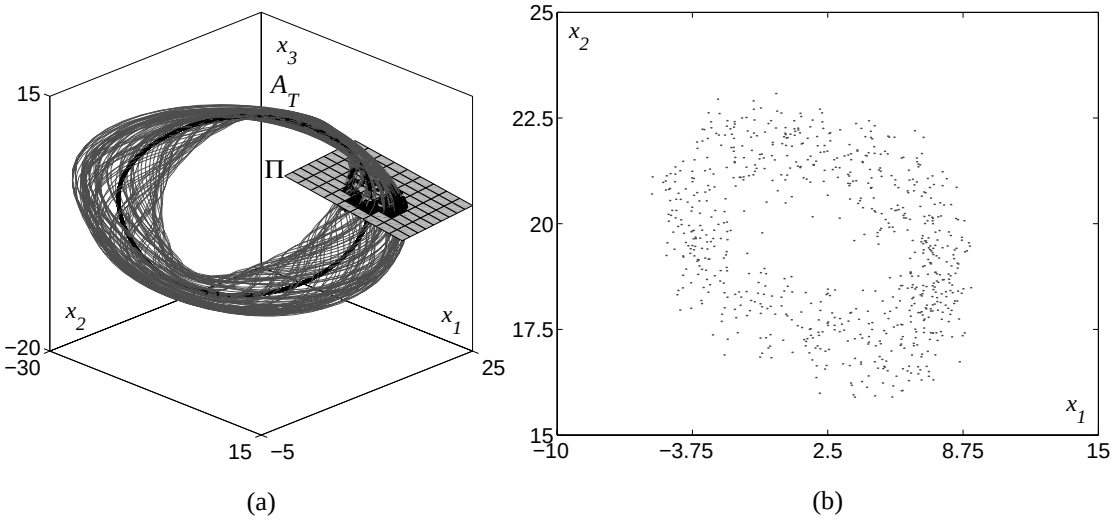

Figure 2.47: *Destroyed-torus-like attractor for Eqs. (2.4), $k = 0.5$, $\alpha = 1$, $Log_{10}(Q) = 1.1$, $\lambda = 0.02$, $\omega = 0.5$ and $Log_{10}(g) = 0.75$. The bold line is the embedded unstable generating cycle: (a) – in the state space; (b) – intersection with the Poincaré section.*

seen in Fig. 2.47(b). This is just a particular case due to the chosen parameter values, varying the parameters a three-star shape or a complex shape can be obtained. Even though that, the following considerations do not depend upon the particular shape.

Once again, each pseudo-period of the attractor A_T is the trajectory segment that goes from Π back to Π. A two-dimensional map for the return time to Π can be computed for the attractor A_T, namely a map that links the current coordinates on the Poincaré section (two-dimensional) with the next pseudo-period, *i.e.* with the elapsed time before the trajectory will hit again Π. Such a map for the attractor A_T is shown in Fig. 2.48(a), as can be noted the return time is rather concentrated about 2π. Once again, such a strong determinism in the pseudo-period is not generic for destroyed-torus-like attractors but it is a peculiarity of the particular model herein considered. Anyway, even for other destroyed-torus-like attractors [Alligood *et al.*, 1993; Ott, 1993], the pseudo-period is almost concentrated around a single value. Thus, the δ-like shown in Fig. 2.48(b) will be in general a peaked distribution. More in detail, given the fact that the period-n cycle and its relatives must have a pseudo-period similar to the one of the torus[30] in order to resonate, it follows that such a distribution does not depend upon the profile shape of the attractor, namely it does not depend upon the fact that the image of the destroyed-torus-like strange attractor on the Poincaré section is of simple, n-point star, or complex shape.

For $y = x_2$ as output function, Fig. 2.49 reports the stroboscopic plot of the destroyed-torus-like attractor A_T and the x_2 time series (bold) while behaving on the generating cycle. The probability distribution of the amplitudes in the different point of the pseudo-period is shown in Fig. 2.50. Note that for the torus destruction case there is not a concentration of the trajectories on some time interval, this is because the supporting geometrical structure of a destroyed-torus-like attractor is a torus, namely a tube, and not a Möbius strip.

To summarize, destroyed-torus-like chaotic system can describe approximately periodic signals with randomness mainly on the amplitude and with little or no randomness of the pseudo-period. From a randomness point of view they are not very different from the Feigenbaum-like chaotic systems except that, for a given approximately periodic signal, the absence of any concentration of the amplitude distribution on a particular time interval of the pseudo-period can be a clue that the source is a destroyed-torus-like attractor rather than being a Feigenbaum-like chaotic source.

[30] The pseudo-period of the torus, which is approximately the period of the generating cycle, determines the peak location of the pseudo-period distribution.

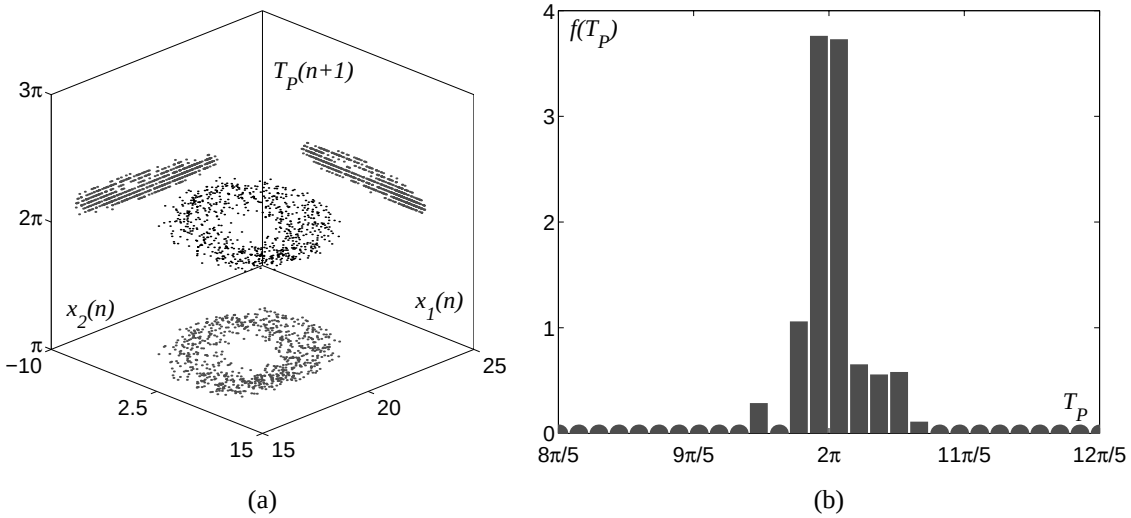

Figure 2.48: *Distribution of the pseudo-period of the destroyed-torus-like attractor A_T* (cfr. *Fig. 2.47*)*: (a) – Poincaré map of the pseudo-period $T_P(n+1)$* vs *the current coordinates on* Π*; (b) – the distribution of the pseudo-period, it is almost a δ centered at 2π.*

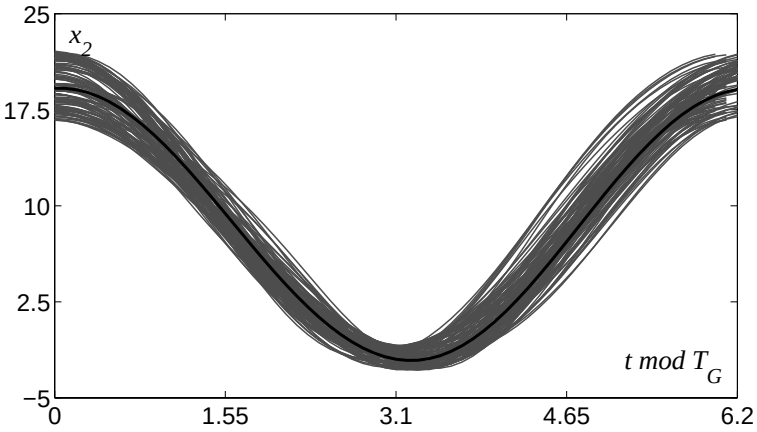

Figure 2.49: *Stroboscopic plot of the x_2 time series while behaving on the destroyed-torus-like attractor A_T* (cfr. *Fig. 2.47*)*. Each plot corresponds to the time series of an orbit starting from and coming back to the Poincaré section* Π*. The bold line is the time series while behaving on the generating cycle.*

2.6 Distribution of Measured Signals

In Sect. 2.2 the natural approximately periodic signals presented in Sect. 2.1.2 have been reconstructed in a three-dimensional state space, the conclusion has been that such signals should be chaotic. To further support this hypothesis, the one-dimensional maps and amplitude distributions over the pseudo-period have been computed[31] for the same seven approximately periodic signals. The results are reported uncommented in the following figures.

To compute the one-dimensional map the peak-to-peak technique described in [Candaten and Rinaldi, 2000] has been used. It is explained in [Candaten and Rinaldi, 2000] that this technique is not always fruitful but in this case it has revealed fairly effective.

The distribution of the amplitudes has been computed with respect to the stereotype obtained from the one-dimensional map. After having computed the one-dimensional map, if such computation succeeds, it is possible to compute the fixed point of such map which in turn corresponds to the period-one cycle that is the generating cycle indeed. After having obtained a point of the time series interval that corresponds to

[31] The pseudo-period distributions have already been shown in Sect. 2.1.2.

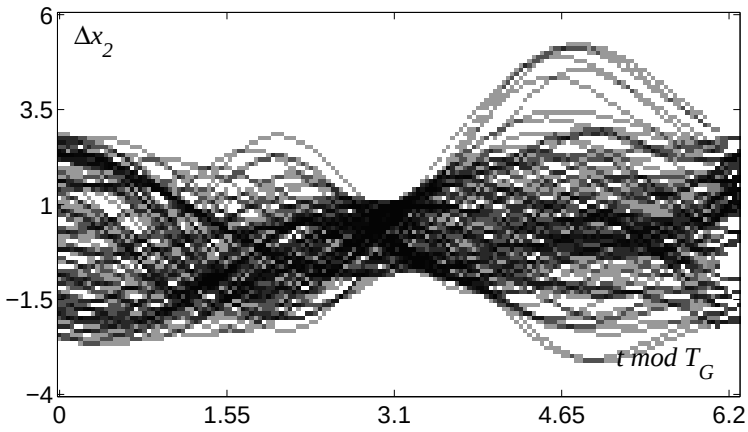

Figure 2.50: *Distributions, along the pseudo-period, of the discrepancies of x_2 while behaving on the destroyed-torus-like attractor A_T* (cfr. *Fig. 2.47*) *from x_2 while behaving on the generating cycle.*

the stereotype it is easy to extract the stereotype itself.

The Electrocardiogram and the Electroencephalogram

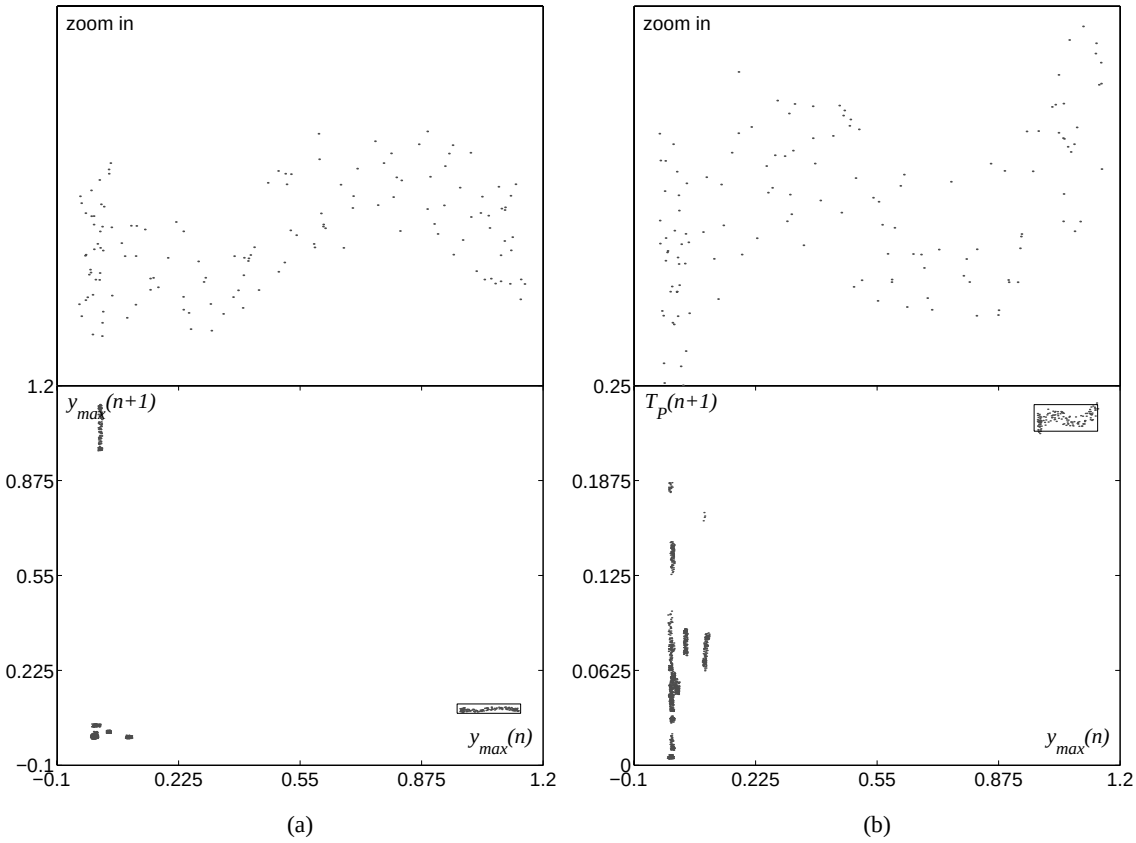

Figure 2.51: *One-dimensional maps obtained from the time series of the ECG shown in Fig. 2.1: (a) – amplitude Poincaré map; (b) – return time Poincaré map.*

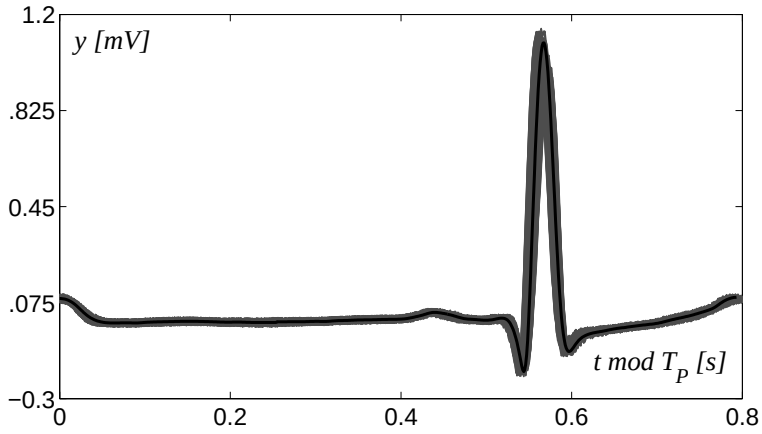

Figure 2.52: *Stroboscopic plot of the pseudo-periods from the time series of the ECG signal shown in Fig. 2.1, the bold line is the stereotype corresponding to the fixed point of the one-dimensional map shown in Fig. 2.51(a).*

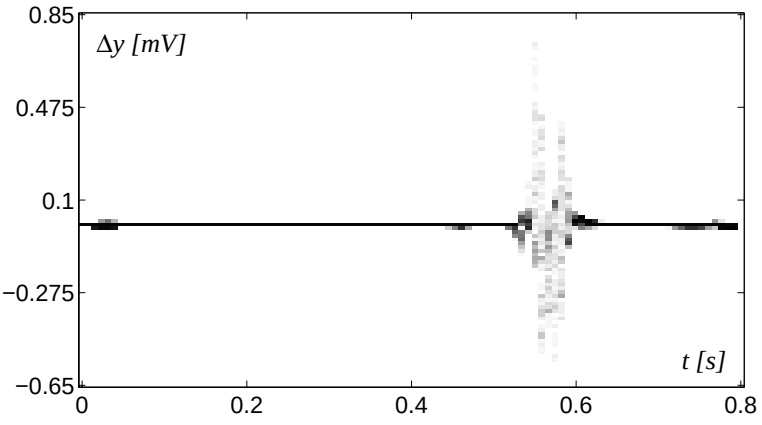

Figure 2.53: *Distributions, along the pseudo-period, of the discrepancies between the pseudo-periods from the time series of the ECG shown in Fig. 2.1 and the time series of the stereotype.*

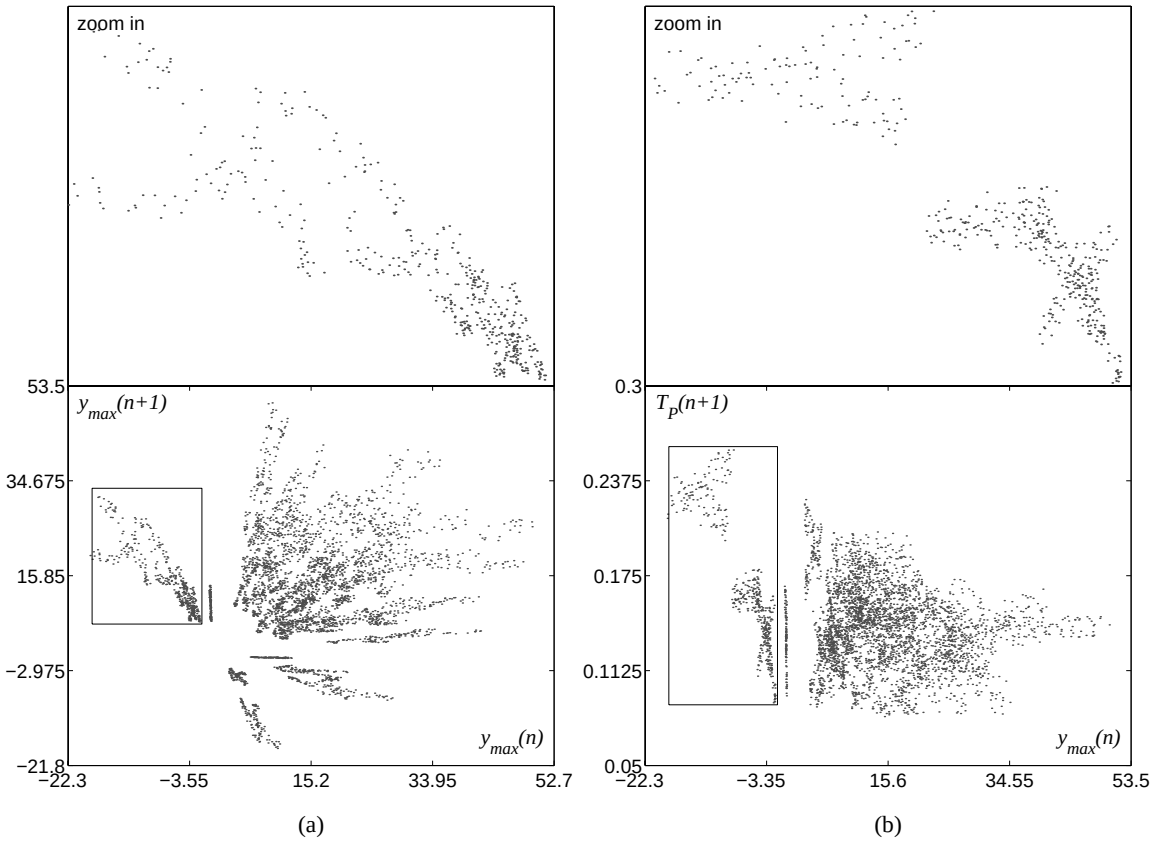

Figure 2.54: *One-dimensional maps obtained from the time series of the EEG shown in Fig. 2.6: (a) – amplitude Poincaré map; (b) – return time Poincaré map.*

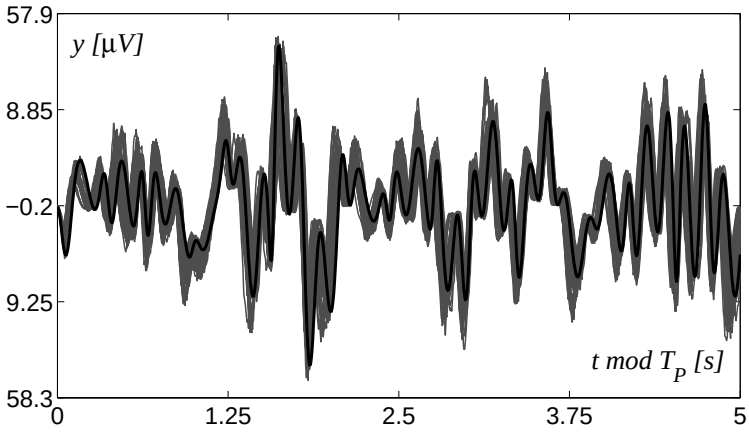

Figure 2.55: *Stroboscopic plot of the pseudo-periods from the time series of the EEG signal shown in Fig. 2.6, the bold line is the stereotype corresponding to the fixed point of the one-dimensional map shown in Fig. 2.54(a).*

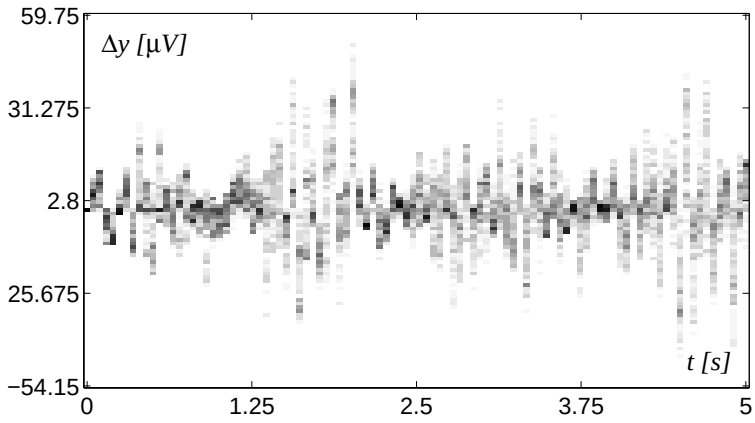

Figure 2.56: *Distributions, along the pseudo-period, of the discrepancies between the pseudo-periods from the time series of the EEG shown in Fig. 2.6 and the time series of the stereotype.*

THE VOWELS IN SPEECH

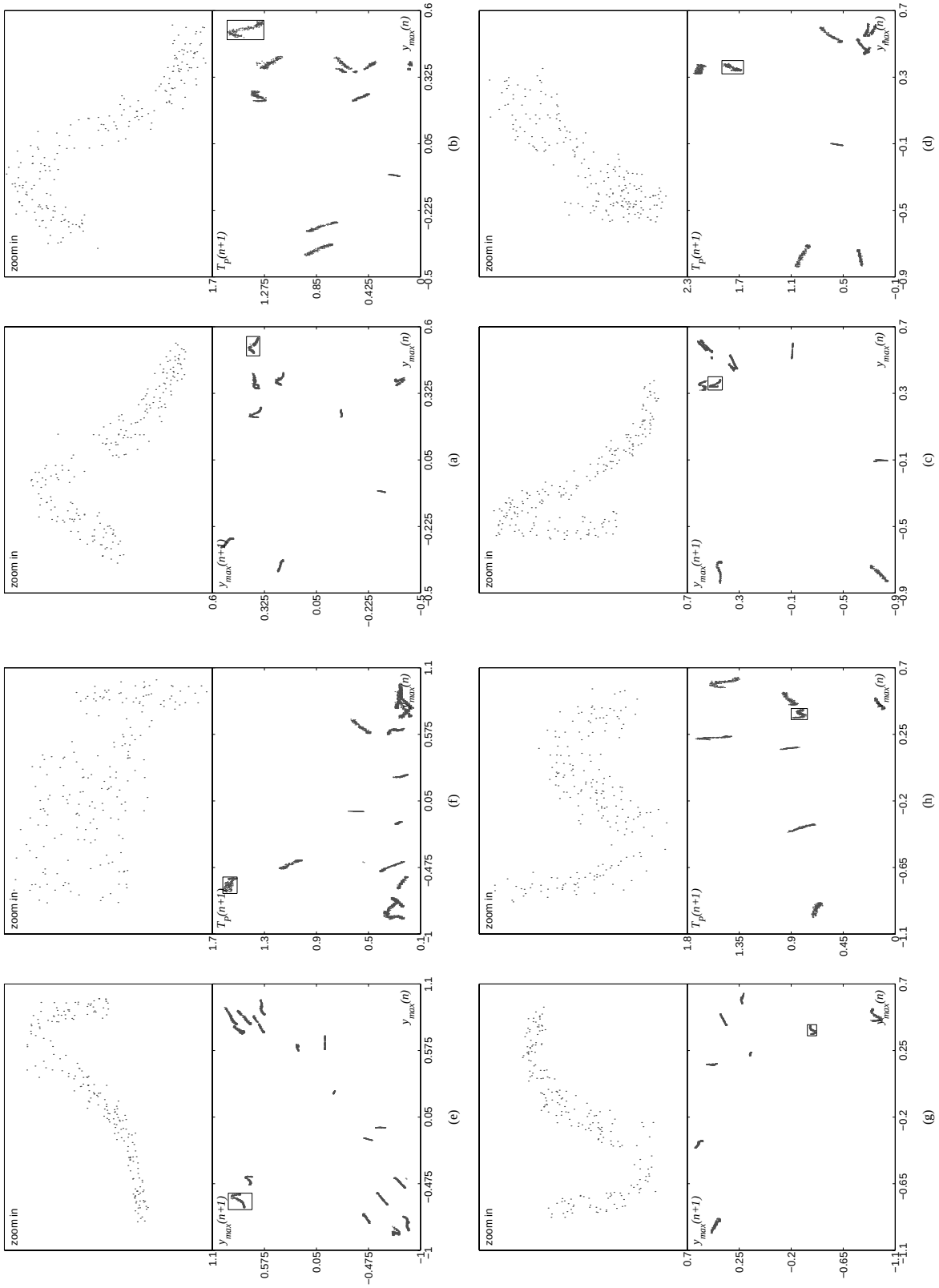

Figure 2.57: *One-dimensional maps obtained from the time series of the sustained vowels shown in Fig. 2.11: amplitude Poincaré maps for [a:], [e], [i], [ɔ] and [u] in (a), (c), (e), (g) and (i), respectively; return time Poincaré map for [a:], [e], [i], [ɔ] and [u] in (b), (d), (f), (h) and (j), respectively.* (continue)

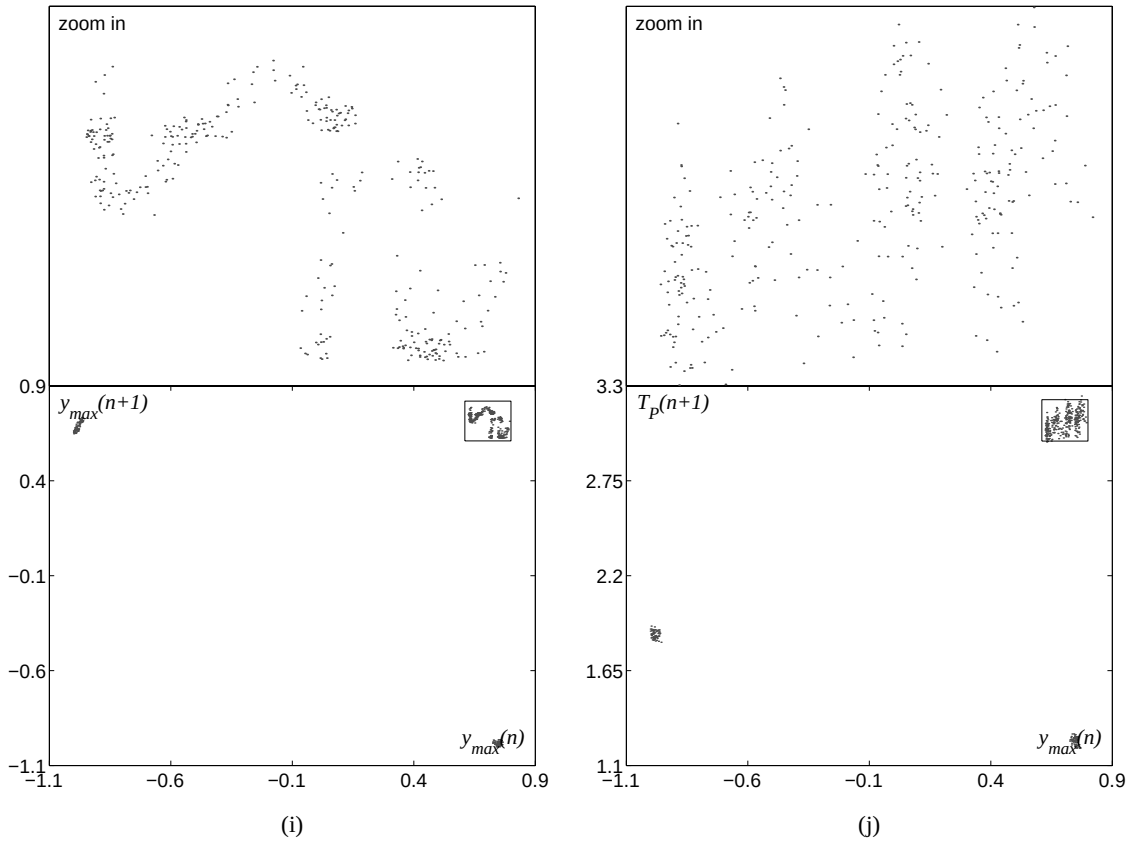

Figure 2.57: *One-dimensional maps obtained from the time series of the sustained vowels shown in Fig. 2.11: amplitude Poincaré maps for [a:], [e], [i], [ɔ] and [u] in (a), (c), (e), (g) and (i), respectively; return time Poincaré map for [a:], [e], [i], [ɔ] and [u] in (b), (d), (f), (h) and (j), respectively.*

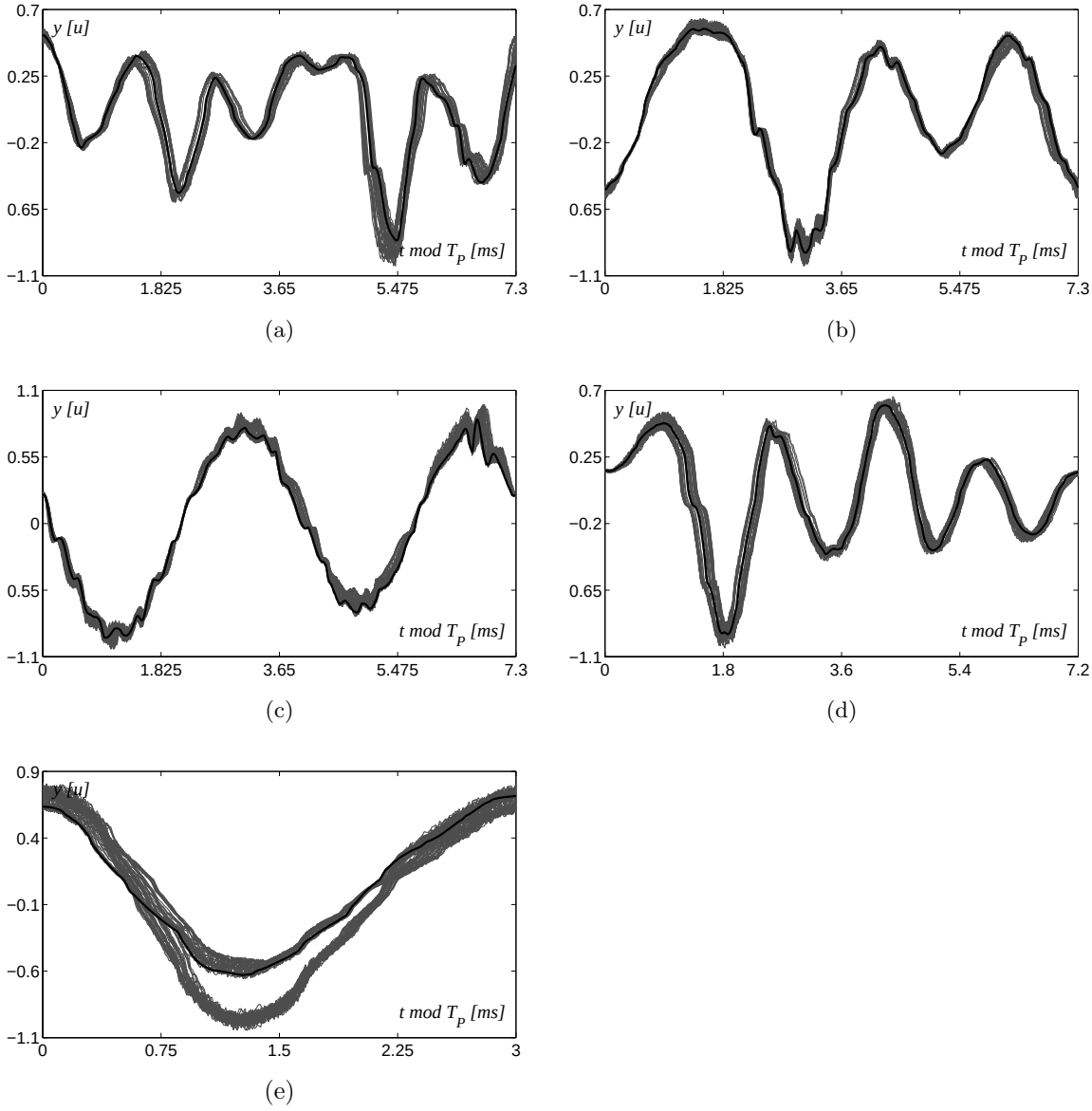

Figure 2.58: *Stroboscopic plots of the pseudo-periods from the time series of the sustained vowels shown in Fig. 2.11, the bold lines are the stereotypes corresponding to the fixed point of the one-dimensional maps shown in Fig. 2.57: (a) – [a:]; (b) – [e]; (c) – [i]; (d) – [ɔ]; (e) – [u].*

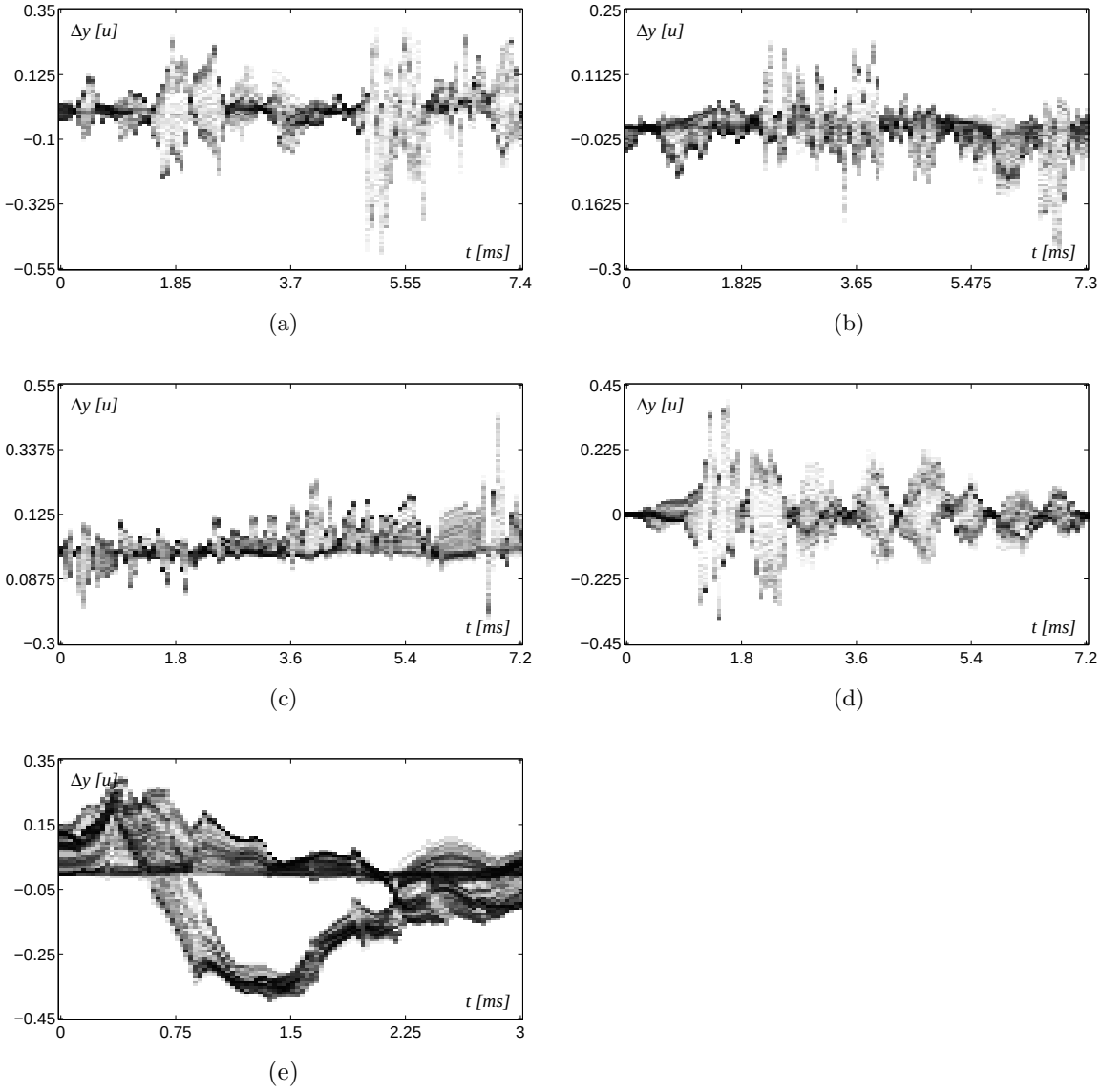

Figure 2.59: *Distributions, along the pseudo-period, of the discrepancies between the pseudo-periods from the time series of the sustained vowels shown in Fig. 2.11 and the time series of the corresponding stereotypes: (a) – [a:]; (b) – [e]; (c) – [i]; (d) – [ɔ]; (e) – [u].*

The previous pictures strongly suggest that all the seven signals considered are of Feigenbaum-like nature. Indeed, the similarity between the figures obtained in the theoretical framework in Sect. 2.5.1 and the one shown here is remarkable. Surely such a strong similarity deserves some reflection about the real nature of randomness.

In the next chapter is shown how Shil'nikov-like strange attractors can be considered as "boxes" where Feigenbaum-like signals are robustly stored.

Bibliography

Alligood, K., T. Sauer, and J. Yorke (1993). *CHAOS: An Introduction to Dynamical System*. Springer-Verlag, New York, NY.

Amerio, L. (1977a). *Analisi Matematica con Elementi di Analisi Funzionale I*. UTET, Torino, Italy. In Italian.

AMERIO, L. (1977b). *Analisi Matematica con Elementi di Analisi Funzionale II*. UTET, Torino, Italy. In Italian.

ANISHCHENKO, V. AND A. NEIMAN (1989). Poincaré return time in the regime of dynamical chaos. *Journal of Technical Physics*, 59, pp. 117–118. In Russian.

ARNOLD, V. (1988). *Geometrical Methods in the Theory of Ordinary Differential Equations*. Springer-Verlag, New York, NY, second edition.

BATESON, G. (1972). *Steps to an Ecology of Mind*. Ballantine, New York, NY.

BITTANTI, S. AND G. PICCI, editors (1996). *Identification, Adaptation, Learning: The Science of Learning Models from Data*. Springer-Verlag, New York, NY.

BRONZINO, J., editor (1995). *The Biomedical Engineering Handbook*. CRC Press for IEEE Press, Boca Raton, FL.

BRUNSDEN, V. AND P. HOLMES (1987). Power spectra of strange attractors near homoclinic orbits. *Physical Review Letters*, 58, pp. 1699–1702.

CALLIER, F. AND C. DESOER (1991). *Linear System Theory*. Springer-Verlag, New York, NY.

CANDATEN, M. AND S. RINALDI (2000). Peak-to-Peak dynamics: A critical survey. *International Journal of Bifurcation and Chaos*, 10(8), pp. 1805–1819.

CVITANOVIĆ, P., editor (1984). *Universality in Chaos*. Adam Hilter, Bristol, UK.

DE FEO, O. AND R. FERRIÈRE (2000). Bifurcation analysis of population invasion: On-off intermittency and basin riddling. *International Journal of Bifurcation and Chaos*, 10, pp. 443–452.

DE FEO, O. AND G. MAGGIO (2000). Bifurcation phenomena in the Colpitts oscillator: A robustness analysis. In *International Symposium on Circuits and Systems ISCAS*. Geneva, Switzerland.

DE FEO, O. AND G. MAGGIO (2001). Bifurcations in the Colpitts oscillator: Theory versus experiments. *IEEE Transaction on Circuit and Systems—I*. Submitted.

DE FEO, O., G. MAGGIO, AND M. KENNEDY (2000). The Colpitts oscillator: Families of periodic solutions and their bifurcations. *International Journal of Bifurcation and Chaos*, 10, pp. 935–958.

DE FEO, O. AND S. RINALDI (1997). Yield and dynamics in tritrophic food chains. *The American Naturalist*, 150, pp. 328–345.

DE LUNA, A. B. (1998). *Clinical Electrocardiography: A Textbook*. Futura Publishing Company, Armonk, NY, second edition.

DELLER, J., J. PROAKIS, AND J. HANSEN (1993). *Discrete-Time Processing of Speech Signals*. Prentice-Hall, Upper Saddle River, NJ.

DOYLE, H. (1996). *Seismology*. John Wiley & Sons, New York, NY.

DREPPER, F., R. ENGBERT, AND N. STOLLENWERK (1994). Nonlinear time series analysis of empirical population dynamics. *Ecological Modelling*, 75, pp. 171–181.

ECKMANN, J. AND D. RUELLE (1985). Ergodic theory of chaos and strange attractors. *Review of Modern Physics*, 57, pp. 617–656.

ELLNER, S. AND P. TURCHIN (1993). *Chaos in a "Noisy" World: New Methods and Evidence from Time Series Analysis*. North Carolina State University Press, Raleigh, NC.

FEIGENBAUM, M. (1979). The universal metric properties of nonlinear transformations. *Journal of Statistical Physics*, 21, pp. 669–706.

GASPARD, P. (1983). Generation of a countable set of homoclinic flows through bifurcation. *Physical letters*, 97A, pp. 1–4.

Gaspard, P., R. Kapral, and G. Nicolis (1984). Bifurcation phenomena near homoclinic systems: A two-parameter analysis. *Journal of Statistical Physics*, 35, pp. 697–727.

Gaspard, P. and G. Nicolis (1983). What can we learn from homoclinic orbits in chaotic dynamics? *Journal of Statistical Physics*, 31, pp. 499–518.

Glendinning, G. and C. Sparrow (1984). Local and global behavior near homoclinic orbits. *Journal of Statistical Physics*, 35, pp. 215–225.

Holton, J. (1992). *An Introduction to Dynamic Meteorology*. Academic Press, New York, NY, third edition.

Hübner, U., C. Weiss, N. Abraham, and D. Tang (1993). *Lorenz-like Chaos in $NH_3 - FIR$ Lasers (Data Set A)*, pp. 73–104. Addison-Wesley, reading, ma edition.

Johansson, R. (1993). *System Modeling Identification*. Prentice-Hall, Englewood Cliffs, NJ.

Johnston, D. and S. Wu (1995). *Foundations of Cellular Neurophysiology*. MIT Press, Cambridge, MA.

Katok, A. and B. Hasselblatt (1995). *Introduction to the Modern Theory of Dynamical Systems*. Cambridge University Press, Cambridge, UK.

Knauss, J. (1997). *An Introduction to Physical Oceanography*. Prentice-Hall, Upper Saddle River, NJ.

Kondepudi, D. and I. Prigogine (1998). *Modern Thermodynamics : From Heat Engines to Dissipative Structures*. John Wiley & Son, Chichester, UK.

Kuznetsov, Y. (1998). *Elements of Applied Bifurcation Theory*. Springer-Verlag, New York, NY, second edition.

Laface, P. (1992). *Speech Recognition and Understanding*. Springer-Verlag, Berlin, Germany.

Laurent, G., M. Wehr, and H. Davidowitz (1996). Temporal representation of odors in an olfactory network. *The Journal of Neuroscience*, 16, pp. 3837–3847.

Lewis, B. and G. von Elbe (1961). *Combustion, Flames and Explosions of Gases*. Academic Press, Orlando, FL.

Ljung, L. (1999). *System Identification: Theory for the User*. Prentice-Hall, Upper Saddle River, NJ, second edition.

MacKay, D. (1999). *Information Theory, Inference, and Learning Algorithms*. Not published. Freely available on the world wide web: http://wol.ra.phy.cam.ac.uk/mackay/itprnn/book.html.

Madan, R., editor (1993). *Chua's Circuit: A Paradigm for Chaos*. World Scientific, Singapore, fourth edition.

Maggio, G., O. De Feo, and M. Kennedy (1998). Applications of bifurcation analysis to the design of a chaotic Colpitts oscillator. In *International Conference on Nonlinear Theory and its Applications $NOLTA$*. Crans-Montana, Switzerland.

Maggio, G., O. De Feo, and M. Kennedy (1999a). An explicit expression for the output amplitude of the Colpitts oscillator. In *European Conference on Circuit Theory and Design $ECCTD$*. Stresa, Italy.

Maggio, G., O. De Feo, and M. Kennedy (1999b). Nonlinear analysis of the Colpitts oscillator and applications to design. *IEEE Transaction on Circuit and Systems—I*, 46, pp. 1118–1130.

Murray, J. (1993). *Mathematical Biology*. Springer-Verlag, New York, NY.

Nunez, P., editor (1995). *Neocortical Dynamics and Human EEG Rhythms*. Oxford University Press, Oxford, UK.

Ott, E. (1993). *Chaos in Dynamical Systems*. Cambridge University Press, New York, NY.

Packard, N., J. Crutchfield, J. Farmer, and R. Shaw (1980). Geometry from a time series. *Physical Review Letters*, 45, pp. 712–716.

POINCARÉ, H. (1892). *Les Méthods Nouvelles de la Mécanique Céleste*. Gauthier-Villars, Paris, France. In French.

POLLICOTT, M. AND Y. MICHIKO (1998). *Dynamical Systems and Ergodic Theory*. Cambridge University Press, Cambridge, UK.

RENSHAW, E. (1993). *Modelling Biological Populations in Space and Time*. Cambridge University Press, Cambridge, UK.

RICKER, W. (1954). Stock and recruitment. *Journal of Fishing Resources Board of Canada*, 11, pp. 559–623.

RILEY, M. (1989). *Speech Time-Frequency Representations*. Kluwer Academic Press, Boston, MA.

RUGH, W. (1990). *Non Linear System Theory , The Volterra/Wiener Approach*. John Hopkins University Press, London, UK.

SCOTT, S. (1994). *Oscillations, Waves and Chaos in Chemical Kinetics*. Oxford University Press, Oxford, UK.

SEDRA, S. AND K. SMITH (1998). *Microelectronic Circuits*. Oxford University Press, New York, NY, fourth edition.

SIGMUND, J. H. K. (1998). *Evolutionary Games and Population Dynamics*. Cambridge University Press, Cambridge, UK.

SILVA, C. (1993). Shil'nikov theorem – a tutorial. *IEEE Transaction on Circuits and Systems—I*, 40, pp. 675–682.

SINAI, Y. (1993). *Topics in Ergodic Theory*. Priceton University Press, Princeton, NJ.

SMITH, R. (1992). Estimating dimension in noisy chaotic time series. *Journal of Royal Statistic Society B*, 54, pp. 329–351.

STROGATZ, S. (1994). *Nonlinear Dynamics and Chaos: With Applications in Physics, Biology, Chemistry, and Engineering*. Addison-Wesley, New York, NY.

TAKENS, F. (1981). *Detecting Strange Attractors in Turbulence*, volume 898, pp. 336–381. Springer-Verlag, Berlin, Germany.

TRESSER, C. (1984). On some theorems of L. P. Shil'nikov and some applications. *Annales de l'Institute Henri Poincaré*, 40, pp. 441–461.

TURBAN, E. (1998). *Decision Support Systems and Intelligent Systems*. Prentice-Hall, London, UK, fifth edition.

WALLER, H. AND R. SCHMIDT (1989). *Schwingungslehre für Ingenieure - Theorie, Simulation, Anwendung*. BI-Wissenschaftsverlag, Mannheim, Germany. In German.

WALPONE, R. (1993). *Probabilty and Statistics for Engineers and Scientists*. Macmillan, New York, NY, fifth edition.

WALTERS, P. (1982). *An Introduction to Ergodic Theory*. Springer-Verlag, New York, NY.

WANG, H. (1993). *Control of Bifurcations and Routes to Chaos in Dynamical Systems*. Ph.D. thesis, University of Maryland, College Park, MD.

WEISS, S. (1991). *Computer Systems that Learn? Classification and Prediction Methods from Statistics, Neural Nets, Machine Learning and Expert Systems*. Morgan Kaufmann, San Mateo, CA.

CHAPTER 3

THE QUALITATIVE RESONANCE OF STRANGE ATTRACTORS

Brief — In this chapter a peculiar resonance property of periodically forced chaotic oscillators is analyzed both from an experimental and from a theoretical point of view. The analysis shows that models which admit Shil'nikov-like chaotic behavior tend to have a quite particular selective property when externally perturbed. If they are slightly perturbed with an external signal which is strongly related with the generating cycle of the strange attractor (*cfr.* Chap. 2), Shil'nikov-like chaotic systems tend to settle on a periodic behavior which is strongly similar to the forcing signal. If, on the contrary, they are slightly perturbed with a generic signal, which has not particular correlation with the generating cycle of the Shil'nikov-like strange attractor, they continue to behave chaotically. This peculiar resonance property has been called *qualitative resonance*.

Personal Contribution — The entire chapter can be considered as original. Although the ideas presented are strongly influenced by similar results in other fields, in particular by the recent results about chaos synchronization and chaos control.

In the last twenty years, since the pioneering works of Pecora and Carroll [Pecora and Carroll, 1990], a lot of investigative efforts has been dedicated to the problem of synchronization of chaotic dynamical systems as well as to the problem of their control. In this chapter a dynamical phenomenon, strongly related with these two problems, is introduced and its analysis, both conducted by means of experiments and theoretically, is presented. In particular, it is shown that different dynamical models described by means of ordinary differential equations which admit Shil'nikov-like chaotic behavior tend to have a quite particular selective property when externally perturbed. Namely, when slightly perturbed with an external signal which is strongly related to the generating cycle of their strange attractor, Shil'nikov-like chaotic systems tend to settle on a periodic behavior which is strongly similar to the forcing signal. On the other hand, when they are slightly perturbed with a generic signal, which has no particular correlation with the generating cycle of the Shil'nikov-like strange attractor, they continue to behave chaotically. This peculiar resonance property has been called here *qualitative resonance*. The name comes from the fact that the chaotic system tends to resonate with signals qualitatively similar to an observable of the system evolving on the generating saddle cycle embedded in the skeleton of the strange attractor. In fact, the term resonance is used in science and engineering to denote a "sympathy" between a perturbing signal and the perturbed dynamical system as, for examples, the case of the sinusoidal resonance in linear systems [Brogan, 1996] or the strong and weak resonance on tori in nonlinear systems[1] [Kuznetsov, 1998; Ott, 1993]. Indeed, the phenomenon considered herein is a particular "sympathetic" relationship between the strange attractors and their generating cycles.

As it will be discussed in Chap. 4 such a phenomenon is of definite interest for the application proposed in

[1] A brief discussion of strong resonance has been given in Sect. 2.5.3.

this thesis; it allows to easily verify the correlation between a signal and a strange attractor that is practically the main topic of this thesis.

For simplicity the chapter has been split into two parts. In the first one the results of an experimental analysis about qualitative resonance are presented. In the second part a geometrical qualitative model and three quantitative mathematical models of the phenomena are presented.

3.1 Experimental Evidence

The experiments, aimed to show the extent of the qualitative resonance phenomenon, have been conducted on two very different dynamical systems which satisfy Shil'nikov's fourth theorem, a Lur'e one and a more complex one. The first one is a model for the Colpitts oscillator [Sedra and Smith, 1998] and the second one is the Rosenzweig—MacArthur [Hastings and Powell, 1991] model for a tritrophic food chain. They have been chosen since they have been deeply studied in the past and, furthermore, they have a very similar qualitative bifurcation diagram drawn by an infinite set of homoclinic bifurcations [De Feo *et al.*, 2000; Kuznetsov *et al.*, 2001] which organizes the global coexistence of geometrically different periodic and chaotic solutions known as n-pulse families [Maggio *et al.*, 1999].

The mathematical equations, the qualitative bifurcation diagrams as well as the n-pulse families of solutions for the two models are very briefly recalled in the next two paragraphs, the interested reader is invited to refer to the previously mentioned works.

3.1.1 The Colpitts Oscillator

The first set of ODE, given by Eqs. (3.1), is a particular instance of the paradigm of simple and complex oscillations assume herein (*cfr.* Appendix A). It comes from the electronic applications and it is the model of a very common electronic oscillator [Sedra and Smith, 1998]. Such a model has been analyzed in detail in [De Feo *et al.*, 2000; Maggio *et al.*, 1999], in particular the model considered there corresponds to Eqs. (3.1) when $\alpha = 0$, namely when the external driving signal $u(t)$, which will be considered later, has no influence on the system.

$$\begin{aligned} \dot{x_1} &= \frac{g}{Q\,(1-k)}\left(-e^{-x_2}+1+x_3\right) \\ \dot{x_2} &= \frac{g}{Qk}x_3 - \Big[\alpha\big(x_2-u(t)\big)\Big] \\ \dot{x_3} &= -\frac{Q\,(1-k)}{g}\left(x_1+x_2\right) - \frac{1}{Q}x_3 \end{aligned} \tag{3.1}$$

In Figure 3.1 the qualitative bifurcation diagram of this model with $\alpha = 0$ with respect to its two parameters[2] Q and g as obtained in [De Feo *et al.*, 2000; Maggio *et al.*, 1999] is represented. The diagram shows how the n-pulse families of solutions [De Feo *et al.*, 2000; Kuznetsov *et al.*, 2001], some of which are shown in Fig. 3.2, are organized in the parameter space. In particular it shows the organization of the parameter space in terms of the i-pulse Feigenbaum chaos regions, Fg_i, and the i-pulse Shil'nikov chaos regions, S_i.

A final remark deserves the choice of the controlling action on the second state variable, namely the term in square braces in the second equation of system (3.1). Actually, and this is not a case, the results reported here have been discovered while conducting a bifurcation analysis of the periodically forced Colpitts oscillator whose aim was to determine the robustness of the chaotic behavior of such an oscillator with respect to the classical amplitude and phase modulation schemes. Indeed, the control action on x_2 corresponds to the most easy amplitude modulation scheme for the Colpitts oscillator. Furthermore, the system is completely observable and reachable[3] from x_2, this is very important as explained later on.

3.1.2 The Rosenzweig—MacArthur Food Chain

The second set of ODE, given by Eqs. (3.2), comes from biology, it is one of the most common models of a tritrophic food chain [De Feo and Rinaldi, 1997; Hastings and Powell, 1991], namely a food chain composed of a prey, a predator, and a super predator. This model has been analyzed in detail in [Kuznetsov and Rinaldi, 1996] and [Kuznetsov *et al.*, 2001]. Similarly to the case of the Colpitts Oscillator, the model deeply studied

[2] The parameter k has no influence on the dynamics and is assumed equal to 1/2.

[3] Observability and reachability are key concepts of linear system theory [Callier and Desoer, 1991].

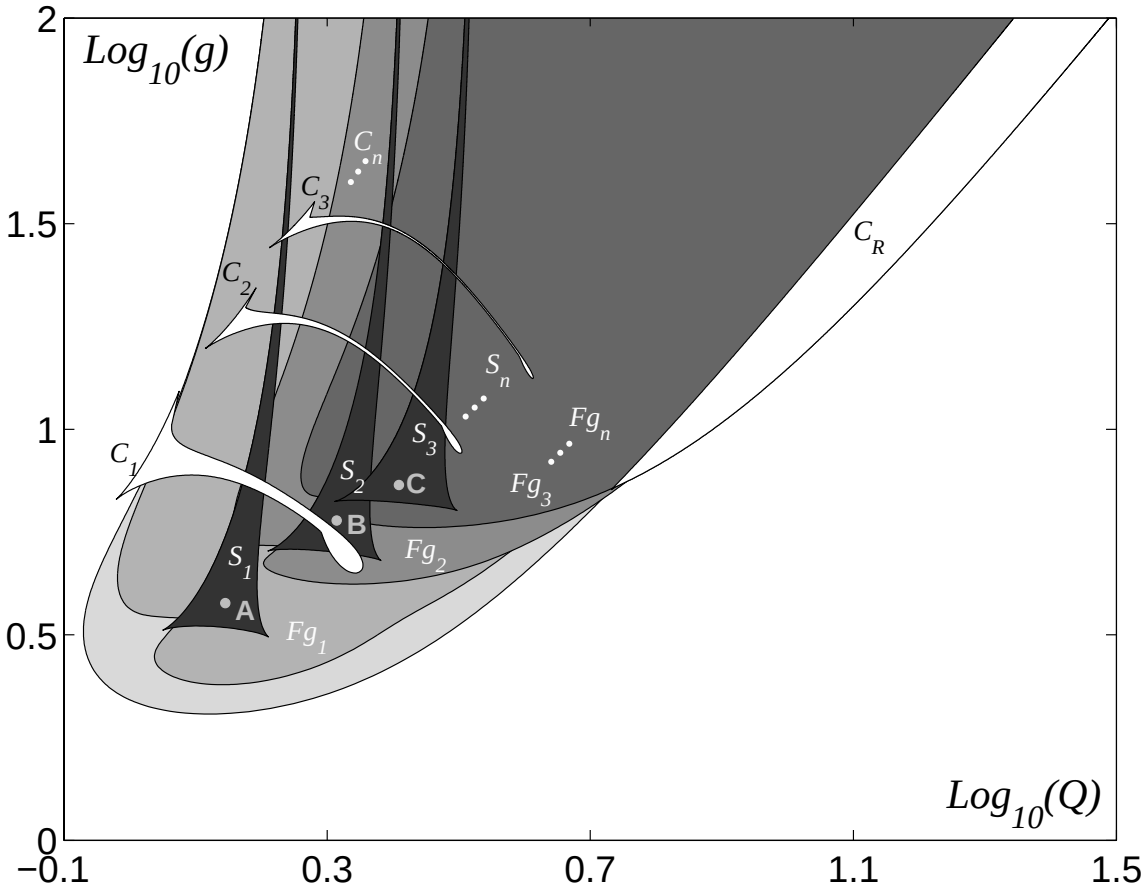

Figure 3.1: *Qualitative bifurcation diagram of the Colpitts oscillator and classification of the parameter space in regions of Feigenbaum-like, Fg_i, and Shil'nikov-like, S_i, chaotic behavior. Coordinates of points:* A *–* $Log_{10}(Q) = 0.1452$, $Log_{10}(g) = 0.5772$; B *–* $Log_{10}(Q) = 0.3144$, $Log_{10}(g) = 0.7778$; C *–* $Log_{10}(Q) = 0.4091$, $Log_{10}(g) = 0.8645$.

in [Kuznetsov *et al.*, 2001] correspond to Eqs. (3.2) when $\alpha = 0$, namely when the external driving signal $u(t)$ has no influence on the system.

$$\begin{aligned} \dot{x_1} &= x_1\left(r\left(1-\frac{x_1}{K}\right)-\frac{a_1x_2}{1+b_1x_1}\right)-\Big[\alpha\big(x_1-u(t)\big)\Big] \\ \dot{x_2} &= x_2\left(\frac{a_1x_1}{1+b_1x_1}-\frac{a_2x_3}{1+b_2x_2}-d_1\right) \\ \dot{x_3} &= x_3\left(\frac{a_2x_2}{1+b_2x_2}-d_2\right) \end{aligned} \tag{3.2}$$

In Figure 3.3 the qualitative bifurcation diagram of this model, with $\alpha = 0$, with respect to two of its parameters, namely K and r is reported [Kuznetsov *et al.*, 2001]. Once again, the diagram shows how the n-pulse families of solutions, some of which are shown in Fig. 3.4, are organized in the parameter space. In particular it shows the organization of the parameter space in terms of the i-pulse Feigenbaum chaos regions, Fg_i, and the i-pulse Shil'nikov chaos regions, S_i.

Again a remark should be made about the choice of the controlling action on the first state variable. Once again, the results reported here have been discovered while conducting a bifurcation analysis of the periodically forced Rosenzweig—MacArthur food chain. The aim of this analysis was to determine the effects of seasonal migration of preys. Indeed, the control action between square braces on the first equation of system (3.2) corresponds to a linear modeling of migration. Furthermore, also in this case the system is completely observable and reachable from x_1.

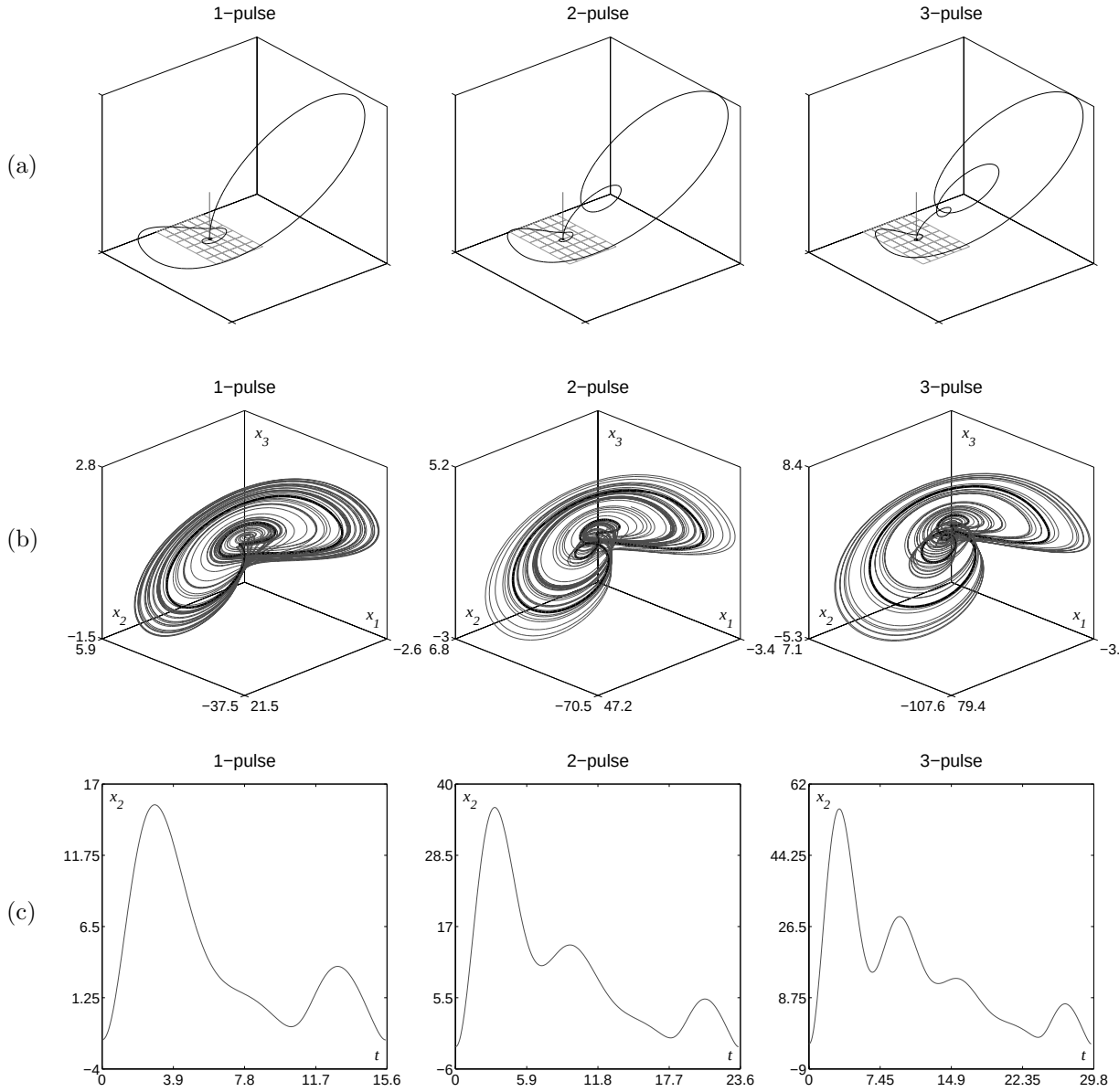

Figure 3.2: *n-pulse families of solution for the Colpitts oscillator: (a) – homoclinic trajectory, in the eigenbases, of the* 1-, 2-, 3*-pulse family in proximity of points* A, B, *and* C *of Fig. 3.1, respectively; (b) – chaotic attractors of the* 1-, 2-, 3*-pulse family at the points* A, B, *and* C *of Fig. 3.1, respectively, the bold lines are the embedded unstable generating cycles; (c) – time series of* x_2 *while evolving on the generating cycles shown in (b).*

A final remark should be made about the main difference between the two qualitative bifurcation diagrams reported in Figs. 3.1 and 3.3. In the case of the Colpitts oscillator the n-pulse families of solution exists for different values of the parameters while in the case of the Rosenzweig—MacArthur model the n-pulse families of solution happens almost in the same region of the parameter space. This fact will be commented in detail in Chap. 4.

3.1.3 Experimental Analysis

The extent of the qualitative resonance phenomenon, described in the introductory paragraph, has been studied by means of several experiments conducted on the two previously introduced models at different parameter values. Briefly, the experiments consisted in slightly (small values of α) perturbing the original

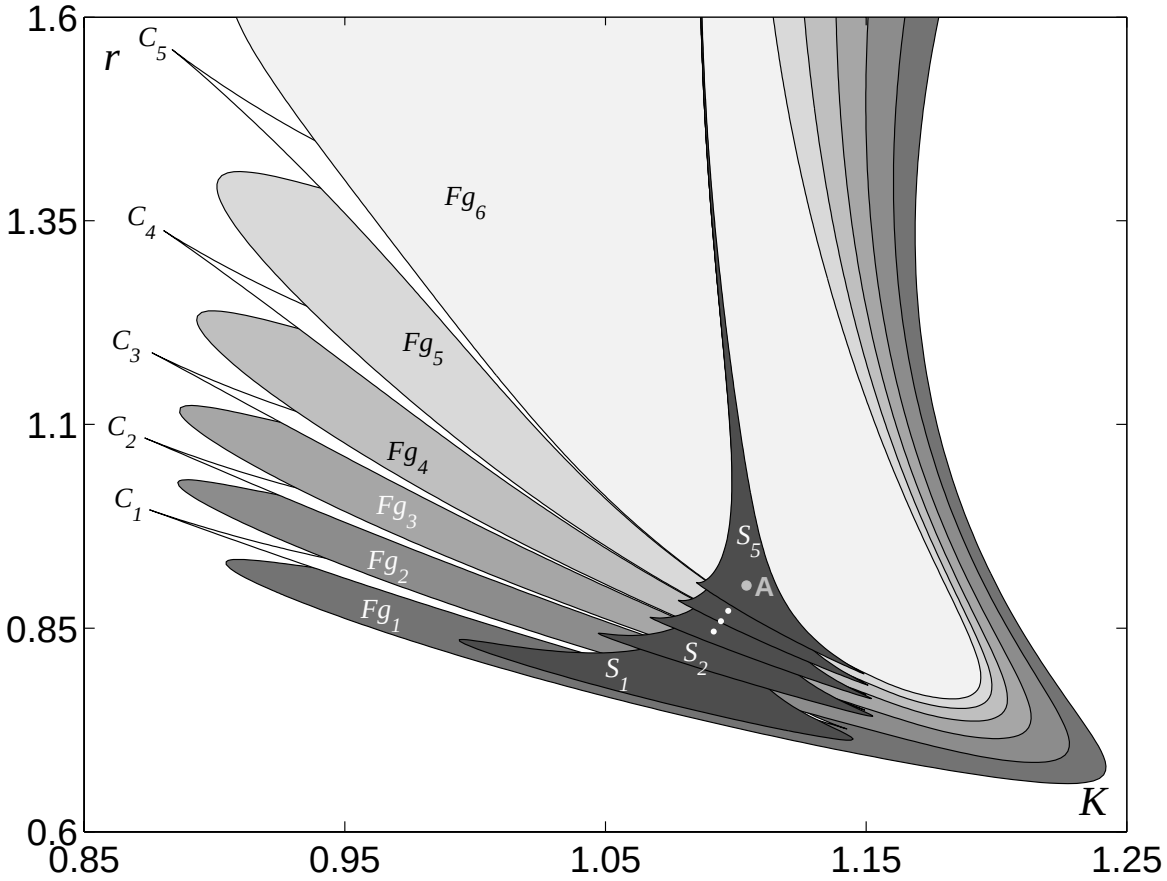

Figure 3.3: *Qualitative bifurcation diagram of the Rosenzweig—MacArthur food chain and classification of the (K, r) parameter space in regions of Feigenbaum-like, Fg_i, and Shil'nikov-like, S_i, chaotic behavior. Coordinates of point* A *– $K = 1.1041$, $r = 0.9022$.*

equations by means of several different external signals $u(t)$. The signals have been chosen in such a way that some of them were strongly related to the generating cycle of the Shil'nikov-like strange attractor(s) existing for the given parameter values, while others were not. For each set of parameter values and driving signal, each one of the two systems has been simulated and its steady state has been classified as follow: whenever the steady state was shrinking to a periodic solution or to a chaotic solution with a very small variance, *i.e.* something very close to a limit cycle, the ensemble has been said to *qualitatively resonate*; on the other hand, whenever the steady state was chaotically wandering, the ensemble has been said to not qualitatively resonate or to *anti-resonate*.

The analysis framework can be summarized as follows, the generic system admitting Shil'nikov-like chaotic behavior for $\alpha = 0$:

$$\dot{x} = F(x) + \alpha e_i\big(x_i - u(t)\big) = \begin{bmatrix} f_1(x) \\ \vdots \\ f_i(x) + \alpha\big(x_i - u(t)\big) \\ \vdots \\ f_n(x) \end{bmatrix}$$

where e_i is the vector with all zeros and a one in the i^{th} position, is *slightly* driven with different kinds of perturbing signals $u(t)$; namely, the part within the square braces in the Eqs. (3.1) and (3.2) is taken into account for very small values of α. In particular, a value of α is small enough if it satisfies the following

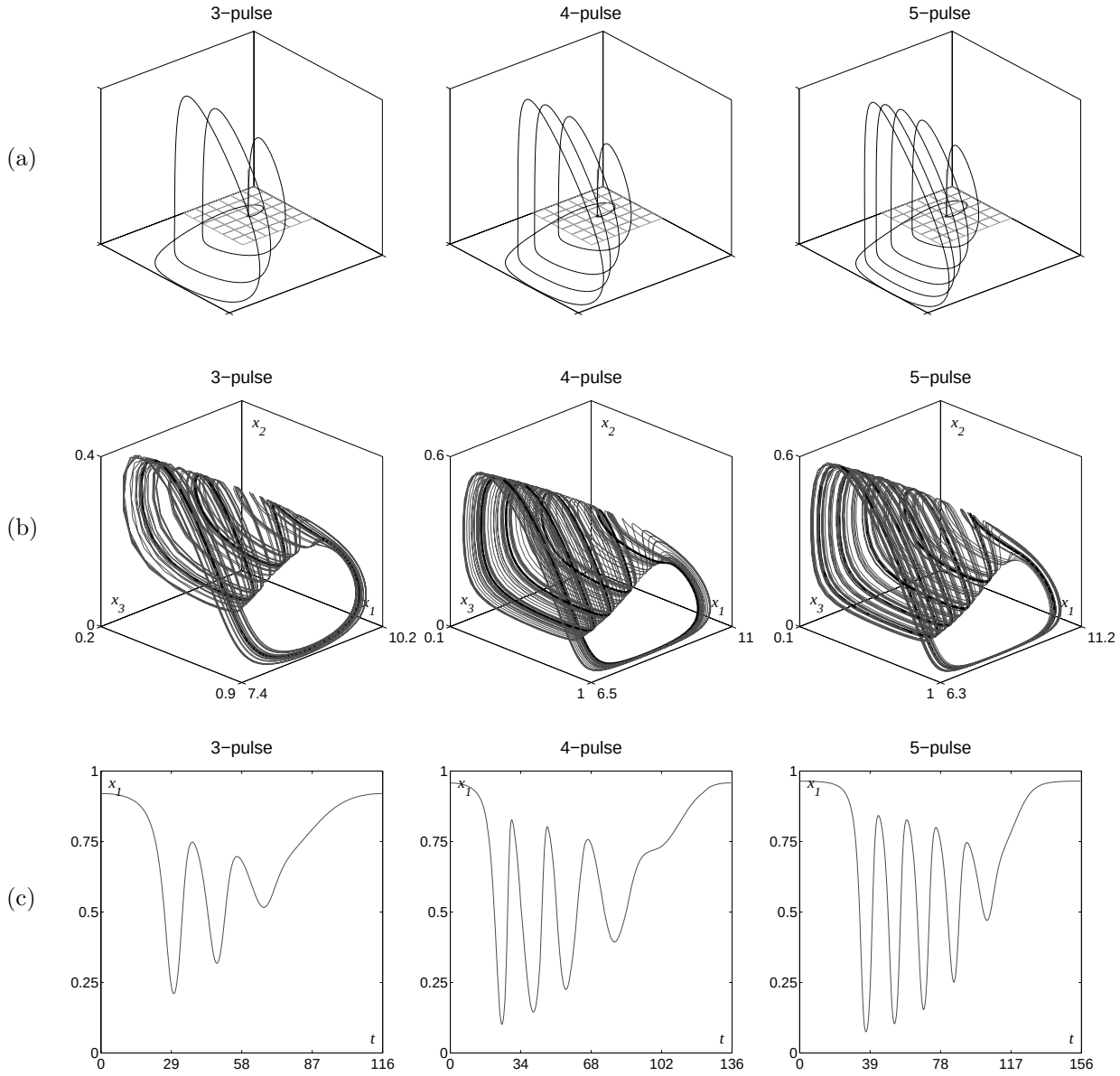

Figure 3.4: *n-pulse families of solution for the Rosenzweig—MacArthur model: (a) – homoclinic trajectory, in the eigenbases, of the* 3*-,* 4*-,* 5*-pulse family in proximity of point* A *of Fig. 3.3; (b) – chaotic attractors of the* 3*-,* 4*-,* 5*-pulse family in proximity of point* A *of Fig. 3.3, in bold the generating cycle; (c) – time series of* x_1 *while evolving on the generating cycle shown in (b).*

condition:

$$\max_{\substack{x_i \in SA \\ u(t)=x_i(t),\, x_i \in GC}} \left(\alpha \Big| \big(x_i - u(t) \big) \Big| \right) \; < \; \frac{1}{\beta} E\Big[\big| f_i(x) \big| \, \Big| x \in SA \Big], \quad \beta > 1$$

for a suitably chosen value of β greater than one. Where $x, x_i \in SA$ means that the state x or the state variable x_i are on the uncontrolled strange attractor (SA); $u(t) = x_i(t), x_i \in GC$ means that the perturbing signal $u(t)$ is the time series of the state variable x_i while evolving on the generating cycle (GC); f_i is the i^{th} components of $\dot{x} = F(x)$; finally, $E[\cdot]$ stands for the averaging operation, *i.e.* the expected value. In other words, the rule means that the maximal external perturbation on the evolution of the i^{th} state variable, left hand side, must be at least β time smaller than the average natural evolution, right hand side. In particular, in the experiments has been considered $\beta = 100$. Furthermore, the system is classified as

qualitatively resonating whenever the following condition is satisfied:

$$\int_{t-nT_G}^{t} \big(x_i(\tau) - u(\tau)\big)^2 d\tau \; < \; \frac{1}{\gamma} E\Big[\int_{t-nT_G}^{t} \Big(x_i(\tau)\big|_{x_i \in SA} - x_i(\tau)\big|_{x_i \in GC}\Big)^2 d\tau\Big], \quad \gamma > 1,\, n \in \mathbb{N} \tag{3.3}$$

for a suitably chosen value of γ greater than one. Where T_G is the period of the generating cycle and the other symbols have the same meaning as before. In simple words, a system is said to be resonant when the driven trajectories, left hand side, are γ time closer to the perturbing signal $u(t)$ than what is expected to be the free strange attractor to the generating cycle, right hand side. In particular, in the experiments has been considered $\gamma = 50$ and $n = 10$.

The perturbing signals $u(t)$ considered in the experiments are periodic signals or perturbations of periodic signals. The signals considered can be easily described by means of a *base signal* u_b defined on an interval that corresponds to the *base period* T_0, namely

$$u_b(\tau),\, u_b(0) = u_b(T_0), \quad \tau \in [0, T_0]$$

then a T-periodic signal of generic period T can be obtained from u_b as

$$u(t) = u_b(t\frac{T_0}{T} \mod T_0)$$

In the experiments different kinds of base signals have been considered, some of them are the evolution of a state variable on a generating cycle, not necessarily the generating cycle of the strange attractor existing for the chosen parameter values. Thus, these signals are somehow related to the perturbed system. Other base signals considered are test signals like sinusoidal and square waves, in general these signals are not related to the perturbed system. In the experiments, for any base signal considered, five possible signals have been constructed as follows.

1. *Clean signal*: it is the periodic signal obtained from the base signal as described before, where T_G is the period of the generating cycle of the strange attractor existing at the chosen parameter settings

$$u_c(t) = u_b(t\frac{T_0}{T_G} \mod T_0)$$

2. *Piecewise linear approximation*: it is the piecewise linear approximation of the clean signal described above, the approximation can be more or less fine depending on the length l of the linear segments. In the experiments $l = L/40$ has been assumed, where $L = \int_0^{T_G} \sqrt{1 + {u'_c}^2(\tau)} d\tau$ is the length of the clean signal

$$u_{pwl}(t) = PWL\Big(u_c(t), l\Big)$$

where

$$\begin{aligned} PWL(u(t), l) \;\; = \;\; & u(t_i)\left(1 - \frac{t - t_i}{t_{i+1} - t_i}\right) + u(t_{i+1})\frac{t - t_i}{t_{i+1} - t_i}, \\ & t_i, t_{i+1} : \sqrt{\big(u(t_{i+1}) - u(t_i)\big)^2 + \big(t_{i+1} - t_i\big)^2} = l,\; t_0 = 0 \end{aligned}$$

3. *Additive Gaussian noise*: it is the clean pattern corrupted by additive white Gaussian noise with zero mean and σ^2 variance. In the experiments the variance has been assumed such that $\sigma^2 = \frac{1}{40}\int_0^{T_G} \left(u(\tau) - \overline{u}\right)^2 d\tau$ where $\overline{u} = \frac{1}{T_G}\int_0^{T_G} u(\tau) d\tau$ is the mean value of the clean signal. Namely, such that the signal to noise ratio is $SNR = 16dB$

$$u(t) = u_c(t) + \varepsilon, \quad \varepsilon \sim WGN(0, \sigma^2)$$

4. *Random amplitude modulation*: it is the clean pattern modulated in amplitude by white Gaussian noise with zero mean and σ^2 variance. In the experiments the variance has been assumed such that $\sigma^2 = 1/900$, *i.e.* has been practically assumed that the maximum modulation index is of $1/10$

$$u(t) = u_c(t)(1 + \varepsilon), \quad \varepsilon \sim WGN(0, \sigma^2)$$

5. *Random phase modulation*: it is the clean pattern modulated in phase by white Gaussian noise with zero mean and σ^2 variance. In the experiments the variance has been assumed such that $\sigma^2 = T_G^2/900$, *i.e.* has been practically assumed that the maximum modulation factor is of 1/10

$$u(t) = u_b(t\frac{T_0}{T_G} + \varepsilon \mod T_0), \quad \varepsilon \sim WGN(0, \sigma^2)$$

The simulations have been run three-hundreds times and an average of the results has been compiled. The detail of the experiments and of their results for the two cases are reported in the two next paragraphs.

Results for the Colpitts Oscillator

For the Colpitts oscillators three sets of experiments have been conducted with the parameters of system (3.1) corresponding to the points A, B, and C in Fig. 3.1. Each experiment set consists of six geometrically different base signals. The first three driving signals are the time evolution, over a period, of x_2 when the system evolves on the generating cycles of a 1-, 2-, and 3-pulse strange attractor existing in the points A, B, and C, as shown in Fig. 3.5(a); the other three are sinusoidal, square, and triangular waves of the same period as the generating cycle existing at the chosen parameter values. For each one of these base signals the set of five driving signals afore mentioned has been considered, Figs. 3.5(b) and (c) show the signal corrupted by additive Gaussian noise and a piecewise linear approximation, respectively.

As examples of qualitative resonance and anti-resonance, Fig. 3.6 shows the behavior in the state space of system (3.1) when perturbed with a fine and a coarse piecewise linear approximation of the time series of x_2 while evolving on the generating cycle of the strange attractor existing at the points A, B, and C of Fig. 3.3, respectively.

The results of qualitative resonance are reported in the Tab. 3.1 where each entry in the table represents the percentage of time that the system was qualitatively resonating for a given input, *i.e.* the percentage of times in which relation (3.3) has been hold true. The row determine the geometry of the base signal while the column determine the class of driving signal obtained from the base signal. In Table 3.1 the peaks of qualitative resonance are highlighted in gray, it can be concluded that the Colpitts model qualitatively resonate with signals strongly related to the generating cycle of the strange attractor existing for the chosen parameters. Indeed a peak of qualitative resonance can be observed for all the generalizations of 1-, 2-, and 3-pulse driving signals when working in points A, B, and C of Fig. 3.1, respectively.

A separate comment deserves the peak of qualitative resonance for the sinusoidal and triangular driving signals that can be observed in correspondence of all the three parameters set. The Colpitts oscillator is indeed a sinusoidal oscillator, or at least has been designed to behave like that in the old forties. Such a strong presence of sinusoidal behavior in this model could be the justification of its "sympathy" for the sinusoid and for the triangular wave which can be thought as a coarse piecewise linear approximation of the sinusoidal wave. Even though a square wave could be thought as an even coarser piecewise linear approximation of a sinusoid, no particular qualitative resonance with respect to such a driving signal has been observed.

Results for the Rosenzweig—MacArthur Model

For the Rosenzweig—MacArthur model the framework of the conducted experiments is almost identical to the one described above for the Colpitts oscillator, the difference is in the fact that for this model a single set of experiments has been conducted, corresponding to the parameters r and K set to the values identified by the point A in Fig. 3.3.

Some of the base signals considered, corresponding to the time series of x_1 when the system evolves on one of the generating cycle of a 3-, 4-, and 5-pulse strange attractors existing in the point A, their additive Gaussian noise corruption, and their piecewise linear approximation are shown in Fig. 3.7.

As examples of qualitative resonance and anti-resonance, Fig. 3.8 shows the behavior in the state space of system (3.2) when perturbed, respectively, with a fine and a coarse piecewise linear approximation of the time series of x_1 while evolving on the generating cycle of the strange attractor existing at the chosen parameter values.

The results of qualitative resonance have been collected in the following table. The peaks of qualitative resonance are again highlighted in gray. From Tab. 3.2 it can be concluded that the Rosenzweig—MacArthur model qualitatively resonate with signals strongly related to the generating cycle of the strange attractors existing for the chosen parameter values. Indeed a peak of qualitative resonance can be observed for all the generalizations of 1-, 2-, 3-, 4- and 5-pulse driving signal. In fact for parameters values nearby point A of

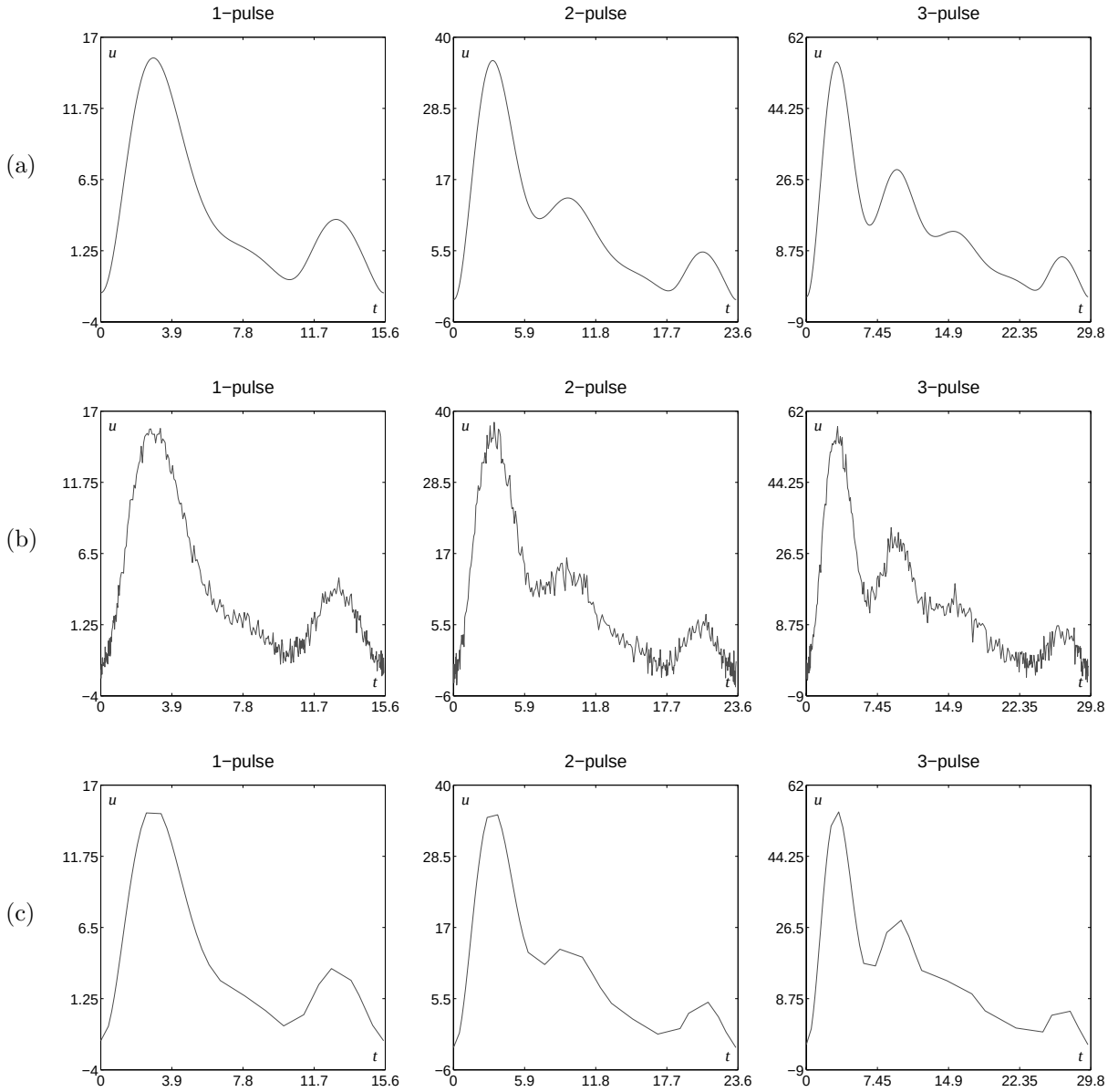

Figure 3.5: *Driving signal, related to the generating cycle, for the Colpitts oscillator: (a) – clean time series of x_2 while evolving on a* 1*-,* 2*-,* 3*-pulse generating cycle of the strange attractors existing at points* A*,* B*, and* C *of Fig. 3.1 respectively; (b) – white Gaussian noise corruption of the base signals shown in (a); (c) – piecewise linear approximation of the base signals shown in (a).*

Fig. 3.3 the model admits a strange attractor for each one of the named n-pulse families of solution. The fact that for this model there is not a particular "sympathy" neither for sinusoidal waves nor for triangular ones, strongly support the previous discussion about the fact that such a "sympathy" in the Colpitts model is related to its primordial design as sinusoidal oscillator.

3.1.4 Remarks on the Results

The results of this experiments, *cfr.* Tab. 3.1 and Tab. 3.2, that have been conducted on two very different dynamical systems highlight a clear evidence of relationship between the kind of driving signals and the phenomenon of qualitative resonance. Indeed, the results show that both the systems admit qualitative resonance and furthermore they show that the qualitative resonance is a quite robust phenomenon. Namely, the systems qualitatively resonate with respect to several signals obtained by distorting/generalizing a signal

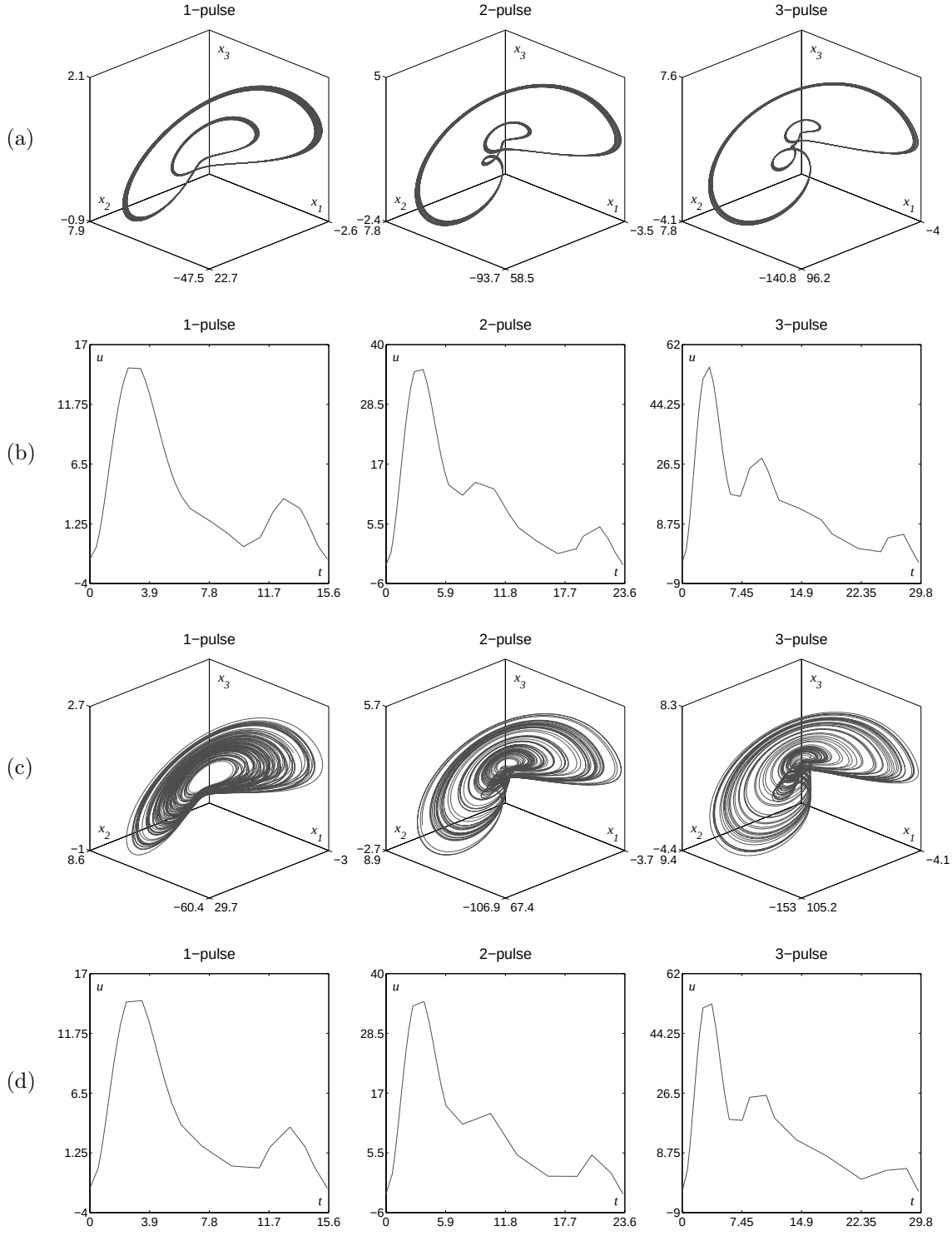

Figure 3.6: *Qualitative resonance and anti-resonance for the Colpitts oscillator when driven with piecewise linear approximations of the x_2 time series while evolving on the n-pulse generating cycle of the strange attractor existing at the points* A, B, *and* C *of Fig. 3.3: (a) – behavior in the state space when qualitatively resonating with a fine piecewise linear approximation; (b) – driving signals corresponding to the behavior shown in (a), piecewise linear approximation with $l = L/40$; (c) – behavior in the state space when qualitatively anti-resonating with a coarse piecewise linear approximation; (d) – driving signals corresponding to the behavior shown in (c), piecewise linear approximation with $l = L/25$;*

A driving signal → base signal ↓	clean	$+\epsilon(t)$	PWL	δA	δt
1-pulse	100%	98%	98%	90%	88%
2-pulse	$< 1\%$	$< 1\%$	$< 1\%$	$< 1\%$	$< 1\%$
3-pulse	$< 1\%$	$< 1\%$	$< 1\%$	$< 1\%$	$< 1\%$
sin	100%	85%	83%	72%	61%
square	2%	$< 1\%$	–	$< 1\%$	$< 1\%$
triangular	58%	$< 1\%$	–	15%	15%

B driving signal → base signal ↓	clean	$+\epsilon(t)$	PWL	δA	δt
1-pulse	$< 1\%$	$< 1\%$	$< 1\%$	$< 1\%$	$< 1\%$
2-pulse	98%	94%	93%	88%	81%
3-pulse	$< 1\%$	$< 1\%$	$< 1\%$	$< 1\%$	$< 1\%$
sin	95%	81%	81%	64%	61%
square	$< 1\%$	$< 1\%$	–	$< 1\%$	$< 1\%$
triangular	48%	$< 1\%$	–	12%	14%

C driving signal → base signal ↓	clean	$+\epsilon(t)$	PWL	δA	δt
1-pulse	$< 1\%$	$< 1\%$	$< 1\%$	$< 1\%$	$< 1\%$
2-pulse	$< 1\%$	$< 1\%$	$< 1\%$	$< 1\%$	$< 1\%$
3-pulse	97%	92%	90%	87%	79%
sin	94%	79%	78%	62%	60%
square	4%	$< 1\%$	–	$< 1\%$	$< 1\%$
triangular	52%	$< 1\%$	–	22%	21%

Table 3.1: *Qualitative resonance results for the Colpitts oscillator for parameter setting corresponding respectively to the points* A, B, *and* C *in Fig. 3.1. Legend of the driving signals: clean = no distortion;* $+\epsilon(t)$ *= additive Gaussian noise; PWL = piecewise linear approximation;* δA *= random amplitude modulation;* δt *= random phase modulation.*

A driving signal → base signal ↓	clean	$+\epsilon(t)$	PWL	δA	δt
1-pulse	100%	94%	97%	89%	73%
2-pulse	99%	92%	95%	87%	72%
3-pulse	97%	89%	93%	86%	65%
4-pulse	94%	85%	90%	86%	60%
5-pulse	91%	84%	90%	84%	55%
sin	$< 1\%$	$< 1\%$	$< 1\%$	$< 1\%$	$< 1\%$
square	$< 1\%$	$< 1\%$	–	$< 1\%$	$< 1\%$
triangular	$< 1\%$	$< 1\%$	–	$< 1\%$	$< 1\%$

Table 3.2: *Qualitative resonance results for the Rosenzweig—MacArthur model for parameter setting corresponding to the point* A *in Fig. 3.3. Legend of the driving signals: clean = no distortion;* $+\epsilon(t)$ *= additive Gaussian noise; PWL = piecewise linear approximation;* δA *= random amplitude modulation;* δt *= random phase modulation.*

obtained from the time series of a generating cycle.

The value of such a phenomenon as a pattern matching test for approximately periodic signals is clear and indeed in the next chapter it is explained how to exploit it for the purposes of this thesis. On the other hand, why and how such a phenomenon take place remain an open questions. Furthermore, in order to develop applications, this phenomenon needs to be quantified, namely it is necessary to quantify and qualify the kind of signals that qualitatively resonate and anti-resonate. The rest of this chapter is dedicated to these crucial points, both a qualitative geometrical explanation and a deeper mathematical analysis are

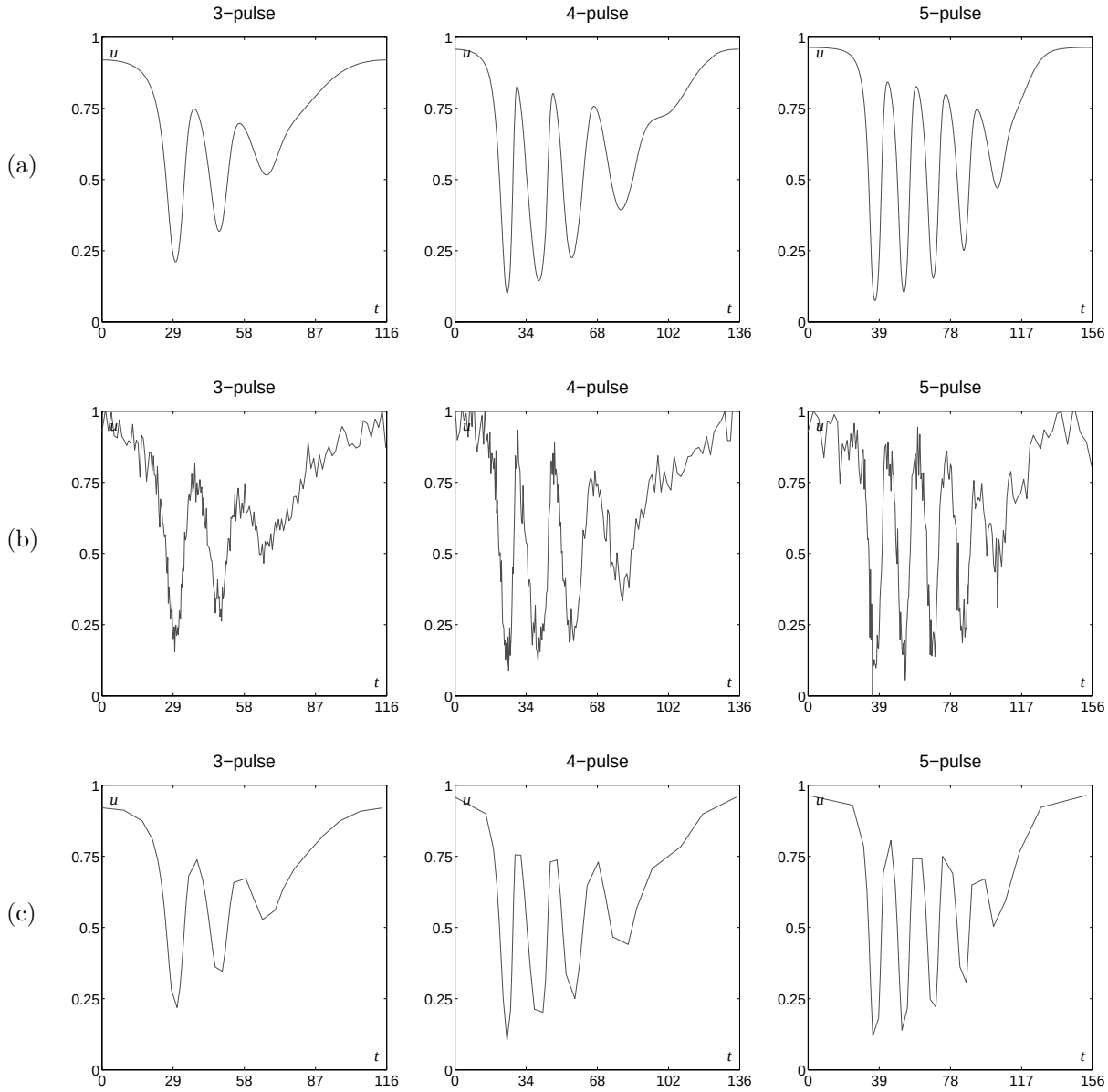

Figure 3.7: *Driving signal, related to the generating cycle, for the Rosenzweig—MacArthur food chain: (a) – clean time series of x_1 while evolving on a* 3*-,* 4*-, and* 5*-pulse generating cycle of the strange attractors existing at point* A *of Fig. 3.3; (b) – white Gaussian noise corruption of the base signals shown in (a); (c) – piecewise linear approximation of the base signals shown in (a).*

presented.

3.2 Geometrical Model of Qualitative Resonance

Before giving an intuitive and geometrical explanation for the apparently "amazing" phenomenon of qualitative resonance it should be noted that there is nothing so amazing in the case of resonance with the clean signal coming from the generating cycle. Indeed, such a case would correspond to a simple reconstruction of a periodic linear system [Bittanti and Colaneri, 1999; Callier and Desoer, 1991] or, for non-control theory people, it would be just a particular case of synchronization between chaotic systems [Hasler, 1994; Lakshmanan and Murali, 1996; Pecora and Carroll, 1990]. In fact, consider an autonomous nonlinear system

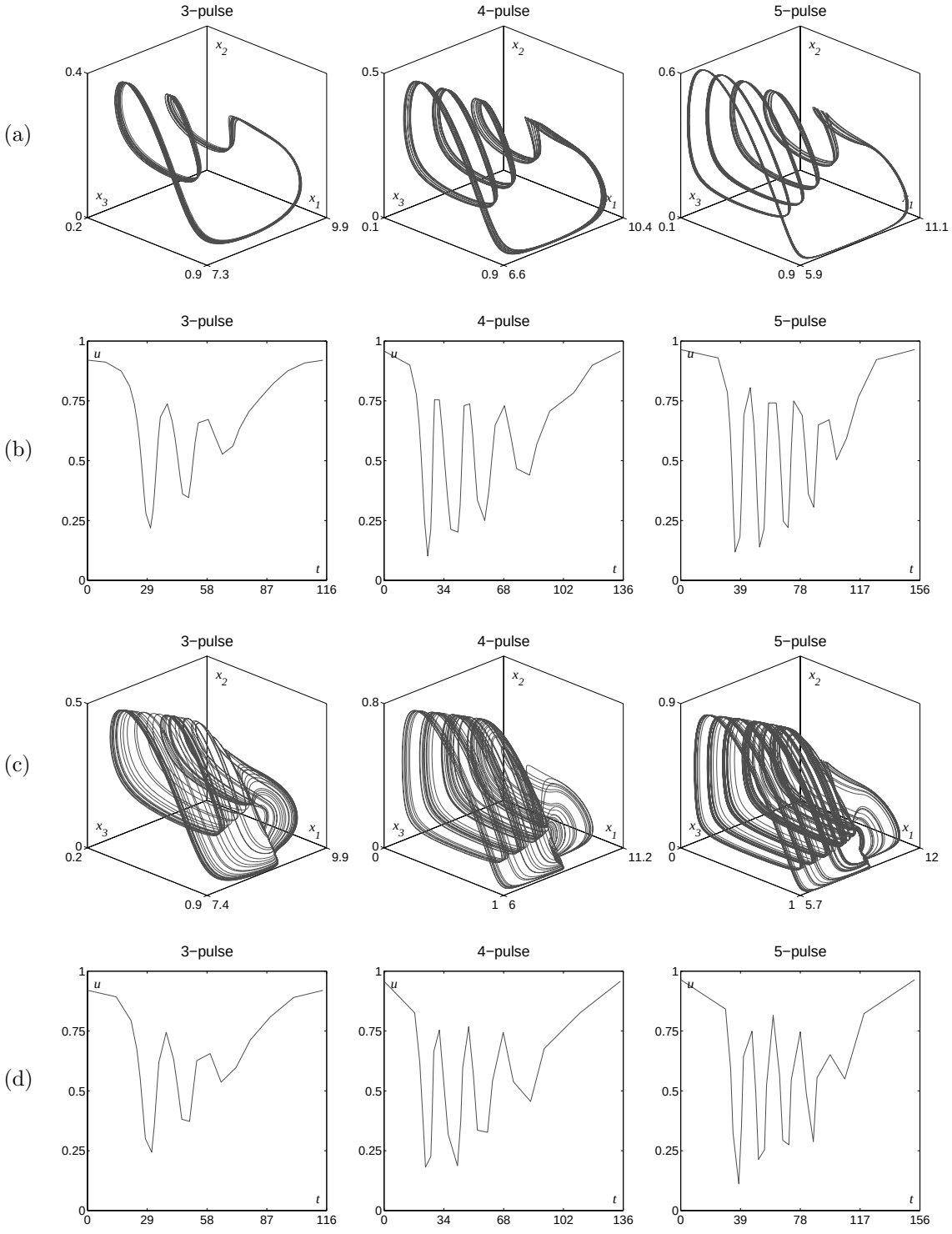

Figure 3.8: *Qualitative resonance and anti-resonance for the Rosenzweig—MacArthur food chain when driven with piecewise linear approximations of the x_1 time series while evolving on the n-pulse generating cycles of the strange attractors existing at the point* A *of Fig. 3.3: (a) – behavior in the state space when qualitatively resonating with a fine piecewise linear approximation; (b) – driving signals corresponding to the behavior shown in (a), piecewise linear approximation with $l = L/40$; (c) – behavior in the state space when qualitatively anti-resonating with a coarse piecewise linear approximation; (d) – driving signals corresponding to the behavior shown in (c), piecewise linear approximation with $l = L/25$;*

of the kind

$$\begin{aligned} \dot{\widetilde{x}} &= F(\widetilde{x}), \quad \widetilde{x} \in \mathbb{R}^n,\ F : \mathbb{R}^n \mapsto \mathbb{R}^n \\ \widetilde{y} &= H(\widetilde{x}), \quad \widetilde{y} \in \mathbb{R}^m,\ H : \mathbb{R}^n \mapsto \mathbb{R}^m,\ m < n \end{aligned} \tag{3.4}$$

where $y(t)$ is an observable of the state. Let suppose that the system admits a T-periodic solution of period T

$$\begin{aligned} &\widehat{x}(t) :\ \widehat{x}(t+T) = \widehat{x}(t),\ \dot{\widehat{x}}(t) = F(\widehat{x}(t)) \\ &\widehat{y}(t) = H(\widehat{x}(t)) \end{aligned}$$

then it is trivial to show that $\widehat{x}(t)$ is a periodic solution also of the following system

$$\begin{aligned} \dot{x} &= F(x) - K\left(y - \widehat{y}\right), \quad \forall K :\ \dim(K) = n \times m \\ y &= H(x) \end{aligned} \tag{3.5}$$

Less evident is the fact that under suitable conditions $\widehat{x}(t)$ is a stable solution of system (3.5) independently from its stability in system (3.4). Indeed, system (3.5) can be linearized around the periodic solution $\widehat{x}(t)$ leading to a periodic linear system

$$\begin{aligned} \dot{\delta x} &= A(t)\delta x - K \underbrace{(y - \widehat{y})}_{\delta y} \\ \delta y &= C(t)\delta x \end{aligned} \tag{3.6}$$

where

$$\begin{aligned} \delta x(t) &= x(t) - \widehat{x}(t) \\ \delta y(t) &= y(t) - \widehat{y}(t) \\ A(t) &= \left.\frac{\partial F(x)}{\partial x}\right|_{x=\widehat{x}(t)}, \quad A(t+T) = A(t) \\ C(t) &= \left.\frac{\partial H(x)}{\partial x}\right|_{x=\widehat{x}(t)}, \quad C(t+T) = C(t) \end{aligned}$$

For such kind of system it is known from control theory [Brogan, 1996; Callier and Desoer, 1991] that if the couple $(A(t), C(t))$ is observable[4] then for an arbitrary n-tuple of multipliers, there exists a T-periodic matrix $K = K(t) :\ K(t+T) = K(t)$ such that the characteristic multipliers[5] of the system (3.6) are exactly those given by n-tuple. In particular, they can be chosen such that the solution $\delta x(t) = 0$ of system (3.6), which corresponds to the periodic solution $\widehat{x}(t)$ of system (3.5), is stable. Furthermore, for the case where the observation matrix $C(t)$ is a constant matrix, $C(t) = \overline{C}$, there exists at least one constant matrix K such that the solution $\delta x(t) = 0$ of system (3.6) is stabilized [Brunovski, 1970; Kučera *et al.*, 1998]. The non-specialist in control theory could think that the stability of the solution $\delta x(t) = 0$ of system (3.6) generically corresponds to the asymptotic stability of the periodic solution $\widehat{x}(t)$ of system (3.5). Unfortunately, this is true only provided that the Jacobian matrix $A(t)$ and the reference signal $\widehat{y}(t)$ are almost in phase. Namely, provided that the state $x(t)$ of system (3.5) is almost in phase with the "hidden" driving state $\widehat{x}(t)$. This condition is due to the fact that while system (3.5) is an autonomous nonlinear system and therefore its Jacobian depends upon the state, system (3.6) is a time-varying linear system, therefore its Jacobian depends upon the time. Thus, the equivalence of the two systems depend upon the fact that the state x of the first system uniquely identifies the time of the second one, *i.e.* the two system must be almost in phase. It should be noted that considering the driving and driven systems together, the asymptotic stability of the $\delta x(t) = 0$ solution implies automatically the "almost in phase" condition. In fact, the suitable neighborhood from which the trajectories tend to $\delta x(t) = 0$, necessary to define the asymptotic stability, defines as well the "almost in phase" condition. On the contrary, considering only the driven system, as a periodically forced

[4] Concept like detectability, stabilizability, controllability, reachability, etc. imply that a particular matrix, commonly called Graminian matrix, has maximal rank [Callier and Desoer, 1991].

[5] The characteristic multipliers of a periodic linear system, known also as Floquet multipliers, are the multipliers of the monodromy matrix of the system. Namely, they are the multipliers of the matrix $\Psi(\tau) = \Phi(\tau + T, \tau)$ where $\Phi(\tau, t)$ is the solution of the following differential matrix equation

$$\frac{\partial}{\partial t}\Phi(t,\tau) = A(t)\Phi(t,\tau), \quad \Phi(\tau,\tau) = I$$

Later in the text, in Sect. 3.3.1, the concept is described in more detail for a particular case.

system, requires to uniquely specify the phases of the input signal, with respect to the phase of the system output, which guarantee the convergence to the $\delta x(t) = 0$ solution.

Going back to the case considered herein, namely the stabilization of the generating cycle in a Shil'nikov-like strange attractor, this condition is almost implicitly satisfied. Indeed, in Sect. 2.5.2 it has been shown that a Shil'nikov-like strange attractor randomly changes its phase. Thus, if the gain matrix K is such that Shil'nikov's conditions are not violated, here the hypothesis of a small α is employed, it can be concluded that sooner or later the driving signal and the state of the driven system will be in phase. At this point the linear control theory just discussed will warrant the convergence to the generating cycle. Thus, concluding, the qualitative resonance with the clean signal coming from the generating cycle[6] of a Shil'nikov-like strange attractor is a straight consequence of a random phase seeking of the Shil'nikov-like chaos and of linear control theory, that is why nothing amazing is in the phenomenon at least for a clean driving signal.

Explaining Qualitative Resonance

The presented control theory argument can be raised to explain the occurrence of the qualitative resonance phenomena for not so clean driving signal as well. Actually, when a feedback matrix gain K is chosen the asymptotic *noise reduction ratio*[7] (NRR) of input Gaussian noise for the filter given by Eqs. (3.6) is uniquely defined. Namely, for a given feedback matrix gain K, feeding the filter (3.6) with a signal $\widehat{y}(t) + \varepsilon_{in}$, where ε_{in} is a white Gaussian noise, the output of the filter (3.6) is a signal $\delta y = \varepsilon_{out}$ where the variance of ε_{out} is NRR times smaller than that of ε_{in}. This means that feeding the system (3.5) with a signal $\widehat{y}(t) + \varepsilon_{in}$, if and when the signal and the system will be in phase, will lead the system to shrink around the periodic solution $\widehat{x}(t)$ as much as predicted by the NRR.

Remembering what has been shown in the previous chapter in Sect. 2.5.1, a very simple generalization of a cycle is a Feigenbaum-like strange attractor. Even though the previous argument is valid for Gaussian perturbations it is still "almost"[8] valid also for non Gaussian perturbations. Taking into account that, for continuity of the vector field, the Jacobian of a Feigenbaum-like strange attractor cannot be very different from that of its generating cycle and remembering that the filtering principle described is based indeed only on a Jacobian approximation (*cfr.* Eqs. (3.6)), it follows that feeding the system (3.5) with a Feigenbaum-like signal coming from a strange attractor lying on a Möbius strip large ε will lead the system to shrink on a strange attractor NRR time narrower than that of the source, similarly as what shown in Figs. 3.6(a) and 3.8(a).

At this point taking into account what explained in Sect. 2.5.2, namely that a Shil'nikov-like strange attractors is a Russian doll containing infinite self-similar Feigenbaum-like strange saddles, the geometrical working principle of the qualitative resonance is easily understandable.

As explained in Sect. 2.5.2, the Shil'nikov-like strange attractors lie on an almost one-dimensional manifold, called the reinjection manifold, which has a transversal attracting direction, the system must tend to this manifold, and is repulsive in the directions that are parallel to this manifold, to let the system be chaotic. Since it has been assumed that the feedback gain matrix K does not alter excessively the dynamic of the system, it follows that the minimal[9] K which stabilizes the periodic solution $\widehat{x}(t)$, contained in the strange attractors, must mainly stabilize the repelling direction, namely the direction parallel to the strange attractor manifold, while leaving almost unaltered the dynamic in the already stable direction. Because of the existence of infinite self similar skeleton saddle cycles that lie on the strange attractor manifold, also a cycle built by a piecewise composition of arcs of skeleton cycles which, consequently, lies on the manifold and satisfies the tachometric law on it, can be stabilized by a similar procedure as the one described above. Obviously, such a new cycle cannot be to much different from the skeleton cycles, because of its construction constraints. Thus, it will be "just a generalization" of the stereotype cycles of the skeleton leading to the qualitative resonance phenomenon. A geometrical sketch of this working principle is given in Fig. 3.9. Therefore, in general, for a given Feigenbaum-like driving signal, namely a generalization of the generating cycle that still have a good correlation with the generating cycle, there must be in the infinite Feigenbaum-like saddles a good source model, then the control law let the system shrink on this solution leading to a

[6] In reality of any skeleton cycle, for this explanation the condition that the periodic solution is the generating cycle has not been used indeed, it will be useful later.

[7] In engineering the NRR is defined, in decibels, as $10Log_{10}\left(\sigma^2_{out}/\sigma^2_{in}\right)$ where $\sigma^2_{in,out}$ are the input and output noise variance. Should be noted that depending upon the chosen K the NRR could be either negative, the noise is indeed reduced, or positive, *i.e.* the noise is amplified. For the herein discussion it is reasonably supposed that the NRR is negative.

[8] There is a myriad of working applications of the Kalman filter where the Gaussian Hypothesis are not satisfied [Petersen and Savkin, 1999].

[9] Minimal to respect to some norm, for instance the small α condition given in Sect. 3.1.3 would corresponds to minimize the $\|\cdot\|_\infty$ norm of K.

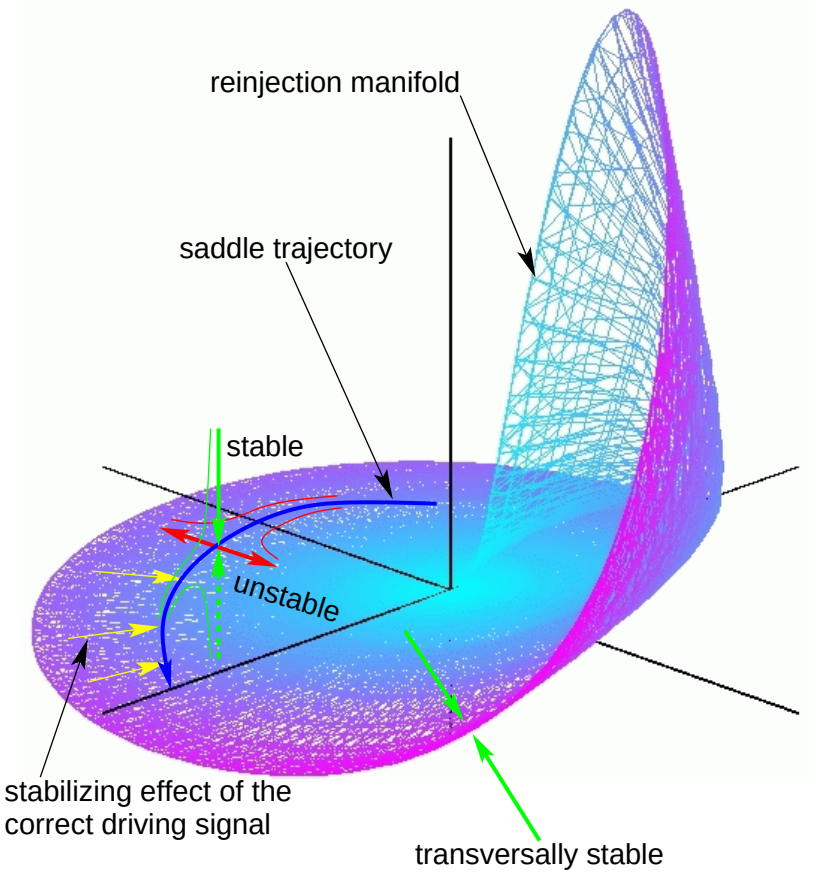

Figure 3.9: *The driving forces of qualitative resonance in a Shil'nikov-like strange attractor.*

very small error between the driving signal and the output signal, therefore the qualitative resonance test is going to be satisfied. In other words, the infinite Feigenbaum-like saddles build a base for signals similar to the generating cycle.

Explaining Qualitative Anti-Resonance

The previous argument explains how the resonance phenomena can be justified but nothing is said about the anti-resonance of signals that are too far from signal corresponding to the generating cycle. The stabilization theory explained before (*cfr.* Eqs. (3.4) to Eqs. (3.6)) is valid as far as the Jacobian of the driven system is close to the Jacobian of the source of the driving signal. Therefore, the only justification for anti-resonance is that there are cases where the Jacobian of the driven system changes significantly; hence, to little changes in the state space coordinate correspond big changes in the Jacobian and it is no longer close to the one of the driving signal. This is the case for Shil'nikov-like systems, indeed the vector field has a singularity in proximity of the equilibrium bearing the homoclinic trajectory that let the Shil'nikov-like attractor exist. Thus, it can be intuitively argued that the cause of an anti-resonance effect is the fact that the trajectory of the driven system approaches excessively the equilibrium or, more in general, the homoclinic trajectory that leads to the equilibrium.

The anti-resonance appears as an explosion of the strange attractor, namely the narrow Feigenbaum-like strange attractor that is observed in the case of resonance, Figs. 3.6(a) and 3.8(a), suddenly become wide, Figs. 3.6(c) and 3.8(c). Such a phenomenon strongly resembles the transition from spiral-type Shil'nikov-like chaos to screw-type Shil'nikov-like chaos as described in Sect. 2.5.2. Since the spiral to screw transition is indeed due to the approaching of the trajectories to the equilibrium bearing the homoclinic trajectory, that confirm the hypothesis that the anti-resonance is due to the driven trajectories approaching the singular point of the vector field, *i.e.* the equilibrium. Indeed, the monotonic to spiral change in the trajectories behavior, introduced by the saddle-focus equilibrium, is at the origin of Shil'nikov-like chaos.

From this intuitive explanation of anti-resonance it should be clear that the distance between the generating cycle and the homoclinic cycle, both embedded in the Shil'nikov-like attractor, plays the main role in

determining those signals that will resonate and those that will not, *i.e.* the distance between generating and homoclinic cycles determine somehow the maximum extent of the perturbations supported by the resonance phenomenon.

Summary of the Working Principle

The previous argument explaining the qualitative resonance in its entirety, resonance and anti-resonance, can be easily summarized as follows.

Resonance: for a driving signal that is a *good pattern* the system will wander until passing to a solution epsilon-close to the driving pattern, at this point due to the control law the system will resonate with (shrink on) the driving signal. Unfortunately, from Sect. 2.5.2, it is clear that the system could wander for an arbitrary long time before shrinking on the driving signal.

Anti-Resonance: for a driving signal that is a *bad pattern* the system will be recurrently forced to visit the expanding direction of the Shil'nikov-like strange attractor. Namely, when the bad stimulus leads the driven system to pass near the equilibrium the Shil'nikov's effect[10] is activated and the system becomes strongly chaotic.

To conclude, there are now strong and reasonable hypotheses about the working principle of qualitative resonance. However, these hypotheses need to be confirmed by a more detailed mathematical analysis that is indeed the subject of the next section. Before starting to present stronger mathematical results there are two noteworthy remarks that should be stated. Firstly, it should be noted that although the linear analysis presented here, and discussed in more detail later, is a correct argument it is neither a necessary nor a sufficient condition for qualitative resonance. Indeed, it is not difficult to perturb the clean signal $\widehat{y}$ by means of a small non Gaussian noise such that anti-resonance will be observed. This is illustrated in Fig. 3.10(a), there it is reported the behavior of the Colpitts oscillator in 1-pulse Shil'nikov conditions (*cfr.* point A in Fig. 3.1) driven by the signal corresponding to the 1-pulse generating cycle perturbed by a random "little" spike in correspondence of the minimum of the signal, as shown in Fig. 3.10(b). As result the driven system behaves chaotically. Vice versa, a strong regular corrupting signal can be designed such that a periodic solution, far from the generating cycle, will be stabilized as shown in Fig. 3.10(c) and (d). Secondly, it should be noted that theoretically it could happen that a system driven with a resonating signal would wander chaotically forever. Nevertheless, practically this has never been observed.

These remarks are given in order to let be clear which kind of answer can be reasonably looked for by a deeper mathematical analysis and which kind of trial would be, on the contrary, worthless.

3.3 Mathematical Analysis of Qualitative Resonance

Intuition has lead to formulate three conjectures about qualitative resonance. First, the resonance phenomenon can be interpreted as a linear periodic state reconstructor with fixed noise reduction ratio. Second, the anti-resonance is due to perturbations that lead the driven system to approach the equilibrium bearing the homoclinic trajectory. Third, the perturbations that lead to anti-resonance are mainly those in the unstable direction of the generating cycle.

The first conjecture is indeed not a conjecture since it can be easily confirmed by means of the results of periodic control [Bittanti and Colaneri, 1999], as done at the beginning of Sect. 3.2 and will be discussed further in Sect. 3.3.3. On the contrary, the other two are nothing more than conjectures that need confirmation by a deep mathematical analysis. Unfortunately, the described phenomena, mainly anti-resonance, are global phenomena that do not allow for a local analysis that is indeed one of the few possible analytical methods in nonlinear analysis. That is why such an analysis has been conducted combining advanced numerically techniques with theoretical arguments. Indeed, to support the conjectures, twenty cases of qualitative resonance have been deeply studied by means of bifurcation analysis in order to identify the main leading forces governing such a phenomenon. The results are presented in the next two sections.

In Section 3.1 it has been shown that some dynamical systems satisfy Shil'nikov's fourth theorem several times with respect to different parameter values and/or different geometries of the homoclinic trajectory. To

[10] The chaotic behavior induced by a sudden change from monotonic to spiral trajectories is sometimes called Shil'nikov's effect. For the specialists this is the effect that allows the existence of a Smale's horseshoe in the dynamic of the systems [Kuznetsov, 1998; Tresser, 1984].

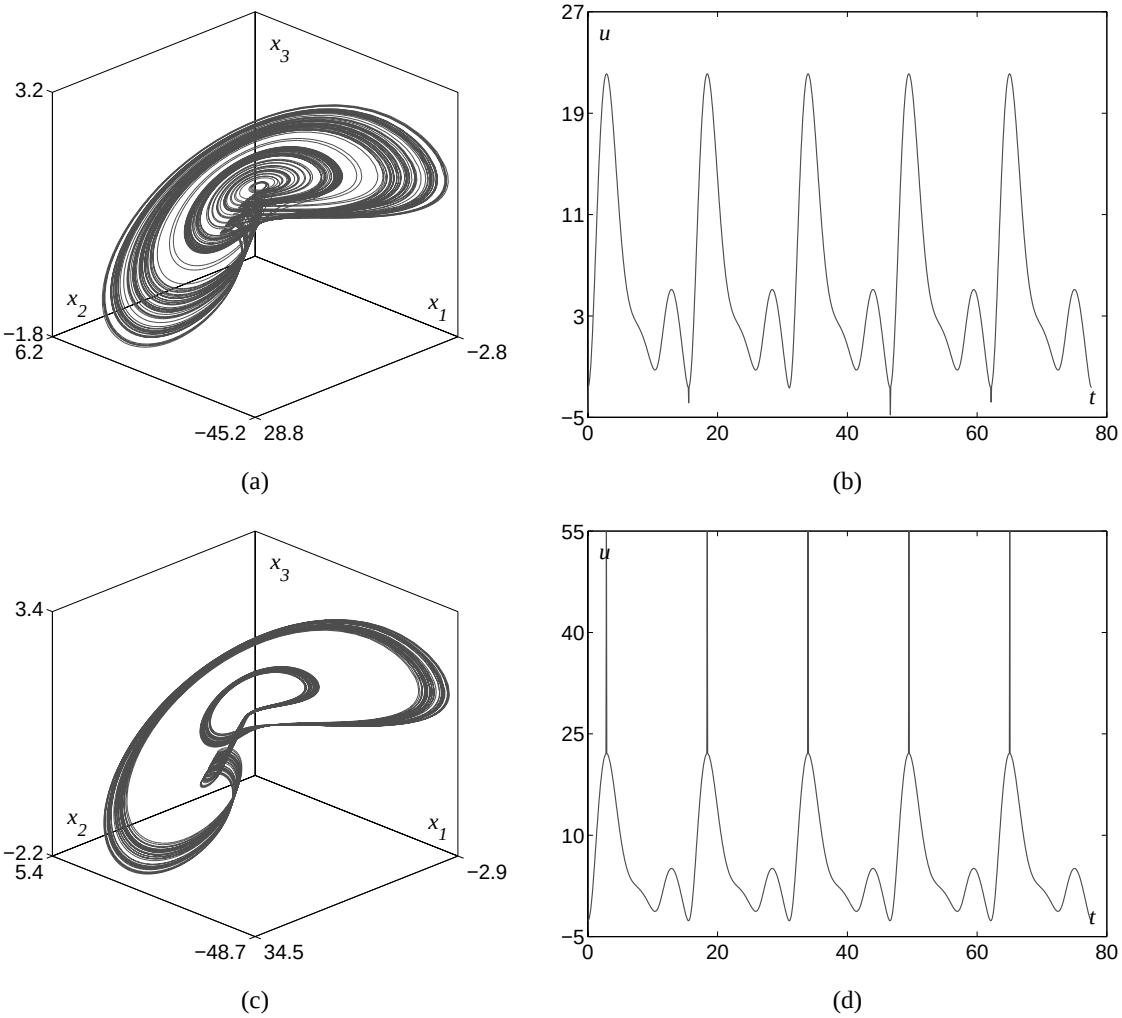

Figure 3.10: *Uncharacteristic qualitative resonance and anti-resonance: (a) – chaotic behavior of the Colpitts oscillator in* 1*-pulse Shil'nikov conditions while driven by the signal shown in (b); (b) – driving signal corresponding to the* 1*-pulse generating cycle of the Colpitts oscillator corrupted by a random "little" spike in correspondence of the minimum; (c) – approximately periodic behavior of the Colpitts oscillator in* 1*-pulse Shil'nikov conditions while driven by the signal shown in (e); (d) – driving signal corresponding to the* 1*-pulse generating cycle of the Colpitts oscillator corrupted by a regular "strong" spike in correspondence of the maximum.*

identify the geometrically different homoclinic trajectories one or more indexes are used. They refer to the number of global turns (loops, pulses) that a given homoclinic trajectory takes in particular regions of the state space [De Feo *et al.*, 2000; Mastumoto, 1993], as it was for the 1- to 5-pulse solutions shown before.

Since each set of homoclinic trajectories (generating cycle[11]) and parameter values satisfying Shil'nikov's fourth theorem is a good candidate for observing qualitative resonance, the same dynamical system can produce more than one case suitable for the mathematical analysis, as shown in Sect. 3.1. In fact, the twenty cases of qualitative resonance studied correspond to only six different dynamical systems that admit geometrical different homoclinic trajectories satisfying Shil'nikov's fourth theorem.

The first ten cases are the 1- to 5-pulse solutions of both the Colpitts oscillator and the Rosenzweig—MacArthur food chain previously presented. The other ten cases considered are famous dynamical systems that satisfy Shil'nikov's fourth theorem: Chua's circuit [Madan, 1993], for 2-1- and 3-2-pulse generating cycles; the Hindmarsh—Rose model for a neuron cell [Hindmarsh and Rose, 1984], for 4- to 6-pulse generating cycles; the Rössler system [Rössler, 1976], for 1- and 2-pulse generating signal; a variation of the Lorenz system [Lorenz, 1963], for parameters values quite far from those usually considered where a n-pulse solutions

[11] Homoclinic trajectory and generating cycle are strong relatives as shown in Sect. 2.5.2.

can be observed, in particular a 5- to 7-pulse generating cycle have been considered. In Appendix C the model equations and the parameter values considered are reported.

For all these cases[12] a deep analysis of the qualitative resonance has been performed, the detail of the analysis and of its results are reported in the next two sections.

3.3.1 Nonlinear Bifurcation Analysis

Bifurcation analysis is a deterministic tool, thus the perturbations of the driving signal that can be studied by means of this tool are only the deterministic ones. This is not a real restriction if the perturbations are chosen in a suitable way such as to bring the maximal insight about the dynamic structure of the phenomenon. Since the resonance, synchronization, of a dynamical system with a signal originating from the generating cycle has been shown to be a simple phenomenon, it is definitely interesting to consider the perturbations of this same signal and try to classify which are those that lead to resonate and which, on the contrary, lead to anti-resonate. Furthermore, it is important to determine which dynamic mechanisms link resonance and anti-resonance.

Analysis Framework

Similarly to what has been done in Sect. 3.2, consider a three dimensional[13] dynamical system in Shil'nikov's condition, *i.e.* close to the homoclinic bifurcation and in chaotic condition, and consider a generic[14] scalar linear observable of its state

$$\begin{aligned} \dot{\widetilde{x}} &= F(\widetilde{x}), \quad \widetilde{x} \in \mathbb{R}^3,\, F : \mathbb{R}^3 \mapsto \mathbb{R}^3 \\ \widetilde{y} &= C\widetilde{x}, \quad y \in \mathbb{R},\, \dim(C) = 1 \times 3 \end{aligned}$$

Let

$$\widehat{x}(t), \quad t \in [0, T_G],\, \widehat{x}(T_G) = \widehat{x}(0)$$

be the generating cycle, of period T_G, associated with the homoclinic trajectory and

$$\widehat{y}(t) = C\widehat{x}(t)$$

the corresponding scalar observable. Considering the following non autonomous system

$$\begin{aligned} \dot{x} &= F(x) - K(y - y_d), \quad \dim(K) = 3 \times 1 \\ y &= Cx \\ y_d(t) &= \widehat{y}(t) + \varepsilon(t) \end{aligned} \tag{3.7}$$

Namely, a driven system where the driving signal $y_d(t)$ is a perturbation of $\widehat{y}(t)$ while the feedback gain matrix K, according to what was presented in Sect. 3.2, is chosen as the ∞-norm minimal stabilizing feedback. The interest is in the behavior of the system depending upon the deterministic perturbation $\varepsilon(t)$. Furthermore, in order to guarantee the periodicity of the driving signal the perturbation $\varepsilon(t)$ must be either constant or a periodic signal with a period in rational ratio with the period of $\widehat{y}(t)$.

The generating cycle $\widehat{x}(t)$, being a saddle cycle at the chosen parameter values, has associated three one-dimensional manifolds: the stable manifold W_s, being the set of initial conditions converging to the cycle forward in time; the unstable manifold W_u, being the set of initial conditions converging to the cycle backward in time; the center manifold W_c, *i.e.* the cycle itself. The tangent vectors at these three manifolds in any point of the cycle

$$\widehat{x}(\tau), \quad \tau \in [0, T_G)$$

are identified by the eigenvectors of the monodromy matrix of the system evaluated at the point $\widehat{x}(\tau)$. Namely, considering

$$A(t) = \left.\frac{\partial F(x)}{\partial x}\right|_{x=\widehat{x}(t)}, \quad A(t + T_G) = A(t)$$

[12] In reality, the analysis presented in the next sections have been performed on more cases than that but a complete and rigorous study has been conducted only for the cited twenty cases.

[13] The restriction to three-dimensional systems simplify the expositions but most of the results found have been verified for systems in $\mathbb{R}^n$ with $n > 3$. Nevertheless, all the systems explicitly considered here are three-dimensional systems.

[14] Namely, a linear observation $\widetilde{y} = C\widetilde{x}$ such that the pair $\left(\frac{\partial F(\widetilde{x})}{\partial \widetilde{x}}, C\right)$ is observable for almost any t.

the monodromy matrix [Callier and Desoer, 1991; Kuznetsov, 1998] of the cycle at a point $\widehat{x}(\tau)$ is defined as

$$\Psi(\tau) = \Phi(\tau + T_G, \tau)$$

where

$$\Phi(\tau, t) : \frac{\partial}{\partial t}\Phi(t, \tau) = A(t)\Phi(t, \tau), \quad \Phi(\tau, \tau) = I$$

The monodromy matrix $\Psi(\tau)$ has three eigenvalues that do not depend on τ, called characteristic multipliers of the cycle [Callier and Desoer, 1991; Kuznetsov, 1998], $\mu_1 = 1$, $|\mu_2| < 1$, and $|\mu_3| > 1$. Their corresponding eigenvectors identify the tangent to the center, stable, and unstable manifolds of the cycle at point $\widehat{x}(\tau)$. Namely, the tangent to the three manifolds are given by

$$\begin{aligned} T\left(W_c(\tau)\right) &= e_p(\tau)\ , \quad e_p(\tau) :\ \Psi(\tau)e_p(\tau) = e_p(\tau) \\ T\left(W_s(\tau)\right) &= e_s(\tau)\ , \quad e_s(\tau) :\ \Psi(\tau)e_s(\tau) = \mu_2 e_s(\tau) \\ T\left(W_u(\tau)\right) &= e_u(\tau)\ , \quad e_u(\tau) :\ \Psi(\tau)e_u(\tau) = \mu_3 e_u(\tau) \end{aligned}$$

Note that because of the periodicity of the monodromy matrix, the characteristic eigendirections are, up to a constant factor, periodic functions of t, namely $e_i(\tau + T_G) = \mu e_i(\tau)$.

For the purpose of this analysis it is convenient to split the generic deterministic perturbation $\varepsilon(t)$ according to these three vectors. Namely,

$$\varepsilon(t) = C\big(e_p\delta_p(t) + e_s\delta_s(t) + e_u\delta_u(t)\big) = C\delta_{\widehat{x}}(t) \tag{3.8}$$

Note that the index "p" stands for phase perturbation. This framework allows to determine separately the influence on resonance given by the perturbation on phase, stable, and unstable directions.

The analysis framework described is not complete as long as the perturbing functions $\delta_i(t)$, $i = p, s, u$ are not given. For this analysis three possible forms for each of the $\delta_i(t)$ functions have been considered

1. *static perturbation*: $\delta_i(t) = \overline{\delta}_i$;
2. *slow sinusoidal*: $\delta_i(t) = \overline{\delta}_i sin(\omega_i t)$, in order to guarantee the periodicity of $y_d(t)$, ω_i must be chosen as a rational fraction of $2\pi/T_G$, in particular for the analysis $\omega_i = \pi/(5T_G)$ has been chosen;
3. *fast sinusoidal*: it is the fast version of the previous case, *i.e.* $\delta_i(t) = \overline{\delta}_i sin(\omega_i t)$ where $\omega_i = 20\pi/T_G$.

Note that the system (3.7) is a non autonomous system, therefore, to determine its initial condition, an initial phase for the signals $\widehat{y}(t)$ and $\varepsilon(t)$, with respect to the initial state $x(0)$ of the driven system, must be chosen. Since the interest is in the resonance and anti-resonance phenomena and not on the phase locking phenomenon, the phase of the main part of the driving signal has always been set to zero, *i.e.* the initial state $\widehat{x}(0)$, which determines the initial phase of the main part of the driving signal $\widehat{y}(t)$, has always been set equal to the initial state $x(0)$. A similar choice has been made for $\varepsilon(t)$, fixing the initial time always at $t = 0$. Since $\overline{\delta}_i$ can be either positive or negative this implies two possible initial phases for sinusoidal perturbations $\delta_i(t)$.

A bifurcation analysis of the system (3.7) and (3.8) with respect $\overline{\delta}_u$ and $\overline{\delta}_s$, at different values of $\overline{\delta}_p$, has been conducted for all the eighty-one (3^3) possible combinations of perturbations and for all the twenty cases introduced above. The bifurcations analysis has been carried out by means of AUTO97 [Doedel *et al.*, 1998] and CONTENT [Kuznetsov and Levitin, 1997] two powerful continuation environments designed for bifurcation analysis. How to implement the bifurcation analysis of such driven systems is quite tricky and is described in Appendix D.

ANALYSIS RESULTS

The overall bifurcation analysis has required about nine months of works but amazingly the result is incredibly compact and synthetic. Indeed, albeit the single bifurcation diagrams for each case are quantitatively different all of them can be qualitatively described by the bifurcation diagrams shown in Fig. 3.11.

The bifurcation diagrams are always approximately symmetric, sometimes they are symmetric with respect to the origin and sometimes they are symmetric with respect to both the x and y axis. Furthermore, the difference in scale of the effect of the two parameters, namely the apparent stretching in the vertical direction of the bifurcation diagram, is generic albeit quantitatively different from case to case. A particular case of this bifurcation diagram is shown in Fig. 3.12.

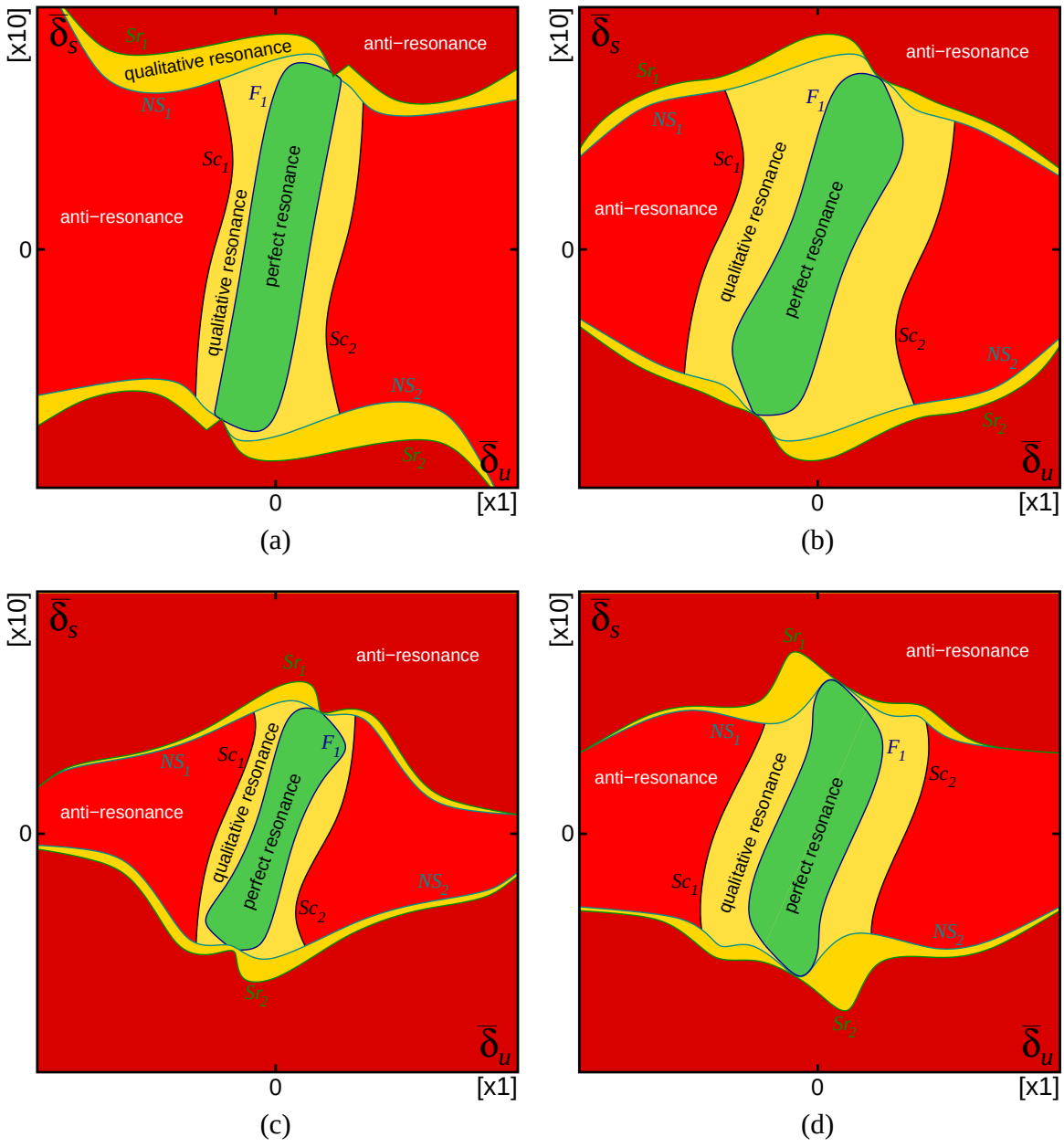

Figure 3.11: *General bifurcation diagram of the qualitative resonance with respect to perturbations in the unstable ($\overline{\delta}_u$) and stable ($\overline{\delta}_s$) directions at different intensities and kind of the phase perturbations ($\overline{\delta}_p$): (a) – any possible stable perturbation with respect to static or slow unstable perturbations at weak phase perturbation, if static or slow, or at medium intensity phase perturbation, if fast; (b) – any possible stable perturbation with respect to fast unstable perturbations at weak phase perturbation, if static or slow, or at medium intensity phase perturbation, if fast; (c) – any possible stable perturbation with respect to static or slow unstable perturbations at any possible strong phase perturbation; (d) – any possible stable perturbation with respect to fast unstable perturbations at any possible strong phase perturbation.*

Disregarding the differences between static/slow and fast perturbations, commented later, the bifurcation diagrams in Fig. 3.11 must be interpreted as follow.

For perturbations such that the parameter vector is inside the green or yellow regions the system qualitatively resonate. In the green region the driving signal and the driven system perfectly resonate, synchronize, and the system behaves on a limit cycle close to the generating cycle $\widehat{x}(t)$. Increasing the perturbations in the unstable directions such that the parameter vector enters, through the line F_1, the region of narrow Feigenbaum-like chaos, light yellow region, the drive system becomes chaotic but the corresponding strange

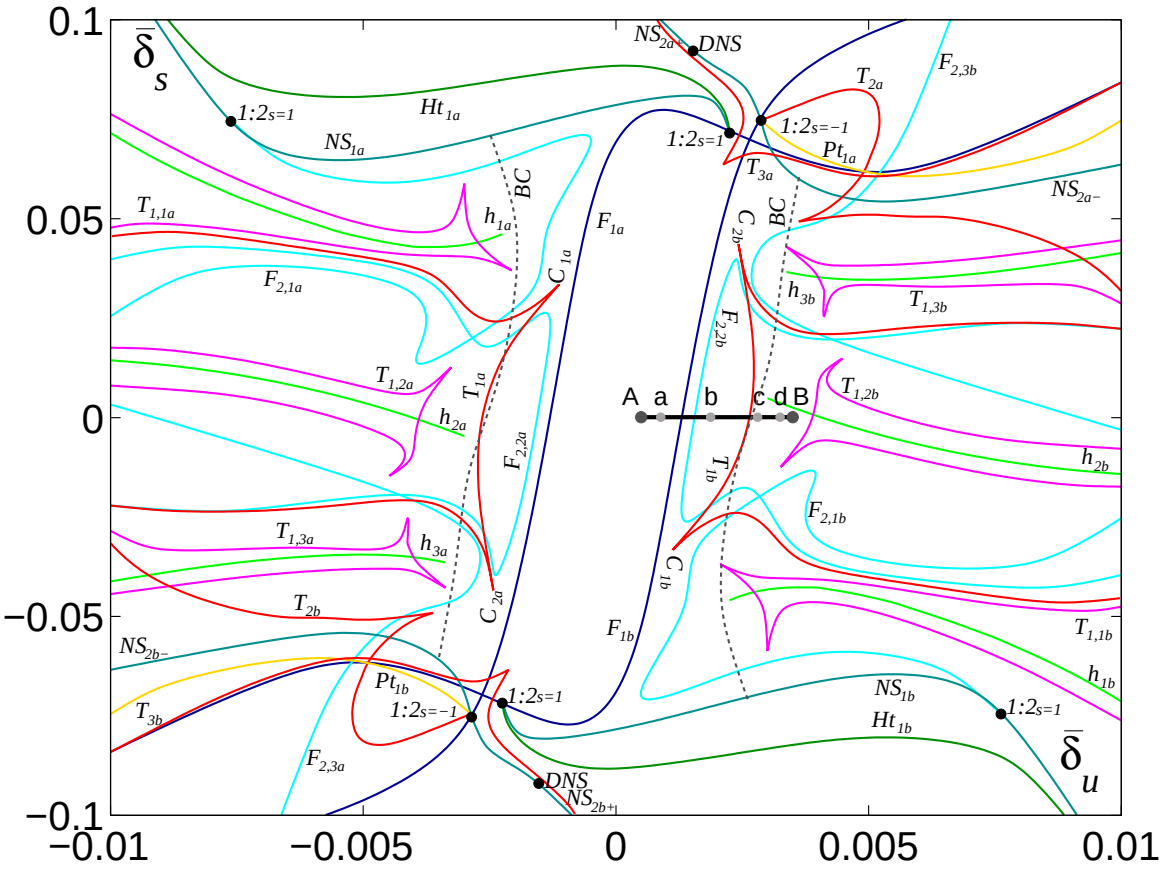

Figure 3.12: *Bifurcation diagram of the qualitative resonance with respect to perturbations in the unstable and stable directions for the case of* 1*-pulse solution in the Colpitts oscillator. All the perturbations are of slow sinusoidal kind while the phase perturbation is rather weak (*$\bar{\delta}_p = 0.03$*). Legend of labels:* F_i *– flip bifurcations (cyan or blue);* NS_i *– Neimark—Sacker bifurcations (dark cyan);* h_i *– homoclinic bifurcations (green);* Ht_i *– heteroclinic bifurcations of limit cycles (dark green);* Pt_i *– homoclinic bifurcations of limit cycles (yellow);* T_i *– tangent bifurcations of limit cycles (red or magenta);* C_i *– cusp codim-2 points;* DNS *– degenerate Neimark—Sacker codim-2 points;* $1:2$ *–* $1:2$ *strong resonance codim-2 points;* BC *– approximate boundary crisis limit (black dashed).*

attractor is a narrow one and containing the generating cycle $\widehat{x}(t)$ such that the system can be classified as resonating. On the other hand, increasing the perturbations in the stable directions such that the parameter vector enters, through the line NS_1, the region of torus behavior, dark yellow region, the drive system become quasi-periodic but the corresponding torus is a narrow one and contains the generating cycle $\widehat{x}(t)$ such that the system can be classified as resonating.

For perturbations such that the parameter vector is inside the red region the system qualitatively anti-resonates. For strong perturbations in the unstable directions such that the parameter vector enters, through the line Sc_1, the region of wide Shil'nikov-like chaos, light red region, the drive system become chaotic and the corresponding strange attractor is a Shil'nikov-like of screw-type, thus is quite spread such that the system can be classified as anti-resonating. For strong perturbations in the stable directions such that the parameter vector enters, through the line Sr_1, the region of torus-destroyed-like chaos, dark red region, the driven system undergoes a $1:n$ strong resonance and the quasi-periodic behavior is destroyed becoming chaotic, the corresponding strange attractor is quite spread such that the system can be classified as anti-resonating.

From Figure 3.11 it is clear that the perturbations in the unstable direction are more effective in leading to anti-resonance than the perturbations in the stable directions. Hence, for a generic perturbed driving signal, where no one of the two components is dominant, it will be definitely the perturbations in the unstable directions which will determine the anti-resonance. The dominance of unstable direction perturbations is not changed by phase perturbations, indeed Fig. 3.11 shows that phase perturbations shrink the bifurcation

diagram in both the x and y direction. Since the perturbations in the unstable directions are the dominant mechanism that drive the system to anti-resonance, the next section has been dedicated to the detailed description of the transition from resonance to anti-resonance along such direction.

The results of this almost exhaustive analysis can be summarized as follow.

Perturbations in the stable direction: could be very strong without effect, when effective lead to the appearance of torus and torus-destroyed-like chaos. Static or slow perturbations are more effective for anti-resonance than fast perturbations.

Perturbations in the unstable direction: even of small intensity lead easily to anti-resonance, the anti-resonance regime is Shil'nikov-like chaos. Static or slow perturbations are more effective for anti-resonance than fast perturbations.

Phase perturbations: when static or slow they anticipate the anti-resonance, *i.e.* they decrease the area of the region of qualitative resonance, if fast they are not very influent.

These results confirm the third of the conjectures formulated at the beginning, indeed they show that the main cause of anti-resonance are perturbation in the unstable direction while perturbation in the stable direction are not so important. Note that phase perturbations are never very strong if phase locking is guaranteed between the driving signal and the driven system, it will be shown later in Chap. 4 how this can be achieved.

The fact that slow perturbations are more effective than fast ones is not so surprising if it is taken into account the fact that all the considered systems (*cfr.* Appendix C) have an integrative effect on the driving signal and not a derivative one. Thus, such a result should not be taken as general but rather associated to the particular fact that no one of the considered system was having a *transmission zero*[15] of the triplet $(A + KC, K, C)$ at a frequency higher than that of the considered frequencies [Brogan, 1996; Callier and Desoer, 1991; De Nicolao *et al.*, 1998]. Even though mathematically this is a particular case, in practice this should be considered the generic case since low pass system are definitely the rule rather than the exception.

3.3.2 One-Dimensional Bifurcation Analysis

Since it has been shown that are the perturbations in the unstable directions that lead a system to anti-resonance, here it is analyzed in detail what happens in the unstable direction that leads the system to anti-resonate.

In Section 2.5.2 it has been shown that the chaotic behavior of Shil'nikov-like strange attractors is determined by the behavior of the trajectories on the almost two-dimensional reinjection manifold on which the attractor lies, Fig. 2.36. As already explained in Sect. 3.2 this manifold is transversally stable and the trajectories on it are unstable in the direction parallel to this manifold. Furthermore, in the previous section it has been shown that the transition from resonance to anti-resonance is mainly determined by the perturbation on this unstable direction, which means that such a transition is mainly determined by the behavior on such a manifold. Thus, the transition is determined by the dynamic behavior and the bifurcations of a one-dimensional map, *i.e.* the Poincaré map of the system in the unstable direction on the reinjection manifold.

Suppose the perturbation of a dynamical system is in the proximity of a Shil'nikov homoclinic bifurcation, the reinjection manifold exists independently from the fact that the trajectories on the final attractors fill it densely or not, namely independently from the fact that the system is chaotic or not. Indeed, such a manifold exists in a whole neighborhood of the homoclinic bifurcation [Gaspard *et al.*, 1984], it is an invariant of the system and it can be computed by means of particular numerical methods [Dellnitz and Hohmann, 1996; Dellnitz and Junge, 1997]. From the computation of the reinjection manifold it is possible to derive the one-dimensional map governing the dynamics of the trajectories on this manifold.

The transition to anti-resonance observed when augmenting the intensity of the perturbations in the unstable direction, *i.e.* moving on the generic line A–B in Fig. 3.12, has been studied on the one dimensional Poincaré map on the reinjection manifold for all the twenty cases under study. Once again, despite of quantitative differences, the qualitative result is synthetic and compact. The analysis has identified four main stages that lead to anti-resonance when increasing the perturbations in the unstable direction. They corresponds to the four behaviors shown in Fig. 3.13(b-e) and to the four one-dimensional maps shown in

[15] Zeros of transfer functions induce derivative effects [Brogan, 1996; Callier and Desoer, 1991; De Nicolao *et al.*, 1998].

Fig. 3.14(b-e). Figure 3.13 shows the Feigenbaum diagram, and the corresponding attractors, of the driven 1-pulse Colpitts oscillator when sliding the parameters along the segment A–B shown in Fig. 3.12 while Fig. 3.14 shows the one-dimensional maps on the reinjection manifold corresponding to the free, autonomous system, and to the driven system in the points a, b, c and d in Fig. 3.12. The results shown in Figs. 3.13 and 3.14 are particular for the case of 1-pulse solution in the Colpitts oscillator but the route to anti-resonance they illustrate is general and has been observed in all the twenty cases under analysis.

The four stages that lead to anti-resonance are the following.

1. *Perfect locking*: case shown in Figs. 3.13(b) and 3.14(b), it corresponds to the green region shown in Fig. 3.11. The driving signal and the driven system perfectly resonate and the system behaves on a limit cycle close to the generating cycle.

2. *Qualitative locking*: case shown in Figs. 3.13(c) and 3.14(c), it corresponds to the light yellow region shown in Fig. 3.11. The driven systems subresonante with the driving system and behaves on a $r2^n$ limit cycle or on a very narrow Feigenbaum-like chaotic attractor very close to the generating cycle.

3. *Boundary crisis*: case shown in Figs. 3.13(d) and 3.14(d), it corresponds to the light red region shown in Fig. 3.11. The narrow chaotic attractor explodes in amplitude, because of a boundary crisis, and the driven system and driving signal are no longer locked neither exactly nor qualitatively.

4. *Swapout*: case shown in Figs. 3.13(e) and 3.14(e), it still corresponds to the light red region shown in Fig. 3.11. After that the narrow chaotic attractor explodes in amplitude, further increase of the perturbations in the unstable directions monotonically increase the width of the strange attractor.

These four stages are described in details in the next paragraphs.

Perfect Locking

In this case, the driving signal is not very different from the generating cycle, as result the generating cycle is stabilized by the control law. Indeed, the point GC in 3.14(b) has a negative slope larger than -1 while the corresponding generating cycle is unstable in the free system, the point GC in 3.14(a) has a negative slope smaller than -1.

The change of slope at point GC is easily explained by the linear control theory as done in Sect. 3.2. On the contrary, the flexure of the Poincaré map faraway from such a point is due to the nonlinearities of the system and cannot be explained with linear arguments. In particular, the nonlinear effects of the driven system are more and more excited as the trajectories pass closer to the equilibrium bearing the homoclinic trajectory. Indeed, as already said, the Jacobian of the system strongly change only in proximity of singular points.

The intensity of the perturbations in the unstable direction is shown by means of the bold segment in Fig. 3.14(b). The bold segment shows the direct maximal deviation from the generating cycle due to the perturbations in the unstable directions of the driving signal. Namely, it shows the projection onto the reinjection manifold of the state determining the driving signal $x_d(t) = \widehat{x}(t) + \delta_{\widehat{x}}(t)$ (*cfr.* system (3.7) and (3.8)).

Since in this case the perturbations are small, the nonlinear effects due to the perturbations are negligible with respect to the linear effects of the control law. Namely, the perturbed Poincaré map is slightly deformed with respect to the free one, Fig. 3.14(a), only in the neighborhood of the generating cycle GC which is therefore stabilized.

Qualitative Locking

Increasing the intensity of the perturbations in the unstable direction lead to excite more and more the nonlinearities of the driven system until the nonlinear effects due to the perturbations become prevalent on the effect of the linear control law. This is shown in Fig. 3.15 where the dependence of the map upon the intensity of the perturbation is reported.

Once again, the intensity of the perturbations in the unstable direction is shown by the bold segment in both Fig. 3.14(c) and in Fig. 3.15. As can be seen comparing the bold segments in Fig. 3.15 with the bold segment in Fig. 3.14(b), the deformation of the Poincaré map in the neighborhood of the point GC is achieved by an imperceptible, in intensity, change in the intensity of the perturbations.

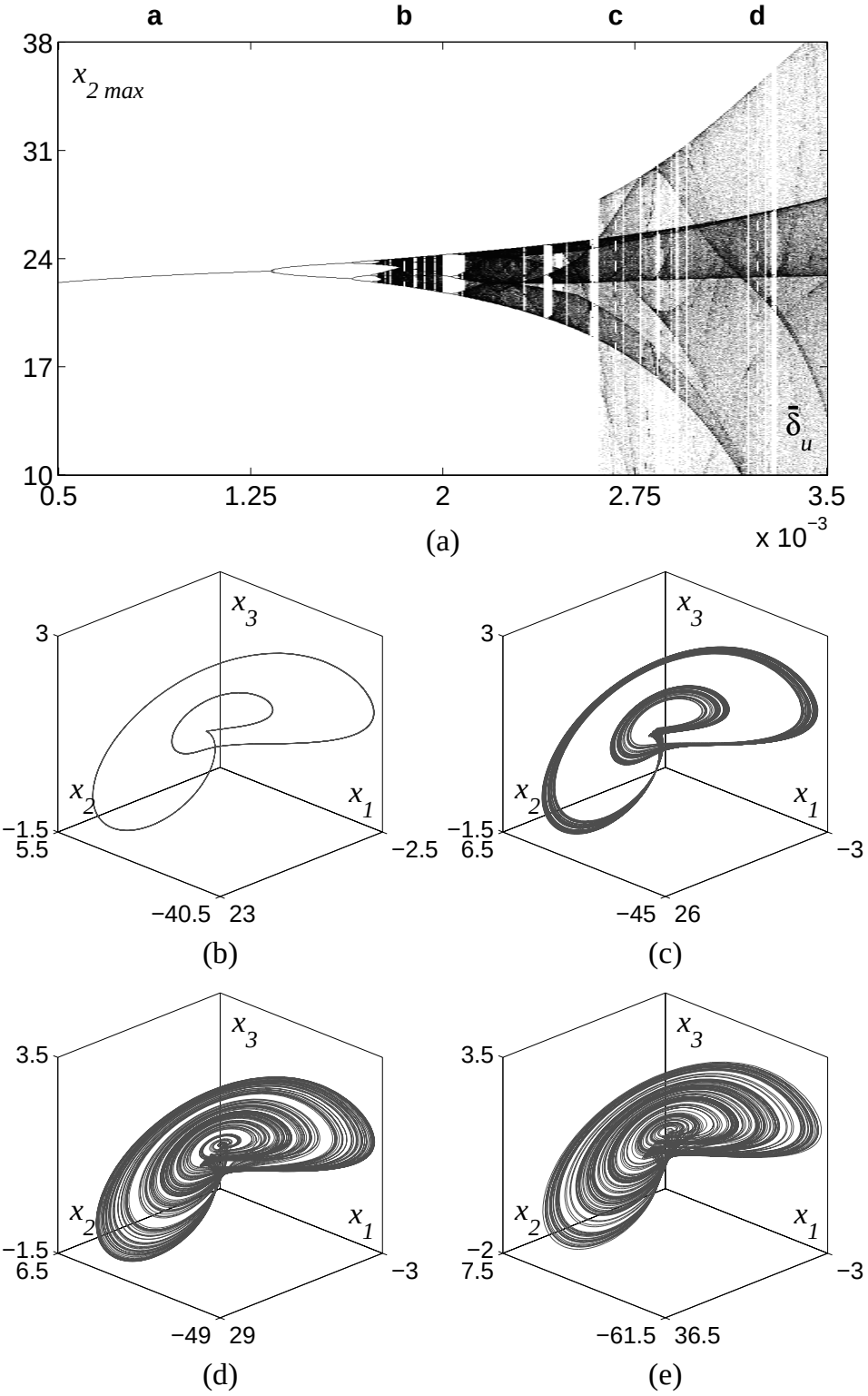

Figure 3.13: *Route from resonance to anti-resonance through chaos crisis and swapout of the unstable manifold, path* A–B *in Fig. 3.12, for the case of* 1*-pulse solution in the Colpitts oscillator: (a) – Feigenbaum's diagram of the attractors along the path* A–B*; (b) – stable limit cycle at* $\overline{\delta}_u = 0.8750E-3$*, point* a *in Fig. 3.12; (c) – Narrow Feigenbaum-like strange attractors at* $\overline{\delta}_u = 1.8470E-3$*, point* b *in Fig. 3.12; (d) – Shil'nikov-like strange attractors at* $\overline{\delta}_u = 2.6740E-3$*, point* c *in Fig. 3.12; (e) – swapout effect on the Shil'nikov-like strange attractors at* $\overline{\delta}_u = 3.2270E-3$*, point* d *in Fig. 3.12.*

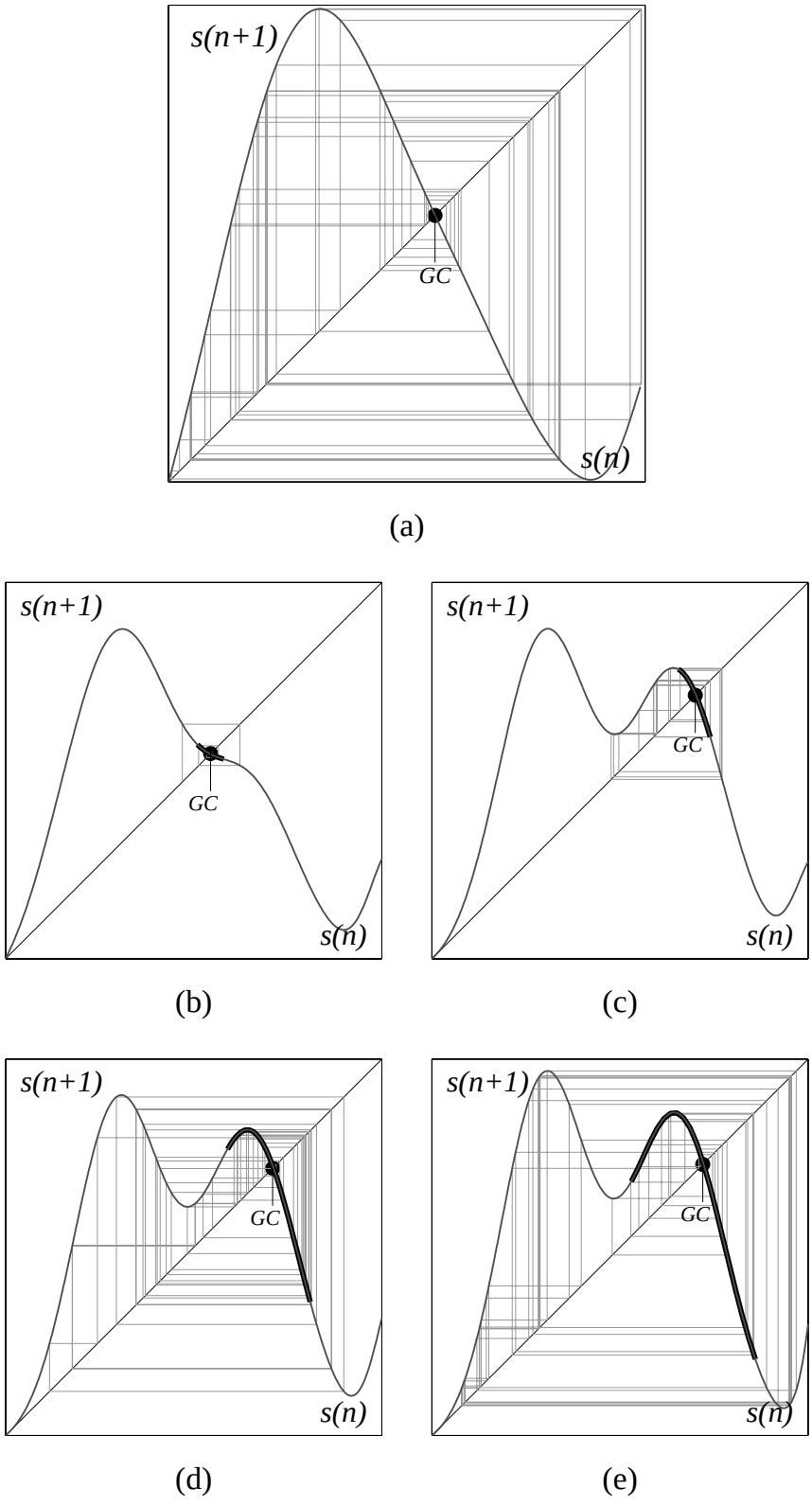

Figure 3.14: *One-dimensional maps on the reinjection manifold for the case of* 1*-pulse solution in the Colpitts oscillator: (a) – free system; (b), (c), (d) and (e) correspond to the points* a, b, c *and* d *in Fig. 3.12 respectively.*

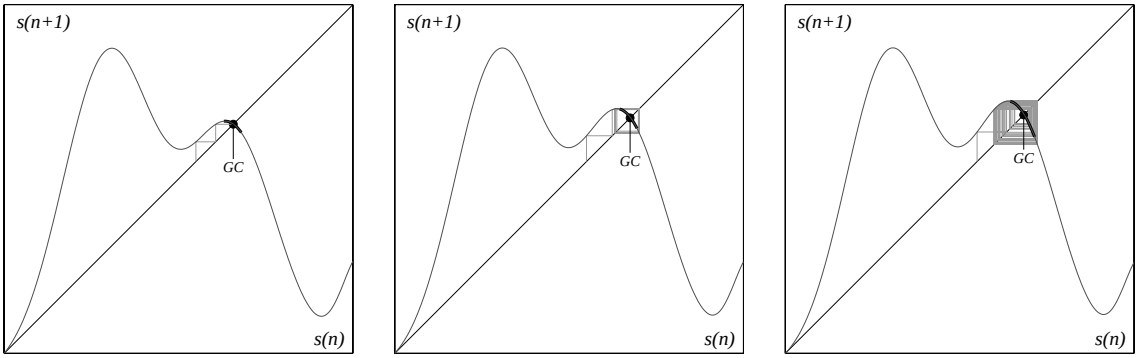

Figure 3.15: *One-dimensional maps on the reinjection manifold for the case of* 1*-pulse solution in the Colpitts oscillator: (a) – linear effects of the control law dominating over the nonlinear effect of the perturbations; (b) – linear effects of the control law and nonlinear effect of the perturbations almost equivalent; (c) – linear effects of the control law dominated by the nonlinear effect of the perturbations.*

Increasing the intensity of the perturbations change the slope of the Poincaré map at point GC until it reaches -1. At this point the generating cycle undergoes a flip bifurcation. Increasing the perturbation further lead the system to chaotic behavior by a "simple" Feigenbaum's cascade. The appearance of Feigenbaum-like chaos is due to the unimodal shape of the second wiggle of the Poincaré map in the neighborhood of the point GC. For the same reason the emerging strange attractor is narrow and close to the generating cycle, *i.e.* the GC point.

Boundary Crisis

Increasing further the intensity of the perturbations increase the effect of the excited nonlinearities that has as effect to increase the amplitude of the second wiggle of the Poincaré map, Fig. 3.16(a). This do not change the qualitative behavior of the driven system until the maximal point M in Fig. 3.16 is mapped onto points on the descending side at the left of point m of the Poincaré map which are lower than M itself.

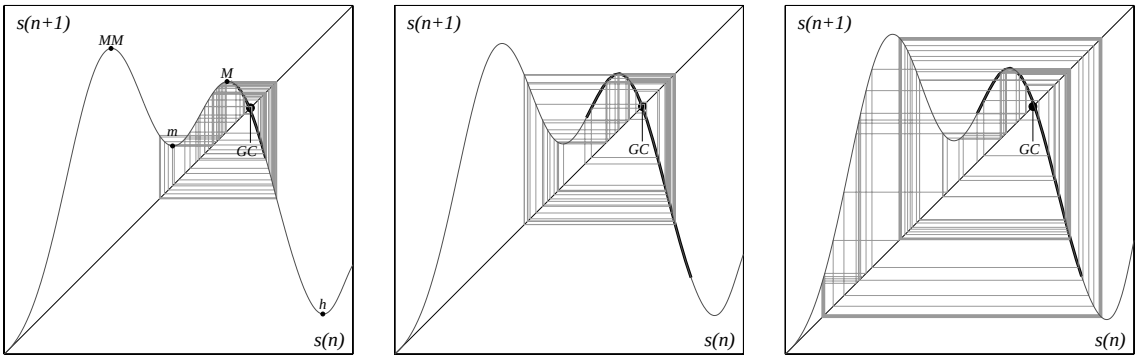

Figure 3.16: *One-dimensional maps on the reinjection manifold for the case of* 1*-pulse solution in the Colpitts oscillator: (a) – increased amplitude of the second wiggle due to the nonlinear effect of the perturbations; (b) – Poincaré map at the boundary crisis; (c) – wide strange attractor after the boundary crisis.*

When the perturbations are strong enough such that the point M is mapped exactly into itself, the system undergoes an important bifurcation, Fig. 3.16(b). This transition is known for four modal maps as those shown herein, it is known to involve several subsidiary bifurcations [Hansen, 1993, 1994; Hansen and Cvitanovič, 1998] and different kinds of exotic phenomena can be observed for parameter values around such a bifurcation depending on the relative values of maxima and minima. Similar bifurcations can be observed in generic system, not necessarily four modal maps, depending on what is the main bifurcation and what is

considered as subsidiary effect these bifurcations take several exotic names among which *boundary crisis* [Osinga and Feudel, 2000], *homoclinic tangency* [Gonchenko *et al.*, 1997], *homoclinic contact* [Kuznetsov, 1998], *superstability crisis* [Zhou and Peng, 2000], *type III intermittency* [Ott, 1993] and other [Robert *et al.*, 2000].

Despite of the colorful variety of phenomena related to this bifurcation there are only two of interest for this analysis. These results are for continuous four modal maps with the first maximum higher than the second and the first minimum higher than the second [Hansen, 1993], that is exactly the configuration shown in Fig. 3.16.

Firstly, after the bifurcation point the strange attractor explodes, namely it becomes wide as shown in Fig. 3.16(c). Thus, this bifurcation marks the threshold between the qualitative resonance and anti-resonance.

The second phenomenon of interest is the fact that, under not so generic condition of the four modal map[16], when this bifurcation happen there is also a trajectory passing arbitrarily close to all the extremants MM, m, M, and h [Hansen, 1993]. Remembering that the point h corresponds to the homoclinic trajectory of the system and arbitrarily[17] inverting cause and effect, the explosion of the attractor can be thought as due to an excessive proximity of the system to the homoclinic trajectory. This is confirmed by the intensity of the perturbation needed to deform the Poincaré map enough to obtain the chaos crisis, reported by the bold segments in Fig. 3.16. As can be seen, the perturbations leads the system to definitely approach the homoclinic trajectory h, this condition has been verified in all the cases under analysis.

Swapout

Increasing further the perturbation over the threshold of the boundary crisis leads to a monotonic enlargement of the strange attractors, as shown in Fig. 3.13(a) for $\overline{\delta}_u > 2.6102E-3$.

This phenomenon is related to the spiral-type to screw-type transition in Shil'nikov-like chaotic systems as discussed in Sect. 2.5.2. The trajectories visiting the part of the Poincaré map on the left of the h point correspond to trajectories that are reinjected on the "other side" of the equilibrium, *cfr.* Sect. 2.5.2. The farther the trajectory of the one-dimensional map is on the left of point h the farer from the equilibria, on the other side, the trajectory is reinjected in the system. This correspond to enlarge the visited portion of the unstable focus manifold of the equilibrium, as illustrated in Fig. 3.18, thus the name swapout effect [Gaspard *et al.*, 1984; Glendinning and Sparrow, 1984].

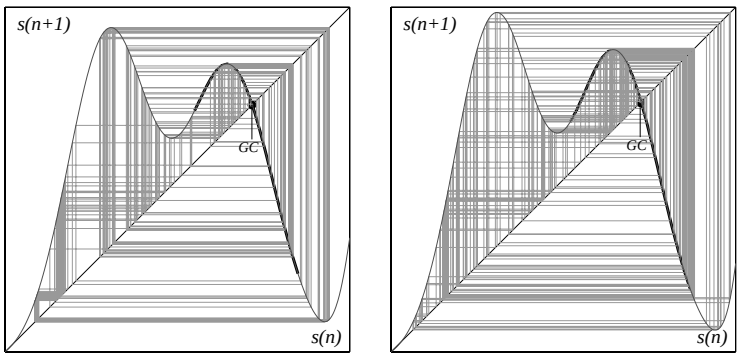

Figure 3.17: *One-dimensional maps on the reinjection manifold for the case of* 1*-pulse solution in the Colpitts oscillator: (a) – a small portion of the opposite reinjection side is visited; (b) – a large portion of the opposite reinjection side is visited.*

Remarks on the Results

These results practically confirm the second of the conjectures formulated at the beginning, indeed they suggest that the main mechanism driving towards anti-resonance is an approaching of the driving signal

[16] Unfortunately, this is often the case for the theoretical results in nonlinear system theory.
[17] Unfortunately, the inverse it is not necessarily true.

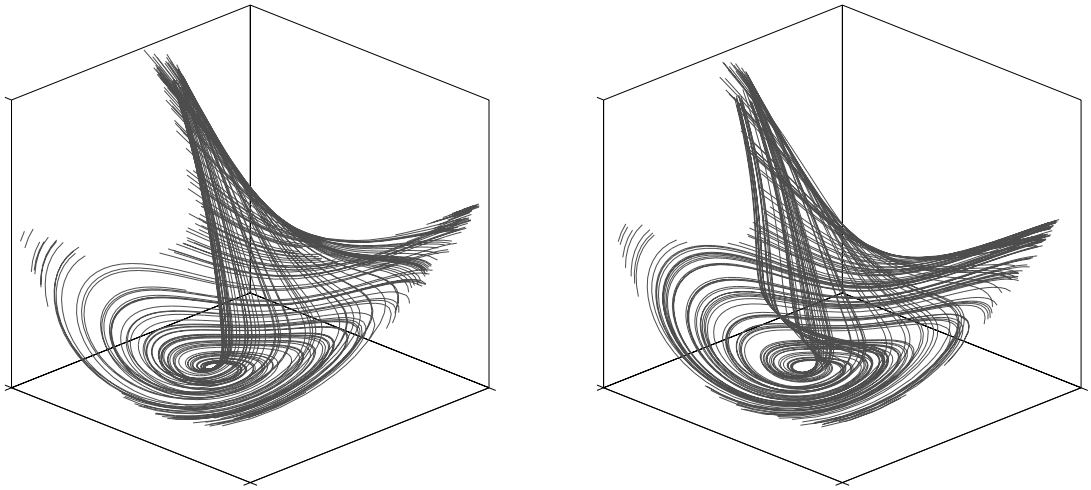

(a) (b)

Figure 3.18: *Behavior in the state space corresponding to the one-dimensional maps shown in Fig. 3.17: (a) – a small portion of the opposite reinjection side is visited; (b) – a large portion of the opposite reinjection side is visited.*

to the homoclinic trajectory. More in particular, they confirm the conjecture that the explosion of anti-resonance is due to the fact that the trajectories of the driven system are forced to pass close to the reinjection point nearby the equilibrium bearing the homoclinic trajectory. In Chapter 6 it will be shown how to exploit this knowledge in order to tune qualitative resonance according to the one's own needs.

A final remark concerns the possibility of multiple attractors of the driven system. It is not very difficult to identify configurations of the maps shown in Figs. 3.14, 3.15, and 3.16 such that multiple attractors are possible. This clearly confirms the remark, about the impossibility of determining necessary and sufficient conditions for qualitative resonance, ending Sect. 3.2.

3.3.3 Linear Analysis

The aim of this paragraph is just to clarify some points about the linear results shown in Sect. 3.2 under the enlightenment given by the nonlinear analysis. In particular, the aim is to show what are the easiest possible techniques to determine the relationships between qualitatively resonating signals and the driven dynamical system. Even though this paragraph is dedicated to any reader, for the sake of shortness, the details are restricted to readers familiar at least with the fundamental concepts of optimal control and filtering theory as well as with the concepts of linear periodic control theory, the esoteric reader can refer to [Bittanti and Colaneri, 1999; Bryson, 1996] for a brief introduction while [Brogan, 1996; Burl, 1999; Feuer and Goodwin, 1996] can give some deeper insight.

In the framework of system (3.7) consider together both the dynamical system generating the driving signal, *i.e.* the tilde system, and the driven system, let $\widehat{x}(t)$ be the *nominal* periodic regime of the driving system and $\widehat{y}(t)$ the corresponding output. Moreover, assume that driving and driven system are initially almost in phase such that a periodic linear approximation, similar to Eqs. (3.6), is valid. Under such assumptions the problem of qualitative resonance can be analyzed using the following linear periodic framework

$$\begin{aligned}
\dot{\delta\widetilde{x}} &= \big[A(t) + \Delta A(t)\big]\delta\widetilde{x} + w(t) \\
\delta\widetilde{y} &= \big[C + \Delta C(t)\big]\delta\widetilde{x} + v(t) \\
\dot{\delta x} &= A(t)\delta x - K\underbrace{\big(\delta y - \delta\widetilde{y}\big)}_{(y-\widetilde{y})} \\
\delta y &= C\delta x
\end{aligned} \tag{3.9}$$

with

$$\begin{aligned}\delta\widetilde{x} &= \widetilde{x} - \widehat{x}\\ \delta\widetilde{y} &= \widetilde{y} - \widehat{y}\\ \delta x &= x - \widehat{x}\\ \delta y &= y - \widehat{y}\end{aligned}$$

$$A(t) = \left.\frac{\partial F(x)}{\partial x}\right|_{x=\widehat{x}(t)}, \quad A(t+T_G) = A(t)$$

where $\widetilde{x}$ and x are the state of the driving and driven system, respectively, and T_G is the period of the nominal periodic regime, *i.e.* the generating cycle $\widehat{x}(t)$.

There are several results in the literature for the framework (3.9), refer for instance to [Bittanti and Colaneri, 1999] and the references therein. Depending upon the particular hypothesis made about the perturbations $\Delta A(t)$, ΔC, $w(t)$ and $v(t)$, the problem of qualitative resonance, *i.e.* the convergence of state $x(t)$ towards the state $\widetilde{x}(t)$, can be formulated as a problem of optimal/robust periodic follower/tracker [Grasselli and Longhi, 1991] or as a problem of optimal/robust periodic filtering [de Souza, 1987]. In this contest it is of particular interest to consider two among all the possible cases. Indeed, these two cases give the simplest hint about how one should proceed to determine the relationships between the driven dynamical system and the driving signals that ensure the qualitative resonance.

Disregarding the structural perturbations, $\Delta A(t) = 0$ and $\Delta C = 0$, and assuming the perturbations w and v to be white Gaussian T_D-periodic noises, of period T_D in rational ratio with T_G, the qualitative resonance can be reduced to the inverse problem of optimal periodic filtering. In automatic control jargon, H_2 periodic filtering [Burl, 1999].

On the other hand, disregarding the observation and modeling perturbations, $v = 0$ and $w = 0$, and assuming the structural perturbations to be deterministic and T_D-periodic, once again of period T_D in rational ratio with T_G, then the qualitative resonance can be reduced to the inverse problem of an optimal periodic follower. In automatic control jargon, H_2 periodic tracking [Burl, 1999].

Several other cases could be considered indeed as those in [De Nicolao, 1994; Xie and de Souza, 1991, 1993], but for the sake of shortness and simplicity only these two are described in more detail.

Filtering Problem

In the case in which the perturbation w and v are assumed to be white[18] Gaussian T_D-periodic noises while $\Delta A(t)$ and ΔC are disregarded, the occurrence of qualitative resonance can be reduced to a periodic Kalman filtering problem [de Souza, 1987].

In this case, the framework given in (3.9) is reduced to

$$\begin{aligned}\dot{\delta\widetilde{x}} &= A(t)\delta\widetilde{x} + w(t)\\ \delta\widetilde{y} &= C\delta\widetilde{x} + v(t)\\ \dot{\delta x} &= A(t)\delta x - K\underbrace{(\delta y - \delta\widetilde{y})}_{(y-\widetilde{y})}\\ \delta y &= C\delta x\end{aligned} \tag{3.10}$$

Let assume that w and v have zero mean and variance given by the T_D-periodic semidefinite positive matrices[19]

$$\begin{aligned}Q(t) &= E\left[w(t)w(t)^T\right], \quad Q(t) = Q(t+T_D), \quad Q \geq 0\,\forall t\\ R(t) &= E\left[v(t)v(t)^T\right], \quad R(t) = R(t+T_D), \quad R > 0\,\forall t\end{aligned}$$

[18] The white hypothesis implies that $E\left[w(t)w(\tau)^T\right] = 0 \quad \forall t \neq \tau$ and the same thing holds for v. Furthermore, note that being periodic, the considered noises are not ergodic.

[19] Here it is assumed that w and v are uncorrelated for simplicity of exposition but it is easy to consider the case where $E\left[wv^T\right] = Z \neq 0$.

Here, for simplicity is assumed that $R(t)$ is strictly definite positive[20] the case in which $R(t) \geq 0$ can be found in [Bell and Jacobson, 1975; Locatelli, 1993].

Under the conditions of observability of the pair $(A(t), C)$ and of rational ratio of periods T_G and T_D, letting T be the least common multiple of T_G and T_D, for any nontrivial T-periodic n-dimensional vector $b(t)$ the T-periodic control gain $K(t)$ which minimizes the following cost functional [Kwakernaak and Sivan, 1972; Locatelli, 1993]

$$J(t) = b(t)^T E\Big[\big(\delta x(t) - \delta\widetilde{x}(t)\big)\big(\delta x(t) - \delta\widetilde{x}(t)\big)^T\Big] b(t) \tag{3.11}$$

is given by

$$K(t) = -P(t)CR(t)^{-1} \tag{3.12}$$

where $P(t)$ is the T-periodic bounded symmetric definite positive stabilizing solution of the following periodic differential Riccati equation [de Souza, 1987]

$$\dot{P}(t) = P(t)A^T(t) + A(t)P(t) - P(t)C^T R^{-1}(t)CP(t) + Q(t) \tag{3.13}$$

The corresponding asymptotic value of the functional (3.11) is indeed given by

$$J_{min}(t) = b^T(t)P(t)b(t), \quad \forall t \in \lim_{k\to\infty}[(k-1)T, kT)$$

namely

$$E\Big[\big(\delta x(t) - \delta\widetilde{x}(t)\big)\big(\delta x(t) - \delta\widetilde{x}(t)\big)^T\Big] = P(t) \tag{3.14}$$

Under quite generic condition, in particular if the matrices C and K are constant, the inverse problem is well defined [Locatelli, 1993; Strauss, 1992]. Namely, given a stabilizing[21] matrix control gain K and an expected variance of the state estimation error $P(t)$ there exist two periodic (semi)definite positive matrices $Q(t)$ and $R(t)$ such that K is the optimal gain for the filtering problem defined by Eqs. (3.10) and (3.11). The fact that these matrices exist does not mean that they are easy to compute [Locatelli, 1993; Strauss, 1992].

Remembering that the previous analysis has shown that the qualitative resonance is achieved when the driven trajectory does not approach the homoclinic trajectory, the solution of the inverse problem suggests a threshold condition for the qualitative resonance, at least in statistical sense. Let ρ be the minimal distance between the generating cycle and the homoclinic trajectory, *i.e.*

$$\rho(t) = \min_{\eta\in HT}\Big\|x(t)\big|_{x\in GC} - \eta\Big\|$$

where HT is the set of states on the homoclinic trajectory. From ρ the matrix of minimal variance of the generating cycle about the homoclinic trajectory can be defined as

$$\Gamma(t) = \rho(t)\rho(t)^T$$

At this point it is easy to provide a statistical threshold, *i.e.* valid most of the time, in asking that the wandering of the reconstruction error, $P(t)$, is smaller than the distance of the generating cycle from the homoclinic trajectory, $\Gamma(t)$. Namely, $\Gamma(t) - P(t) > 0$. In fact, if the homoclinic trajectory is not approached then the linearization holds true and, consequently, the determined threshold. In other words it is a snake biting its own tail, if the homoclinic trajectory is not approached, then the results obtained under the linearized framework are valid. Consequently, the noise is guaranteed to be attenuated enough such to stay away from the homoclinic trajectory satisfying the initial hypothesis. In this way a stochastic threshold for qualitative resonance has been constructed. In other words, given the driven system (described by K, $A(t)$, and $\Gamma(t)$) the maximal Gaussian noise on the driving signal (described by $Q(t)$ and $R(t)$) that "usually" ensures qualitative resonance (*i.e.* $\Gamma(t) - P(t) > 0$) can be determined.

[20] Here it is used the standard notation for (semi)definite positive matrices, *i.e.* $A > B$ means that $A - B$ is definite positive.

[21] In filtering and control theory, a gain matrix K is said to be stabilizing with respect to a pair $(A(t), B(t))$ iff $A(t) - B(t)K(t)$ is stable [Callier and Desoer, 1991].

Control Problem

In the case in which the structural perturbations $\Delta A(t)$ and $\Delta C(t)$ are assumed to be T_D-periodic and deterministic while the observation/modeling perturbations $v = 0$ and $w = 0$ are disregarded, the occurrence of qualitative resonance can be reduced to a finite horizon optimal tracking problem [Grasselli and Longhi, 1991; Locatelli, 1993].

Let refer to the following feedforward plus closed loop control framework

$$\begin{aligned} \dot{\delta\widetilde{x}} &= \big(A(t)+\Delta A(t)\big)\delta\widetilde{x} \\ \delta\widetilde{y} &= \big(C+\Delta C\big)\delta\widetilde{x} \\ \dot{\delta x} &= A(t)\delta x - K_1(t)\underbrace{\big(\delta y-\delta\widetilde{y}\big)}_{(y-\widetilde{y})}+K_2(t)\delta\widetilde{y} \\ \delta y &= C\delta x \end{aligned} \tag{3.15}$$

under the assumptions that T_G and T_D are in rational ratio and let call T the least common multiple of T_G and T_D.

Given two T-periodic (semi)definite positive matrices

$$\begin{aligned} Q(t) &\geq 0\,\forall t, \quad Q(t)=Q(t+T), \quad \dim(Q)=m\times m \\ R(t) &> 0\,\forall t, \quad R(t)=R(t+T), \quad \dim(R)=n\times n \end{aligned}$$

Under the conditions of detectability of the pair $(A(t), C)$ and boundness of the driving signal $\delta\widetilde{y}(t)$, *i.e.* $A(t)+\Delta A(t)$ is stable, for any positive integer n the nT-periodic control gains $K_1(t)$ and $K_2(t)$ which minimize[22] for any time $\tau > \sigma > t_0$ the following cost functional [Kwakernaak and Sivan, 1972; Locatelli, 1993]

$$\begin{aligned} J(\tau,n) &= \int_{\tau}^{\tau+nT}\big[\delta y(t)-\delta\widetilde{y}(t)\big]^T Q(t)\big[\delta y(t)-\delta\widetilde{y}(t)\big]+u^T(t)R(t)u(t)dt \\ u(t) &= K_1(t)(\delta y-\delta\widetilde{y})+K_2(t)\delta\widetilde{y} \end{aligned} \tag{3.16}$$

are given by

$$\begin{aligned} K_1(t) &= R^{-1}(t)C'\overline{P}(t) \\ K_2(t) &= R^{-1}(t)C'\overline{\Delta P}(t) \end{aligned} \tag{3.17}$$

where $\overline{P}(t)$ is the C decomposition

$$P(t) = C^T\overline{P}(t)C$$

of the nT-periodic bounded symmetric definite positive stabilizing solution of the following periodic differential Riccati equation [Grasselli and Longhi, 1991; Locatelli, 1993]

$$\dot{P}(t) = -P(t)A(t) - A^T(t)P(t) + P(t)R^{-1}(t)P(t) - C'Q(t)C \tag{3.18}$$

while $\overline{\Delta P}(t)$ is the C decomposition

$$\Delta P(t) = C^T\overline{\Delta P}(t)C$$

of the nT-periodic solution of the following periodic differential Sylvester equation [Kwakernaak and Sivan, 1972; Locatelli, 1993]

$$\dot{\Delta P}(t) = \Delta P(t)A(t) + \big[A(t)+\Delta A(t)+R^{-1}(t)P(t)\big]^T\Delta P(t) - P(t)\Delta A(t) + C^TQ(t)\Delta C(t) \tag{3.19}$$

For any receding horizon time $\tau > \sigma > t_0$, the corresponding value of the functional (3.16) is given by

$$J_{min}(\tau,n) = \delta x^T(\tau)P(T)\delta x(\tau) + 2\delta\widetilde{x}^T(\tau)\big[P(t)+\Delta P(t)\big]\delta x(\tau) + 2v(\tau) \tag{3.20}$$

where $v(t)$ is the unique nT-periodic solution of the following differential equation

$$\dot{v}(t) = \frac{1}{2}\delta\widetilde{x}^T(t)\Big[\big(P(t)+\Delta P(t)\big)R^{-1}\big(P(t)+\Delta P(t)\big) - \big(C+\Delta C(t)\big)^TQ(t)\big(C+\Delta C(t)\big)\Big]\delta\widetilde{x}(t)$$

[22] In coherence with finite horizon periodic control theory, these are not the optimal gains but the best ones among those that are periodic [De Nicolao, 1994].

while $\delta\widetilde{x}(\tau)$ and $\delta x(\tau)$ are the initial conditions, at the begin of the receding horizon interval, of the driving and driven system, respectively. Note that such receding horizon control is asymptotically stable, for t tending to infinite $\delta y(t)$ tends to $\delta\widetilde{y}(t)$, which implies that asymptotically the cost functional is dominated by the cost of the control, *i.e.* the second term of the right hand side of Eq. (3.16). Therefore, the cost functional (3.16) is meaningful for the qualitative resonance framework only for small τ that is indeed not restrictive since the interest is not in the asymptotic behavior but in that occurring in finite time.

Once again, under quite general conditions, in particular if the matrices C, K_1, and K_2 are constant, the inverse problem is well defined [Locatelli, 1993; Strauss, 1992]. Namely, given two matrix control gains K_1 and K_2, with K_1 stabilizing, there exist two periodic (semi)definite positive matrices $Q(t)$ and $R(t)$ such that K_1 and K_2 are the optimal control for the tracking problem given by Eqs. (3.15) and (3.16). Once again, the fact that these matrices exist does not mean that they are easy to compute, indeed they are not [Locatelli, 1993; Strauss, 1992]. To summarize, given the dynamics of driving and driven system (described by $A(t)$ and $\Delta A(t)$), together with a control gain (described by K_1 and K_2) on an observable of the state (described by C) uniquely identify the minimized quadratic functional (identified by $Q(t)$ and $R(t)$). Once the matrices $Q(t)$ and $R(t)$ are obtained from the direct problem, the value of the functional for the given control law follows. Unfortunately, the solution of the inverse problem cannot be used straightforward for obtaining some conditions for the occurrence of qualitatively resonance or anti-resonance. Indeed, the control problem considered (*cfr.* Eqs. (3.15)) coincides with that of qualitative resonance (*cfr.* Eqs. (3.15)) only if the forward gain K_2 can be disregarded, *i.e.* $K_2 \equiv 0$. Thus, to determine the occurrence of qualitative resonance or anti-resonance it is necessary to evaluate the contribution of the forward gain to the overall performance, *cfr.* Eq. (3.20). This can be done considering the following three cases.

1. *Unperturbed driving system*: this is the case $\Delta A(t) = 0$ and $\Delta C(t) = 0$. The optimal follower (3.15-3.20) regress to a simple periodic observer [Callier and Desoer, 1991]. Thus, for this trivial case the condition for the occurrence of qualitative resonance, *i.e.* perfect synchronization, is that the gain matrix $K_1 = K$ is stabilizing.

2. *Nonobservable perturbations*: this is the case in which $\Delta A(t)$ and $\Delta C(t)$ are such that $\widetilde{y}(t)$ is a non reachability Zero of the couple $(A(t), K_2(t))$ [De Nicolao *et al.*, 1998]. Hence, the perturbations do not reach (perturb) the state of the driven system and the results for the optimal follower (3.15-3.20) hold also for $K_2(t) = 0$. Therefore, for this case, the condition for the occurrence of qualitative resonance, *i.e.* perfect synchronization, is once again that the gain matrix $K_1 = K$ is stabilizing.

   It should be noted that, for a given gain matrix K, this case implicitly defines the class of periodic perturbations $\delta\widetilde{y}(t)$ on $\widehat{y}(t)$ which do not affect the perfect synchronization of the driving and driven system.

3. *Generic perturbations*: this is the generic case in which $\Delta A(t)$ and $\Delta C(t)$ do not have any of the above singularity. In such a case, it follows, from the result of robust control [Wang and Speyer, 1990], that imposing $K_2(t) = 0$ the following bounds hold for any receding horizon time $\tau > \sigma > t_0$ [Bolzern *et al.*, 1994; De Nicolao, 1994; Freiling *et al.*, 1996; Kwon *et al.*, 1996; Locatelli, 1993]

$$\begin{aligned} \left[\delta x(t)\delta\widetilde{x}(t)\right]^T Q(t)\left[\delta x(t)\delta\widetilde{x}(t)\right] &\geq Tr\big(P(t)\big)^2 = L_b \\ J(n,\tau) &\leq \overline{Z}(t) = H_b \end{aligned} \tag{3.21}$$

   where $\overline{Z}(t)$ is the nT-periodic bounded symmetric definite positive solution of the following periodic differential Riccati equation

$$\dot{\overline{Z}}(t) = -\overline{Z}(t)A(t) - A^T(t)\overline{Z}(t) + \frac{\overline{Z}(t)\overline{Z}(t)}{\beta} + \beta\overline{A} - K_{2n}(t)K_{2n}(t)^T$$

   with $\overline{A}:\ \Delta A(t)\Delta A^T(t) < \overline{A}$, β is a positive number such that $A(t) + \overline{Z}(t)/\beta$ is stable, and $K_{2n}(t)$ is the nominal optimal $K_2(t)$ corresponding to the considered $K_1(t)$.

   From these two bounds, considering the straightforward physical meaning of the functional (3.16), two thresholds can be obtained, one for the occurrence of resonance and one for the occurrence of anti-resonance. Indeed, in Eq. (3.16) the matrix Q weights the mean square error between the driven trajectory and the generating cycle over many turns, while the matrix R weights the mean square control action, namely it weights how much cost to alter the dynamic of the driven system. Since they are all positive

and summed together, it is clear that each one of the terms of functional (3.16) must be smaller than the lower bound given in Eqs. (3.21).

Remembering that resonance [anti-resonance] is achieved when the driven trajectory does not [does] approach the homoclinic trajectory and calling $\gamma(t)$ the $C^T Q(t) C$ weighted square distance of the generating cycle from the homoclinic trajectory, *i.e.*

$$\gamma(t) = \rho(t)^T C^T Q(t) C \rho(t)$$

the interpretation of the previous results in terms of qualitative resonance is straightforward. For a given control gain matrix K and a periodic driving signal (described by the matrices $A(t)$, $\Delta A(t)$, C and $\Delta C(t)$) the qualitative resonance [anti-resonance] of the driven system (described by the matrix $A(t)$) is surely achieved whenever the value of the high [low] bound H_b [L_b], given by the solution of the inverse problem, is smaller [larger] than $\gamma(t)$ for any time t.

Thresholds for Qualitative Resonance

The control/filtering frameworks described above allows to define, implicitly, the conditions for qualitative resonance or anti-resonance. For a given gain matrix K, the solution of the inverse filtering [control] problem provide the matrices Q and R, that, by means of the corresponding minimized functional, give a statistic [deterministic] *measure* of how much the driven trajectory wander around the generating cycle. In other words, the solution of the inverse problem provide a measure of the distance of the driving signal from the natural dynamics of the system. If such a distance is smaller [smaller or larger] than the average [deterministic] distance of the generating cycle from the homoclinic trajectory, then the qualitative resonance [resonance or anti-resonance] is guaranteed, *provided the phase synchronization* take place. Furthermore, the case of nonobservable perturbations implicitly define those additive deterministic perturbations of the ideal driving signal ($\widehat{y}(t)$) which do not alter at all the perfect synchronization (resonance) of driving and driven system.

The very same argument can be used with any invertible optimal/robust periodic tracking/filtering framework [Colaneri and Geromel, 1997; Locatelli, 1993]. Indeed, in any of these frameworks the cost functional define a sort of *distance* of the regulated/reconstructed state from the ideal one, namely the driving signal. Therefore, for a given stabilizing gain matrix K and the maximal admissible deviation of the driven trajectory from the driving one, *i.e.* the distance from the generating cycle and the homoclinic trajectory, the inversion of the filtering/tracking problem give the maximal perturbation compatible with such a condition, thus the threshold for the occurrence of qualitative resonance. Sometimes, as shown above, even a bound for qualitative anti-resonance can be obtained.

To conclude it should be noted that the provided threshold conditions are neither necessary nor sufficient in the generic case. Actually, the thresholds are valid under the condition of phase locking between driving signal and driven system. Such a condition is not necessarily achieved (*cfr.* final remarks in Sect. 3.2). Furthermore, the thresholds have been obtained under pure deterministic or Gaussian conditions, as already mentioned, it is not difficult to perturb the clean signal $\widehat{y}$ by means of a small non Gaussian noise such that anti-resonance will be observed, and, vice versa, build a strong regular corrupting signal such that a coexisting periodic solution, far from the generating cycle, will be stabilized. Indeed, these conditions do not take into account the possibility of multiple attractors that are more the rule than the exception in nonlinear systems. Unfortunately, this is the price to pay for "playing" with nonlinear systems. Despite of this limitations in Chap. 6 it will be shown that this simple model reveals to be sufficient for building applications.

3.4 Remarks on Qualitative Resonance

Before concluding this chapter there are some remarks about the phenomenon illustrated herein, and its analysis too, that need to be stated.

The presented analysis has been quite tedious but it has been necessary. In fact all the methods presented in the following are based on the conjectures about the working principles of qualitative resonance; without the confirmation of these conjectures the methods would lack a solid basis. Furthermore, the phenomenon of qualitative resonance and the analysis of its extent has a value *in se*. In fact, numerous are nowadays the works in the literature dedicated to the information processing and propagation in *biological neural networks*

[Elbert *et al.*, 1994; Rabinovich *et al.*, 2000]. Indeed, there are strong arguments sustaining that the dominating mechanisms governing this propagation and processing are generalized phenomena of synchronization among clusters of neurons [Basar, 1990; Elbert *et al.*, 1994; Freeman, 2000; Getting, 1989; Hopfield, 1991, 1995, 1996; Izhikevich, 2000; Rabinovich *et al.*, 2000]. In this respect the discovery and study of qualitative resonance could open new doors for the understanding of biological neural networks.

The hypothesis that the behavior of the free, *i.e.* not forced, system is chaotic of Shil'nikov type is everywhere present but never explicitly justified. There are two main reasons for such a statement.

1. *Phase locking*: all the arguments spent above are valid only under the assumption that the driving signal and the driven system will lock in phase. In order to achieve this condition it is necessary that the free system changes randomly its phase. The only system known, shown in the previous chapter, with such a property is indeed the Shil'nikov-like chaos.

2. *Anti-resonance*: in order to obtain anti-resonance it is necessary to have a singularity in the flow. Thus, an equilibrium, which is the simplest singularity of flow, in the proximity of a bounded flow leads almost automatically to homoclinic trajectories that in turn lead to Shil'nikov-like chaos.

About the first reason, experiments of qualitative resonance conducted on Feigenbaum-like and torus-destroyed-like chaos have indeed highlighted difficulties for these systems to reach the phase locking condition. In general, the experiments show that these systems tend to have a spread chaotic or quasi-periodic, *i.e.* torus, behavior, rather than shrinking on the driving signal, when perturbed under qualitative resonance conditions. In some sense the "too regular" behavior of these systems can be thought of a periodic behavior and it is known that the periodic perturbation of periodic systems usually leads to quasi-periodic behavior indeed. For the second assumptions there are no *a priori* conditions for excluding other kinds of chaos based on other singularities in the vector field such as Blue-Sky chaos [Izhikevich, 2000] or heteroclinic chaos [Kuznetsov, 1998] but it should be noted that the singularity alone is not enough. Actually, torus-destroyed chaos is associated with a homoclinic to a cycle, thus satisfy the singularity requirement. This singularity does not introduce any phase randomness, since the torus and the cycle bearing the homoclinic have similar frequencies, *cfr.* to Sect. 2.5.3. Indeed, for torus-destroyed-like chaos an emergent phenomenon of qualitative resonance has not been observed. Therefore, it can be conjectured that qualitative resonance needs singularities of the flow both in time and in state space.

To conclude, some words are appropriate for the relationship between qualitative resonance, chaos synchronization, and chaos control problems [Chen, 1999; Chen and Dong, 1988; Hasler, 1994]. Despite of their similarity, the occurrence of qualitative resonance can be considered as a separate problem even though it is obviously strongly related to the previous two. On the one hand, in chaos control the problem is to find a closed loop[23] control law that will stabilize a given unstable periodic orbit. Usually, no a priori constraints on the shape of the control signal are given other than a maximal amplitude constraint or, sometimes, a piecewise constant constraint. In the qualitative resonance problem the control, *i.e.* the perturbing signal, is given and the question is what kind of, maybe chaotic, attractor will be stabilized by that signal under the constraint that the perturbation must be a "weak" one. In this sense the occurrence of qualitative resonance can be seen as a solution of the typical inverse problem of control theory, as indeed shown in Sect. 3.3.3. On the other hand, the synchronization problem usually consists of finding the maximal parameter mismatch between two identical systems such that the two systems will synchronize even when they behave chaotically. Another typical problem of synchronization is to find the maximal additive unstructured noise over the synchronizing signal such that the systems will synchronize, this time in statistical sense. This is very similar to qualitative resonance imagining that the perturbing signal has been generated by a system similar to the driven one. The main difference lies in the intensity of the perturbations on the driving signal. In a qualitative resonance problem they are stronger than those usually considered in synchronization. On the other hand, they can be more structured. Furthermore, the aim of synchronization can be summarized as keeping the total system, master and slave, as close as possible on the hyper-diagonal, *i.e.* state of the master equal to the state of the slave. On the contrary in qualitative resonance the aim is definitively weaker, namely to keep the input (driving) signal close to the output one. Thus, in general, the qualitative resonance can be seen as a subcase of synchronization.

[23] There is another problem known in literature as chaos entrainment that refer to open loop control laws [Guevara and Glass, 1982].

Bibliography

Basar, E. (1990). *Chaotic Dynamics and Resonance Phenomena in Brain Function: Progress, Perspectives, and Thoughts*, pp. 1–30. Springer-Verlag, Berlin, Germany.

Bell, D. and D. Jacobson (1975). *Singular Optimal Control Problems*. Academic Press, London, UK.

Bittanti, S. and P. Colaneri (1999). *Periodic Control*, pp. 59–74. John Wiley & Sons, New York, NY.

Bolzern, P., P. Colaneri, and G. De Nicolao (1994). On the computations of upper covariance bounds for perturbed linear systems. *IEEE Transactions on Automatic Control*, 39, pp. 623–626.

Brogan, W. (1996). *Modern Control Theory*. Prentice-Hall, New York, NY, third edition.

Brunovski, P. (1970). A classification of linear controllable systems. *Kybernetica*, 3, pp. 173–187.

Bryson, A. (1996). Optimal control-1950 to 1985. *IEEE Control Systems Magazine*, 16, pp. 26–33.

Burl, J. (1999). *Linear Optimal Control: H_2 and H_∞ Methods*. Addison-Wesley, Menlo Park, CA.

Callier, F. and C. Desoer (1991). *Linear System Theory*. Springer-Verlag, New York, NY.

Chen, G., editor (1999). *Controlling Chaos and Bifurcations in Engineering Systems*. CRC Press, Cambridge, UK.

Chen, G. and X. Dong (1988). *From Chaos to Order: Methodologies, Perspectives and Applications*. World Scientific, Singapore.

Colaneri, P. and A. L. J. Geromel (1997). *Control Theory and Design. A $RH_2 - RH_\infty$ Viewpoint*. Academic Press, London, UK.

De Feo, O., G. Maggio, and M. Kennedy (2000). The Colpitts oscillator: Families of periodic solutions and their bifurcations. *International Journal of Bifurcation and Chaos*, 10, pp. 935–958.

De Feo, O. and S. Rinaldi (1997). Yield and dynamics in tritrophic food chains. *The American Naturalist*, 150, pp. 328–345.

De Nicolao, G. (1994). Cyclomonotonicity, Riccati eqution and periodic receding horizon control. *Automatica*, 30, pp. 1375–1388.

De Nicolao, G., G. Ferrari-Trecate, and S. Pinzoni (1998). Zeros of continuous-time linear periodic systems. *Automatica*, 34, pp. 1651–1655.

de Souza, C. (1987). Riccati differential equation in optimal filtering of periodic non-stabilizing systems. *Intrnational Journal of Control*, 46, pp. 1235–1250.

Dellnitz, M. and A. Hohmann (1996). *The Computation of Unstable Manifolds Using Subdivision and Continuation*, pp. 449–459. Birkhauser, Boston, MA.

Dellnitz, M. and O. Junge (1997). Almost invariant sets in Chua's circuit. *International Journal of Bifurcation and Chaos*, 7, pp. 2475–2486.

Doedel, E., A. Champneys, T. Fairgrieve, Y. Kuznetsov, B. Sandstede, and X. Wang (1998). *AUTO 97: Continuation and Bifurcation Software for Ordinary Differential Equations withHomCont*. Computer Science Department, Concordia University, Montreal, Canada, Motreal, Quebec, Canada.

Elbert, T., W. Ray, Z. Kowalik, J. Skinner, K. Graf, and N. Birbaumer (1994). Chaos and physiology: Deterministic chaos in excitable cell assemblies. *Physiological Reviews*, 74, pp. 1–47.

Feuer, A. and G. Goodwin (1996). *Sampling in Digital Signal Processing and Control*. Birkauser, Boston, MA.

Freeman, W. (2000). Characteristics of the synchronization of brain activity imposed by finite conduction velocities of axons. *International Journal of Bifurcation and Chaos*, 10, pp. 2307–2322.

Freiling, G., G. Jank, and H. Abou-Kandil (1996). Generalized Riccati difference and differential equations. *Linear Algebra and Its Applications*, 241, pp. 243–291.

Gaspard, P., R. Kapral, and G. Nicolis (1984). Bifurcation phenomena near homoclinic systems: A two-parameter analysis. *Journal of Statistical Physics*, 35, pp. 697–727.

Getting, P. (1989). Emerging principles governing the operation of neural network. *Annual Review of Neuroscience*, 12, pp. 185–204.

Glendinning, G. and C. Sparrow (1984). Local and global behavior near homoclinic orbits. *Journal of Statistical Physics*, 35, pp. 215–225.

Gonchenko, S., L. Shil'nikov, and D. Turaev (1997). Quasiattractors and homoclinic tangencies. *Computers & Mathematics with Applications*, 34, pp. 195–227.

Grasselli, O. and S. Longhi (1991). Robust tracking and regulation of linear periodic discrete-time systems. *Intrnational Journal of Control*, 54, pp. 613–633.

Guevara, M. and L. Glass (1982). Phase locking, period doubling bifurcations and chaos in a mathematical model of a periodically driven oscillator: A theory for the entrainment of biological oscillators and the generation of cardiac dysrhythmias. *Journal of Mathematical Biology*, 14, pp. 1–23.

Hansen, K. (1993). *Symbolic Dynamics in Chaotic Systems*. Ph.D. thesis, University of Oslo, Blindern, Norway.

Hansen, K. (1994). Bifurcations of homoclinic orbits in bimodal maps. *Physica E*, 50, pp. 1653–1656.

Hansen, K. and P. Cvitanovič (1998). Bifurcation structures in maps of Hénon type. *Nonlinearity*, 11, pp. 1233–1261.

Hasler, M. (1994). *Synchronization Principles and Applications*, pp. 314–327. IEEE Press, New York, NY.

Hastings, H. and T. Powell (1991). Chaos in three species food chain. *Ecology*, 72, pp. 896–903.

Hindmarsh, J. and R. Rose (1984). A model of neuronal bursting using three coupled first order differential equations. *Philosophical Transaction of the Royal Society of London*, B221, pp. 87–102.

Hopfield, J. (1991). Olfactory computation and object perception. *Proceedings of the National Academy of Science USA*, 88, pp. 6462–6466.

Hopfield, J. (1995). Pattern recognition computation using action potential timing for stimulus representation. *Nature*, 376, pp. 33–36.

Hopfield, J. (1996). Transforming neural computations and representing time. *Proceedings of the National Academy of Science USA*, 93, pp. 15440–15444.

Izhikevich, E. (2000). Neural excitability, spiking and bursting. *International Journal of Bifurcation and Chaos*, 10, pp. 1171–1266.

Kučera, V., P. Colaneri, and C. de Souza (1998). Output stabilizability of periodic systems: Necessary and sufficient condidtions. In *Proceedings of the American Control Conference 1998*, pp. 2795–2796. IEEE Press, Piscataway, NJ.

Kuznetsov, Y. (1998). *Elements of Applied Bifurcation Theory*. Springer-Verlag, New York, NY, second edition.

Kuznetsov, Y., O. De Feo, and S. Rinaldi (2001). Belyakov homoclinic bifurcations in a tritrophic food chain model. *SIAM Journal of Applied Mathematics*. Submitted.

Kuznetsov, Y. and V. Levitin (1997). CONTENT: A multiplatform environment for continuation and bifurcation analysis of dynamical systems. Dynamical systems laboratory, CWI, Centrum voor Wiskunde en Informatica, National Research Institute for Mathematics and Computer Science, Amsterdam, The Netherlands.

Kuznetsov, Y. and S. Rinaldi (1996). Remarks on food chain dynamics. *Mathematical Biosciences*, 134, pp. 1–33.

Kwakernaak, H. and R. Sivan (1972). *Linear Optimal Control Systems*. John Wiley & Sons, New York, NY.

Kwon, W., Y. Moon, and S. Ahn (1996). Bounds in algebraic Riccati and Lyapunov equations - a survey and some new results. *International Journal of Control*, 64, pp. 377–389.

Lakshmanan, M. and K. Murali (1996). *Chaos in Nonlinear Oscillators: Controlling and Synchronization*. World Scientific, Singapore.

Locatelli, A. (1993). *Elementi di Controllo Ottimo*. UTET, Torino, Italy. In Italian.

Lorenz, E. (1963). Deterministic nonperiodic flow. *Journal of Atmospheric Science*, 20, pp. 130–141.

Madan, R., editor (1993). *Chua's Circuit: A Paradigm for Chaos*. World Scientific, Singapore, fourth edition.

Maggio, G., O. De Feo, and M. Kennedy (1999). Nonlinear analysis of the Colpitts oscillator and applications to design. *IEEE Transaction on Circuit and Systems—I*, 46, pp. 1118–1130.

Mastumoto, T. (1993). *Bifurcations: Sights, Sounds and Mathematics*. Springer-Verlag, Tokyo, Japan.

Osinga, H. and U. Feudel (2000). Boundary crisis in quasiperiodically forced systems. *Physica D*, 141, pp. 54–64.

Ott, E. (1993). *Chaos in Dynamical Systems*. Cambridge University Press, New York, NY.

Pecora, L. and T. Carroll (1990). Synchronization in chaotic systems. *Physical Reviw Letters*, pp. 821–824.

Petersen, I. and A. Savkin (1999). *Robust Kalman Filtering for Signals and Systems with Large Uncertainties*. Birkhauser, Boston, MA.

Rabinovich, M., P. Varona, and H. Abarbanel (2000). Nonlinear cooperative dynamics of living neurons. *International Journal of Bifurcation and Chaos*, 10, pp. 913–933.

Robert, C., T. Alligoodb, E. Ott, and J. Yorke (2000). Explosions of chaotic sets. *Physica D*, 144, pp. 44–61.

Rössler, O. (1976). An equation for continuous chaos. *Physics Letters*, 57A, pp. 397–398.

Sedra, S. and K. Smith (1998). *Microelectronic Circuits*. Oxford University Press, New York, NY, fourth edition.

Strauss, M. (1992). *Introduction to Optimal Control Theory*. Springer-Verlag, New York, NY.

Tresser, C. (1984). On some theorems of L. P. Shil'nikov and some applications. *Annales de l'Institute Henri Poincaré*, 40, pp. 441–461.

Wang, Q. and J. Speyer (1990). Necessary and sufficient conditions for local optimality of a periodic process. *SIAM Journal on Control and Optimization*, 28, pp. 482–497.

Xie, L. and C. de Souza (1991). Robust H_∞ filtering for a class of uncertain periodic systems. *IEE Proceedings on Control Theory and Applications*, 138, pp. 479 –483.

Xie, L. and C. de Souza (1993). H_∞ state estimation for linear periodic systems. *IEEE Transaction on Automatic Control*, 38, pp. 1704–1707.

Zhou, Z. and S. Peng (2000). Cyclic star products and universalities in symbolic dynamics of trimodal maps. *Physica D*, 140, pp. 213–226.

CHAPTER 4

CHAOS BASED PATTERN RECOGNIZERS

Brief — In this chapter the specific technique proposed for dealing with the *Thesis* of this research work is presented. In particular, on the basis of the results obtained on the phenomenon of qualitative resonance, a new conjecture about a dynamical interpretation of the associative behaviors is proposed. This conjecture is therefore exploited to conceive a two-step dynamical approach to pattern recognition problems. The first step regards the modeling of the periodic temporal patterns diversity by means of chaotic dynamical models. The second step proposes to exploit such chaotic dynamical models in pattern recognition problems by means of the qualitative resonance phenomenon. In this direction a pattern recognition technique based on a nonlinear chaotic filter is proposed, a filter which resonates when excited with patterns that should be recognized and, vice versa, does not resonate when the patterns should not be recognized. The above mentioned filter has been called *qualitatively resonating filter*.

Personal Contribution — The entire chapter can be considered as original. Nonetheless, it is definitely influenced by ideas, from several other fields, that are rather similar to those presented here.

As mentioned in Chap. 1, this research work deals with pattern recognition, or better, classification. In particular, this thesis proposes a chaos-based technique for dealing with the classification of approximately periodic temporal patterns. This is because the pattern recognition, or better, the classification ability is often assumed as the atomic operation a cognitive agent must be capable to perform [Alder, 1994; Newman, 1998; Russell and Norvig, 1999; Schalkoff, 1992].

On the basis of the argument presented in Chap. 2 and Chap. 3 the following *Thesis* can be conjectured

> *The diversity of approximately periodic signals found in nature can be modeled by means of Feigenbaum-like strange attractors. This kind of modeling technique together with the phenomenon of qualitative resonance could be exploited for pattern recognition purposes.*

The rest of this work will be dedicated to defend this Thesis.

Since the qualitative resonance phenomenon has been deeply explained and discussed in the previous chapter, it is natural that the chaos-based technique that this thesis proposes is obviously based on this phenomenon. Nonetheless, it should be noted that it is not the only possible way of exploiting chaos for such a purpose [Andreyev *et al.*, 1996a, 1992, 1996b, 1995, 1999, 1997; Dmitriev *et al.*, 1991; Goertzel, 1994; Rouabhi, 2000].

In exploiting qualitative resonance for pattern recognition purposes a hypothesis/conjecture about cognitive agents, in particular about the dynamical origin of their associative behavior, is conceived; besides,

implicitly a hypothesis about a possible schematic functional decomposition of cognitive agents is made. Actually, it is assumed that a cognitive agent is composed, as shown in Fig. 4.1, of an intelligent sensory system which feeds with almost symbolic information a high-level pattern recognizer, possibly symbolic/statistic-based [Mitchell, 2000, 2001]. In particular, this latter hypothesis will be discussed more in detail in the Chaps. 7 and 8. Furthermore, exploiting qualitative resonance for pattern recognition purposes implies automatically to have, in first place, a chaotic model of the considered temporal pattern and, moreover, a feedback gain K (*cfr.* Chap. 3) tuned such as to let the chaotic model qualitatively resonate with the patterns of interest. All these topics are addressed in detail in this chapter.

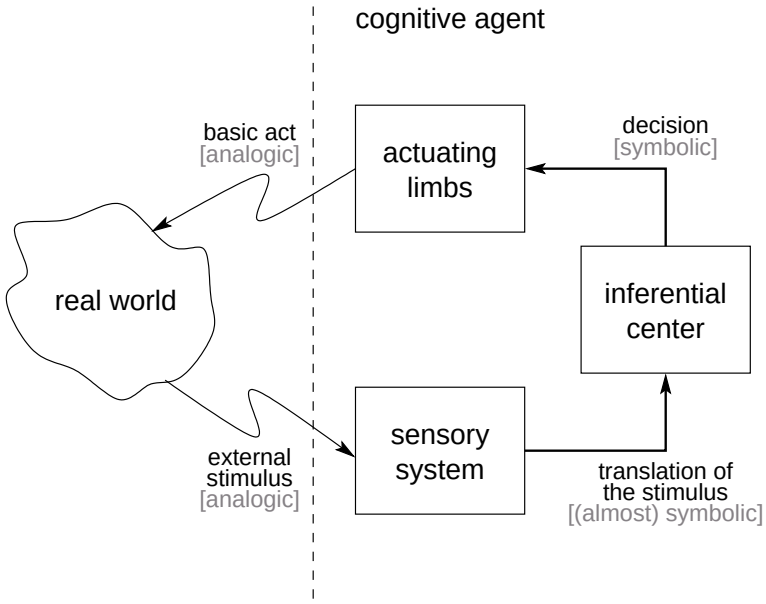

Figure 4.1: *Schematic functional decomposition of a cognitive agent.*

4.1 A New Conjecture for Associative Behavior

The *associative behavior* of a cognitive agent is its ability to *generalize* its own knowledge [Alder, 1994; Russell and Norvig, 1999; Thagard, 1996]. A cognitive agent usually possesses an *a priori* knowledge on which it bases those speculations/inferences necessary to achieve its apparently intelligent behavior. The associative behavior is its ability in generalizing this knowledge such as to achieve the robustness of its intelligent behavior despite of the inaccuracy of its *a priori* knowledge with respect to the real world. An example can help to clarify this abstract concept: the mathematical concept of a circle is definitely different from those real shapes that usually an engineer, an architect or whoever else, *associates* with a circle. This is indeed the associative ability, the imprecise, inaccurate, reality can be associated to a precise concept[1].

A pattern recognizer possesses an *a priori* knowledge, usually suitable stereotypes (*cfr.* Chap. 2), about the classes of patterns that it is supposed to recognize. As discussed in Chap. 2, one of the main properties of a pattern recognizer is indeed the ability to generalize these stereotypes such as to match those relevant patterns that can be observed in the real world. With regard to that, and especially in the optic of exploiting the qualitative resonance as pattern matching technique, there is a noteworthy remark. In the previous chapter, in particular during the presentation of the experimental results about qualitative resonance (*cfr.* Sect. 3.1), a fundamental difference in the behavior of the two models considered in the experiments emerged. Actually, the Colpitts oscillator, which is characterized by weak coexistence of geometrically different strange attractors (*cfr.* Fig. 3.1), resonates with only one of the patterns related with these strange attractors, at time, namely, with the one that corresponds to the strange attractor existing at the chosen parameter

[1] Engineers are champions in doing that. The first step to solve a problem in the everyday work of an engineer is indeed to fit an imprecise vague reality to the closest precise and accurate mathematical model which corresponds to the given problem [Shinskey, 1996].

values[2]. On the other hand, the Rosenzweig—MacArthur model, which on the contrary is characterized by strong coexistence of geometrically different strange attractors (*cfr.* Fig. 3.3), has revealed to resonate with patterns related to each one of these strange attractors at the same time. This difference implies strong consequences in the dynamical perception of associative behavior which, consequently, deserves a separated consideration herein discussed.

In the past years several efforts have been devoted at linking the deterministic chaos to the associative behavior of cognitive agents [Andreyev *et al.*, 1996b; Kelso, 1995; Robertson *et al.*, 1993]. The majority of such works has always been based, implicitly or explicitly, on the fact that strange, *i.e.* chaotic, attractors are composed of an infinite number of limit cycles which composes their skeleton. Thus, associating a different information to each cycle, the *storing capacity* of a strange attractor should be infinite [Andreyev *et al.*, 1992]. Consequently, the characterization of the generalization capabilities, *i.e.* the associative behavior, of such a kind of pattern recognizers[3] has always been linked to a problem of feedback chaos control [Rouabhi, 2000]. In other words, the robustness/generalization ability of the pattern matching action has always been reduced to the problem of stabilizing this or that unstable periodic orbit once the sampling pattern is given; namely, once the reference for the feedback is given [Rouabhi, 2000].

Despite of the attractiveness of such an idea, it has not been exceedingly satisfactory in practice. One of the main reasons of this failure has to be found in the self-similarity of the unstable periodic orbits embedded in the strange attractors. In fact, even if a strange attractor contains an infinite number of limit cycles they are not very different from each other; indeed, they are self-similar [Ott, 1993], therefore the information that can be associated to each one of them cannot be very different[4].

An alternative hypothesis about the role of deterministic chaos in the emergence of associative behavior can be found in the qualitative resonance phenomenon. Actually, in the previous chapter (*cfr.* Sect. 3.2), it has been shown that the self-similarity of strange attractors, rather than being considered as a problem, can indeed be exploited, by means of phenomena such as qualitative resonance, in order to obtain associative behavior. It is indeed this associative behavior that is at the origin of the adjective "qualitative" in the purposely coined term "qualitative resonance". Moreover, it has been shown that multiple qualitative resonances are possible. Indeed, models like the Rosenzweig—MacArthur one, *i.e.* models which admit multiple attractors, resonate with signals related to the generating cycles of each one of these strange attractors.

The possibility of multiple qualitative resonances, which is associated with multiple coexisting attractors, allows for a new dynamical conjecture about the storing capacity of cognitive agents; more simply, of associative memories or pattern recognizers. Namely, it can be conjectured that the storing capacity, rather than being associated with the infinite limit cycles embedded in a strange attractor, is related to the multiplicity of coexisting attractors. An intuitive, and quite naive, justification of such a conjecture can be given by an analogy with digital computer memories, *i.e.* the flip-flops [Christiansen, 1997]. In fact, the flip-flops, which are often called bistables, are able to store a binary information by means of two alternative stable equilibria in which they can be driven by an external signal. Another similar example is given by the n-ary dynamical quantizers [Christiansen, 1997], which are indeed the n-ary generalization of a flip-flop.

The previous two considerations allow for a new conjecture about the dynamical origins of associative behavior which can be summarized as follows

$$\begin{array}{lcl} \text{multiple attractors} & \Longleftrightarrow & \textit{storing capacity} \\ \text{chaotic behavior} & \Longleftrightarrow & \textit{associative behavior} \end{array}$$

In other words, the associative behavior, *i.e.* the ability to generalize, is linked to a chaotic self-similar redundant representation of the information while the amount of knowledge that can be stored in a cognitive agent is linked to the number of multiple attractors that it can possess.

This conjecture is rather useless from an engineering point of view. In fact, as it will be shown later, it is already difficult to store one given pattern, together with its diversity, in a chaotic model; to store simultaneously several patterns in a single model would be practically impossible. Nevertheless, this conjecture could

[2] In reality, the resonance has been observed with respect to the sinusoidal pattern too, which is indeed strongly coexisting, even if in the form of an unstable strange attractor, with all the other strange attractors [De Feo *et al.*, 2000].

[3] In reality, this approach is usually adopted in the development of dynamical-based associative memories [Rouabhi, 2000]. Despite of some slight difference, the associative memories and the pattern recognizers are the two sides of the same medal [Alder, 1994]. In fact an associative pattern recognizer is the basic component necessary to realize a content addressed memory, *i.e.* an associative memory; vice versa, an associative memory can be used as a pattern recognizer, or better as a classifier, classifying the patterns according to its content.

[4] This is not the case in noncontinuous discrete maps [Gumowski and Mira, 1980; Mira *et al.*, 1996; Rouabhi, 2000], which are indeed, as discussed later in the chapter, one of the effective alternatives to that proposed in this thesis.

have a strong impact in the cognitive sciences or in the analysis of biological neural networks [Elbert *et al.*, 1994; Rabinovich *et al.*, 2000; Thiran, 1996].

Before exploiting this conjecture for the aim of this thesis, there is a conceptual difference between the common conjecture and this new one that needs to be highlighted. At first sight the two conjectures could appear rather similar, both of them imagine information stored in strange attractors, a chaotic box where to deposit information, and both of them rely on some synchronization/stabilization phenomena for retrieving such information, *i.e.* qualitative resonance for the conjecture proposed here and synchronization or chaos control for the classic conjecture. The conceptual difference between the two conjectures lies in what is represented by the unstable orbits that need to be stabilized at retrieving time.

The classic approach [Andreyev *et al.*, 1997] works at symbolic level, it associates to each unstable periodic orbit a different symbolic information. The signal used as reference for driving the system is a fragmentary information of what has to be retrieved from the associative memory [Rouabhi, 2000]. In general, such a signal will be a symbolic representation of an external stimulus. Hence, the occurrence of synchronization corresponds to the matching of the fragmentary symbolic information with one of the patterns stored in the strange attractor.

On the contrary, the new conjecture works directly at stimulus level, it associates an entire strange attractor to a single information. The unstable periodic orbits embedded in the strange attractor represent, by means of the self-similarity, multiple instances of the same pattern; somehow they represent the stereotype of the pattern together with a stereotype of its possible variations. In other words the strange attractors *in todo* represents the stereotype of the entire class of patterns. In this case, the signal used as reference for driving the system is a real stimulus that has to be compared with the class of patterns represented by the entire strange attractor. Hence, the occurrence of qualitative resonance, thus the approximative stabilization of a particular unstable orbit, corresponds to recognizing in the sampling signal used as external stimulus those dynamical features that are characteristic in the given class of patterns .

Thus, summarizing, the main conceptual difference between the two conjectures is that the classic one works at symbol level, associating one strange attractor to several information items $(1 : n)$, while the one herein proposed works directly at the stimulus level, associating one strange attractor to one information $(1 : 1)$.

4.2 Application of Chaos to Pattern Recognition

The exploitation of chaotic behavior for pattern recognition purposes that is proposed here involves, obviously, qualitative resonance. Actually, the qualitative resonance property can be interpreted as a generalization capability of Shil'nikov strange attractors with respect to a given reference stereotype, *i.e.* the generating cycle. More precisely, the entire strange attractor represent a generalized stereotype, namely an entire class of patterns together with their diversity. This property is of interest for pattern recognition purposes and even for more general artificial intelligence applications based on nonlinear dynamical systems. In fact, this qualitative resonance phenomenon can be imagined as the very basic way of associative retrieval of information stored in strange attractors. Qualitative resonance can be easily exploited to decide, on the basis of simple correlation methods, if the perturbing signal is contained or not in the perturbed strange attractors.

Before going further, it should be noted that this proposed method is certainly not the only possible one of exploiting chaos for pattern recognition purposes. As mentioned above, changing from a signal to a symbolic approach, there would be all those techniques of storing symbolic patterns inside discontinues chaotic maps as proposed in [Andreyev *et al.*, 1996a]. Besides, even remaining at signal level, there are other possibilities of exploiting the material presented in Chap. 2 for pattern recognition purposes. For instance, the one-dimensional maps associated with the peak-to-peak properties [Candaten and Rinaldi, 2000] of approximately periodic signals, as illustrated in Sect. 2.2.1, could be an interesting alternative. Some essays in this direction are reported in [Casagrandi and Rinaldi, 1999] and [Rinaldi *et al.*, 2001] where this technique has been exploited for the forest fire prevention and for the prediction of extremes episodes, respectively. In the same direction some unpublished trials have been conducted by the colleague Rosario Pittarelli and the author for the detection of cardiac diseases [Pitarelli, 2001].

As suggested by the title of this thesis, what is proposed here is a two step approach of exploiting chaos. The first step regards the automatic modeling of the diversity of real approximately periodic signals by means of chaotic attractors, this is strictly related with the conjecture given above and it is the modeling part of

this thesis. The second step proposes to exploit the so obtained chaotic model, by means of qualitative resonance, for pattern recognition purposes, this clearly represent the applicative part of this thesis.

4.3 Pattern Recognition by Means of Filtering

Before dealing with the problem of building a chaotic model representing a class of patterns together with their diversity, *i.e.* the first step mentioned above, it is necessary to precisely define the topology of the method in which this model will be exploited for pattern recognition purposes, *i.e.* the second step mentioned above.

In order to exploit the qualitative resonance for pattern recognition purposes it is first of all necessary to detect its occurrence. This can be done, as suggested in Sect. 3.1.3, by means of a receding horizon integral measure of the mismatch between the driving signal, *i.e.* the sampling pattern, and the output of the driven system. Calling $u(t)$ the pattern under test and $y(t)$ the output of the driven system, this would correspond to a generic expression of the kind

$$\sigma(u,y) = h\left(\int_{t-T_r}^{t} f\big(u(\tau)-y(\tau)\big)d\tau\right) \tag{4.1}$$

where T_r is the receding horizon on which the test detecting the occurrence of qualitative resonance is run, $f(\cdot)$ is a general enough[5] function, which must be always positive for the functional to make sense, and $h(\cdot)$ is a positive function monotonically increasing, *i.e.* $\big(h(\cdot)>0\big)\wedge\big(h'(\cdot)>0\big)$. A particular choice could be, for instance, $f(\cdot)=(\cdot)^2$ and $h(\cdot)=\sqrt{\cdot}$ in which case $\sigma(u,y)=\|u-y\|_{L^2[t-T_r,t]}$. Such functional is a generalized finite horizon standard deviation of the output with respect to the input, that is why the symbol σ has been chosen to denote the functional result. Hence, the smaller is the value of the functional the more qualitative resonance is taking place. That it is why the method to decide if the qualitative resonance occurs or not will be always supposed to be of the following form

$$\sigma < \sigma_{th} \tag{4.2}$$

where σ is of the form given by Eq. (4.1) while σ_{th} is a suitably chosen threshold. The test given by Eq. (4.2) will be referred to henceforth as *qualitative resonance test* while the functional given by Eq. (4.2) will be referred to as *qualitative resonance functional*.

Exploiting qualitative resonance for pattern recognition would mean to execute the pattern matching by means of filtering. In fact, the ensemble of the qualitatively resonating model, the feedback loop, and the qualitative resonance functional can be imagined as resonating filter whose output, *i.e.* the result of the qualitative resonance functional, is not null only for not resonating signals[6]. Hence, the pattern matching test is executed running the sampling signal through the filter and verifying the intensity of the output; the smaller it is the more the pattern is similar to what is represented by the strange attractor. This filter is called henceforth the *qualitatively resonating filter*.

The conjecture given above (*cfr.* Sect. 4.1) suggests to have coexistence of multiple strange attractors in the qualitatively resonating model in order to represent more than one class of patterns at a time. This idea, albeit biologically attractive [Rabinovich *et al.*, 2000], is quite problematic from an engineering point of view. This is mainly for two reasons, one related to the modeling and one related to the problem of classification. Firstly for the problem of building such a model from data, it is already challenging to store a given information in a chaotic model and it is almost impossible to deal with the problem of storing multiple strange attractors at once. Secondly, while the coexistence of multiple attractors gives the possibility to a single model to resonate with more than one class of patterns, on the other hand, in such a case the

[5] The functional $\sigma(u,y)$ given in Eq. (4.1) define a metric if the following three conditions are all satisfied

$$\big(\sigma(u,y)\geq 0\big)\wedge\big(\sigma(u,y)=0\Leftrightarrow u(\tau)=y(\tau)\quad\forall\,\tau\in[t-T_r,t]\big)$$

$$\sigma(u,y)=\sigma(y,u)$$

$$\sigma(u,y)\leq\sigma(u,z)+\sigma(z,y)\quad\forall\,u,y,z$$

[6] A simple analogy is a series LC filter whose voltage at the terminals is not null only for stimulating currents which are not at the resonating frequency.

occurrence of qualitative resonance gives no insights about the resonating class of patterns; namely, it gives only a binary information: "yes, the pattern belongs to one of the stored classes", but does not say to which class in particular. Hence, it is not possible to perform n-ary classification.

From the engineering point of view, both problems could be easily solved using a bank of parallel chaotic systems as shown in Fig. 4.2, one for each class of patterns that are to be tested, namely a bank of qualitatively resonating filters. This means a filter for each given class of patterns that must be recognized. Namely, one class of patterns is represented by means of one strange attractor, this strange attractor is given by means of one system of ordinary differential equations (ODE), and in turn this ODE is used to build one qualitatively resonating filter. Hence, in general, given a problem of classifying approximately periodic temporal patterns over n classes of patterns, called the $\mathcal{I}$ classes, a filter bank composed of n filters, called the $\mathbf{i}$ filters, must be considered. Each one of the filters in the bank represents a particular class of patterns and tests the sampling pattern against this and only this one class. It reports, by means of the qualitative resonance functional, how much the sampling pattern is similar to the class represented by the strange attractor used in the filter. Thus, the output of the filter bank will be a vector of n numbers quantifying the similarity between the sampling pattern with each one of the n classes of patterns. In a certain way, the filter bank can be considered as a sort of fuzzyfier [Kosko, 1992] saying how much the sampling pattern is likely to belong to this or that class of patterns. Since each particular class of patterns can be associated with a symbol, the vector resulting from the filter bank can be mapped into a probability distribution over a finite alphabet of symbols. Namely, the output of the filter bank can be considered as a probability distribution[7] saying how much likely a pattern corresponds to each one of the symbols of a finite alphabet [Alder, 1994; Kosko, 1992; Vapnik, 1995].

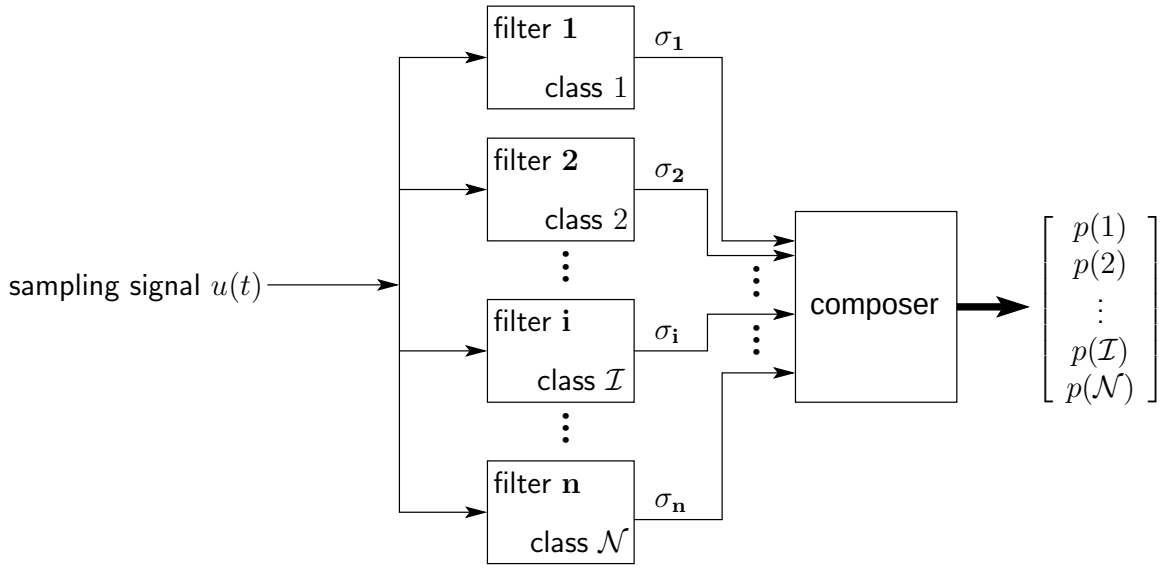

Figure 4.2: *Bank of qualitatively resonating filters as solution for problems of n-ary classification. The sampling signal is presented as input to all the filters at once while the qualitative resonance functional outputs are used to compose a vector of likelihood components.*

In this sense, the filter bank maps the external stimuli to an almost symbolic information. This kind of information, *i.e.* a probability distribution over symbols, is particularly suitable for cascading the filter bank with more abstract pattern recognizers based on symbolic and/or statistic techniques such as fuzzy systems [Kosko, 1992], support vector machines [Cortes and Vapnik, 1995; Schölkopf *et al.*, 1999], neural networks [Dayhoff, 1990], hidden Markov models [Rabiner, 1989], factor graphs [Kschischang *et al.*, 1998], and many others [Bittanti and Picci, 1996; Cherkassky and Mulier, 1998; MacKay, 1999; Michalski *et al.*, 1983, 1986; Vapnik, 1995; Weiss, 1991]. To this higher-level of artificial intelligence the exploitation of all that unexploited information would be left, that is necessary to the accomplishment of the real aim of

[7] It should be noted that even if the output of the filter is considered as a probability distribution over the considered symbols there is no reason why the output should correctly estimate this probability distribution; indeed, in general it would not. Despite of this incorrectness, it is conceptually helpful to consider the output as a likelihood vector.

the artificial cognitive agent for which the stimuli preclassification, performed by the filter bank, is just a subproblem[8].

This idea is perfectly coherent with the former proposal given in Chap. 1 and with the functional schematic of cognitive agent as hypothesized in Fig. 4.1. In fact, in this sense, the filter bank would not be the final pattern recognizer but the implementation of an intelligent sensory system which can processes the incoming stimuli providing to the higher levels of the cognitive agent a highly formatted information, *i.e.* an almost symbolic one, necessary for the accomplishment of more interesting and complex intelligent tasks.

No matter how the qualitative resonance functional is conceived, namely independently from the particular $f(\cdot)$ and $h(\cdot)$ functions chosen for Eq. (4.1), the vector of the qualitative functional results can be easily mapped on a probability distribution. In fact, there is a very natural way to perform such a mapping. Let $\sigma_{\mathbf{i}}$ be the qualitative resonance functional result of the $\mathbf{i}$ filter, namely the i^{th} filter of the filter bank. For the same filter $\mathbf{i}$, let $\sigma_{f\,\mathbf{i}}$ be the value of the same functional when applied on the difference between the output while evolving on the free, *i.e.* not driven, strange attractor and the output while evolving on the generating cycle, namely

$$\sigma_{f\,\mathbf{i}} = \max_{\substack{t \\ \vartheta(t)=y(x(t)):\, x(t)\in SA \\ \psi(t)=y(x(t)):\, x(t)\in GC}} h\left(\int_{t-T_r}^{t} f\big(\vartheta(\tau)-\psi(\tau)\big)d\tau \right)$$

which, in some sense, represents the maximal natural variance of the class $\mathcal{I}$ of patterns.

When the functional answer $\sigma_{\mathbf{i}}$ is null or very small the sampling pattern is very likely to be of the class $\mathcal{I}$, indeed it almost perfectly resonates. On the contrary, when the functional answer is of the magnitude of $\sigma_{f\,\mathbf{i}}$ or even larger it is very unlikely that the sampling signal could belong to the class $\mathcal{I}$; indeed, it almost perfectly anti-resonates since the system wanders at least as it would wander if it would be left free. Exploiting the meaning of $\sigma_{\mathbf{i}}$, an unconditional probability of the sampling pattern to belong to the class $\mathcal{I}$ can be given by the function

$$p_{u\,\mathbf{i}}(\sigma_{\mathbf{i}}), \quad p_{u\,\mathbf{i}} \;:\; \Big(\mathbb{R}^{+} \mapsto [0,1]\Big) \wedge \Big(p_{u\,\mathbf{i}}(\sigma_{\mathbf{i}}) = 0\,\forall \sigma_{\mathbf{i}} \geq \sigma_{f\,\mathbf{i}}\Big) \wedge \Big(p_{u\,\mathbf{i}}(0) = 1\Big) \wedge$$
$$\wedge \Big(p'_{u\,\mathbf{i}}(\sigma_{\mathbf{i}}) < 0\,\forall \sigma_{\mathbf{i}} \in [0, \sigma_{f\,\mathbf{i}}]\Big)$$

The function $p_{u\,\mathbf{i}}$ maps the qualitative resonance functional result $\sigma_{\mathbf{i}}$ *monotonically* into an unconditioned probability of the sampling signal to belong to the class $\mathcal{I}$ of patterns. The probability is one if the resonance error is zero while the probability is zero if the driven system wanders more than what it wanders when left free. Furthermore, the probability diminishes as the resonance error increases. A simple choice of the function $p_{u\,\mathbf{i}}$ is a linear decreasing function from one at zero to zero at $\sigma_{f\,\mathbf{i}}$, saturating at zero for every argument greater of $\sigma_{f\,\mathbf{i}}$.

Such a probability is not yet the value of the probability distribution at the symbol/class $\mathcal{I}$. There are two main reasons for that. First, the integral of a probability density must be one and the sum of the $p_{u\,\mathbf{i}}$ over all the filter bank is clearly not satisfying such a constraint. Second, the value of the probability distribution at the symbol $\mathcal{I}$, *i.e.* the probability of the sampling signal to belongs to the class $\mathcal{I}$, should be a conditional probability; namely, it should be the probability of being this symbol given that it is in one of the available classes. The two reasons in reality coincide, in fact the conditioning of the probability obliges the sum of the probabilities over all the symbols to be one, *i.e.* the tautology "a symbol must be a symbol[9]". A simple normalization of the probabilities $p_{u\,\mathbf{i}}(\sigma_{\mathbf{i}})$ over the entire filter bank leads to the probability distribution over the symbols $\mathcal{I}$

$$p(\mathcal{I}) = \frac{p_{u\,\mathbf{i}}(\sigma_{\mathbf{i}})}{\sum\limits_{j=\mathbf{i}} p_{u\,\mathbf{i}}(\sigma_{\mathbf{j}})} \tag{4.3}$$

[8] As far as unattainable at this stage, an example would be an application in speech recognition in which the different phonemes would be preclassified by such a kind of qualitatively resonating filter bank. After the filtering, the left information necessary to identify the precise pronounced word, as the phoneme occurrence probability and/or the probability of a sequence of phonemes, would be left to a higher-level of artificial intelligence as, for instance, the hidden Markov chains, which are normally used for speech recognition [Rabiner, 1989].

[9] On this topic a big discussion about the recognition of the so called foreigners could be opened [Alder, 1994; Schalkoff, 1992; Vapnik, 1995], namely patterns that do not belong to any of the considered classes. Actually, the detection of foreigners, sometimes called *novelty detection*, is a nontrivial task that can be better performed on statistical argument by the higher-level pattern recognizer that should follow the filter bank [Schölkopf *et al.*, 2001]. Hence, this case is not considered here.

Since $p(\mathcal{I})$ is wanted to be a conditional probability, this normalization has a precise statistical meaning. It means that the occurrence of a symbol is independent from the occurrence of any other symbol. Namely, assuming Eq. (4.3) as true implies that there are no reasons other than the results of the qualitative resonance functionals over the entire filter bank to suppose that a sampling pattern should belong more likely to a class rather than another. In other words, the symbols are supposed equilikely to occur. This is natural in absence of any other information. In regard to that, it should be noted that any *a priori* statistical information about the probability of occurrence of the symbols can be included in Eq. (4.3) using the Bayes formula [Walpone, 1993] for computing the conditional probability of the symbols.

4.3.1 Filter Topologies

On the basis of what is presented in the previous chapter and on the basis of what is just discussed above, the proposed general topology for one qualitatively resonating filter is shown in Fig. 4.3. It is characterized of eight elements which are not necessarily all present in a real implementation of the filter.

1. *Chaotic model*: is the Shil'nikov-like chaotic model of the patterns that must be recognized by the filter; namely, it is the chaotic model of the patterns which should let the filter resonate. It is the main component of the filter.

2. *Filter gain*: is the feedback gain matrix K, discussed in detail in the previous chapter, which tunes the occurrence of qualitative resonance and anti-resonance.

3. *Qualitative resonance functional*: is the functional used to detect the occurrence of qualitative resonance between the driving signal and the Shil'nikov-like chaotic model.

4. *Phase detector (optional)*: it is necessary if the adopted filter gain is periodic. Its aim is to detect the phase of the driving signal and to lock the phase of the filter gain on it.

5. *Control loop switch (optional)*: it switches on and off the control feedback loop depending upon the phase synchronization between the driving signal and the free Shil'nikov-like chaotic signal.

6. *Phase lock detector (optional)*: it is necessary if the control loop switch is used. Its aim is to detect when the driving signal and the chaotic model are almost in phase.

7. *Frequency modulator (optional)*: it is useful when the considered temporal patterns are not stationary in frequency. Namely, it is useful in case of temporal patterns which do not change in shape but that can change in frequency. Its aim is to modulate the temporal scale of the chaotic model, and eventually of the filter gain, such as to match that of the driving signal.

8. *Period detector (optional)*: it is necessary if the frequency modulator is adopted. Its aim is to detect the nominal pseudo-period of the driving signal.

Several different kinds of topologies/filters can be obtained from the general topology shown in Fig. 4.3 depending upon the particular choices adopted for each one of these elements.

Chaotic Model

There is nothing special to say about that, almost everything has been already said above. The main problem is to build it starting from data, Sect. 4.4.1 and the entire next chapter are dedicated to this.

Filter Gain

The aim of the filter gain K is to tune the occurrence of qualitative resonance and anti-resonance, *cfr.* Chap. 3. It determines which patterns qualitatively resonate and which do not. Its role has been discussed in Sect. 3.3.3; moreover, Sect. 4.4.2 and the entire Chap. 6 are dedicated to the problem of tuning it.

As it can be imagined on the basis of what has been presented in Sect. 3.3.3, the arguments that will be adopted later to tune the filter gain K will be those of optimal linear periodic control theory. Thus, besides all the particulars, there are two main kinds of possible filter gains, constant or periodic.

The main advantage of using a periodic filter gain rather than a fixed one is from Sect. 3.3.3. Independently of the particular technique chosen for designing the filter gain, *i.e.* filtering/reconstruction or control/tracking techniques, to restrict the solution on a fixed feedback gain implies that only the stability

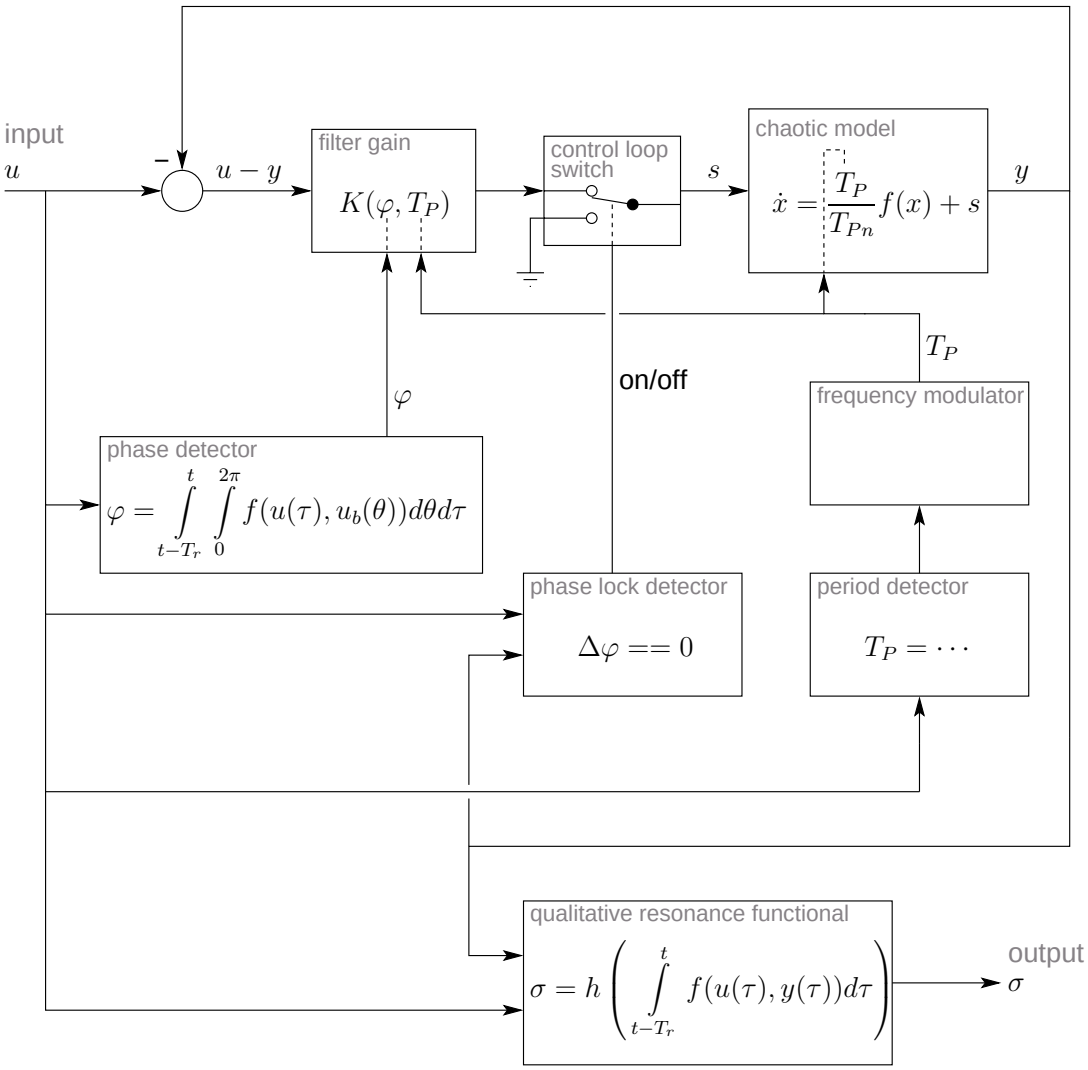

Figure 4.3: *General topology of one qualitatively resonating filter.*

can be warranted, *cfr.* Sect. 3.3.3. Namely, the filter gain can be tuned such as to guarantee the qualitative resonance (reconstruction/tracking) of the signal associated with the clean generating cycle but no constraints can be imposed on the perturbations that will be supported by the filter without hurting the homoclinic trajectory, *i.e.* the class of resonating patterns cannot be specified. In other words, once the stabilizing fixed filter gain is determined, the class of perturbations which stay away from the homoclinic trajectory (class of qualitatively resonating signals) and those that lead the system to approach it (class of qualitative anti-resonating signals) are determined, there are no degrees of freedom. The fixed filter gain fixes the two classes of qualitatively resonating and anti-resonating patterns. On the contrary, as will be shown in Chap. 6, considering a periodic feedback gain allows to give some specifics on the classes of resonating and anti-resonating signals. Furthermore, the design of a periodic filter gain is, paradoxically, easier than the design of a fixed gain. This is simply because in the linear periodic control theory [Bittanti and Colaneri, 1999] it is assumed as hypothesis that the feedback gain is, for both control and filtering problems, periodic. Hence, all the algorithms available in the literature, refer to the references in [Bittanti and Colaneri, 1999], for the design of an optimal and/or robust periodic reconstructor/follower return, by definition, a periodic feedback gain. Few cases are available for the case of fixed gain [Aeyels and Willems, 1995; Tornambé and Valigi, 1996].

On the other side of the medal, the clear disadvantage of a periodic gain is the necessity of synchronizing

its phase with that of the input signal. Indeed, the gain is optimal only under this condition. If a periodic filter gain is adopted then the *phase detector*, discussed later in the text, is devoted to solve this particular problem.

Qualitative Resonance Functional

The role and aim of the qualitative resonance functional has already been discussed in detail in Sect. 4.3. Here three particular interesting forms of qualitative resonance functionals, which comply with the general form given by Eq. (4.1), are proposed.

The first one, which is very simple, corresponds to assume $f(\cdot) = (\cdot)^2$ and $h(\cdot) = \sqrt{\cdot}$. This means that the qualitative resonance functional is the finite horizon quadratic error of the driven system output with respect to the driving signal. Such a choice is very interesting keeping in account the simple physical meaning of the functional.

The second proposed form, which is slightly more complex, finds its reason in the following remark. The driven strange attractor has not uniform sensitivity with respect to the external perturbations. Indeed, the local sensitivity to external perturbations depends upon the local expansion of the strange attractor, the more the trajectories are locally expanding the more sensitive is the strange attractor to the external perturbations. This can lead to conclude that the intensity of the resonance error $(u(t) - y(t))$ should not be weighted always in the same way. A large error in a very sensitive region could be not so important as a small error in a relatively insensitive region. The simplest possible qualitative resonance functional taking into account the local expansion of the strange attractor is

$$\sigma = \sqrt{\int_{t-T_r}^{t} \frac{1}{\varepsilon + e^{Tr(J(x(\tau)))}} \big(u(\tau) - y(\tau)\big)^2 d\tau}$$

which uses as a weight for the resonance error the inverse of the local expansion of the strange attractor. In fact, the first approximation of the local expansion is given by the exponential of the local divergence, which is indeed the trace of the local Jacobian.

The aim of the third proposed functional is simply to measure how much the strange attractor of the driven system shrinks, independently from the driving signal. Namely, it measures the natural variance of the driven system and not the variance relative to the input signal. The reason for such a measure has to be found in the qualitative resonance itself; as it has been shown in the previous chapter, the main effect of qualitative resonance is a shrinking of the strange attractor, the fact that it shrinks around a signal similar to the driving one is a further condition. Hence, a finite horizon integral measure for such shrinking could be, for instance, the following

$$\sigma = \sqrt{\int_{t-T_r}^{t} \left(y(\tau) - \frac{1}{n} \sum_{k=1}^{n} y(\tau - kT_P) \right)^2 d\tau}$$

where T_P is the nominal pseudo-period and n an integer positive number; namely, the inner sum compute the mean of $y(t)$ along n pseudo-periods and the outer integral compute the variance. A simpler integral variant is

$$\sigma = \sqrt{\int_{t-T_r}^{t} \big(y(\tau) - y(\tau - nT_P) \big)^2 d\tau}$$

where the variance is simply relativized to the output $y(t)$ n pseudo-periods earlier.

Phase Detector

In the case that a periodic filter gain is adopted it is necessary, to satisfy the conditions under which the filter gain has been obtained, to synchronize the phase of the filter with the phase of the input signal [Feuer and Goodwin, 1996].

Any periodic function can be described by a base function (*cfr.* Sect. 3.1.3) defined over the interval $[0, 2\pi)$ [Amerio, 1977a,b]. In particular this is true for the periodic signal $u(t)$, *i.e.* the output while evolving

on the generating cycle, which has been used to tune the periodic gain $K(t)$ and the periodic gain itself, namely

$$\begin{aligned} u(t) &= u_b(\frac{2\pi t}{T_G} \mod 2\pi) \\ K(t) &= K_b(\frac{2\pi t}{T_G} \mod 2\pi + \varphi_0) \end{aligned}$$

where T_G is the period of the generating cycle. The filter gain $K(t)$ is obtained assuming a given initial relative phase φ_0 with respect to the input signal, usually $\varphi_0 = 0$. Thus, at control time the filter gain $K(t)$[10] must run with this same relative phase with respect to the input signal if the control is to be effective. To synchronize in phase the input signal and the filter gain means to obtain the absolute phase of the input signal from measurements of it and then to synchronize the absolute phase of the control gain on it. Thus, obtaining a relative phase $\varphi_0 = 0$.

This can be achieved with standard techniques [Feuer and Goodwin, 1996] as, for instance, a *main component phase locked loop (PLL)* [Christiansen, 1997; Taub and Schilling, 1986]. Another technique, purely nonlinear, is to exploit the two peak-to-peak one-dimensional maps described in Sect. 2.6. In fact, from the amplitudes of subsequent peaks it is possible to extract the phase of the input signal and then to synchronize the phase of the filter gain on it.

Whatever the chosen method is, to avoid any kind of stability problem, the overall phase control must be a feedforward method. Namely, it must correct the phase of the filter gain on the only basis of the input signal. It is not forbidden to use also, for instance, the resonance error but this is in some sense unnecessary and furthermore *taboo*. In fact, if any information on the output of the filter is used for the phase locking, a new loop is closed; thus, its stability must be guaranteed [Brogan, 1996] and this it is not an easy task.

The general form suggested for the phase detector is a receding horizon one, namely a phase detector that determines the phase of the input signal on the basis of measurements of the input signal over a finite interval, *e.g.*

$$\varphi(t) = \int_{t-T_r}^{t} \int_{0}^{2\pi} f\big(u(\tau), u_b(\theta)\big) d\theta d\tau$$

where T_r is the receding horizon used to determine the phase. The two methods proposed above are indeed of this kind.

Both the techniques proposed above have been tested giving satisfactory results. Since the peak-to-peak based technique is closer to the chaotic methods, the author prefers it.

Control Loop Switch

As largely explained in Chap. 3, the arguments on which the filter gain is designed are valid only when the state of the driven system and the driving signal are almost phase locked.

Based on this argument could be the idea to activate (switch on) the feedback loop only when this condition is satisfied and, on the contrary, to deactivate (switch off) the feedback loop when the two phases excessively diverge.

Two subsidiary subsystems are necessary to implement such an idea. First of all, a phase locking detector. It can be composed of two phase detectors, one for the phase of the driving signal and one for the phase of the output of the driven system. This is not particularly complex and could be realized with techniques similar to those described above for the *phase locker*. The second subsystem, is definitely more complex.

The control loop switch is a bang-bang kind of control (all or nothing) [Atherton, 1982]; it is known that for such a kind of control system a hysteresis is necessary in order to avoid rippling problems [Atherton, 1982]. The aim of such a hysteresis would be, in one direction, to decide when the phase locking has been kept long enough and then to switch on the feedback loop; vice versa, it should, in the other direction, detect an excessively prolonged phase drift before switching off the feedback loop. The tuning of the two thresholds for the hysteresis is not particularly easy [Atherton, 1982]. In fact, this kind of bang-bang with hysteresis control ignites oscillations in the overall system; the frequency of these oscillations depends on the two thresholds of the hysteresis. Since these control oscillations are going to excite the modes of the driven system, it is necessary that they are uncoupled in frequency from the useful signal considered [Atherton, 1982]. Even warranting the frequency uncoupling, the risk of exciting some subharmonic effects due to the

[10] Since the control gain $K(t)$ depend only on the data of the model and not on the measurements, it is usually precomputed and stored. Thus, it is read sequentially according to the current phase of the input signal [Feuer and Goodwin, 1996].

nonlinearity is always present, complicating further the tuning of the hysteresis. Summarizing, the tuning of such a kind of control loop switch is a mess[11].

This technique has been tested and the results have been everything but promising. In particular, no advantages given by the control loop switch have been observed. On the contrary, the occurrence of qualitative resonance is slackened by the presence of the switch. Namely, the qualitative convergence synchronization of the driven system state towards the (hidden) state of the driving system is faster when the control feedback loop is always on. This clearly indicates that the linear analysis of the qualitative resonance is not enough to explain all its intrinsic properties, there are a lot of nonlinear properties of qualitative resonance that remain unexplained and, even worse, unexploited.

Even though it has proved to be unnecessary and even performance degrading, it is necessary to keep this technique available since it is the only way to guarantee the condition under which the filter gain is tuned. It cannot be said *a priori* that there are not cases where it turns out to be fruitful or even necessary.

Phase Locking Detector

As described above, if the control loop switch is adopted, it is necessary to detect the occurrence of the phase locking between the driving signal and the driven system. This can easily be done by means of two phase detector realized with, more or less, standard techniques as described in the *phase detector* section.

Frequency Modulator

There are particular classes of approximately periodic signals which are not stationary in frequency. These are approximately periodic signals which preserve their shape in amplitude but that change their time scale. For instance in a ECG the heart beating rate is not always the same due to the fact that the heart accelerates and decelerates according to the oxygen demand [Despopoulos and Silbernagl, 1991]. Also the pitch of the vowels pronounced by the same person augments and diminishes depending on the prosody [Deller *et al.*, 1993].

When dealing with this kind of signals it can be useful to modulated the time scale of the driven system such as to adapt it to the time scale of the driving system. The time scale modulation, which is in fact a frequency modulation [Taub and Schilling, 1986], of the driven system can be realized very easily once the instantaneous nominal pseudo-period T_M is known. Indeed, suppose that the following ODE admits a periodic solution of period T_0

$$\dot{x} = F(x)$$

then the ODE

$$\dot{x} = \frac{T_0}{T_M} F(x)$$

admits a periodic solution of period T_M. Hence, the time scale of the driven system can be easily controlled by using a multiplicative coefficient on its right hand side [Kuznetsov, 1998].

In the case in which a periodic filter gain is adopted its time scale must be modulated as well. Since the filter gain is simply precomputed and run locked in phase with the input signal, this is not very difficult; indeed, once it has been precomputed with sufficient temporal resolution, the modulation of its time scale it is just a matter of running through its values more or less rapidly [Feuer and Goodwin, 1996].

Clearly, to adapt the natural frequency of the driven system to the frequency of the driving signal, it is necessary to detect the period/frequency of the driving signal. The *period detector*, discussed hereafter, is devoted to solve this particular problem.

Period Detector

In the case that the frequency modulation of the driven system, and eventually of the filter gain, is adopted, it is necessary to determine the natural frequency/period of the driving signal.

This can easily be done as soon as an approximate base function $u_b(\varphi)$ of the driving signals is known, which is indeed the case knowing at least the base function of the generating cycle. The problem of the period detection is not very different from that of the phase detection discussed above for the *phase locker*. Actually, all the techniques used for detecting the phase can be used as well for the detection of the pseudo-period of the driving signal [Taub and Schilling, 1986]. Alternatively, the pseudo-period of a signal can be determined by means of standard frequency analysis [Baher, 1990; Proakis and Manolakis, 1992] or slightly

[11] The author is sorry but this is the best technical term to describe the problem.

more complex convolutive techniques [Blatter, 1998]. Another, purely nonlinear, technique is to exploit the two peak-to-peak one-dimensional maps described in Sect. 2.6. In fact, from the amplitudes of subsequent peaks, and the measure of the elapsed time between them, it is possible to determine the time scaling factor necessary to fit the one-dimensional map of the return time (*cfr.* Sect. 2.6) to the measurements.

Once again, whatever the method chosen is, to avoid any kind of stability problem, the overall time scale control must be a feedforward method. Namely, it must modulate the time scale of the driven system of the filter gain on the only basis of the input signal. It is not forbidden to use also, for instance, the resonance error but this is in some sense unnecessary and furthermore *taboo*. In fact, if any information on the output of the filter is used for the frequency modulation a new loop is closed; thus, its stability must be guaranteed and this it is not an easy task.

Again, a general form for the period detector can be suggested. It is a receding horizon one, namely a period detector that determines the pseudo-period of the input signal on the basis of measurements of the input signal over a finite interval, *e.g.*

$$T_M(t) = \int_{t-T_r}^{t} \int_{0}^{2\pi} f\big(u(\tau), u_b(\theta)\big) d\theta d\tau$$

where T_r is the receding horizon used to determine the pseudo-period. Frequency analysis methods, more complex convolutive ones, as well as the peak-to-peak-based one can be mapped onto this general form.

Three techniques have been tested: one based on principal component analysis and finite time Fourier transform [Proakis and Manolakis, 1992]; one based on multi-resolution technique, practically a wavelet [Blatter, 1998] transform where as wavelet function the base signal has been used; and the peak-to-peak-based one. All of them gave satisfactory results. Since the peak-to-peak based technique is more close to the chaotic methods, the author prefers this one.

4.3.2 Degrees of Freedom Summary

The general topology of the qualitatively resonating filter shown in Fig. 4.3 has a total of six free parameters, three binary and three analog parameters which depend on the binary choices.

Because of the binary choices, there are $2^3 = 8$ specific topologies of qualitatively resonating filter.

Filter gain: can be fixed (F) or periodic (T).

Feedback loop: can be always on (F) or switched on phase locking (T).

Natural frequency: can be fixed (F) or modulated (T).

Each one of the true (T) binary choices induces a subproblem with infinite solutions which determines a further degree of freedom.

Phase locker: necessary if a periodic filter gain is adopted.

Period detector: necessary if the natural frequency is modulated.

Phase lock detector: necessary if the feedback loop is switched.

4.4 Building the Filter

After having chosen the desired topology of the qualitatively resonating filter from those proposed in the previous section, the filter must be tuned to fit the data of the application in which it is to be used.

This means mainly two things, to build a Shil'nikov-like chaotic model of the class of temporal patterns that are to be recognized by the filter and to tune the filter gain such as to guarantee resonance and anti-resonance with the patterns of the correct classes. The two next chapters are dedicated to these two subproblems but, before discussing the particularities of them, there are some general noteworthy remarks. Indeed, this two subproblems address specifically the first and second step of the chaos based approach to pattern recognition as proposed in Sect. 4.2.

4.4.1 Modeling

This task addresses specifically the modeling part of this thesis, its aim is to store a class of approximately periodic temporal patterns, together with their diversity, inside a strange attractor. Namely the first step proposed in Sect. 4.3.

In particular, this task should provide as results the dynamical model of a Shil'nikov-like chaotic model fitting at best the data. This is the chaotic model necessary to build the qualitatively resonating filter used to recognize the class of patterns stored in the strange attractor, *cfr.* Sect. 4.3.1.

To build a dynamical model, chaotic or not, from observations means identification. In fact, nonlinear identification methods will be used.

Three main problems can be identified *a priori* about the nonlinear identification problem spanned by this task.

1. *Constrained identification*: the aim is not to identify any kind of chaotic model fitting the data but a particular one, namely a Shil'nikov-like one. Even admitting that the signals that are to be fitted are, as discussed in Chap. 2, from a Feigenbaum-like strange attractor, an identification based on these data will lead, at best, to a chaotic model of this kind that, as discussed in the previous chapter, is not enough for the qualitative resonance. The Feigenbaum-like strange attractors are simpler than the Shil'nikov-like ones (*cfr.* Chap. 2); hence, it is clear that a constraint leading the identified model to be more complex than what it should be, *i.e.* Shil'nikov-like rather than Feigenbaum-like, is needed.

2. *Stability*: even admitting to succeed in fitting the data to a Shil'nikov-like strange invariant by means of a constrained identification, the stability of this strange object remains a serious and tough problem. It could be, for instance, that the identified dynamical model admits a strange saddle rather than a strange attractor.

3. *Overfitting*: a strange attractor is composed of infinite saddle limit cycles but it is itself a compact set [Ruelle, 1989]. The typical trajectory of a strange attractor jumps between the saddle cycles of its skeleton; hence, the observations from a strange attractor are segments of limit cycle. Since the data available for the identification are finite, *i.e.* they do not cover the entire strange attractor, it could happen that the identification rather than providing a model with a single compact chaotic invariant set provides a model with several isolated invariants, namely limit cycles.

Finally, it should be noted that for dealing with this task only instances (examples) of patterns from the class that is to be stored in the strange attractor are needed. With respect to the qualitatively resonating filter, which is the final aim, these patterns can be considered as the *good patterns* since they are those that must by recognized by the filter. In antithesis, the *bad patterns* can be defined, namely those that must not be recognized when tested with this specific filter.

4.4.2 Tuning Qualitative Resonance

This task addresses specifically the part of the thesis which proposes to exploit the chaotic model obtained from the modeling part for pattern recognition purposes. Namely the second step proposed in Sect. 4.3.

In particular, this task should provide as a result the filter gain necessary to build the qualitatively resonating filter, *cfr.* Sect. 4.3.1.

This task has been already largely discussed in Sect. 4.3.1 and in Sect. 3.3.3. In particular, it has been shown that the achievement of this task passes by techniques proper to the optimal/robust linear periodic filtering/control theory.

Two main problems can be identified *a priori* about the optimal/robust filtering/control problem spanned by this task.

1. *Too large filter gain*: as discussed in Chap. 3, the filter gain should be small enough such that it does not alter excessively the free dynamics of the driven system. The solution provided by the optimal/robust periodic control theory may not satisfy this constraint.

2. *Indistinguishability*: it could happen that the constraints defining the robust control/filtering problem[12], are too tight. Hence, the solution to the control/filtering problem does not exists. In this case the two classes of good and bad patterns cannot be distinguished by the qualitatively resonating filter.

[12] Repetitat juvat. The constraints are the class of perturbation that must be beard by the tracker/reconstructor without touching the homoclinic trajectory (qualitative resonance) and the class of perturbations that must lead to touch the homoclinic trajectory (anti-resonance).

Finally, it should be noted that for dealing with this task both instances of good and bad patterns are necessary. Indeed, the aim of tuning the filter gain is not only the robustness of the qualitative resonance but also the occurrence of the anti-resonance in presence of bad patterns.

4.5 Remarks

Before going to the details of the proposed techniques developed to address the two above mentioned sub-problems, it should be noted that together they correspond to the learning phase of a supervised learning algorithm [Bishop, 1995; Vapnik, 1995]. In fact, it could be said that what is proposed in this thesis is a chaos-based supervised learning algorithm; in this respect, more comments are given in the introduction of Chap. 7. Indeed, the modeling phase corresponds to learn the diversity of the patterns that are to be stored into the strange attractor in such a way to be able to recognize them in the future. On the other hand, the filter gain tuning corresponds to learn the differences between the class of patterns that are to be stored in the strange attractor and the other classes of patterns considered in the specific application.

Bibliography

Aeyels, D. and J. Willems (1995). Pole assignment for linear periodic systems by memoryless output feedback. *IEEE Transactions of Automatic Control*, 40, pp. 735–739.

Alder, M. (1994). *Principles of Pattern Classification: Statistical, Neural Net and Syntactic Methods of Getting Robots to See and Hear*. Not published. Freely available on the world wide web: ftp://ciips.ee.uwa.edu.au/pub/syntactic/book,http://ciips.ee.uwa.edu.au/ mike/PatRec/.

Amerio, L. (1977a). *Analisi Matematica con Elementi di Analisi Funzionale I*. UTET, Torino, Italy. In Italian.

Amerio, L. (1977b). *Analisi Matematica con Elementi di Analisi Funzionale II*. UTET, Torino, Italy. In Italian.

Andreyev, Y., Y. Belsky, A. Dmitriev, and D. Kuminov (1996a). Information processing using dynamical chaos. *IEEE Transactions on Neural Networks*, 7, pp. 290–299.

Andreyev, Y., A. Dmitriev, L. Chua, and C. Wu (1992). Associative and random access memory using one-dimensional maps. *International Journal of Bifurcation and Chaos*, 2, pp. 483–504.

Andreyev, Y., A. Dmitriev, D. Kuminov, L. Chua, and C. Wu (1996b). 1-D Maps, chaos and neural networks for information processing. *International Journal of Bifurcation and Chaos*, 6, pp. 627–646.

Andreyev, Y., A. Dmitriev, and M. Matveev (1995). Application of chaotic dynamical systems to the problems of recognition and classification. In *Proceedings of the 3rd International Workshop on Nonlinear Dynamics in Electronic Systems NDES*, pp. 249–252. Dublin, Ireland.

Andreyev, Y., A. Dmitriev, and A. Ovsyannikov (1999). Chaotic processors and content-based search of information in unstructured data bases. *Interdisciplinary Journal of Nonlinear Phenomena in Complex Systems*, 2, pp. 48–53.

Andreyev, Y., A. Dmitriev, and S. Starkov (1997). Information processing in 1-D systems with chaos. *IEEE Transactions on Circuits and Systems—I*, 44, pp. 21–28.

Atherton, D. (1982). *Nonlinear Control Engineering*. Van Nostrand Reinhold, Melburne. Australia.

Baher, H. (1990). *Analog & Digital Signal Processing*. John Wiley & Sons, New York, NY.

Bishop, C. (1995). *Neural Networks for Pattern Recognition*. Clarendon Press, Oxford, UK.

Bittanti, S. and P. Colaneri (1999). *Periodic Control*, pp. 59–74. John Wiley & Sons, New York, NY.

Bittanti, S. and G. Picci, editors (1996). *Identification, Adaptation, Learning: The Science of Learning Models from Data*. Springer-Verlag, New York, NY.

Blatter, C. (1998). *Wavelet's : A Primer*. A K Peters, Natick, MA.

Brogan, W. (1996). *Modern Control Theory*. Prentice-Hall, New York, NY, third edition.

Candaten, M. and S. Rinaldi (2000). Peak-to-Peak dynamics: A critical survey. *International Journal of Bifurcation and Chaos*, 10(8), pp. 1805–1819.

Casagrandi, R. and S. Rinaldi (1999). A minimal model for forest fire regimes. *American Naturalist*, 153, pp. 527–539.

Cherkassky, V. and F. Mulier (1998). *Learning from Data: Concepts, Theory and Methods*. John Wiley & Sons, New York, NY.

Christiansen, D., editor (1997). *Electronics Engineers' Handbook*. McGraw-Hill for IEEE Press, New York, NY.

Cortes, C. and V. Vapnik (1995). Support vector networks. *Machine Learning*, 20, pp. 273–297.

Dayhoff, J. (1990). *Neural Networks Architectures: An Introduction*. Van Nostrand Reinhold, New York, NY.

De Feo, O., G. Maggio, and M. Kennedy (2000). The Colpitts oscillator: Families of periodic solutions and their bifurcations. *International Journal of Bifurcation and Chaos*, 10, pp. 935–958.

Deller, J., J. Proakis, and J. Hansen (1993). *Discrete-Time Processing of Speech Signals*. Prentice-Hall, Upper Saddle River, NJ.

Despopoulos, A. and S. Silbernagl (1991). *Color Atlas of Physiology*. Thieme, Stuttgart, Germany, fourth edition.

Dmitriev, A., A. Panas, and S. Starkov (1991). Storing and recognizing information based on stable cycles of one-dimensional maps. *Physics Letters*, 155A, pp. 494–499.

Elbert, T., W. Ray, Z. Kowalik, J. Skinner, K. Graf, and N. Birbaumer (1994). Chaos and physiology: Deterministic chaos in excitable cell assemblies. *Physiological Reviews*, 74, pp. 1–47.

Feuer, A. and G. Goodwin (1996). *Sampling in Digital Signal Processing and Control*. Birkauser, Boston, MA.

Goertzel, B. (1994). *Chaotic Logic: Language, Thought and Reality From the Perspective of Complex Systems Science*. Plenum, New York, NY.

Gumowski, J. and C. Mira (1980). *Dynamique Chaotique*. Capadues, Toulouse, France. In French.

Kelso, J. (1995). *Dynamic Patterns: The Self-Organization of Brain and Behavior*. MIT Press, Cambridge, MA.

Kosko, B. (1992). *Neural Networks and Fuzzy Systems*. Prentice-Hall, Englewood Cliffs, NJ.

Kschischang, F., B. Frey, and H. Loeliger (1998). Factor graphs and the sum-product algorithm. *IEEE Transactions on Information Theory*. Submitted.

Kuznetsov, Y. (1998). *Elements of Applied Bifurcation Theory*. Springer-Verlag, New York, NY, second edition.

MacKay, D. (1999). *Information Theory, Inference, and Learning Algorithms*. Not published. Freely available on the world wide web: http://wol.ra.phy.cam.ac.uk/mackay/itprnn/book.html.

Michalski, R., J. Carbonell, and T. Mitchell, editors (1983). *Machine learning: An Artificial Intelligence Approach volume I*. Tioga, Palo Alto, CA.

Michalski, R., J. Carbonell, and T. Mitchell, editors (1986). *Machine learning: An Artificial Intelligence Approach Volume II*. Morgan Kaufmann, Los Altos, CA.

Mira, C., L. Gardini, A. Bugola, and J. Cathala (1996). *Chaotic Dynamics in Two-Dimensional Noninvertible Maps*. World Scientific, Singapore.

MITCHELL, M. (2000). Theories of structure versus theories of change (Commentary on T. van Gelder, "The dynamical hypothesis in cognitive science)". *Behavioral and Brain Sciences*. Submitted.

MITCHELL, M. (2001). A complex-systems perspective on the "Computation vs. Dynamics" debate in cognitive science. In *Proceedings of the Twentieth Annual Conference of the Cognitive Science Society*. To Appear.

NEWMAN, D. (1998). Chaos, classification, and intelligence. In COLUMBO, R., editor, *Origine Della Vita Intelligente Nell'Universo: Atti del Convegno Internazionale*, pp. 93–106. New Press, Como, Italy.

OTT, E. (1993). *Chaos in Dynamical Systems*. Cambridge University Press, New York, NY.

PITARELLI, R. (2001). *Methods to Design and Assess Monitoring Processes for Complex Systems: Application to Cardiovascular Intensive Care Early Detection of Pathophysiological Events*. Ph.D. thesis, Swiss Federal Institute of Technology Lausanne, Lausanne, Switzerland.

PROAKIS, J. AND D. MANOLAKIS (1992). *Digital Signal Processing: Priciples, Algorithms and Applications*. Maxwell Macmillan, New York, NY, second edition.

RABINER, L. (1989). A tutorial on hidden Markov models and selected applications in speech recognition. *Proceedings of the IEEE*, 77, pp. 257–286.

RABINOVICH, M., P. VARONA, AND H. ABARBANEL (2000). Nonlinear cooperative dynamics of living neurons. *International Journal of Bifurcation and Chaos*, 10, pp. 913–933.

RINALDI, S., R. CASAGRANDI, AND A. GRAGNANI (2001). Reduced order models for the prediction of extreme episodes. *Chaos, Solitons & Fractals*, 12, pp. 313–320.

ROBERTSON, S., A. COHEN, AND G. MAYER-KRESS (1993). *Behavioural Chaos: Beyond the Metaphor. A Dynamic Systems Approach to Development: Applications*. MIT Press, Cambridge, MA.

ROUABHI, S. (2000). Storage of information in one-dimensional piecewise-continuous maps. *International Journal of Bifurcation and Chaos*, 10, pp. 1127–1137.

RUELLE, D. (1989). *Chaotic Evolution and Strange Attractors : The Statistical Analysis of Time Series for Deterministic Nonlinear Systems (Lezioni Lincee)*. Cambridge University Press, Cambridge, UK.

RUSSELL, S. AND P. NORVIG (1999). *Artificial Intelligence: A Modern Approach*. Prentice-Hall, New York, NY.

SCHALKOFF, R. (1992). *Pattern Recognition: Statistical, Structural and Neural Approaches*. John Wiley & Sons, New York, NY.

SCHÖLKOPF, B., C. BURGES, AND A. SMOLA (1999). *Advances in Kernel Methods: Support Vector Learning*. MIT Press, Cambridge, MA.

SCHÖLKOPF, B., J. PLATT, J. SHAWE-TAYLOR, A. SMOLA, AND R. WILLIAMSON (2001). Estimating the support of a high-dimensional distribution. *Neural Computation*. To appear.

SHINSKEY, F. (1996). *Process Control Systems: Application, Design, and Tuning*. McGraw-Hill, New York, NY.

TAUB, H. AND D. SCHILLING (1986). *Principles of Communication Systems*. McGraw-Hill, New York, NY, second edition.

THAGARD, P. (1996). *Mind: Introduction to Cognitive Science*. MIT Press, Cambridge, MA.

THIRAN, P. (1996). *Dynamics and Self-Organization of Locally Coupled Neural Networks*. Ph.D. thesis, Swiss Federal Institute of Technology Lausanne, Lausanne, Switzerland.

TORNAMBÉ, A. AND P. VALIGI (1996). Asymptotic stabilization of a class of continuous-time linear periodic systems. *Systems and Control Letters*, 28, pp. 189–196.

VAPNIK, V. (1995). *The Nature of Statistical Learning Theory*. Springer-Verlag, New York, NY.

WALPONE, R. (1993). *Probabilty and Statistics for Engineers and Scientists*. Macmillan, New York, NY, fifth edition.

WEISS, S. (1991). *Computer Systems that Learn? Classification and Prediction Methods from Statistics, Neural Nets, Machine Learning and Expert Systems*. Morgan Kaufmann, San Mateo, CA.

CHAPTER 5

AUTOMATIC CHAOS-BASED MODELING OF DIVERSITY

Brief — In this chapter one among the possible algorithms to model a class of approximately periodic temporal patterns by means of a chaotic attractor is presented. The chosen algorithm is presented since it is easy, based on standard known theories, and, furthermore, fairly well performing. No one of the other considered algorithms has revealed noticeably superior performance to this one despite of an increased complexity. Hence, in some sense, the proposed technique represents the best quality/price compromise. The proposed algorithm decomposes the chaotic modeling into two steps. The first step is devoted to obtain a Feigenbaum-like chaotic model from the data while the second step is dedicated to drive the model resulting from the first step towards Shil'nikov-like chaotic conditions. The first step decomposes the nonlinear identification problem into a linear identification and a nonlinear optimization assuming a Lur'e structure for the model to identify. The second step exploits the theoretical relationships between Feigenbaum-like and Shil'nikov-like systems to drive, by means of continuation techniques, the result of the first step towards Shil'nikov-like conditions.

Personal Contribution — The nonlinear identification algorithm presented in this chapter is original. Nonetheless, it can be considered as a fitting of fairly similar algorithms already known in literature to the purposes of this thesis.

This chapter deals with the construction of a Shil'nikov-like chaotic model for the class of good patterns, its aim is to store a class of approximately periodic temporal patterns, together with their diversity, inside a strange attractor of Shil'nikov's kind.

Although several algorithms to accomplish this duty have been considered, in this chapter only one of them is presented, a few of the others are briefly mentioned in Appendix E. The algorithm presented here is the one with the best quality/complexity ratio among those that have been considered; it is simple, based on standard known theories, and fairly well performing. Indeed, despite of its simplicity, the proposed algorithm reveals to be effective in most of the cases (*cfr.* Chap. 7); more in particular, no one of the other considered algorithms has revealed noticeably superior performance to this one despite of an increased complexity.

The idea followed in developing such algorithms is to decompose the given task, *i.e.* building the Shil'nikov-like chaotic model for the class of patterns considered, into subproblems that have been already solved in other fields of science or engineering. This is the common *divide et impera*[1] approach dear to the engineers. As mentioned in Sect. 4.4.1, building models from data is the aim of identification; thus, the decomposition will inevitably lead to some kind of identification subproblem. In order to decompose a problem into subproblems it is usually necessary to assume some hypotheses which allow indeed the decomposition

[1] Divide and conquer.

itself. The first decomposition here considered relies on the following hypothesis.

(H.1) The data considered for building the model, *i.e.* the instances of good patterns, are indeed of Feigenbaum's kind.

This means that the data available for the accomplishment of this task, *i.e.* the good patterns, are assumed to be produced by a Feigenbaum-like chaotic system. This is coherent with all that presented in Chap. 2 where it has been shown that the diversity of approximately periodic signals seems to be related to Feigenbaum-like attractors, *cfr.* Sect. 2.2.1. As mentioned at the end of the previous chapter (*cfr.* Sect. 4.4.1) this implies already a problem, the data available (Feigenbaum-like) are simpler than the aimed result (Shil'nikov-like). The solution of this problem is the aim of the first decomposition; in particular, the construction of the Shil'nikov-like chaotic model is decomposed into the following two steps.

1. *Feigenbaum-like chaotic model identification*: the aim of this step is to build a Feigenbaum-like chaotic model for and from the Feigenbaum-like patterns available. The result of this step should be a parameter dependent ODE together with a set of parameter values at which the given ODE is Feigenbaum-like chaotic. Obviously, the resulting Feigenbaum-like strange attractor should span those dynamical properties of the patterns used for the identification.

2. *Shil'nikov driving*: the aim of this second step is to drift the parameter values of the model resulting from the first step such as to drive the system to Shil'nikov's conditions. This step is conceivable because of the theoretical relationships between Feigenbaum-like chaos and Shil'nikov-like chaos, *cfr.* Sect. 2.5.2.

5.1 Feigenbaum-like Model Identification

The technique that is described here does not consist simply of the identification algorithm, besides it there are other points that need clarification, among them are the following.

The input data: the data used for the identification needs to be specified. In particular, it is necessary to specify which kind of properties they must satisfy and which kind of treatment they must undergo before being used for the identification.

The modeling technique: which kind of modeling technique to use; in particular, continuous time or discrete time.

The nonlinear identification: the identification of a Feigenbaum-like chaotic model remains a complex task, it is necessary to decompose it into simpler subproblems.

The algorithm: this is mainly what provides the result of this first step; it is the identification algorithm resulting from the decomposition of the nonlinear Feigenbaum-like identification task into easier subproblems.

These points are addressed in details in the following sections.

5.1.1 The Input Data

Details about how to treat the data used for the identification are given in the Sect. 7.1.2 of the Chap. 7. Besides these details, there are some general considerations about the data that should be used and, in particular, about the treatment that they should undergo before their use.

First of all, as mentioned in Sect. 4.4.1, the data considered must be representatives of good patterns. Namely, they must be observations, *i.e.* measurements, of temporal patterns indeed belonging to the class of patterns that are to be stored into the qualitatively resonating filter. This could sound quite obvious but actually, it implies a certain degree of confidence about the source of measurements considered; namely, it must be certain that the measurements considered are of the considered class of patterns (*cfr.* Chap. 7).

The hypothesis (H.1), namely the fact that the observations are of Feigenbaum's origin, implies that the measurements considered must satisfy the following conditions.

1. Each considered observation must be long enough in time such as to describe a significative portion of the underlining Feigenbaum-like strange attractor.

For instance, an observation containing about thirty-two pseudo-periods[2] should be long enough. Since the data are supposed to be generated by a Feigenbaum-like strange attractor, it is natural to consider time lengths of their observations of $q * 2^r$ times the nominal pseudo-period, where q is prime number and r a positive integer [Ott, 1993].

2. The observations must be long enough such to span a significative part of the strange attractor but, on the other hand, they must not be too long in order to avoid any kind of nonstationariness in the signals. The data must remain contextual, *cfr.* Chaps. 2 and 7.

3. Since its period-doubling structure, it is conceivable to approximate a Feigenbaum-like strange attractor with a periodic orbit of long enough period, *cfr.* Sect. 2.5.1. Thus, the observations, which on the base of the previous point should be sensible to be long enough in such sense, should be adjusted at the boundaries, begin and end, such to become periodic.

4. On the base of the previous point, whenever necessary, the data should be considered periodic. Namely, whenever example signals longer than their real length are needed, the observations can be considered as ring closed starting reading them from the beginning when their end is reached.

As in any kind of identification application, it is recommended to perform a preliminary filtering and a scaling of the signals [Ljung, 1999, 2000]. The filtering has as aim to remove those frequency components that are more likely to be due to real external noise, as *e.g.* the noise due to the measuring instrumentation, rather than being an intrinsic part of the signal [Ljung, 1999, 2000]. The aim of scaling, on the other hand, is to avoid any kind of numerical problems in the identification algorithm due to too small or too large numbers. Since identification relies, implicitly or explicitly, on matrix inversion problems, an excessive excursion of the signals can lead to a diminished reliability of the numerical computations. Furthermore, since the identification algorithm must deal with both the signals and their dynamics, the scaling is meant on both amplitude and time scale, *cfr.* Sect. 7.1.2.

The data considered are real measurements; in general they are the sampled version, *i.e.* discrete time, of an analog, *i.e.* continuous time, signal [Brogan, 1996; Proakis and Manolakis, 1992; Rinaldi and Piccardi, 1998]. More precisely, every observation is a vector containing the regularly sampled measurements, *i.e.* sampled at fixed rate, of a continuous time source [Proakis and Manolakis, 1992].

In this respect, it should be noted that it is not sufficient for the sampling rate to satisfy the Shannon's theorem. Indeed, as specified later in Sect. 5.1.2, the vector of measurements must be dynamically equivalent to the observed continuous time system and not simply containing the same frequency information [Feuer and Goodwin, 1996; Guardabassi, 1990; Proakis and Manolakis, 1992].

Finally, the available observations must substantially represent the class of patterns that are to be stored into the qualitatively resonating filter. Namely, sufficiently enough observations must be available such that they richly describe the intrinsic diversity of the class of patterns considered. Thus, in practice, there are several vector of measurements which must be considered all at once and not as a single very long observation vector, this imply particular choices in the identification strategies that can be considered, as explained lately in the text.

5.1.2 The Modeling Technique

Since the measurements, as well as the most common identification algorithms, are in the discrete time domain [Ljung, 1999], it is clear that the most convenient modeling technique is also in the discrete time domain. However, this does not correspond to what was presented until now; indeed, the chaotic attractors considered, as well as the qualitative resonance, are continuous time phenomena. This does not represent a real problem; it is known [Feuer and Goodwin, 1996; Guardabassi, 1990] that the continuous time systems and their sampled discrete time versions are indeed equivalent [Feuer and Goodwin, 1996; Guardabassi, 1990] under the assumption of a sufficiently high sampling rate.

The cited equivalence does not refer to the well-known theorem of Shannon [Proakis and Manolakis, 1992] which states the sampling condition for an equivalence between a continuous time signal and its sampled version based on their frequency content. What is meant here is the *qualitative dynamical* equivalence between the discrete time system resulting form the sampling of a continuous time system and the sampled system itself, which is slightly different from the equivalence at an information theoretic level. In fact, it is well-known [Feuer and Goodwin, 1996; Guardabassi, 1990] that discrete time systems are richer in features than

[2]Remember that pseudo-period is used to address both an entire oscillation and the average of the oscillation periods.

their continuous time counterpart of the same order. A simple example is given by the oscillating behavior which is already possible in first order discrete time systems while at least a second order continuous time dynamical system is necessary to exhibit such behavior [Callier and Desoer, 1991].

In order to guarantee the qualitative dynamical equivalence between the sampled (discrete time) system and the original (continuous time) system, none of these additional features characteristic of discrete time systems must appear in the sampled system[3] [Feuer and Goodwin, 1996; Guardabassi, 1990]. This condition is automatically satisfied whenever the sampling frequency is high enough such as to oversample even the fastest possible phenomena in the continuous time system [Guardabassi, 1990]. A practical rule in this direction is, usually, to consider a sampling frequency at least two orders of magnitude greater than the fastest phenomenon of interest in the continuous time system [Feuer and Goodwin, 1996; Lambert, 1991; Schwarz, 1989].

It should be noted that this equivalence rule is the same as the one used to determine the minimal integration step in a numerical integrator [Lambert, 1991; Schwarz, 1989] that guarantees the reliability of its result.

5.1.3 Nonlinear Identification

The nonlinear identification, especially of a chaotic system, is a difficult topic [Juditsky *et al.*, 1995; Sjoberg *et al.*, 1995]. Most of the algorithms available in the literature are quite specific to particular cases [Akritas *et al.*, 2000; Yuan, 1995; Yuan and Feeny, 1998] and/or quite complicated [Aguirre and Billings, 1995; Aguirre *et al.*, 1996; Al-Zamel, 1999; Dedieu and Ogorzalek, 1997]. Since neither the development of general nonlinear identification algorithms nor the verification of the effective applicability of those cumbersome algorithms that are already available in the literature is the aim of this thesis, it is necessary to somehow simplify this task. Once again, the simplification is achieved by a decomposition of the complex task into easier subproblems. In particular, the decomposition proposed here relies on the following hypothesis.

(H.2) The data considered for building the model, *i.e.* the instances of good patterns, are generated by a scalar Lur'e-type dynamical system [Atherton, 1982].

This would not represent a restrictive hypothesis if a generalized Lur'e system, *i.e.* a Lur'e system with a vectorial (n-dimensional) nonlinearity, was considered. In fact, every ODE can be rewritten in the form of a generalized Lur'e system [Slotine and Li, 1991]. The effective limitation is due to the restriction to scalar Lur'e systems. In reality, this hypothesis is not a methodological hypothesis but rather an operative one. In theory, the algorithm, which is explained later, can be applied in the case of vectorial nonlinearity too, *i.e.* to generalized Lur'e systems. Unfortunately, the complexity of the algorithm grows exponentially with respect to the nonlinearity domain and codomain dimensions. Thus, to keep the complexity to a reasonable level, only the scalar case has been considered here. Theoretically, nothing but the computation time prevents from considering higher-dimensional nonlinearities.

A Lur'e system is composed of two clearly distinct parts, as shown in Sect. 5.1, the linear dynamical system and the algebraic, *i.e.* static, nonlinearity. The algorithm presented in the next section exploits this to decompose the nonlinear identification problem into two easier and well-known subproblems.

5.1.4 The Algorithm

The main idea exploited by this algorithm is to simplify the task of the nonlinear identification by opening the feedback loop of the Lur'e system, and then to identify the two parts, the dynamical and the static one, separately. Opening the feedback loop, the nonlinear identification of the ensemble can be reduced to an iterative method which works alternatively on two very basic problems; namely, *linear identification* and *nonlinear optimization*.

The working principle can be easily explained referring to Fig. 5.1. Consider a parameterized nonlinear function $f_p(\cdot)$ where the index p highlights the dependence upon the parameter vector p of m elements, *i.e.* $p \in \mathbb{R}^m$. Open the feedback loop in the point A and consider a reference signal(s) $y(t)$ on the two sides of the of the open loop, *i.e.* A' and A''. Applying the nonlinearity $f_p(\cdot)$ to the reference signal(s) $y(t)$ the input $u(t)$ of the linear dynamical system $G(Z)$ is obtained. At this point it is possible to apply a parametric linear identification technique [Ljung, 1999, 2000] on the pair $(u(t), y(t))$ such as to obtain an

[3] Roughly speaking, the sampled system should not exhibit negative characteristic multipliers associated with its dynamic [Feuer and Goodwin, 1996; Guardabassi, 1990].

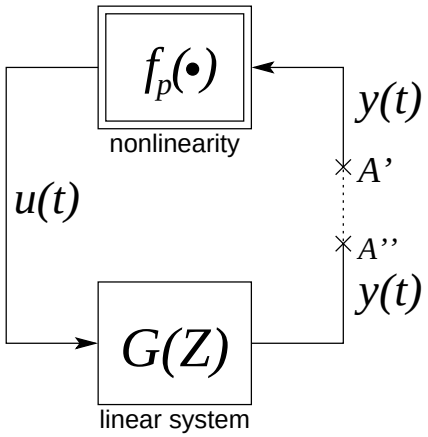

Figure 5.1: *Decomposition of a Lur'e dynamical system into its elementary parts.*

estimation $\widehat{G}(Z)$ of the linear system[4]. Besides the estimate of the transfer function $\widehat{G}(t)$, every serious linear identification techniques [Johansson, 1993; Ljung, 1999, 2000] returns also a measure of the quality of the identification result; namely, a measure that says how much reliable is the identified transfer function $\widehat{G}(t)$. Hence, it is possible to alter the parameters describing the nonlinear function p such as to improve this quality measure. In other words, it is possible to optimize the identification quality with respect to the guessed nonlinearity. Then, the procedure can be iteratively repeated until, hopefully, the best possible pair $(p, \widehat{G}(Z))$ is determined.

The described method is an iterative forward method, namely the information propagates always forward on the open feedback loop. In fact, the guess of the nonlinearity is used to compute the input of the linear system used in the linear identification, and then the confidence measure of the identification is used to correct the guess about the nonlinearity. This represents the simplest method, more complex variants where the information propagates backward, forward-backward, and roundly, are briefly illustrated in Appendix E.

To summarize, the nonlinear identification problem is decomposed into a linear identification whose quality determines the value of a nonlinear objective function which must be optimized acting on the parameters describing the nonlinearity.

Before passing to describe in detail how to deal with the two subproblems, there are two noteworthy general remarks.

First, iterative algorithms as the one described should be proved to converge. For the particular case considered, *i.e.* Lur'e systems, there exist a general theoretical result about the convergence of iterative methods similar to the one described [Wigren, 1994, 1997]. In particular, the theoretical result affirms that if a solution exists the iterative method will converge to it. A solution exists if the considered reference signal(s) $y(t)$ is indeed issued from a Lur'e system or, at least, if its dynamics can be described by such kind of systems.

Secondly, opening the feedback loop, the Lur'e system becomes a Wiener [Rugh, 1990], or a Hammerstein, system. Hence, it seems natural to exploit one of the identification algorithms available for this particular kind of dynamical systems [Bai, 1998; Greblicki, 1998; Ledoux, 1996] to identify both the parts at once. However, this idea cannot be exploited since most, if not all, these algorithms rely on the fact that the identification runs on an open loop [Juditsky *et al.*, 1995; Ledoux, 1996], *i.e.* the input is independent of the output, which is definitely not the case here. Furthermore, it should be noted that these algorithms do not differ substantially from the one proposed here; with the difference that in these algorithms it is not possible, or it is not easy, to include constraints that keep in account the fact that the loop is indeed closed, as explained later in the text.

[4]Keeping in account the scalar hypothesis (H.2) on the nonlinearity, it follows that $G(Z)$ describe a single-input—single-output linear (SISO) relation. Since identification algorithms for multi-input—multi-output (MIMO) relations exists, the described algorithm can be adopted, as mentioned above, for generalized Lur'e systems; obviously, at the price of an augmented complexity.

Linear Identification

The identification of linear dynamical systems is a common problem of control theory [Callier and Desoer, 1991; Johansson, 1993] and literally tons of literature are available on this topic. For what is relevant here, the linear identification is a subproblem; hence, the choice of a particular identification algorithm from those available in literature is subordinate to the accomplishment of the final goal, *i.e.* the Lur'e identification. In particular, with respect to the final aim[5], four points must be taken into account when employing an identification algorithm.

1. *Data use*: as mentioned above (*cfr.* Sect. 5.1.1) there are several reference vectors ($y(t)$) which have to be taken into account for the identification. There are two possible ways in which several input—output relations can participate to the identification of a single dynamical system [Ljung, 1999; Ljung and Söderström, 1983]. First, they can be used alternatively in an iterative method, but it is known that this kind of methods do not work very effectively [Johansson, 1993; Ljung, 1999; Söderström and Stoica, 1989]; this is mainly because each input—output relation has been obtained starting from a different initial condition of the dynamical system, and these iterative methods do not discern between these different initial conditions. The second method to exploit several independent input—output relations for a single identification is all at once. It is, usually, possible to extent the standard techniques to consider several input—output relations [Johansson, 1993; Söderström and Stoica, 1989], each one with its own initial condition, and then to consider the dynamical system which fits at best, on the basis of some least square error or similar criterion, all of them[6].

2. *Model*: there are several ways to model a linear input—output relation[7]. In particular, these models differ in the way in which the effect of a possible exogenous noise is taken into account. According to

[5] In reality, these four points are quite general for any application of identification algorithms. However, here they are specifically interpreted with respect to the final aim to which the linear identification is devoted here.

[6] The linear parametric identification algorithms are in general based, implicitly or explicitly, on the solution of an overdimensioned linear system, *i.e.* a linear system with more equations than unknowns, which links the parameters of the linear system to the measurements. The solution of this linear system passes by the computation of the pseudo-inverse of a matrix which keeps the measurements in account. The term *pseudo* takes into account that there are more relations, *i.e.* measurements, than unknowns, *i.e.* parameters. Thus, from the kind of particular pseudo-inverse chosen it depends in which sense the measurements must be fitted, least square error, maximal error etc. [Meyer, 2000; Schwarz, 1989]. In all the nonrecursive identification algorithms this matrix can be extended to keep in account as many independent input—output relations as desired [Ljung and Glad, 1994]. A simple example is the identification of an ARMA input—output relation

$$y(t) = -\sum_{i=1}^{n} a_i y(t-i) + \sum_{i=1}^{n} b_i u(t-i)$$

which corresponds to the transfer function

$$G(Z) = \frac{\sum_{i=1}^{n} b_i Z^{n-i}}{Z^n + \sum_{i=1}^{n} a_i Z^{n-i}}$$

Suppose to have an ordered pairs of observations $(u(k), y(k))\ k = 0, 1, \ldots, r$ with $r \gg n$. Then the complete ARMA relationships can be rewritten as

$$\begin{bmatrix} y(n-1) & y(n-2) & \cdots & y(0) & u(n-1) & u(n-2) & \cdots & u(0) \\ y(n) & y(n-1) & \ddots & y(1) & u(n) & u(n-1) & \ddots & u(1) \\ y(n+1) & \ddots & \ddots & y(2) & u(n+1) & \ddots & \ddots & u(2) \\ \vdots & \ddots & \ddots & \vdots & \vdots & \ddots & \ddots & \vdots \\ y(r-1) & y(r-2) & \cdots & y(r-n) & u(r-1) & u(r-2) & \cdots & u(r-n) \end{bmatrix} \begin{bmatrix} -a_1 \\ -a_2 \\ \vdots \\ -a_n \\ b_1 \\ b_2 \\ \vdots \\ b_n \end{bmatrix} = \begin{bmatrix} y(n) \\ y(n+1) \\ y(n+2) \\ \vdots \\ y(r) \end{bmatrix}$$

or

$$T\theta = Y$$

where T, θ, and Y are the corresponding Toeplitz matrix and vectors shown above. Hence, the maximum likelihood estimation of the parameter vector $\theta = [-a_i\ b_i]^T$ is given by

$$\theta = T^{-1\dagger} Y$$

where $T^{-1\dagger}$ is the pseudo-inverse of the Toeplitz matrix T. It should be clear that such an approach can easily take into account several pairs of independent observations $(u_i(k), y_i(k))$.

[7] Since hypothesis (H.2), here only SISO linear relations are considered but, as explained in the footnote 4, similar arguments are valid in the case of MIMO linear relations.

the way in which the exogenous noise acts on the system, there are the *generic SISO linear relation*, the *ARMAX*, the *ARX*, the *Output-Error*, and the *Box-Jenkins* models [Ljung, 1999, 2000]. Which one of them to consider depend on the suspected nature of the data and is one of the skills required to the control engineers [Ljung, 1999, 2000; Söderström and Stoica, 1989]. For the application here considered, of particular interest are the Output-Error models in which only a measuring noise is kept in account and no modeling noise is considered. A model of this kind is in agreement with the hypothesis assumed in this thesis, more precisely with the *Thesis* itself. In fact, as assumed in Chaps. 1 and 2, and reasserted in the previous chapter, the diversity of the considered signals must be deterministically modeled by means of the strange attractor, whose identification is the final aim to which the linear identification is devoted, and not by means of exogenous modeling noise as usually done. That is why here only the Output-Error model has been considered; even though that, one of the other models could result necessary in a particular application [Johansson, 1993; Ljung, 1999; Söderström and Stoica, 1989], *cfr.* Chap. 7.

3. *Order*: whatever model for the linear input—output relation is chosen a critical problem is the choice of its order [Ljung, 1999, 2000]. The choice of the order in linear identification is a very complex problem; indeed, there are entire books dedicated to this topic [Burnham and Anderson, 1998; McQuarrie and Tsai, 1998]. Once again, which order to consider depends on the suspected nature of the data and is one of the skills required to the control engineers. Since the final aim is a (continuous time) chaotic system, it is clear that no less than a third order can be considered [Ott, 1993]. On the other hand, tests run on several data (*cfr.* Chap. 7) have indicated that most of the time a fourth order system appears to be enough. There is a geometrical intuition that can justify such a remark. The considered model of diversity is Feigenbaum-like chaos (*cfr.* Sect. 2.2.1) which lies on a Möbius' strip. The next complexity step for modeling diversity, restricting to Feigenbaum-like strange attractors, is the so-called *doubly flipped* Feigenbaum-like chaos[8] [Kuznetsov, 1998]. This kind of strange attractor lies on a Klein's bottle which is indeed embedded into a four-dimensional space. Probably, this model of diversity is already complex enough to model any kind of observable endogenous diversity, which could be the reason why the fourth models have proved to be sufficient in most cases. Even though that, it could be that an order higher than four is necessary to model possible integral effects which are not at the origin of the diversity but that are anyway present. In this respect, the role of the employed dimensions (order) can be easily determined once the identification has been ended; indeed, the dimension of the identified strange attractor gives a hint of how many dimensions are devoted to model the endogenous diversity, *i.e.* $\lceil d \rceil$ where d is the Haußdorf dimension of the strange attractor [Ott, 1993], and how many are devoted to model linear filtering effects, *i.e.* $n - d$ where n is the order considered for the system.

4. *Method*: there are several linear identification algorithms available in literature [Johansson, 1993; Ljung, 1999, 2000; Söderström and Stoica, 1989], they differ in several points: in the domain in which they work, time or frequency; the model they consider, input—output or state space; the way in which operate, recursive or single shot; etc. [Johansson, 1993; Ljung, 1999; Ljung and Söderström, 1983]. Most of them are optimized for a particular input—output model, for instance the *general instrument* method is suited for ARX models [Ljung, 1999, 2000], the *prediction error* based methods are suited for Output-Error and ARMAX models, etc. [Ljung, 1999, 2000]. For the application here considered, the frequency based identification algorithms must be considered *taboo*, this because they cannot be used in closed loop identification [Ljung, 1999, 2000]. On the other hand, recursive algorithms are of no interest since the identification must not be performed online; moreover, the recursive algorithms are, obviously, not suited for considering several input—output relations at once. Finally, since the Output-Error model is mainly considered, the prediction-error and the maximum-likelihood [Ljung, 1999, 2000] algorithms (*cfr.* the footnote 6) are to be considered the most suitable ones for this application.

Nonlinear Optimization

As the identification, the optimization of nonlinear static functions is a common problem and is one of the main topics of *operations research* [Hillier and Lieberman, 1990; Wagner, 1975; Winston, 1991]; in the literature there are several algorithms dedicated to solve this problem. Once again, here, the nonlinear function optimization is a subproblem; hence, the choice of a particular optimization algorithm from those available in literature is subordinate to the accomplishment of the final goal, *i.e.* the Lur'e identification.

[8] The doubly flipped Feigenbaum-like attractors [Kuznetsov, 1998] are obtained by a cascade of period doubling bifurcations in two alternatively directions. The doubly flipped Feigenbaum attractor has its Shil'nikov-like counterpart in the focus-focus Shil'nikov-like strange attractors [Kuznetsov, 1998].

In particular, with respect to the final aim[9], three points must be kept in account in employing a nonlinear optimization algorithm.

1. *Nonlinearity parameterization*: the aim of the optimization is to find the nonlinearity $f(\cdot)$ whose application on the reference signal(s) $y(t)$ (*cfr.* Fig. 5.1) results in the best possible linear identification. Given as such, this would be a problem of functional analysis; it can be reduced to a problem of function optimization approximating the generic function $f(\cdot)$ with a parameter dependent function $f_p(\cdot)$, *i.e.* parameterizing the nonlinearity. Consequently, the problem is reduced to finding the combination of parameters $\overline{p}$, *i.e.* the description of the approximating nonlinearity, which results in the best linear identification.

   The considered parameterization of the function $f(\cdot)$, *i.e.* $f_p(\cdot)$, should satisfy at least the following two properties.

   — It should be *complete* [Amerio, 1977a,b,c; Arfken and Weber, 1995]. Namely, there must exist a measure with respect to which $f_p(\cdot)$ converges to $f(\cdot)$ when the dimension of p tends to infinity. Loosely speaking, augmenting the number of parameters used should augment the precision with which $f_p(\cdot)$ approximates $f(\cdot)$.

   — The parameterization should be *unique* [Amerio, 1977a,b,c; Arfken and Weber, 1995]. Namely, given the order of approximation, *i.e.* the dimension of p, the approximated function $f(\cdot)$ uniquely identifies the parameters p which determine the best approximating function $f_p(\cdot)$ with respect to a given norm. Roughly speaking, the effect of each parameter p_i on the shape of $f_p(\cdot)$ should be independent of the effects of the other parameters $p_{j\neq i}$.

   In this sense, any orthonormal bases of the Hilbert space L^2 represents a good candidate parameterization of the nonlinearity [Amerio, 1977b,c; Arfken and Weber, 1995]. Therefore, any finite generalized series expansion of functions [Arfken and Weber, 1995] represents a suitable parameterization of the nonlinearity, as, for instance, the standard orthonormal polynomials series, commonly used in engineering, of *Gegenbauer*, *Hermite*, *Laguerre*, *Legendre*, *Jacobi*, and *Tchebyshev* [Szegö, 1975]. Clearly, using one of these orthonormal bases would imply to assume, implicitly, the hypothesis that the nonlinear function $f(\cdot)$ is a continuous[10] member of L^2 [Arfken and Weber, 1995]. As an alternative to the series-based approximations of the nonlinearity are the geometrical-based ones, which are easily conceivable especially in the case of a scalar nonlinearity. Examples of this kind of approximations are the cubic *splines* [de Boor, 2000; Schwarz, 1989]; the *piecewise linear functions* [Chua and Kang, 1977]; and the *piecewise polynomials*, *i.e.* the generic splines, [de Boor, 2000; Schwarz, 1989]. This kind of approximations does not require to the function $f(\cdot)$ to be a continuous member of[11] L^2.

   To be effective with respect to the final aim, the parameterized nonlinearity should satisfy two further conditions.

   — The parameterization of the nonlinearity must compose, together with the linear transfer function, a unique parameterization of the Lur'e system. In particular, to guarantee such an uniqueness, the slope of f_p, *i.e.* f'_p, must be assigned in a point[12], for instance $f'_p(\overline{0}) = 1$. In fact, since the transfer function has its own static gain ρ, the static loop gain, given by $\rho f'_p(y)$, is not unique, it can be altered either acting on ρ or on f'_p. In this respect, it should be noted that fixing the slope in the wrong point could jeopardize the entire identification. For instance, fixing the slope of f_p in the origin such that $f'_p(0) = 1$ while the data require this slope to be zero or very small would lead to have a badly conditioned overall identification; in fact, to compensate the nonzero loop gain at the origin, the linear identification will result in very small static gain ρ which, in turn, will compel the nonlinearity to very high values off the origin.

   — To avoid problems in the overall nonlinear identification algorithm, the regression of the nonlinearity to a linear function must be forbidden. In fact, in several possible parameterizations there exists a suitable combination of the parameters such that the nonlinearity $f_p(\cdot)$ regresses to a linear function, *i.e.* $f_{\overline{p}}(x) = mx$; this combination of parameters must be removed from the search space on which the

[9] In reality, these three points are quite general for the application of nonlinear optimization algorithms. However, here they are specifically interpreted with respect to the final aim to which the nonlinear optimization is devoted here.

[10] The effective discontinuity is obtained only when the entire series expansion is considered, *i.e.* $dim(p) \to \infty$.

[11] In reality the examples given here implicitly imply that the approximated function $f(\cdot)$ is a continuous member of L^2; nevertheless, there are other cases, as noncontinuous piecewise linear functions, which do not imply that.

[12] The uniqueness condition in the case of vectorial nonlinearity and MIMO transfer function becomes less evident.

optimization algorithm works. The reason for this is rather simple, the iterative nonlinear identification method above described works in a closed loop; in particular, the reference signal(s) at input and output, points A' and A'' in Fig. 5.1, are exactly the same, namely $y(t)$. Therefore, if the nonlinearity is allowed to regress to a linear function, then the overall iterative method will converge to the trivial solution $f_p(x) = mx$ and $\widehat{G}(Z) = \frac{1}{mZ}$. In fact, because of the dense sampling condition (*cfr.* Sect. 5.1.2) the delay of a sampling period (T_S), *i.e.* the Z at the denominator, is very small. Hence, the overall loop transfer function, *i.e.* $(1/Z)$, regresses, up to a very small delay, to the identity *input equals output*, which is, obviously, the best possible solution satisfying the data. In addition, a second constraint is necessary; actually, this one is on the transfer function but it is logic to discuss it here. To avoid the convergence of the overall method to trivial loop solutions, of the kind $f_p \bullet \widehat{G}(Z) = \frac{1}{Z^r}$, it is not enough to restrict the nonlinearity to be indeed nonlinear; actually, it is necessary to forbid the degeneracy of the linear transfer function as well. This can be done in several ways [Bittanti, 2000a], for instance: prohibiting too many cancellations between the poles and zeros of $\widehat{G}(Z)$; prohibiting too many poles at the origin; prohibiting the annihilation of the a_i (b_i) coefficients (*cfr.* the footnote 6); etc. [Bittanti, 2000a]. In particular, pure delay solutions, as well as poles and zeros with negative real part, should always be forbidden since they do not correspond to any continuous time ODE (*cfr.* Sect. 5.1.2).

The two parameterizations that have been considered (*cfr.* Chap. 7) are the Tchebyshev polynomials of first kind [Arfken and Weber, 1995; Szegö, 1975] and the smoothed piecewise linear functions [Doedel *et al.*, 1998]; examples of them are given in Fig. 5.2. The smoothed piecewise linear functions are simply piecewise linear functions in which the absolute value operator is substituted by the smooth operator

$$|x| \rightarrow \frac{2x}{\pi} atan(ax)$$

where the parameter a is called *attraction* since it determines as much close to the break point of the piecewise linear function the smoothed function will pass. Hence, an n-segment smoothed piecewise linear function is characterized by $3n-1$ parameters; namely, n slopes, $n-1$ parameters for the break points, one parameter for the vertical shift and $n-1$ attractions. Therefore, fixing the slope in a point, as required above, gives $3n-2$ parameters to characterize an n-segment smoothed piecewise linear function.

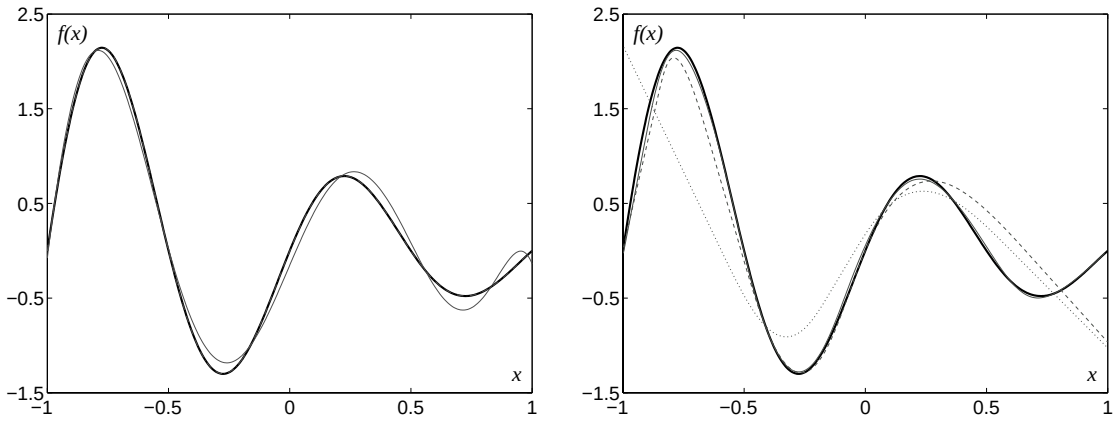

Figure 5.2: *Parameterization of the nonlinearity,approximation of* $sin(2\pi x)e^{-x}$ *(bold line) in the interval* $[-1, 1]$*: (a) – by means of Tchebyshev polynomials, eight (dotted), eleventh (dashed), and fourteenth (solid) order; (b) – by means of piecewise linear smoothed function, three (dotted), four (dashed), and five (solid) segments.*

2. *Objective function*: any measure of the quality of the linear identification can be used as objective function to be minimized by the optimization algorithm. In this regard, it should be noted that the aim of the objective function is not simply to account for the quality of the linear identification result. In fact, as explained in the next point, the algorithms that have been considered in this thesis are suited for *unconstrained* optimization; hence, the objective function must be altered, by means of penalty functions

[Hillier and Lieberman, 1990; Winston, 1991], such as to take into account the degree of compliance of the considered solution, *i.e.* the parameters vector p, to the imposed constraints, *cfr.* previous point. Thus, in general, the objective function $f_C(p)$ will be the sum of two terms

$$f_C(p) = f_I(p) + \sum_{j=1}^{r} f_{P\,j}(p)$$

The first term ($f_I(p)$) measures the quality of the linear identification result while the second term ($\sum_{j=1}^{r} f_{P\,j}(p)$) weights the satisfaction of the imposed constraints, *i.e.* the degree of compliance to the j constraint is measured by means of the penalty function $f_{P\,j}$ [Hillier and Lieberman, 1990; Winston, 1991].

A simple formulation of f_I can be obtained by considering that every serious parametric linear identification algorithm returns both the mean value and the covariance matrix of the identified parameters [Bittanti, 2000a; Ljung, 1999]. From these two information items it is possible to compute the *tolerance*, or the interval of confidence [Walpone, 1993], of every estimated parameter. Call $\overline{\theta}$ the average parameter value vector of the estimated parameters and Θ the corresponding covariance matrix, namely

$$\Theta = E[(\theta - \overline{\theta})(\theta - \overline{\theta})^T]$$

Consider the following matrix, *i.e.* the relative tolerance matrix,

$$R_T = \Theta./\overline{\theta\theta}^T$$

where ./ is the pairwise division of matrices; any norm of such matrix can be used as measure of badness of the identification, namely

$$f_I(p) = \left\|R_T\right\|_X \tag{5.1}$$

In fact, the higher the norm of the relative tolerances matrix the higher are the tolerances within it, thus the worse is the identification. Another possible formulation of f_I can be given evaluating the prediction ability of the identified model [Bittanti, 2000b; Ljung and Söderström, 1983]. Once the linear system ($\widehat{G}(Z)$) is obtained, it can be used to forecast the output at k steps ahead $\widehat{y}(t+k|t)$, given the input $u(t)$ up to the time $t+k$ and the output $y(t)$ up to the time t, thus the $t+k|t$ notation. The prediction error $e(t) = \widehat{y}(t+k|t) - y(t+k)$ can be used to compute a measure of the badness of the identified model, the higher the prediction error the worse is the prediction ability of the model, thus the worse is the identified model. Given the approximative periodicity of the involved signals $u(t)$ and $y(t)$, it results of particular interest to consider the prediction error in predictions a number of steps ahead coinciding with the elapsing of a multiple of the pseudo-period, *i.e.* $k : kT_S = mT_P$ where T_S is the sampling period, T_P is the nominal pseudo-period, and m is an integer greater than zero. By means of the same argument, it is reasonable to evaluate an integral measure of this prediction error over a finite horizon of time that is a multiple of the pseudo-period. Hence, for instance, a receding horizon mean square error can result in a suitable formulation of f_I, namely

$$f_I(p) = \frac{1}{r}\sum_{i=1}^{r}\left(\widehat{y}(t+k|t) - y(t+k)\right)^2 \tag{5.2}$$

where $k : kT_S = mT_P$ and similarly $r : rT_S = nT_P$, with m and n integer numbers greater than zero. In reality, Eq. (5.2) would not result in a good objective function. In fact, the prediction, thus the prediction error, is computed assuming the standard initial condition for the transfer function [Brogan, 1996; Rinaldi and Piccardi, 1998], *i.e.* everything at zero. Thus, the prediction error would include, in general, the effect of the wrong initial condition. Since an error in the initial condition results in a static systematic error, *i.e.* $E[e(t)] \neq 0$, rather than considering the prediction error its derivative should be considered that indeed removes the static systematic error due to the wrong initial condition, alternatively an AC coupled measure of the prediction can be considered instead, *i.e.* $e(t) - E[e(t)]$. Hence, a correct badness measure of the identification would be

$$f_I(p) = \frac{1}{r}\sum_{i=1}^{r} e'(i)^2 \tag{5.3}$$

where $e'(t)$ is either the derivative of the prediction error or the AC coupled measure of it.

On the other hand, examples of penalty functions can be given for the constraints mentioned above. The parameters p determining the nonlinearity must always be different from the combination that let the nonlinear function regress to a linear one, the parameter combination leading to such regression can be given in implicit form of the kind $g(p) = 0$; thus, a possible penalty function for this constraint is

$$f_{P\,1} = \frac{1}{g^2(p)}$$

Analogously, the constraint on the poles and zeros, or the other parameters as the a_i and b_i, of the identified linear transfer function warranting the non degeneracy, namely the non lowering of order, can be easily given by functions of the following kind

$$\begin{aligned} f_{P\,i} &= \frac{1}{|\mu_i|} \\ f_{P\,ij} &= \frac{1}{|\mu_i - \nu_j|} \\ f_{P\,i} &= \frac{1}{|a_i|} \\ f_{P\,i} &= \frac{1}{|b_i|} \end{aligned}$$

where μ_i is the i^{th} pole and ν_j is the j^{th} zero of the identified transfer function $\widehat{G}(Z)$, while the a_i and b_i are the coefficients of the denominator and numerator polynomials of $\widehat{G}(Z)$; namely, the first penalty function forbids to the poles to reach the origin (pure delay), the second one prohibits the annihilation of poles and zeros, while the third and fourth ones constraint the identified transfer function to be indeed of the chosen order,they avoid the lowering of the order. Definitely more complex, is a penalty function to keep in account the stability of the identified (closed loop) strange attractor [Devaney, 1995; Kapitaniak and Brindley, 1996; Ruelle, 1989].

3. *Method*: there are several optimization algorithms available in literature [Hillier and Lieberman, 1990], they can be divided into two big classes, locally searching and globally searching methods [Winston, 1991]. The locally searching methods search in the neighborhood of an initial guess to find those changes in the argument values which reduce the value of the objective function, of this kind are all the *gradient descent-like* and *Newton-like* methods [Wagner, 1975]. The globally searching methods are, usually, heuristics devoted to explore, in a more or less intelligent manner, the entire searching space such to find the global minima(maxima) of the objective function [Colorni *et al.*, 1996]. For the application here considered, the locally searching methods are to be considered *taboo*, because the objective function that is to be optimized is, generally, strongly wrinkled; thus, globally searching methods must be considered in order to find the global optimum. Examples of globally searching methods that could be considered are the *genetic algorithms*, the *simulated annealing*, the *adaptive random search*, and the *taboo search* [Colorni *et al.*, 1996]. The only optimization method considered in this thesis is the genetic algorithm; in particular, it has been considered in the variant suggested in [Dasgupta and McGregor, 1992, 1994]. There are three reasons for such a choice: their intrinsic parallelism improve substantially their searching ability [Bertoni and Dorigo, 1993]; having available strong computational facilities[13] they result more performing than sequentially searching algorithm as the simulated annealing, furthermore their parallel implementation [Alander, 1995; Schwehm, 1993] on a cluster of computers is reasonably easy; finally, the author prefer it to the others.

5.1.5 Problems

As already mentioned here and there in the previous sections, there are three main problems which may occur in the proposed algorithm.

Stability: the obtained system (closed loop) could possess a strange saddle or a repellor rather than a strange attractor. In such a case, a penalty function accounting for the instability becomes necessary.

Overfitting: the obtained system (closed loop) could result in having several isolated stable and unstable periodic orbits rather than a simple strange attractor [Ott, 1993; Ruelle, 1989]. In such a case, a simpler

[13] Thanks to the Helvetic Confederation.

matching model should be considered; namely, a lower order of the linear transfer function and/or of the nonlinearity. Alternatively, a complete reformatting of the identified data is advisable [Ljung, 1999, 2000]; namely, reconsider, with different parameters, the sampling, the filtering, the normalization, etc., *cfr.* Sect. 5.1.1.

Degeneration: despite of the precautions taken, it could happen that the iterative algorithm insists in converging to a trivial degenerate solution, *cfr.* to the point "Nonlinearity parameterization" above. In such a case, stronger penalty functions for anti-degeneracy must be adopted; alternatively, other parameterizations of the nonlinearity can be considered, approximating functions which cannot describe linear functions should be preferred, for instance trigonometric or exponential expansions [Arfken and Weber, 1995].

5.1.6 Remarks

Since the next step, the Shil'nikov driving, expects as initial guess a parameter dependent continuous time ODE, the discrete time input—output Lur'e model identified must be converted into such a form. This can be performed very easily by means of three steps two of which are very common in control theory [Brogan, 1996; Feuer and Goodwin, 1996; Rinaldi and Piccardi, 1998].

In the first step, the discrete time transfer function $\widehat{G}(Z)$ is transformed into a state space model by means of one of the standard SISO realizations [Matlab, 2000; Rinaldi and Piccardi, 1998] as, for instance, the controller canonical form. The controller canonical form of a general proper[14] transfer function

$$\widehat{G}(Z) = \frac{\sum_{i=1}^{n} b_i Z^{n-i}}{Z^n + \sum_{i=1}^{n} a_i Z^{n-i}}$$

is given by

$$\begin{aligned} x(t+1) &= \widetilde{A}x(t) + \widetilde{b}u(t) \\ y &= \widetilde{c}^T x(t) \end{aligned}$$

where

$$\widetilde{A} = \begin{bmatrix} 0 & 1 & 0 & \cdots & 0 \\ 0 & 0 & 1 & \cdots & 0 \\ \vdots & \vdots & \vdots & \ddots & \vdots \\ 0 & 0 & 0 & \cdots & 1 \\ -a_n & -a_{n-1} & -a_{n-2} & \cdots & -a_1 \end{bmatrix} \quad \widetilde{b} = \begin{bmatrix} 0 \\ 0 \\ \vdots \\ 0 \\ 1 \end{bmatrix}$$

$$\widetilde{c}^T = \begin{bmatrix} b_n & b_{n-1} & b_{n-2} & \cdots & b_1 \end{bmatrix}$$

In the second step, the discrete time state space realization $(\widetilde{A}, \widetilde{b}, \widetilde{c}^T)$ is transformed into a continuous time one (A, b, c^T) by means of one of the standard approximations [Matlab, 2000; Rinaldi and Piccardi, 1998] as, for instance, the *zero order holder (ZOH)* approximation. Using the ZOH approximation, the discrete time system

$$\begin{aligned} x(t+1) &= \widetilde{A}x(t) + \widetilde{b}u(t) \\ y &= \widetilde{c}^T x(t) \end{aligned}$$

is mapped into the continuous time system

$$\begin{aligned} \dot{x} &= Ax + bu \\ y &= c^T x \end{aligned}$$

where

$$A = \tfrac{1}{T_S} log(\widetilde{A}) \qquad b = \widetilde{A}^{-1}\widetilde{b}$$

$$c^T = \widetilde{c}^T$$

[14] Roughly, with more poles than zeros.

Note that the *log* of a matrix is defined only if the argument matrix has not multipliers with negative real part, coherently with what required above when dealing with the sampling time choice, *cfr.* Sect. 5.1.1.

The third step is quite trivial and simply consists in rendering the nonlinear dependence inside the state space model explicit, namely

$$\begin{cases} \dot{x} &= Ax + bu \\ y &= c^T x \\ u &= f_p(y) \end{cases} \qquad \mapsto \dot{x} = Ax + f_p(Cx) = F(x,p) \tag{5.4}$$

It can results useful, not for the next step of automatic modeling but for the filter gain tuning (*cfr.* Chap. 6), to compute at this point the natural standard deviation of the identified Feigenbaum-like strange attractor with respect to its generating cycle; namely, the semi-width of the Möbius strip on which it lies[15], *i.e.*

$$\sigma_{Fg}(\theta) = \max_{\substack{\eta \in SA \\ \gamma \in GC}} \sqrt{\big(\eta(\theta) - \gamma(\theta)\big)^T \big(\eta(\theta) - \gamma(\theta)\big)}$$

where θ is the phase along the generating cycle as well as the strange attractor (*cfr.* Sect. 2.5.1), $\eta \in SA$ means that η belongs to the Feigenbaum-like strange attractor, and $\gamma \in GC$ means that γ belongs to the generating cycle. Note that γ and η must have the same phase θ while computing the maximum.

As can be imagined, this can be done numerically fairly easily once the generating cycle is detected. Since the detection of the generating cycle is a step necessary to the next step, as described in the next section, it is convenient to perform this computation at this point.

5.2 Shil'nikov Driving

The aim of this second step is to drive the Feigenbaum-like chaotic model obtained with the identification algorithm described above, *i.e.* the first step (*cfr.* Sect. 5.1), towards Shil'nikov-like chaotic conditions; thus, obtaining the chaotic model of the class of patterns which, as before explained (*cfr.* Sect. 4.4) is indeed the result needed to build a qualitatively resonating filter.

The initial guess, from which this step starts, is the parametric ODE describing the identified Feigenbaum-like chaotic model, *cfr.* Sect. 5.1.6. In this regard, it should be noted that for this step the parameters are not simply the parameters used to describe the nonlinearity but all the parameters on which the ODE depends; namely, the parameters of the nonlinearity as well as those of the linear transfer function, *i.e.* the p, a_i, and b_i parameters all together.

Driving a Feigenbaum-like chaotic system towards Shil'nikov-like chaotic conditions is conceivable because of the theoretical results illustrated in [De Feo *et al.*, 2000; Gaspard *et al.*, 1984; Glendinning and Sparrow, 1984]. A regularly behaving system, *i.e.* a periodic system, must pass necessarily by Feigenbaum-like conditions in order to approach Shil'nikov's chaoticity [Gaspard *et al.*, 1984; Gaspard and Nicolis, 1983]. In other words, the region in the parameter space where the system shows Shil'nikov-like chaotic behavior is surrounded by a region where the system shows Feigenbaum-like chaotic behavior [De Feo *et al.*, 2000; Gaspard *et al.*, 1984]. In some sense, the Shil'nikov-like chaotic region is at the core of the Feigenbaum-like chaotic region. Hence, the hypothesis on which this step relies is that the Feigenbaum-like chaotic model identified at the first step is in a parameter region surrounding a Shil'nikov-like region; this is not necessarily true, there exists Feigenbaum-like chaotic systems that never becomes Shil'nikov-like chaotic [Cvitanović, 1984], they are quite particular, *i.e.* not generic, but indeed possible.

Before starting to drift the parameters, it is necessary at first to determine in which direction to change them; namely, it must be determined in which direction the Shil'nikov-like chaotic region is situated in the parameter space with respect the current parameter values, *i.e.* the identified Feigenbaum-like ones. Loosely speaking, being in Boston and wanting to go in New York the first knowledge needed is to know where is New York with respect to Boston; namely, South in a South-South-East direction. This information can be easily obtained since the organization of the parameter space imposed by a fourth type Shil'nikov's homoclinic bifurcation (*cfr.* Sect. 2.5.2) [Gaspard *et al.*, 1984; Tresser, 1984]; namely, as shown in Fig. 5.3(a),

[15] Practically, this is the width in the state space of the stroboscopic plot of the Feigenbaum-like strange attractor, *cfr.* Sect. 2.5.1

the homoclinic bifurcation locus (h) is at the core of the Shil'nikov-like chaotic region which is, in turn, surrounded by the Feigenbaum-like chaotic region.

Actually, since the homoclinic bifurcations can be seen as the collision of the generating cycle with an equilibrium [Kuznetsov, 1998]; it follows that approaching the homoclinic bifurcation, the period of the generating cycle tends to infinity, as the trajectory spends more and more time in the neighborhood of the equilibrium that is approaching, *cfr.* Sect. 2.5.2. In particular, in the case of a Shil'nikov's homoclinic bifurcation of fourth type [Kuznetsov, 1998; Tresser, 1984], chosen a generic, *i.e.* transversal to h, direction in the parameter space, *i.e.* a straight line Γ (*cfr.* Fig. 5.3(a)), and called μ the coordinate along it, the dependence of the generating cycle period upon μ is illustrated in Fig. 5.3(b). Namely, the period of the generating cycle tends to infinite swinging around the coordinate value μ_0 at which the homoclinic bifurcation occurs, *i.e.* the intersection between Γ and h. Therefore, the idea for reaching the core of the Shil'nikov-like chaotic region, *i.e.* the homoclinic locus h, starting from a point inside the Feigenbaum-like chaotic region is to fix a direction, *i.e.* a straight line, in the parameter space and to move along it in the sense in which the period of the generating cycle augments. Since that, the proposed Shil'nikov driving technique can be called *period climbing*; in fact, the generating cycle period must increase towards infinity.

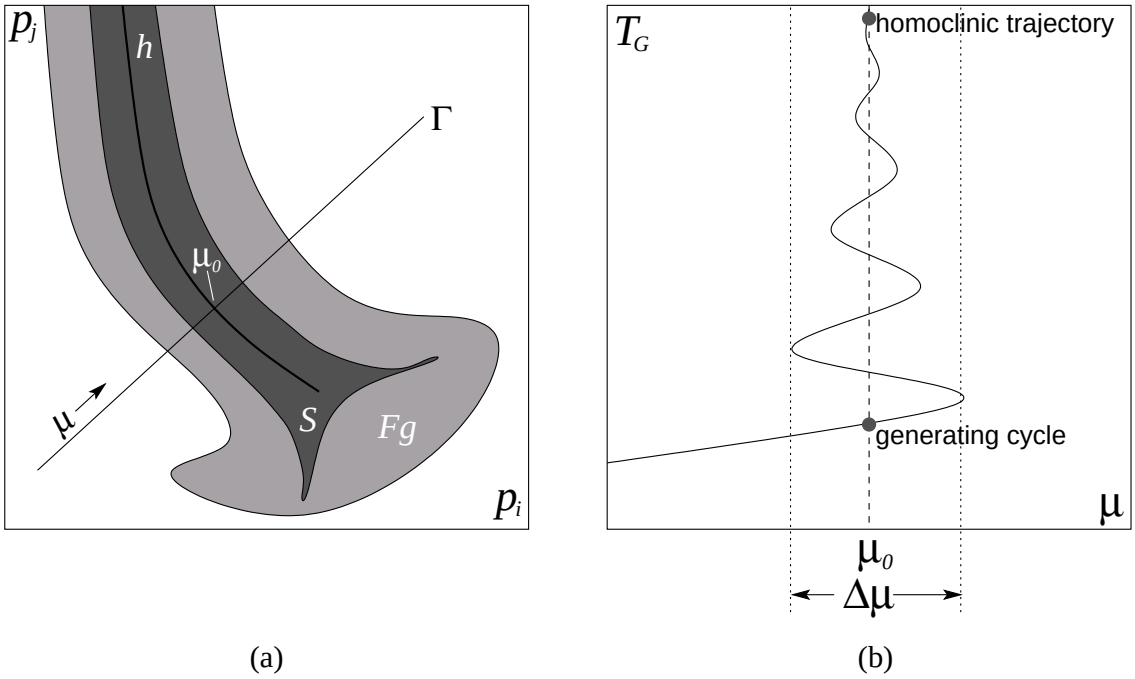

Figure 5.3: *Organization of the parameter space by means of a Shil'nikov's homoclinic bifurcation of the fourth type: (a) – organization of the parameter space into three regions, homoclinic bifurcation locus (h), Shil'nikov-like chaotic region (S), and Feigenbaum-like chaotic region (Fg); (b) – behavior of the generating cycle period while moving along the generic line Γ as shown in (a), μ is the coordinate along Γ.*

The period climbing can be easily implemented by means of continuation techniques. Indeed, the continuation of a limit cycle with respect to its period and another parameter is a standard operation implemented in any continuer, as AUTO97 [Doedel *et al.*, 1998] and CONTENT [Kuznetsov and Levitin, 1997], devoted to bifurcation analysis [Champneys and Kuznetsov, 1994; Champneys *et al.*, 1996; Doedel *et al.*, 1991a,b; Kuznetsov, 1998]. In particular, before adopting a continuer to perform the period climbing two subproblems must be solved.

To perform the continuation of the generating cycle it is necessary in first place to determine it. Indeed, what is available as result of the first step is the ODE at Feigenbaum-like chaotic condition and, eventually, the Feigenbaum-like strange attractor, but not the generating cycle. Actually, an initial guess of the generating cycle, suitable for a continuation algorithm [Doedel *et al.*, 1998; Kuznetsov, 1998], can be obtained from the two mentioned information items, *i.e.* ODE and strange attractor, by means of a homotopy method [Doedel *et al.*, 1998; Kuznetsov, 1998] combined with one of those algorithms, available in literature, for the extraction of unstable periodic orbits from the time series of strange attractors [Farantos, 1995; Galias, 1999; Ogorzalek, 1995].

Secondly, since the continuation of a cycle with free period is a one parameter continuation, an oriented one-dimensional line in the r-dimensional[16] parameter space must be spotted; namely, the Γ line above mentioned, characterized by one parameter μ as, for instance, its curvilinear coordinate. Actually, this line does not need to be a straight line; it just needs to be generic enough to transversely cross the homoclinic bifurcation locus h. Hence, this line can be characterized in several ways. Here, only two simple, but rather effective, ones are considered.

1. *Straight greedy direction*: by means of the continuation algorithm it is possible to numerically compute the gradient of the generating cycle period with respect to all the parameters [Doedel *et al.*, 1998; Kuznetsov, 1998]. Thus, computing the gradient at the initial point, *i.e.* that provided by the identification step, it is possible to determine the maximal ascending direction in the parameter space. The straight line determined by this direction can be fixed, once for all in the name of some greedy approach [Kuznetsov, 1998], as the one-dimensional path along which to perform the continuation.

2. *Adaptive greedy direction*: this is simply the adaptive version of the above mentioned way of proceeding [Kuznetsov, 1998]. Namely, rather than fixing a straight line in the parameter space once for all at the beginning, the direction can be corrected every N_c continuation steps according to a gradient ascend technique. This should, theoretically, improve the performance of the period climbing algorithm [Champneys and Kuznetsov, 1994; Champneys *et al.*, 1996; Kuznetsov, 1998], *i.e.* it should lead the continuation to approach the homoclinic bifurcation locus h using less continuation steps.

These two algorithms can be considered as pathfinders, in fact they find the path along which to proceed with the continuation.

The described period climbing methods have been tested (*cfr.* Chap. 7) giving satisfactory results. In particular, both the pathfinder algorithms have proved to be valid. More in particular, the adaptive direction has been indeed more effective than the fixed direction but at the price of an increased tendency to run into some, not too serious, problem.

5.2.1 Problems

During the test run to ascertain the real effectiveness of the above described method, two main problems emerged.

First, it can happen that the period does not climb at all, the continuation begin increasing the period but after reaching a maximum the period decreases. There are two possible reasons for that to happen. One is a structural reason; namely, the Feigenbaum-like strange attractor obtained at the first step is not a relative of a Shil'nikov-like one. Precisely, the considered Feigenbaum-like chaotic region of the parameter space does not surround a Shil'nikov-like one. This means that the hypothesis on which the entire algorithm is based is not satisfied; therefore, obviously, the algorithm does not work. If this is the case, there is no other solution than starting again from the beginning of the first step, *i.e.* the Feigenbaum-like model identification, trying to obtain an alternative model without this problem. A second, less dramatic, reason for the algorithm to fail in increasing the period is simply that a wrong path has been chosen. In this case, the alternative pathfinder to the one used can be tried, or, in the case of the adaptive pathfinder, the adaptation step N_c can be changed. If no one of these two alternatives lead to a solution, a more complex, or a more "stupid", pathfinder, as a random one, can be tried. Failing with several pathfinders can be a serious index of a structural unachievability as just explained.

The second problem that can be encountered in the use of this algorithm is that the period increases but without swinging, *cfr.* Sects. 5.2 and 2.5.2. There are two possible main reasons for that to happen. First, the adaptive pathfinder has found the only possible path [Gaspard *et al.*, 1984; Glendinning and Sparrow, 1984] along which the period tends to infinity without swinging along the path. In fact, theoretically, there exists a spiral path in the parameter space along which this is possible [Gaspard *et al.*, 1984]. To hit it with the adaptive pathfinder is quite improbable but not impossible. If this is the case, a simple test on the eigenvalues of the equilibrium[17] which is colliding with the generating cycle can determine the type of homoclinic bifurcation. If the leading eigenvalues are complex and conjugate (*cfr.* Sect. 2.5.2) [Kuznetsov, 1998; Tresser, 1984], then there is no problem since the system has been driven to Shil'nikov condition indeed.

[16] The dimension of the parameter space is $r = \dim(p) + 2n$ where n is the order of the linear transfer function used in the identification, *i.e.* the order of the identified system.

[17] The equilibrium bearing the homoclinic, *i.e.* the one colliding with the generating cycle, can be automatically extracted from the continuation results [Champneys and Kuznetsov, 1994; Champneys *et al.*, 1996; Kuznetsov, 1998].

On the contrary, if the leading eigenvalue is real, then it means that the homoclinic bifurcation is of tame type (*cfr.* Sect. 2.5.2) [Kuznetsov, 1998; Tresser, 1984]. Actually, this is the second reason that can lead the period to increase without swinging along the path. This means that the Feigenbaum-like chaos is not relative to a "simple" Shil'nikov homoclinic bifurcation of fourth type but is related to a codimension-two (or higher) degeneracy of the homoclinic bifurcation [Champneys and Kuznetsov, 1994; Kuznetsov, 1998] as, just to cite few of them, *inclination flip* [Deng, 1993], *Belyakov resonance* [Belyakov, 1981; Kuznetsov *et al.*, 2001], and *Nozdrachova resonance* [Chow *et al.*, 1990; Nozdrachova, 1982]. In this case, the parameter region where the homoclinic bifurcation becomes a Shil'nikov type IV can be found by means of a two parameter continuation of the homoclinic bifurcation itself. Although this is possible, to find the "good" two-dimensional surface in the parameter space where to perform such a continuation is not so obvious. Alternatively, is preferable trying to reach the homoclinic locus h along another path, acting on the pathfinder, and hoping that this time the homoclinic bifurcation will be hit in a Shil'nikov type IV region.

5.2.2 Remarks

First of all, it should be noted that this step is in open loop, namely no feedback from the data is used to drive the period climbing. Therefore, it could happen that the generating cycle of the Shil'nikov-like strange attractor found does not describe very well the patterns represented by the data used for the identification; namely, the period climbing drift the parameters excessively and the obtained Shil'nikov-like strange attractor is no longer a good model for the diversity of the patterns considered. This does not represent a real problem since once a point on the h manifold is obtained, a two parameter continuation of h can be performed in order to find a Shil'nikov-like strange attractors well fitting the data. Namely, once a point on the homoclinic bifurcation manifold h has been found it is possible to proceed to a continuation constrained on it whose aim is to find a better data fitting strange attractor. In other words, it is possible to proceed to a fine-tuning of the strange attractor to the data. In particular, using Auto97 [Doedel *et al.*, 1998], it is possible, for instance, to continue the generating cycle along h looking for the solutions which fit at best, with respect to an integral measure[18] [Doedel *et al.*, 1998], the data considered, *cfr.* Sect. 5.1.1.

Finally, the fact that this step is based on continuation allows to obtain very easily those information items which are needed by the filter gain (*cfr.* Sect. 4.4.2) tuning algorithm proposed in the next chapter. Actually, these information items are the generating cycle, the homoclinic trajectory, and the Jacobians along these two solutions. In particular, the generating cycle is the periodic solution with lowest period, *i.e.* the farthest from the equilibrium, which exists at the parameter values considered; namely, since the period climbing is stopped in a close neighborhood of the homoclinic bifurcation h, the generating cycle is, as shown in Fig. 5.3(b), the solution with the lowest period existing at $\mu = \mu_0$. Thus, it can be easily extracted from the results of the continuation performed for the period climbing. On the other hand, the homoclinic trajectory is fairly well approximated by the periodic solution with the highest period at the same parameter values μ_0, *cfr.* Fig. 5.3(b). Eventually, the approximation of the homoclinic trajectory can be improved starting with this approximation and refining it by means of a homotopy method, as the one implemented in HomCont [Champneys *et al.*, 1996; Doedel *et al.*, 1998]. Finally, the Jacobians along the two solutions have been already computed by the continuation algorithm, it needs them to perform the continuation. Thus, it is simply a matter of letting the continuation algorithm dump this internal information. Anyway, it would not be difficult to compute them since the trajectory and the model are both known.

5.3 Degrees of Freedoms Summary

The general idea, as presented in the introduction of this chapter, implies two main degrees of freedom. In fact, any suitable algorithm to solve the two subproblems, *i.e.* Feigenbaum-like chaotic identification and Shil'nikov driving, can be adopted. Here, only one solution for each of the two subproblems has been considered but the proposed one is not the only combination possible. Actually, any nonlinear identification technique suitable for the identification of a Feigenbaum-like chaotic system can be indeed adopted to solve the first step; for instance, techniques based on nonlinear state space modeling [Ljung, 1999, 2000] or on adapted linear periodic identification [Arambel and Tadmor, 1994; Hench, 1995; McLernon, 1989], as

[18] Indeed, Auto97 can evaluate integral conditions of the continued periodic solution. Furthermore, it can detect the extrema of the integral condition, *i.e.* minima and maxima, and can perform the continuation of the periodic solution constrained on the extrema of the integral condition.

mentioned in Appendix E, can be considered as well. As well, any technique suitable to drive a Feigenbaum-like chaotic system towards Shil'nikov's conditions can be considered for dealing with the second step; here, the simplest one has been considered but other methods, *e.g.* based on simulation or on singular perturbation analysis [De Feo and Rinaldi, 1998; O'Malley, 1974; Pontryagin, 1957; Tikhonov, 1952] can be considered as well.

More specifically, restricting to the algorithm presented here for the Lur'e system identification, there are more than twenty degrees of freedom distributed among the two steps.

For the Feigenbaum-like chaotic identification, there are the following choices to consider.

Linear model type: the type of linear model. For instance, ARMA, ARMAX, Box-Jenkins, Output-Error, etc. [Ljung, 1999, 2000].

Linear model order: the order for each part of the chosen linear model. In particular, the order of the main input—output relation and the order of the eventual input-noise—output relation [Ljung, 1999, 2000].

Nonlinearity type: the parameterization of the nonlinearity. For instance, geometrical-based as splines, piecewise linear function, Bézier curves, etc. [Schwarz, 1989]; or series-based as Laguerre polynomials, Tchebyshev ones, Hermite ones, etc. [Szegö, 1975].

Nonlinearity order: the number of parameters used to approximate the nonlinearity.

Linear identification algorithm: the identification algorithm used to solve the linear identification subproblem. For instance, Maximum likelihood, subspace projections, error prediction, etc. [Ljung, 1999, 2000].

Optimization objective function: the objective function whose maximization (minimization) corresponds to improving the overall identification; in particular, the two parts which compose it. First, the linear identification quality measure as, for instance, the relative tolerance of the identified parameters or the prediction error (*cfr.* Sect. 5.1.4). Second, the penalty functions for all the constraints imposed, *cfr.* Sect. 5.1.4.

Globally searching optimization algorithm: the (global) optimization algorithm used to solve the optimization subproblem. For instance, genetic algorithms, simulated annealing, random search, adaptive random search, etc. [Colorni *et al.*, 1996; Winston, 1991].

On the other hand, to accomplish the Shil'nikov driving there are the following choices to consider.

Continuation technique: the periodic solution of ODE continuation technique considered to accomplish the period climbing. For instance, shooting, multiple shooting, Gaussian collocation, etc. [Kuznetsov, 1998].

Intrinsic degrees of freedom of the continuation: all the tuning parameters specific to the continuation technique considered. For instance, in the shooting technique there are the integrator, its minimal step, maximal step etc. [Kuznetsov *et al.*, 1992; Kuznetsov, 1998]; in the Gaussian collocation method there are the number of meshes, the number of collocations points for mesh, the weights, etc. [Doedel *et al.*, 1998; Kuznetsov, 1998].

Pathfinder: the pathfinder used. For instance, fixed greedy, adaptive greedy, random searching, etc., *cfr.* Sect. 5.2. Eventually, the parameters intrinsic to the pathfinder technique considered as, for instance, in the case of adaptive greedy the number of continuation steps to take before correcting the direction.

From the previous list it can be easily deduced that there are overall numerous degrees of freedom indeed. Most of the possible combinations have been tested during the last years of research without ever noticing the existence of a *super winning combination*. Hence, the easiest combination has been the most often considered one. This combination is, without going in the particulars of the intrinsic parameters of the continuation, as follow (*cfr.* Chap. 7).

— Linear model type: Output-Error.

— Linear model order: fourth or fifth.

— Nonlinearity type: smoothed piecewise linear or Tchebyshev polynomials.

— Nonlinearity order: about thirteenth.

— Linear identification algorithm: maximum likelihood in least square error sense.

— Optimization objective function: relative tolerance on the identified parameters of the linear transfer function as identification quality measure; furthermore, penalty functions to implement three constraints, first the non regression to linear of the nonlinearity, second a maximum of three/four annihilating coefficients of the identified transfer function (*i.e.* , at maximum three or four of all the a_i b_i can annihilate) and third, to augment the probabilities of having a stable strange attractor as a result, the time derivative of the output ($y(t)$) must be such as to enter the visited segment of the nonlinearity from its borders.

— Globally searching optimization algorithm: genetic algorithms.

— Continuation technique: Gaussian collocation method as implemented in AUTO97.

— Pathfinder: adaptive greedy every ten continuation steps.

This combination is very easy to implement and gives very satisfactory results as reported in Chap. 7. It should be remarked that the Output-Error model reflects the hypothesis of an endogenous diversity, *i.e.* the only noise is the measurement noise. Finally, more complex combinations that have been tested did not show improvements in the performance such as to justify the increased complexity.

5.4 TESTS

The two tests considered here serve to illustrate the effective employability of the considered algorithm at least in almost ideal conditions. In Chapter 7, more realistic and interesting tests have been performed.

The two tests considered here consist in constructing a Shil'nikov-like chaotic model for two Feigenbaum-like chaotic time series issuing from numerical simulations of mathematical models. Hence, both the cases considered satisfy the hypothesis (H.1). On the contrary, not both the time series considered satisfy the hypothesis (H.2). More precisely, the first time series considered is the one associated with the 2-pulse Feigenbaum-like attractor that can be observed in the Colpitts oscillator (*cfr.* Sect. 3.1.1 and Appendix A) [De Feo *et al.*, 2000]; thus, it satisfies both the hypothesis (H.1) and (H.2). The second time series is generated by the 3-pulse Feigenbaum-like attractor that can be observed in the Rosenzweig—MacArthur food chain model (*cfr.* Sect. 3.1.2) [Kuznetsov *et al.*, 2001]; thus, it satisfies the first hypothesis (H.1) while it does not satisfy the hypothesis (H.2). In fact, the Rosenzweig—MacArthur model cannot be mapped into a scalar Lur'e-like form by any invertible diffeomorphism [Kuznetsov, 1998; Kuznetsov and Rinaldi, 1996].

5.4.1 TEST FRAMEWORK

In both the tests the same framework has been considered, very similar to the one considered for more realistic applications considered in Chap. 7.

For what regards the data, twenty independent observations of thirty-two pseudo-periods each have been considered in each identification; the sampling of the observations is of two-hundred samples for each pseudo-period, *cfr.* Sect. 5.1.1. More in particular, the measurements have been scaled in amplitude and in time, the whole set of twenty measurements together, such as to have the amplitude between ± 1 and a unitary nominal pseudo-period. Furthermore, the mean value has been removed and the boundary conditions have been adapted such as that every observation is periodic. Finally, whenever necessary, the observations have been considered periodic. Namely, whenever an example signal longer than thirty-two pseudo-periods has been necessary, the vectors have been completed starting reading them from the beginning when the end is reached.

For the Feigenbaum-like identification step, the following choices have been taken, *cfr.* Sect. 5.3. A third order (exact matching) Output-Error model has been considered for the linear dynamical system. The nonlinearity has been modeled with a three segments smooth piecewise linear function, *i.e.* $3 \cdot 3 - 2 = 7$ parameters. The linear identification algorithm used is a maximum likelihood in least square error sense as that described in [Bittanti, 2000a; Söderström and Stoica, 1989]. It has been implemented modifying the MATLAB function `ARX` [Ljung, 2000]. Such an identification method allows to fit several input—output relations at once, namely it can make ensemble identification. Thus, all the observations are used at once in the identification, as described in Sect. 5.1.4. The objective function is exactly the one considered above in Sect. 5.3, *cfr.* Chap. 7. It has been optimized with a genetic algorithm, in the variant considered by

[Dasgupta and McGregor, 1994], working for five-hundreds evolution steps on hundred individuals of seven chromosomes each, which in turn are composed of eighty binary genes each, *i.e.* the IEEE representations of reals. The reproduction function is governed by a reproduction probability, given by the normalized fitness, and a standard Monte Carlo method, excepting the best three individuals which are surely reproduced at the next generation [Koza, 1992]. The crossover operator is applied with probability $P_C = 0.7$ while the mutation operator is applied with a probability $P_M = 0.1$. The crossover works at chromosome level while the mutation works at gene level. The cut point, over the chromosomes, for the crossover and the gene, over the genes, for the mutation are randomly drawn with an uniform distribution. Finally, whenever the state space of the identified model is considered it corresponds to the reconstructor[19] canonical form realization of the linear transfer function [Brogan, 1996; Rinaldi and Piccardi, 1998], similarly to what described in Sect. 5.1.6.

On the other hand, for the Shil'nikov driving step, the following choices have been taken. The continuation algorithm is the Gaussian collocation method implemented in AUTO97 which has been run with forty meshes and four collocation point for each mesh [Doedel *et al.*, 1998]. The pathfinder considered is the adaptive greedy one with the direction corrected every ten continuation steps.

5.4.2 Colpitts Oscillator

The first time series considered, satisfying both the hypotheses (H.1) and (H.2), are those issuing from the Colpitts oscillator mathematical model given by Eqs. (3.1) with $Log_{10}(Q) = 0.2432$ and $Log_{10}(g) = 0.5697$. Namely, the x_2 time series (*cfr.* Sect. 3.1.1) associated with the 2-pulse Feigenbaum-like strange attractor shown in Fig. 5.4.

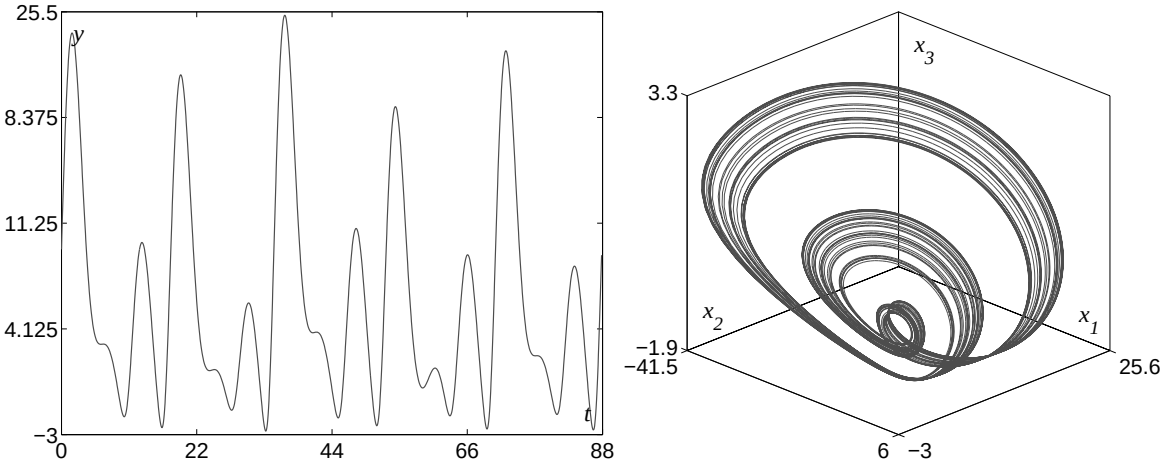

(a) (b)

Figure 5.4: *The Feigenbaum-like data issuing from the Colpitts Oscillator mathematical model (3.1), when* $Log_{10}(Q) = 0.2432$ *and* $Log_{10}(g) = 0.5697$*, which have been considered for the first test session: (a) – the 2-pulse* x_2 *time series; (b) – the corresponding Feigenbaum-like strange attractor in the state space.*

The result of the first step of the automatic chaos-based modeling of diversity, *i.e.* Feigenbaum-like chaotic model identification, is shown in Figs. 5.5 and 5.6. Figure 5.5 shows the identified Feigenbaum-like strange attractor in the state space (b) and the corresponding output signal (a) while Fig. 5.6 compares the stroboscopic plot of the identified system (b) with that of the data used for the identification (a). The two stroboscopic plots look very similar to each other, highlighting the quality of the constructed model. Moreover, as can be deduced from comparing Figs. 5.5(b) and 5.4(b), the model constructed by the algorithm looks geometrically different from the one generating the considered signals.

The result of the second step, *i.e.* period climbing, is shown in Figs. 5.7 and 5.8. Figure 5.7 shows the resulting Shil'nikov-like strange attractor in the state space (b) and the corresponding output signal (a) while Fig. 5.8 shows the peak-to-peak maps of the corresponding output time series. The bimodal form of the amplitude map, Fig. 5.8(a), as well as the phase skips in the return time map, Fig. 5.8(b), confirms the Shil'nikov-like nature of the obtained strange attractor.

[19] For the computations it is rather convenient to use the controller canonical form since, as it will be clear in the next chapter, some computation remain easier. On the other hand, the reconstructor canonical form gives nicer three-dimensional portraits.

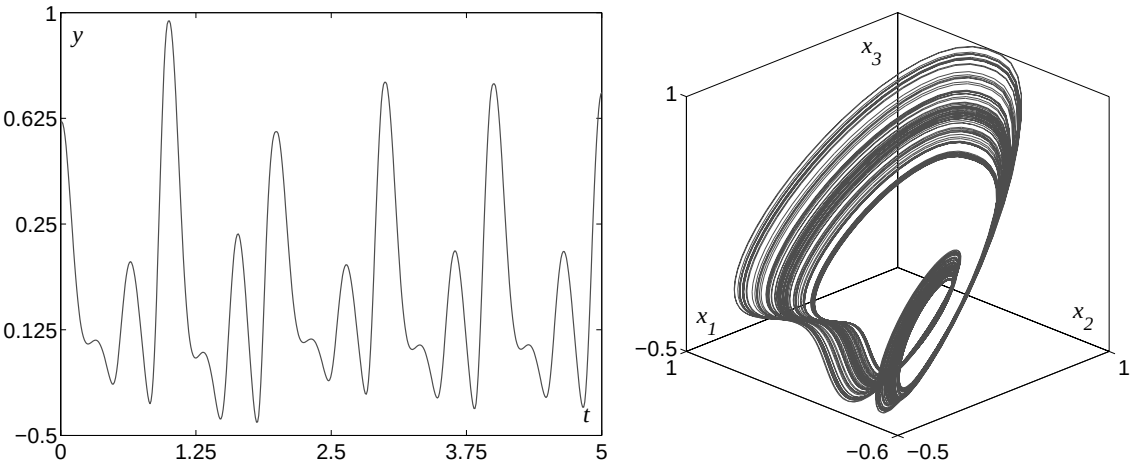

(a) (b)

Figure 5.5: *The 2-pulse Feigenbaum-like strange attractor of the identified system: (a) – the output time series; (b) – the strange attractor in the state space.*

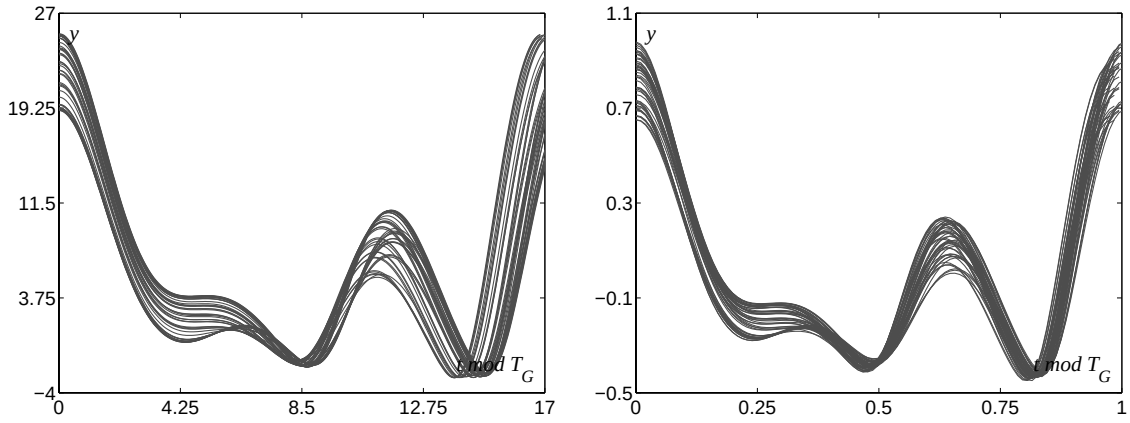

(a) (b)

Figure 5.6: *Stroboscopic plot of the Feigenbaum-like time series: (a) – of the data used for the identification; (b) – of the time series issuing from the identified system.*

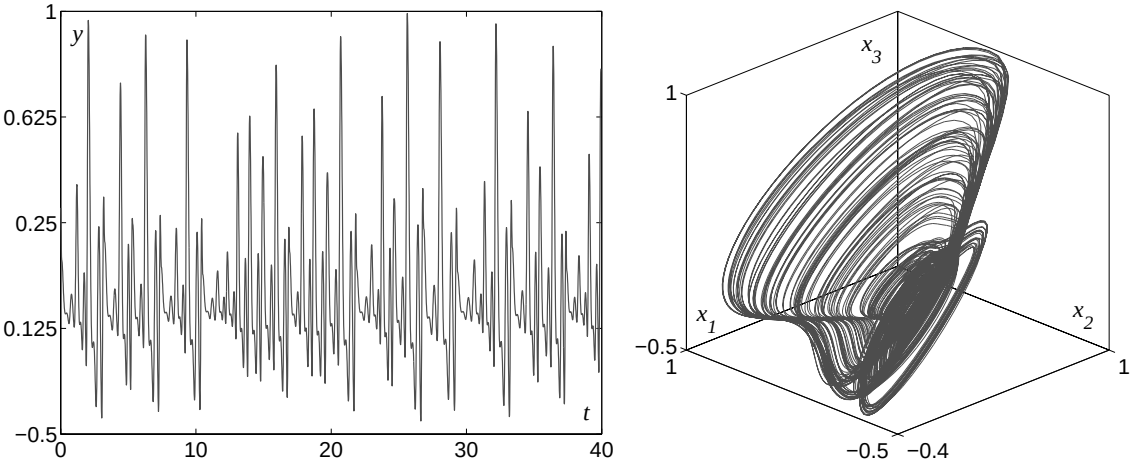

(a) (b)

Figure 5.7: *The 2-pulse Shil'nikov-like strange attractor of the identified system: (a) – the output time series; (b) – the strange attractor in the state space.*

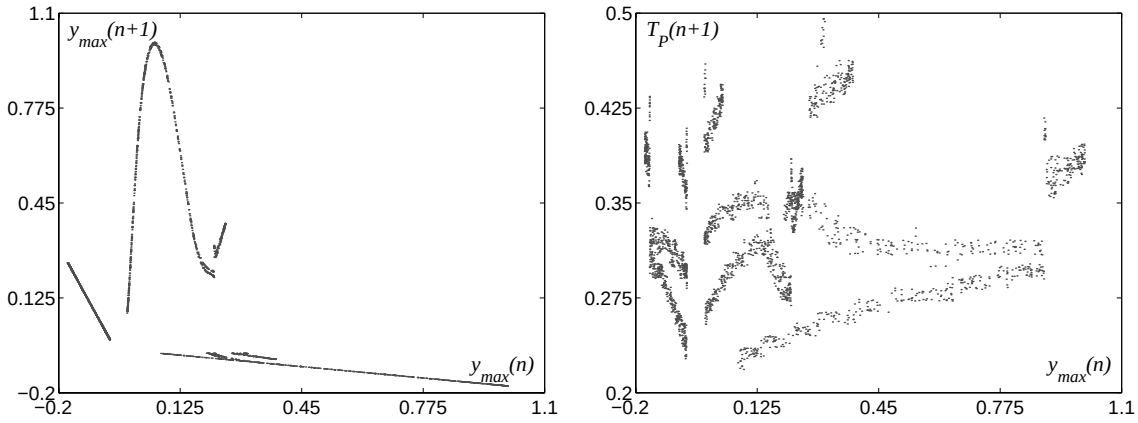

(a) (b)

Figure 5.8: *One-dimensional peak-to-peak maps of the time series issuing from the system resulting from the Shil'nikov driving: (a) – amplitude* vs *amplitude map; (b) – amplitude* vs *return time map.*

5.4.3 Rosenzweig—MacArthur Food Chain

The second time series considered, satisfying the hypothesis (H.1) but not (H.2), are those generated by the Rosenzweig—MacArthur food chain model given by Eqs. (3.2) with $K = 0.9583$ and $r = 1.0374$. Namely, the x_1 time series (*cfr.* Sect. 3.1.2) associated with the 3-pulse Feigenbaum-like strange attractor shown in Fig. 5.9.

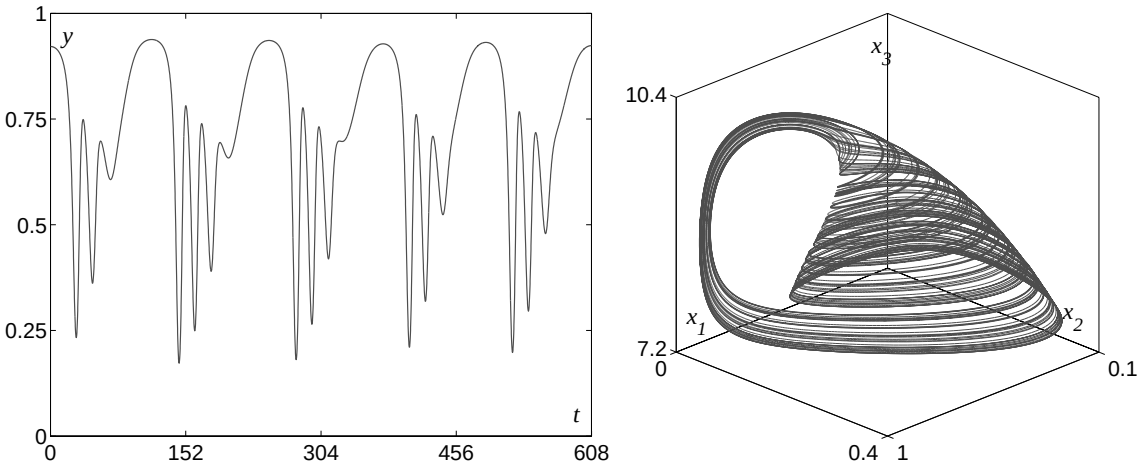

(a) (b)

Figure 5.9: *The Feigenbaum-like data issuing from the Rosenzweig—MacArthur food chain model (3.2), when $K = 0.9583$ and $r = 1.0374$, which have been considered for the second test session: (a) – the 3-pulse x_1 time series; (b) – the corresponding Feigenbaum-like strange attractor in the state space.*

The result of the first step of the automatic chaos-based modeling of diversity, *i.e.* Feigenbaum-like chaotic model identification, is shown in Figs. 5.10 and 5.11. Figure 5.10 shows the identified Feigenbaum-like strange attractor in the state space (b) and the corresponding output signal (a) while Fig. 5.11 compares the stroboscopic plot of the identified system (b) with that of the data used for the identification (a). The two stroboscopic plots look very similar to each other, highlighting the quality of the constructed model despite of the fact that in this case the data were not generated by a Lur'e system. Moreover, it can be deduced by comparing Figs. 5.10(b) and 5.9(b) that the model constructed by the algorithm looks geometrically different from the one generating the considered signals.

The result of the second step, *i.e.* period climbing, is shown in Figs. 5.12 and 5.13. Figure 5.12 shows the resulting Shil'nikov-like strange attractor in the state space (b) and the corresponding output signal (a) while Fig. 5.13 shows the peak-to-peak maps of the corresponding output time series. The bimodal form of

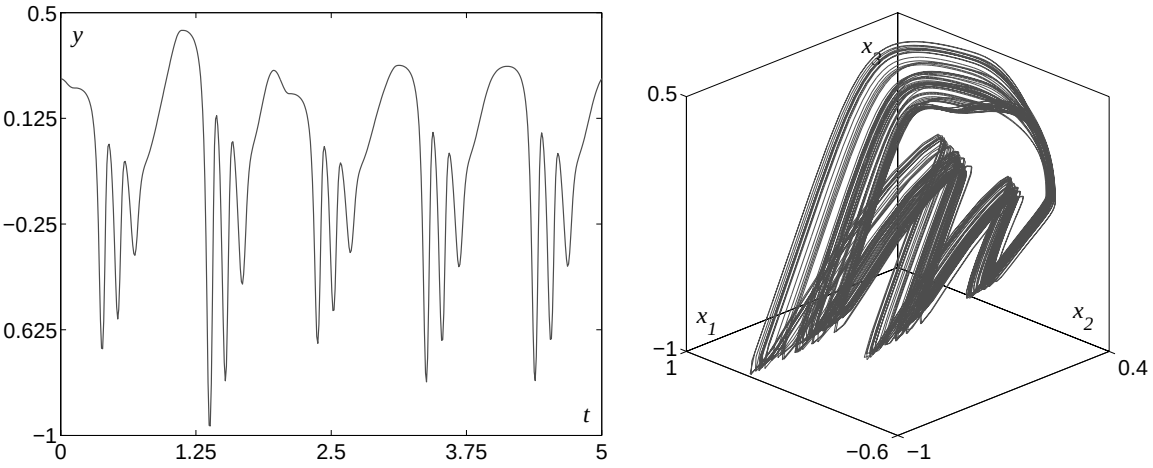

Figure 5.10: *The 3-pulse Feigenbaum-like strange attractor of the identified system: (a) – the output time series; (b) – the strange attractor in the state space.*

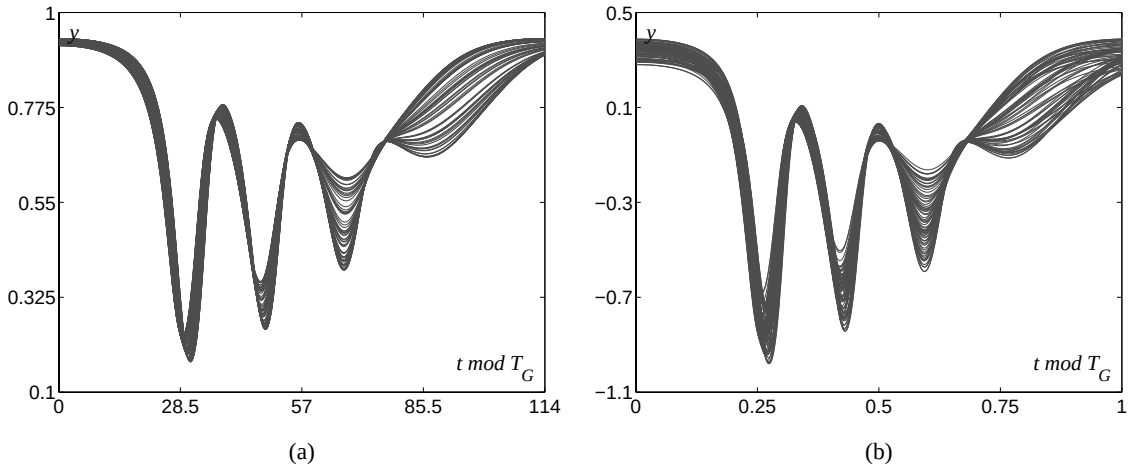

Figure 5.11: *Stroboscopic plot of the Feigenbaum-like time series: (a) – of the data used for the identification; (b) – of the time series issuing from the identified system.*

the amplitude map, Fig. 5.13(a), as well as the phase skips in the return time map, Fig. 5.13(b), confirms the Shil'nikov-like nature of the obtained strange attractor.

5.4.4 Comments

The results of the two test runs illustrate that the proposed algorithm for the automatic chaos-based modeling of diversity works at least when the Feigenbaum's nature of the diversity of the considered signals is guaranteed. Indeed, both the two sets of Feigenbaum-like signals, the set of signals generated by a Lur'e system as well as the set of those generated by a non Lur'e system, have been correctly modeled by the proposed algorithm.

5.5 Final Remarks

Specific remarks about the two subproblems composing the overall algorithm have been reported in the corresponding sections (*cfr.* Sects. 5.1.6 and 5.2.2), as general remark it should be simply said that, taken into account everything, the algorithm is rather simple and, in particular, relies on standard techniques which are well-known in engineering. Furthermore, it has enough degrees of freedom (*cfr.* Sect. 5.3) which allow to adapt it to fit several of the possible real applications. Finally, it has revealed indeed effective on

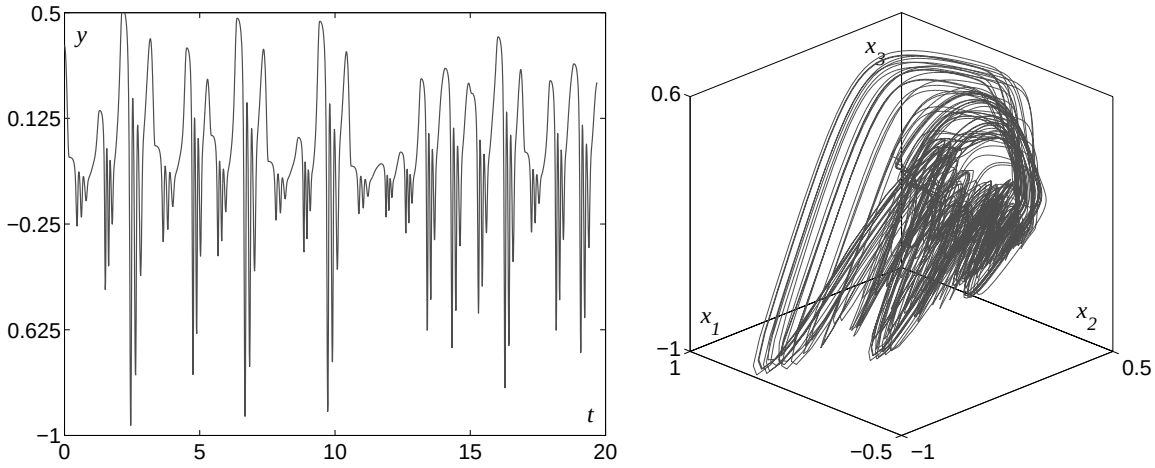

(a) (b)

Figure 5.12: *The* 3*-pulse Shil'nikov-like strange attractor of the identified system: (a) – the output time series; (b) – the strange attractor in the state space.*

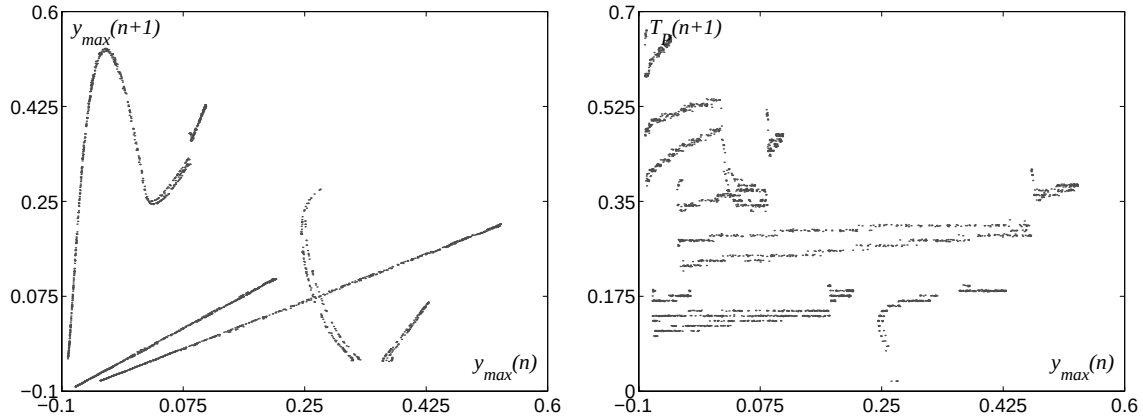

(a) (b)

Figure 5.13: *One-dimensional peak-to-peak maps of the time series issuing from the system resulting from the Shil'nikov driving: (a) – amplitude* vs *amplitude map; (b) – amplitude* vs *return time map.*

real data as reported later in Chap. 7.

Bibliography

Aguirre, L. and S. Billings (1995). Identification of models for chaotic systems from noisy data: Implications for performance and nonlinear filtering. *Physica D*, 85, pp. 239–258.

Aguirre, L., E. Mendes, and S. Billings (1996). Smoothing data with local instabilities for the identification of chaotic systems. *International Journal of Control*, 63, pp. 483–505.

Akritas, P., I. Antoniou, and V. Ivanov (2000). Identification and prediction of discrete chaotic maps applying a Chebyshev neural network. *Chaos, Solitons, & Fractals*, 11, pp. 337–344.

Al-Zamel, Z. (1999). *Unstable Periodic Orbit Extraction Error and its Effect on Nonlinear System Parametric Identification*. Ph.D. thesis, Michigan State University, MI, East Lansing.

Alander, J. (1995). Indexed bibliography of genetic algorithm implementations. Department of information technology and production economics, University of Vaasa, Vaasa, Finland.

Amerio, L. (1977a). *Analisi Matematica con Elementi di Analisi Funzionale II*. UTET, Torino, Italy. In Italian.

Amerio, L. (1977b). *Analisi Matematica con Elementi di Analisi Funzionale III Parte I*. UTET, Torino, Italy. In Italian.

Amerio, L. (1977c). *Analisi Matematica con Elementi di Analisi Funzionale III Parte II*. UTET, Torino, Italy. In Italian.

Arambel, P. and G. Tadmor (1994). Robust H_∞ identification of linear periodic discrete-time systems. *International Journal of Robust and Nonlinear Control*, 4, pp. 595–612.

Arfken, G. and H. Weber, editors (1995). *Mathematical Methods for Physicists*. Academic Press, Orlando, FL, fourth edition.

Atherton, D. (1982). *Nonlinear Control Engineering*. Van Nostrand Reinhold, Melburne. Australia.

Bai, E. (1998). An optimal two-stage identification algorithm for Hammerstein-Wiener nonlinear systems. *Automatica*, 34, pp. 333–338.

Belyakov, L. (1981). The bifurcation set in a system with a homoclinic saddle curve. *Matematicheskie Zametki*, 28, pp. 910–916. In Russian.

Bertoni, A. and M. Dorigo (1993). Implicit parallelism in genetic algorithms. *Artificial Intelligence*, 61, pp. 307–314.

Bittanti, S. (2000a). *Identificazione dei Modelli e Controllo Adattativo*. Pitagora, Bologna, 2000.

Bittanti, S. (2000b). *Teoria della Predizione e del Filtraggio*. Pitagora, Bologna, 2000.

Brogan, W. (1996). *Modern Control Theory*. Prentice-Hall, New York, NY, third edition.

Burnham, K. and D. Anderson (1998). *Model Selection and Inference: A Practical Information-theoretic Approach*. Spinger-Verlag, New York, NY.

Callier, F. and C. Desoer (1991). *Linear System Theory*. Springer-Verlag, New York, NY.

Champneys, A. and Y. Kuznetsov (1994). Numerical detection and continuation of codimension-two homoclinic bifurcations. *International Journal of Bifurcation and Chaos*, 4, pp. 795–822.

Champneys, A., Y. Kuznetsov, and B. Sandstede (1996). A numerical toolbox for homoclinic bifurcation analysis. *International Journal of Bifurcation and Chaos*, 5, pp. 867–887.

Chow, S., B. Deng, and B. Fiedler (1990). Homoclinic bifurcation at resonant eigenvalues. *Journal of Dynamics and Differential Equations*, 2, pp. 177–244.

Chua, L. and S. Kang (1977). Section-wise piecewise-linear functions: Canonical representation, properties, and applications. *Proceedings of the IEEE*, 65, pp. 915–929.

Colorni, A., M. Dorigo, F. Maffioli, V. Maniezzo, G. Righini, and M. Trubian (1996). Heuristics from nature for hard combinatorial optimization problems. *International Transactions in Operational Research*, 3, pp. 1–21.

Cvitanović, P., editor (1984). *Universality in Chaos*. Adam Hilter, Bristol, UK.

Dasgupta, D. and D. McGregor (1992). SGA: A structured genetic algorithm. Department of computer science, University of Strathclyde, Glasgow, UK.

Dasgupta, D. and D. McGregor (1994). A more biologically motivated genetic algorithm: The model and some results. *Cybernetics and Systems*, 25, pp. 447–469.

de Boor, C. (2000). *Spline Toolbox For Use with MATLAB*. The MathWorks, Natick, MA. For the Toolbox version 3.0 $MatlabR12$.

De Feo, O., G. Maggio, and M. Kennedy (2000). The Colpitts oscillator: Families of periodic solutions and their bifurcations. *International Journal of Bifurcation and Chaos*, 10, pp. 935–958.

De Feo, O. and S. Rinaldi (1998). Singular homoclinic bifurcations in tri-trophic food chains. *Mathematical Biosciences*, 148, pp. 7–20.

Dedieu, H. and M. Ogorzalek (1997). Identifiability and identification of chaotic systems based on adaptive synchronization. *IEEE Transactions on Circuits and Systems—I*, 44, pp. 948–962.

Deng, B. (1993). Homoclinic twisting bifurcations and cusp horseshoe maps. *Journal of Dynamics and Differential Equations*, 5, pp. 417–468.

Devaney, R. (1995). *Chaotic Dynamical Systems*. Addison-Wesley, New York, NY.

Doedel, E., A. Champneys, T. Fairgrieve, Y. Kuznetsov, B. Sandstede, and X. Wang (1998). *AUTO 97: Continuation and Bifurcation Software for Ordinary Differential Equations withHomCont*. Computer Science Department, Concordia University, Montreal, Canada, Motreal, Quebec, Canada.

Doedel, E., H. Keller, and J. Kernévez (1991a). Numerical analysis and control of bifurcation problems, part I: Bifurcation in finite dimensions. *International Journal of Bifurcation and Chaos*, 1, pp. 493–520.

Doedel, E., H. Keller, and J. Kernévez (1991b). Numerical analysis and control of bifurcation problems, part II: Bifurcation in infinite dimensions. *International Journal of Bifurcation and Chaos*, 1, pp. 745–772.

Farantos, S. (1995). Methods for locating periodic orbits in highly unstable systems. *Journal of Molecular Structure: THEOCHEM*, 341, pp. 91–100.

Feuer, A. and G. Goodwin (1996). *Sampling in Digital Signal Processing and Control*. Birkauser, Boston, MA.

Galias, Z. (1999). Comparison of interval methods for finding periodic orbits. In *International Conference on Nonlinear Theory and its Applications NOLTA*. Crans-Montana, Switzerland.

Gaspard, P., R. Kapral, and G. Nicolis (1984). Bifurcation phenomena near homoclinic systems: A two-parameter analysis. *Journal of Statistical Physics*, 35, pp. 697–727.

Gaspard, P. and G. Nicolis (1983). What can we learn from homoclinic orbits in chaotic dynamics? *Journal of Statistical Physics*, 31, pp. 499–518.

Glendinning, G. and C. Sparrow (1984). Local and global behavior near homoclinic orbits. *Journal of Statistical Physics*, 35, pp. 215–225.

Greblicki, W. (1998). Continuous-time Wiener system identification. *IEEE Transactions on Automatic Control*, 43, pp. 1488–1493.

Guardabassi, G. (1990). *Elementi di Controllo Digitale*. CLUP, Milano, Italy. In Italian.

Hench, J. (1995). Technique for the identification of linear periodic state-space models. *International Journal of Control*, 62, pp. 289–301.

Hillier, F. and G. Lieberman (1990). *Introduction to Operations Research*. McGraw-Hill, New York, NY, fifth edition.

Johansson, R. (1993). *System Modeling Identification*. Prentice-Hall, Englewood Cliffs, NJ.

Juditsky, A., H. Hjalmarsson, A. Benveniste, B. Delyon, L. Ljung, J. Sjöberg, and Z. Qinghua (1995). Nonlinear black-box models in system identification: Mathematical foundations. *Automatica*, 31, pp. 1725–1750.

Kapitaniak, T. and J. Brindley (1996). Practical stability of chaotic attractors. *Chaos, Solitons, & Fractals*, 7, pp. 1569–1581.

Koza, J. (1992). *Genetic Programming: On the Programming of Computers by Means of Natural Selection*. MIT Press, Cambridge, MA.

Kuznetsov, A. K. Y., V. Levitin, and E. Nikolav (1992). *Interactive Local Bifurcation Analyzer*. CAN Expertise Centre, Amsterdam, The Netherlands. For LOCBIF Version 2.0.

Kuznetsov, Y. (1998). *Elements of Applied Bifurcation Theory*. Springer-Verlag, New York, NY, second edition.

Kuznetsov, Y., O. De Feo, and S. Rinaldi (2001). Belyakov homoclinic bifurcations in a tritrophic food chain model. *SIAM Journal of Applied Mathematics*. Submitted.

Kuznetsov, Y. and V. Levitin (1997). CONTENT: A multiplatform environment for continuation and bifurcation analysis of dynamical systems. Dynamical systems laboratory, CWI, Centrum voor Wiskunde en Informatica, National Research Institute for Mathematics and Computer Science, Amsterdam, The Netherlands.

Kuznetsov, Y. and S. Rinaldi (1996). Remarks on food chain dynamics. *Mathematical Biosciences*, 134, pp. 1–33.

Lambert, J. (1991). *Numerical Methods for Ordinary Differential Systems*. John Wiley & Sons, New York, NY.

Ledoux, C. (1996). Identification of SISO nonlinear Wiener systems. Department of electrical engineering, Linköping University, Linköping, Sweden.

Ljung, L. (1999). *System Identification: Theory for the User*. Prentice-Hall, Upper Saddle River, NJ, second edition.

Ljung, L. (2000). *System Identification Toolbox For Use with MATLAB*. The MathWorks, Natick, MA. For the Toolbox version 5.0 $MatlabR12$.

Ljung, L. and T. Glad (1994). *Modeling of Dynamic Systems*. Prentice-Hall, Englewood Cliffs, NJ.

Ljung, L. and T. Söderström (1983). *Theory and Practice of Recursive Identification*. MIT Press, Cambridge, MA.

Matlab (2000). *Control System Toolbox For Use with MATLAB*. The MathWorks, Natick, MA. For the Toolbox version 1.0 $MatlabR12$.

McLernon, D. (1989). Parameter estimation of autoregressive processes with periodic coefficients. In *International Symposium on Circuits and Systems ISCAS*, pp. 1350–1353. Portland, OR.

McQuarrie, A. and C. Tsai (1998). *Regression and Time Series Model Selection*. World Scientific, Singapore.

Meyer, C. (2000). *Matrix Analysis and Applied Linear Algebra*. SIAM Press, Philadelphia, PA.

Nozdrachova, V. (1982). Bifurcation of a noncourse separatrix loop. *Differential Equations*, 18, pp. 1098–1104.

Ogorzalek, M. (1995). Chaos control: How to avoid chaos or take advantage of it. *Journal of the Franklin Institute*, 331, pp. 681–704.

O'Malley, R. (1974). *Introduction to Singular Perturbations*. Academic Press, New York, NY.

Ott, E. (1993). *Chaos in Dynamical Systems*. Cambridge University Press, New York, NY.

Pontryagin, L. (1957). Asymptotic behavior of solutions of systems of differential equations with small parameters at higher derivatives. *Izvestija Akademii Nauk SSSR*, 21, pp. 605–626. In Russian.

Proakis, J. and D. Manolakis (1992). *Digital Signal Processing: Priciples, Algorithms and Applications*. Maxwell Macmillan, New York, NY, second edition.

Rinaldi, S. and C. Piccardi (1998). *I Sistemi Lineari*. UTET, Torino, Italy. In Italian.

Ruelle, D. (1989). *Chaotic Evolution and Strange Attractors : The Statistical Analysis of Time Series for Deterministic Nonlinear Systems (Lezioni Lincee)*. Cambridge University Press, Cambridge, UK.

RUGH, W. (1990). *Non Linear System Theory , The Volterra/Wiener Approach*. John Hopkins University Press, London, UK.

SCHWARZ, H. (1989). *Numerical Analysis: A Comprehensive Introduction*. John Wiley & Sons, New York, NY.

SCHWEHM, M. (1993). *A Massively Parallel Genetic Algorithm on the MasPar MP-1*, pp. 503–507. Springer-Verlag, New York, NY.

SJOBERG, J., Q. ZHANG, L. LJUNG, A. BENVENISTE, B. DELYON, P. GLORENNEC, H. HJALMARSSON, AND A. JUDITSKY (1995). Nonlinear black-box modeling in system identification: A unified overview. *Automatica*, 31, pp. 1691–1724.

SLOTINE, J. AND W. LI (1991). *Applied Nonlinear Control*. Prentice-Hall, Englewood Cliffs, NJ.

SÖDERSTRÖM, T. AND P. STOICA (1989). *System Identification*. Prentice-Hall, London, UK.

SZEGÖ, G. (1975). *Orthogonal Polynomials*. American Mathematical Society, Providence, RI, fourth edition.

TIKHONOV, A. (1952). System of differential equations containing small parameters at derivatives. *Matematiceskij Sbornik*, 31, pp. 575–586. In Russian.

TRESSER, C. (1984). On some theorems of L. P. Shil'nikov and some applications. *Annales de l'Institute Henri Poincaré*, 40, pp. 441–461.

WAGNER, H. (1975). *Principles of Operations Research*. Prentice-Hall, Englewood Cliffs, NJ.

WALPONE, R. (1993). *Probabilty and Statistics for Engineers and Scientists*. Macmillan, New York, NY, fifth edition.

WIGREN, T. (1994). Convergence analysis of recursive identification algorithms based on the nonlinear Wiener model. *IEEE Transactions on Automatic Control*, 39, pp. 2191–2206.

WIGREN, T. (1997). Circle criteria in recursive identification. *IEEE Transactions on Automatic Control*, 42, pp. 975–979.

WINSTON, W. (1991). *Operations Research: Applications and Algorithms*. PWS-Kent, Boston, MA, second edition.

YUAN, C. (1995). *A Method of Parametric Identification of Chaotic Systems*. Ph.D. thesis, Michigan State University, MI, East Lansing.

YUAN, C. AND B. FEENY (1998). Parametric identification of chaotic systems. *Journal of Vibration and Control*, 4, pp. 405–426.

CHAPTER 6

AUTOMATIC FILTER GAIN TUNING

Brief — In this chapter one among several possible algorithms is presented to automatically design the filter gain that guarantees the resonance with input signal exemplars of good patterns and anti-resonance with input signal exemplars of bad patterns. The chosen algorithm is presented since it is easy, based on standard theories about robust filtering, and, furthermore, fairly well performing. No one of the other considered algorithms has proved to be noticeably superior to this one despite of an increased complexity. Hence, in some sense, the proposed technique represents the best quality/price compromise. The proposed algorithm for tuning the filter gain consists of four steps. In the first step, the requirement of qualitative resonance with signals belonging to the class of good patterns is transformed into a problem of robust H_∞ linear periodic filtering with structured and unstructured perturbations. The set of possible solutions for this problem is characterized by the solutions of a one parameter dependent family of periodic Riccati differential equations. In the second step, the anti-resonance requirement for bad pattern signals is reduced to a problem of anti-robust H_∞ linear periodic filtering with unstructured perturbations. The set of possible solutions for this problem is characterized by a Riccati-like matrix inequality. The third step consists in computing the family of solutions for the filtering problem given at the first step, *i.e.* the resonance requirement, selecting among them only those which satisfy the matrix inequality imposed by the anti-resonance requirement given at the second step. This step obtains the set of filter gains compatible with the resonance and anti-resonance requirements. Finally, at the fourth step, the smallest, with respect to a given norm, filter gain from those belonging to the set computed at the previous step is selected.

Personal Contribution — The algorithm for the tuning of the filter gain presented in this chapter is original. Nevertheless, it is based on well-known results of periodic control theory.

In the previous chapter it has been shown how to construct automatically a Shil'nikov-like chaotic model for the class of good patterns. In order to complete the construction of the qualitatively resonating filter, as described in Sect. 4.4, it is now necessary to tune the filter gain such as to guarantee that the qualitatively resonating filter resonates when driven with signals belonging to the class of good patterns and anti-resonates when driven with signals belonging to the class of the bad patterns. This is the second step of the qualitatively resonating filter construction as described in Sect. 4.4.2.

Even though several algorithms to accomplish this duty have been considered, in this chapter only one of them is presented, some of the others are presented in Appendix E. The algorithm presented here is the one with the best quality/price ratio among those that have been considered; it is simple, based on standard theories about robust filtering, and fairly well performing. Indeed, despite of its simplicity the proposed

algorithm proves to be effective in most cases (*cfr.* Chap. 7); moreover, none of the other considered algorithms has proved to be noticeably superior to this one despite of an increased complexity.

The idea followed in developing this algorithm is to satisfy the two requirements, *i.e.* the resonance and anti-resonance, independently determining two families of filter gains, one satisfying the resonance requirement and one satisfying the anti-resonance requirement and then to select a filter gain from the intersection of these two families, which is hoped to be nonempty. Actually, from Sect. 3.3.3, it should be clear that the computation of the two families of filter gains passes by those techniques proper to the optimal/robust linear periodic filtering/control.

The idea is to rely on filtering techniques rather than control ones. There is one main reason that justify this choice. Although the filtering and the control problem are very similar to each other [Bryson, 1996; Mitter, 1996], in fact their solutions are obtained by means of the same mathematical tools [Kwakernaak and Sivan, 1972; Locatelli, 1993], there is a conceptual difference between them. A tracking, *i.e.* control, problem is usually meant for letting two different dynamical systems to behave in the same way [Levine, 1996]. Namely, there is a master (driver) and a slave (driven) system which are substantially different; the aim of the control law (tracking law) is to let the slave system behave as the master one despite of their diversity. On the other hand, a filter, *i.e.* reconstruction, problem is usually meant for letting two almost equal systems synchronize with each other [Levine, 1996]. Once again, there is a master (driver) and a slave (driven) system which are substantially identical; the aim of the filtering law (reconstruction law) is to let the slave system state to converge towards (reconstruct, synchronize) the state of the master system despite of the modeling and measurement noises.

Keeping in account the way in which the qualitatively resonating filter is conceived, it is clear that is more logic to deal with its tuning by means of a reconstruction problem rather than a tracking problem. Indeed, the model constructed at the previous step (*cfr.* Chap. 5) is meant to be a chaotic repulsive[1] model for the generation mechanism of the good patterns. Thus, if the model of the good patterns has been well built it is meant to be qualitatively equivalent to the driving system. Therefore, to oblige the driven system, *i.e.* the qualitatively resonating filter, to synchronize, *i.e.* qualitatively resonate, with the driving signal, *i.e.* the driving system, is definitely more a problem of filtering rather than one of control since the two systems, master and slave, are meant to be (qualitatively) equal.

Before passing to describe the developed algorithm in detail, it should be noted that the qualitatively resonating filter can be thought as a sort of reconstructor with a nonlinear saturation. It contains the dynamical model of the class of good patterns in the form of an unstable Feigenbaum-like strange attractor embedded into a Shil'nikov-like one (*cfr.* Sect. 3.4 for the explanation why a Shil'nikov-like strange attractor is needed).

The resonance requirement asks the filtering gain to be tuned in such a way as to stabilize the unstable Feigenbaum-like strange attractor whenever the system is excited with a signal from the class of good patterns. Namely, under the condition of qualitative resonance, the state of the driven system, which is qualitatively equal to the driving one, is required to converge to the state of the driving system despite of the modeling and measurement noises; this is exactly a reconstruction (filtering) problem, *cfr.* Sect. 3.3.3.

On the other hand, because of the Shil'nikov's nature of the driven model, the performance of the reconstructor does not degrade linearly with the modeling and measuring noise as for a linear reconstructor [Grewal and Andrews, 1993]. In fact, if the difference between the driving signal and the corresponding Feigenbaum-like trajectory of the driven system becomes excessive, then the homoclinic mode of the driven system gets excited leading to an explosion of the chaotic behavior and thus loosing any convergence between the two states; in other words, leading to the occurrence of anti-resonance. Hence, in some sense, the model used in the qualitatively resonating filter saturates with respect to the maximal diversity that is supported. In this respect it should be noted that exactly this nonlinear phenomenon is exploited for pattern recognition purposes. The occurrence of qualitative resonance is mainly a phenomenon of linear stability; on the contrary, the occurrence of anti-resonance is a saturating phenomenon that does not occur in linear systems.

6.1 The Filter Gain Tuning Algorithm

The idea on which the filter gain tuning algorithm is based is rather simple. It decomposes the tuning into four steps. The first two are linked to optimal/robust periodic linear filtering while the third and fourth ones consist of a, rather trivial, solution selection criterion.

[1] The Feigenbaum-like strange attractor, which is indeed the model of the diversity of the good patterns, is a repulsive invariant embedded inside the Shil'nikov-like strange attractor.

1. *Resonance requirement*: the requirement of qualitative resonance with signals belonging to the class of good patterns is transformed into a problem of robust linear periodic filtering with structured and unstructured perturbations; it is required that the state of the system that generates the good patterns is reconstructed, by the qualitatively resonating filter, with a noise reduction ratio guaranteeing that the reconstructed state stays away from the homoclinic trajectory. Namely, the measurement and modeling noises are *attenuated* enough such as to stay away from the homoclinic trajectory. The set of possible solutions for this problem is characterized by the solutions of a one parameter dependent family of periodic Riccati differential equations. This step determine as well the relationship between the periodic Riccati differential equation solution and the filter gain.

2. *Anti-resonance requirement*: the anti-resonance with bad pattern signals requirement is reduced to a problem of anti-robust linear periodic filtering with unstructured perturbations; it is required that the state of the system generating the bad patterns is reconstructed, by the qualitatively resonating filter, with a noise reduction ratio guaranteeing that the reconstructed state surely approaches, sooner or later, the homoclinic trajectory. Namely, the measurement and modeling noises are *amplified* enough such as to reach touching the homoclinic trajectory. The set of possible solutions for this problem is characterized by a Riccati-like matrix inequality.

3. *Potential solutions set*: in this step the potential solutions compatible with both requirements (imposed at the first and second step) are determined. Namely, the intersection between the one parameter family of periodic Riccati differential equations and the Riccati-like matrix inequality is computed. Sequentially, using the relation given at the first step, the potential solutions of the periodic Riccati differential equations are transformed into filter gain candidates.

4. *Solution extraction*: the smallest filter gain candidate, with respect to a given norm, is selected from those obtained at the previous step.

The presented algorithm depends on the way in which the first two requirements are imposed. Theoretically, the first two step can be faced by means of any robust filtering technique; in particular, with any robust H_X filtering approach using the ℓ_X Hardy norm [Burl, 1999; Colaneri and Geromel, 1997]. Here, only the tuning of the filter gain by means of robust H_∞ filtering is presented [Petersen and Savkin, 1999].

Before starting to describe in details the four steps it should be noted that for the filter gain tuning, as already mentioned in Sect. 4.4.2, both instances, *i.e.* observations, of good and bad patterns are necessary. How the observations of good patterns should be chosen and how they should be treated before their employment has been already largely discussed in Sect. 5.1.1. Clearly, *mutando mutandis*, the arguments adopted there for the good patterns are valid as well for the representatives of the bad patterns.

6.1.1 Good Patterns H_∞ Robust Filtering

This first step has two goals. The first aim is the satisfaction of the resonance requirement while the second one is to provide the rule for computing the filter gain from the constraints. As it is now described in detail, this step is faced by means of robust H_∞ linear periodic filtering with structured and unstructured perturbations.

The Pattern Generation Framework

To reduce the resonance requirement to a robust filtering problem it is first of all necessary to hypothesize a linear periodic model for the generation of the good patterns. Similarly to Sect. 3.3.3, such a linear system can be obtained by linearizing the generating system in the neighborhood of its nominal periodic trajectory. Since the only considered variables are the linearized ones, to simplify the already heavy notation the δ indicating the linearization have been omitted in the following.

From the modeling step (*cfr.* Chap. 5) a lot of information is available about the generation of good patterns; thus, a model hypothesizing both structured, *i.e.* approximately known, and unstructured, *i.e.* completely unknown, uncertainties can be assumed, namely

$$\begin{aligned} \dot{x}_{GP}(t) &= \big[A_{GP}(t) + \Delta A_{GP}(t)\big] x_{GP}(t) + B_{GP\,w}(t) w_{GP}(t) \\ y_{GP}(t) &= \big[C_{GP}(t) + \Delta C_{GP}(t)\big] x_{GP}(t) + D_{GP\,w}(t) w_{GP}(t) \end{aligned} \tag{6.1}$$

where $x_{GP}(t) \in \mathbb{R}^n$ is the state, $w_{GP}(t) \in \mathbb{R}^m$ is the noise which is assumed to belong[2] to $L^2(0,\infty]$, and $y_{GP}(t)$ is the output signal, *i.e.* the variation of the driving signal with respect to the nominal periodic regime; $A_{GP}(\cdot)$ and $C_{GP}(\cdot)$ are real piecewise continuous bounded matrix functions of period[3] T_P that describe the nominal system, *i.e.* the right hand side and output function Jacobians along the nominal periodic trajectory; $B_{GP\,w}(\cdot)$ and $D_{GP\,w}(\cdot)$ are real piecewise continuous bounded matrix functions of period T_P which describe the unstructured uncertainties about the model; finally, $\Delta A_{GP}(\cdot)$ and $\Delta C_{GP}(\cdot)$ represent the time-varying structured uncertainties about the model. In particular, the structured uncertainties, which are not necessarily T_P-periodic functions, are supposed (to be used in the standard H_∞ framework) to have the following structure

$$\begin{bmatrix} \Delta A_{GP}(t) \\ \Delta C_{GP}(t) \end{bmatrix} = \begin{bmatrix} H_{GP\,1}(t) \\ H_{GP\,2}(t) \end{bmatrix} F_{GP}(t) E_{GP}(t) \tag{6.2}$$

where $H_{GP\,1}(\cdot)$, $H_{GP\,2}(\cdot)$, and $E_{GP}(\cdot)$ are known real piecewise continuous bounded matrix functions of period T_P while $F_{GP}(\cdot)$ is an unknown matrix function with Lebesgue measurable elements satisfying

$$F_{GP}(\cdot)^T F_{GP}(\cdot) \leq I \tag{6.3}$$

It should be noted that the matrix function $F_{GP}(\cdot)$ is not necessarily a T_P periodic function. In fact, it can be any arbitrary time-varying matrix which is even allowed to depend on the state $x_{GP}(t)$ as long as the Eq. (6.3) is satisfied.

The index GP given to all the variables is meant to remind that this is the model for the good pattern generation. Since it will be necessary to hypothesize a similar model for the generation of bad patterns, the purpose of this index is, obviously, to discriminate the data about the generation of good patterns from the data about the generation of bad patterns, which, logically, will have index BP.

As described in the next section, the exact knowledge of the matrix functions describing the generation of the good patterns, *i.e.* $A_{GP}(\cdot)$, $C_{GP}(\cdot)$, $H_{GP\,1}(\cdot)$, $H_{GP\,2}(\cdot)$, $E_{GP}(\cdot)$ $B_{GP\,w}(\cdot)$ and $D_{GP\,w}(\cdot)$, is necessary to solve the robust filtering problem used to impose the resonance requirement as well as to determine the explicit formula to compute the periodic filter gain $K(t)$; it will be shown later how to determine these information items on the basis of the constructed chaotic model (*cfr.* Chap. 5) and the good pattern observations.

The H_∞ Filtering with Structured and Unstructured Perturbations

Given the generating system (6.1) and a prescribed level of noise attenuation $\gamma > 0$, the estimation $\widehat{x}(t)$ of $x_{GP}(t)$ such that the estimation error dynamics is quadratically stable [Barmish, 1985; Xie and de Souza, 1991] and satisfies the H_∞ performance criterion

$$\left\|\widehat{x}(t) - x_{GP}(t)\right\|_2 < \gamma \left\|w_{GP}(t)\right\|_2 \tag{6.4}$$

for all the admissible uncertainties $F(\cdot)$ satisfying Eq. (6.3) and for any nonzero $w_{GP}(\cdot)$, where $\|\cdot\|_2$ stands for the usual $L^2[0,\infty)$ norm, is given by the modified Luemberger observer [Xie and de Souza, 1991]

$$\begin{aligned} \dot{\widehat{x}}(t) &= \widehat{A}(t)\widehat{x}(t) + \widehat{K}_{GP}(t)\left[y_{GP}(t) - \widehat{y}(t)\right] \\ \widehat{y}(t) &= \widehat{C}(t)\widehat{x}(t) \end{aligned} \tag{6.5}$$

The matrix functions specifying the observer are given by

$$\begin{aligned} \widehat{A}(\cdot) &= A_{GP}(\cdot) + \gamma^{-2}\widehat{B}(\cdot)\widehat{B}^T(\cdot)S(\cdot) \\ \widehat{C}(\cdot) &= C_{GP}(\cdot) + \gamma^{-2}\widehat{D}(\cdot)\widehat{B}^T(\cdot)S(\cdot) \\ \widehat{K}_{GP}(\cdot) &= \left[P(\cdot)\widehat{C}^T(\cdot) + \widehat{B}(\cdot)\widehat{D}^T(\cdot)\right]\widehat{R}^{-1}(\cdot) \end{aligned} \tag{6.6}$$

where the matrix functions $\widehat{R}(\cdot)$, $\widehat{B}(\cdot)$ and $\widehat{D}(\cdot)$ are given by

$$\begin{aligned} \widehat{D}(\cdot) &= \left[D_{GP\,w}(\cdot) \quad \frac{\gamma}{\varepsilon}H_{GP\,2}(\cdot)\right] \\ \widehat{B}(\cdot) &= \left[B_{GP\,w}(\cdot) \quad \frac{\gamma}{\varepsilon}H_{GP\,1}(\cdot)\right] \\ \widehat{R}(\cdot) &= \widehat{D}(\cdot)\widehat{D}^T(\cdot) \end{aligned} \tag{6.7}$$

[2] The noise is assumed simply to be energy bounded and not necessarily Gaussian.
[3] Reminder: T_P is the nominal pseudo-period of the approximately periodic patterns.

while the matrix functions $S(\cdot)$ and $P(\cdot)$ are the stabilizing periodic symmetric semidefinite positive solutions of the following two periodic Riccati differential equation, respectively

$$\dot{S}(t) + A_{GP}^T(t)S(t) + S(t)A_{GP}(t) + \gamma^{-2}S(t)\widehat{B}(t)\widehat{B}^T(t)S(t) + \varepsilon^2 E_{GP}^T(t)E_{GP}(t) = 0 \tag{6.8}$$

and

$$\begin{aligned}\dot{P}(t) = \; & P(t)\big[\widehat{A}(t) - \widehat{B}(t)\widehat{D}^T(t)\widehat{R}^{-1}(t)\widehat{C}(t)\big]^T + \big[\widehat{A}(t) - \widehat{B}(t)\widehat{D}^T(t)\widehat{R}^{-1}(t)\widehat{C}(t)\big]P(t) + \\ & + P(t)\big[\gamma^{-2}I - \widehat{C}^T(t)\widehat{R}^{-1}(t)\widehat{C}(t)\big]P(t) + \widehat{B}(t)\big[I - \widehat{D}^T(t)\widehat{R}^{-1}(t)\widehat{D}(t)\big]\widehat{B}^T(t)\end{aligned} \tag{6.9}$$

Since in Eqs. (6.6) and (6.9) the inverse of $\widehat{R}(\cdot)$ is computed, it follows that the condition for the filtering problem to be well posed[4] is the existence of a positive real number ε such that the periodic matrix function $\widehat{R}(\cdot)$, defined in Eqs. (6.7), is strictly definite positive for any time t. Furthermore, it should be noted that the Eqs. (6.5-6.9) define a family of potential solutions to the robust filtering problem (6.1-6.4). Indeed, for any $\varepsilon > 0$ such that $\widehat{R}(\cdot) > 0$, the Eqs. (6.5-6.9) give an observer candidate. In particular, for any $\varepsilon > 0$ such that $\widehat{R}(\cdot) > 0$, the solutions of the Eqs. (6.9) gives a potential filter gain candidate for the observer (6.5).

The idea proposed by this algorithm is to consider as candidate qualitatively resonating filter gains satisfying the resonance requirement the filter gain candidate for the observer (6.5). Namely, the ε dependent family of gains $\widehat{K}_{GP}(\cdot)$ as given by Eqs. (6.6-6.9). This is conceivable since the filter gain operates on the difference between the outputs, *i.e.* $y_{GP}(t) - \widehat{y}(t)$, thus it does not matter if the $y(t)$ variables refer to the real outputs or to their variation with respect to a nominal value.

Finally, note that this represents a strongly conservative approach. In fact, in the qualitatively resonating filter the matrices governing the local dynamics depend upon the state and not on the time; namely, the equivalents of the qualitatively resonating filter to the matrices $\widehat{A}(\cdot)$ and $\widehat{C}(\cdot)$ of the observer (6.5) are the local Jacobians of the dynamics and the output functions (*cfr.* Sect. 3.3.3) which indeed depend only upon the state and not on the time. Thus, under resonance conditions, *i.e.* approximate synchronization, the local dynamic matrices of the qualitatively resonating filter, *i.e.* those corresponding to $\widehat{A}(\cdot)$ and $\widehat{C}(\cdot)$, synchronize with those of the driving system, *i.e.* $\big[A_{GP}(t) + \Delta A_{GP}(t)\big]$ and $\big[C_{GP}(t) + \Delta C_{GP}(t)\big]$. Therefore, the local dynamic matrices of the qualitatively resonating filter are certainly better approximations of the real local dynamic matrices than what the worst case approximates [Xie and de Souza, 1991] given by $\widehat{A}(\cdot)$ and $\widehat{C}(\cdot)$, used in the robust observer (6.5), are. Concluding, the proposed filter gain remains conservative with respect the application since it considers an admissible worst case [Xie and de Souza, 1991] which is definitely more dramatic than the reality.

Computing the Necessary Data

In order to compute the family of filter gain candidates as given by the Eqs. (6.6-6.9), the matrices which describe the dynamical model generating the good pattern, *i.e.* $A_{GP}(\cdot)$, $C_{GP}(\cdot)$, $H_{GP\,1}(\cdot)$, $H_{GP\,2}(\cdot)$, $E_{GP}(\cdot)$ $B_{GP\,w}(\cdot)$ and $D_{GP\,w}(\cdot)$, must be given. Furthermore, as will be explained in the next section, to impose the resonance condition a hypothesis on the norm of $w(\cdot)$ is as well necessary.

These information items must be extracted from the available data as the good pattern observations and the chaotic model obtained in the modeling step. Before starting to give the details on how to extract these information items from the available data, it should be noted that, since the reference model for good patterns (as obtained in the previous chapter) is a scalar Lur'e system, it remains very easy to merge measurements and model knowledge in order to obtain the required information items. In fact, since in a scalar Lur'e system the Jacobian depend only upon the output, the Jacobian of the system corresponding to a given observation can be computed without reconstructing the corresponding state. Namely, referring to Eqs. (5.4), the Jacobian of a scalar Lur'e system is given by

$$J\big(x(t)\big) = \left.\frac{\partial F(x)}{\partial x}\right|_{x=x(t)} = A + b\left.\frac{\partial f(c^T x)}{\partial x}\right|_{x=x(t)} = A + bc^T\left.\frac{\partial f(y)}{\partial y}\right|_{y=y(t)} \tag{6.10}$$

Where the matrices A, b and c^T are those obtained in Sect. 5.1.6. In this respect, note that if the reference model was not a scalar Lur'e system, it would be necessary to apply an extended Kalman filter

[4] In reality, the existence of the observer given in Eqs. (6.5) is subordinate to the existence of the two stabilizing periodic symmetric semidefinite positive solutions for the two differential Riccati equations Eqs. (6.8) and (6.9) [Bittanti *et al.*, 1984; Chen *et al.*, 1998; Xie and de Souza, 1991].

[Grewal and Andrews, 1993; Petersen and Savkin, 1999] in order to extract together the parameters, *i.e.* the Jacobian, and the state at once from the observations.

Here, a rather arbitrary, but fairly logic, way is proposed to compute these information items starting from the chaotic model, as constructed in the previous chapter, and the good pattern observations.

The nominal dynamical matrices, *i.e.* $A_{GP}(\cdot)$ and $C_{GP}(\cdot)$, can be easily assumed to be the right hand side and output function Jacobians of the system along the generating cycle, namely

$$\begin{aligned} A_{GP}(t) &= \left.\frac{\partial F(x)}{\partial x}\right|_{x\in GC} \\ C_{GP}(t) &= c^T \end{aligned} \tag{6.11}$$

It is reminded that the Jacobian along the generating cycle is a side product of the modeling step, *cfr.* Sect. 5.2.2. Furthermore, because of the Lur'e structure of the considered model, no computations are needed to obtain $C_{GP}(t)$; it is simply the output matrix of the controller canonical form; namely a constant matrix[5]. Finally, note that a reference phase, as explained in Sect. 4.3.1, must be chosen to uniquely determine the matrix function $A_{GP}(\cdot)$; on the other hand, since $C_{GP}(\cdot)$ is a constant matrix, it is not necessary to chose a reference phase for it.

Assuming a unitary base noise, namely $\left\|w_{GP}(t)\right\|_2 = 1$, it is rather simple to determine two matrices modeling the effects of the unstructured uncertainties, *i.e.* $B_{GP\,w}(\cdot)$ and $D_{GP\,w}(\cdot)$. Actually, a natural measure of the unstructured uncertainty is given by the parameter covariance matrix of the identified linear transfer function, *cfr.* Sect. 5.1.4. In other words, the unstructured uncertainties are due to the imprecision with which the transfer function $G(Z)$ is known; namely, they are modeled by the standard deviations of the parameters a_i and b_i of the identified transfer function $\widehat{G}(Z)$, *cfr.* Sect. 5.1.4. Actually, since the identified discrete time linear transfer function $\widehat{G}(Z)$ has been converted into a continuous time state space model (*cfr.* Sect. 5.1.6), it follows that the uncertainty on the a_i and b_i parameters must undergo the same transformation as well. In particular, neglecting the cross-variances[6] and keeping in account the controller canonical form, as given in Sect. 5.1.6, it follows that

$$\begin{aligned} B_{GP\,w} &= \widetilde{A}^{-1}\widetilde{b}_w \\ D_{GP\,w} &= \widetilde{d}_w \end{aligned} \tag{6.12}$$

where the matrix $\widetilde{b}_w$ and the scalar $\widetilde{d}_w$ are given by

$$\widetilde{b}_w = \begin{bmatrix} 0 \\ \vdots \\ 0 \\ \mathrm{sum}\big(\mathrm{diag}(\Theta_a)\big) \end{bmatrix}$$

$$\widetilde{d}_w = \mathrm{sum}\big(\mathrm{diag}(\Theta_b)\big)$$

where the matrices Θ_a and Θ_b are the square root[7] of the covariance matrices, as reported by the linear identification algorithm (*cfr.* Sect. 5.1.4), of the denominator and numerator coefficients of the discrete time transfer function, respectively. The so obtained two matrix functions $B_{GP\,w}(\cdot)$ and $D_{GP\,w}(\cdot)$ are constant matrices; namely, the easiest kind of periodic matrices. Thus, for them it is not necessary to chose a reference phase which, in case they would be needed, should be chosen coherent with that chosen for $A_{GP}(\cdot)$.

Since it has been assumed that the good patterns are of Feigenbaum-like nature (*cfr.* Chap. 5 hypothesis (H.1)), it follows that the main source of structured uncertainty is the chaotic, but deterministic, wandering of the trajectories around the nominal periodic trajectory, *i.e.* the generating cycle. Therefore, it is rather simple to obtain the matrices describing the structured uncertainties from the observations; in particular, exploiting Eq. (6.10).

[5] Obviously, constant matrices are particular cases of periodic matrices.

[6] If the identification has been well performed the cross variances should be quite small; indeed, they are considered a sign of a bad identification [Bittanti, 2000; Ljung, 1999].

[7] The principal square root of a definite positive matrix M is the symmetric semidefinite positive matrix S such that $S*S = M$

Before starting with the formulae, it should be noted that keeping in account the Lur'e structure of the reference model, it follows that the structured uncertainties on the output function vanish. Namely, since the output function is fixed[8] at $c^T x$ it follows that $\Delta C_{GP}(\cdot) \equiv 0$; consequentially, $H_{GP\,2}(\cdot) \equiv 0$ as well. This simplifies notably all the computations as explained in the next section.

The computation of the remaining matrices $H_{GP\,1}(\cdot)$ and $E_{GP}(\cdot)$ passes by the computation of the set of the structured uncertainty matrices $\Delta A_{GP}(\cdot)$ admissible according to the measurements. More in particular, for any given observation $y_i(t)$ it is computed the corresponding Jacobian, then subtracting from it the nominal Jacobian, *i.e.* $A_{GP}(\cdot)$, the corresponding structural uncertainty is obtained, namely

$$\Delta A_{GP\,i}(t) = A + bc^T \frac{\partial f(y)}{\partial y}\bigg|_{y=y_i(t)} - A_{GP}(t) = bc^T \left(\frac{\partial f(y)}{\partial y}\bigg|_{y=y_i(t)} - \frac{\partial f(y)}{\partial y}\bigg|_{y:x\in GC} \right)$$

For a correct computation of the matrices $\Delta A_{GP\,i}(t)$ the reference phase for the $y_i(t)$ signals must be chosen coherent with the one chosen for $A_{GP}(\cdot)$. The matrices $H_{GP\,1}(\cdot)$ and $E_{GP}(\cdot)$ are obtained by a multi-kernel factorization of the $\Delta A_{GP\,i}(t)$ matrices, namely

$$\begin{bmatrix} \Delta A_{GP\,1}(t) \\ \Delta A_{GP\,2}(t) \\ \vdots \\ \Delta A_{GP\,r}(t) \end{bmatrix} = H_{GP\,1}(t) \begin{bmatrix} \Delta F_{GP\,1}(t) \\ \Delta F_{GP\,2}(t) \\ \vdots \\ \Delta F_{GP\,r}(t) \end{bmatrix} E(\cdot) \tag{6.13}$$

where each F_i must satisfies (*cfr.* Eq. (6.3))

$$F_{GP\,i}(\cdot)^T F_{GP\,i}(\cdot) \leq I$$

The mentioned factorization can be easily implemented in MATLAB discretizing, in time, the $\Delta A_{GP\,i}(t)$ matrices and recursively applying the generalized singular value decomposition on the result. Finally, note that choosing the reference phase of $y_i(t)$ coherent with that of $A_{GP}(\cdot)$, as suggested above, guarantees the phase coherency of the matrices $H_{GP\,1}(\cdot)$ and $E_{GP}(\cdot)$ as well.

It should be noted, that any alternative method for extracting these information items from the available data other than the one proposed here could be considered instead without changing the general idea for the tuning of the filter gain; for instance, methods based on extended Kalman filtering [Grewal and Andrews, 1993; Petersen and Savkin, 1999] or on state covariance bounds formulae [Bolzern *et al.*, 1994] could be considered. Here, only the proposed method has been tested.

The Filtering Problem

Giving the prescribed level of noise attenuation γ such to guarantee the qualitative resonance requirement, the data computed at the previous section allow to compute the family of the candidate qualitatively resonating filter gains satisfying the resonance requirement. Namely, the ε dependent family of gains $\widehat{K}_{GP}(\cdot)$ as given by Eqs. (6.6-6.9).

Since the unstructured noise $w_{GP}(t)$ has been chosen unitary, *i.e.* $\left\|w_{GP}(t)\right\|_2 = 1$, from the H_∞ performance criterion (6.4) it follows that, in order to guarantee the qualitative resonance with good patterns, the noise attenuation must be such that

$$\gamma < \min_{\theta}(\left|\rho(\theta) - \sigma_{Fg}(\theta)\right|) \tag{6.14}$$

where $\rho(\theta)$ (*cfr.* Sect. 3.3.3) is the minimal distance between the point on the generating cycle at phase θ and the homoclinic trajectory; and $\sigma_{Fg}(\theta)$ (*cfr.* Sect. 5.1.6) is the natural standard deviation of the Feigenbaum-like strange attractor, modeling the diversity of the good patterns, at the phase θ.

The condition given by Eq. (6.14) requires that the maximal wandering due to the model imprecision, *i.e.* γ, added to the natural diversity of the good patterns, *i.e.* $\sigma_{Fg}(\theta)$, is not enough to reach the homoclinic trajectory. Hence, if the qualitatively resonating filter is initially almost in phase (*cfr.* Sect. 3.3.3) with a driving signal belonging to the class of good patterns, then any filter gain candidate given by Eqs. (6.6-6.9) will guarantee the quadratically stable [Barmish, 1985; Xie and de Souza, 1991] convergence of the filter output to the driving signal; namely, qualitative resonance.

[8] The uncertainties on the b_i parameters have already been taken into account into $D_{GP\,w}$.

It should be noted that the identical annihilation of the $H_{GP\,2}(\cdot)$ matrix notably simplifies the computations necessary to determine the set of filter gain candidates which satisfy the resonance requirement. In fact, because of the annihilation of $H_{GP\,2}(\cdot)$, it follows that

$$\widehat{R}(\cdot) = \widehat{D}(\cdot)\widehat{D}^T(\cdot) = D_{GP\,w}D_{GP\,w}^T = \mathrm{sum}\big(\mathrm{diag}(\Theta_b)\big)^2$$

which is independent from ε; therefore, $\widehat{R}(\cdot)$ is strictly positive for any value of ε. Hence, there is a filter gain candidate for any positive value of ε. In other words, it is not necessary to determine the ε for which the robust filtering problem is well posed.

Finally, not shown here, because of the annihilation of $H_{GP\,2}(\cdot)$ the second Riccati equation, *i.e.* Eq. (6.9), is notably simplified especially for numerical computations.

6.1.2 Bad Patterns H_∞ Anti-Robust Filtering

The aim of this step is to restrict the potential solutions determined at the first step to those solutions guaranteeing a minimal anti-resonance requirement. As it is now described in detail, this step is faced by means of a problem of anti-robust H_∞ linear periodic filtering with unstructured perturbations.

The Pattern Generation Framework

To reduce the anti-resonance requirement to an anti-robust filtering problem it is first of all necessary to hypothesize a linear periodic model for the generation of the bad patterns. Once again, similarly to Sect. 3.3.3, such a linear system can be obtained linearizing the generating system in the neighborhood of its nominal periodic trajectory. Since the only considered variables are the linearized ones, to simplify the already heavy notation the δ indicating the linearization have been omitted.

The linear periodic model here assumed for the generation of the bad patterns does not exploit any knowledge about structured uncertainties; namely, it models only unstructured uncertainties. There are two reasons for neglecting the structured uncertainties. Firstly, this information is unavailable; in fact, there are not too many information items about the generation of bad patterns; actually, they have not been considered until now. Thus, it would be difficult to obtain the information about their structured uncertainties. Secondly, this information should not be exploited on purpose; in fact, the anti-resonance requirement is not so precise as the resonance requirement. Actually, since the resonance must be as selective as possible, it is logic to exploit as much information as available to tune it. Ideally, the resonance should be constrained to occur only with good patterns and only with them. On the contrary, the ideal anti-resonance should occur with any non good pattern. In reality, imposing such a stringent requirement is practically impossible; therefore, only a restricted class of bad patterns is considered, *i.e.* the considered generating model, for tuning the anti-resonance. Nevertheless, this class should not be too selective; thus, a model hypothesizing only unstructured uncertainties can be assumed, namely

$$\begin{aligned} \dot{x}_{BP}(t) &= A_{BP}(t)x_{BP}(t) + B_{BP\,w}(t)w_{BP}(t) \\ y_{BP}(t) &= C_{BP}(t)x_{BP}(t) + D_{BP\,w}(t)w_{BP}(t) \end{aligned} \tag{6.15}$$

where $x_{BP}(t) \in \mathbb{R}^n$ is the state, $w_{BP}(t) \in \mathbb{R}^m$ is the noise which is assumed to belong[9] to $L^2(0,\infty]$, and $y_{BP}(t)$ is the output signal, *i.e.* the variation of the driving signal with respect to the nominal periodic regime; $A_{BP}(\cdot)$ and $C_{BP}(\cdot)$ are real piecewise continuous bounded matrix functions of period T_P that describe the nominal system, *i.e.* the right hand side and output function Jacobians along the nominal periodic trajectory; finally, $B_{BP\,w}(\cdot)$ and $D_{BP\,w}(\cdot)$ are real piecewise continuous bounded matrix functions of period T_P which describe the unstructured uncertainties about the model.

As described in the next section, the exact knowledge of the matrix functions describing the generation of the bad patterns, *i.e.* $A_{BP}(\cdot)$, $C_{BP}(\cdot)$, $B_{BP\,w}(\cdot)$ and $D_{BP\,w}(\cdot)$, is necessary to impose the anti-robust filtering condition corresponding to the anti-resonance requirement. It will be shown later how to determine such information on the base of the constructed chaotic model (*cfr.* Chap. 5) and the bad pattern observations.

The H_∞ Filtering with Unstructured Perturbations

Fortunately enough, the solution for the problem of anti-robust H_∞ filtering in the presence of unstructured uncertainties results simpler than the solution, given above, for the problem of robust H_∞ filtering in presence of structured uncertainties.

[9] The noise is assumed simply to be energy bounded and not necessarily Gaussian.

Given the generating system (6.15), a prescribed level of noise amplification $\beta > 0$, and a Luemberger observer [Xie and de Souza, 1993] of the form

$$\begin{aligned} \dot{\widehat{x}}(t) &= A_{BP}(t)\widehat{x}(t) + K_{BP}(t)\big[y_{GP}(t) - \widehat{y}(t)\big] \\ \widehat{y}(t) &= C_{BP}(t)\widehat{x}(t) \end{aligned} \tag{6.16}$$

where $K_{BP}(\cdot)$ is a real piecewise continuous bounded matrix function of period T_P. The periodic filter gain $K_{BP}(\cdot)$ guarantees the stable[10] [Wang and Speyer, 1990; Xie and de Souza, 1993] anti-robustness performance

$$\big\|\widehat{x}(t) - x_{BP}(t)\big\|_2 > \beta\big\|w_{BP}(t)\big\|_2 \tag{6.17}$$

if [Xie and de Souza, 1993] it can be decomposed into the following form

$$K_{BP}(t) = \big[Q(t)C_{BP}^T(t) + B_{BPw}(t)D_{BPw}^T(t)\big]\big(D_{BPw}(t)D_{BPw}^T(t)\big)^{-1} \tag{6.18}$$

where $Q(\cdot)$ is a stabilizing periodic symmetric semidefinite positive matrix function which satisfies the following matrix inequality

$$Q(t)\widetilde{M}^T(t) + \widetilde{M}(t)Q(t) + Q(t)\widetilde{N}(t)Q(t) + \widetilde{W}(t) \geq 0 \quad \forall t \tag{6.19}$$

where the matrices $\widetilde{M}(\cdot)$, $\widetilde{N}(\cdot)$, and $\widetilde{W}(\cdot)$ are given by

$$\begin{aligned} \widetilde{M}(\cdot) &= \big[A_{BP}(\cdot) - B_{BPw}(\cdot)D_{BPw}^T(\cdot)\big(D_{BPw}(\cdot)D_{BPw}^T(\cdot)\big)^{-1}C_{BP}(\cdot)\big] \\ \widetilde{N}(\cdot) &= \big[\beta^{-2}I - C_{BP}^T(\cdot)\big(D_{BPw}(\cdot)D_{BPw}^T(\cdot)\big)^{-1}C_{BP}(\cdot)\big] \\ \widetilde{W}(\cdot) &= B_{BPw}(\cdot)\big[I - D_{BPw}^T(\cdot)\big(D_{BPw}(\cdot)D_{BPw}^T(\cdot)\big)^{-1}D_{BPw}(\cdot)\big]B_{BPw}^T(\cdot) \end{aligned} \tag{6.20}$$

Using the periodic Schur's complement Lemma [Boyd *et al.*, 1994], the nonlinear inequality (6.19) can be reduced to a periodic linear matrix inequality, namely

$$\begin{bmatrix} \big[Q(t)\widetilde{M}^T(t) + \widetilde{M}(t)Q(t) + \widetilde{W}(t)\big] & Q(t) \\ Q(t) & \widetilde{N}(t) \end{bmatrix} \geq 0 \quad \forall t \tag{6.21}$$

Since in Eqs. (6.18) and (6.20) the inverse of $\big(D_{BPw}(t)D_{BPw}^T(t)\big)$ is computed, it follows that the condition for the filtering problem to be well posed is that there does not exist a clean (without noise) linear combination of the output vector $y(t)$ [Kwakernaak and Sivan, 1972; Locatelli, 1993]. Similarly to the case before, since here a scalar output case is considered this condition results rather trivial. Furthermore, it should be noted that in the case in which the measurement noise and modeling noise are independent, *i.e.* $B_{BPw}(t)D_{BPw}^T(t) \equiv 0$, the Eqs. (6.20), and consequently Eq. (6.21), simplifies notably.

The idea proposed by this algorithm is to consider a candidate qualitatively resonating filter gain satisfying the resonance requirement, as given above in Sect. 6.1.1, compatible with the anti-resonance requirement when it satisfies the conditions given by Eqs. (6.18) and (6.21).

Unfortunately, this does not represent a conservative approach, but rather an optimistic one. In fact, as explained above, the local dynamics matrices of the qualitatively resonating filter have tendency to synchronize with that of the driving system. Therefore, the real situation is not so dramatic as thought by the filter given in Eqs. (6.16). Hence, the anti-resonance condition given remains rather optimistic.

This condition has been considered mainly for two reasons. First, the author did not find an alternative one which is not excessively complex and/or unpractical. Second, as shown in the next section, the pessimistic way of computing the data needed for testing the condition Eqs. (6.18) and (6.21), *i.e.* $A_{BP}(\cdot)$, $C_{BP}(\cdot)$, $B_{BPw}(\cdot)$ and $D_{BPw}(\cdot)$, compensate somehow the optimism of the considered condition, or at least it is hoped so.

[10] Unstable anti-robustness is a trivial problem.

Computing the Necessary Data

In order to test a filter gain candidate against the anti-resonance requirement, given by Eqs. (6.18) and (6.21), the matrices which describe the dynamical model generating the bad patterns, *i.e.* $A_{BP}(\cdot)$, $C_{BP}(\cdot)$, $B_{BP\,w}(\cdot)$ and $D_{BP\,w}(\cdot)$, as well as the hypothesized L^2-norm of the base noise $w_{BP}(\cdot)$, must be known.

Clearly, these information items must be extracted from available data as the bad pattern observations and, eventually, the chaotic model obtained in the modeling step. In this regard, it could sound absurd to use the reference chaotic model of the good patterns generation to determine the model generating the bad patterns. There are mainly two reasons justifying such approach. The first one, quite practical, is that there is no other information available[11]. The second reason is that such an approach results quite pessimistic and, therefore, can, hopefully, compensate somehow the optimism, as explained above, of the considered constraint. Namely, bad patterns which are very different, dynamically speaking, from the good patterns do not give any problem in satisfying the anti-resonance requirement, it follows almost automatically. The worst cases to consider are those patterns which, dynamically speaking, are rather similar to the good patterns but belong anyway to the class of bad patterns. Thus, testing the anti-resonance requirement compliancy with respect to the bad patterns by extracting from them those dynamical features corresponding to the good patterns results, in some sense, in a worst case approach. In particular, the dynamical features used to distinguish the two cases are the linear dynamic differences. In fact, while the nonlinear system, namely the reference chaotic system, is assumed to be equal for the two cases, bad and good patterns, this is not the case for the corresponding linear system determining the filtering framework; in general, the matrices with BP index will be different from their GP counterpart. Hence, this practically means that resonance and anti-resonance are tuned on the linear (periodic) dynamical differences of the two considered classes of patterns.

Under these assumptions, and keeping in account the Lur'e structure of the nonlinear chaotic reference model, *i.e.* Eq. (6.10), it remains rather simple to determine the required information.

The nominal dynamical matrices, *i.e.* $A_{BP}(\cdot)$ and $C_{BP}(\cdot)$, can be easily assumed to be the right hand side and output function Jacobians of the system along the nominal periodic orbit, namely

$$\begin{aligned} A_{BP}(t) &= A + bc^T \frac{\partial f(y)}{\partial y}\bigg|_{y=y_n(t)} \\ C_{BP}(t) &= c^T \end{aligned} \tag{6.22}$$

where $y_n(t)$ is the nominal periodic observation of bad patterns; for instance, it can be chosen to be simply the average of the bad observations. Once again, since the Lur'e structure of the considered model, no computations are needed to obtain $C_{GP}(t)$; it is simply the output matrix of the controller canonical form. Moreover, note that, once again, a reference phase for the $y_n(t)$ signal must be chosen such as to uniquely determine the matrix function $A_{BP}(\cdot)$. Furthermore, this same reference phase must be coherently used for the computation of the other two matrix functions $B_{BP\,w}(\cdot)$ and $D_{BP\,w}(\cdot)$.

Assuming a more than unitary base noise, namely $\left\|w_{BP}(t)\right\|_2 \geq 1$, it is rather simple to determine two matrices modeling the effects of the unstructured uncertainties in a very similar way as above have been determined the structured uncertainties. Note that the noise intensity must be assumed greater than a given quantity to let the anti-resonance condition be conservative.

For the good patterns, the diversity of the considered patterns has been modeled by means of structured uncertainty, *cfr.* Sect. 6.1.1. On the contrary, the diversity of bad patterns, coherently with the remark above, is modeled by means of unstructured uncertainty. This difference is simply conceptual since, as it will be immediately shown, the computation techniques for the matrices describing the two kind uncertainties are very similar. Actually, the real difference is in the use of the information in the filter gain tuning, as can be noticed comparing the robust filters given by Eqs. (6.5) and (6.16).

Before proceeding, it should be noted that the way for splitting the diversity of the bad pattern signals among the two possible causes is not uniquely determined; namely, it is not uniquely determined in which extent the diversity must be ascribed to the modeling noise and to which extent to the measuring noise [Grewal and Andrews, 1993]. In the case of good patterns, where the diversity was attributed to structural uncertainties, the diversity as been ascribed completely to the modeling noise annihilating the measuring

[11] In the cases in which the qualitatively resonating filters are used for n-ary classification, as those considered in Chap. 7, this is not the case and a more accurate model for the bad patterns is available; hence, more complex methods for extracting the needed information from the available one can be considered instead of the one proposed here.

noise. In this case this choice cannot be taken as such since, for the anti-robust filtering problem to be well posed (*cfr.* previous section), the measuring noise must be nonzero. A simple assumption satisfying this condition and simplifying notably all the computations [Grewal and Andrews, 1993] is to assume the measuring noise given by the accuracy of the measurement instrument used for performing the observations and to attribute all the diversity of the bad patterns to the modeling noise. Hence, the measuring noise matrix, actually is a scalar since the SISO system, $B_{BP\,w}(\cdot)$ is given by

$$D_{BP\,w}(t) = \mathcal{A}_m \tag{6.23}$$

where $\mathcal{A}_m$ is the nominal accuracy, *i.e.* the nominal standard deviation, of the measurement instrument used to perform the bad patterns observations. As already mentioned several time, the fact that the matrix is a constant one does not represent a problem.

The computation of the remaining matrix $B_{BP\,w}(\cdot)$ passes by the computation of the set of the uncertainty matrices $\Delta A_{BP}(\cdot)$ admissible according to the measurements. More in particular, for any given observation $y_i(t)$ the corresponding Jacobian is computed, then subtracting from it the nominal Jacobian, *i.e.* $A_{BP}(\cdot)$, the corresponding uncertainty is obtained, namely

$$\Delta A_{BP\,i}(t) = A + bc^T \left.\frac{\partial f(y)}{\partial y}\right|_{y=y_i(t)} - A_{BP}(t) = bc^T \left(\left.\frac{\partial f(y)}{\partial y}\right|_{y=y_i(t)} - \left.\frac{\partial f(y)}{\partial y}\right|_{y=y_n(t)} \right)$$

For a correct computation of the matrices $\Delta A_{BP\,i}(t)$ the reference phase for the $y_i(t)$ signals must be chosen coherent with the one chosen above for $y_n(t)$. The matrix $B_{BP\,w}(\cdot)$ is then obtained by a multi-kernel factorization of the $\Delta A_{BP\,i}(t)$ matrices, namely

$$\begin{bmatrix} \Delta A_{BP\,1}(t) \\ \Delta A_{BP\,2}(t) \\ \vdots \\ \Delta A_{BP\,r}(t) \end{bmatrix} = B_{BP\,w}(t) \begin{bmatrix} w_1 \\ w_2 \\ \vdots \\ w_r \end{bmatrix} \tag{6.24}$$

where each w_i must satisfies

$$w_i^T w_i \geq I$$

Assuming, arbitrarily, the dimension of the matrices $B_{BP\,w}(t)$ and w_i to be

$$\dim\big(B_{BP\,w}(\cdot)\big) = n \times n$$

$$\dim\big(w_i\big) = 1 \times 1$$

where n is the dimension of the reference system, *i.e.* $\dim\big(A\big) = n \times n$, it is easy to perform the mentioned factorization in MATLAB, discretizing, in time, the $\Delta A_{BP\,i}(t)$ matrices and recursively applying the generalized singular value decomposition on the result. Finally, note that choosing the reference phase of $y_i(t)$ coherent with that of $y_n(t)$, as suggested above, guarantees the phase coherency between the matrices $B_{BP\,w}(t)$ and $A_{BP}(t)$.

It should be noted that any alternative method for extracting these information items from the available data, other than the one proposed here, could be considered instead without changing the general idea for the testing of a filter gain candidate against the anti-resonance condition; for instance, methods based on extended Kalman filtering [Grewal and Andrews, 1993; Petersen and Savkin, 1999] or on state covariance bounds formulae [Bolzern *et al.*, 1994] could be considered. For what is concerned here, only the proposed method has been tested.

The Filtering Problem

Giving the prescribed level of noise amplification β such as to guarantee the qualitative anti-resonance, the data computed at the previous section allow to test any filter gain candidate, provided by the first step described in Sect. 6.1.1, against the compliancy to the anti-resonance requirement using the Eqs. (6.18) and (6.21).

Since the unstructured noise $w_{BP}(\cdot)$ has been imposed to be stronger than unitary, *i.e.* $\big\|w_{BP}(t)\big\|_2 > 1$, from the anti-robust H_∞ performance (6.17) it follows that, in order to guarantee the qualitative anti-resonance with bad patterns, the noise amplification must be such that

$$\beta > \max_{\theta}(\rho(\theta)) \tag{6.25}$$

where $\rho(\theta)$ (*cfr.* Sect. 3.3.3) is the minimal distance between the point on the generating cycle at phase θ and the homoclinic trajectory.

The condition given by Eq. (6.25) require that the minimal wondering due to the model imprecision, *i.e.* β, is enough to reach the homoclinic trajectory. Hence, even if the qualitatively resonating filter is initially almost in phase (*cfr.* Sect. 3.3.3) with a driving signal belonging to the class of bed patterns, then the noise amplification will lead to approach the homoclinic trajectory, exciting in this way the chaotic mode of the filter; namely, leading to qualitative anti-resonance.

Finally, since $D_{BP\,w}(t)$ is given by the real measuring noise on the observation while $B_{BP\,w}(t)$ is the noise modeling the diversity of the bad patterns, it follows that there is no reasonable reason why these two noises should be correlated. Hence, it can be easily assumed that[12] $D_{BP\,w}(t)B^T_{BP\,w}(t) \equiv 0$. Therefore, the Riccati-like inequality (6.19), as well as the linear matrix inequality (6.21), simplifies notably. Namely, the matrices $\widetilde{M}(\cdot)$, $\widetilde{N}(\cdot)$, and $\widetilde{W}(\cdot)$ given by Eqs. (6.20) reduce to

$$\begin{aligned} \widetilde{M}(\cdot) &= A_{BP}(\cdot) \\ \widetilde{N}(\cdot) &= \left[\beta^{-2} I - C^T_{BP}(t) R^{-1} C_{BP}(t)\right] \\ \widetilde{W}(\cdot) &= B_{BP\,w}(\cdot) R^{-1} B^T_{BP\,w}(\cdot) \end{aligned} \tag{6.26}$$

where the measurement noise covariance matrix R is simply the scalar $\mathcal{A}^2_m$ which, as given in the previous section, is the nominal accuracy, *i.e.* the nominal standard deviation, of the measurement instrument used to perform the bad patterns observations. Analogously, the filter gain decomposition given in Eq. (6.18) reduces to

$$K_{BP}(t) = Q(t) C^T_{BP}(t) R^{-1} \tag{6.27}$$

6.1.3 Computing the Set of Potential Solutions

The third step consists in computing the family of filter gain candidates as given at the first step, *i.e.* satisfying the resonance requirement (*cfr.* Sect. 6.1.1), selecting among them only those solutions which satisfy the compliancy to the anti-resonance requirement as given at the second step, *i.e.* satisfying the anti-resonance requirement (*cfr.* Sect. 6.1.2). Namely, the aim of this step is to obtain the set of filter gains compatible with both the resonance and anti-resonance requirements.

The accomplishment of this duty is rather simple and is, as matter of fact, simply a problem of numerical exhaustive computation. Namely, this step is performed by the following algorithm

[12] Since in the considered case $D_{BP\,w}(t)$ is a scalar the condition $D_{BP\,w}(t)B^T_{BP\,w}(t) \equiv 0$ does not make any sense mathematically, it is simply used to mean that the measuring noise and modeling noise are assumed to be uncorrelated.

BEGIN

select a positive range for ε, $I = [\ \varepsilon_{min}, \varepsilon_{max}\ ]$

for every $\varepsilon \in I$,

compute a solution $S(t)$ for the periodic Riccati Eq. (6.8);

compute a solution $P(t)$ for the periodic Riccati Eq. (6.9);

compute a filter gain candidate $K_\varepsilon(t)$ according to Eq. (6.6);

decompose $K_\varepsilon(t)$ according to Eq. (6.27) obtaining a
stabilizing symmetric periodic semidefinite positive matrix $Q(t)$;

test the matrix $Q(t)$ against the inequality (6.21);

if the test fail,
dump the candidate;
else,
add the candidate to the set of potential filter gain $\mathcal{K}$;
end;

end;

END

The only specific problem to this step is how to solve numerically, the Eqs. (6.8), (6.9), and (6.18); and how to test the matrix inequality (6.21).

Actually, the periodic Riccati differential equations Eqs. (6.8) and (6.9) can be solved by the algorithm given in [Hench and Laub, 1994; Morera *et al.*, 1995; Yao and Chen, 2000]. The filter gain decomposition Eq. (6.18), necessary to determine $Q(t)$, is trivial since Eq. (6.18) is reduced to Eq. (6.27). Finally, the linear matrix inequality test can be performed iteratively, with respect to the time discretization, using the inequality test available in the LMI toolbox of MATLAB [Matlab, 2000].

6.1.4 Selection of the Solution

This step is rather trivial, it consists simply in selecting the smallest, with respect to a given norm, filter gain from those belonging to the set $\mathcal{K}$ of potential filter gains computed at the previous step. In fact, as discussed in Chap. 3, the filter gain should be small enough in order not to alter excessively the free dynamics of the driven system.

For instance, the norm considered could be the ∞-norm [Meyer, 2000], choosing in this way the filter gain minimizing the maximal influence on the free dynamics of the filter.

Even though other norms can be considered only the ∞-norm has been used.

6.1.5 Problems

As mentioned elsewhere (*cfr.* Sect. 4.4.2) there are two main problems which can incur in the proposed algorithm.

The first is the indistinguishability between the good and bad pattern signals. It could happen that the constraints, *i.e.* the measurements and the reference chaotic model, defining the robust and anti-robust filtering problems are too tight leading the set $\mathcal{K}$ to be empty. Namely, there does not exist a filter gain that complies with both the resonance and anti-resonance requirements; in this sense, the filter gain tuning fails. There are two possible reasons for this to happen. One is a structural reason; namely, the two classes of good and bad patterns considered cannot be distinguished by any qualitatively resonating filter[13]. In the case of structural indistinguishability with respect to the qualitatively resonating filters, there is no other solution than changing method. A second, less dramatic, reason for the algorithm to fail is a bad choice of

[13]It is not difficult to imagine an example of such a case. Consider, for instance, the classification of Feigenbaum-like and Shil'nikov-like signals issued by the same system, in this case it is clear that for tautology, the box and its content coincide, the system would fail. An example of application which requires such a kind of classification is given in [Maggio and De Feo, 2000].

the data and/or of the constraints considered. In this case the constraints can be relaxed such as to see if a solution can be determined. For instance, some of the observations, especially bad patterns, can be dumped and disregarded in the tuning; this is equivalent to consider less strong unstructured uncertainty in the anti-resonance test. Alternatively, a reference chaotic model for the bad patterns can be determined as well such as to relax the anti-resonance requirement. This alternative model for the bad patterns comes for free when qualitatively resonating filters are considered for binary, or n-ary, classification purposes, *cfr.* Chap. 7. Continuing to fail in determining a compatible filter gain despite of the relaxation of the constraints can be a symptom of structural indistinguishability.

The second problem that can occur is an excessively large filter gain. As discussed in Chap. 3, the filter gain should be small enough in order not to alter excessively the free dynamics of the driven system. The solution provided by the above described algorithm could be not satisfactory in this sense. Once again, there are two main reasons for this to happens. The first reason is an excessive instability of the identified Shil'nikov-like strange attractor (*cfr.* Chap. 5); namely, a strong control action, thus a large filter gain, is required to stabilize the unstable Feigenbaum-like strange attractor embedded into the Shil'nikov-like one. In such a case, the construction of the qualitatively resonating filter should be reconsidered starting again from the modeling step. The second reason is very similar to the indistinguishability problem. Namely, the two classes of patterns considered are too similar dynamically speaking; therefore, a strong control action, thus a large filter gain, is required to separate the good from the bad patterns. In such a case, the same remedies as suggested for the indistinguishability can be taken; namely, the relaxation of the constraints. Once again, continuing to obtain too strong filter gain despite of the relaxation of the constraints can be symptom of a badly conditioned problem; namely, the two classes considered are close to the structural indistinguishability.

6.1.6 Remarks

Despite of its apparent complexity, the algorithm for the tuning of the filter gain proposed here is rather simple. Indeed, it exploits theoretical results which are common in control theory; namely, the robust control in the Hardy spaces and the Hardy sensitivity measure of dynamical systems [Burl, 1999; Colaneri and Geromel, 1997; Eslami, 1994], *i.e.* the control theory in H_2 and H_∞. In particular, the methods proposed here to impose the resonance (*cfr.* Sect. 6.1.1) and anti-resonance (*cfr.* Sect. 6.1.2) requirements rely on robust H_∞ filtering. Alternative algorithms very similar to the one proposed can be obtained by considering the robust filtering in any other of the Hardy spaces H_X [Colaneri and Geromel, 1997].

It should be noted that the filter gain obtained by means of the proposed algorithm is periodic, thus time varying, but it does not depend upon the input data; namely, it does not depend on the driving signal. Therefore, it can be precomputed once for all and stored into the qualitatively resonating filter. On the other hand, since the filter gain is periodic there remains the need for synchronizing its phase with that of the input signal. Indeed, the obtained filter gain has been obtained under such condition. As explained in Sect. 4.3.1, the phase locking can be achieved by means of a phase detector.

It should be noted that, albeit here the base period has been assumed to be the nominal pseudo-period as determined by the generating cycle, nothing forbids to consider a periodic filter gain tuned on a base period which is a multiple of the nominal pseudo-period. Obviously, in such a case the phase detector needed to lock its phase on the input signal would result more complex.

6.2 The Degrees of Freedom Summary

Albeit only one of the possible combinations has been considered herein, the general idea, as presented in Sect. 6.1, implies three main degrees of freedom. Namely, the robust filtering technique considered to impose the resonance constraint; the anti-robust filtering technique considered to impose the anti-resonance constraints; and, finally, the norm used to select one among the filter gain candidates.

More specifically, restricting to the method proposed here for the tuning of the filter gain, *i.e.* working in H_∞, it consists of about eleven degrees of freedom mainly concentrated in the first two steps. Namely, these are the techniques considered for extracting the generating model information items, *i.e.* $A_{GP}(\cdot)$, $C_{GP}(\cdot)$, $H_{GP\,1}(\cdot)$, $H_{GP\,2}(\cdot)$, $E_{GP}(\cdot)$, $B_{GP\,w}(\cdot)$, $D_{GP\,w}(\cdot)$, $A_{BP}(\cdot)$, $C_{BP}(\cdot)$, $B_{BP\,w}(\cdot)$, and $D_{BP\,w}(\cdot)$, from the available data, *i.e.* the two set of observations[14].

[14]Note that the reference chaotic model for the good patterns has been obtained from the good patterns observations; thus, the two set of observations can be considered as the real basic available data.

As it was the case for the chosen continuation algorithm in the previous chapter, further degrees of freedoms are associated to each one of the numerical algorithms considered for solving the specific subproblems (*cfr.* Sect. 6.1.3); namely, the integration of the periodic Riccati equations, the filter gain factorization, and the definite positive test.

As already mentioned above, only one combination of these degree of freedom has been considered herein; namely, the one described in this chapter.

6.3 Tests

The two tests considered here serve to illustrate the robustness of the proposed technique for the automatic tuning of the filter gain. In Chapter 7, more realistic and interesting tests will be considered.

The two tests considered here consist in tuning two filter gains such as to oblige the Shil'nikov-like models obtained in the previous chapter (*cfr.* Sect. 5.4) to qualitatively resonate with fine piecewise linear approximations of the pattern corresponding to the generating cycle (*cfr.* Sect. 3.1.3) and to anti-resonate with too coarse approximations of it.

Note that this does not represent a correct application of this algorithm. Indeed, the class of good patterns, *i.e.* the fine piecewise linear approximations of the pattern corresponding to the generating cycle of the Shil'nikov-like strange attractor, are not the good patterns that have been used to construct the chaotic reference model. In some sense, the meaning of these tests is a robustness assessment; namely, if it works in this case it will certainly work in the cases satisfying the hypothesis under which it has been developed.

6.3.1 Test Framework

In both the tests the same framework has been considered, very similar to the one considered in Sect. 3.1.3 for the preliminary experiments of qualitative resonance.

As good patterns fine piecewise linear approximations of the pattern corresponding to the generating cycle of the Shil'nikov-like strange attractor have been considered; namely, piecewise linear approximations of the linear system output when the complete system, *i.e.* the closed loop Lur'e one, evolves on the generating cycle. In particular, twenty observations of thirty-two pseudo-periods each have been considered. Each observation is approximated with a different degree of approximation[15] l (*cfr.* Sect. 3.1.3) linearly scaling from a minimum of $L/70$ to a maximum of $L/30$ where L is the length of the original pattern, *cfr.* Sect. 3.1.3.

Similarly, as bad patterns coarse piecewise linear approximations of the same reference pattern have been considered; namely, the one corresponding to the generating cycle of the Shil'nikov-like strange attractor. Once again, twenty observations of thirty-two pseudo-periods each have been considered. Each observation is approximated with a different degree of approximation l which is linearly scaling from a minimum of $L/25$ to a maximum of $L/10$. Hence, the interval of approximations between $L/30$ and $L/25$ is left as cache where to place the qualitative resonance threshold.

Since in this case there is no measurement noise associated with the observations, the accuracy of the measurement system, which is necessary for the tuning (*cfr.* Sect. 6.1.2) has been, arbitrarily, fixed at $\mathcal{A} = 0.1$, namely the $SNR = 20dB$.

Finally, the phase of the filter gain is locked on the one of the input signal by means of a peak-to-peak phase predicting feedforward control. The receding horizon used for this control is of $10T_P$ where T_P is the nominal pseudo-period.

The results of the tuning for the two considered cases are shown in the next two sections.

6.3.2 Colpitts Oscillator

The first tests have been run considering the Shil'nikov-like chaotic system modeling the 2-pulse signals, generated by the Colpitts oscillator mathematical model, as identified in the previous chapter, *cfr.* Sect. 5.4.2.

The result provided by the filter gain tuning algorithm is shown in Fig. 6.1 where the Feigenbaum-like scenario of the driven system, *i.e.* the qualitatively resonating filter, with respect the degree of approximation of the driving signal is reported.

As it can be seen the qualitative resonance threshold have been correctly placed between the two considered limits; namely, the boundary crisis (*cfr.* Sect. 3.3.2) occurs for approximation degrees l between $L/30$

[15] The piecewise linear approximation can be more or less fine depending on the length l of each linear segment, Sect. 3.1.3.

and $L/25$. Furthermore, it can be remarked how sharp is the transition from resonance to anti-resonance; actually, it is sharper than what usually observed using static filter gain confirming the goodness of periodic filter gains.

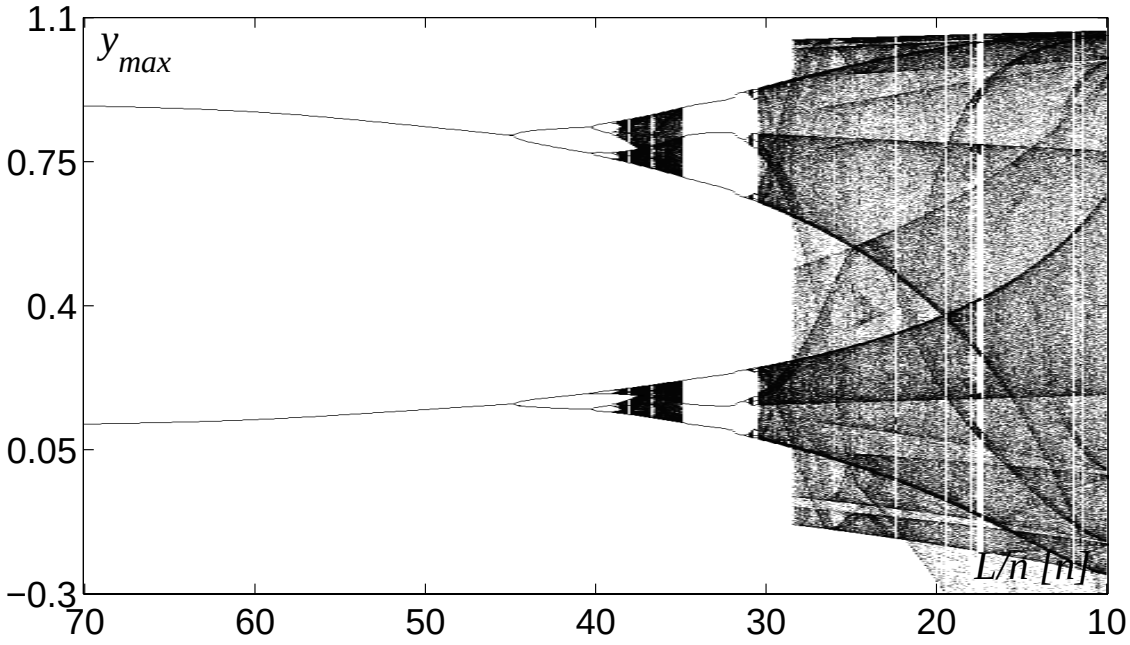

Figure 6.1: *Feigenbaum-like scenario of the output's* (y) *peaks of the driven system,* i.e. *the qualitatively resonating filter, with respect the degree of approximation of the driving signal.*

6.3.3 Rosenzweig—MacArthur Food Chain

The second test has been run considering the Shil'nikov-like chaotic system modeling the 3-pulse signals, generated by the Rosenzweig-MacArthur food chain model, as identified in the previous chapter, *cfr.* Sect. 5.4.3.

The result provided by the filter gain tuning algorithm is shown in Fig. 6.2 where the Feigenbaum-like scenario of the driven system, *i.e.* the qualitatively resonating filter, with respect the degree of approximation of the driving signal is reported.

Once again, the qualitative resonance threshold have been correctly placed between the two considered limits; namely, the boundary crisis (*cfr.* Sect. 3.3.2) occurs for approximation degrees l between $L/30$ and $L/25$. Again, the transition from resonance to anti-resonance is rather sharp.

6.3.4 Remarks

The considered algorithm for the automatic filter gain tuning proves to be rather conservative. In fact, it has been able to correctly place the resonance threshold in the two "fake" tests considered above which do not satisfy at all the hypothesis under which the algorithm has been developed.

Moreover, as can be deduced observing Figs. 6.1 and 6.2, the periodic filter gains obtained appear to be impressively effective. In fact, the state of the qualitatively resonating filter results to be shrunk on a very thin (strange) attractor for all the parameter values corresponding to qualitative resonance conditions, *i.e.* $l \in [L/70, L/30]$, while it results rather spread for all the parameter values corresponding to qualitative anti-resonance conditions, *i.e.* $l \in [L/25, L/10]$. Furthermore, a very sharp transition separates the two cases.

6.4 Final Remarks

Specific remarks to the subproblems composing the overall algorithm have been reported in the corresponding sections (*cfr.* Sects. 6.1.1, 6.1.2, 6.1.3, 6.1.4 and 6.1.6), as general remark it should simply be said that,

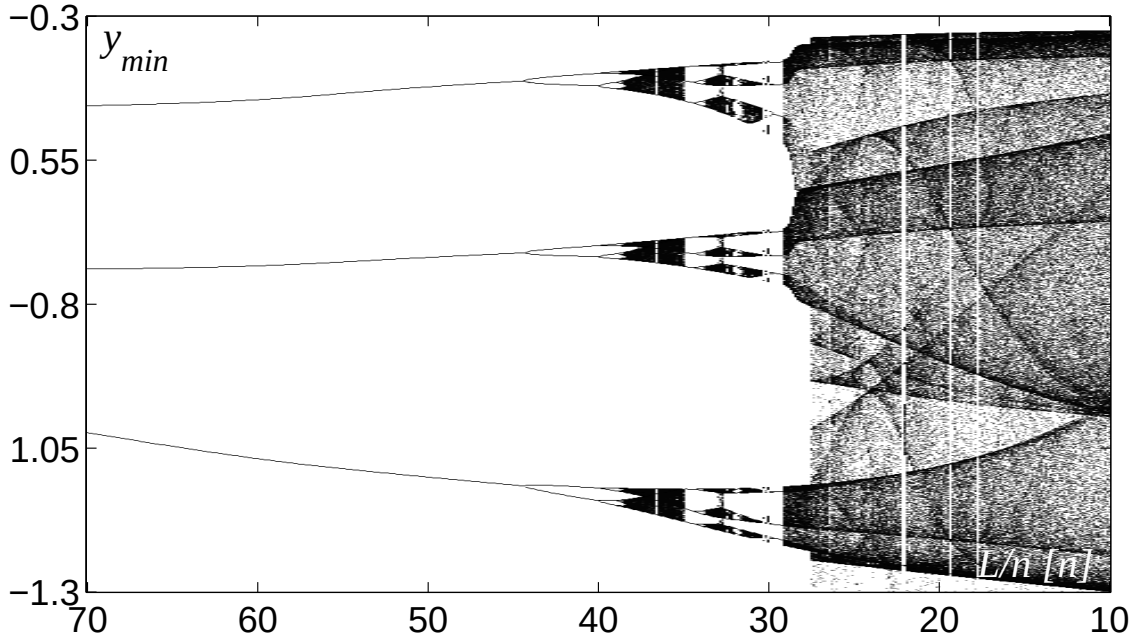

Figure 6.2: *Feigenbaum-like scenario of the output's* (y) *valleys of the driven system,* i.e. *the qualitatively resonating filter, with respect the degree of approximation of the driving signal.*

taken into account everything, the algorithm is rather simple and it relies on standard techniques which are well-known in control engineering. Furthermore, it has enough degrees of freedom (*cfr.* Sect. 6.2) which would allow to fit it to several of the possible real applications. Finally, it has revealed indeed effective on real data as reported later in Chap. 7.

Bibliography

Barmish, B. (1985). Necessary and sufficient conditions for quadratic stability of uncertain systems. *Journal of Optimization Theory and Application*, 46, pp. 399–408.

Bittanti, S. (2000). *Identificazione dei Modelli e Controllo Adattativo*. Pitagora, Bologna, 2000.

Bittanti, S., P. Colaneri, and G. Guardabassi (1984). Periodic solutions of periodic Riccati equations. *IEEE Transactions on Automatic Control*, 29, pp. 665–667.

Bolzern, P., P. Colaneri, and G. De Nicolao (1994). On the computations of upper covariance bounds for perturbed linear systems. *IEEE Transactions on Automatic Control*, 39, pp. 623–626.

Boyd, S., L. El Ghaoui, E. Feron, and V. Balakrishnan (1994). *Linear Matrix Inequalities in System and Control Theory*. SIAM Press, Philadelphia, PA.

Bryson, A. (1996). Optimal control-1950 to 1985. *IEEE Control Systems Magazine*, 16, pp. 26–33.

Burl, J. (1999). *Linear Optimal Control: H_2 and H_∞ Methods*. Addison-Wesley, Menlo Park, CA.

Chen, Y., J. Liu, and S. Chen (1998). Comparison and uniqueness theorems for periodic Riccati differential equations. *International Journal of Control*, 69, pp. 467–473.

Colaneri, P. and A. L. J. Geromel (1997). *Control Theory and Design. A $RH_2 - RH_\infty$ Viewpoint*. Academic Press, London, UK.

Eslami, M. (1994). *Theory of Sensitivity in Dynamic Systems*. Springer-Verlag, Berlin, Germany.

Grewal, M. and A. Andrews (1993). *Kalman Filtering Theory and Practice*. Prentice-Hall, Englewood Cliffs, NJ.

Hench, J. and A. Laub (1994). Numerical solution of the discrete-time periodic Riccati equation. *IEEE Transactions on Automatic Control*, 39, pp. 1197–1210.

Kwakernaak, H. and R. Sivan (1972). *Linear Optimal Control Systems*. John Wiley & Sons, New York, NY.

Levine, W., editor (1996). *The Control Handbook*. CRC Press for IEEE Press, Boca Raton, FL.

Ljung, L. (1999). *System Identification: Theory for the User*. Prentice-Hall, Upper Saddle River, NJ, second edition.

Locatelli, A. (1993). *Elementi di Controllo Ottimo*. UTET, Torino, Italy. In Italian.

Maggio, G. and O. De Feo (2000). T-CSK: A robust approach to chaos-based communications. In *IEEE Workshop on Nonlinear Dynamics of Electronic Systems NDES*. Catania, Italy.

Matlab (2000). *Control System Toolbox For Use with MATLAB*. The MathWorks, Natick, MA. For the Toolbox version 1.0 *MatlabR*12.

Meyer, C. (2000). *Matrix Analysis and Applied Linear Algebra*. SIAM Press, Philadelphia, PA.

Mitter, S. (1996). Filtering and stochastic control: A historical perspective. *IEEE Control Systems Magazine*, pp. 67–76.

Morera, J., G. Rubio, and L. Jódar (1995). Accurate numerical integration of stiff differential Riccati equations. *Applied Mathematics and Computation*, 72, pp. 183–203.

Petersen, I. and A. Savkin (1999). *Robust Kalman Filtering for Signals and Systems with Large Uncertainties*. Birkhauser, Boston, MA.

Wang, Q. and J. Speyer (1990). Necessary and sufficient conditions for local optimality of a periodic process. *SIAM Journal on Control and Optimization*, 28, pp. 482–497.

Xie, L. and C. de Souza (1991). Robust H_∞ filtering for a class of uncertain periodic systems. *IEE Proceedings on Control Theory and Applications*, 138, pp. 479 –483.

Xie, L. and C. de Souza (1993). H_∞ state estimation for linear periodic systems. *IEEE Transaction on Automatic Control*, 38, pp. 1704–1707.

Yao, G. and S. Chen (2000). The precise integration of the Riccati equation and its application in the optimal shape control. *Computer Methods in Applied Mechanics and Engineering*, 189, pp. 141–148.

CHAPTER 7

APPLICATIONS

Brief — This chapter deals with the effective employability of the methods proposed in the previous two chapters in real applications. Both, the modeling of the diversity of approximately periodic signals by means of strange attractors, as well as the pattern recognition method based on the phenomenon of qualitative resonance, are assessed with respect to those simplifying assumptions adopted at the time in which these methods have been developed. In particular, the modeling technique and the pattern recognition method are shown to be effective when dealing with real field signals.

Personal Contribution — While the experiments presented in this chapter are original their corresponding inspiring applications are well-known pattern recognition problems.

In Chapter 4 it has been argued how it would be possible to exploit the phenomenon of qualitative resonance for pattern recognition purposes; more precisely, it has been explained how to realize an "intelligent" system, *i.e.* the qualitatively resonating filter bank, which can preprocess field signals such to feed, with almost symbolic information, a high-level pattern recognizer, possibly symbolic/statistic-based [Alder, 1994; Schalkoff, 1992; Vapnik, 1995]. Sequentially, in Chaps. 5 and 6, it has been shown that it is indeed possible, at least conceptually, to build and tune automatically a qualitatively resonating filter starting from *field* data. In reality, the previous three chapters are based on a hidden hypothesis that is indeed the main *Thesis* of this work, namely

> The diversity of approximately periodic signals found in nature can be modeled by means of Feigenbaum-like strange attractors. This kind of modeling technique together with the phenomenon of qualitative resonance can be exploited for pattern recognition purposes.

In fact, as suggested by the title of this work, and as largely discussed in the first two chapters, what is proposed here is a chaos-based modeling technique for diversity and a possible application of it. That is why here the qualitatively resonating filter is meant to be both a modeling technique and a pattern recognizer.

The previous two chapters have been mainly devoted to automating the design and tuning of the qualitatively resonating filter for approximately periodic signal, *i.e.* the building of the chaotic model for the diversity of signals, assuming the chaoticity of the signals as true. Indeed, the data used in the previous two chapters to validate the proposed algorithms were synthetic data satisfying the main hypotheses by definition.

The real value and the possible applications of this modeling technique would remain at a speculative level if the above mentioned methods would not be tested on "real" data. In other words, to validate the Thesis it is now necessary to verify that both the modeling technique, *i.e.* the identification algorithm, and its application, *i.e.* the tuning method of the filter gain of the qualitatively resonating filter, work indeed on real signals that can be found in nature. A series of test runs with the aim of validating indeed the real power of the proposed modeling technique when dealing with real data is presented in this chapter.

Since the final aim of the qualitatively resonating filters is pattern recognition[1], *i.e.* an artificial intelligence application, there are several things that would need to be verified and validated. In particular, two distinct classes of items needing validation can be identified.

1. The items, methods and results, mainly related to the proposed modeling technique and to the qualitatively resonating filter itself.

2. The items related to the proposed artificial intelligence application of this modeling technique.

Taking into account that what is discussed here is definitely a pioneering proposal of chaos-based modeling technique of temporal signals, it is of more interest, for what concerns this work, to validate the modeling technique itself before venturing in the validation of its possible applications. It would be quite illogical to build an entire application exploiting the qualitatively resonating filter before having the effectiveness of the principle itself verified in a controlled, almost aseptic, environment. This is why what is discussed herein are not real pattern recognition applications but rather laboratory experiments, indeed suggested by real pattern recognition problems, aimed to verify the effective employability of qualitatively resonating filters as preprocessors for statistical pattern recognizers. In particular, the following are the items and the possible problems intrinsic to the proposed modeling technique that are to be assessed when dealing with real data.

Occurrence of chaos: even if assumed as main hypothesis in this thesis, the fact that real signal are indeed chaotic cannot be taken for granted, this is one of the tough questions of the last ten years [Costa *et al.*, 1999; Duke and Pritchard, 1991; Guzzetti *et al.*, 1996; Kanters *et al.*, 1994; Pijn *et al.*, 1991; Popivanov and Mineva, 1999; Pritchard *et al.*, 1995; Rapp, 1993; Soong and Stuart, 1989]. Thus, it is not certain that the first step of modeling, *i.e.* identification (*cfr.* Chap. 5), will lead to Feigenbaum-like strange attractors when dealing with real data. Namely, it is not sure that the proposed method will really employ chaos to model the diversity of real approximately periodic signals. Furthermore, it is not necessarily true that the second step of modeling, *i.e.* period climbing, will be able, sequentially, to drive the system towards Shil'nikov-like chaos.

Qualitative resonance: the occurrence of qualitative resonance has been extensively, both theoretically and practically, discussed, *cfr.* Chap. 3. The theoretical arguments hold true for Shil'nikov-like chaos in the neighborhood of its generating cycle; the proposed theory does not contemplate other nonlinear phenomena as, for instance, coexisting alternative attractors. Nothing ensures that in the automatically constructed model, *i.e.* the identified one, these undesired nonlinear phenomena would not be the dominating ones. Consequently, the effective occurrence of qualitative resonance in the artificially constructed models is not certain.

Model complexity: for real signals, the hypothesis of an underling generating dynamical system of scalar Lur'e type is not necessarily true, namely sufficient. Thus, the first step of modeling, *i.e.* identification, which is based on this hypothesis (*cfr.* Chap. 5) will not necessarily succeed when dealing with real signals.

Filter gain tuning: obviously, since qualitative resonance does not necessarily occur in the identified models, the tuning of the filter gain, which is at first based on the arguments about the qualitative resonance, will not necessarily work in the case of real signals, *cfr.* Chap. 6. Moreover, it is not necessarily true that each pseudo-period can be effectively modeled by means of the learned generating cycle plus some structural perturbations of it, as indeed assumed for tuning the filter gain by means of robust control theory.

The following are, on the other hand, the items and the possible problems of the proposed application, *i.e.* pattern recognition, which are anyway strictly related to the modeling technique. Thus, it is duty of this thesis to assess their validity when dealing with real data.

Basic classification: the main aim of a pattern recognizer, a classifier, is obviously the recognition/classification of objects. The method proposed herein is based on automatic learning of correct training examples, *i.e.* it learns to classify by examples [Cherkassky and Mulier, 1998; Michalski *et al.*, 1983, 1986]. Such methods are called *supervised learning* algorithms [Michalski *et al.*, 1983]. The minimal requirement for them is that they are able to correctly classify a substantial majority of those instances that has been used for their training, *i.e.* during the learning. For the proposed method, this item is both related to the chaotic model identified and to the occurrence of qualitative resonance; more precisely, the assessment of this item passes by the assessment of the modeling method (*cfr.* Chap. 5) and of the proposed filter gain tuning method (*cfr.* Chap. 6).

[1] At least this is what was in the intentions of the author but any other possible application is welcome.

Weak generalization: a pattern recognizer must be able to classify not only those examples that have been shown at learning time but also other instances belonging to the considered class. Namely, as discussed in Chaps. 4 and 6, for the proposed method this item is directly related to the qualitative resonance and its generalization ability. More in particular, the assessment of this item passes by the assessment of the proposed tuning method of the filter gain.

Indistinguishability: in problems of binary classification, *i.e.* given two classes of signal to distinguish, a choice of too simple models at modeling time, *i.e.* too low order or a too simple nonlinearity of the model used for the identification, could results in two identified dynamical systems which are not sufficiently different to ensure the distinction of the two classes of signals on the basis of qualitative resonance. A similar problem could happen at the tuning of the filter gain. Namely, the requested robustness could result excessive leading one or both the filters to resonate with signals of both classes. This problem is quite particular. On the one hand it can be due to a bad design of the filters, too simple models or excessive robustness of qualitative resonance. On the other hand it can be structural, namely it can be because the two classes of signals are indeed not distinguishable by means of models of the underlining dynamical processes producing them.

Overfitting: when modeling, in particular at the identification step, it could happen that using a too complex model, *i.e.* a too high order or a too complex nonlinearity, the identified system would not results in a compact strange attractor containing the learned signals in the form of embedded unstable periodic orbits but rather in isolated stable and unstable periodic orbits. That would corresponds to the overfitting of an automatic learning algorithm [Cherkassky and Mulier, 1998; Michalski *et al.*, 1983, 1986], namely the system learns by heart each example rather than constructing a compact model of all them.

Finally, the following are those items that are more specific to a real application, they are common items of pattern recognition and artificial intelligence [Cherkassky and Mulier, 1998; Michalski *et al.*, 1983, 1986; Russell and Norvig, 1999], thus are not addressed by the following tests, they are left as future research.

Complex classification: among the aims of pattern recognition and classification theories is, other than the automatic basic classification, the automatic generation of classes and subclasses starting from an unstructured presentation of the instances of the considered objects [Alder, 1994; Cherkassky and Mulier, 1998; Schalkoff, 1992]. That is often the argument of *unsupervised learning* [Russell and Norvig, 1999; Weiss, 1991].

Strong generalization: among the purposes of supervised learning, other than the classification of objects, is the automatic discovery of properties, unknown before, of the objects of a given class [Cherkassky and Mulier, 1998; Schalkoff, 1992].

Wrong learning robustness: when evaluating a new classification method based on supervised learning it is always necessary to assess the robustness of the method with respect to wrong teaching [Cherkassky and Mulier, 1998; Schalkoff, 1992]. Namely, it is necessary to evaluate the effect, on the overall performance, of one or more training examples wrongly presented, *i.e.* presented as belonging to a class while they belong to another one.

7.1 Validation Framework

To keep the comparison of the different tests as simple as possible all the test runs are very similar, they differ simply by the application from which they are inspired and for the real signals treated which are, obviously, different from test to test. Moreover, all those degrees of freedom, *i.e.* order of the system, nonlinearity model, identification method, etc., present in the design of the qualitatively resonating filter, both at modeling and filter gain tuning time, have been chosen equal for all the tests. In particular, they have been chosen to be the combination whose performance has proved to be fairly good and application independent[2]. This choice has been determined by the desire of evaluating the intrinsic power of the proposed modeling techniques rather than that of the particular choices used.

[2]Indeed, as illustrated in the previous chapters, the methods proposed for the automatic construction/tuning of qualitatively resonating filters have a lot of degrees of freedom associated with all the possible choices about the particular techniques used to solve the subproblems of which they are composed, *i.e.* order of the system, nonlinearity model, identification method, etc. Tests similar to those herein described have been run in order to discover which one of the possible combinations of these degrees of freedom is the best one. As is to be expected, the answer is application specific, namely it depends upon the particular signals that are to be modeled. Even though that, as already mentioned in the previous chapters, a particular combination of

The conditions under which the tests have been conducted, namely the validation framework, are reported in the following.

7.1.1 Application Type

Except for one of them, all the tests are inspired by applications of *binary classification*. Namely, they are the classification of temporal approximately periodic signals, similar among them, into two predefined classes, the class $\mathcal{A}$ and the class $\mathcal{B}$. Thus, with respect to what is discussed in Chap. 4, the input signals are used to feed two suitably tuned qualitatively resonating filters, the **A** and **B** filters, which map the input signals into a probability distribution over an alphabet of two symbols.

7.1.2 Data Type

According to the standard nomenclature [Schalkoff, 1992; Vapnik, 1995], each example signal is referred as *signal vector* or simply as *vector*. Since the tests are applications of binary classification, it follows that the vectors necessary for the tuning of the filters and their test are obviously from two classes, namely from the class $\mathcal{A}$ and the class $\mathcal{B}$. They are organized into four sets, more in particular into two sets, which in turn are divided into two subsets each

Set A: Vectors belonging to the class $\mathcal{A}$.

Subset A_{Tr} (training set): Vectors *used* for both the tuning of the qualitatively resonating filters and for the test of their classification ability.

Subset A_{Ts} (test set): Vectors *not used* for the tuning of the qualitatively resonating filters but used for the test of their classification ability.

Set B: Vectors belonging to the class $\mathcal{B}$.

Subset B_{Tr} (training set): Vectors *used* for both the tuning of the qualitatively resonating filters and for the test of their classification ability.

Subset B_{Ts} (test set): Vectors *not used* for the tuning of the qualitatively resonating filters but used for the test of their classification ability.

In other words, the available signal vectors from the two classes are divided into two nonoverlapping sets, those used for learning/training the qualitatively resonating filters and those that are used only at test time. Furthermore, as mentioned above, the vectors are *a priori* correctly classified, namely those vectors that belong to the set A describe indeed signals from the class $\mathcal{A}$ and analogously for B.

The vectors of the two sets exchange their role in the tuning of the two filters. Namely, the vector from set A are the *good patterns* when tuning the **A** filter while they are the *bad patterns* when tuning the **B** filter and vice versa for the vectors from set B.

The signal vectors are long enough in time; in particular, they are sixty-four pseudo-periods long each. The cardinality of the two sets of vectors (A and B) is of hundred vectors in each set. The two subset are exactly half the entire set, namely they have a cardinality of fifty vectors each.

Whenever necessary, the signal vectors are considered periodic. Namely, whenever an example signal longer than sixty-four pseudo-periods is necessary, the vectors are ring closed starting reading them from the beginning when the end is reached.

For sake of clearness, here the symbolism is summarized: $\mathcal{X}$ is the X class; X is the set of vectors belonging to the class $\mathcal{X}$; **X** is the filter tuned to recognize vectors from the class $\mathcal{X}$; X_{Tr} is the set of vectors used to tune and test **X**; and finally X_{Ts} is the set of vectors used to test but not to tune **X**.

Construction of the Vector Sets

The vectors for the two sets are constructed from field observations as follow.

AC coupling: from each observation the mean value is first removed, in jargon it is AC (alternative current) coupled, namely the DC (direct current) component is removed from the signal.

techniques has proved to be in average satisfactory. Namely, even if it is not the absolute best one, this choice has proved to be fairly performing in all the cases and the difference in performance with respect to the best one is marginal. The tests here considered have been run using this *a priori* good combination of techniques.

Low-pass filtering: each observation is split into nonoverlapping vectors of sixty-four pseudo-periods each, *i.e.* of sixty-four complete oscillations each[3]. Then each vector is slightly modified at the boundaries such to become periodic, *i.e.* it becomes a periodic signal vector with very long period[4] $T \approx 64T_P$, where T_P is the nominal pseudo-period. Sequentially, each vector is lowpass filtered to reduce the high frequency noise. The filtering is done in the frequency domain removing all the angular frequencies higher than thirty-two times the pseudo-angular frequency[5]. Namely, the T-periodic signal vector is transformed according to Fourier [Arfken and Weber, 1995; Baher, 1990] computing all the harmonics up to the one that is thirty-two time the pseudo-angular frequency, namely

$$k : k\omega \leq 32\omega_P, \quad \omega = \frac{2\pi}{T}, \omega_P = \frac{2\pi}{T_P}$$

Then, the signal vector is anti-transformed obtaining a T-periodic signal vector with frequencies only up to thirty-two times the pseudo-angular frequency.

According to what is discussed in Sect. 5.1.2, the sampling of the signals must be dense enough such as to warrant the equivalence with a continuous time system; more in particular, the sampling frequency as been chosen such that there are two-hundred observations per pseudo-period.

Normalization: each vector is normalized, after the filtering, both in time and in amplitude. The amplitude is normalized such that the range of the vector is contained between minus one and plus one; in particular, the normalization is done guaranteeing a zero mean of the resulting signal. The time is scaled such that the pseudo-angular frequency ω_P is one, *i.e.* $T = 128\pi$.

The normalization at vector level allows supposing that a single observation is not necessarily stationary. Namely, it is not necessary to suppose that an entire observation is coming from a single Feigenbaum-like strange attractor but only that sixty-four pseudo-periods are observation of the very same strange attractor. Obviously, this introduces the problem of the segmentation of the observations in almost stationary segments [Deller *et al.*, 1993]. In the applications that follow, whenever such a segmentation has been necessary, since the observations were clearly nonstationary, the segmentation has been performed manually.

7.1.3 Filter Type

The filter type considered for the tests is the one shown in Fig. 4.3. In particular, here are the specific features considered, *cfr.* Sect. 4.3.1.

1. *Filter gain*: the filter gain is time varying and periodic. The phase of the filter gain is locked on the phase of the input by means of a peak-to-peak phase predicting feedforward control. The receding horizon used for this control is of $10\overline{T}_P$ where $\overline{T}_P$ is the expected value of the nominal pseudo-period.

2. *Feedback loop*: the control loop is always on.

3. *Natural frequency*: the time scale is adjusted online by means of a feedforward peak-to-peak-based control[6]. The receding horizon used for this control is of $10\overline{T}_P$ where $\overline{T}_P$ is the expected value of the nominal pseudo-period.

4. *Qualitative resonance functional*: the qualitative resonance functional considered consists in a simple *receding horizon mean square error* between the input (driving signal) and the output (resonating signal) of the qualitatively resonating filter. The receding horizon is assumed to be $10\overline{T}_P$. Namely, referring to Eq. (4.1), $f(\cdot) = (\cdot)^2$ while $h(\cdot)$ is not applied. The result is retrieved/sampled after hundred-thirty-eight pseudo-periods, *i.e.* after two length of the vector in test plus a receding horizon.

5. *Probability distribution map*: The results of the qualitative resonance functional from the two filters is mapped into a probability distribution over an alphabet of two symbols by means of the following linear

[3] Remember that pseudo-period is used to address both an entire oscillation and the average of the oscillation periods.
[4] It is a rough approximation of a Feigenbaum-like strange attractor.
[5] In a strange attractor, the subharmonics are definitely more important than the superharmonics.
[6] Since the signal vectors considered have been normalized in frequency separately, it follows that this feature is not really indispensable but it has been implemented anyway in order to verify its stability.

transformation (*cfr.* Eq. (4.3))

$$\begin{aligned} p_{\mathrm{A}} &= \frac{\sigma^2_{f\,\mathbf{B}}\left(\sigma^2_{f\,\mathbf{A}} - \sigma^2_{\mathbf{A}}\right)}{2\sigma^2_{f\,\mathbf{A}}\sigma^2_{f\,\mathbf{B}} - \sigma^2_{\mathbf{A}}\sigma^2_{f\,\mathbf{B}} - \sigma^2_{\mathbf{B}}\sigma^2_{f\,\mathbf{A}}} \\ p_{\mathrm{B}} &= \frac{\sigma^2_{f\,\mathbf{A}}\left(\sigma^2_{f\,\mathbf{B}} - \sigma^2_{\mathbf{B}}\right)}{2\sigma^2_{f\,\mathbf{A}}\sigma^2_{f\,\mathbf{B}} - \sigma^2_{\mathbf{A}}\sigma^2_{f\,\mathbf{B}} - \sigma^2_{\mathbf{B}}\sigma^2_{f\,\mathbf{A}}} \end{aligned} \tag{7.1}$$

where $\sigma^2_{f\,\mathbf{X}}$ is the variance of the output, while evolving on the free strange attractor, with respect to the output, while evolving on the generating cycle, in the $\mathbf{X}$ filter. $\sigma^2_{\mathbf{X}}$ is the saturated qualitative resonance functional result of the filter $\mathbf{X}$, *i.e.*

$$\sigma^2_{\mathbf{X}} = \begin{cases} \sigma^2_{QR\,\mathbf{X}} & \text{if } \sigma^2_{QR\,\mathbf{X}} < \sigma^2_{f\,\mathbf{X}} \\ \sigma^2_{f\,\mathbf{X}} & \text{if } \sigma^2_{QR\,\mathbf{X}} \geq \sigma^2_{f\,\mathbf{X}} \end{cases}$$

where $\sigma^2_{QR\,\mathbf{X}}$ is the output of the receding horizon mean square error used for testing the qualitative resonance of the filter $\mathbf{X}$.

7.1.4 Tuning Methods

The qualitatively resonating filters are built/tuned under the following assumptions.

Modeling — Automatic Construction of the Model

The chaotic model used by the qualitatively resonating filter is built using the method described in Chap. 5 consisting of two steps.

1. *Identification*

   The method used for the first step of modeling is the Lur'e system identification described in Sect. 5.1. Here are the details regarding the two subproblems, namely linear identification and optimization.

   1.1. *Linear identification*: the model used is an output error OE(4,3), *i.e.* four poles and three zeros from input to output and noise directly on the output.

   The identification methods used is a maximum likelihood in least square error sense as that described in [Bittanti, 2000; Söderström and Stoica, 1989]; it has been implemented modifying the Matlab function `ARX` [Ljung, 2000]. This identification method allows to fit several input—output relations at once, namely it can make ensemble identification. Thus, all the training vectors are used in the identification at once, as described in Sect. 5.1.4.

   1.2. *Nonlinear optimization*: the nonlinearity is modeled by a five segment smoothed piecewise linear function as described in Sect. 5.1.4. The slope of the middle segment is fixed at one[7]. Thus, the nonlinearity is described by $3 \cdot 5 - 2 = 13$ parameters.

   The term of the objective function measuring the quality of the linear identification is the norm L^∞ of the relative standard deviation of the identified parameters, *cfr.* Sect. 5.3. Namely, it is the maximal tolerance on the identified parameters.

   The optimization is achieved by means of a genetic algorithm, in the variant considered by [Dasgupta and McGregor, 1992, 1994], working for five-hundreds evolution steps on hundred individuals of thirteen chromosomes each (the parameters of the nonlinearity), which in turn are composed of eighty binary genes each, *i.e.* the IEEE representations of reals *cfr.* Sect. 5.4.1. The reproduction function is governed by a reproduction probability, given by the normalized fitness, and a standard Monte Carlo method, excepting the best three individuals which are surely reproduced at the next generation [Koza, 1992]. The crossover operator is applied with probability $P_C = 0.7$ while the mutation operator is applied with a probability $P_M = 0.1$. The crossover works at chromosome level while the mutation works at gene level. The cut point, over the chromosomes, for the crossover and the choice of gene, over the genes, for the mutation are randomly drawn with an uniform distribution.

   The optimization is run with three constraints. The first two are dedicated to avoid the convergence of the system to the trivial solution (*cfr.* Sects. 5.1.4 and 5.3); namely, to avoid the regression of the

[7] As described in Sect. 5.1.4 this is to fix the gain of the linear transfer function.

overall system to a linear system only two pairs of the segments of the nonlinearity can be aligned and no more than three coefficients of the linear transfer function can annihilate. The third constraint is to augment the probabilities of having a stable strange attractor as a result; namely, the time derivative of the output ($y(t)$) must be such as to enter the visited segment of the nonlinearity from its borders.

2. *Shil'nikov constraint*

   The dynamical system resulting from the previous identification is driven towards the Shil'nikov condition using the continuation-based period climbing algorithm described in Sect. 5.2.

   The initial guess for the generating cycle is obtained from the method given in [Pierson and Moss, 1995], *cfr.* Sect. 5.2.

   The initial direction in the thirteen-dimensional parameter space is obtained from the greedy approach choosing the maximal gradient direction (*cfr.* Sect. 5.2) which is adapted every ten continuation steps.

   No post fine-tuning is performed, the Shil'nikov-like strange attractor obtained is taken as good as it gets, *cfr.* Sect. 5.2.2.

   As described in Sect. 5.2.2, this technique returns as side results the generating cycle, the Jacobian along it, the homoclinic trajectory and the Jacobian along it. These elements are necessary for tuning the filter gain.

Filter Gain Tuning

Accordingly to what is described in Chap. 6, the filter gain K is practically tuned by means of a multi-constrained robust Kalman filter. Just as a reminder, the robust control problem described by Sect. 6.1, Eqs. (6.4), (6.14), (6.17), (6.25), and Sect. 6.1.4, can be, approximately, summarized as follow. The multi-constrained periodic robust observer requires the periodic, of period equal to the nominal pseudo-period, gain K with the largest component over the period as small as possible (*cfr.* Sect. 6.1.4) which maximizes the minimal square distance of the reconstructed trajectory ($x(t)$) from the homoclinic trajectory (HT) whenever the input signal ($u(t)$) is a good pattern (GP) (*cfr.* Sect. 6.1.1) and, at the same time, minimize the maximal square distance of the reconstructed trajectory ($x(t)$) from the homoclinic trajectory (HT) whenever the input signal ($u(t)$) is a bad pattern (GP) (*cfr.* Sects. 6.1.2 and 6.1.3).

The nominal accuracy, *i.e.* the nominal standard deviation $\mathcal{A}_m$, of the measuring instrument, which is necessary to test the compliancy to the anti-resonance requirement, has been assumed, arbitrarily, equal for all the tests. In particular, a signal to noise ratio of the measurements of $20dB$ has been supposed; namely, $\mathcal{A}_m = 0.1$.

As already mentioned, all the data needed for this step, the generating cycle, the homoclinic trajectory, and the Jacobians along them are obtained as side results from the second step of modeling.

7.1.5 Learning Conditions

As mentioned above, the two sets of signal vectors are always divided into two equal parts. One of these parts is used for the training/tuning of the filter while the other half is used only for testing the pattern recognition ability of the tuned qualitatively resonating filter.

Obviously, the vectors of the two sets exchange their role in the tuning of the two filters. Namely, the vector from set A are the *good patterns* when tuning the **A** filter while are the *bad patterns* when tuning the **B** filter and vice versa for the vectors from set B.

7.1.6 Classification Test Conditions

After having tuned the two filters, two classification tests are run.

1. *Basic test*: in this test only the vectors that have been used in the training are classified, *i.e.* those belonging to A_{Tr} and B_{Tr}. The particular aim of this test is to assess the basic classification ability of the filters. Indeed, only those vectors that have been seen are tested.

2. *Blind test*: in this test only the vectors that have not been used in the training are classified, *i.e.* those belonging to A_{Ts} and B_{Ts}. The particular aim of this test is to assess the weak generalization ability of the filter. Indeed, only those vectors that have never been seen are tested.

It should be noted that most of the other possible problems addressed in the introductory paragraph are assessed at tuning time. This is obvious for all those items directly related to the qualitatively resonating filter, *i.e.* the first list in the introduction, but this is true also for problems as the overfitting and the indistinguishability (*cfr.* Sects. 5.1.5 and 6.1.5). Indeed, if the tuning overfits, no chaos will be observed in the identified filter after the first step of modeling and in general the period climbing, second step of modeling, will fail. On the other hand, if the vectors from the two classes are indistinguishable the tuning of the robust observer will fail since the two requirements of qualitative resonance and anti-resonance cannot be satisfied at the same time. In general, the tuning does not really fail in such a case but its result is quite particular; namely, the gain K is not so small as expected[8].

Classification Test

The classification test considered is very simple and no statistic postprocessing is done. The tested vector is classified to be of the class corresponding to the filter with the maximum probability. Namely, given the probability distribution over the two symbol composed of the two probabilities p_{A} and p_{B}, the signal is classified as belonging to $\mathcal{A}$ if $p_{\mathsf{A}} > p_{\mathbf{B}}$ and vice versa. This corresponds to a *maximum a posteriori* criterion [Walpone, 1993].

7.1.7 Results Compilation

For a given application, at first the observations from the field are preprocessed such as to compose the sets A and B, as described in Sect. 7.1.2. Then, a single test run consists of the following steps.

1. *Random splitting of the data sets*: fifty vectors are randomly drawn from the set A such to compose the subset of the vectors used for the training, *i.e.* A_{Tr}, while the set of the vectors used only for test is simply the A complementary of A_{Tr}, *i.e.* $\mathsf{A}_{\mathsf{Ts}} = \mathsf{A} - \mathsf{A}_{\mathsf{Tr}}$. Analogously, the set B_{Tr} and B_{Ts} are randomly drawn from the vectors in B.

2. *Filter tuning*: the qualitatively resonating filters $\mathbf{A}$ and $\mathbf{B}$ are tuned, according to what is described in Sects. 7.1.3 and 7.1.4, using the vectors from the A_{Tr} and B_{Tr} sets. All the encountered problems and manual adjustments necessary to let the system working are recorded.

3. *Basic classification test*: classification of the vectors belonging to A_{Tr} and B_{Tr}. The overall performance is recorded.

4. *Blind classification test*: classification of the vectors belonging to A_{Ts} and B_{Ts}. The overall performance is recorded.

The overall performance of the tuned classifier during one of the two tests is recorded in a matrix, usually called *confusion matrix*, as follow

$$P = \begin{bmatrix} P_{\mathcal{A},\mathcal{A}} & P_{\mathcal{A},\mathcal{B}} \\ P_{\mathcal{B},\mathcal{A}} & P_{\mathcal{B},\mathcal{B}} \end{bmatrix} \tag{7.2}$$

The elements $P_{i,j}, i, j = \mathcal{A}, \mathcal{B}$ give the percentage in which i has been recognized as j. Thus, the elements along the diagonal represent the correct classification rates while those on the anti-diagonal give the failure rates. The information reported in the table is redundant since the sum of the rows must be one. Finally, since the sets A and B have the same cardinality, the average of the elements on the diagonal gives the overall score of correctly classified vectors. This score must be compared with the score of the blind random classifier that, in such a case, would have a score of 50% of correctly classified vectors.

A complete test session consists in running hundred times the complete single test. The overall performances of the classifier in the two classification tests are compiled during each run and then the results of the hundred runs are synthesized in six matrices, *i.e.* the following three matrices for each one of the classification tests (basic and blind).

Average case: the average of all the results obtained in the hundred tests.

Worst case: the worst result obtained among the results obtained in the hundred tests.

Best case: the best result obtained among the results obtained in the hundred tests.

[8] It should be remembered that the control action K should be very small in order not to alter excessively the free dynamics, *cfr.* Sect. 6.1.5.

7.2 Result Presentation Scheme

In the following section the results of the test runs on six different applications are reported. The results are always presented according the to following scheme.

1. *Introduction*: as first, the application inspiring the test is briefly introduced.

2. *Signals*: the stereotype and typical observations of the signals from the two classes $\mathcal{A}$ and $\mathcal{B}$ are illustrated.

3. *Modeling results*: the results of the two phases of modeling are illustrated separately. For both filters **A** and **B**, first the two free Feigenbaum-like strange attractors, and their corresponding output patterns, resulting from the Lur'e identification are shown. Then, the two free Shil'nikov-like strange attractors, and their corresponding free output patterns, resulting from the period climbing are shown.

   Since the filters are four-dimensional what is shown are the projection of the four-dimensional strange attractors onto the last three state variables (x_2, x_3, x_4) of the reconstructor canonical form realization [Brogan, 1996; Rinaldi and Piccardi, 1998] of the transfer function of the linear part of the two filters (*cfr.* Sects. 5.1.6 and 5.4.1). On the other hand, the free temporal patterns shown are obviously the output of the linear part of the two filters.

4. *Filter gain tuning results*: the results of the filter gain tuning are illustrated showing eight typical results. Namely, the behaviors, in the state space, of the filter **A** and **B** when correctly or wrongly resonating are shown. In particular, eight pictures, four for each filter, are shown: **A** correctly resonating with a class $\mathcal{A}$ signal; **A** correctly anti-resonating with a class $\mathcal{B}$ signal; **A** wrongly resonating with a class $\mathcal{B}$ signal; **A** wrongly anti-resonating with a class $\mathcal{A}$ signal; **B** correctly resonating with a class $\mathcal{B}$ signal; **B** correctly anti-resonating with a class $\mathcal{A}$ signal; **B** wrongly resonating with a class $\mathcal{A}$ signal; **B** wrongly anti-resonating with a class $\mathcal{B}$ signal.

   Once again, since the filters are four-dimensional, the behavior of the two filters is illustrated showing the projection of the behavior in the four-dimensional state space onto the last three state variables (x_2, x_3, x_4) of the reconstructor canonical form realization [Brogan, 1996; Rinaldi and Piccardi, 1998] of the transfer function of the linear part of the two filters (*cfr.* Sect. 5.1.6).

5. *Classification tests results*: the results of the classification tests are reported by means of the six matrices discussed in Sect. 7.1.7.

6. *Problems and discussion*: all the problems encountered in the tuning phases and the results are commented at the end.

7.3 Applications

In this section, in order of increasing complexity and veracity of the considered signals, the applications developed with the aim of testing the proposed modeling technique and its application to pattern recognition are presented.

7.3.1 Square Sinus Detection

Although this application, as the tests presented in the previous two chapters, does not correspond to any real application directly, it is inspired by those problems of shape detection that occur in artificial vision which are quite common in robotics [Alder, 1994].

The problem is to distinguish approximately square waves, class $\mathcal{A}$, from approximately sinusoidal waves, class $\mathcal{B}$. For doing that, the generalized square waves produced by the generalized Van Der Pol oscillator [Belhaq and Fahsi, 1996], shown in Fig. 7.1, and the generalized sinusoidal waves produced by the Colpitts oscillator [Maggio *et al.*, 1999], shown in Fig. 7.2, have been considered.

The observations to compose the A and B sets of vectors have been artificially generated simulating the two above cited models. Even though that, no information about these models has been employed to deal with the tuning of the qualitatively resonating filters.

To some extent, this application can be considered as the most aseptic test for the proposed method. Namely, everything satisfies the hypotheses. It would be worrying if the proposed technique did not work for such an application.

SIGNALS

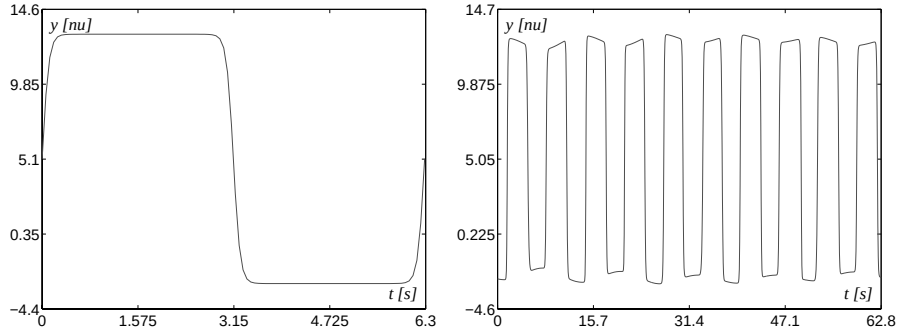

Figure 7.1: *The class $\mathcal{A}$ patterns, approximately square waves: (a) – the pattern prototype; (b) – a typical observation.*

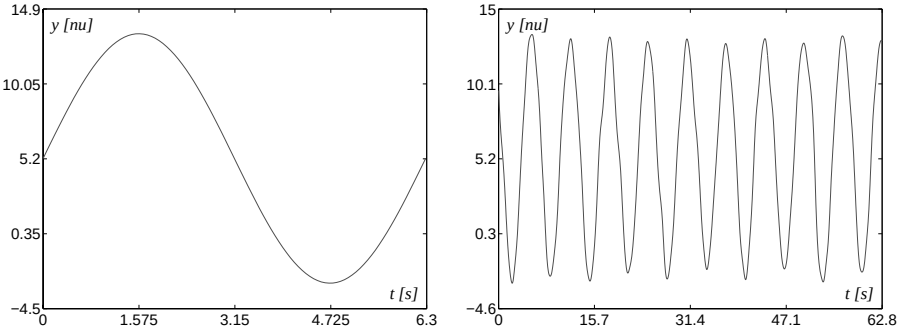

Figure 7.2: *The class $\mathcal{B}$ patterns, approximately sinusoidal waves: (a) – the pattern prototype; (b) – a typical observation.*

MODELING RESULTS

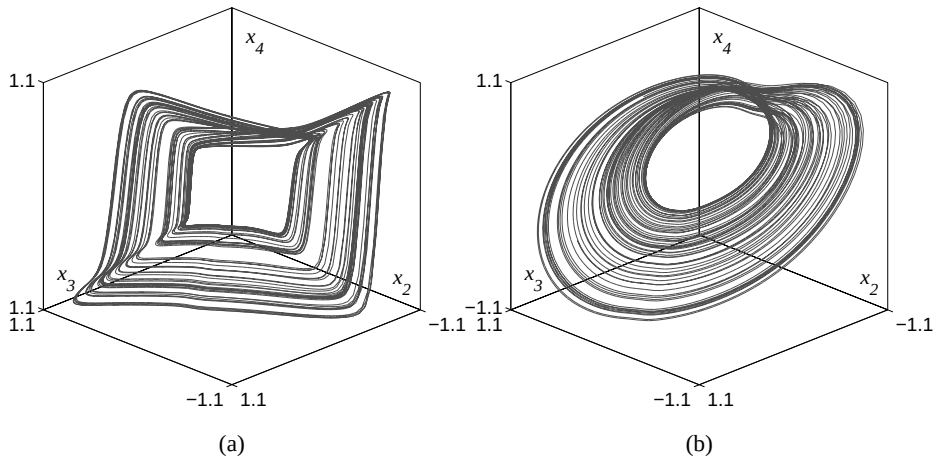

Figure 7.3: *Three-dimensional projection of the free Feigenbaum-like strange attractors resulting from the first step of modeling,* i.e. *identification: (a) – filter* **A**, *approximately square waves; (b) – filter* **B**, *approximately sinusoidal waves.*

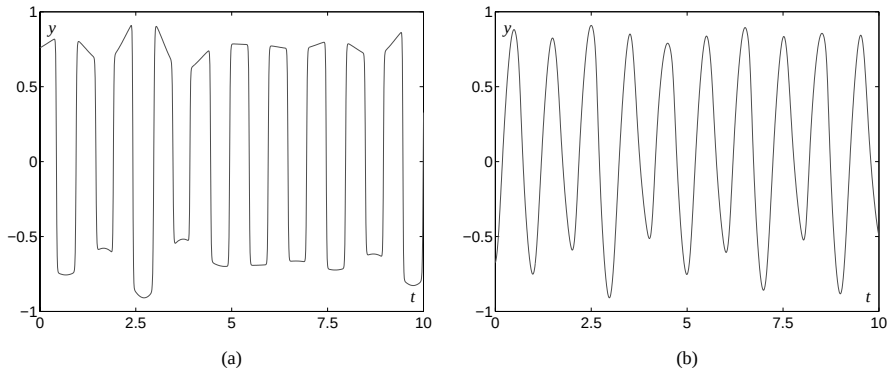

Figure 7.4: *Output of the filters corresponding to the free Feigenbaum-like strange attractors shown in Fig. 7.3: (a) – filter* **A**, *approximately square waves; (b) – filter* **B**, *approximately sinusoidal waves.*

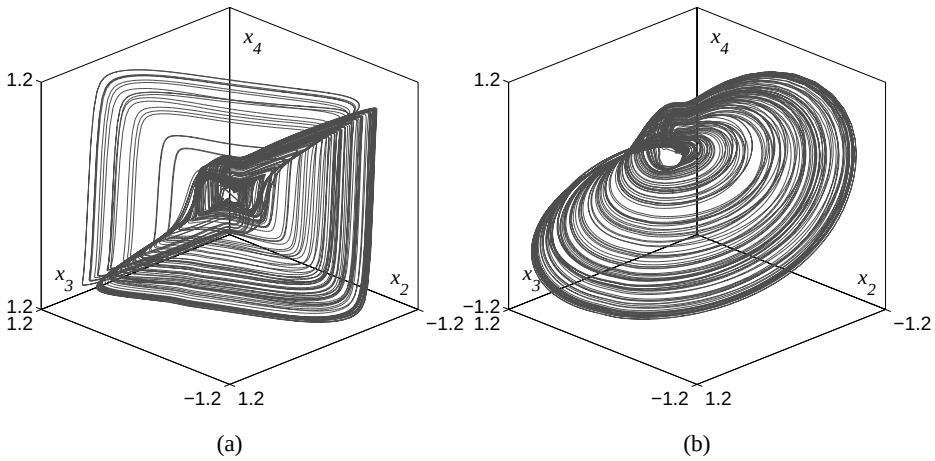

Figure 7.5: *Three-dimensional projection of the free Shil'nikov-like strange attractors resulting from the second step of modeling,* i.e. *period climbing: (a) – filter* **A**, *approximately square waves; (b) – filter* **B**, *approximately sinusoidal waves.*

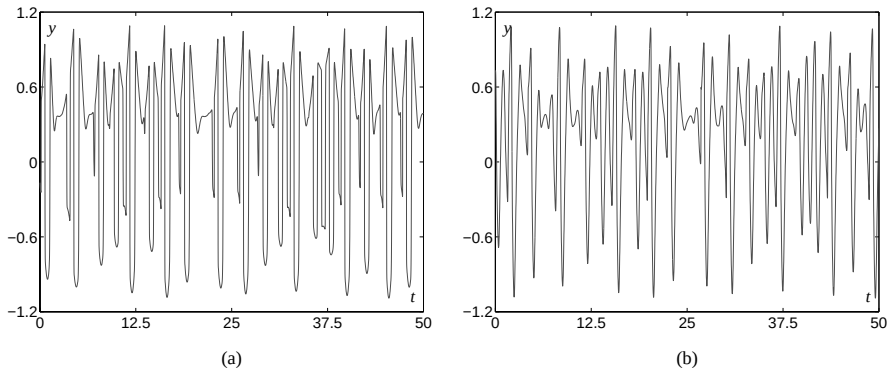

Figure 7.6: *Output of the filters corresponding to the free Shil'nikov-like strange attractors shown in Fig. 7.5: (a) – filter* **A**, *approximately square waves; (b) – filter* **B**, *approximately sinusoidal waves.*

FILTER GAIN TUNING RESULTS

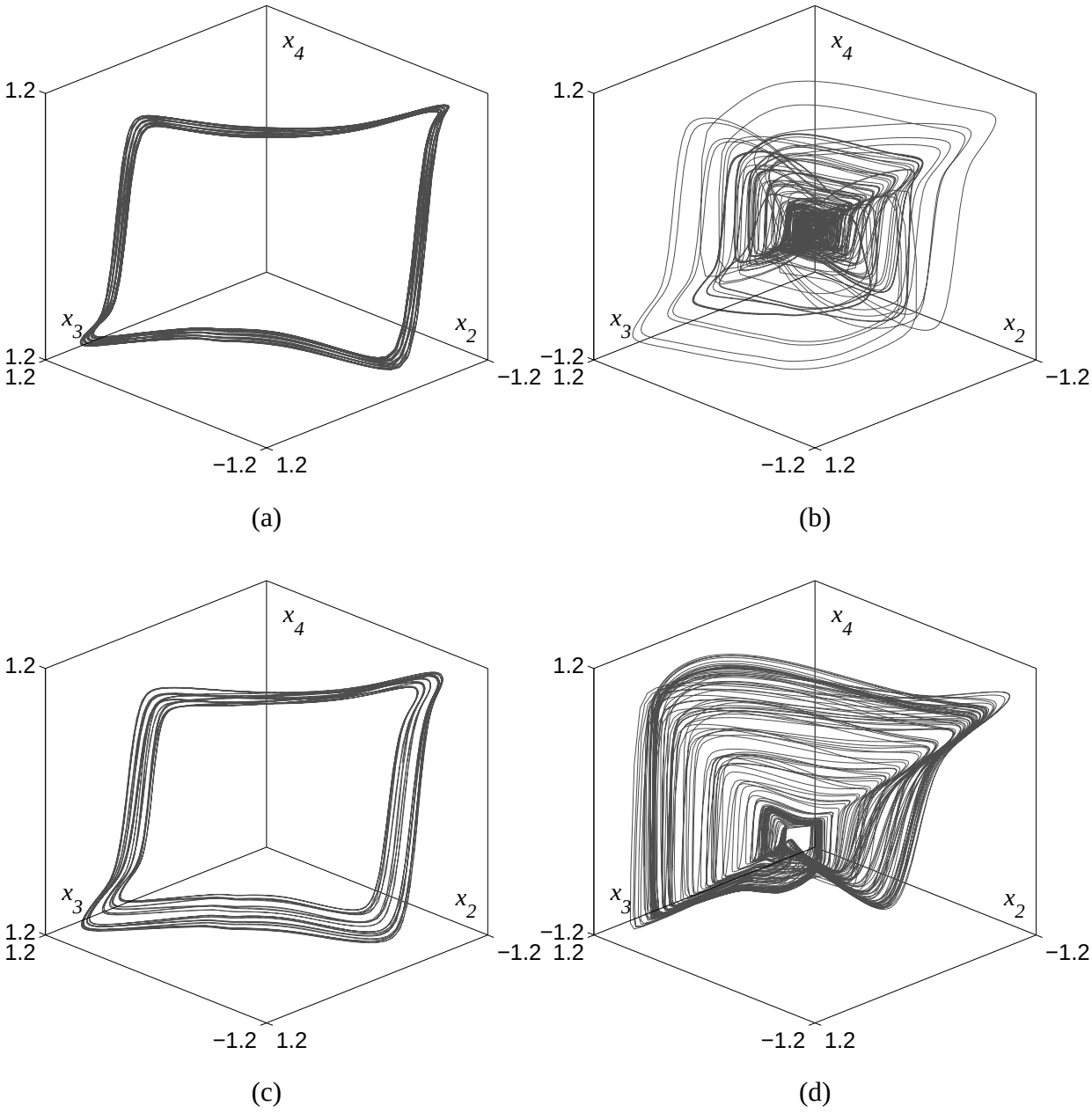

Figure 7.7: *Three-dimensional projection of the behavior in the state space of the driven filter* $\mathbf{A}$, i.e. *the approximately square waves detector: (a) – correctly resonating with a class* $\mathcal{A}$ *signal,* i.e. *an approximately square wave; (b) – correctly anti-resonating with a class* $\mathcal{B}$ *signal,* i.e. *an approximately sinusoidal wave; (c) – wrongly resonating with a class* $\mathcal{B}$ *signal,* i.e. *an approximately sinusoidal wave; (d) – wrongly anti-resonating with a class* $\mathcal{A}$ *signal,* i.e. *an approximately square wave.*

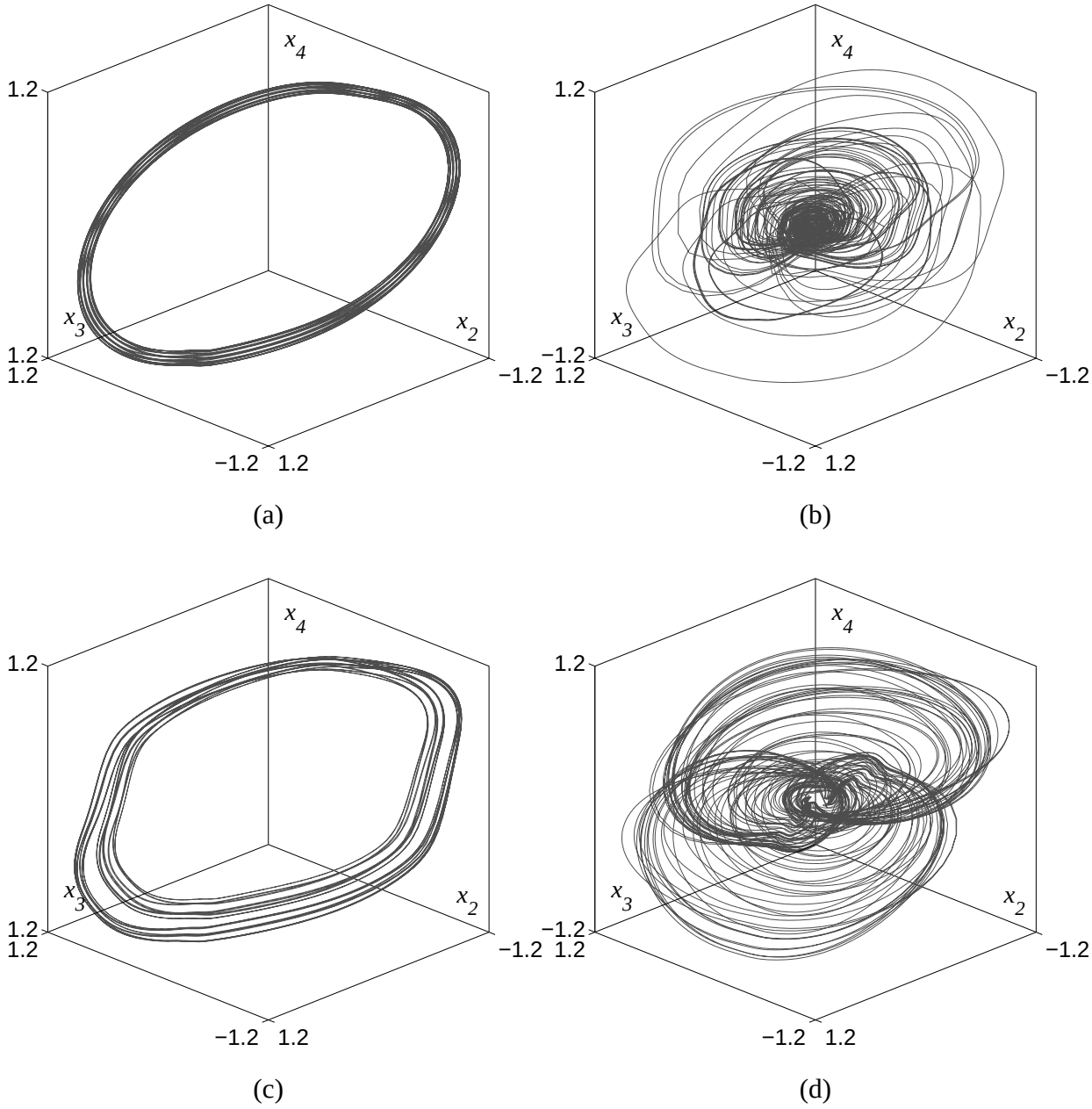

Figure 7.8: *Three-dimensional projection of the behavior in the state space of the driven filter* $\mathbf{B}$, i.e. *the approximately sinusoidal waves detector: (a) – correctly resonating with a class* $\mathcal{B}$ *signal,* i.e. *an approximately sinusoidal wave; (b) – correctly anti-resonating with a class* $\mathcal{A}$ *signal,* i.e. *an approximately square wave; (c) – wrongly resonating with a class* $\mathcal{A}$ *signal,* i.e. *an approximately square wave; (d) – wrongly anti-resonating with a class* $\mathcal{B}$ *signal,* i.e. *an approximately sinusoidal wave.*

Classification Tests Results

average

in \ as	$\mathcal{A}$	$\mathcal{B}$
$\mathcal{A}$	99.66%	0.34%
$\mathcal{B}$	0.22%	99.78%

best

in \ as	$\mathcal{A}$	$\mathcal{B}$
$\mathcal{A}$	99.88%	0.12%
$\mathcal{B}$	0.06%	99.94%

worst

in \ as	$\mathcal{A}$	$\mathcal{B}$
$\mathcal{A}$	99.32%	0.68%
$\mathcal{B}$	1.10%	98.90%

Table 7.1: *Results on the training set, only the vectors used for learning are classified,* i.e. *the vectors belonging to* A_{Tr} *and* B_{Tr}.

average

in \ as	$\mathcal{A}$	$\mathcal{B}$
$\mathcal{A}$	99.14%	0.86%
$\mathcal{B}$	1.06%	98.94%

best

in \ as	$\mathcal{A}$	$\mathcal{B}$
$\mathcal{A}$	99.69%	0.31%
$\mathcal{B}$	0.14%	99.86%

worst

in \ as	$\mathcal{A}$	$\mathcal{B}$
$\mathcal{A}$	98.75%	1.25%
$\mathcal{B}$	2.10%	97.90%

Table 7.2: *Results on the test set, only the vectors not used for learning are classified,* i.e. *the vectors belonging to* A_{Ts} *and* B_{Ts}.

Problems and Discussion

No particular problems have been encountered for this application. If that had been the case the author would be ashamed to present the proposed chaos-based modeling technique for diversity and its application to pattern recognition as a Ph.D Thesis.

As can be seen from the result tables, for this fake application the method in practice works perfectly. This was expected since, for this application, all the hypotheses, under which the proposed method has been developed, are satisfied.

7.3.2 Chaos-Based Communication Scheme

This application has been suggested by one of the research projects in which it is involved the laboratory[9] that hosted the author during the development of this thesis, namely the transmission of information by means of chaotic carriers [Hasler, 1998]. A simplified version, but better performing, of what is proposed here has been presented in [Maggio and De Feo, 2000].

Here, the main idea is reported very briefly, the interested reader can refer to [Schweizer, 1999]. A transmission scheme is composed of four elements: the information that is to be transmitted; the propagation channel trough which the information must be transmitted, which corrupts the signals propagating through it; the modulator which, at one side of the channel, transform the information in a signal suitable for the transmission through the channel; the demodulator which, on the other side of the channel, retrieves the original information from the received corrupted signal. The simple problem of designing the best modulator-demodulator pair for a given channel is an argument of tough discussion and is at the origin of the modern communication engineering [Gibson, 1993] as well as of the information theory [MacKay, 1999]. Dumping all the difficulties related with a real communication scheme, what is here considered is the transmission of a binary information, zero or one, over a very simple channel, namely some meter of electrically conducting cable.

The idea is the following, a binary information (bit) zero or one is transmitted on the channel sending one of two geometrically different chaotic signals, generated by two different strange attractors, coming from the Colpitts oscillator. This idea has been introduced in [Maggio and De Feo, 2000] under the name of *topological chaos shift keying* (T-CSK) and is a particular case of the most common *chaos shift keying* described in [Dedieu *et al.*, 1993].

What is proposed here is to demodulate, *i.e.* retrieve, the binary information by means of the proposed pattern recognition method. Namely, to classify the two chaotic patterns, *i.e.* the received signals, associated to the two geometrically different chaotic attractors chosen to code the zero and the one. In particular, the problem is to distinguish approximately 2-pulse signals, class $\mathcal{A}$, from approximately 3-pulse signals, class $\mathcal{B}$, which are shown in Figs. 7.9 and 7.10, respectively.

The observations to compose the A and B sets of vectors have been obtained measuring one of the state variables in a physical realization of the Colpitts oscillator[10] [De Feo and Maggio, 2001]. Hence, this time the patterns considered are real electrical signals and not the result of simulations. It should be noted that also this time no information about the source of the signals has been exploited for the tuning of the qualitatively resonating filters.

To some extent, this application can be considered as the next generation of the previous one. The hypotheses are theoretically all satisfied but this time the observed signals come from real measurements and not from a computer simulation.

[9] The Laboratory of NOnlinear Systems (LANOS) of the Department of Communication Systems (DSC) at the Swiss Federal Institute of Technology (EPFL).

[10] A Colpitts oscillator has been physically implemented in such a way that its state variables can be measured by means of a data acquisition system and such that its parameters can be easily controlled by means of a computer [De Feo and Maggio, 2001].

Signals

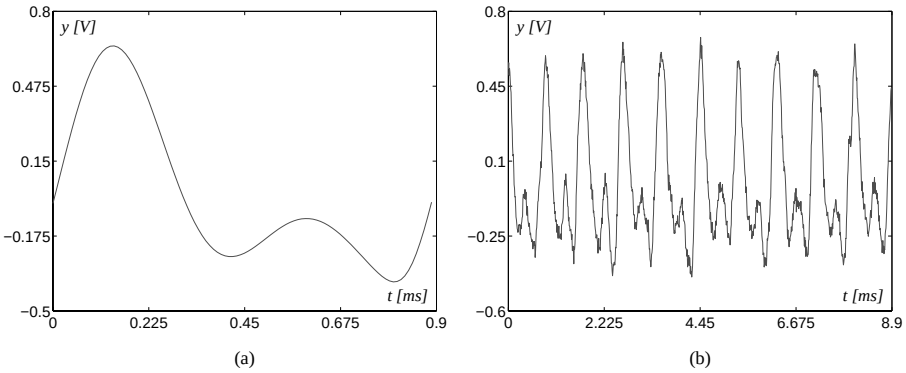

Figure 7.9: *The class $\mathcal{A}$ patterns, approximately* 2*-pulse signals: (a) – the pattern prototype; (b) – a typical observation.*

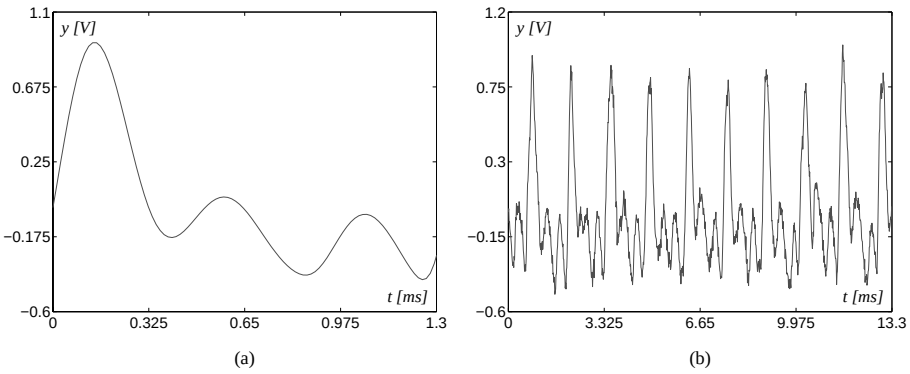

Figure 7.10: *The class $\mathcal{B}$ patterns, approximately* 3*-pulse signals: (a) – the pattern prototype; (b) – a typical observation.*

Modeling Results

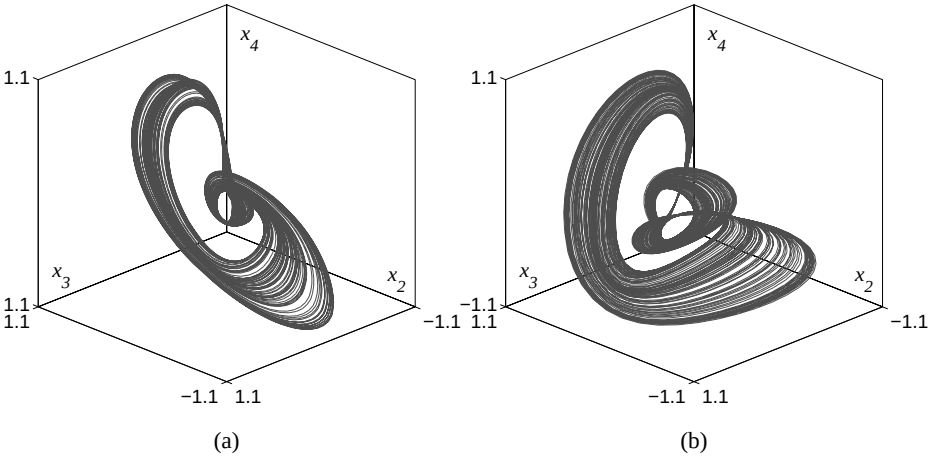

Figure 7.11: *Three-dimensional projection of the free Feigenbaum-like strange attractors resulting from the first step of modeling,* i.e. *identification: (a) – filter* **A***, approximately* 2*-pulse signals; (b) – filter* **B***, approximately* 3*-pulse signals.*

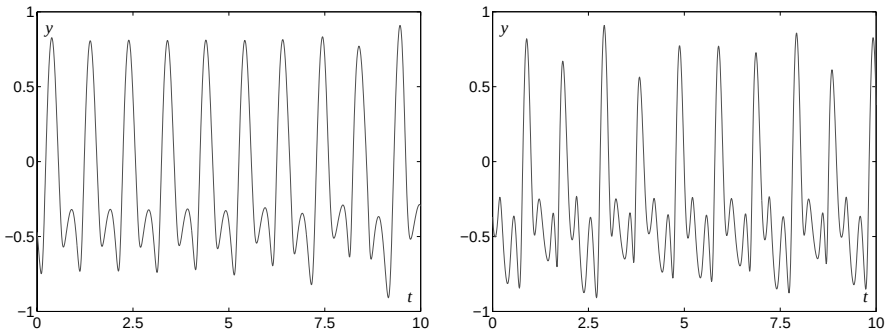

Figure 7.12: *Output of the filters corresponding to the free Feigenbaum-like strange attractors shown in Fig. 7.11: (a) – filter* **A**, *approximately* 2*-pulse signals; (b) – filter* **B**, *approximately* 3*-pulse signals.*

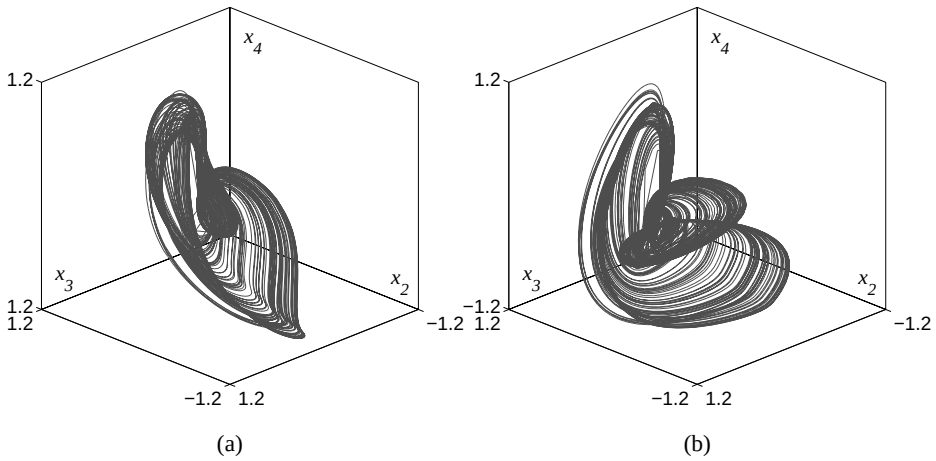

Figure 7.13: *Three-dimensional projection of the free Shil'nikov-like strange attractors resulting from the second step of modeling,* i.e. *period climbing: (a) – filter* **A**, *approximately* 2*-pulse signals; (b) – filter* **B**, *approximately* 3*-pulse signals.*

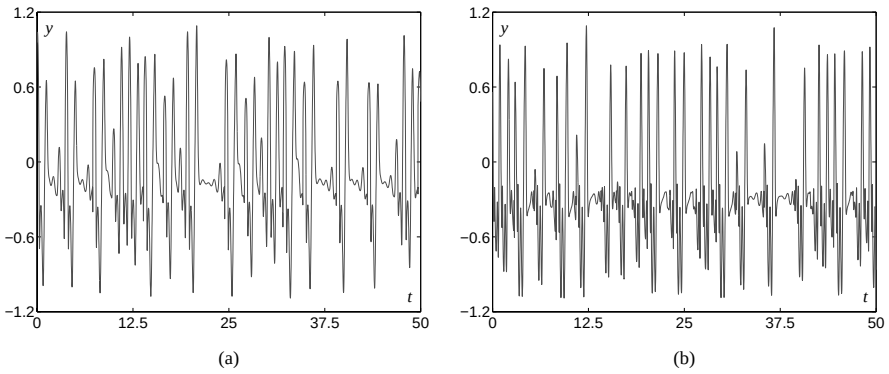

Figure 7.14: *Output of the filters corresponding to the free Shil'nikov-like strange attractors shown in Fig. 7.13: (a) – filter* **A**, *approximately* 2*-pulse signals; (b) – filter* **B**, *approximately* 3*-pulse signals.*

Filter Gain Tuning Results

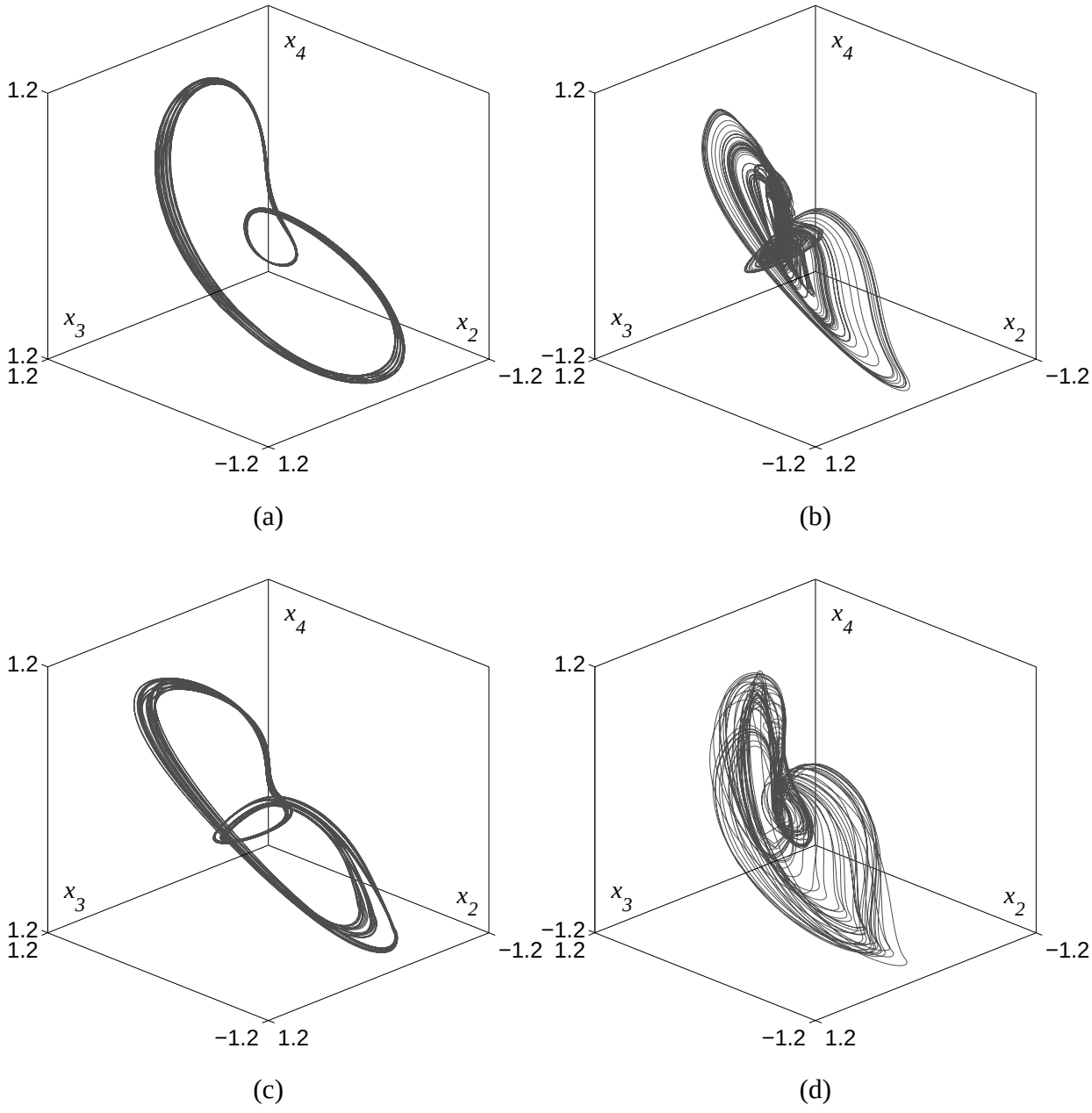

Figure 7.15: *Three-dimensional projection of the behavior in the state space of the driven filter* $\mathbf{A}$, i.e. *the approximately* 2*-pulse signals detector: (a) – correctly resonating with a class* $\mathcal{A}$ *signal,* i.e. *an approximately* 2*-pulse signal; (b) – correctly anti-resonating with a class* $\mathcal{B}$ *signal,* i.e. *an approximately* 3*-pulse signal; (c) – wrongly resonating with a class* $\mathcal{B}$ *signal,* i.e. *an approximately* 3*-pulse signal; (d) – wrongly anti-resonating with a class* $\mathcal{A}$ *signal,* i.e. *an approximately* 2*-pulse signal.*

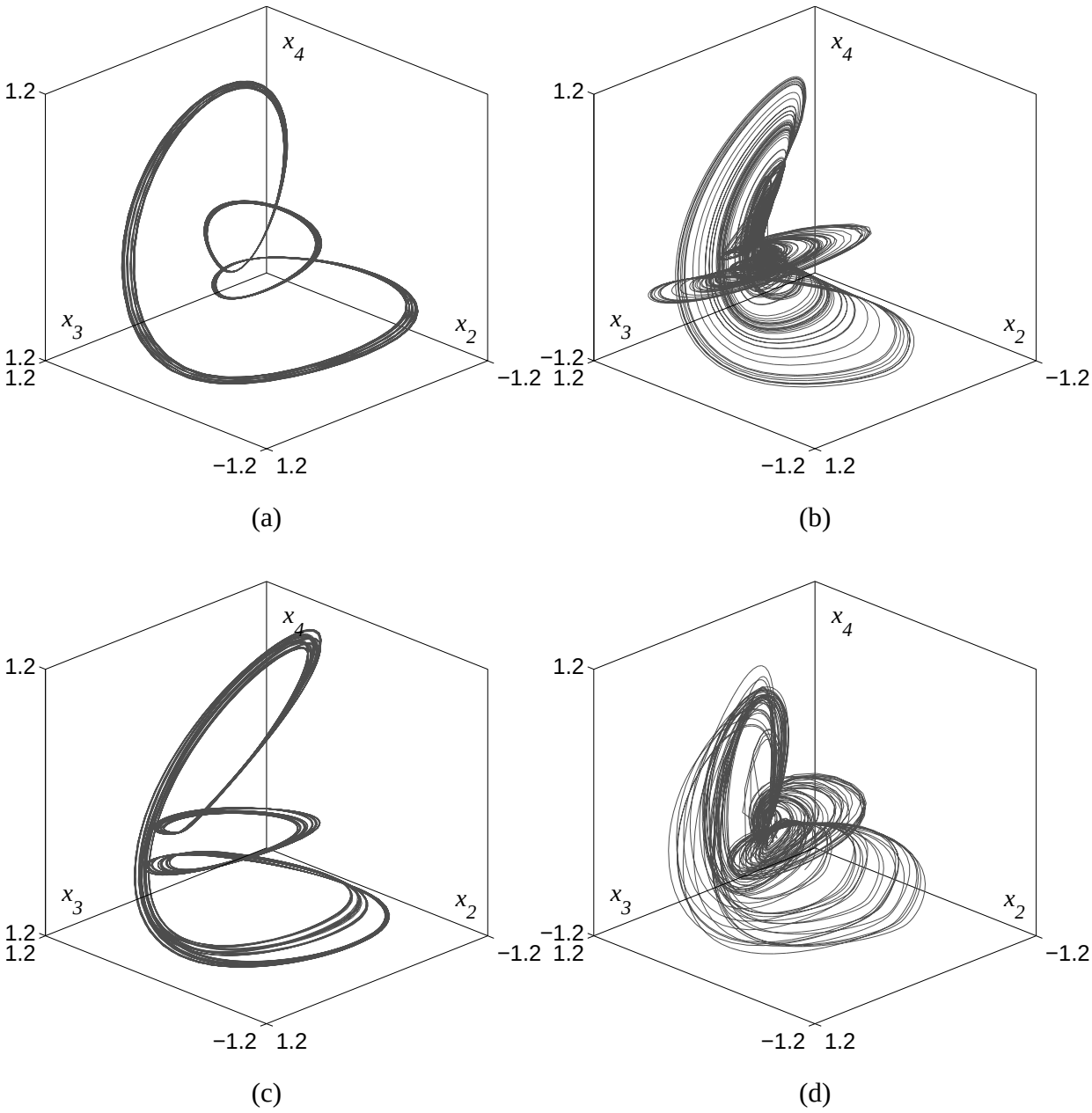

Figure 7.16: *Three-dimensional projection of the behavior in the state space of the driven filter* $\mathbf{B}$, i.e. *the approximately* 3*-pulse signals detector: (a) – correctly resonating with a class* $\mathcal{B}$ *signal,* i.e. *an approximately* 3*-pulse signal; (b) – correctly anti-resonating with a class* $\mathcal{A}$ *signal,* i.e. *an approximately* 2*-pulse signal; (c) – wrongly resonating with a class* $\mathcal{A}$ *signal,* i.e. *an approximately* 2*-pulse signal; (d) – wrongly anti-resonating with a class* $\mathcal{B}$ *signal,* i.e. *an approximately* 3*-pulse signal.*

Classification Tests Results

average

in \ as	$\mathcal{A}$	$\mathcal{B}$
$\mathcal{A}$	99.55%	0.45%
$\mathcal{B}$	0.51%	99.49%

best

in \ as	$\mathcal{A}$	$\mathcal{B}$
$\mathcal{A}$	99.97%	0.03%
$\mathcal{B}$	0.09%	99.91%

worst

in \ as	$\mathcal{A}$	$\mathcal{B}$
$\mathcal{A}$	99.08%	0.92%
$\mathcal{B}$	1.14%	98.86%

Table 7.3: *Results on the training set, only the vectors used for learning are classified,* i.e. *the vectors belonging to* A_{Tr} *and* B_{Tr}.

average

in \ as	$\mathcal{A}$	$\mathcal{B}$
$\mathcal{A}$	98.75%	1.25%
$\mathcal{B}$	0.81%	99.19%

best

in \ as	$\mathcal{A}$	$\mathcal{B}$
$\mathcal{A}$	99.18%	0.82%
$\mathcal{B}$	0.37%	99.63%

worst

in \ as	$\mathcal{A}$	$\mathcal{B}$
$\mathcal{A}$	96.61%	3.39%
$\mathcal{B}$	1.99%	98.01%

Table 7.4: *Results on the test set, only the vectors not used for learning are classified,* i.e. *the vectors belonging to* A_{Ts} *and* B_{Ts}.

Problems and Discussion

The only problem encountered, a minor one, has been the noise on the measured signals. The quality of the Colpitts implementation was quite poor and the measurements were corrupted by strong noise. A further lowpass filtering, other than the one described in Sect. 7.1.2, has been necessary to let the system work.

Also in this case, as can be drawn from the result tables, the method practically works perfectly. This confirms the results obtained in the previous application showing that these results are indeed proper to the method and not the due to some numerical "ghost" hidden in the simulations. Nevertheless, it should be noted that the measured performance would not be sufficient for being considered in a real communication scheme.

7.3.3 Pathology Detection in the Electrocardiogram

As the previous one, also this application has been suggested by one of the research projects in which the author's laboratory is involved, namely the diagnosis of cardiac pathologies based on nonlinear identification techniques [Pitarelli, 2001].

The main idea is to recognize automatically some cardiac pathology on a pattern recognition base. This would not be very different from what expert cardiologists do when they examine the track of an ECG or generated by some more sophisticated instrument. The idea is to automate this examination using a pattern recognizer.

In this application, what is proposed is to distinguish the ECG of a pathological patient from that of a healthy patient. The pathology considered is a harmless and very common one, namely the *mitral stenosis* or *mid-diastolic heart murmur* [AHA, 2001]. Furthermore, it is a pathology that any general physician could recognize from a simple visual inspection of the ECG track of the pathological patient [de Luna, 1998].

Taking into account the apparent chaoticity of the ECG track, as shown in Sect. 2.6, and the fact that the mitral stenosis is easily detectable from the ECG track, this application represents a good candidate for the approach described in this work.

The problem is to distinguish the pathological ECG tracks which look approximately as in Figs. 7.17, class $\mathcal{A}$, from the healthy ECG tracks which look approximately as in Figs. 7.18, class $\mathcal{B}$.

The observations to compose the A and B sets of vectors have been obtained by courtesy of Dr. Raffaella Bartolini[11], they are forty normal lead II ECG tracks (*cfr.* Sect. 2.6) of five minutes each, *i.e.* about three-hundreds pseudo-periods each, of patients at rest. Twenty of the ECG are from healthy patients while the other twenty are from pathological patients affected by mitral stenosis and unaffected by any other cardiac disease, at least by knowledge of Dr. Bartolini. The ECG have been recorded with a digital electrocardiograph with a resolution of twenty-four bits.

This application is now a real one in which no one of the required hypotheses is guaranteed to hold true.

[11] Department of Advanced Medical Devices, Hospital San Raffaele, Milan, Italy.

SIGNALS

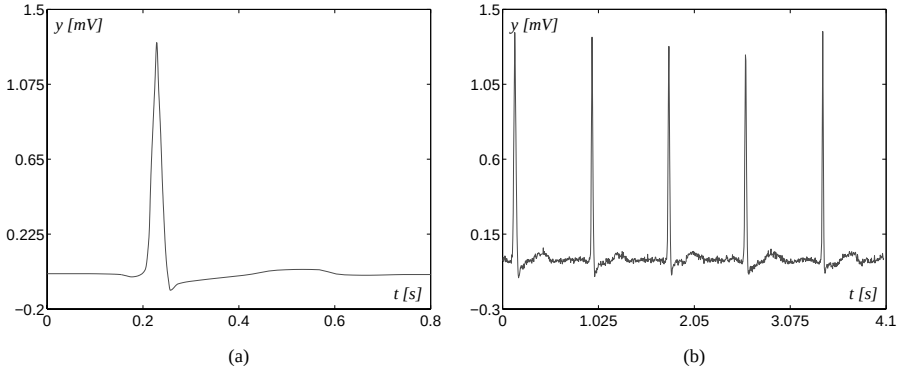

Figure 7.17: *The class $\mathcal{A}$ patterns, pathological ECG tracks: (a) – the pattern prototype; (b) – a typical observation.*

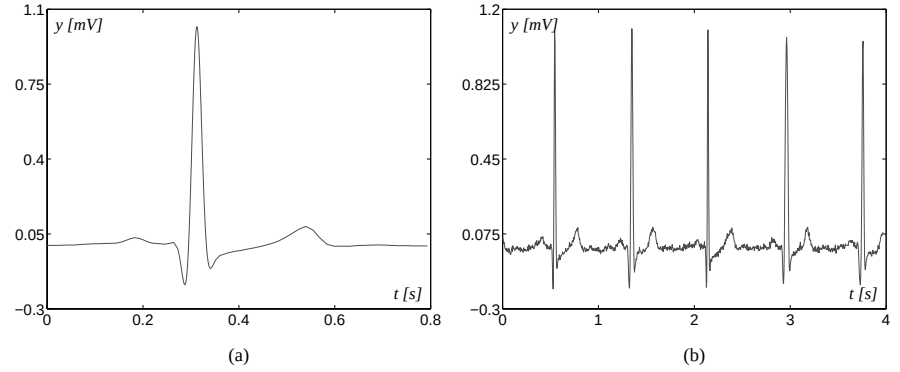

Figure 7.18: *The class $\mathcal{B}$ patterns, healthy ECG tracks: (a) – the pattern prototype; (b) – a typical observation.*

MODELING RESULTS

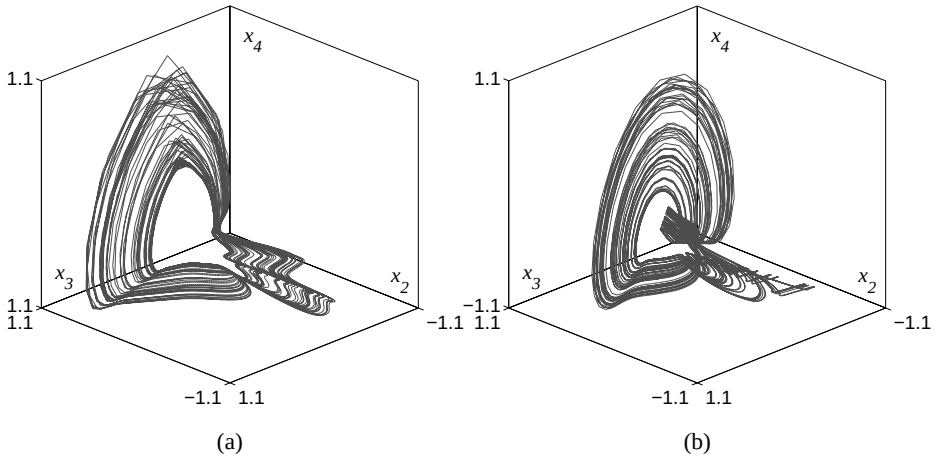

Figure 7.19: *Three-dimensional projection of the free Feigenbaum-like strange attractors resulting from the first step of modeling,* i.e. *identification: (a) – filter* $\mathbf{A}$*, pathological ECG tracks; (b) – filter* $\mathbf{B}$*, healthy ECG tracks.*

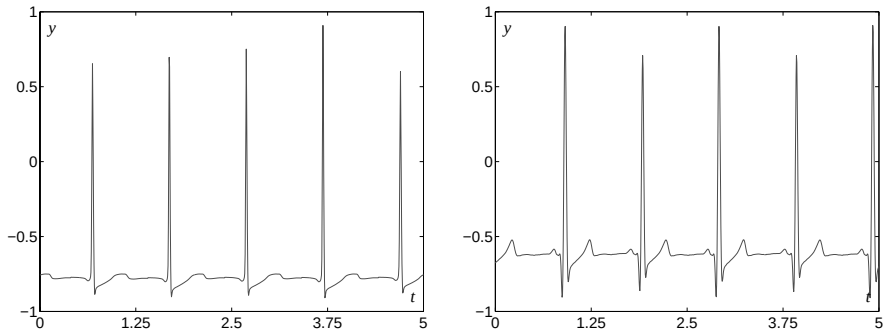

Figure 7.20: *Output of the filters corresponding to the free Feigenbaum-like strange attractors shown in Fig. 7.19: (a) – filter* **A**, *pathological ECG tracks; (b) – filter* **B**, *healthy ECG tracks.*

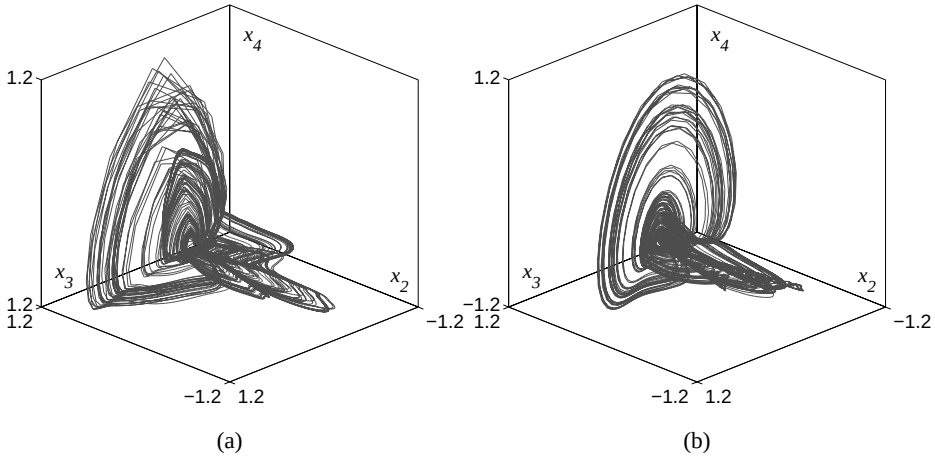

Figure 7.21: *Three-dimensional projection of the free Shil'nikov-like strange attractors resulting from the second step of modeling,* i.e. *period climbing: (a) – filter* **A**, *pathological ECG tracks; (b) – filter* **B**, *healthy ECG tracks.*

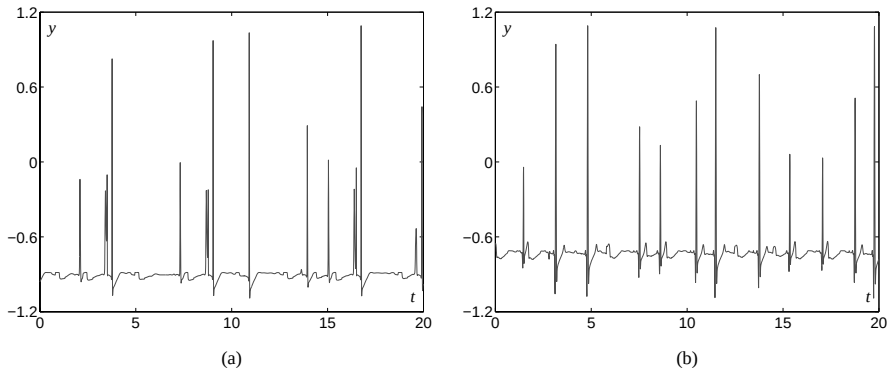

Figure 7.22: *Output of the filters corresponding to the free Shil'nikov-like strange attractors shown in Fig. 7.21: (a) – filter* **A**, *pathological ECG tracks; (b) – filter* **B**, *healthy ECG tracks.*

Filter Gain Tuning Results

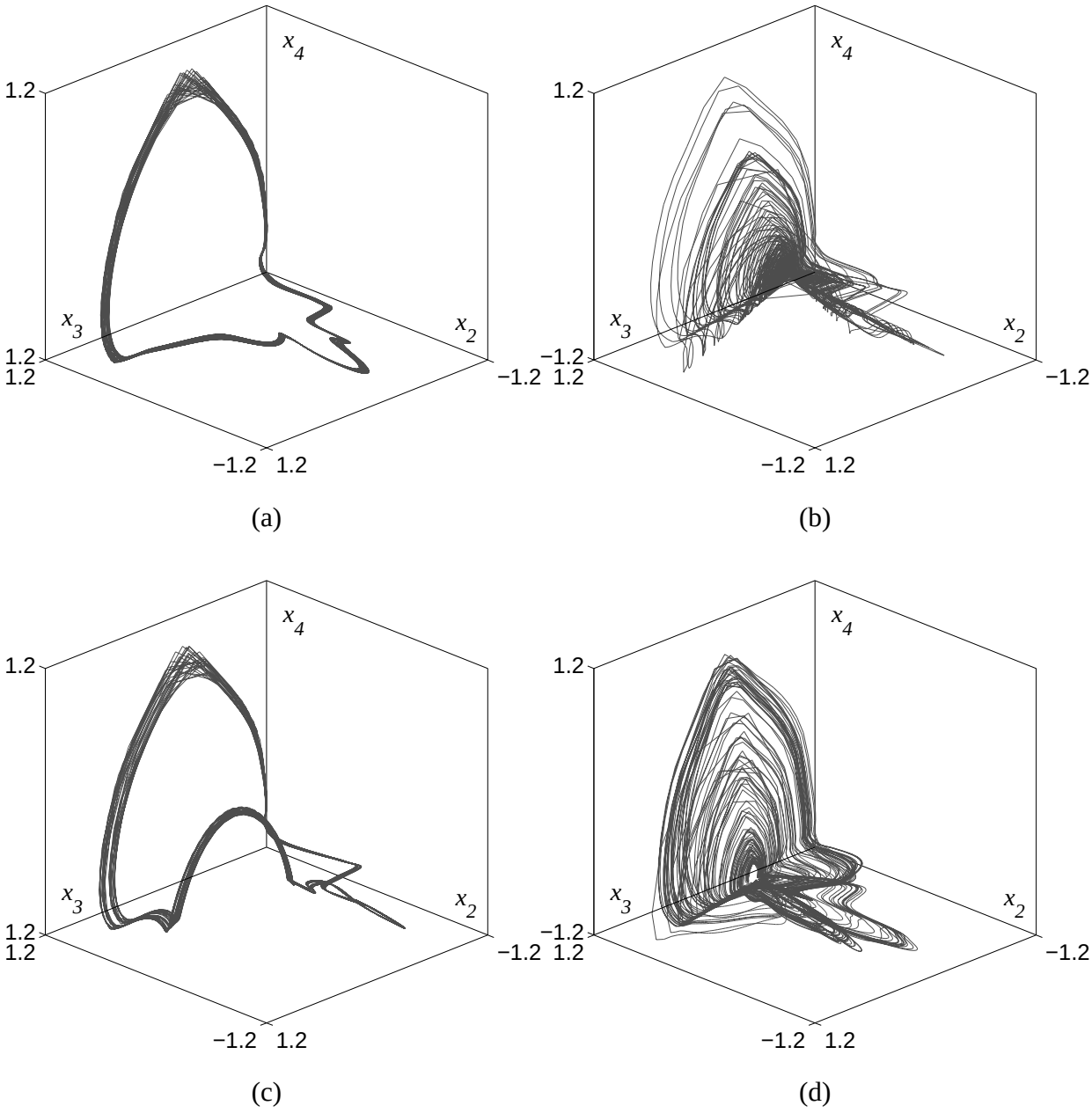

Figure 7.23: *Three-dimensional projection of the behavior in the state space of the driven filter* $\mathbf{A}$, i.e. *the* mitral stenosis *ECG detector: (a) – correctly resonating with a class* $\mathcal{A}$ *signal,* i.e. *a pathological ECG track; (b) – correctly anti-resonating with a class* $\mathcal{B}$ *signal,* i.e. *a healthy ECG track; (c) – wrongly resonating with a class* $\mathcal{B}$ *signal,* i.e. *a healthy ECG track; (d) – wrongly anti-resonating with a class* $\mathcal{A}$ *signal,* i.e. *a pathological ECG track.*

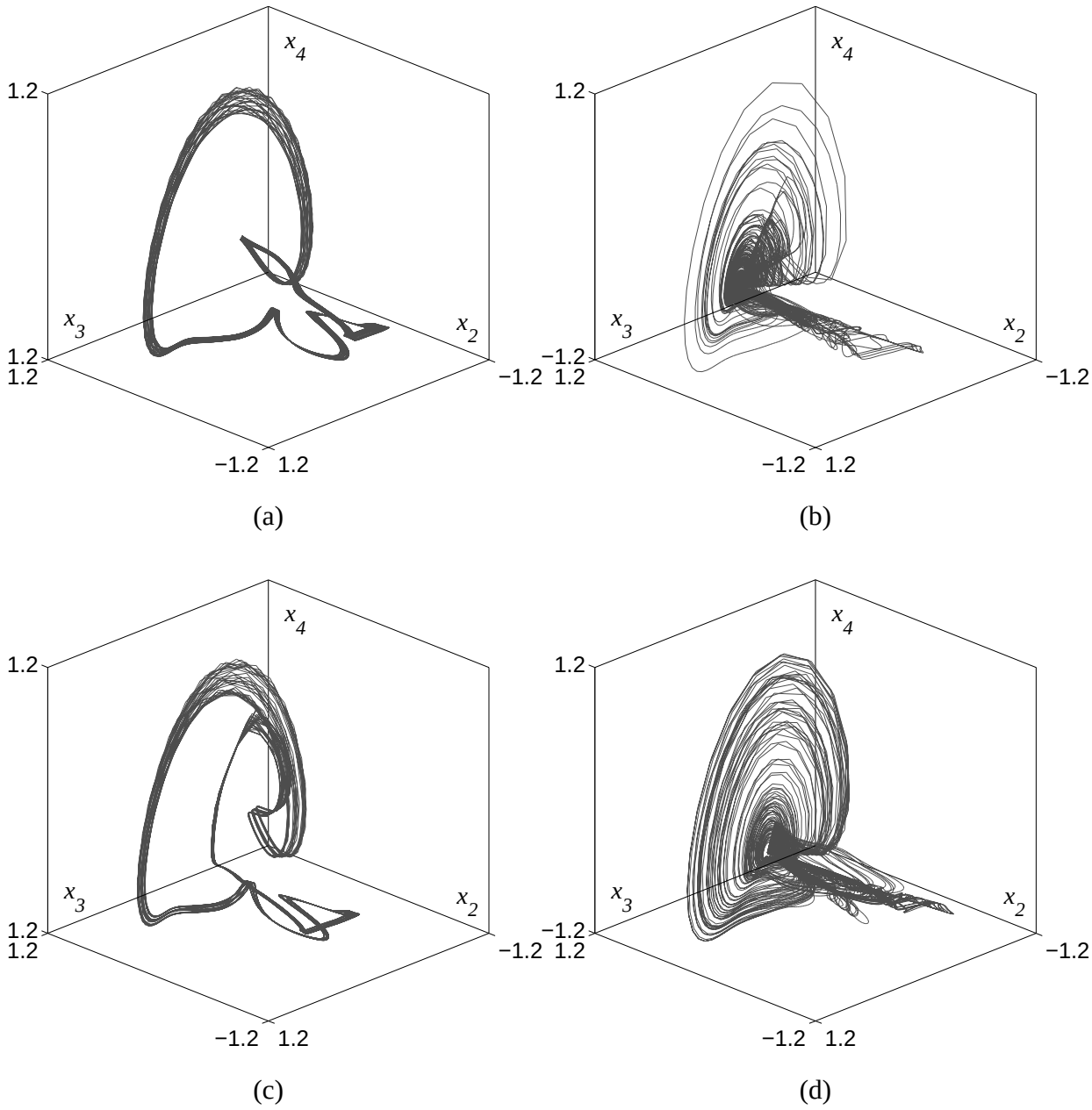

Figure 7.24: *Three-dimensional projection of the behavior in the state space of the driven filter* $\mathbf{B}$*,* i.e. *the healthy ECG detector: (a) – correctly resonating with a class* $\mathcal{B}$ *signal,* i.e. *a healthy ECG track; (b) – correctly anti-resonating with a class* $\mathcal{A}$ *signal,* i.e. *a pathological ECG track; (c) – wrongly resonating with a class* $\mathcal{A}$ *signal,* i.e. *a pathological ECG track; (d) – wrongly anti-resonating with a class* $\mathcal{B}$ *signal,* i.e. *a healthy ECG track.*

Classification Tests Results

average

in \ as	$\mathcal{A}$	$\mathcal{B}$
$\mathcal{A}$	90.31%	9.69%
$\mathcal{B}$	7.41%	92.59%

best

in \ as	$\mathcal{A}$	$\mathcal{B}$
$\mathcal{A}$	92.91%	4.09%
$\mathcal{B}$	6.77%	93.23%

worst

in \ as	$\mathcal{A}$	$\mathcal{B}$
$\mathcal{A}$	90.10%	9.90%
$\mathcal{B}$	7.50%	92.50%

Table 7.5: *Results on the training set, only the vectors used for learning are classified,* i.e. *the vectors belonging to* A_{Tr} *and* B_{Tr}*.*

average

in \ as	$\mathcal{A}$	$\mathcal{B}$
$\mathcal{A}$	88.19%	11.81%
$\mathcal{B}$	14.98%	85.02%

best

in \ as	$\mathcal{A}$	$\mathcal{B}$
$\mathcal{A}$	93.33%	6.67%
$\mathcal{B}$	10.36%	89.64%

worst

in \ as	$\mathcal{A}$	$\mathcal{B}$
$\mathcal{A}$	84.82%	15.18%
$\mathcal{B}$	15.40%	84.60%

Table 7.6: *Results on the test set, only the vectors not used for learning are classified,* i.e. *the vectors belonging to* A_{Ts} *and* B_{Ts}.

Problems and Discussion

Three main problems have been encountered when dealing with this application. The first was the stability of the filters, most of the time the models obtained from the first step of modeling, *i.e.* the Lur'e identification, were unstable. It has been necessary to modify the objective function used in the optimization in order to keep the stability in account. The second problem encountered was the fifty Hz noise in the observations, the automatic modeling had tendency to model it rather than the useful signal causing problems of indistinguishability. A notch filtering, other than the lowpass filtering described in Sect. 7.1.2, has been necessary to let the system work. The last problem has been the intrinsic "homoclinic" nature of the ECG; namely, the ECG is naturally composed of long stationary periods followed by brutal fast spikes exactly as a homoclinic-like signal[12], this intrinsic homoclinic nature has somehow interfered with the period climbing. Some forcing has been necessary to get the period climbing, *i.e.* the second step of modeling, to work.

Before identifying in the fifty Hz noise the real cause of indistinguishability, this problem has been addressed trying to augment the complexity of the model used. Namely, augmenting the segments used for the model of the nonlinearity, the order of the filter, or both them. Any of this trials immediately ran into the problem of overfitting. This highlights a delicate problem of this modeling technique, namely the sensitivity with respect to the complexity of the model used for the identification.

From the pattern recognition performance, the results are definitely promising, especially those of the blind tests which point out the effective generalization ability of qualitative resonance.

7.3.4 State Detection in the Electroencephalogram

This application is very similar to the previous one, it is mainly suggested by the same kind of medical application of pattern recognition techniques.

The idea is to distinguish automatically the drowsiness from the sleeping state, of a human being, on a pattern recognition base. Once again, this would not be very different from what expert neurologists do when they examine the track of an EEG or generated by some more sophisticated instrument. The idea is to automate this examination using a pattern recognizer.

In this application, what is proposed is to distinguish the EEG of a drowsy but still awake healthy human being, mainly slow θ-waves in the EEG [Nunez, 1995; Pradhan *et al.*, 1995], from that of a sleeping at stage three or four healthy human being, mainly slow δ-waves in the EEG [Nunez, 1995; Pradhan *et al.*, 1995]. These two states can be distinguished by visual inspection of the EEG track by any general physician [Johnston and Wu, 1995].

The apparent chaoticity of the EEG track, as shown in Sect. 2.6, and the fact that the two states are easily detectable from the EEG track make this application a good candidate for the qualitative resonance approach.

The problem is to distinguish the θ-waves-like EEG tracks which look approximately as in Figs. 7.25, class $\mathcal{A}$, from the δ-waves-like EEG tracks which look approximately as in Figs. 7.26, class $\mathcal{B}$.

The observations to compose the A and B sets of vectors have been obtained by the Massachusetts Institute of Technology (MIT) open source database[13]. They are thirty *O1* EEG [Bronzino, 1995] (*cfr.* Sect. 2.1.2) tracks of two minutes each, *i.e.* about four-hundreds-eighty pseudo-periods each, of patients at rest. Fifteen of the EEG are from healthy drowsy but still awake subjects while the other fifteen are from sleeping at stage four subjects. The EEG have been recorded with a digital electroencephalograph with a resolution of twelve bits and are sampled at two-hundred-fifty Hz.

[12] Homoclinic-like does not mean necessary Shil'nikov-like, there are also nonchaotic homoclinic bifurcations [Kuznetsov, 1998].

[13] Accessible from internet at `http://www.physionet.org/`

As the previous one, this application is now a real one in which no one of the required hypotheses is guaranteed to hold true.

Signals

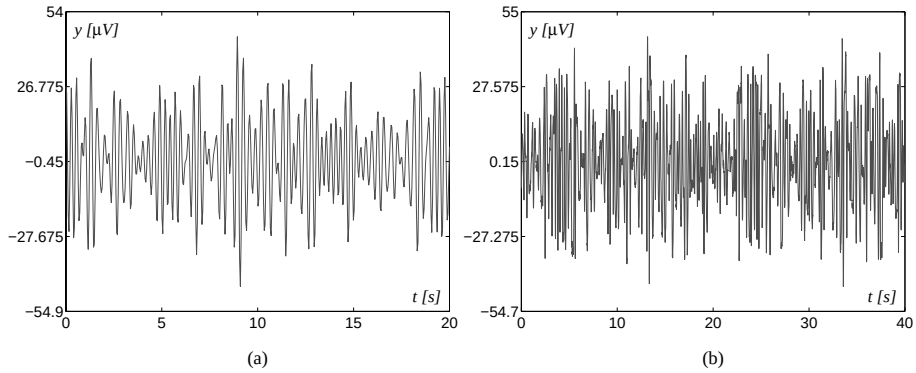

Figure 7.25: *The class $\mathcal{A}$ patterns, θ-waves-like EEG; (a) – the pattern prototype; (b) – a typical observation.*

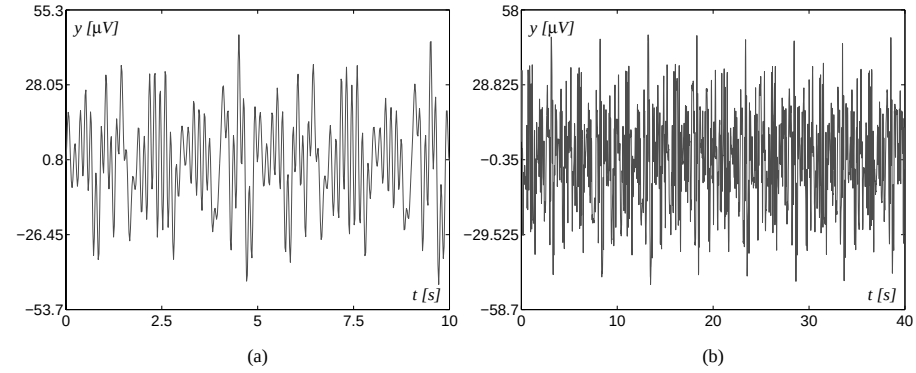

Figure 7.26: *The class $\mathcal{B}$ patterns, δ-waves-like EEG: (a) – the pattern prototype; (b) – a typical observation.*

Modeling Results

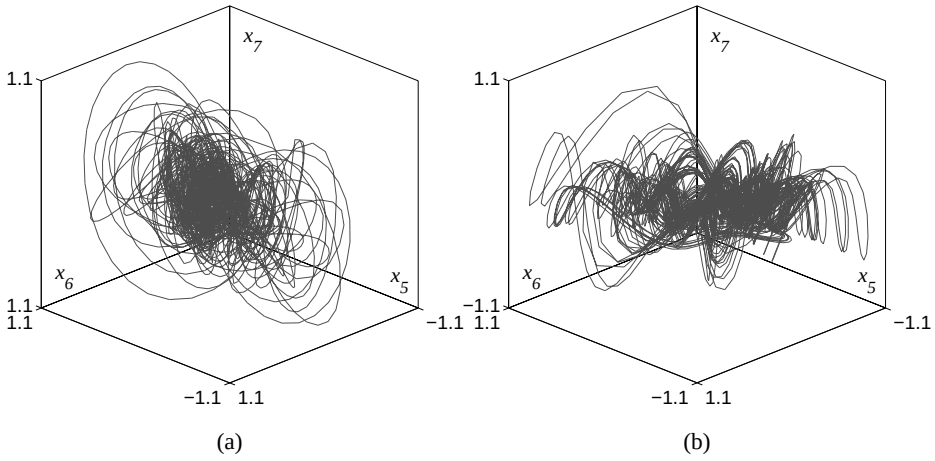

Figure 7.27: *Three-dimensional projection of the free Feigenbaum-like strange attractors resulting from the first step of modeling,* i.e. *identification: (a) – filter* **A**, *θ-waves-like EEG; (b) – filter* **B**, *δ-waves-like EEG.*

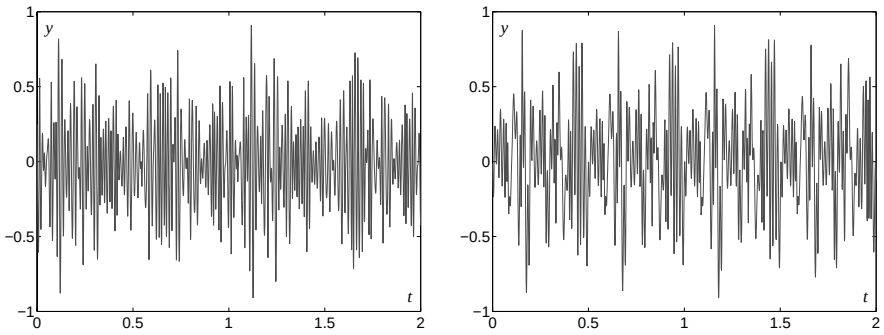

Figure 7.28: *Output of the filters corresponding to the free Feigenbaum-like strange attractors shown in Fig. 7.27: (a) – filter* **A**, *θ-waves-like EEG; (b) – filter* **B**, *δ-waves-like EEG.*

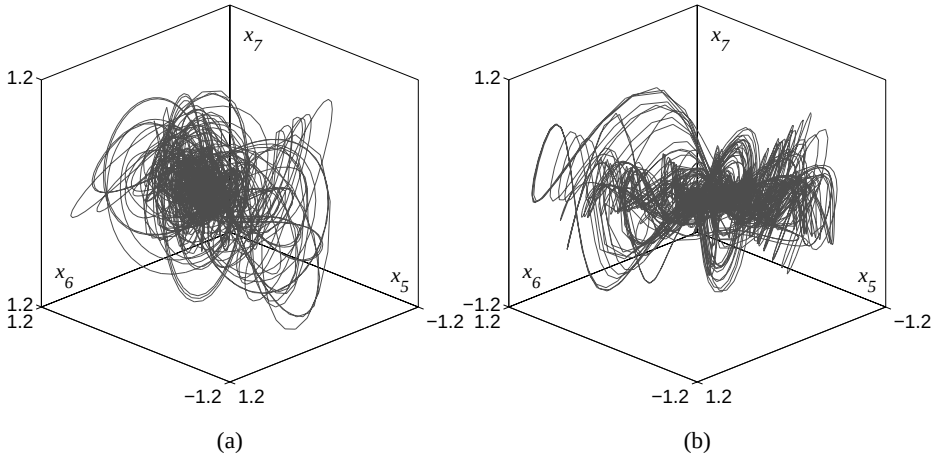

Figure 7.29: *Three-dimensional projection of the free Shil'nikov-like strange attractors resulting from the second step of modeling,* i.e. *period climbing: (a) – filter* **A**, *θ-waves-like EEG; (b) – filter* **B**, *δ-waves-like EEG.*

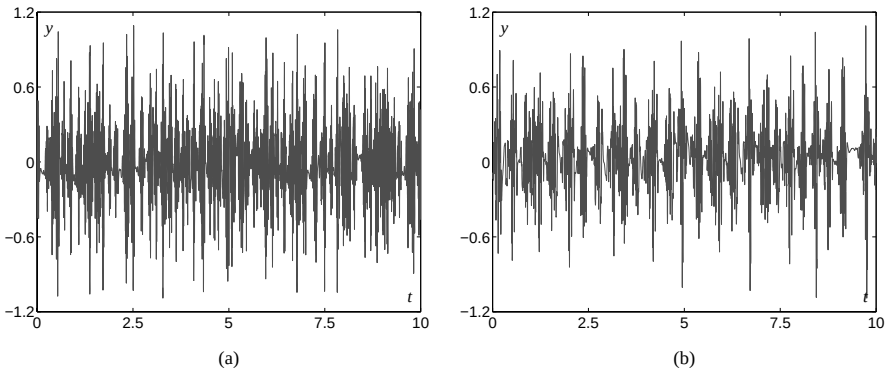

Figure 7.30: *Output of the filters corresponding to the free Shil'nikov-like strange attractors shown in Fig. 7.29: (a) – filter* **A**, *θ-waves-like EEG; (b) – filter* **B**, *δ-waves-like EEG.*

Filter Gain Tuning Results

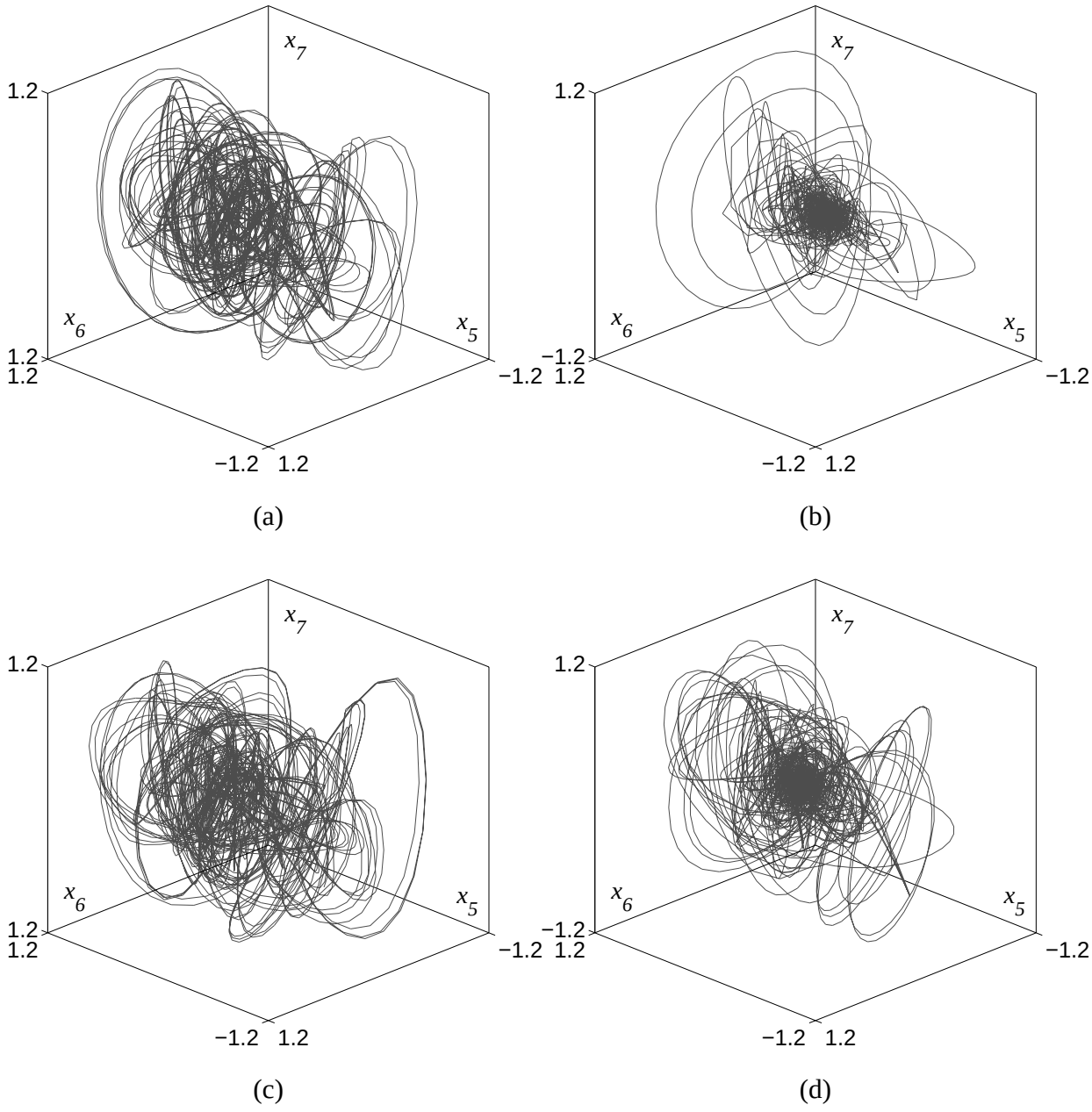

Figure 7.31: *Three-dimensional projection of the behavior in the state space of the driven filter* $\mathbf{A}$, i.e. *the drowsiness detector: (a) – correctly resonating with a class* $\mathcal{A}$ *signal,* i.e. *an* θ*-waves-like EEG track; (b) – correctly anti-resonating with a class* $\mathcal{B}$ *signal,* i.e. *a* δ*-waves-like EEG track; (c) – wrongly resonating with a class* $\mathcal{B}$ *signal,* i.e. *a* δ*-waves-like EEG track; (d) – wrongly anti-resonating with a class* $\mathcal{A}$ *signal,* i.e. *an* θ*-waves-like EEG track.*

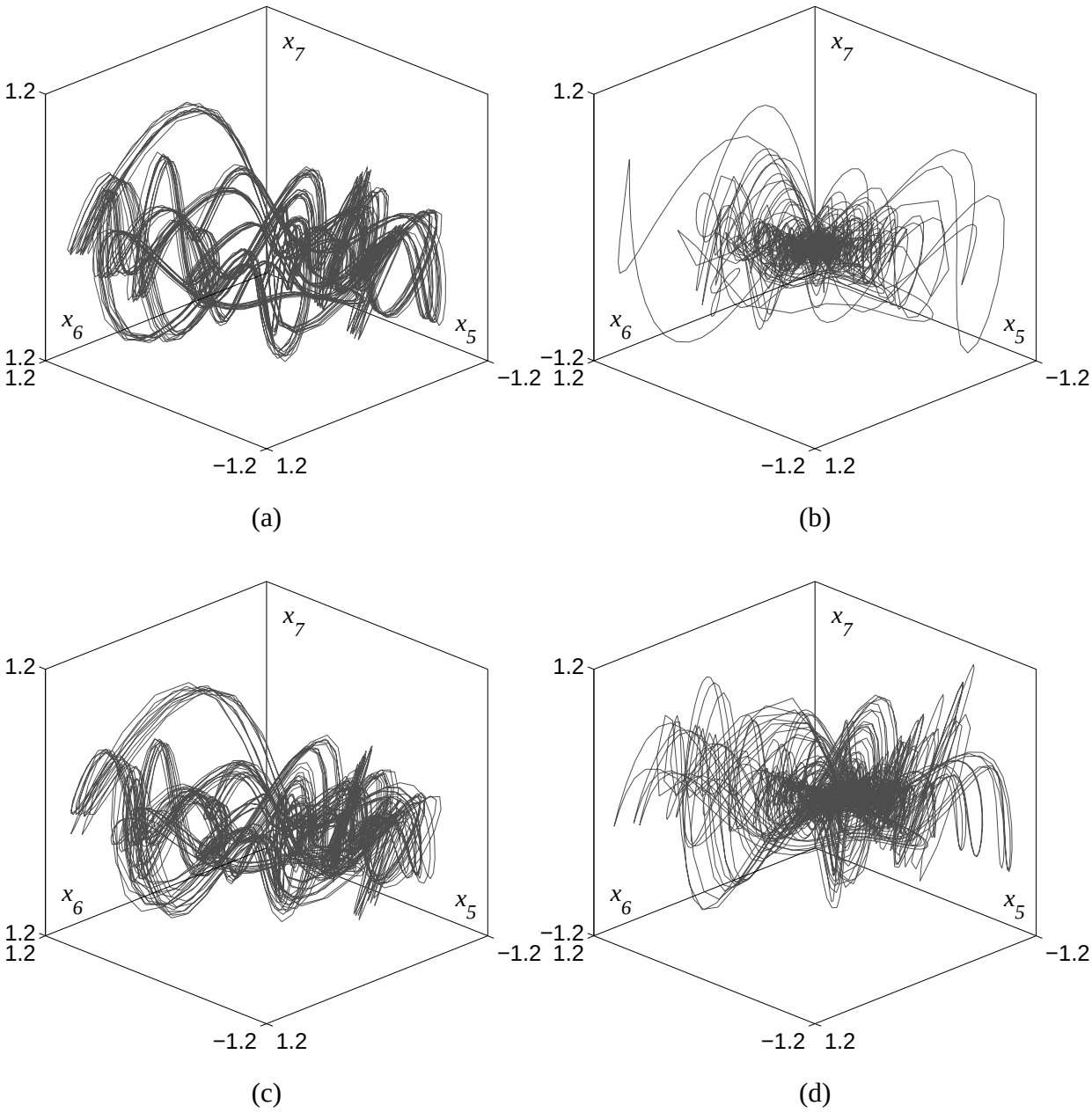

Figure 7.32: *Three-dimensional projection of the behavior in the state space of the driven filter* $\mathbf{B}$*,* i.e. *the sleepiness detector: (a) – correctly resonating with a class* $\mathcal{B}$ *signal,* i.e. *a* δ*-waves-like EEG track; (b) – correctly anti-resonating with a class* $\mathcal{A}$ *signal,* i.e. *an* θ*-waves-like EEG track; (c) – wrongly resonating with a class* $\mathcal{A}$ *signal,* i.e. *an* θ*-waves-like EEG track; (d) – wrongly anti-resonating with a class* $\mathcal{B}$ *signal,* i.e. *a* δ*-waves-like EEG track.*

Classification Tests Results

average

in \ as	$\mathcal{A}$	$\mathcal{B}$
$\mathcal{A}$	85.56%	14.44%
$\mathcal{B}$	15.57%	84.43%

best

in \ as	$\mathcal{A}$	$\mathcal{B}$
$\mathcal{A}$	91.75%	8.25%
$\mathcal{B}$	14.34%	85.66%

worst

in \ as	$\mathcal{A}$	$\mathcal{B}$
$\mathcal{A}$	83.88%	16.12%
$\mathcal{B}$	16.41%	83.59%

Table 7.7: *Results on the training set, only the vectors used for learning are classified,* i.e. *the vectors belonging to* A_{Tr} *and* B_{Tr}*.*

average

in \ as	$\mathcal{A}$	$\mathcal{B}$
$\mathcal{A}$	79.73%	20.27%
$\mathcal{B}$	22.77%	77.23%

best

in \ as	$\mathcal{A}$	$\mathcal{B}$
$\mathcal{A}$	84.38%	15.62%
$\mathcal{B}$	18.76%	81.24%

worst

in \ as	$\mathcal{A}$	$\mathcal{B}$
$\mathcal{A}$	76.76%	23.24%
$\mathcal{B}$	25.75%	74.25%

Table 7.8: *Results on the test set, only the vectors not used for learning are classified,* i.e. *the vectors belonging to* A_{Ts} *and* B_{Ts}.

Problems and Discussion

This application has been definitely the most troubled one. Several problems have been encountered while trying to fit the given data by means of the standard approach described in Sect. 7.1, namely using those "usually good" choices for the degrees of freedom available.

This application has been the author's personal nightmare for several months. It has been definitely useful to point out the limits of the particular choices described in Sect. 7.1 highlighting the real need of keeping all the mentioned degrees of freedom indeed open. In other words, this application has shown that trying to fix all the mentioned degree of freedom for the sake of simplicity would definitely lead to a degradation of the employability of the proposed technique. Despite of such a dramatic debut, with a lot of patience it has been possible to come to a satisfactory solution, which leads indeed to the reasonably good results just illustrated.

As for the previous application, the toughest problem has been the stability of the filter. Despite of the modification of the objective function used in the optimization in order to keep the stability in account, two-thousands evolutionary steps on a population of two-hundreds individuals have been necessary to obtain a stable satisfactory model for the signals considered. Namely, it has been necessary to increase the search time/complexity of an order of magnitude to achieve a solution. This result confirms the power of the genetic algorithms rather than the quality of the proposed modeling technique.

The smoothed piecewise linear nonlinearity has revealed inept for modeling this kind of signals retaining their distinguishability. A nonlinear analysis of the considered signals has highlighted the need of ripples in the nonlinearity. On these bases, the nonlinearity has been modeled with the first fourteen Tchebyshev polynomials [Szegö, 1975] obtaining immediately satisfactory results. In this case, the complexity has not been increased since the number of parameters used for the nonlinearity stays at thirteen[14]. The order of the model has revealed as well insufficient for the distinguishability, to obtain satisfactory results it has been necessary to consider a seventh order model. This, somehow, confirms the suspicion of several researcher that seven should be the embedding dimension of the EEG [Duke and Pritchard, 1991; Pereda *et al.*, 1998; Pradhan *et al.*, 1995; Röschke *et al.*, 1997]. In reality, the dimension of the obtained strange attractors is four (*cfr.* Sect. 5.1.4 and [Ferri *et al.*, 1996]) while the remaining three orders are used for modeling linear integral effects.

Before achieving the solution for the distinguishability by means of the Tchebyshev polynomials with a seventh order model, it has been tried to augment either the order of the system or the number of segments for the smoothed piecewise linear nonlinearity incurring immediately in the problem of overfitting. Thus, reinforcing the suspicion of some delicate sensitivity problem with respect to the complexity of the model used for the identification.

After having solved all the problems linked to the modeling technique, the final pattern recognition performance has been satisfactory, surely not exalting as in the case of the previous applications but definitely remarkable. In particular, the results are very satisfactory if the fact is taken into account that there is a tough discussion about the *real nature* of the EEG signals [Duke and Pritchard, 1991; Pijn *et al.*, 1991; Popivanov and Mineva, 1999; Soong and Stuart, 1989]. Indeed, there are several works [Jaeseung Jeong *et al.*, 1998a,b; Lopes da Silva *et al.*, 1997; Pritchard *et al.*, 1995] claiming that the EEG signals should be embedded in a fifteen/twenty-dimensional space. Thus, because of such a high dimensionality, they can be considered indeed randomly corrupted. Even though that, the proposed modeling technique has been able to fit the interesting features in a simple scalar Lur'e system of seventh order, that in the author's opinion is quite remarkable.

[14] Fourteen parameters minus the constraint of the slope at one point leave thirteen free parameters.

7.3.5 Vowels Detection

This application is suggested by two distinct sources. On one hand, as the other applications, it has been suggested by one of the research projects in which the author's laboratory is involved, namely the speech recognition [Hennebert, 1998; Robert, 1999]. On the other hand, it is suggested by some recent published results [Baier *et al.*, 2000; Miyano *et al.*, 2000], which point definitely in the direction of this thesis showing that the signals associated with vowels can be modeled by chaotic signals.

The main aim of this application is to verify the employability of the proposed technique in n-class classification problems. Indeed, while the previous considered application were binary classification problem the one here considered is a penta-classification problem.

The main idea is to recognize automatically the five Italian vowels (*cfr.* Sect. 2.1.2) using the pattern recognition technique based on qualitative resonance. Taking into account the apparent chaoticity of the signals associated with these vowels, as shown in Sect. 2.1.2, this application represents a good candidate for the approach described in this work.

Obviously, since in this case there are five classes of signals, the framework described in Sect. 7.1 needs to be modified in consequence. The details given in Sect. 7.1.2 remain valid adapting them to a case where five classes are considered. In particular, in this case there are five classes $\mathcal{A}, \mathcal{B}, \mathcal{C}, \mathcal{D}$ and $\mathcal{E}$; five vectors set $\mathsf{A}, \mathsf{B}, \mathsf{C}, \mathsf{D}$ and E with their corresponding training and test subsets X_{Tr} and X_{Ts} ($\mathsf{X} = \mathsf{A}, \mathsf{B}, \mathsf{C}, \mathsf{D}, \mathsf{E}$); and, obviously, there are five qualitatively resonating filters $\mathbf{A}, \mathbf{B}, \mathbf{C}, \mathbf{D}$ and $\mathbf{E}$. The details given in Sect. 7.1.3 remain valid, too, but in this case, the Eq. (7.1), which map the five qualitative resonance functionals in a probability distribution over five symbols, is more complex. In particular, it is given by (*cfr.* Sect. 4.3 and Eq. (4.3))

$$p_{\mathsf{x}} = \frac{\left(\sigma^2_{f\,\mathbf{X}} - \sigma^2_{\mathbf{X}}\right) \prod\limits_{\mathbf{i} \neq \mathbf{X}} \sigma^2_{f\,\mathbf{i}}}{5 \prod\limits_{\mathbf{i}=\mathbf{A}}^{\mathbf{E}} \sigma^2_{f\,\mathbf{i}} - \sum\limits_{\mathbf{i}=\mathbf{A}}^{\mathbf{E}} \prod\limits_{\mathbf{j}=\mathbf{A}}^{\mathbf{i}} \sigma^2_{\mathbf{j}} \prod\limits_{\mathbf{j}=\mathbf{i}}^{\mathbf{E}} \sigma^2_{f\,\mathbf{j}}}$$

where $\sigma^2_{f\,\mathbf{X}}$ and $\sigma^2_{\mathbf{X}}$ $\mathbf{X} = \mathbf{A}, \ldots, \mathbf{E}$ have the same meaning as in Sect. 7.1.3. The learning conditions given in Sect. 7.1.5 need to be modified for this case. In fact, given a filter to tune, which are the good patterns remains clear but it is no longer clear which are the bad patterns. In order not to alter the cardinalities of the sets used for the training, the set of hundred bad patterns has been composed randomly drawing twenty-five vectors from each one of the four sets complementary to the good patterns set. Finally, for this application the results of the classification tests will be given by means of 5×5 matrices. All the rest stays as described in Sect. 7.1.

The problem is to distinguish from each other the five vowels signals which approximately look as in Figs. 7.33-7.37. In particular, the [a:] vowels which look approximately as in Fig. 7.33, class $\mathcal{A}$; the [e] vowels which look approximately as in Fig. 7.34, class $\mathcal{B}$; the [i] vowels which look approximately as in Fig. 7.35, class $\mathcal{C}$; the [ɔ] vowels which look approximately as in Fig. 7.36, class $\mathcal{D}$; the [u] vowels which look approximately as in Fig. 7.37, class $\mathcal{E}$.

The observations to compose the $\mathsf{A} - \mathsf{E}$ sets of vectors have been obtained recording fifty sustained pronunciations, of two seconds each (*i.e.* about four-hundreds pseudo-period each), for each of the above mentioned vowels, *cfr.* Sect. 2.1.2. The recording has been done using the sound card[15] of a personal computer with a normal microphone[16]. The recording has been done at a sampling frequency of $44.1 KHz$ and at a resolution of sixteen bits/sample.

[15] A SoundBlaster compatible.
[16] Not a professional microphone.

SIGNALS

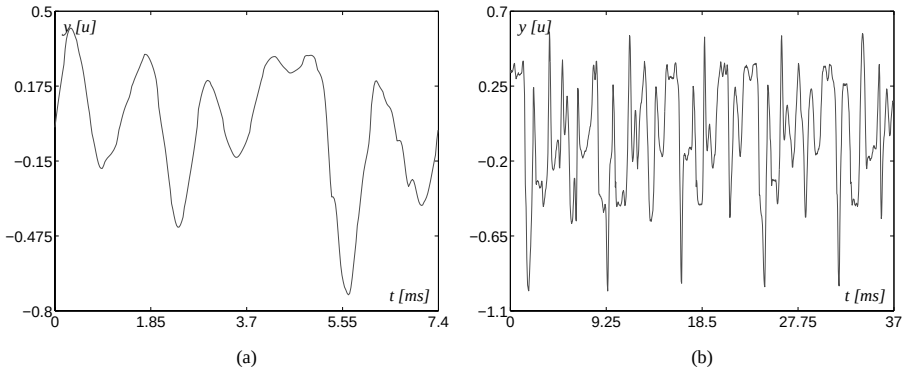

Figure 7.33: *The class $\mathcal{A}$ patterns, the [a:] vowels: (a) – the pattern prototype; (b) – a typical observation.*

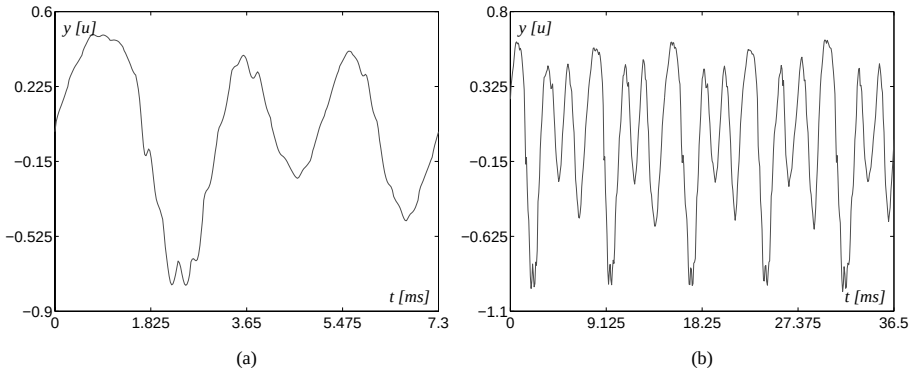

Figure 7.34: *The class $\mathcal{B}$ patterns, the [e] vowels: (a) – the pattern prototype; (b) – a typical observation.*

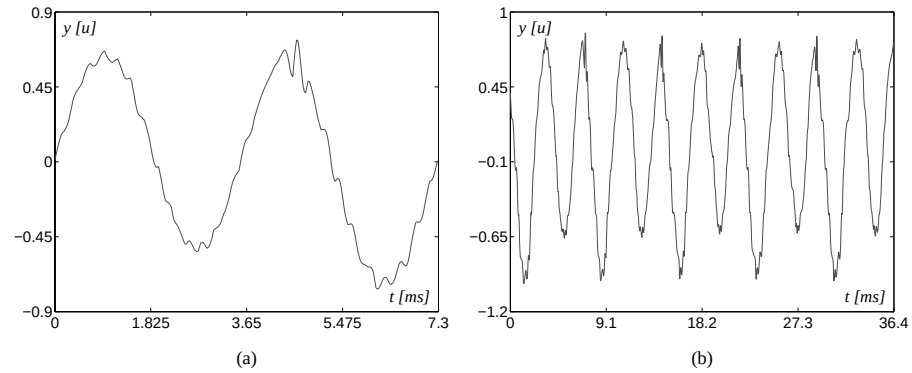

Figure 7.35: *The class $\mathcal{C}$ patterns, the [i] vowels: (a) – the pattern prototype; (b) – a typical observation.*

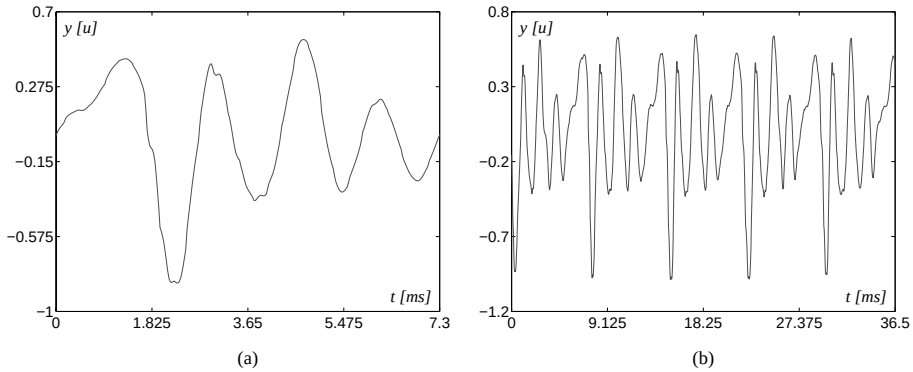

Figure 7.36: *The class $\mathcal{D}$ patterns, the [ɔ] vowels: (a) – the pattern prototype; (b) – a typical observation.*

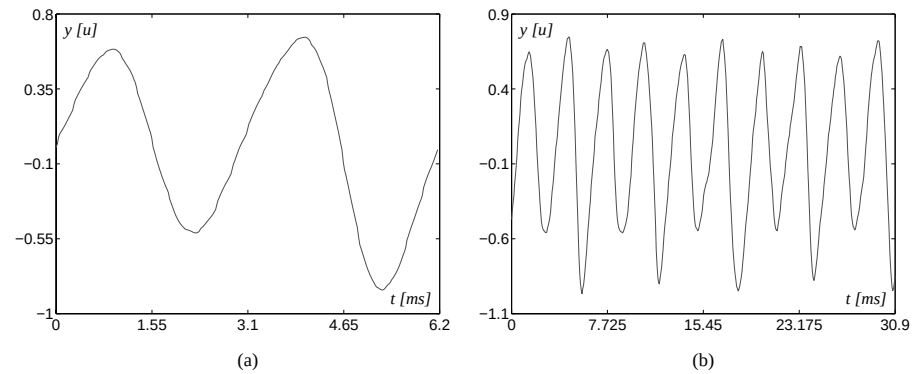

Figure 7.37: *The class $\mathcal{E}$ patterns, the [u] vowels: (a) – the pattern prototype; (b) – a typical observation.*

Modeling Results

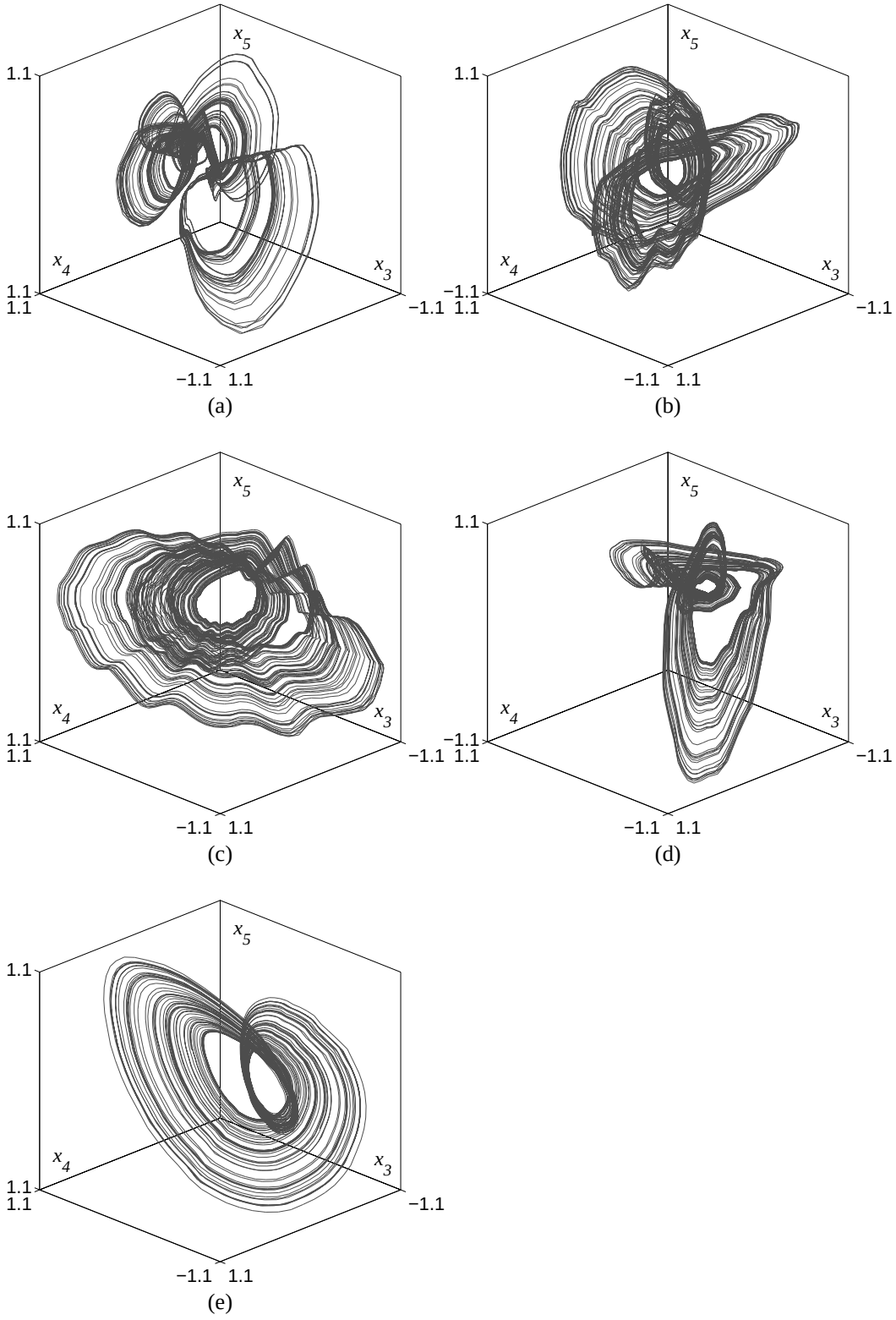

Figure 7.38: *Three-dimensional projection of the free Feigenbaum-like strange attractors resulting from the first step of modeling,* i.e. *identification: (a) – filter* **A**, *the [a:] vowels; (b) – filter* **B**, *the [e] vowels; (c) – filter* **C**, *the [i] vowels; (d) – filter* **D**, *the [ɔ] vowels; (e) – filter* **E**, *the [u] vowels.*

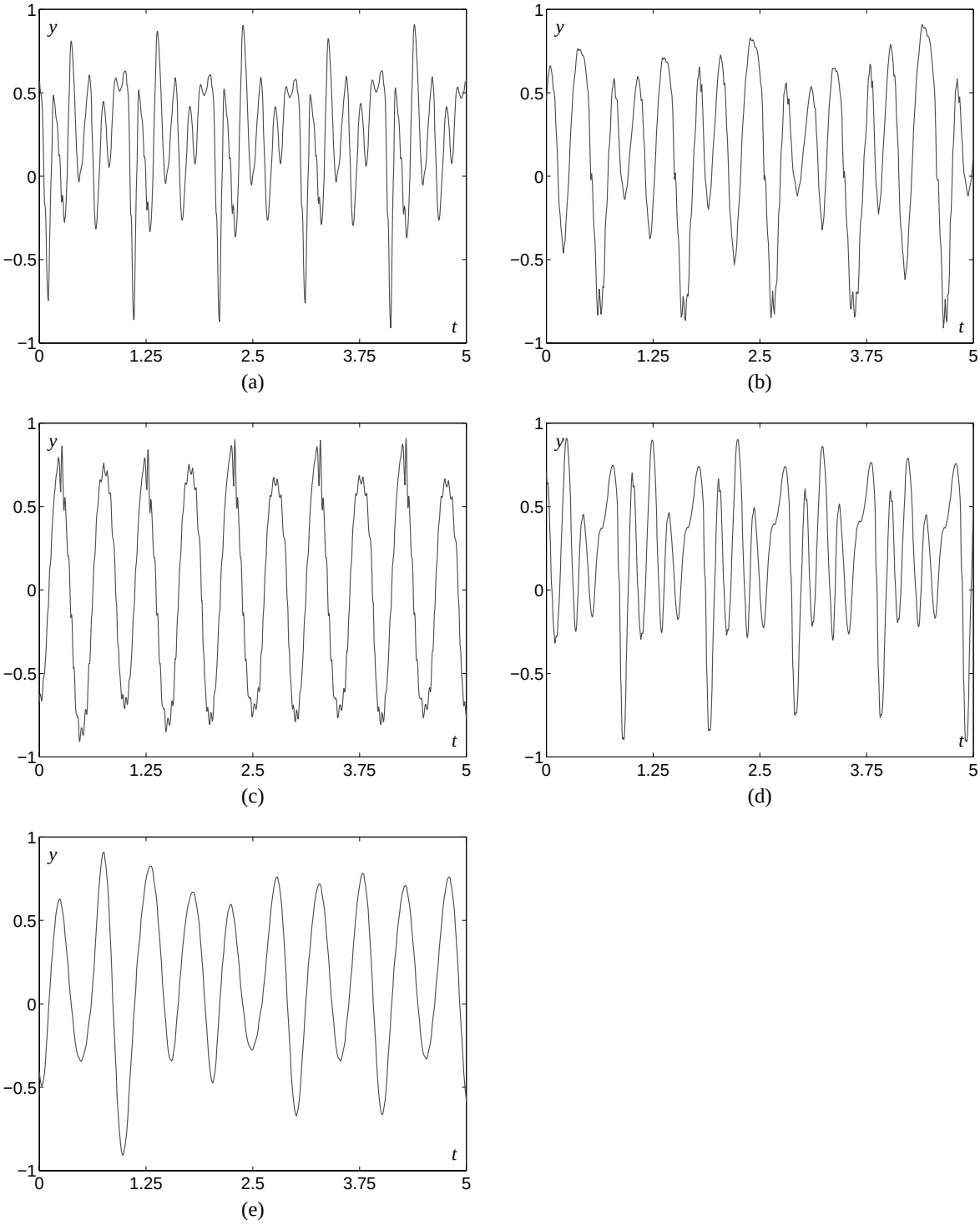

Figure 7.39: *Output of the filters corresponding to the free Feigenbaum-like strange attractors shown in Fig. 7.38: (a) – filter* **A**, *the [a:] vowels; (b) – filter* **B**, *the [e] vowels; (c) – filter* **C**, *the [i] vowels; (d) – filter* **D**, *the [ɔ] vowels; (e) – filter* **E**, *the [u] vowels.*

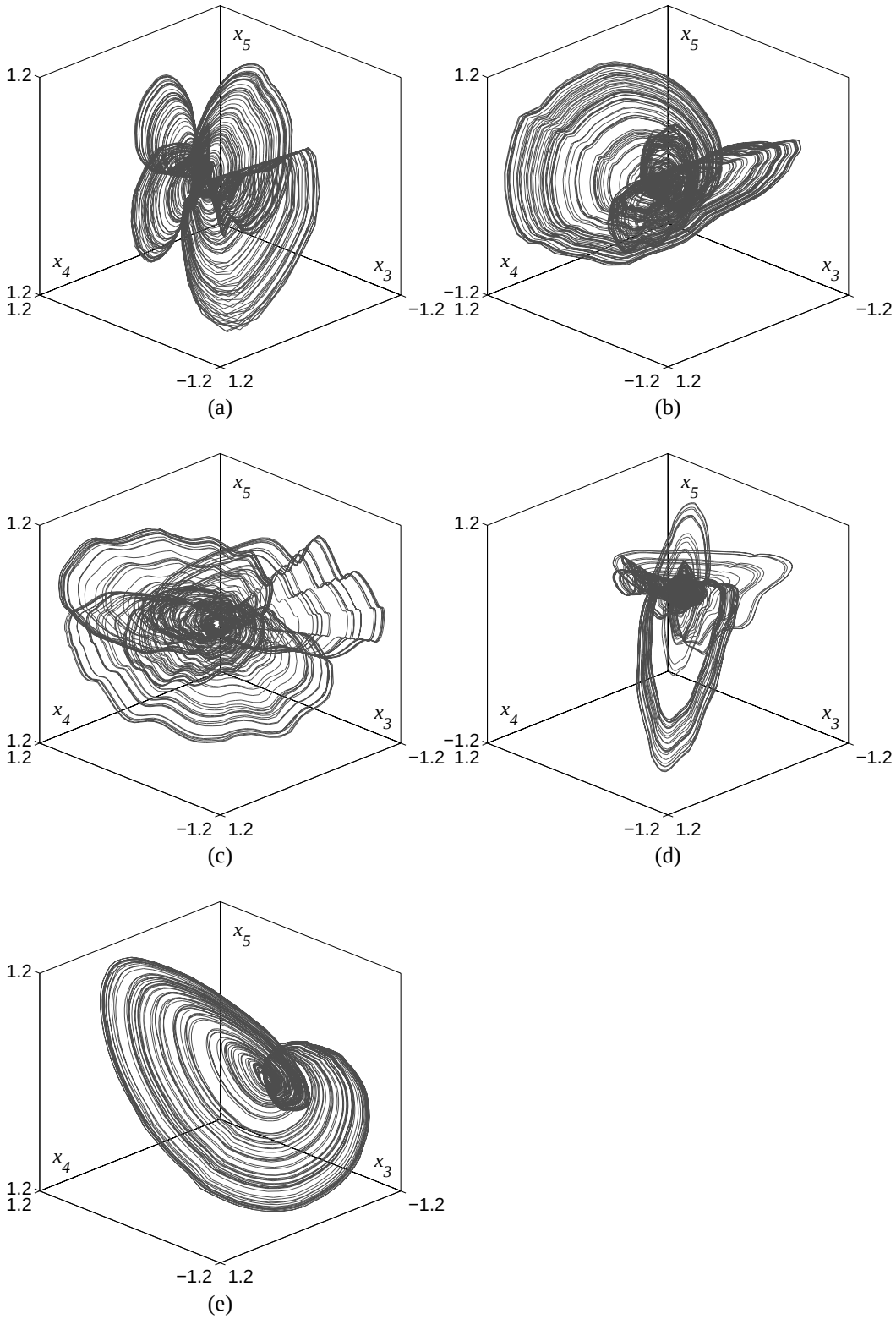

Figure 7.40: *Three-dimensional projection of the free Shil'nikov-like strange attractors resulting from the second step of modeling,* i.e. *period climbing: (a) – filter* **A**, *the [a:] vowels; (b) – filter* **B**, *the [e] vowels; (c) – filter* **C**, *the [i] vowels; (d) – filter* **D**, *the [ɔ] vowels; (e) – filter* **E**, *the [u] vowels.*

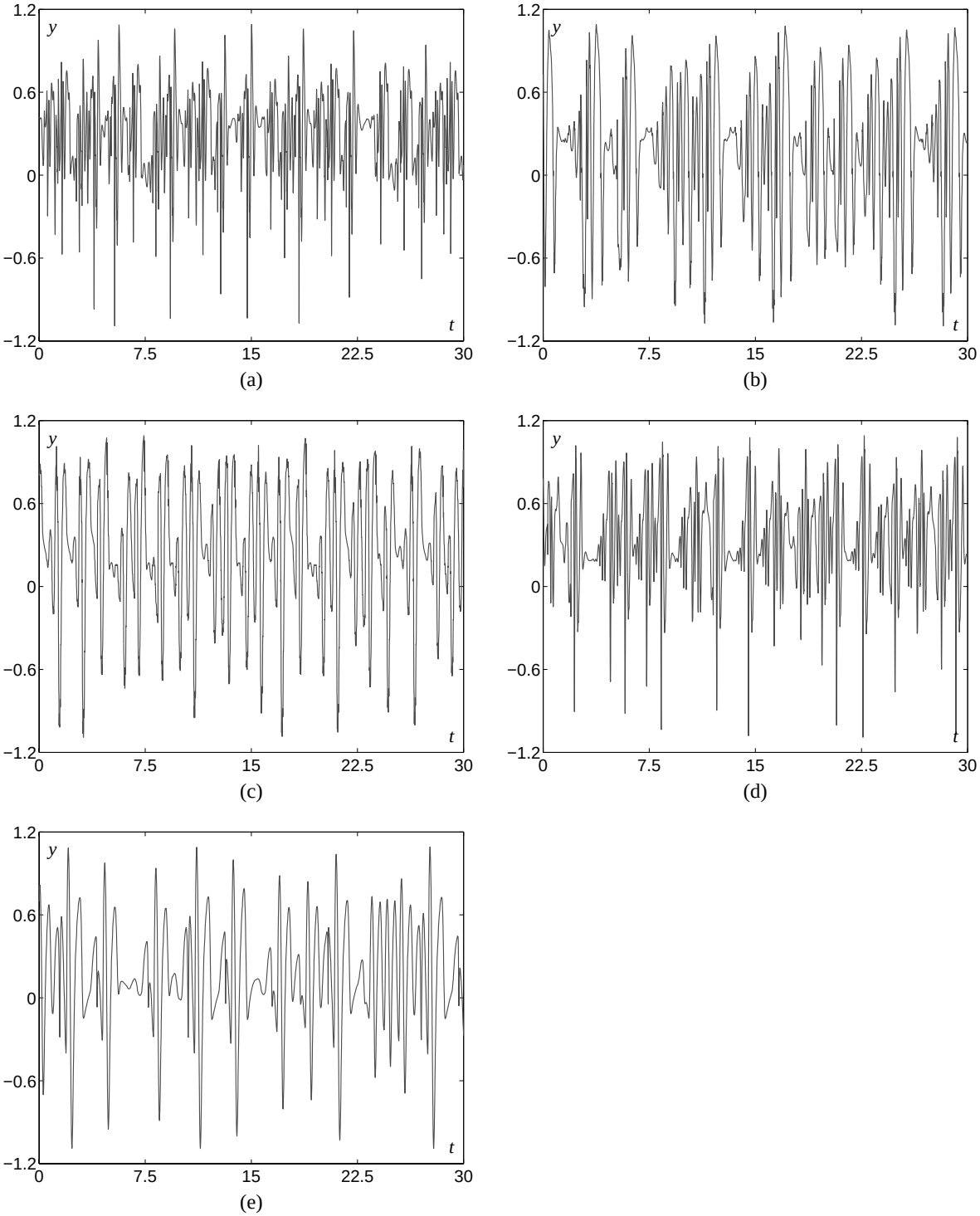

Figure 7.41: *Output of the filters corresponding to the free Shil'nikov-like strange attractors shown in Fig. 7.40: (a) – filter* **A**, *the [a:] vowels; (b) – filter* **B**, *the [e] vowels; (c) – filter* **C**, *the [i] vowels; (d) – filter* **D**, *the [ɔ] vowels; (e) – filter* **E**, *the [u] vowels.*

FILTER GAIN TUNING RESULTS

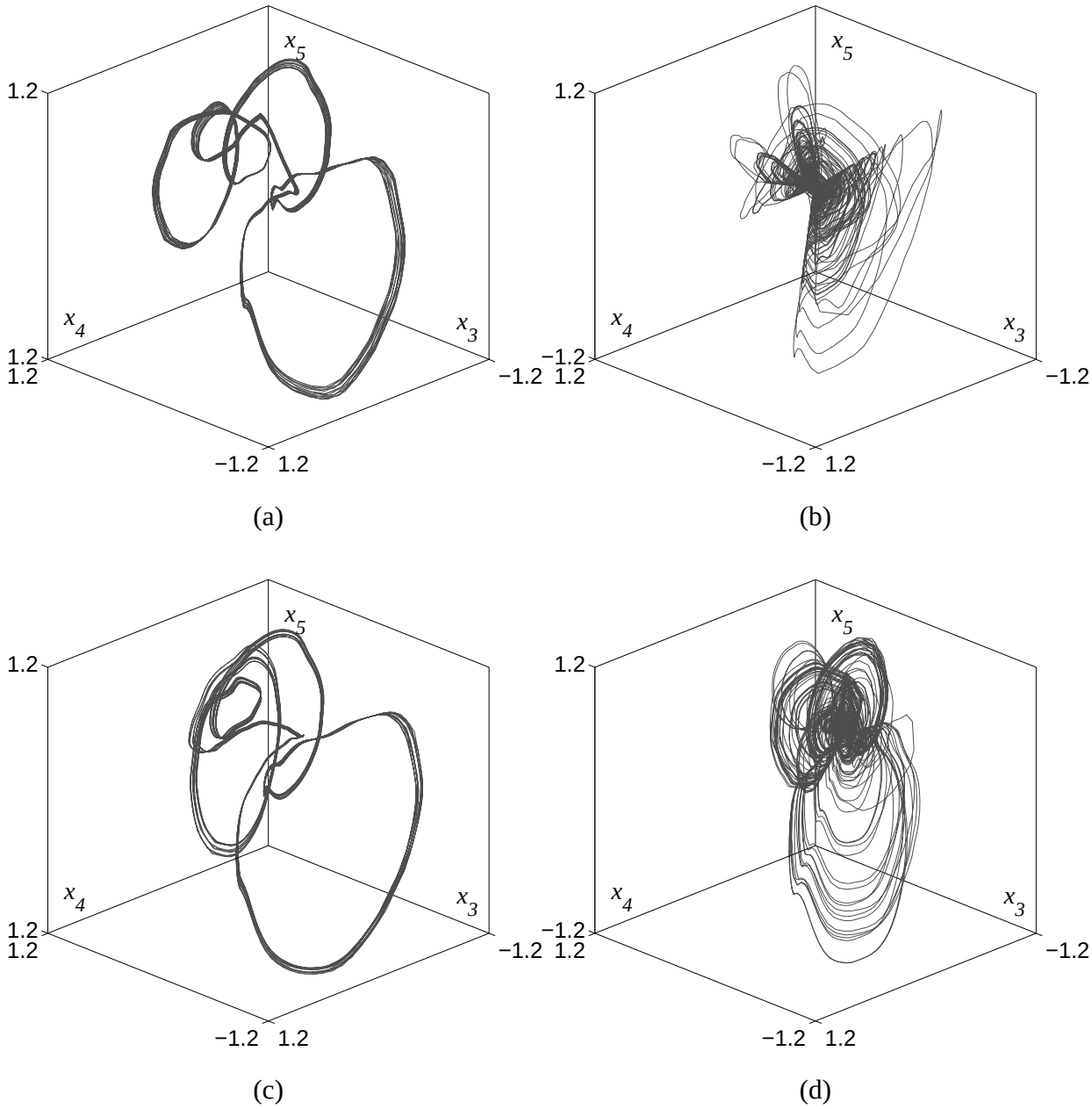

Figure 7.42: *Three-dimensional projection of the behavior in the state space of the driven filter* $\mathbf{A}$, i.e. *the [a:] vowel detector: (a) – correctly resonating with a class* $\mathcal{A}$ *signal,* i.e. *a [a:] vowel; (b) – correctly anti-resonating with a class* $\mathcal{B} \uplus \mathcal{C} \uplus \mathcal{D} \uplus \mathcal{E}$ *signal,* i.e. *another vowel; (c) – wrongly resonating with a class* $\mathcal{B} \uplus \mathcal{C} \uplus \mathcal{D} \uplus \mathcal{E}$ *signal,* i.e. *another vowel; (d) – wrongly anti-resonating with a class* $\mathcal{A}$ *signal,* i.e. *a [a:] vowel.*

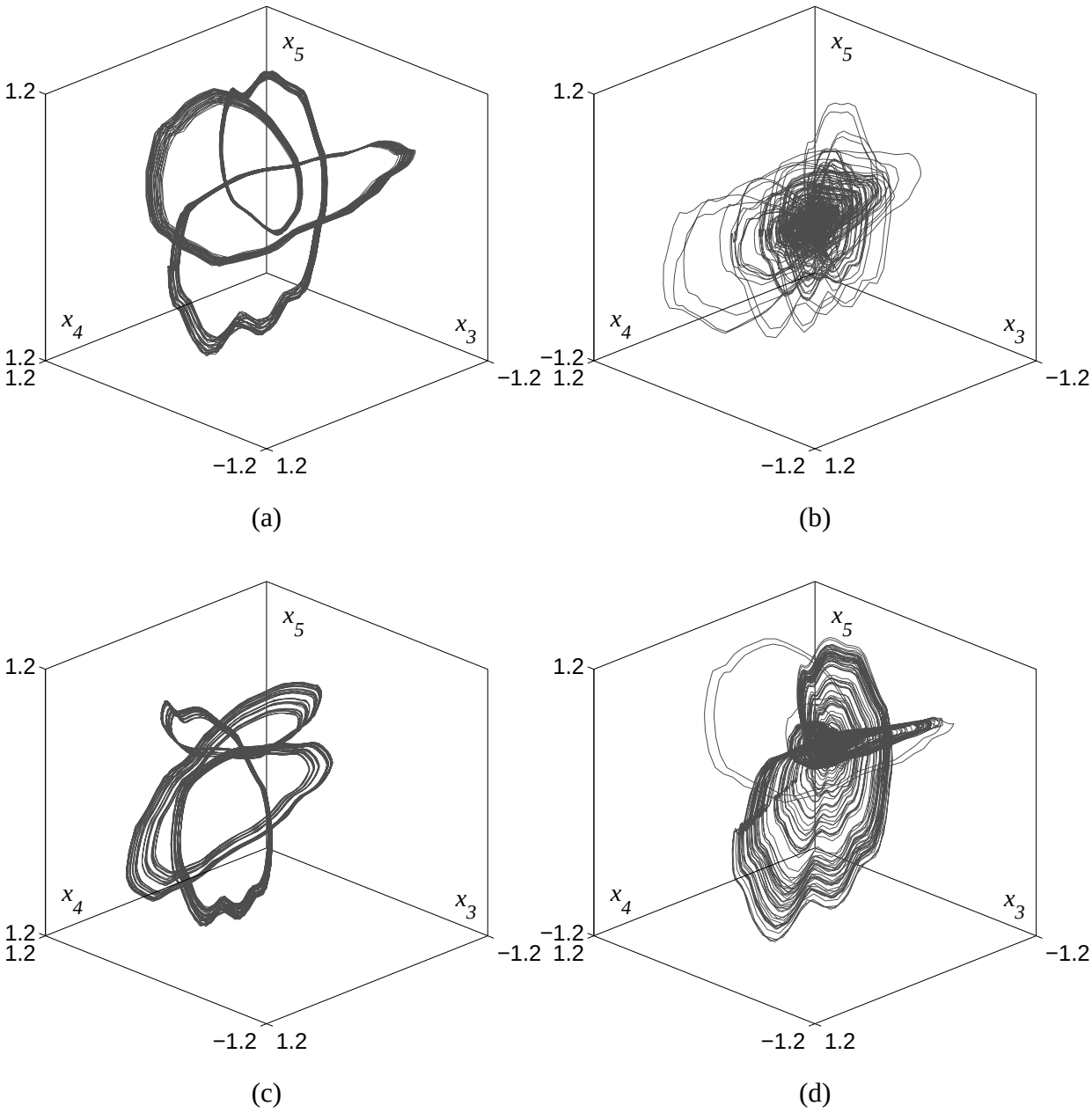

Figure 7.43: *Three-dimensional projection of the behavior in the state space of the driven filter* $\mathbf{B}$, i.e. *the [e] vowel detector: (a) – correctly resonating with a class* $\mathcal{B}$ *signal,* i.e. *a [e] vowel; (b) – correctly anti-resonating with a class* $\mathcal{A} \uplus \mathcal{C} \uplus \mathcal{D} \uplus \mathcal{E}$ *signal,* i.e. *another vowel; (c) – wrongly resonating with a class* $\mathcal{A} \uplus \mathcal{C} \uplus \mathcal{D} \uplus \mathcal{E}$ *signal,* i.e. *another vowel; (d) – wrongly anti-resonating with a class* $\mathcal{B}$ *signal,* i.e. *a [e] vowel.*

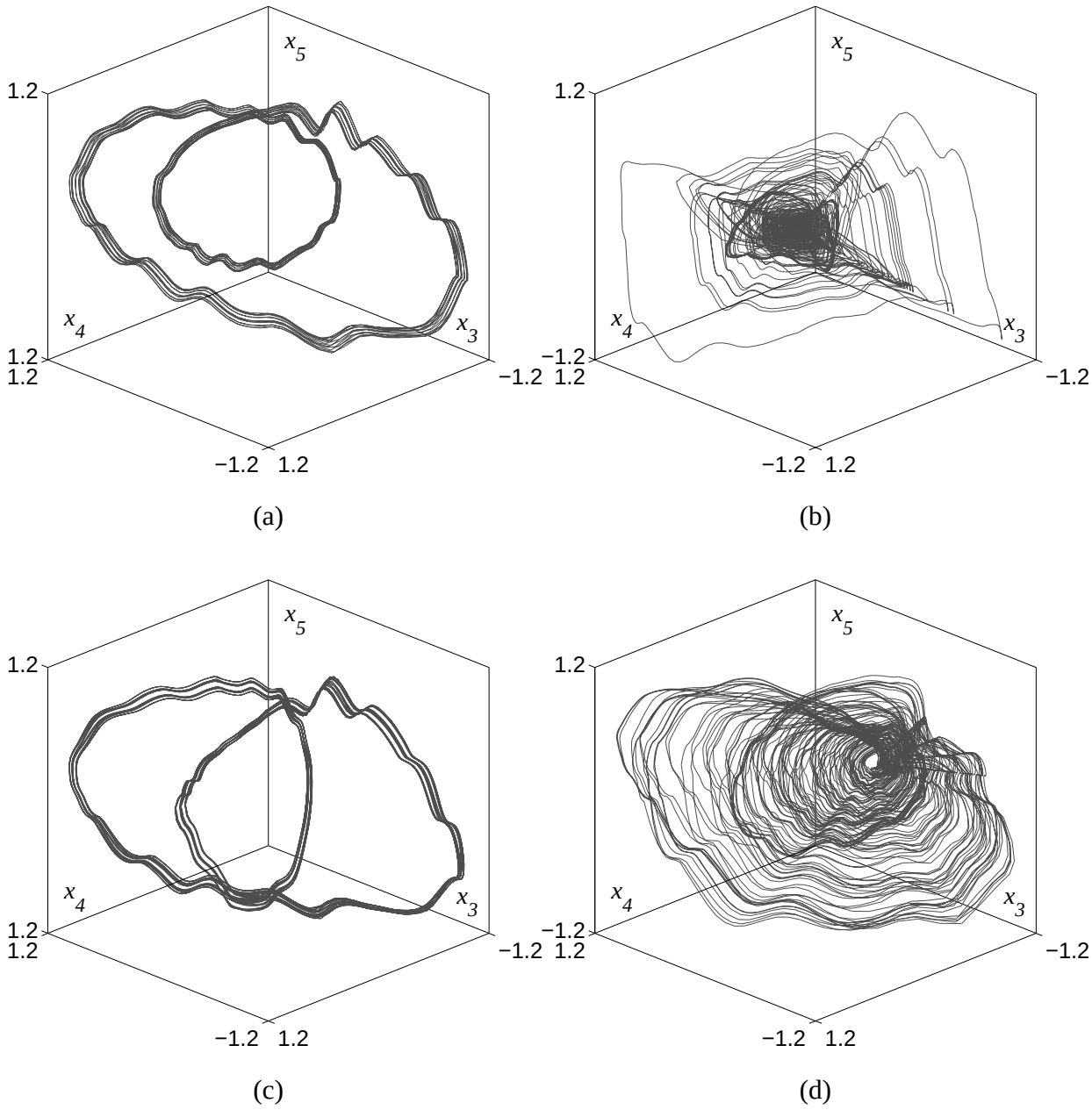

Figure 7.44: *Three-dimensional projection of the behavior in the state space of the driven filter* $\mathbf{C}$*,* i.e. *the [i] vowel detector: (a) – correctly resonating with a class* $\mathcal{C}$ *signal,* i.e. *a [i] vowel; (b) – correctly anti-resonating with a class* $\mathcal{A} \uplus \mathcal{B} \uplus \mathcal{D} \uplus \mathcal{E}$ *signal,* i.e. *another vowel; (c) – wrongly resonating with a class* $\mathcal{A} \uplus \mathcal{B} \uplus \mathcal{D} \uplus \mathcal{E}$ *signal,* i.e. *another vowel; (d) – wrongly anti-resonating with a class* $\mathcal{C}$ *signal,* i.e. *a [i] vowel.*

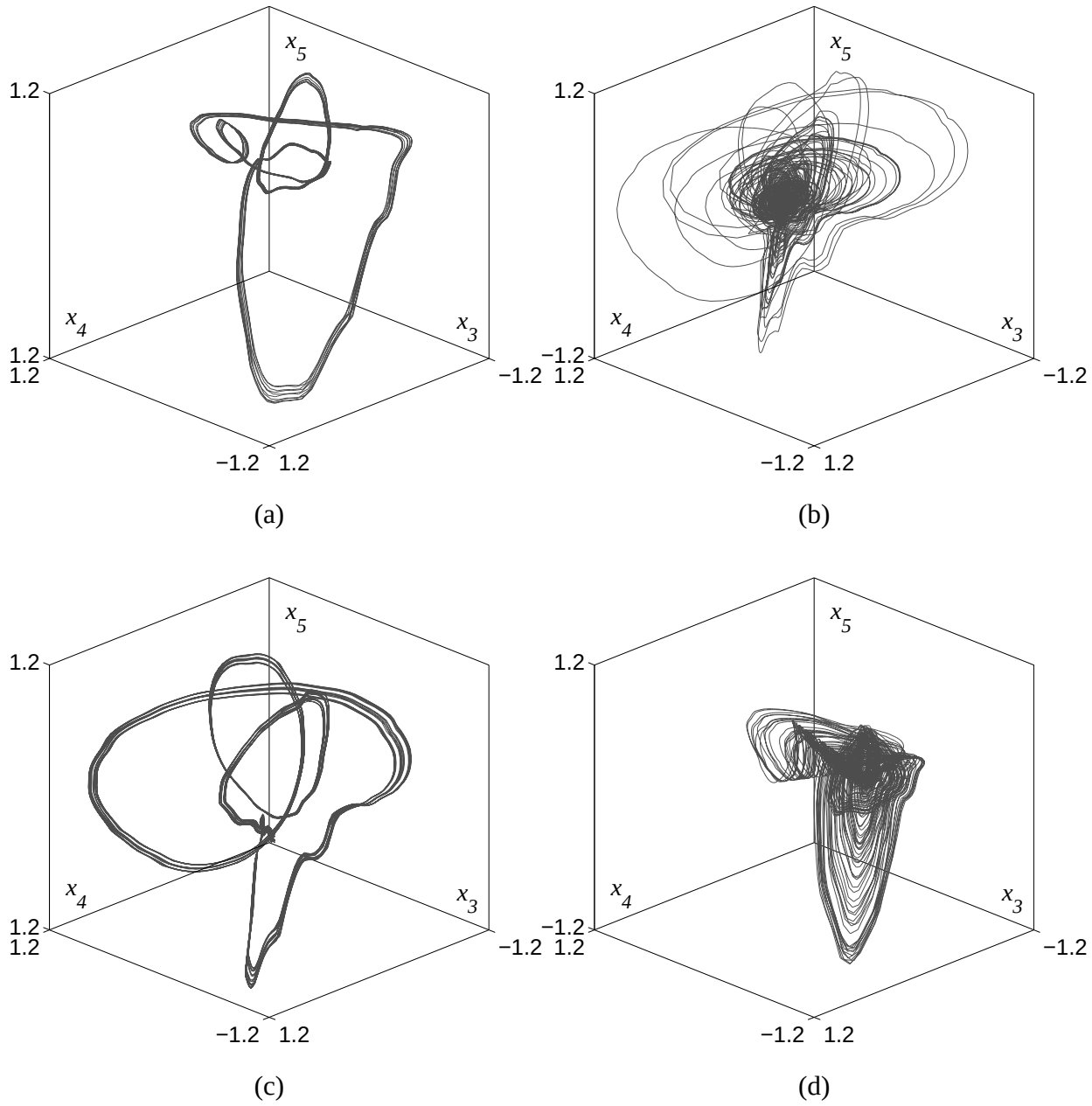

Figure 7.45: *Three-dimensional projection of the behavior in the state space of the driven filter* $\mathbf{D}$*,* i.e. *the [ɔ] vowel detector: (a) – correctly resonating with a class* $\mathcal{D}$ *signal,* i.e. *a [ɔ] vowel; (b) – correctly anti-resonating with a class* $\mathcal{A} \uplus \mathcal{B} \uplus \mathcal{C} \uplus \mathcal{E}$ *signal,* i.e. *another vowel; (c) – wrongly resonating with a class* $\mathcal{A} \uplus \mathcal{B} \uplus \mathcal{C} \uplus \mathcal{E}$ *signal,* i.e. *another vowel; (d) – wrongly anti-resonating with a class* $\mathcal{D}$ *signal,* i.e. *a [ɔ] vowel.*

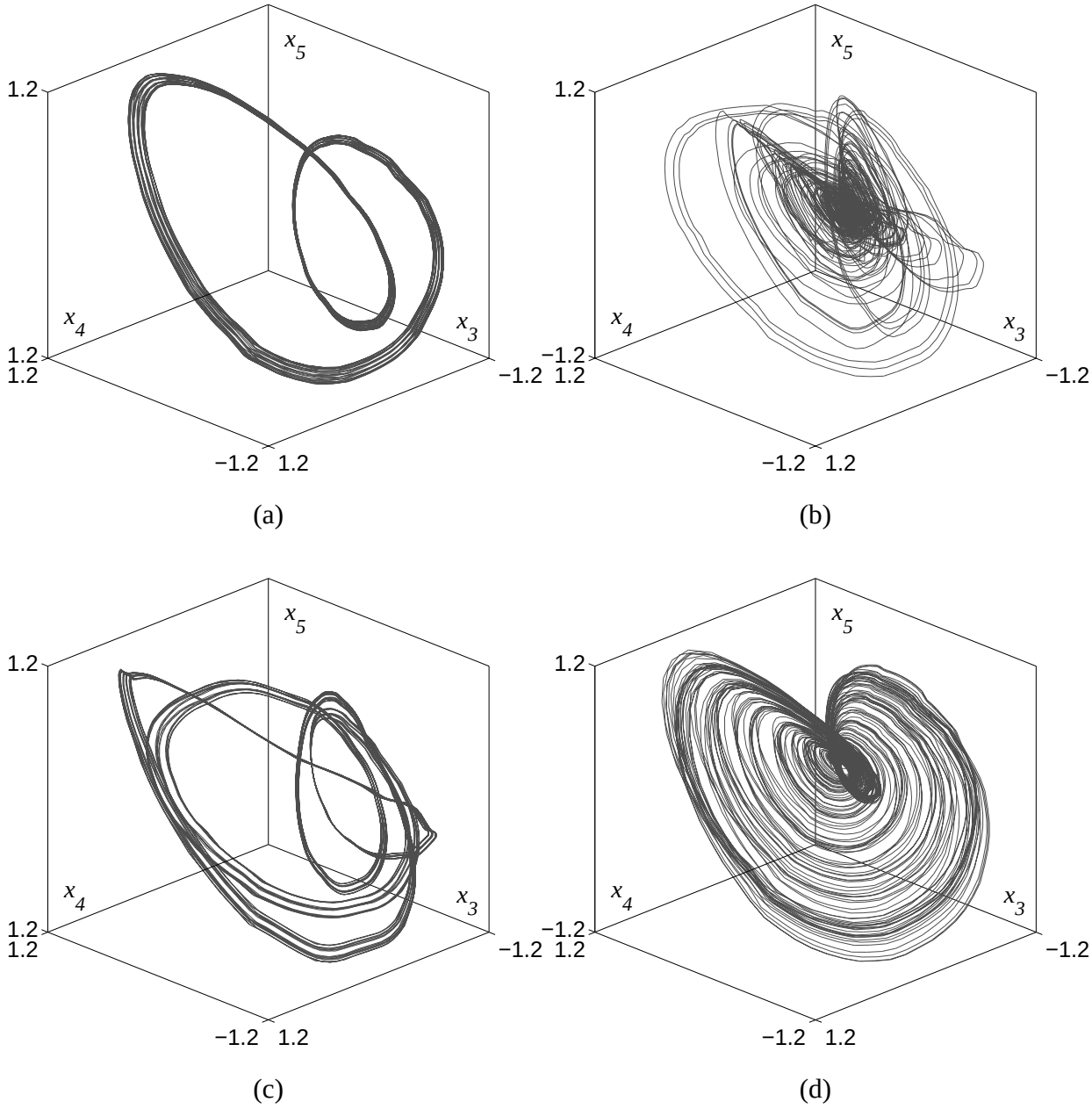

Figure 7.46: *Three-dimensional projection of the behavior in the state space of the driven filter* $\mathbf{E}$*,* i.e. *the [u] vowel detector: (a) – correctly resonating with a class* $\mathcal{E}$ *signal,* i.e. *a [u] vowel; (b) – correctly anti-resonating with a class* $\mathcal{A} \uplus \mathcal{B} \uplus \mathcal{C} \uplus \mathcal{D}$ *signal,* i.e. *another vowel; (c) – wrongly resonating with a class* $\mathcal{A} \uplus \mathcal{B} \uplus \mathcal{C} \uplus \mathcal{D}$ *signal,* i.e. *another vowel; (d) – wrongly anti-resonating with a class* $\mathcal{E}$ *signal,* i.e. *a [u] vowel.*

Classification Tests Results

average

in \ as	$\mathcal{A}$	$\mathcal{B}$	$\mathcal{C}$	$\mathcal{D}$	$\mathcal{E}$
$\mathcal{A}$	90.88%	5.47%	1.90%	0.51%	1.24%
$\mathcal{B}$	3.15%	93.27%	0.33%	2.76%	0.49%
$\mathcal{C}$	2.16%	2.11%	91.82%	2.09%	1.82%
$\mathcal{D}$	1.48%	1.68%	1.49%	93.62%	1.73%
$\mathcal{E}$	1.40%	1.28%	1.18%	1.39%	94.75%

best

in \ as	$\mathcal{A}$	$\mathcal{B}$	$\mathcal{C}$	$\mathcal{D}$	$\mathcal{E}$
$\mathcal{A}$	94.50%	3.30%	0.74%	1.33%	0.13%
$\mathcal{B}$	2.00%	93.61%	0.39%	3.09%	0.91%
$\mathcal{C}$	0.19%	0.18%	99.29%	0.19%	0.15%
$\mathcal{D}$	1.32%	1.27%	1.45%	94.54%	1.42%
$\mathcal{E}$	0.87%	0.84%	0.86%	0.76%	96.67%

worst

in \ as	$\mathcal{A}$	$\mathcal{B}$	$\mathcal{C}$	$\mathcal{D}$	$\mathcal{E}$
$\mathcal{A}$	90.11%	5.94%	0.58%	1.53%	1.84%
$\mathcal{B}$	4.47%	91.08%	0.04%	2.78%	1.63%
$\mathcal{C}$	2.63%	2.68%	89.73%	2.47%	2.49%
$\mathcal{D}$	1.86%	1.81%	1.83%	92.79%	1.71%
$\mathcal{E}$	1.91%	1.90%	1.73%	1.91%	92.55%

Table 7.9: *Results on the training set, only the vectors used for learning are classified,* i.e. *the vectors belonging to* X_{Tr}, $\mathsf{X} = \mathsf{A}, \mathsf{B}, \mathsf{C}, \mathsf{D}, \mathsf{E}$.

average

in \ as	$\mathcal{A}$	$\mathcal{B}$	$\mathcal{C}$	$\mathcal{D}$	$\mathcal{E}$
$\mathcal{A}$	85.33%	8.80%	2.60%	1.09%	2.18%
$\mathcal{B}$	6.05%	87.38%	1.19%	3.56%	1.82%
$\mathcal{C}$	3.71%	2.39%	86.41%	2.41%	5.08%
$\mathcal{D}$	3.05%	2.54%	3.23%	89.52%	1.66%
$\mathcal{E}$	1.92%	2.06%	2.92%	3.18%	89.92%

best

in \ as	$\mathcal{A}$	$\mathcal{B}$	$\mathcal{C}$	$\mathcal{D}$	$\mathcal{E}$
$\mathcal{A}$	93.52%	3.89%	0.74%	0.60%	1.25%
$\mathcal{B}$	4.33%	94.10%	0.29%	0.33%	0.95%
$\mathcal{C}$	2.46%	2.73%	91.05%	2.17%	1.59%
$\mathcal{D}$	1.46%	1.71%	1.34%	94.72%	0.77%
$\mathcal{E}$	2.28%	1.81%	1.45%	1.68%	92.78%

worst

in \ as	$\mathcal{A}$	$\mathcal{B}$	$\mathcal{C}$	$\mathcal{D}$	$\mathcal{E}$
$\mathcal{A}$	83.36%	9.98%	3.81%	1.92%	0.93%
$\mathcal{B}$	8.52%	85.81%	1.98%	0.71%	2.98%
$\mathcal{C}$	4.43%	6.30%	80.05%	4.33%	4.89%
$\mathcal{D}$	2.21%	2.39%	2.72%	89.47%	3.21%
$\mathcal{E}$	3.37%	3.68%	3.52%	3.63%	85.80%

Table 7.10: *Results on the test set, only the vectors not used for learning are classified,* i.e. *the vectors belonging to* X_{Ts}, $\mathsf{X} = \mathsf{A}, \mathsf{B}, \mathsf{C}, \mathsf{D}, \mathsf{E}$.

Problems and Discussion

The application presented here is definitely the most complex one that has been considered in this work. Despite of this complexity, only one new problem emerged dealing with this application. This has been the problem of nonstationary of the recorded signals, because of that it has been necessary to manually segment them. On the other hand, practically, only those problems already mentioned occurred.

More precisely, the main problem has been, once again, the stability of the filter. The solution to this problem has been the same as for the case of the previous application (Sect. 7.3.4).

The problem of indistinguishability has been mainly caused by the [a:] vowel signals. Indeed, for this signal, as for the EEG, the smoothed piecewise linear nonlinearity, as well as the fourth order model, has proved to be insufficient. The problem has been solved using the first fourteen Tchebyshev polynomials with a fifth order model. Although only the [a:] vowel signals needed this more complex modeling, for the other

vowel signals the model described in Sect. 7.1.4 was sufficient, for sake of symmetry[17] all the signals have been modeled with this model.

No particular cases of overfitting have been observed during the test sessions. It is the author's opinion that the reason for this is that the indistinguishability problem has been immediately addressed with the Tchebyshev polynomials without trying to augment the segments of the smoothed piecewise linear nonlinearity.

The results summarized in the Tabs. 7.9-7.10 are definitely remarkable. Indeed, the diagonals of all the matrices clearly highlight a peak of qualitative resonance, thus of correct classification. This was not taken for granted given the complexity of the overall filter.

From attentive examination of the Tabs. 7.9-7.10 would emerge a slight problem of indistinguishability of the [a:] and [e] vowels. Indeed, the corresponding entries in the matrices are oddly high. This problem in particular has not been addressed during the tests.

7.4 Final Remarks on the Overall Results

On the bases of the results obtained in the previous sections it is possible to draw some general conclusion about the proposed chaos-based modeling technique of diversity, about its possible application in pattern recognition, and about the main problems concerning it.

7.4.1 Assessing the Modeling Technique

The modeling technique has proved to be definitely successful. Indeed, for all the applications considered it has been possible, more or less easily, to build a chaotic model for the diversity of the approximately periodic signals considered.

Obviously, the chosen applications were the most promising ones for this technique, *cfr.* Sect. 2.6. Therefore, the enthusiasm for the results must be counterbalanced by the awareness that in other applications this technique could be less successful.

7.4.2 Assessing the Pattern Recognition Application

The results of the pattern recognition tests show that the average results are definitely meaningful. Indeed, they are not very different from the results in the worst and best case. Since the average scores are rather good, usually more than the 85% of vectors are correctly classified, it follows that the proposed technique could indeed be taken into account for real applications.

The effective employability of the proposed technique is further confirmed by the definitely good score in the worst case, usually more than 75%. Such a good score for the worst case confirms the fact that the qualitatively resonating filters indeed perform some association between the driving signal and their internal model and seldom draw randomly their answer, which would correspond to a score of 50% of right classification.

On the other hand, unfortunately, the definitely not exciting score of the best case should be taken into account. Indeed, it could suggests that whatever is possible to squeeze from this technique is already squeezed. In reality, this is not true since there are a lot of unexploited degrees of freedom that are still available, *cfr.* Sect. 7.1. Furthermore, it should not be forgot that the qualitatively resonating filter is supposed to be just a preprocessor, all the statistical-based postprocessing, *i.e.* the statistical-based pattern recognition [Duda and Hart, 1973; Kosko, 1992; Vapnik, 1995], is still available to improve the score.

7.4.3 Problems

As already mentioned in the introductory paragraph, there are mainly two classes of problems. Those related to the tuning of the qualitatively resonating filters and those related to the pattern recognition application. From the tests clearly two main recurrent problems emerged, one for each of these two classes.

[17] The author hates asymmetries.

Problems at Tuning Level

When building the qualitatively resonating filter the main problem encountered has been to ensure the stability of the strange invariant embedded in the filter. Indeed, the simple constraint used (*cfr.* Sect. 7.1.5) has proved to be insufficient most of the time. Note that ensuring the stability of a locally unstable object, *i.e.* a strange attractor, is not a trivial task (*cfr.* Sects. 5.1.4 and 5.1.5) [Kapitaniak and Brindley, 1996].

The second problem that could occur is that of overfitting the filters. Practically, this problem has never been seriously met in the test runs. This does not mean that this problem is negligible. Indeed, it does not occur so often in the tests simply because of the very simple model considered for the filters, which is more easily insufficient rather than overperforming. In the tentative of pushing the performances, the overfitting could turn out to be a tough problem in tradeoff with the indistinguishability problem, as already mentioned and further discussed later.

Problems at Pattern Recognition Level

From the application point of view, the strongest problem encountered has been the indistinguishability of the signals from the two considered classes. Namely, it has happened often that the construction of the two isolated chaotic models for the two considered classes of signals perfectly succeeded. Unfortunately, the two obtained models resulted too similar to each other such that it was not possible to use them to distinguish the two classes of signals exploiting the qualitative resonance, *i.e.* the filters were resonating with signals coming from both the classes. As previously mentioned in the introductory paragraph, there are mainly three possible reasons for the occurrence of this problem.

1. *Too simple model*: the model considered for the identification is too simple. This could be because the linear dynamical system has too low order or because the nonlinearity considered is too simple. If, on the one hand, this problem could be solved by augmenting the complexity of the considered model, on the other hand this could lead to the problem of overfitting. This has been indeed the case in the applications considered.

2. *Lur'e restriction*: this is just another side of the *too simple model* medal. Indeed, the considered model could result too simple not because of its order or because of the nonlinearity but because the scalar Lur'e model could be structurally insufficient.

3. *Structural indistinguishability*: it could happen that the two classes of signals are indeed produced by the very same dynamical system or by two very similar ones. In such a case, it would be the entire method that would be structurally inapt for the classification of the two kinds of signals. A deeper discussion of this problem is given in [Pitarelli, 2001].

   It is not difficult to imagine an example of such a case. Consider, for instance, the classification of Feigenbaum-like and Shil'nikov-like signals coming from the same system, in this case it is clear that for tautology[18] the system would fail. An example of application which requires such a kind of classification is given in [Maggio and De Feo, 2000].

From the problems encountered when dealing with the specific applications it could be concluded that the indistinguishability problem is simply the peak of an iceberg. Namely, an oddly strong sensitivity of the proposed technique with respect to the complexity of the model used for the identification.

7.4.4 General Remarks

Before concluding there are two general remarks which deserve attention.

In all the applications considered above, the two classes of signals are usually easily distinguishable by means of more common techniques as frequency domain analysis and similar[19]. As already mentioned several times, the aim of this thesis is not to compete with the common techniques of pattern recognition but rather to propose a new chaos-based modeling technique for diversity. Hence, the fact that these signals could be classified with other techniques is not of main importance for this work. The important result is that the diversity of these signals can indeed be modeled by means of a chaotic dynamical system and the fact that this kind of model can be successfully employed for pattern recognition purposes.

[18] In this case the box and its content would coincide.
[19] Multi-resolution analysis as with wavelets or with finite time FFT.

Referring to the pattern recognition application of the proposed modeling technique it should be noted that all the tests have been run offline. In particular, the signals have been normalized and filtered before being used, both for the training and for the tests. While on a theoretical base it should not be a problem to implement the filter online, in practice this could reserve some undesired surprise. It is clear that time and amplitude scaling should not alter the results as well as the lowpass filtering that could be realized online. The real problem would reside in the time length of the signal that needs to be recognized. Indeed, as discussed in Sect. 3.4, for the qualitative resonance to happen it is necessary that the randomly changing phase of the filter and the fixed phase of the feeding signal align. While in the tests run this has never been a problem, the hundred-thirty-eight pseudo-periods have been always enough to achieve such a condition, in real applications, for instance pattern spotting, so many pseudo-periods might be not available.

Bibliography

AHA (2001). *Heart and Stroke A-Z Guide*. American Heart Association, http://www.americanheart.org/.

Alder, M. (1994). *Principles of Pattern Classification: Statistical, Neural Net and Syntactic Methods of Getting Robots to See and Hear*. Not published. Freely available on the world wide web: ftp://ciips.ee.uwa.edu.au/pub/syntactic/book,http://ciips.ee.uwa.edu.au/ mike/PatRec/.

Arfken, G. and H. Weber, editors (1995). *Mathematical Methods for Physicists*. Academic Press, Orlando, FL, fourth edition.

Baher, H. (1990). *Analog & Digital Signal Processing*. John Wiley & Sons, New York, NY.

Baier, N., T. Schimming, and O. De Feo (2000). Nonlinear structures in voiced speech signals. In *International Conference on Nonlinear Theory and its Applications NOLTA*. Dresden, Germany.

Belhaq, M. and A. Fahsi (1996). Homoclinic bifurcations in self-excited oscillators. *Mechanics Research Communications*, 23, pp. 381–386.

Bittanti, S. (2000). *Identificazione dei Modelli e Controllo Adattativo*. Pitagora, Bologna, 2000.

Brogan, W. (1996). *Modern Control Theory*. Prentice-Hall, New York, NY, third edition.

Bronzino, J., editor (1995). *The Biomedical Engineering Handbook*. CRC Press for IEEE Press, Boca Raton, FL.

Cherkassky, V. and F. Mulier (1998). *Learning from Data: Concepts, Theory and Methods*. John Wiley & Sons, New York, NY.

Costa, M., I. Pimentel, T. Santiago, P. Sarreira, J. Melo, and E. Ducla-Soares (1999). No evidence of chaos in the heart rate variability of normal and cardiac transplant human subjects. *Journal of Cardiovascular Electrophysiology*, 10, pp. 1350–1357.

Dasgupta, D. and D. McGregor (1992). SGA: A structured genetic algorithm. Department of computer science, University of Strathclyde, Glasgow, UK.

Dasgupta, D. and D. McGregor (1994). A more biologically motivated genetic algorithm: The model and some results. *Cybernetics and Systems*, 25, pp. 447–469.

De Feo, O. and G. Maggio (2001). Bifurcations in the Colpitts oscillator: Theory versus experiments. *IEEE Transaction on Circuit and Systems—I*. Submitted.

de Luna, A. B. (1998). *Clinical Electrocardiography: A Textbook*. Futura Publishing Company, Armonk, NY, second edition.

Dedieu, H., M. Kennedy, and M. Hasler (1993). Chaos shift keying: Modulation and demodulation of a chaotic carrier using self-synchronizing Chua's circuits. *IEEE Transaction on Circuit and Systems—I*, 40, pp. 634–642.

Deller, J., J. Proakis, and J. Hansen (1993). *Discrete-Time Processing of Speech Signals*. Prentice-Hall, Upper Saddle River, NJ.

Duda, R. and P. Hart (1973). *Pattern Classification and Scene Analysis*. John Wiley & Sons, New York, NY.

Duke, D. and W. Pritchard, editors (1991). *Proceedings of the Conference on: Measuring Chaos in the Human Brain*. World Scientific, Singapore.

Ferri, R., F. Alicata, S. Del Gracco, M. Elia, S. Musumeci, and M. Stefanini (1996). Chaotic behavior of EEG slow-wave activity during sleep. *Electroencephalography and Clinical Neurophysiology*, 99, pp. 539–543.

Gibson, J. (1993). *Principles of Digital and Analog Communications*. Macmillan, New York, NY, second edition.

Guzzetti, S., M. Signorini, C. Cogliati, S. Mezzetti, A. Porta, S. Cerutti, and M. A (1996). Non-linear dynamics and chaotic indices in heart rate variability of normal subjects and heart-transplanted patients. *Cardiovascular Research*, 31, pp. 441–446.

Hasler, M. (1998). Synchronization of chaotic systems and transmission of information. *International Journal of Bifurcation and Chaos*, 8, pp. 647–659.

Hennebert, J. (1998). *Hidden Markov Models and Artificial Neural Networks for Speech and Speaker Recognition*. Ph.D. thesis, Swiss Federal Institute of Technology Lausanne, Lausanne, Switzerland.

Jaeseung Jeong, Dai-Jin Kim, Jeong-Ho Chae, Soo Yong Kim, Hyo-Jin Ko, and In-Ho Paik (1998a). Nonlinear analysis of the EEG of schizophrenics with optimal embedding dimension. *Medical Engineering & Physics*, 20, pp. 669–676.

Jaeseung Jeong, Soo Yong Kim, and Seol-Heui Han (1998b). Non-linear dynamical analysis of the EEG in Alzheimer's disease with optimal embedding dimension. *Electroencephalography and Clinical Neurophysiology*, 106, pp. 220–228.

Johnston, D. and S. Wu (1995). *Foundations of Cellular Neurophysiology*. MIT Press, Cambridge, MA.

Kanters, J., N. Holstein-Rathlou, and E. Agner (1994). Lack of evidence for low-dimensional chaos in heart rate variability. *Journal of Cardiovascular Electrophysiology*, 5, pp. 591–601.

Kapitaniak, T. and J. Brindley (1996). Practical stability of chaotic attractors. *Chaos, Solitons, & Fractals*, 7, pp. 1569–1581.

Kosko, B. (1992). *Neural Networks and Fuzzy Systems*. Prentice-Hall, Englewood Cliffs, NJ.

Koza, J. (1992). *Genetic Programming: On the Programming of Computers by Means of Natural Selection*. MIT Press, Cambridge, MA.

Kuznetsov, Y. (1998). *Elements of Applied Bifurcation Theory*. Springer-Verlag, New York, NY, second edition.

Ljung, L. (2000). *System Identification Toolbox For Use with MATLAB*. The MathWorks, Natick, MA. For the Toolbox version 5.0 $MatlabR12$.

Lopes da Silva, F. H., J. Pijn, D. Velis, and P. Nijssen (1997). Alpha rhythms: Noise, dynamics and models. *International Journal of Psychophysiology*, 26, pp. 237–249.

MacKay, D. (1999). *Information Theory, Inference, and Learning Algorithms*. Not published. Freely available on the world wide web: http://wol.ra.phy.cam.ac.uk/mackay/itprnn/book.html.

Maggio, G. and O. De Feo (2000). T-CSK: A robust approach to chaos-based communications. In *IEEE Workshop on Nonlinear Dynamics of Electronic Systems NDES*. Catania, Italy.

Maggio, G., O. De Feo, and M. Kennedy (1999). Nonlinear analysis of the Colpitts oscillator and applications to design. *IEEE Transaction on Circuit and Systems—I*, 46, pp. 1118–1130.

Michalski, R., J. Carbonell, and T. Mitchell, editors (1983). *Machine learning: An Artificial Intelligence Approach volume I*. Tioga, Palo Alto, CA.

MICHALSKI, R., J. CARBONELL, AND T. MITCHELL, editors (1986). *Machine learning: An Artificial Intelligence Approach Volume II*. Morgan Kaufmann, Los Altos, CA.

MIYANO, T., A. NAGAMI, I. TOKUDA, AND K. AIHARA (2000). Detecting nonlinear determinism in voiced sounds of japanese vowel /a/. *International Journal of Bifurcation and Chaos*, 10, pp. 1973–1979.

NUNEZ, P., editor (1995). *Neocortical Dynamics and Human EEG Rhythms*. Oxford University Press, Oxford, UK.

PEREDA, E., A. GAMUNDI, R. RIAL, AND J. GONZÁLEZ (1998). Non-linear behaviour of human EEG: Fractal exponent versus correlation dimension in awake and sleep stages. *Neuroscience Letters*, 250, pp. 91–94.

PIERSON, D. AND F. MOSS (1995). Detecting periodic unstable points in noisy chaotic and limit cycle attractors with applications to biology. *Physical Review Letters*, 75, pp. 2124–2127.

PIJN, J., J. V. NEERVEN, A. NOEST, AND F. LOPES DA SILVA (1991). Chaos or noise in the EEG signals: Dependence on state and brain site. *Electroencephalographic Clinical Neurophysiology*, 79, pp. 371–381.

PITARELLI, R. (2001). *Methods to Design and Assess Monitoring Processes for Complex Systems: Application to Cardiovascular Intensive Care Early Detection of Pathophysiological Events*. Ph.D. thesis, Swiss Federal Institute of Technology Lausanne, Lausanne, Switzerland.

POPIVANOV, D. AND A. MINEVA (1999). Testing procedures for non-stationarity and non-linearity in physiological signals. *Mathematical Biosciences*, 157, pp. 303–320.

PRADHAN, N., P. SADASIVAN, S. CHATTERJI, AND D. NARAYANA DUTT (1995). Patterns of attractor dimensions of sleep EEG. *Computers in Biology and Medicine*, 25, pp. 455–462.

PRITCHARD, W., D. DUKE, AND K. KRIEBLE (1995). Dimension analysis of resting human EEG II: Surrogate-data testing indicates nonlinearity but not low-dimensional chaos. *Psychophysiology*, 32, pp. 486–491.

RAPP, P. (1993). Chaos in the neurosciences: Cautionary tales from the frontier. *The Biologist*, 40, pp. 89–94.

RINALDI, S. AND C. PICCARDI (1998). *I Sistemi Lineari*. UTET, Torino, Italy. In Italian.

ROBERT, A. (1999). *Perception and Applications in Audio Processing*. Ph.D. thesis, Swiss Federal Institute of Technology Lausanne, Lausanne, Switzerland.

RÖSCHKE, J., J. FELL, AND K. MANN (1997). Non-linear dynamics of alpha and theta rhythm: Correlation dimensions and Lyapunov exponents from healthy subject's spontaneous EEG. *International Journal of Psychophysiology*, 26, pp. 251–261.

RUSSELL, S. AND P. NORVIG (1999). *Artificial Intelligence: A Modern Approach*. Prentice-Hall, New York, NY.

SCHALKOFF, R. (1992). *Pattern Recognition: Statistical, Structural and Neural Approaches*. John Wiley & Sons, New York, NY.

SCHWEIZER, J. (1999). *Application of Chaos to Communications*. Ph.D. thesis, Swiss Federal Institute of Technology Lausanne, Lausanne, Switzerland.

SÖDERSTRÖM, T. AND P. STOICA (1989). *System Identification*. Prentice-Hall, London, UK.

SOONG, A. AND C. STUART (1989). Evidence of chaotic dynamics underlying the human alpha-rhythm electroencephalogram. *Biological Cybernetic*, 62, pp. 55–62.

SZEGÖ, G. (1975). *Orthogonal Polynomials*. American Mathematical Society, Providence, RI, fourth edition.

VAPNIK, V. (1995). *The Nature of Statistical Learning Theory*. Springer-Verlag, New York, NY.

WALPONE, R. (1993). *Probabilty and Statistics for Engineers and Scientists*. Macmillan, New York, NY, fifth edition.

WEISS, S. (1991). *Computer Systems that Learn? Classification and Prediction Methods from Statistics, Neural Nets, Machine Learning and Expert Systems*. Morgan Kaufmann, San Mateo, CA.

CHAPTER 8

FINAL DISCUSSION

Brief — Here the general conclusion about the specific results that have been presented in this thesis are drawn. Furthermore, hints for possible future research projects are given.

With this chapter, the thesis ends. Hence, it is time to draw some conclusion about the specific results obtained during these last three years of research. Before coming to the final remarks specific to what has been presented here, it should be noted that, as often happens in Ph.D theses, what is presented here does not represent the entirety of the work conducted. More in particular, there are two classes of results that have been completely omitted or simply mentioned in Appendix E. In the first place is all the subsidiary work necessary to reach an acceptable sensitivity on continuous time chaos, especially on Shil'nikov-like chaos, without which it would have been quite impossible to correctly interpret the phenomenon of qualitative resonance; a hint of what implied by this work is given by the two publications [De Feo *et al.*, 2000; Kuznetsov *et al.*, 2001], which indeed are the direct result of this acquired sensitivity. In the second place, there is a portion of the research conducted, which has not even been mentioned here, that it is related with the third proposal for future research; in particular, it is related to the representation of randomness in deterministic cognitive agents by means of chaotic dynamics (*cfr.* Sect. 8.4). No mention has been given since, despite of the promising preliminary results, this part of research is still at an embryonic stage. The hope is to continue working on this topic in the future.

Coming back to the specific material presented here, in the author's opinion the Thesis, namely

> The diversity of approximately periodic signals found in nature can be modeled by means of Feigenbaum-like strange attractors. This kind of modeling technique together with the phenomenon of qualitative resonance can be exploited for pattern recognition purposes.

is definitely supported by the results that have been presented. It can be concluded that indeed the diversity of approximately periodic signals can be modeled by means of a chaotic dynamical system; besides, this kind of model can be successfully employed, by means of the qualitative resonance phenomenon, for pattern recognition purposes.

Furthermore, from the overall results, three main general remarks, both from engineering and philosophical point of view, can be drawn. One, which is mainly mathematical/engineeristic, is about the specific modeling technique adopted; a second one is about the role of the sensory system in cognitive agents; and, finally, one is about the role of chaos in knowledge representations. They are discussed in detail in the following sections.

The hope of a final engineering application of the presented techniques is the basic motivation throughout this entire work, by means of the decomposition of big problems into basic simple problems, of the particular techniques chosen for solving the subproblems, etc. Despite of this attention given to the final practical employability, this work remains a pioneering exploration of a chaos-based modeling technique. Hence, it is clear that from an engineering point of view, and not only from that one, there is a lot of work that must be accomplished before this technique will be indeed employed.

In this sense, it could be said that these are *not concluding conclusions*. From the application point of view this is not the concluding but the introductory chapter; that is why the chapter ends with a series of research proposals, which, in the author's opinion, are the engineering, and not only, natural continuation of what has been proposed here.

8.1 A Control Theory Approach

To the proposed method of temporal pattern recognition, *i.e.* qualitative resonance, a precise meaning can be given if it is interpreted in the right terms. As mentioned in Chap. 2, to recognize a pattern can often be thought of comparing the observed pattern with an idealized stereotype of it. Keeping that in mind, recognizing a temporal pattern by means of qualitative resonance can be thought of performing the comparison of the observed pattern with the suspected stereotype in the dynamical space, in which the patterns are generated, rather than in the static space of the observations. In other words, a given temporal pattern $y(t)$ is recognized in the space

$$\begin{aligned} \dot{x}(t) &= F(x(t)) \\ y(t) &= H(x(t)) \end{aligned}$$

where it has been generated rather than working on the particular temporal observation. Namely, for the comparison it is considered a dynamical stereotype $\widehat{F}(\cdot)$ rather than a temporal stereotype $\widehat{y}(t)$.

This technique is decidedly not new; in particular, it is the common approach of *automatic control engineering* [Brogan, 1996]. Indeed, a regulator, which is the typical product of control engineering, can be thought of a black box that, on the basis of the available measurements, decides what is the best action to perform on the controlled system in order to obtain the desired behavior. In some sense, this means that the regulator recognizes particular patterns coming from the controlled system and responds to them with the best counteraction.
How does the regulator know about the possible incoming patterns?
How does the regulator recognize them in order to know about the effect of its counteractions?
The answer to these two questions is known in control engineering as the concept of *internal model* [Berber, 1995; Marro, 1997; Shinskey, 1996]. Namely, the regulator knows *"what is going on"* since it has internally a model of the controlled system.

With this analogy in mind, that must be handled with due caution, it should be clear that the qualitative resonance is not very far. In particular, the two steps of the technique presented here, *i.e.* modeling and pattern recognition, can be reinterpreted as follows. At first a dynamical model for the generation of $y(t)$ is built (modeling). The obtained model is used to realize a reconstructor of the internal state corresponding to $y(t)$ (qualitatively resonating filter). This reconstructor is then used for the pattern recognition: if the reconstruction of the state succeeds (qualitative resonance) the pattern is matched; on the contrary, if the reconstruction fails (qualitative anti-resonance) the pattern is rejected.

Bearing in mind how a Kalman regulator[1] works [Grewal and Andrews, 1993; Kwakernaak and Sivan, 1972; Locatelli, 1993], it can be concluded that the proposed method is an interpretation, for pattern recognition purposes, of the automatic control theory concept of internal model.

8.2 A New Role of the Sensory System

The results presented here, especially those reported in Chap. 3 go in the direction of revaluating the role of the sensory system in the cognitive agents. In particular, it points in the direction of supposing some intelligence associated with the sensory system [Chiel and Beer, 1997].

This conclusion emerges combining the results shown in the previous chapter (*cfr.* Chap. 7) and a quite ambitious analogy.

There are recent results in experimental physiology leading to believe that phenomena of generalized synchronization are indeed the dominating mechanism used by biological neural cells for processing information [Basar, 1990; Elbert *et al.*, 1994; Freeman, 2000; Getting, 1989; Hopfield, 1991, 1995, 1996; Izhikevich, 2000; Rabinovich *et al.*, 2000; Singer and Gray, 1995]. More in particular, there are similar results in experiments conducted on the neural cells of the sensory system of living beings [Bressler, 1988; Elson *et al.*, 1998;

[1] A Kalman regulator is composed of two parts. The first part can drive the controlled system as desired if it knows the state of the controlled system. The second part reconstructs the state of the controlled system, needed by the first part, starting from the available observations. For doing that the second part has a dynamical model of the controlled system inside.

Engel *et al.*, 1991; Kay and Freeman, 1998; Laurent *et al.*, 1996; Prechtl *et al.*, 1997]. Keeping in account that the phenomenon of qualitative resonance is indeed a kind of synchronization, an ambitious analogy comes immediately to mind:

> *as the qualitatively resonating preprocessing transforms external stimuli in symbolic information, more specifically in a probability distribution over a finite alphabet of symbols, it could be that the synchronization phenomena observed in the sensorial neural cells of living beings could realize a similar transformation; namely, it could transform the external stimuli in a more symbolic internal representation useful for the brain,* i.e. *the inferential engine.*

Furthermore, from the results shown in the previous chapter, it emerges that the symbolic information provided by the qualitatively resonating preprocessing is of high quality, denoting some intelligence in this preprocessing; indeed, the preprocessor almost realizes the complete pattern recognition without needing a postprocessing, *cfr.* Chap. 7.

These two remarks lead to conclude that the sensing system of living beings is definitely more than a simple transducer converting external stimuli into internal electric potentials, as often thought by engineers [McKerrow, 1991]; it is a sophisticated, intelligent, system by itself. Hence, the role of the sensory system in the emergence of intelligent behavior in cognitive agents should be revisited.

As final remark, it should be noted that despite of its attractiveness, this ambitious analogy, comparing a qualitatively resonating filter followed by a higher system at symbolic level with the sensory system of living beings feeding the brain with high level information, is not necessarily likely to be observed in nature.

8.3 Chaos and Knowledge Representation

Probably, the main result of this thesis has been the possibility of exploiting chaotic behavior in representing imprecise knowledge. This result goes supporting the conjecture given in Sect. 4.1 about the dynamical nature of associative behavior. In fact, there it is supposed that chaos is necessary to robustly represent imprecise knowledge.

It should be noted that a priori this result is unlinked to the more general and tough item about the real nature of randomness. Indeed, as shown in the previous chapter where some of the modeled signals are not necessarily really chaotic, the chaos-based modeling is beyond the real nature of the diversity of the modeled signals. In other words, the chaos-based modeling of diversity is a disjoint topic from the investigation about the real nature of diversity; namely, it is disjoint from knowing if the random fluctuations of the real world are indeed exogenous random perturbations or if they are the result of endogenous nonlinear dynamics.

Positively enough this is an important result; indeed, being able to represent the fluctuations of the signals independently from the real nature of their randomness represents definitely a step ahead. In this respect, it should be noted that the important result is not being able to build such a chaotic model but its subsequent practical employability. Clearly, the chaotic model alone, *i.e.* being able to write its equations, has no sense; it is the essence of chaos itself: the knowledge of the equations gives no insight on the behavior described. The model becomes important together with phenomena, as qualitative resonance, which allow to forecast qualitatively surprising behaviors independently from the particular equations considered. In this sense the modeling technique and its application are in symbiosis. Indeed, for the particular case considered here, to have the chaotic model by itself is of no use; what makes it useful is the qualitative resonance that allows to exploit the knowledge of the model for pattern recognition purposes.

8.4 Propositions of Future Research

Three main veins can be pursued starting from the results of this thesis. Each one of them is more related to a specific field of science, that is why they are presented separately as research in this or that particular field; even though that, it should be clear that this separation is fictitious and these research projects are definitely all linked to each other.

8.4.1 Engineering

This project for future research is mainly linked to the connection of a dynamic-based sensory system to a second level cognitive system of symbolic nature. More closely to the specific problem discussed in this thesis,

this research project would deal with the cascading of a qualitatively resonating preprocessor with second level pattern recognizer of symbolic nature; namely, a statistic-based or a more general symbolic-based one.

Several questions can be raised in this direction, among them are the following.

- Is this mixed dynamic-symbolic approach effective?

  The inspiration of this approach comes from biology and from cognitive science, namely from the hypothesis of a dynamic-based sensory system followed by a symbolic-based inferential engine. Despite of its origin, the value of this approach in engineering should be evaluated separately from its likelihood to be observed in nature. Indeed, it could happen that this method proves to be successful for the engineering of artificial intelligence applications while this kind of decomposition is hardly observed in nature. The opposite is, obviously, possible as well.

- How can such a mixed system be tuned?
  Would a separate tuning, in agreement with the *divide et impera* approach, be sufficient or a mixed tuning would be necessary?

  More closely to the specific problem discussed in this thesis, would it be sufficient to tune at best the qualitatively resonating preprocessor and then the statistical pattern recognizer or would it be necessary to consider an iterative loop of tuning for the two?

8.4.2 Biology & Cognitive Science

As mentioned above, an interesting question for biologist and cognitive scientist would be to evaluate the likelihood of the mixed dynamic-symbolic hypothesis in nature. The justification for a research effort in such a direction should be found in those recent results reporting the observation of synchronization phenomena, among several cells, when dealing with biological neural cells; in particular, in the observed synchronization of the sensorial neurons in presence of external stimuli [Elbert *et al.*, 1994; Rabinovich *et al.*, 2000]. It would be of definitive interest to interpret such phenomena in terms of qualitative resonance. In words that are more emphatic: *looking for qualitative resonance in biological systems.* In this respect, this could be the main question in this direction.

- Are the external stimuli transformed into an internal representation useful for the brain by a mechanism similar to the qualitative resonance?

8.4.3 Cognitive Science & Philosophy

Definitely more related to cognitive science, and at the limit of philosophy, would be the investigation about the real role of chaos in knowledge representation. In this direction, the author mainly imagines three points.

1. *The chaos for representing randomness*: this would stay in the direction followed in this thesis and suggested by David Ruelle in [Ruelle, 1991, 1995].

   - Is chaos the way in which a deterministic cognitive agent can conceive randomness?

   To understand better this question consider game theory [Maynard Smith, 1982], which is commonly used in theoretical biology [Sigmund, 1998; Weibull, 1996], psychology [Colman, 1995; de Waal, 1998], and cognitive science to model, just for instance, problems of cooperation among agents [Colman, 1982]. From game theory, it is known that, often enough, the best strategies that the players, *i.e.* the playing agents, should play are statistical strategies [Weibull, 1996]; namely, they should make some random decision. Now it comes a question, if the agents are perfectly *deterministic* how could they represent internally a statistical strategy? Roughly speaking, if a program that makes some random choice must be written and the `rand()`function is not available how can the problem can be solved?

   In this direction points the research conducted at the Sony and Nec laboratories cited in the introductory chapter (*cfr.* Sect. 1.4) [Giles and Omlin, 1993; Tani, 1996].

2. *Chaos as robust response to randomness*: this is mainly the conjecture proposed in Chap. 4. Namely, independently from the fact that the real word is random or is chaotic; chaos can be a versatile representation of imprecise knowledge. In this direction, there are the following questions.

- Can any generalization of qualitative resonance be imagined?
  In particular, there exist a chaos-based knowledge representation of nonperiodic information or the periodicity is a necessary condition?
- If periodicity is a necessary condition, is there any link to the natural cyclic behavior of neural cells [Li *et al.*, 1995]?
  In other words, is the internal representation of knowledge of the brain based on the cyclic behavior?

3. *The unification*: this would be the unification of the previous two points. Is the apparent randomness of nature really noise or is it the fingerprint of an intrinsic chaotic behavior that is necessary to be robust with respect to the unforecasted events? In more emphatic words:

   - Is chaos the evolutionary answer to the need of robustness with respect to unforecastable events?

It is in these last topics that the author hopes to spend some of his time in the near and more farther future.

Bibliography

Basar, E. (1990). *Chaotic Dynamics and Resonance Phenomena in Brain Function: Progress, Perspectives, and Thoughts*, pp. 1–30. Springer-Verlag, Berlin, Germany.

Berber, R., editor (1995). *Methods of Model Based Process Control*. Kluwer Academic.

Bressler, S. (1988). Changes in electrical activity of rabbit olfactory bulb and cortex to conditioned odor stimulation. *Journal of Neurophysiology*, 62, pp. 740–747.

Brogan, W. (1996). *Modern Control Theory*. Prentice-Hall, New York, NY, third edition.

Chiel, H. and R. Beer (1997). The brain has a body: Adaptive behavior emerges from interactions of nervous system, body, and environment. *Trends in Neurosciences*, 20, pp. 553–557.

Colman, A. (1982). *Game Theory and Experimental Games: The Study of Strategic Interaction*. Pergamon, Oxford, UK.

Colman, A. (1995). *Game Theory and its Application in the Social and Biological Sciences*. Butterworth-Heinemann, Oxford, UK, second edition.

De Feo, O., G. Maggio, and M. Kennedy (2000). The Colpitts oscillator: Families of periodic solutions and their bifurcations. *International Journal of Bifurcation and Chaos*, 10, pp. 935–958.

de Waal, F. (1998). *Chimpanzee Politics*. Johns Hopkins University Press, Baltimore, MD.

Elbert, T., W. Ray, Z. Kowalik, J. Skinner, K. Graf, and N. Birbaumer (1994). Chaos and physiology: Deterministic chaos in excitable cell assemblies. *Physiological Reviews*, 74, pp. 1–47.

Elson, R., A. Selverston, R. Huerta, M. Rabinovich, and H. Abarbanel (1998). Synchronous behavior of two coupled biological neurons. *Physical Review Letters*, 81, pp. 5692–5695.

Engel, A., A. Kreiter, P. König, and W. Singer (1991). Synchronization of oscillatory neuronal responses between striate and extrastriate visual cortical areas of the cat. *Proceedings of the National Academy of Science USA*, 88, pp. 6048–6052.

Freeman, W. (2000). Characteristics of the synchronization of brain activity imposed by finite conduction velocities of axons. *International Journal of Bifurcation and Chaos*, 10, pp. 2307–2322.

Getting, P. (1989). Emerging principles governing the operation of neural network. *Annual Review of Neuroscience*, 12, pp. 185–204.

Giles, C. and C. Omlin (1993). Extraction, insertion and refinement of symbolic rules in dynamically driven recurrent neural networks. *Connection Science*, 5, pp. 307–337.

Grewal, M. and A. Andrews (1993). *Kalman Filtering Theory and Practice*. Prentice-Hall, Englewood Cliffs, NJ.

Hopfield, J. (1991). Olfactory computation and object perception. *Proceedings of the National Academy of Science USA*, 88, pp. 6462–6466.

Hopfield, J. (1995). Pattern recognition computation using action potential timing for stimulus representation. *Nature*, 376, pp. 33–36.

Hopfield, J. (1996). Transforming neural computations and representing time. *Proceedings of the National Academy of Science USA*, 93, pp. 15440–15444.

Izhikevich, E. (2000). Neural excitability, spiking and bursting. *International Journal of Bifurcation and Chaos*, 10, pp. 1171–1266.

Kay, L. and W. Freeman (1998). Bidirectional processing in the olfactory-limbic axis during olfactory behavior. *Behavioral Neuroscience*, 112, pp. 541–553.

Kuznetsov, Y., O. De Feo, and S. Rinaldi (2001). Belyakov homoclinic bifurcations in a tritrophic food chain model. *SIAM Journal of Applied Mathematics*. Submitted.

Kwakernaak, H. and R. Sivan (1972). *Linear Optimal Control Systems*. John Wiley & Sons, New York, NY.

Laurent, G., M. Wehr, and H. Davidowitz (1996). Temporal representation of odors in an olfactory network. *The Journal of Neuroscience*, 16, pp. 3837–3847.

Li, Y., J. Rinzel, L. Vergara, and S. Stojilkovi (1995). Spontaneus electrical and calcium oscillations in unstimulated pituitary gonadotrophs. *Biophysical Journal*, 69, pp. 785–795.

Locatelli, A. (1993). *Elementi di Controllo Ottimo*. UTET, Torino, Italy. In Italian.

Marro, G. (1997). *Controlli Automatici*. Zanichelli, Bologna, Italy, fourth edition. In Italian.

Maynard Smith, J. (1982). *Evolution and the Theory of Games*. Cambridge University Press, Cambridge, UK.

McKerrow, P. (1991). *Introduction to Robotics*. Addison-Wesley, Reading, MA.

Prechtl, J., L. Cohen, B. Pesaran, and P. Mitra (1997). Visual stimuli induce waves of electrical activity in turtle cortex. *Proceedings of the National Academy of Science USA*, 94, pp. 7621–7626.

Rabinovich, M., P. Varona, and H. Abarbanel (2000). Nonlinear cooperative dynamics of living neurons. *International Journal of Bifurcation and Chaos*, 10, pp. 913–933.

Ruelle, D. (1991). *Hasard et Chaos*. Odile Jacob, Paris, France.

Ruelle, D. (1995). *Turbulence, Strange Attractors and Chaos*. World Scientific, Singapore.

Shinskey, F. (1996). *Process Control Systems: Application, Design, and Tuning*. McGraw-Hill, New York, NY.

Sigmund, J. H. K. (1998). *Evolutionary Games and Population Dynamics*. Cambridge University Press, Cambridge, UK.

Singer, W. and C. Gray (1995). Visual feature integration and the temporal correlation hypothesis. *Annual Review of Neuroscience*, 18, pp. 555–586.

Tani, J. (1996). Model-based learning for mobile robot navigation from the dynamical systems perspective. *IEEE Transacions on System, Man and Cybernetics Part B*, 26, pp. 421–436. Special issue on learning autonomous robots.

Weibull, J. (1996). *Evolutionary Game Theory*. MIT Press, Cambridge, MA.

APPENDIX A

THE GENERALIZED COLPITTS OSCILLATOR

Brief — In this Appendix the paradigm which is considered in this thesis for the generation of simple and complex oscillations is presented. It is the generalization of the well-known Colpitts oscillator considered in electronics.

Personal Contribution — The material here presented is original from the author but it has already been published elsewhere.

The Colpitts oscillator is a representative of those oscillators usually known under the term of *Class-C* oscillators. These oscillators work according a *Kick-and-Resonate* principle [Christiansen, 1997]; namely, they are composed, as shown in Fig. A.1(a), of an active device which synchronously, *i.e.* on feedback, strongly stimulate a dissipative resonant network which in consequence behaves in an almost harmonic, *i.e.* sinusoidal, manner. A colorful analogy of the class-C oscillators working principle is given in Fig. A.1(b); a child play with a pendulum, composed of a rope tied on the one side to a ball and keeping the other end of the rope in his hand. The child strongly kick the ball with enough energy such to let the pendulum accomplish at least one complete rotation. In absence on any friction, after an initial transient, the pendulum would settle to a harmonic regime which would be preserved forever. In reality, the friction wastes energy and in consequence the pendulum decelerate until stopping. The harmonic regime could be preserved if the child would kick the ball whenever it passes in front of its foot providing instantaneously the energy dissipated during the accomplished rotation. This is indeed a quite colorful explanation of the class-C oscillators working principle: a dissipative resonant network is provided of an active feedback circuit supplying, in very brief time with respect to the oscillating frequency, *i.e.* almost instantaneously, the energy dissipated by the resonant network during an integer number of oscillations.

The generalized Colpitts oscillator is simply the generalization, such to remain a class-C oscillator, of the mathematical model corresponding to the circuit schematic of Colpitts oscillator usually considered in electronic engineering [Sedra and Smith, 1998].

A.1 The Colpitts Oscillator

Although the Colpitts oscillator was originally designed to be an almost-sinusoidal oscillator [Sedra and Smith, 1998], it has been shown to exhibit a rich dynamical behavior at certain parameter values [Elwakil and Kennedy, 1999; Kennedy, 1994; Lindberg, 1996; Maggio *et al.*, 1999]; that is why a generalization of it has been considered here as paradigm for the generation of simple, *i.e.* almost sinusoidal, and complex, *i.e.* chaotic, oscillations.

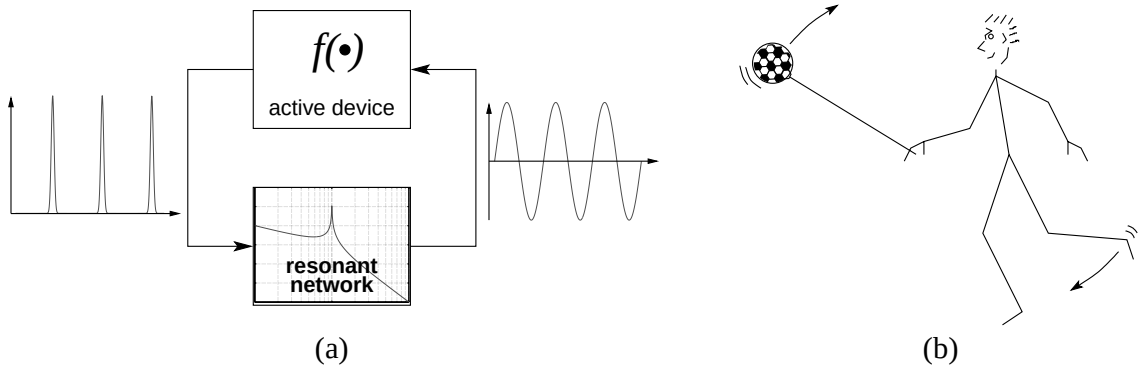

Figure A.1: *The class-C oscillators working principle: (a) – functional schematic of a class-C oscillator; (b) – mechanical analogy of a class-C oscillator.*

The schematic of the Colpitts oscillator usually considered in electronic engineering is shown in Fig. A.2(a). The circuit comprises a (BJT) bipolar junction transistor (T), acting as the active element, and a resonant network consisting of an inductor (L) and a pair of capacitors (C_1 and C_2). The circuit bias is provided by the voltage supply V_{cc} and the current source I_0, the latter being characterized by a Norton-equivalent conductance G_0.

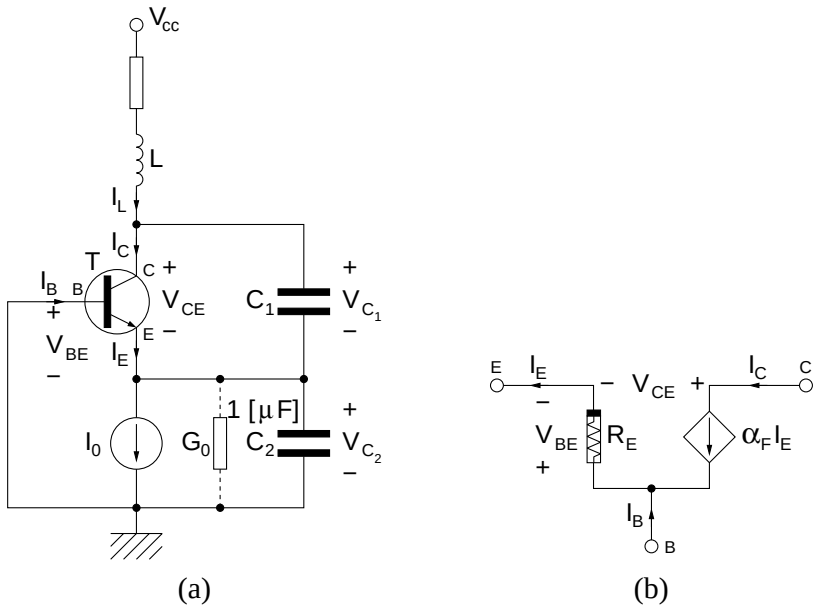

Figure A.2: *The Colpitts oscillator: (a) circuit schematic; (b) bipolar junction transistor (BJT) model in common-base configuration.*

A.1.1 The State Equations

Consistently with the usual assumptions made in electronic engineering [De Feo *et al.*, 2000; Maggio *et al.*, 1999; Sedra and Smith, 1998], the following simplifying hypothesis can be made.

(H.1) The BJT is modeled by a voltage-controlled nonlinear resistor R_E and a linear current-controlled current source, that is all the parasitic effects are discarded.

This is illustrated in Fig. A.2(b) showing the BJT model, with α_F denoting the common-base (CB) short-circuit forward current gain of the BJT. The nonlinear characteristic of R_E is approximated by diode exponential function [Sedra and Smith, 1998]:

$$I_E = f(V_{BE}) = I_S \exp\left(\frac{V_{BE}}{V_T}\right) \tag{A.1}$$

where I_S is the saturation current of the base-emitter junction and V_T is the thermal voltage which is about 27 $[mV]$ at room temperature.

Under the hypothesis (H.1) the state equations of the schematic shown in Fig. A.2(a) can be written as

$$\begin{aligned} C_1 \frac{V_{C_1}}{dt} &= -\alpha_F f\left(-V_{C_2}\right) + I_L \\ C_2 \frac{V_{C_2}}{dt} &= \left(1-\alpha_F\right) f\left(-V_{C_2}\right) + I_L - I_0 - G_0 V_{C_2} \\ L \frac{I_L}{dt} &= -V_{C_1} - V_{C_2} - R I_L + V_{cc} \end{aligned} \tag{A.2}$$

A.1.2 The Normalized State Equations

By means of a linear transformation of the state and time variables, the state equations (A.2) of the Colpitts oscillator can be rewritten as

$$\begin{aligned} \dot{x}_1 &= \frac{g^*}{Q(1-k)}\left[-\alpha_F n(x_2) + x_3\right] \\ \dot{x}_2 &= \frac{g^*}{Qk}\left[(1-\alpha_F) n(x_2) + x_3\right] - Q_0(1-k)x_2 \\ \dot{x}_3 &= -\frac{Qk(1-k)}{g^*}\left[x_1 + x_2\right] - \frac{1}{Q}x_3 \end{aligned} \tag{A.3}$$

where

$$n(x_2) = e^{-x_2} - 1$$

while the dimensionless variables $[x_1, x_2, x_3]$ are obtained by setting the equilibrium point of Eqs. (A.2) to be the origin of the new coordinate system and by normalizing voltages, currents, and time with respect to $V_{ref} = V_T$, $I_{ref} = I_0$, and $t_{ref} = 1/\omega_0$, respectively, with $\omega_0 = 1\Big/\sqrt{L\frac{C_1 C_2}{C_1+C_2}}$, *i.e.* the resonant frequency of the unloaded tank circuit. Finally, the parameters Q, k, and Q_0 are given by

$$\begin{aligned} Q &= \frac{\omega_0 L}{R} \\ k &= \frac{C_2}{C_1 + C_2} \\ Q_0 &= \omega_0 L G_0 \end{aligned} \tag{A.4}$$

Usually, the conductance G_0 is very small and the value of Q_0 can be neglected leading to

$$\begin{aligned} \dot{x}_1 &= \frac{g^*}{Q(1-k)}\left[-\alpha_F n(x_2) + x_3\right] \\ \dot{x}_2 &= \frac{g^*}{Qk}\left[(1-\alpha_F) n(x_2) + x_3\right] \\ \dot{x}_3 &= -\frac{Qk(1-k)}{g^*}\left[x_1 + x_2\right] - \frac{1}{Q}x_3 \end{aligned} \tag{A.5}$$

Note that Q represents the quality factor of the resonant network, while g^* is the loop gain of the oscillator when the phase condition of the Barkhausen criterion [Sedra and Smith, 1998] is satisfied and it is, in general, a complicated function of the circuit parameters. It should be emphasized that system (A.5)) depends only upon the two parameters Q and g^*, while k is just a scaling factor for the state variables [Maggio *et al.*, 1999], hence has no influence on the oscillator dynamics.

A.1.3 The Lur'e Formulation

The state equations given by Eqs. (A.5) can be easily reformatted into a scalar Lur'e form as shown in Fig. A.3 where the linear transfer function is given by

$$G(s) = \frac{Y(s)}{U(s)} = \frac{g^*(1-\alpha)}{kQ} \frac{s^2 + \frac{s}{Q} + \frac{k}{1-\alpha}}{s\left(s^2 + \frac{s}{Q} + 1\right)} \tag{A.6}$$

while the nonlinearity is given by

$$f(y) = e^{-y} - 1 \tag{A.7}$$

For values of α near one the transfer function $G(S)$ is an integrating resonant filter. Namely,

$$\lim_{\alpha \to 1} G(s) = \frac{g^*}{s\left(Qs^2 + s + Q\right)}$$

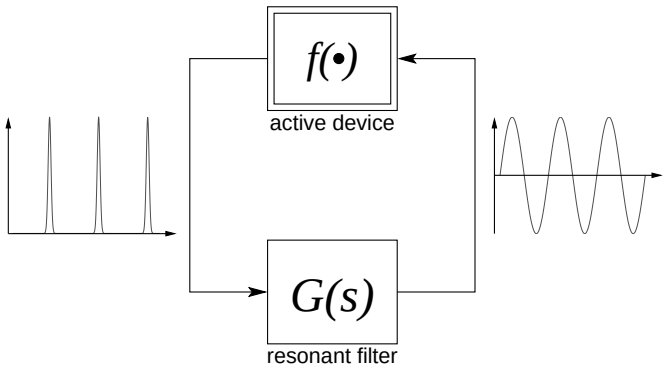

Figure A.3: *Scalar Lur'e formulation of the Colpitts oscillator mathematical model given by Eqs. (A.5).*

A.2 The Generalized Colpitts Oscillator

As can be easily noticed, the Colpitts oscillator as given by Fig. A.3, Eq. (A.6), and Eq. (A.7) results composed of the feedback connection of a integrating resonant linear system, with a couple of anti-resonating zeros, *i.e.* the $G(s)$, by a rectifying function, *i.e.* the $f(\cdot)$.

The generalized Colpitts oscillator is simply the generalization of this scheme; namely, the feedback connection of a generic integrating resonant filter, with a couple of anti-resonating zeros, by means of a generic rectifying nonlinear function. In other words, the generalized Colpitts oscillator is given by the Lur'e system shown in Fig. A.3 where

$$G(s) = \frac{Y(s)}{U(s)} = \frac{g\left((1-\alpha)\frac{s^2}{\omega_n^2} + (1-\alpha)\frac{s}{Q\omega_n} + 1\right)}{s\left(\frac{s^2}{\omega_n^2} + \frac{s}{Q\omega_n} + 1\right)} \tag{A.8}$$

and the nonlinearity $f(\cdot)$ satisfying the following conditions

$$\begin{aligned} f: \quad & \left(f: \mathbb{R} \mapsto (-K, +\infty) \right) \wedge \left(f'(x) < 0 \ \forall x \right) \wedge \left(f(0) = 0 \right) \wedge \\ & \wedge \left(\lim_{x \to +\infty} f(x) = -K \right) \wedge \left(\lim_{x \to -\infty} f(x) \to +\infty \right) \end{aligned} \tag{A.9}$$

These conditions on $f(\cdot)$ require that the Lur'e system works indeed in a Class-C manner. Indeed, when the output $y \gg 0$ the action of the active feedback, *i.e.* $f(\cdot)$, is simply dissipating ($\lim_{x \to +\infty} f(x) = -K$); while, on the other hand, when the output decreases below zero the active function at first compensate the losses ($f(0) = 0$) and then kick the resonant system ($(f'(x) < 0 \forall x) \wedge (\lim_{x \to -\infty} f(x) \to +\infty)$).

Once the rectifying nonlinearity is fixed, the generalized Colpitts oscillator depends upon three parameters.

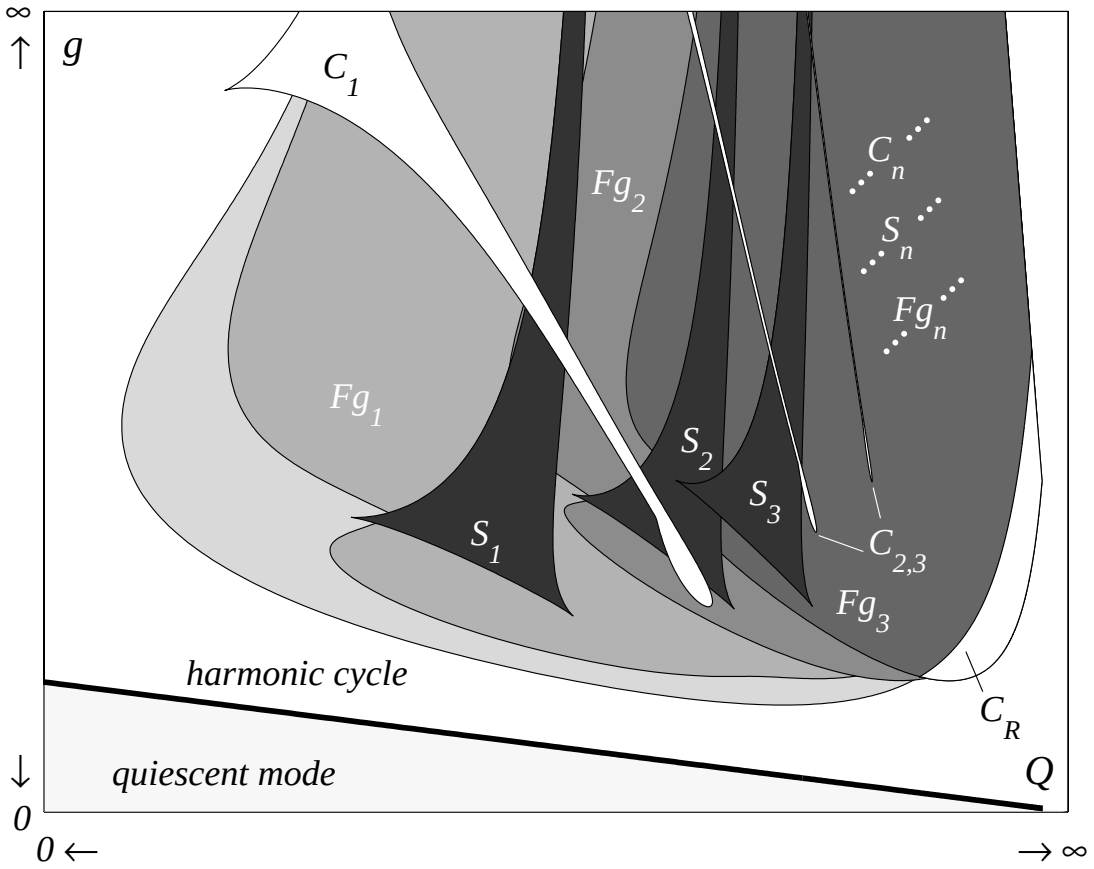

Figure A.4: *Qualitative bifurcation diagram of the generalized Colpitts oscillator with respect to the parameters Q and g for a given value, not too low, of* α*. The circuit does not oscillate for parameter values in the light gray region denoted by* quiescent mode*. The white region labeled* harmonic cycle *corresponds to* 1*-pulse behavior, which includes the nearly-sinusoidal oscillation. The darker gray regions are characterized by more complex behavior. Namely, in the regions indicated by* Fg_n *and* S_n *the system exhibits n-pulse Feigenbaum and Shil'nikov chaos, respectively. The cusp regions,* C_n*, are characterized by coexistence of the* 1*-pulse solution with one or more attractors belonging to different solution families. The former is more likely to be observed in practice because of its larger basin of attraction. For this reason, such regions and the outer region labeled* C_R *have been assigned the white color.*

1. *Energy transfer efficiency* α: it describes how efficiently the energy is transferred from the active device to the dissipative resonant filter. Namely, it determines the percentage of the energy rendered available from the active network that is wasted while transferring it to the resonant network. It is the analogous of the common-base short-circuit forward current gain of the BJT.

2. *Resonant filter quality factor* Q: it summarizes the dissipative effects of the resonant linear system. Namely, it determines the percentage of energy owned by the resonant filter which is dissipated over one oscillation. It is the analogous of the quality factor Q of a RLC resonant network.

3. *Loop gain* g: it describes the conversion of the energy from the form available to the active device in the form in which is stored into the resonant filter. It determines how the transfer factor from active device to the resonant network of the energy which is which is effectively transferred, *i.e.* the *alpha* fraction. It is the analogous of the g^* in the Colpitts oscillator.

4. *The natural pulsatance* ω_n: it determine the pulsatance at which the oscillator resonate. It is simply a time scale factor and can be assumed equal to one without loss of generality.

For fixed, not too low, values of the energy transfer efficiency α, *i.e.* for values about or superior to 90%, the qualitative bifurcation diagram of the generalized Colpitts oscillator with respect to the two

parameters Q and g has been shown to be practically independent of the particular rectifying nonlinearity $f(\cdot)$ [De Feo and Maggio, 2001; De Feo *et al.*, 2000; Maggio *et al.*, 1999; Maggio, 1999; Yang and Chua, 2000]. In particular, the peculiarities of such qualitative bifurcation diagram are summarized in Fig. A.4 [De Feo and Maggio, 2001; De Feo *et al.*, 2000; Maggio *et al.*, 1999]. Namely, the qualitative bifurcation diagram affirms that augmenting the loop gain g leads the generalized Colpitts oscillator to oscillate in irregular, *i.e.* chaotic, n-pulse manner where n augments as the quality factor Q augments.

Bibliography

Christiansen, D., editor (1997). *Electronics Engineers' Handbook*. McGraw-Hill for IEEE Press, New York, NY.

De Feo, O. and G. Maggio (2001). Bifurcations in the Colpitts oscillator: Theory versus experiments. *IEEE Transaction on Circuit and Systems—I*. Submitted.

De Feo, O., G. Maggio, and M. Kennedy (2000). The Colpitts oscillator: Families of periodic solutions and their bifurcations. *International Journal of Bifurcation and Chaos*, 10, pp. 935–958.

Elwakil, A. and M. Kennedy (1999). A family of Colpitts-like chaotic oscillators. *Journal of the Franklin Institute*, 336, pp. 687–700.

Kennedy, M. (1994). Chaos in the Colpitts oscillator. *IEEE Transactions on Circuits and Systems—I*, 41, pp. 771–74.

Lindberg, E. (1996). Colpitts and chaos. In *Proceedings of the 5th Biennial Baltic Electronics Conference BEC'96*. Tallinn, Estonia.

Maggio, G., O. De Feo, and M. Kennedy (1999). Nonlinear analysis of the Colpitts oscillator and applications to design. *IEEE Transaction on Circuit and Systems—I*, 46, pp. 1118–1130.

Maggio, G. M. (1999). *Nonlinear Dynamics and Chaos in Electronic Oscillators*. Ph.D. thesis, University College Dublin, Dublin, Ireland.

Sedra, S. and K. Smith (1998). *Microelectronic Circuits*. Oxford University Press, New York, NY, fourth edition.

Yang, T. and L. Chua (2000). Piecewise-linear chaotic systems with a single equilibrium point. *International Journal of Bifurcation and Chaos*, 10, pp. 2015–2060.

APPENDIX B

NONMINIMAL PHASE RECONSTRUCTION

Brief — This Appendix presents a very simple trick for reconstructing time series in the state space in such a way to obtain very nice figures.

Personal Contribution — The idea here presented is an original "geometrical intuition" of the author.

Among the several aims of the state space reconstruction from the measurements of a single observable [Abarbanel *et al.*, 1993; Kantz and Schreiber, 1997; Packard *et al.*, 1980], there is the attainment of pictures, usually three-dimensional ones, highlighting the eventual chaotic origin of the signal under analysis (*cfr.* Sect. 2.2.1). In other words, the aim of state space reconstruction is to create a state space portrait from a single data series $y(t)$.

The most common tool used for this purpose is the successive lag state space reconstruction proposed by Takens [Takens, 1981], commonly known as *delay coordinate embedding*. It proposes to create a state space portrait from a single data series $y(t)$ plotting the delayed coordinates $(y(t), y(t-\tau), y(t-2\tau))$ for a fixed value of τ. Namely,

$$y(t) \implies \begin{cases} x_1(t) &= y(t) \\ x_2(t) &= y(t-\tau) \\ x_3(t) &= y(t-2\tau) \end{cases}$$

Despite of the fact that it could seem remarkable at first that a picture topologically equivalent to an entire strange attractor can be obtained from a scalar observable, this does not represent something new. Indeed, such a technique rely on the same arguments of the Kalman observability for linear system [Brogan, 1996; Callier and Desoer, 1991; Rinaldi and Farina, 1995; Rinaldi and Piccardi, 1998; Rugh, 1996] and is, somehow, the generic nonlinear case of it. Furthermore, it is important to emphasize that the idea of using derivatives or delay coordinates in time series modeling is nothing new. It goes back at least to the work of Yule [Yule, 1927], who in 1927 used an autoregressive (AR) model to make a predictive model for the sunspot cycle. Autoregressive models are nothing more than delay coordinates used within a linear model. Delays, derivatives, principal components, and a variety of other methods of reconstruction have been widely used in time series analysis since the early fifties, and are described in several hundred books [Box *et al.*, 1994; Granger and Hatanaka, 1964; Hamilton, 1994; Ljung and Söderström, 1983; Shumway and Stoffer, 2000]. The new aspects raised by dynamical systems theory is the implied geometric view of temporal behavior [Kantz and Schreiber, 1997; Packard *et al.*, 1980].

B.1 Tuning the Takens Method

There are several works [Ding *et al.*, 1993; Ellner and Turchin, 1993; Packard *et al.*, 1980; Smith, 1992] dedicated to the tune of the lag value for the Takens reconstruction technique. Depending upon the application to which the reconstruction is aimed, these tuning methods can be very simple [Ding *et al.*, 1993; Packard *et al.*, 1980] or rather complex [Ellner and Turchin, 1993; Smith, 1992].

One of the simpler tuning method [Packard *et al.*, 1980] can be easily illustrated referring to an almost sinusoidal signal $y(t)$ as the one shown in Fig. B.1(a). Called T the pseudo-period (*cfr.* Fig. B.1(a)) of the signal $y(t)$, a good tuning for the time lag such to obtain a nice three-dimensional representation of the signal $y(t)$ is $\tau = T/4$; namely,

$$y(t) \implies \begin{cases} x_1(t) &= y(t) \\ x_2(t) &= y(t - T/4) \\ x_3(t) &= y(t - T/2) \end{cases} \tag{B.1}$$

The state space reconstruction of $y(t)$ corresponding to Eqs. (B.1) is reported in Fig. B.1(b).

There is a simple geometry-frequency explanation to justify this lag value; the signal $y(t)$ is almost sinusoidal. The spatial structure of an almost sinusoidal, *i.e.* harmonic, signal is represented by a circle; namely, in a two-dimensional space, the two reconstructed components should be a cos-like signal and sin-like one, *i.e.* the original signal and one with a relative phase lag of $\frac{\pi}{2}$ with respect to it, the time lag corresponding to such phase lag is indeed $T/4$.

Thus, the state space reconstruction as given in Eqs. (B.1) splits the given signal $y(t)$ according to the following rules.

Plane (x_1, x_2)**:** in this plane it is highlighted the harmonic structure of the signal; namely, the corresponding main circle.

Plane (x_1, x_3)**:** in this plane it is highlighted the eventual period doubling structure of the signal; namely, the period doubled circle. Indeed, a time lag of $T/2$ corresponds to a $\frac{\pi}{2}$ phase lag for a signal of pseudo-period $2T$.

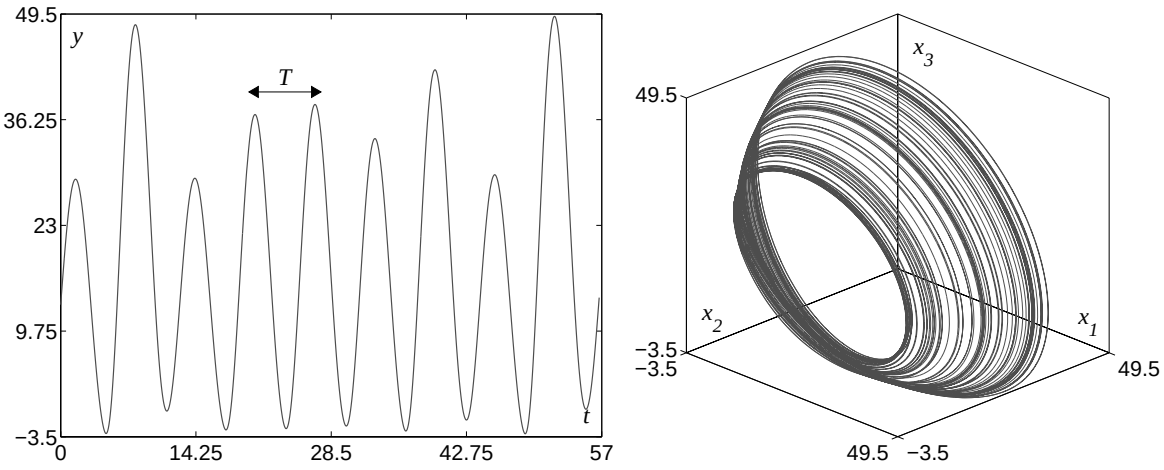

Figure B.1: *Almost,* i.e. *chaotic, sinusoidal signal: (a) – time series; (b) – Takens state space reconstruction.*

B.2 Variation of the Takens Method

The tuning method described above (*cfr.* Sect. B.1) works very well for approximately periodic signals, as the one reported in Fig. B.1(a), but, on the other hand, is quite inefficient for n-pulse-like signals as the one shown in Fig. B.2. In fact, as shown in Fig. B.3(a), this reconstruction technique does not highlight at all the tea-cup structure usually associated with bursting signals [Izhikevich, 2000; Kuznetsov and Rinaldi, 1996].

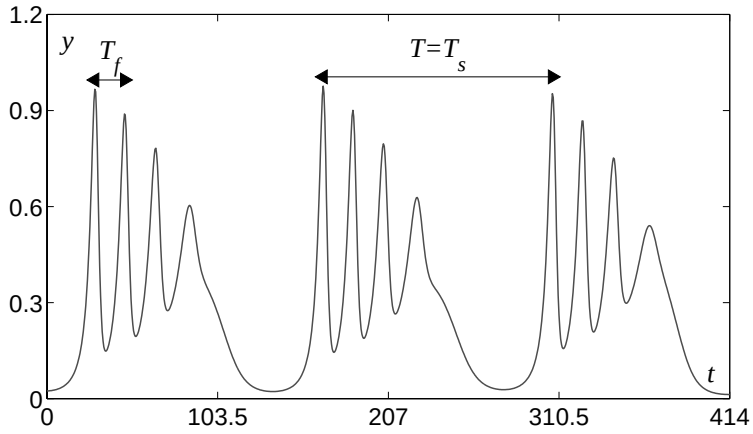

Figure B.2: *An approximately periodic bursting signal,* i.e. *a chaotic n-pulse-like signal.*

The why is quite evident since this reconstruction method tries to highlight only the main slow component but does not try to isolate the fast, bursting, component.

An alternative state space reconstruction method, which meets the requirement of highlighting the bursting structure, is to use the Takens method with two different time lags. Referring to Fig. B.2, called T_s the slow component pseudo-period and T_f the fast, *i.e.* bursting, component pseudo-period, a good tuning for the two time lags such to obtain a nice three-dimensional representation of the signal $y(t)$ is $\tau_1 = T_f/4$ and $\tau_1 = T_s/4$; namely,

$$y(t) \implies \begin{cases} x_1(t) &= y(t) \\ x_2(t) &= y(t - T_s/4) \\ x_3(t) &= y(t - T_f/4) \end{cases} \tag{B.2}$$

The state space reconstruction of $y(t)$ corresponding to Eqs. (B.2) is reported in Fig. B.3(b).

Thus, keeping in account the geometrical explanation given in the previous section, the state space reconstruction as given in Eqs. (B.2) splits the given signal $y(t)$ according to the following rules.

Plane (x_1, x_2)**:** in this plane it is highlighted the harmonic structure of the slow component of the signal; namely, the corresponding main circle.

Plane (x_1, x_3)**:** in this plane it is highlighted the harmonic structure of the bursting component of the signal; namely, the corresponding secondary circle.

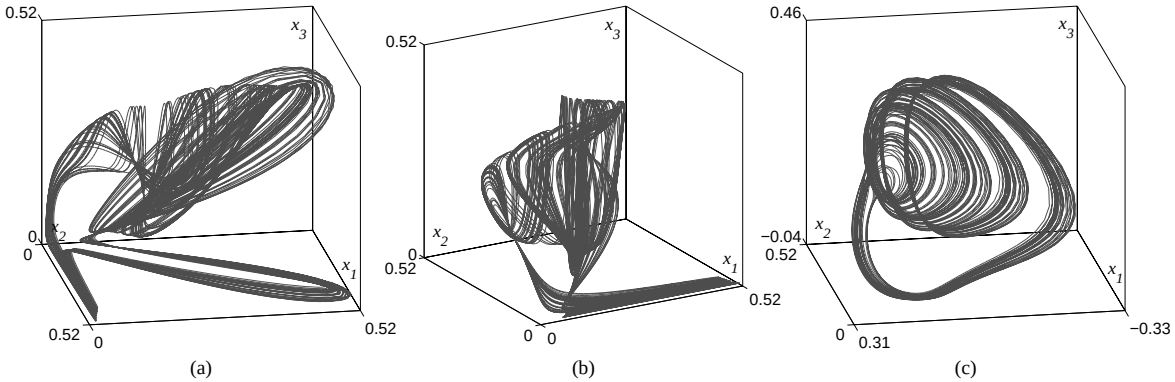

Figure B.3: *State space reconstruction of an approximately periodic bursting signal,* i.e. *a chaotic n-pulse-like signal: (a) – Takens state space reconstruction; (b) – modified Takens state space reconstruction; (c) – nonminimal phase state space reconstruction.*

B.3 The Nonminimal Phase State Space Reconstruction

Albeit already rather effective, the reconstruction method described above (*cfr.* Sect. B.2) does not highlight any of the eventual chaotic features of the given signal. In fact, the period doubling structure is not split in anyone of the directions of the reconstruction state space.

Referring to the geometrical explanation given in Sect. B.1, to highlight the eventual period doubling, *i.e.* chaotic, structure of the given signal $y(t)$, it should be used a longer time lag such to highlight the period doubled components; on the other hand, the corresponding phase lag should short with the frequency such to do not introduce an excessive phase lag at the main frequency. In other words, the lag introduced should depend on the frequency such to highlight the different frequency components. Such a requirement can be very easily met using the $(1,1)$ Padé approximation [Marro, 1997] of the time lag, rather than the time lag itself, for obtaining the x_2 and x_3 state space components in Eqs. (B.2).

In fact, the $(1,1)$ Padé approximation of a time lag τ is given, in the Laplace domain, by

$$e^{-s\tau} \approx G_P(s) = \frac{1 - s\frac{\tau}{2}}{1 + s\frac{\tau}{2}} \tag{B.3}$$

Figure B.4 compares the amplitude and phase Bode plots [Marro, 1997] of the time lag τ, *i.e.* $e^{j\omega\tau}$ (thin line), with those of the corresponding $(1,1)$ Padé approximation, *i.e.* $G_P(j\omega)$ (bold line). As it can be noticed, the amplitude factor is constant at one for both the finite time lag and the corresponding Padé

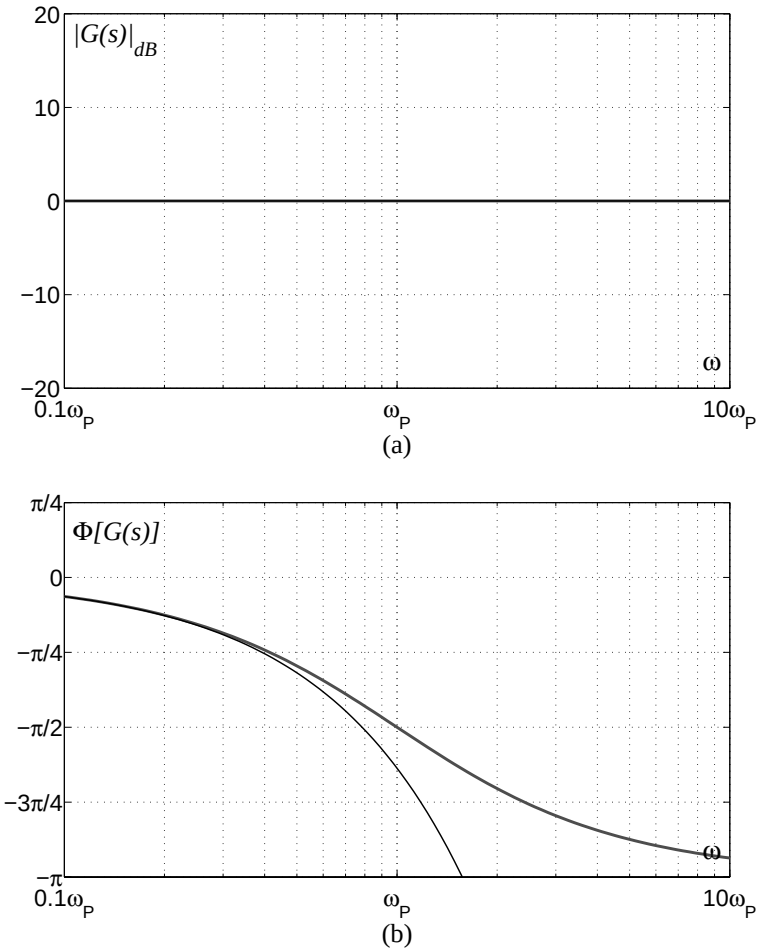

Figure B.4: *Frequency behavior of a finite time lag τ and of the corresponding $(1,1)$ Padé approximation: (a) – amplitude Bode plot, the thin line is the finite time lag τ while the bold line is the corresponding $(1,1)$ Padé approximation; (b) – phase Bode plot, the thin line is the finite time lag τ while the bold line is the corresponding $(1,1)$ Padé approximation.*

approximation. Obviously, the phase lag of the finite time lag is linearly proportional to the frequency of the stimulus. On the contrary, the phase lag of the corresponding Padé approximation is approximately equal to the one of the finite time lag for very low pulsatances while it shorter for pulsatances higher than $\omega_P = 2/\tau$ saturating at $-\pi$. Therefore, tuning, the time lag τ on the period doubled component of interest, *i.e.* $\tau = 2T_i/4\, i = s, f$, it follows that the phase lag is about $\pi/2$ at both the period doubled and the main pulsatance, exactly as required.

Hence, referring to Eqs. (B.2), the proposed state space reconstruction triplet of the signal $y(t)$ shown in Fig. B.2 is given by

$$y(t) \implies \begin{cases} x_1(t) &= y(t) \\ x_2(t) &= \mathcal{L}^{-1}\left[\dfrac{1 - s\dfrac{T_f}{4}}{1 + s\dfrac{T_f}{4}}\mathcal{L}\big[y(t)\big]\right] \\ x_3(t) &= \mathcal{L}^{-1}\left[\dfrac{1 - s\dfrac{T_s}{4}}{1 + s\dfrac{T_s}{4}}\mathcal{L}\big[y(t)\big]\right] \end{cases} \tag{B.4}$$

where $\mathcal{L}$ is the Laplace transform operator and $\mathcal{L}^{-1}$ is the corresponding antitransform operator.

The state space reconstruction of $y(t)$ corresponding to Eqs. (B.4) is reported in Fig. B.3(c). As can be noticed, it is substantially nicer than the corresponding Takens-like state space reconstructions reported in Fig. B.3(a-b). Indeed, both the Feigenbaum-like structure as well as the n-pulse structure of the signal are definitely highlighted in Fig. B.3(c) while hardly perceivable in Fig. B.3(a-b).

Since the Padé filter is a nonminimal phase linear filter [Marro, 1997], *i.e.* it has a positive zero, the corresponding reconstruction method has been called *nonminimal phase reconstruction*.

B.4 Analogic Realization of the Padé Filter

Other than the nicer pictures obtained, there is also a practical advantage in using the nonminimal phase state space reconstruction method.

Indeed, once the two pseudo-period T_s and T_f are determined, the corresponding two Padé filters can be analogically implemented by means of the simple circuit shown in Fig. B.5 where the two components R and C must be chosen such that $RC = T_i/4\, i = s, f$.

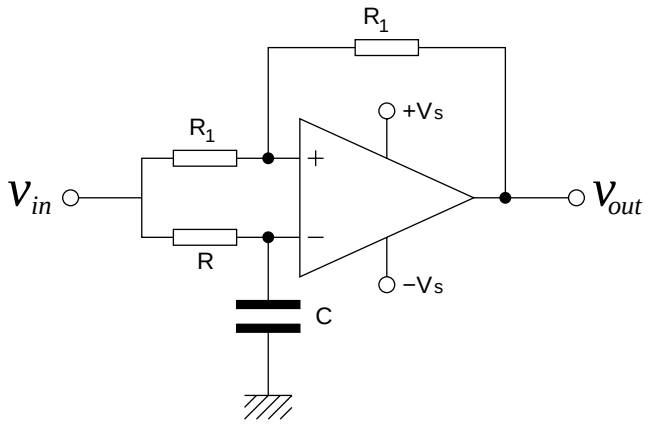

Figure B.5: *Operational amplifier based electronic realization of the* $(1, 1)$ *Padé filter.*

Therefore, the nonminimal state space reconstruction can be realized acting directly on analogic, *i.e.* continuous time, signals without employing data acquisition systems and digital signal processors (DSP) [Christiansen, 1997]. Moreover, it should be noted that to implement analogically the Takens-like methods, based on finite time delay, it is necessary to employ rather complex delayers as those based on bucket brigade technology [Christiansen, 1997].

Finally, it should be noted that the two periods T_s and T_f can be obtained by a simple spectral analysis. Indeed, they are the inverse of the two stronger independent[1] frequency components of the given signal $y(t)$.

Bibliography

Abarbanel, H., R. Brown, J. Sidorowich, and L. Tsimring (1993). The analysis of observed chaotic data in physical systems. *Review of Modern Physics*, 65, pp. 1331–1392.

Box, G., G. Jenkins, G. Reinsel, and G. Jenkins (1994). *Time Series Analysis: Forecasting & Control*. Prentice-Hall, New York, NY.

Brogan, W. (1996). *Modern Control Theory*. Prentice-Hall, New York, NY, third edition.

Callier, F. and C. Desoer (1991). *Linear System Theory*. Springer-Verlag, New York, NY.

Christiansen, D., editor (1997). *Electronics Engineers' Handbook*. McGraw-Hill for IEEE Press, New York, NY.

Ding, M., C. Grebogi, E. Ott, T. Sauer, and J. Yorke (1993). Plateau onset for correlation dimension: When does it occur? *Physical Review Letters*, 7, pp. 3872–3875.

Ellner, S. and P. Turchin (1993). *Chaos in a "Noisy" World: New Methods and Evidence from Time Series Analysis*. North Carolina State University Press, Raleigh, NC.

Granger, C. and M. Hatanaka (1964). *Spectral Analysis of Economic Time Series*. Princeton University Press, Princeton, NJ.

Hamilton, J. (1994). *Time Series Analysis*. Princeton University Press, Princeton, NJ.

Izhikevich, E. (2000). Neural excitability, spiking and bursting. *International Journal of Bifurcation and Chaos*, 10, pp. 1171–1266.

Kantz, H. and T. Schreiber (1997). *Nonlinear Time Series Analysis*. Cambridge University Press, Cambridge, UK.

Kuznetsov, Y. and S. Rinaldi (1996). Remarks on food chain dynamics. *Mathematical Biosciences*, 134, pp. 1–33.

Ljung, L. and T. Söderström (1983). *Theory and Practice of Recursive Identification*. MIT Press, Cambridge, MA.

Marro, G. (1997). *Controlli Automatici*. Zanichelli, Bologna, Italy, fourth edition. In Italian.

Packard, N., J. Crutchfield, J. Farmer, and R. Shaw (1980). Geometry from a time series. *Physical Review Letters*, 45, pp. 712–716.

Rinaldi, S. and L. Farina (1995). *I Sistemi Lineari Positivi: Teoria e Applicazioni*. UTET, Torino, Italy. In Italian.

Rinaldi, S. and C. Piccardi (1998). *I Sistemi Lineari*. UTET, Torino, Italy. In Italian.

Rugh, W. (1996). *Linear System Theory*. Prentice-Hall, New York, NY, second edition.

Shumway, R. and D. Stoffer (2000). *Time Series Analysis and Its Applications*. Springer-Verlag, New York, NY.

Smith, R. (1992). Estimating dimension in noisy chaotic time series. *Journal of Royal Statistic Society B*, 54, pp. 329–351.

Takens, F. (1981). *Detecting Strange Attractors in Turbulence*, volume 898, pp. 336–381. Springer-Verlag, Berlin, Germany.

Yule, G. (1927). On a method of investigating periodicity in disturbed series with special reference to Wolfer's sunspot numbers. *Philosophical Transaction of the Royal Society of London*, A 226, pp. 267–298.

[1] Namely, not in rational ratio.

APPENDIX C

MODELS ADMITTING n-PULSE SHIL'NIKOV-LIKE CHAOS

Brief — This Appendix reports the mathematical models, together with their corresponding parameter values, admitting n-pulse Shil'nikov-like chaos which have been considered in Sect. 3.3 for the bifurcation analysis of the qualitative resonance phenomenon.

As already mentioned in Section 3.1, some dynamical system satisfies the Shil'nikov's fourth theorem [Kuznetsov, 1998; Silva, 1993; Tresser, 1984] several times with respect to different parameter values and/or different geometries of the homoclinic trajectory. To identifies the geometrically different homoclinic trajectories are often used, here as well, one or more indexes that refer to the number of global turns (loops, pulses) that a given homoclinic trajectory does in particular regions of the state space [De Feo *et al.*, 2000; Kuznetsov *et al.*, 1993], as it was for the 1- to 5-pulse solutions shown in Sects. 3.1.1 and 3.1.2.

Since each parameter values set showing a homoclinic trajectory satisfying the Shil'nikov's fourth theorem is a good candidate for observing qualitative resonance, it follows that the same dynamical system can produce more than one case suitable for the mathematical analysis of qualitative resonance, *cfr.* Sect. 3.1. Hence, the twenty cases of qualitative resonance studied in Sect. 3.3 correspond to only six different dynamical systems which indeed admit geometrical different homoclinic trajectories all satisfying the Shil'nikov's fourth theorem.

C.1 Colpitts Oscillator

The first set of ODE, given by Eqs. (C.1), comes from the electronic applications and it is the model of a very common electronic oscillator [Sedra and Smith, 1998]. Such a model has been analyzed in detail in [De Feo *et al.*, 2000; Maggio *et al.*, 1999].

$$\begin{aligned} \dot{x}_1 &= \frac{g^*}{Q(1-k)}\left[-\alpha_F n(x_2) + x_3\right] \\ \dot{x}_2 &= \frac{g^*}{Qk}\left[(1-\alpha_F)n(x_2) + x_3\right] \\ \dot{x}_3 &= -\frac{Qk(1-k)}{g^*}\left[x_1 + x_2\right] - \frac{1}{Q}x_3 \end{aligned} \tag{C.1}$$

In the experiments α_F and k have been kept at a constant value, namely $\alpha_F = 0.996$ and $k = 0.5$, while g^* and Q have been varied to obtain the geometrically different Shil'nikov-like chaotic conditions. In particular, the considered parameter values are

	$Log_{10}(Q)$	$Log_{10}(g)$
1-pulse	0.1602	0.5659
2-pulse	0.3331	0.7530
3-pulse	0.4493	0.8875
4-pulse	0.5808	1.0121
5-pulse	0.6555	1.1368

C.2 The Rosenzweig—MacArthur Food Chain

The second set of ODE, given by Eqs. (C.2), comes from biology, it is one of the most common model of a tritrophic food chain [De Feo and Rinaldi, 1997; Hastings and Powell, 1991; Rinaldi and De Feo, 1999], namely a food chain composed of a prey, a predator, and a super-predator. This model has been analyzed in detail in [Kuznetsov *et al.*, 2001; Kuznetsov and Rinaldi, 1996].

$$\begin{aligned} \dot{x_1} &= x_1 \left[r\left(1 - \frac{x_1}{K}\right) - \frac{a_1 x_2}{1 + b_1 x_1} \right] \\ \dot{x_2} &= x_2 \left[\frac{a_1 x_1}{1 + b_1 x_1} - \frac{a_2 x_3}{1 + b_2 x_2} - d_1 \right] \\ \dot{x_3} &= x_3 \left[\frac{a_2 x_2}{1 + b_2 x_2} - d_2 \right] \end{aligned} \tag{C.2}$$

In the experiments all the parameters but r and K have been kept at constant value [De Feo, 1995; De Feo and Rinaldi, 1997; Kuznetsov *et al.*, 2001], namely

$$\begin{array}{lll} a_1 = 5.0 & b_1 = 3.0 & d_1 = 0.4 \\ a_2 = 0.1 & b_2 = 2.0 & d_1 = 0.01 \end{array}$$

while K and r have been varied to obtain the geometrically different Shil'nikov-like chaotic conditions. In particular, the considered parameter values are

	K	r
1-pulse	1.0713	0.8015
2-pulse	1.0829	0.8273
3-pulse	1.0888	0.8522
4-pulse	1.0925	0.8742
5-pulse	1.0943	0.8904

C.3 The Chua's Circuit

The third set of ODE, given by Eqs. (C.3), comes from the electronic applications and it is the model of the very famous Chua's circuit [Madan, 1993; Mastumoto, 1993]. Such a model has been analyzed in detail in several paper, among them are [Bykov, 1998; Khibnik *et al.*, 1993].

$$\begin{aligned} r\dot{x}_1 &= -vx_1 + \beta(x_2 - x_1) - Ax_3 - B(x_2 - x_1)^3 \\ \dot{x}_2 &= -\beta(x_2 - x_1) - x_3 - B(x_2 - x_1) \\ \dot{x}_3 &= x_2 \end{aligned} \tag{C.3}$$

In the experiments all the parameters but v and β have been kept at constant value [Freire *et al.*, 1993], namely

$$A = 0.3286 \quad B = 0.9336 \quad r = 0.6$$

while a and b have been varied to obtain the geometrically different Shil'nikov-like chaotic conditions. In particular, the considered parameter values are

	v	β
2-1-pulse	−0.8126	0.399
3-2-pulse	−0.7096	0.401

C.4 The Hindmarsh—Rose Neuron

The fourth set of ODE, given by Eqs. (C.4), comes from physiology, it is one of the most common model of a neuron cell [Hindmarsh and Rose, 1984]. This model has been analyzed in detail in [Belykh *et al.*, 2001; Kaas-Peteresen, 1986].

$$\begin{aligned} \dot{x}_1 &= x_2 - ax_1^3 + bx_1^2 + I - x_3 \\ \dot{x}_2 &= c - dx_1^2 - x_2 \\ \dot{x}_3 &= r\big[S(x_1 - \overline{x}_1) - x_3\big] \end{aligned} \tag{C.4}$$

In the experiments all the parameters but I and r have been kept at constant value [Fan and Holden, 1993; Holden and Fan, 1992], namely

$$\begin{array}{lll} a = 1.0 & b = 3.0 & c = 1.0 \\ d = 5.0 & S = 4.0 & \overline{x}_1 = -1.6 \end{array}$$

while I and r have been varied to obtain the geometrically different Shil'nikov-like chaotic conditions. In particular, the considered parameter values are

	I	r
4-pulse	2.9	0.0073
5-pulse	3.1	0.0052
6-pulse	3.25	0.0048

C.5 The Rössler Reaction

The fifth set of ODE, given by Eqs. (C.5), comes from chemistry, it is a very famous model of a (fake) chemical reaction [Rössler, 1976a,b,c,d]. It is one of the first chaotic model that have been discovered and several books and articles deal with these equations [Mastumoto, 1993].

$$\begin{aligned} \dot{x}_1 &= -x_1 - x_3 \\ \dot{x}_2 &= x_1 + ax_2 \\ \dot{x}_3 &= bx_1 + x_3(x_1 - c) \end{aligned} \tag{C.5}$$

In the experiments c has been held fixed, namely $c = 4.5$ while a and b have been varied to obtain the geometrically different Shil'nikov-like chaotic conditions. In particular, the considered parameter values are [Mastumoto, 1993]

	a	b
1-pulse	0.36	0.35
2-pulse	0.45	0.20

C.6 The Lorenz Atmospheric Model

The sixth set of ODE, given by Eqs. (C.6), comes from meteorology, it is a variation of the famous approximation of the Navier—Stokes equations given by Lorenz in the 1969 [Lorenz, 1963]. It has been analyzed in detail in [Shil'nikov *et al.*, 1995].

$$\begin{aligned} \dot{x}_1 &= -x_2^2 - x_3^2 - ax_1 + aF \\ \dot{x}_2 &= x_1x_2 - bx_1x_3 - x_2 + G \\ \dot{x}_3 &= bx_1x_2 + x_1x_3 - x_3 \end{aligned} \tag{C.6}$$

In the experiments a and b have been held fixed, namely $a = 0.25$ and $b = 4$, while F and G have been varied to obtain the geometrically different Shil'nikov-like chaotic conditions. In particular, the considered parameter values are [Shil'nikov *et al.*, 1995]

	F	G
5-pulse	5.012	1.077
7-pulse	4.791	1.063

It should be noted that the parameter values considered here [Shil'nikov *et al.*, 1995] are quite far from those usually considered for this model [Lorenz, 1987, 1990].

Bibliography

Belykh, V., I. Beklykh, M. Colding-Jørgensen, and E. Mosekilde (2001). Homoclinic bifurcations leading to the emergence of bursting oscillations in cell models. *European Journal of Physics B*. To Appear.

Bykov, V. (1998). On bifurcations leading to chaos in Chua's circuit. *International Journal of Bifurcation and Chaos*, 8, pp. 685–699.

De Feo, O. (1995). *Arrichimento nelle Catene Alimentari: Nessi tra Produzione Media e Biforcazioni*. Master's thesis, Politecnico di Milano, Milano, Italy. In Italian.

De Feo, O., G. Maggio, and M. Kennedy (2000). The Colpitts oscillator: Families of periodic solutions and their bifurcations. *International Journal of Bifurcation and Chaos*, 10, pp. 935–958.

De Feo, O. and S. Rinaldi (1997). Yield and dynamics in tritrophic food chains. *The American Naturalist*, 150, pp. 328–345.

Fan, Y. and A. Holden (1993). Bifurcations, burstings, chaos and crises in the Rose—Hindmarsh model for neuronal activity. *Chaos, Solitons and Fractals*, 3, pp. 439–449.

Freire, E., A. Rodriguez-Luis, E. Gamero, and E. Ponce (1993). A case study for homoclinic chaos in an autonomous electronic circuit. *Physica D*, 62, pp. 230–253.

Hastings, H. and T. Powell (1991). Chaos in three species food chain. *Ecology*, 72, pp. 896–903.

Hindmarsh, J. and R. Rose (1984). A model of neuronal bursting using three coupled first order differential equations. *Philosophical Transaction of the Royal Society of London*, B221, pp. 87–102.

Holden, A. and Y. Fan (1992). Crises-induced chaos in the Rose—Hindmarsh model for neuronal activity. *Chaos, Solitons and Fractals*, 2, pp. 583–595.

Kaas-Peteresen, C. (1986). *Bifurcations in the Rose—Hindmarsh and Chay models*, pp. 183–190. Plenum Press, New York, NY.

Khibnik, A., D. Roose, and L. Chua (1993). On periodic orbits and homoclinic bifurcations in Chua's circuit with a smooth nonlinearity. *International Journal of Bifurcation and Chaos*, 3, pp. 363–384.

Kuznetsov, A., S. Kuznetsov, I. Sataev, and L. Chua (1993). Two-parameter study of transition to chaos in Chua's circuit: Renormalization group, universality and scaling. *International Journal of Bifurcation and Chaos*, 3, pp. 943–962.

Kuznetsov, Y. (1998). *Elements of Applied Bifurcation Theory*. Springer-Verlag, New York, NY, second edition.

Kuznetsov, Y., O. De Feo, and S. Rinaldi (2001). Belyakov homoclinic bifurcations in a tritrophic food chain model. *SIAM Journal of Applied Mathematics*. Submitted.

Kuznetsov, Y. and S. Rinaldi (1996). Remarks on food chain dynamics. *Mathematical Biosciences*, 134, pp. 1–33.

Lorenz, E. (1963). Deterministic nonperiodic flow. *Journal of Atmospheric Science*, 20, pp. 130–141.

Lorenz, E. (1987). *Deterministic and Stochastic Aspects of Atmospheric Dynamics*, pp. 159–179. Reidel, Dordrecht, Germany.

Lorenz, E. (1990). Can chaos and intransitivity lead to interannual variability? *Tellus*, 42A, pp. 378–389.

Madan, R., editor (1993). *Chua's Circuit: A Paradigm for Chaos*. World Scientific, Singapore, fourth edition.

Maggio, G., O. De Feo, and M. Kennedy (1999). Nonlinear analysis of the Colpitts oscillator and applications to design. *IEEE Transaction on Circuit and Systems—I*, 46, pp. 1118–1130.

Mastumoto, T. (1993). *Bifurcations: Sights, Sounds and Mathematics*. Springer-Verlag, Tokyo, Japan.

Rinaldi, S. and O. De Feo (1999). Top-predator abundance and chaos in tritrophic food chains. *Ecology Letters*, 2, pp. 6–10.

Rössler, O. (1976a). Chaotic behavior in simple reaction systems. *Zeitschrift für Naturforschung*, 31A, pp. 259–264.

Rössler, O. (1976b). Chemical turbulence: Chaos in a simple reaction-diffusion system. *Zeitschrift für Naturforschung*, 31A, pp. 1168–1172.

Rössler, O. (1976c). Different types of chaos in two simple differential equations. *Zeitschrift für Naturforschung*, 31A, pp. 1664–1670.

Rössler, O. (1976d). An equation for continuous chaos. *Physics Letters*, 57A, pp. 397–398.

Sedra, S. and K. Smith (1998). *Microelectronic Circuits*. Oxford University Press, New York, NY, fourth edition.

Shil'nikov, A., G. Nicolis, and C. Nicolis (1995). Bifurcation and predictability analysis of a low-order atmospheric circulation model. *International Journal of Bifurcation and Chaos*, 5, pp. 1701–1711.

Silva, C. (1993). Shil'nikov theorem – a tutorial. *IEEE Transaction on Circuits and Systems—I*, 40, pp. 675–682.

Tresser, C. (1984). On some theorems of L. P. Shil'nikov and some applications. *Annales de l'Institute Henri Poincaré*, 40, pp. 441–461.

APPENDIX D

MODEL FOR THE QUALITATIVE RESONANCE ANALYSIS

Brief — This Appendix explains how to implement the model necessary for the continuation-based bifurcation analysis of qualitative resonance.

The continuation problem defined by the systems (3.7) and (3.8) proposed in Sect. 3.3.1 cannot be implemented automatically in AUTO97. Namely, AUTO97 is suited for the bifurcation analysis of the periodic solutions of ODE or for the continuation of ODE boundary value problems [Doedel *et al.*, 1998, 1991a,b] (*cfr.* Appendix F) but cannot deals directly with the continuation problem defined by Eqs. (3.7) and (3.8). Hence, it is necessary to reformulate such a problem in the form of an ODE boundary value problem (BVP) with integral and instantaneous constraints which is then treatable by means of AUTO97.

This reformulation is not very difficult, even if rather tricky, once the playing actors are correctly spotted. Actually, for the bifurcation analysis of qualitative resonance there are five dynamical invariants that need to be determined.

1. *The generating cycle*: a copy of the driven system must be used in order to determine the generating cycle which is necessary to know since it is the skeleton of the driving signal.

2. *The stable eigendirection of the generating cycle*: the perturbations considered (*cfr.* Eq. (3.8)) are composed of perturbations in three possible directions, the stable, unstable, and tangent direction of the generating cycle. Therefore, it is necessary to compute the corresponding eigendirections in order to correctly compose the driving signal.

3. *The unstable eigendirection of the generating cycle*: same as above.

4. *The tangent eigendirection of the generating cycle*: same as above. Actually, the tangent eigendirection is trivial to compute since is given by the local Jacobian, *i.e.* by the right hand side (RHS) defining the ODE.

5. *The driving signal*: the generating cycle, its eigendirections, and the bifurcations parameter must be composed into a driving signal.

6. *The periodic solution of the driven system*: the driving signal must be injected into the driven system and the corresponding periodic solution must be continued.

Keeping that in mind, the continuation problem is correctly defined by the following ODE boundary

value problem with integral constraints

$$
\begin{cases}
\text{(I)} & \begin{cases} 0 = \dot{\widetilde{x}}(\tau) - T_G F\big(\widetilde{x}(\tau)\big) \\ 0 = \widetilde{x}(0) - \widetilde{x}(1) \\ 0 = \displaystyle\int_0^1 \langle \widetilde{x}(\tau), \dot{v}(\tau)\rangle d\tau \end{cases} \\
\text{(II)} & \begin{cases} 0 = \dot{e}_p(\tau) - T_G F_x\big(\widetilde{x}(\tau)\big) e_p(\tau) \\ 0 = e_p(1) - \mu_0 e_p(0) \\ 0 = \displaystyle\int_0^1 \langle e_p(\tau), e_p(\tau)\rangle d\tau - 1 \\ 0 = \dot{e}_s(\tau) - T_G F_x\big(\widetilde{x}(\tau)\big) e_s(\tau) \\ 0 = e_s(1) - \mu_1 e_s(0) \\ 0 = \displaystyle\int_0^1 \langle e_s(\tau), e_s(\tau)\rangle d\tau - 1 \\ 0 = \dot{e}_u(\tau) - T_G F_x\big(\widetilde{x}(\tau)\big) e_u(\tau) \\ 0 = e_u(1) - \mu_2 e_u(0) \\ 0 = \displaystyle\int_0^1 \langle e_u(\tau), e_u(\tau)\rangle d\tau - 1 \end{cases} \\
\text{(III)} & \begin{cases} \widetilde{y}(\tau) = C\widetilde{x}(\tau) \\ \varepsilon(\tau) = C\big[e_p(\tau)\delta_p(\tau) + e_s(\tau)\delta_s(\tau) + e_u(\tau)\delta_u(\tau)\big] \\ y_d(\tau) = \widetilde{y}(\tau) + \varepsilon(\tau) \end{cases} \\
\text{(IV)} & \begin{cases} 0 = \dot{x}(\tau) - T_0\Big[F\big(x(\tau)\big) - K\big(Cx(\tau) - y_d(\tau)\big)\Big] \\ 0 = x(0) - x(1) \\ 0 = \displaystyle\int_0^1 \langle x(\tau), \dot{w}(\tau)\rangle d\tau \end{cases}
\end{cases}
\tag{D.1}
$$

where $\langle x, y\rangle$ stands for the standard scalar product between x and y while F_x stands for the Jacobian of the RHS, *i.e.* $F_x = \frac{\partial F(x)}{\partial x}$. The boundary value problem defined by Eqs. (D.1) is composed of four blocks.

The first block is a periodic BVP defining the continuation of the generating cycle [Doedel *et al.*, 1998, 1991a,b; Kuznetsov, 1998], *i.e.* the clean driving signal. This block is, in turn, composed of three constraints. The dynamical constraint defined by the RHS, the periodic boundary constraint, and the phase constraint which is necessary to uniquely determine the periodic solution. In fact, there are infinite solutions satisfying the first two constraints, one for each possible initial phase; hence, it is necessary to chose one among them: this is the meaning of the phase constraint [Doedel *et al.*, 1998, 1991a,b; Kuznetsov, 1998]. Actually, the given constraint select the periodic solution $x(t)$ which is closest to the reference periodic function $v(t)$. Theoretically, $v(t)$ can be any vector-valued function with period one; in practice, it can be chosen to be the periodic solution $x(t)$ at the previous continuation step [Doedel *et al.*, 1998, 1991a,b; Kuznetsov, 1998]. Note that the period of the generating cycle has been factorized in front of the RHS such to have it available as continuation parameter and to uniquely fix the temporal boundaries at zero and one [Kuznetsov, 1998]. Finally, the continuation of this block provide automatically the Floquet multipliers μ_0, μ_1, and μ_2 of the generating cycle [Doedel *et al.*, 1998, 1991a,b; Kuznetsov, 1998]. In particular, $\mu_0 = 1$, $|\mu_1| < 1$, and $|\mu_2| > 1$; namely, μ_0 identifies the eigendirection tangent to the generating cycle, while μ_1 [μ_2] identifies the stable [unstable] eigendirection tangent of the generating cycle. The Floquet multipliers are necessary to compute the eigendirections in the next continuation block.

The second block is a nonperiodic boundary value problem defining the continuation of the eigendirections

of the generating cycle. This block is composed of nine constraints; namely, three for each eigendirection. The variational dynamical constraint, the Poincaré constraint, and the norm constraint which is necessary to uniquely determine the eigendirection. In fact, similarly to the phase in the previous block, the eigendirection can be specified up to a constant factor; therefore, it is necessary a norm condition to uniquely determine it [Kuznetsov, 1998]. Note that the eigendirections are functions of the time since they change along the generating cycle [Kuznetsov, 1998].

The third block determines the driving signal according to the perturbation parameters (*cfr.* Sect. 3.3.1).

The fourth, and last, block is the boundary value problem defining the continuation of the periodic solutions of the driven system. This block is very similar to the first block.

Finally, it should be noted that the boundary value problem defined by Eqs. (D.1) involves double or triple the number of the differential equations involved in the cycle continuation. This kind of boundary value problems are called *extended augmented BVP* [Kuznetsov, 1998]. It is possible to derive a *minimally augmented BVP* to perform the same continuation using a *bordering technique* [Kuznetsov, 1998]. Indeed, the continuations have been performed using a minimal system and not the one reported in Eqs. (D.1) but its attainment is behind the scope of this Appendix and can be found [Kuznetsov, 1998].

Bibliography

Doedel, E., A. Champneys, T. Fairgrieve, Y. Kuznetsov, B. Sandstede, and X. Wang (1998). *AUTO 97: Continuation and Bifurcation Software for Ordinary Differential Equations withHomCont*. Computer Science Department, Concordia University, Montreal, Canada, Motreal, Quebec, Canada.

Doedel, E., H. Keller, and J. Kernévez (1991a). Numerical analysis and control of bifurcation problems, part I: Bifurcation in finite dimensions. *International Journal of Bifurcation and Chaos*, 1, pp. 493–520.

Doedel, E., H. Keller, and J. Kernévez (1991b). Numerical analysis and control of bifurcation problems, part II: Bifurcation in infinite dimensions. *International Journal of Bifurcation and Chaos*, 1, pp. 745–772.

Kuznetsov, Y. (1998). *Elements of Applied Bifurcation Theory*. Springer-Verlag, New York, NY, second edition.

APPENDIX E

ADDENDA

Brief — This Appendix reports, in a brainstorm style, remarks and ideas that, for one reason or another, have not been "officially" reported in the main text. The reason for that is to somehow leave a trace of certain ideas that at first sight were genial but which afterward reveal to be fallacious. The failures are never officially reported but knowing about them would allow to a lot of people to save time.

E.1 Chapter 1

The state of the art which has been reported is rather addressed to the specific approach of exploiting chaos that has been presented in this thesis. Nonetheless, there are several essays of exploiting chaos in cognitive science, take a look on the bibliography reported in Appendix G.

E.2 Chapter 2

There exist several other kinds of strange attractors which have not been mentioned since they are not related with the goal of this thesis. Nonetheless, the class of the so-called *multi-wings* strange attractors [Gumowski and Mira, 1980], which are rather common in the discrete time dynamical systems, could results rather interesting for the problems of grammar detection and automata identification [Giles and Omlin, 1993; Tani and Fukumura, 1995].

Trying to prove that the joint probability distribution of phase skip lengths and pattern interval lengths (Fig. 2.43) fails since there is no apparent simple way to determine when a phase skip trajectory segment finishes escaping the equilibria and start to run along a pattern trajectory segment.

E.3 Chapter 3

Almost all the trials to make a global analysis, in contrary to the linear analysis which is local, of the qualitative resonance failed since the real problem is to determine the probability distribution with which the different regions of the Shil'nikov-like strange attractors are visited. This is a typical unsolved problem of ergodic theory; therefore also a deep understanding of the qualitative resonance remains an open problem too. Developing a global theory, maybe a Lyapunov-like one, about qualitative resonance would give definitely stronger power for mastering the application exploiting it. Several trials have been made in this direction without any success.

E.4 Chapter 4

The qualitative resonance could be used at symbol level as well, using a strange attractor to represent a symbolic sequence and transforming the fragmentary symbolic information in a driving signal. Some experiment has been made in this direction but has not been very successful.

The peak-to-peak pattern recognition would reduce the recognition of the entire pattern to the recognition of its peak-to-peak maps. This means a drastic reduction of data. Nevertheless, the problem remains since afterward the qualitative shape of the peak-to-peak map must be recognized. Thus, this technique would be a transposition of the problem not its solution.

It is not very difficult to extend the qualitatively resonating filter such as to recognize n-dimensional patterns. Once again, a filter bank can be used to solve problems of n-dimensional temporal patterns recognition. Somehow summing together the results of the qualitative resonance functionals of a filter bank it is possible to verify that a vector input is resonating with the entire filter bank. In this case the filter have a multi-input and a single-output. Each filter has its own input and the outputs are summed[1] together. Each components of the vectorial input is presented as input to a different filter while the outputs are combined together to form a scalar likelihood. Obviously, it can be imagined to realize a filter bank of filter banks to solve a problem of n-ary classification of m-dimensional temporal patterns.

E.5 Chapter 5

Several other techniques have been tried to solve the identification problem. In particular, efforts have been made trying to avoid the step that must lead the system in Shil'nikov conditions. Most of the tried techniques, not all of them, have proved to be fallacious.

E.5.1 Fitting by Continuation

The continuation techniques, and in particular the optimization capabilities of Auto97 can be exploited to solve the identification problem all at once. In fact, the identification problem can be formulated as a boundary value problem with dynamical and integral constraint that must be somehow "optimized". This is a rather interesting technique, it has been tested and it works but it is awfully complicated.

E.5.2 Fake Shil'nikov

One of the first ideas of the author was to build a reference Shil'nikov strange attractors starting from the description of a temporal stereotype and of the stochastic requirement about its diversity. Believe, it is not a good idea. The method is a big failure; the geometrical structures of the "fake" Shil'nikov have nothing to do with those of the real signals considered. Thus, the system never works.

E.5.3 Backward Lur'e Identification

In the same framework of Lur'e identification as presented in Sect. 5.1.3, the information can be propagated backward rather than forward in the loop. In the backward propagation of the information the parameters of the linear transfer function are drifted to improve the identification of the nonlinear static function. Namely, there are three step which are iterated: 1 — inverse filtering $y(t) \to \widehat{G}^{-1}(Z) \to u(t)$ which obtains u from y; 2 — curve fitting $(u, y) \to f_p(\cdot)$ which obtains $f_p(\cdot)$ from the pair (u, y); 3 — the optimization which drift the parameters of $\widehat{G}(Z)$, *i.e.* poles and zeros, to improve the data fitting at the second step.
The method has been tested and it works, but not very well.

E.5.4 Forward-Backward Lur'e Identification

The game should be rather clear now. In forward-backward, the transfer function $\widehat{G}(Z)$ is inverted to obtain the $u(t)$ from $y(t)$ then the new estimate of $u(t)$ is used to correct the nonlinearity (backward step). Now, it starts again in a forward step from the new guess of u, which should be equal to y, $y \to f \to u$ then $(u, y) \to \widehat{G}(Z)$ and again iterating $y \to \widehat{G}^{-1}(Z) \to u$. In this approach no optimization is exploited. It has

[1] Not necessarily a simple sum it could be a weighted sum or whatever else, the point is to summarize the outputs in a single one.

been tested and does not work, the procedure is unstable most of the time. Furthermore, it is strictly local therefore it strongly depends on the initial guess.

E.5.5 Round Lur'e Identification

The round propagation is the forward-backward in which the optimization is exploited. 1 — $y \rightarrow f_p(\cdot) \rightarrow u$; 2 — $(u, y) \rightarrow \widehat{G}(Z)$; 3 — $quality(\widehat{G}) \rightarrow \Delta p_1$, first optimization; 4 — $y \rightarrow \widehat{G}^{-1}(Z) \rightarrow u$; 5 — $(u, y) \rightarrow f_p(\cdot)$; 6 — $quality(f_p) \rightarrow \Delta p_2$, second optimization; 6 — $f_p \rightarrow f_{p+\Delta p_1+\Delta p_2}$ then iterate. There are two optimization at each step. It has been tested, it works but the results do not justify the increased complexity.

E.5.6 Periodic Linear Identification

Methods of periodic linear identification [Arambel and Tadmor, 1994; Hench, 1995] can be exploited to determine a non autonomous linear periodic system from the data. Subsequently, a state space to time transformation $x \mapsto t$ can be determined such as to obtain an autonomous nonlinear ODE. Some experience with this method has been made but it reveals to be rather complicated to master.

E.5.7 Neural Network Identification

The idea is rather trivial. First the signal y is filtered with the nonminimal phase filters described in Appendix B such to obtain an n-dimensional vector $y \mapsto x$ then a *radial basis function* neural network is used trying to determine F such that $\dot{x} = F(x)$. It has never been seriously tried. Nevertheless, some essays in a similar direction where also the qualitative resonance and anti-resonance requirements are imposed at the same time gave very promising results.

E.6 Chapter 6

There are two ideas about the filter gain tuning that have never been seriously tried.

1. Conversion of K from periodic to state dependent. Namely, a state space to time transformation $x \mapsto t$ can be searched such to obtain an autonomous nonlinear ODE for (F, K). The few trials in this direction have not been very exciting. Usually, the overall system becomes unstable.

2. As mentioned above (*cfr.* Sect. E.5.7) the filter gain tuning can be performed at the same time of the identification such that is the anti-resonance requirement that lead to the Shil'nikov conditions. In this way the Shil'nikov-like chaos should emerge rather than being imposed. Few trials but very promising.

E.7 Chapter 7

Not all the tests ran during these years have been reported, only those that were composing a coherent set.

In reality most of the variants proposed for the algorithms have been tried on the same kind of data as those considered in Chap. 7. These are the tests that have allowed to say that the proposed technique was effective enough with respect to the other techniques.

A trial not reported here but noteworthy is the "writing signals" test since the idea was to extent to n-dimensional case the qualitative resonance. The idea was to determine a circle and a square drawn continuously by hand, *i.e.* continuing drawing a circle. The x and y coordinate must be considered together in such a case. Only a simple trial has been made in such direction not a complete test but the results were promising.

E.8 Chapter 8

An engineering mathematical research path could be to discover the exact extent of qualitative resonance. In particular, to find, if it exists, a necessary[2] condition for resonance and a sufficient condition for anti-resonance. About this last one, it could be that a necessary condition could be found too since anti-resonance involve chaos the it should be easier.

[2] A sufficient condition would be quite difficult to obtain

Bibliography

Arambel, P. and G. Tadmor (1994). Robust H_∞ identification of linear periodic discrete-time systems. *International Journal of Robust and Nonlinear Control*, 4, pp. 595–612.

Giles, C. and C. Omlin (1993). Extraction, insertion and refinement of symbolic rules in dynamically driven recurrent neural networks. *Connection Science*, 5, pp. 307–337.

Gumowski, J. and C. Mira (1980). *Dynamique Chaotique*. Capadues, Toulouse, France. In French.

Hench, J. (1995). Technique for the identification of linear periodic state-space models. *International Journal of Control*, 62, pp. 289–301.

Tani, J. and N. Fukumura (1995). Embedding a grammatical description in deterministic chaos: An experiment in recurrent neural learning. *Biological Cybernetics*, 72, pp. 365–370.

APPENDIX F

CONTINUATION SOFTWARE

Brief — This Appendix reports a very brief description of the two continuation software packages that have been employed in this thesis.

Continuation methods allow one to translate the bifurcation analysis of equilibria and cycles into the solution of a system of implicit algebraic equations, which can be then computed systematically. Hence, the bifurcation analysis is reduced to locating the zeroes of some functions, which can be found, with the desired precision, by using Newton-based algorithms.

Continuation methods permit the analysis of the dependence of the invariants of a dynamical system (like equilibria or cycles) on the control parameters. Namely, given a dynamical system, for instance an ODE

$$\dot{x}(t) = F\big(x(t), p\big), \qquad f(\cdot,\cdot), x(\cdot) \in \mathbb{R}^n,\ t \in \mathbb{R}$$

where x is the state vector and p represents the parameter set. The aim of the continuation techniques is to determine how the qualitative properties of the system invariants change when varying the parameters. For example, they can predict the stability changes of an equilibrium point, depending on the parameters.

For certain invariants, namely equilibria and cycles, it is possible to express their existence in an algebraic implicit form of the kind

$$G(X) = 0$$

where X is a suitable space that, in general, is obtained by combining the control parameters, the state variables and the dummy[1] variables [Doedel *et al.*, 1991a,b; Kuznetsov, 1998].

The defining function G can be very simple (for equilibria)

$$G\left(X\right) = F\left(x, p\right), \qquad X \equiv [x, p]^T$$

or incredibly complex (for cycles) and can be obtained by special procedures such as the collocation method [de Boor and Swartz, 1973; Kuznetsov, 1998; Russell and Christiansen, 1978]. In the case of cycles the X space is constructed by extending the (x, p) space with variables obtained from the discretization of the cycle itself.

However, the main point is that given an initial solution (e.g. an equilibrium or a cycle), by using an appropriate continuation algorithm, which is usually based upon prediction-correction methods for locating zeroes of functions, it is possible to vary one parameter p_i and to follow the locus in the X space satisfying the condition $G(X) = 0$. In other words, this process consists of determining how the invariant moves and deforms with variations of one parameter. Furthermore, it is possible to monitor, along the continuation path, a certain number of so-called *test functions* [Champneys and Kuznetsov, 1994; Kuznetsov, 1998] whose zeroes correspond to bifurcations of the invariants. By appending an annihilated test function to the defining functions vector it is even possible to "follow" (*i.e.* to continue, as stated before) the locus of the bifurcations of the invariant with respect to two or more parameters.

There are several advantages to using continuation methods as opposed to simulation in systems analysis

[1] Auxiliary variables used in the continuation process either for discretization or monitoring purposes.

— The solutions can be followed in the parameter space even if they are unstable while simulation allows the observation of stable solutions only. In this regard it should be noted that unstable periodic orbits, and in particular saddles, are involved in many bifurcation phenomena. Furthermore, the saddles' invariants separate the basins of attraction of different attractors.

— There is no need to wait for transients to settle before studying the invariants.

— The results are independent of the choice of Poincaré section.

— Numerical problems associated with sensitivity to the initial conditions are avoided.

— Continuation makes it possible to detect hysteretic phenomena due to coexisting attractors while this is difficult to achieve by simulation methods.

In this work mainly two continuation softwares have been used: AUTO97 [Doedel *et al.*, 1998, 1991a,b] and CONTENT [Kuznetsov and Levitin, 1997] which are briefly described in the next two sections.

F.1 AUTO97

AUTO97, which is freely available at `http://indy.cs.concordia.ca/auto/`, can do a limited bifurcation analysis of algebraic systems

$$F(x,p)=0, \qquad F(\cdot,\cdot), x\in\mathbb{R}^n \tag{F.1}$$

and of systems of ordinary differential equation (ODEs) of the form

$$\dot{x}(t)=F\big(x(t),p\big), \qquad F(\cdot,\cdot), x(\cdot)\in\mathbb{R}^n,\ t\in\mathbb{R} \tag{F.2}$$

Here p denotes one or more free parameters.

It can also do certain stationary solution and wave calculations for the partial differential equation (PDE)

$$\frac{\partial x}{\partial t}=D\frac{\partial u}{\partial r}+F\big(u(t),p\big), \qquad F(\cdot,\cdot), u(\cdot)\in\mathbb{R}^n,\ t,r\in\mathbb{R} \tag{F.3}$$

where D denotes a diagonal matrix of diffusion constants.

The basic algorithms used in the package, as well as related algorithms, can be found in [Doedel *et al.*, 1991a,b; Keller, 1977, 1986].

Below, the basic capabilities of AUTO97 are specified in more detail.

F.1.1 ALGEBRAIC SYSTEMS

Specifically, for system (F.1) AUTO97 can

— Compute solution branches.

— Locate branch points and automatically compute bifurcating branches.

— Locate Hopf bifurcation points and continue these in two parameters.

— Locate folds (limit points) and continue these in two parameters.

— Do each of the above for fixed points of the discrete dynamical system

$$x(k+1)=F\big(x(x(k)),p\big), \qquad F(\cdot,\cdot), x\in\mathbb{R}^n \tag{F.4}$$

— Find extrema of an objective function along solution branches and successively continue such extrema in more parameters.

F.1.2 Ordinary Differential Equations

For the ODE system (F.2) Auto97 can

— Compute branches of stable and unstable periodic solutions and compute the Floquet multipliers, that determine stability, along these branches. Starting data for the computation of periodic orbits are generated automatically at Hopf bifurcation points.

— Locate folds, branch points, period doubling bifurcations, and bifurcations to tori, along branches of periodic solutions. Branch switching is possible at branch points and at period doubling bifurcations.

— Continue folds and period-doubling bifurcations, in two parameters. The continuation of orbits of fixed period is also possible. This is the simplest way to compute curves of homoclinic orbits, if the period is sufficiently large.

— Do each of the above for *rotations*, *i.e.* when some of the solution components are periodic modulo a phase gain of a multiple of 2π.

— Follow curves of homoclinic orbits and detect and continue various codimension-2 bifurcations, using the HomCont algorithms of [Champneys and Kuznetsov, 1994; Champneys *et al.*, 1996].

— Locate extrema of an integral objective functional along a branch of periodic solutions and successively continue such extrema in more parameters.

— Compute curves of solutions to system (F.2) on $[0,1]$, subject to general nonlinear boundary and integral conditions. The boundary conditions need not be separated, *i.e.* they may involve both $x(0)$ and $x(1)$ simultaneously. The side conditions may also depend on parameters. The number of boundary conditions plus the number of integral conditions need not equal the dimension of the ODE, provided there is a corresponding number of additional parameter variables.

— Determine folds and branch points along solution branches to the above boundary value problem. Branch switching is possible at branch points. Curves of folds can be computed in two parameters.

F.1.3 Distributions on the Unit Interval

For system (F.3) Auto97 can

— Trace out branches of spatially homogeneous solutions. This amounts to a bifurcation analysis of the algebraic system system (F.1). However, Auto97 uses a related system instead, in order to enable the detection of bifurcations to wave train solutions of given wave speed. More precisely, bifurcations to wave trains are detected as Hopf bifurcations along fixed point branches of the related ODE

$$\begin{aligned} \dot{u}(z) &= v(z) \\ \dot{v}(z) &= -D^{-1}\Big[cv(z) + f\big(u(z),p\big)\Big] \end{aligned} \tag{F.5}$$

where $z = r - ct$, with the wave speed c specified by the user.

— Trace out branches of periodic wave solutions to system (F.3) that emanate from a Hopf bifurcation point of system (F.5). The wave speed c is fixed along such a branch, but the wave length L, *i.e.* the period of periodic solutions to system (F.5), will normally vary. If the wave length L becomes large, *i.e.* if a homoclinic orbit of system (F.5) is approached, then the wave tends to a solitary wave solution of system (F.3).

— Trace out branches of waves of fixed wave length L in two parameters. The wave speed c may be chosen as one of these parameters. If L is large then such a continuation gives a branch of approximate solitary wave solutions to system (F.3).

— Do time evolution calculations for system (F.3), given periodic initial data on the interval $[0,L]$. The initial data must be specified on $[0,1]$ and L must be set separately because of internal scaling. The initial data may be given analytically or obtained from a previous computation of wave trains, solitary waves, or from a previous evolution calculation. Conversely, if an evolution calculation results in a stationary wave then this wave can be used as starting data for a wave continuation calculation.

— Do time evolution calculations for system (F.3) subject to user-specified boundary conditions. As above, the initial data must be specified on $[0, 1]$ and the space interval length L must be specified separately. Time evolution computations of system (F.3) are adaptive in space and in time. Discretization in time is not very accurate: only implicit Euler. Indeed, time integration of system (F.3) has only been included as a convenience and it is not very efficient.

— Compute curves of stationary solutions to system (F.3) subject to user-specified boundary conditions. The initial data may be given analytically, obtained from a previous stationary solution computation, or from a time evolution calculation.

In connection with periodic waves, note that system (F.5) is just a special case of system (F.2) and that its fixed point analysis is a special case of system (F.1). One advantage of the built-in capacity of AUTO97 to deal with problem system (F.3) is that the user need only specify f, D, and c. Another advantage is the compatibility of output data for restart purposes. This allows switching back and forth between evolution calculations and wave computations.

F.1.4 DISCRETIZATION

AUTO97 discretizes ODE boundary value problems (which includes periodic solutions) by the method of orthogonal collocation using piecewise polynomials with 2-7 collocation points per mesh interval [de Boor and Swartz, 1973]. The mesh automatically adapts to the solution to equidistribute the local discretization error [Russell and Christiansen, 1978]. The number of mesh intervals and the number of collocation points remain constant during any given run, although they may be changed at restart points. The implementation is AUTO97-specific. In particular, the choice of local polynomial basis and the algorithm for solving the linearized collocation systems were specifically designed for use in numerical bifurcation analysis.

F.2 CONTENT

CONTENT, which is freely available at `ftp://ftp.cwi.nl/pub/CONTENT`, is rather similar to AUTO97; indeed, it can be considered as its "easy to use" successor [Kuznetsov and Levitin, 1997]. Despite of its increased portability and user friendship with respect to its ancestor, the current available version is definitely less powerful, in terms of features, than AUTO97; that it is why it cannot be considered alone.

Below, the basic capabilities of CONTENT are specified in more detail.

F.2.1 ITERATED MAPS

Specifically, for system (F.4) CONTENT can

— Simulate, *i.e.* numerically integrate, system (F.4).

— Continue fixed points and cycles in one parameter.

— Detect, and automatically perform the normal form analysis, of branching and limit points, flip and torus, *i.e.* Neimark-Sacker, bifurcations of fixed points and cycles.

— Continue all codimension-1 bifurcations of fixed points and cycles in two parameter.

— Detect, and automatically perform the normal form analysis, of all the known codimension-2 bifurcations of fixed points and cycles; *i.e.* cusp, degenerate flip, degenerate Neimark-Sacker, fold-flip, fold-Neimark-Sacker, flip-Neimark-Sacker, double Neimark-Sacker, resonance $1 : 1$, resonance $1 : 2$, resonance $1 : 3$ and resonance $1 : 4$.

— Switch branch at branching and flip points of fixed point and cycles.

F.2.2 ORDINARY DIFFERENTIAL EQUATIONS

For system (F.2) CONTENT can

— Simulate, numerically integrate, system (F.2) by means of Euler, Runge-Kutta, or the *RADAU5* stiff integrators.

— Continue equilibria and limit cycles in one parameter.

— Detect, and automatically perform the normal form analysis, of branching, limit and Hopf points for equilibria.

— Continue fold and Hopf bifurcations of equilibria in two parameters.

— Detect, and automatically perform the normal form analysis, of all the known codimension-2 bifurcations of equilibria; *i.e.* cusp, Bogdanov-Takens, generalized Hopf, zero-Hopf and double Hopf.

— Continue all the codimension-2 bifurcations of equilibria in three parameters.

— Detect, and automatically perform the normal form analysis, of all the known codimension-3 bifurcations of equilibria; *i.e.* triple zero, triple zero degenerate Bogdanov-Takens, double zero degenerate Bogdanov-Takens, Hopf-Bogdanov-Takens, swallow tail, resonant degenerate Hopf and zero degenerate Hopf.

— Detect, and automatically perform the normal form analysis, of the branching, limit points, flip and torus (Neimark-Sacker) bifurcations of limit cycles.

— Perform a conditional continuation of equilibria and codimension-1,2 bifurcations of equilibria.

— Switch branch at equilibrium and limit cycle bifurcations, including switching to the limit cycle continuation at Hopf points.

F.2.3 Differential Algebraic Equations

For a system of differential algebraic equations (DAE) as

$$M\dot{x}(t) = F\big(x(t), p\big), \qquad F(\cdot,\cdot), x(\cdot) \in \mathbb{R}^n,\ t \in \mathbb{R} \tag{F.6}$$

where M denotes an eventually singular mass matrix, Content can

— Simulate, numerically integrate, system (F.4) by means of the *RADAU5* stiff integrators.

F.2.4 Distributions on the Unit Interval

For system (F.3) Content can

— Simulate with respect to time, *i.e.* numerically integrate, an initial spatial distribution trough system (F.3).

— Continue the steady states distributions in one parameter.

— Detect branching and limit points of steady states distributions.

F.2.5 Discretization and Advanced Features

Content implements the discretization of the ODE boundary value problems, which includes periodic solutions, with the same method implemented in Auto97 [de Boor and Swartz, 1973; Russell and Christiansen, 1978].

Furthermore, Content provides an automatic generation of the generating function (*cfr.* the above $G(X)$) derivatives by means of either a C++ routine [Levitin, 1997] or eventually exploiting the Maple libraries.

Bibliography

Champneys, A. and Y. Kuznetsov (1994). Numerical detection and continuation of codimension-two homoclinic bifurcations. *International Journal of Bifurcation and Chaos*, 4, pp. 795–822.

Champneys, A., Y. Kuznetsov, and B. Sandstede (1996). A numerical toolbox for homoclinic bifurcation analysis. *International Journal of Bifurcation and Chaos*, 5, pp. 867–887.

de Boor, C. and B. Swartz (1973). Collocation at Gaussian points. *SIAM Journal of Numerical Analysis*, 10, pp. 582–606.

Doedel, E., A. Champneys, T. Fairgrieve, Y. Kuznetsov, B. Sandstede, and X. Wang (1998). *AUTO 97: Continuation and Bifurcation Software for Ordinary Differential Equations withHomCont*. Computer Science Department, Concordia University, Montreal, Canada, Motreal, Quebec, Canada.

Doedel, E., H. Keller, and J. Kernévez (1991a). Numerical analysis and control of bifurcation problems, part I: Bifurcation in finite dimensions. *International Journal of Bifurcation and Chaos*, 1, pp. 493–520.

Doedel, E., H. Keller, and J. Kernévez (1991b). Numerical analysis and control of bifurcation problems, part II: Bifurcation in infinite dimensions. *International Journal of Bifurcation and Chaos*, 1, pp. 745–772.

Keller, H. (1977). *Numerical solution of bifurcation and nonlinear eigenvalue problems*, pp. 359–384. Academic Press, New York, NY.

Keller, H. (1986). *Lectures on Numerical Methods in Bifurcation Problems*. Springer-Verlag, New York, NY. Notes by A. K. Nandakumaran and Mythily Ramaswamy, Indian Institute of Science, Bangalore.

Kuznetsov, Y. (1998). *Elements of Applied Bifurcation Theory*. Springer-Verlag, New York, NY, second edition.

Kuznetsov, Y. and V. Levitin (1997). CONTENT: A multiplatform environment for continuation and bifurcation analysis of dynamical systems. Dynamical systems laboratory, CWI, Centrum voor Wiskunde en Informatica, National Research Institute for Mathematics and Computer Science, Amsterdam, The Netherlands.

Levitin, V. (1997). Computation of functions and their derivatives in CONTENT. Dynamical systems laboratory, CWI, Centrum voor Wiskunde en Informatica, National Research Institute for Mathematics and Computer Science, Amsterdam, The Netherlands.

Russell, R. and J. Christiansen (1978). Adaptive mesh selection strategies for solving boundary value problems. *SIAM Journal of Numerical Analysis*, 15, pp. 59–80.

APPENDIX G

FURTHER READING

Brief — This Appendix reports the bibliography that has not been mentioned elsewhere in order to limit the already heavy bibliographic lists. Nevertheless, the literature here reported has influenced, directly or indirectly, the development of this thesis.

Bibliography

Arsten, A. and V. Braitenberg, editors (1991). *Information Processing in the Cortex*. Springer-Verlag, Berlin, Germany.

Basar, E., editor (1990). *Chaos in Brain Function*. Springer-Verlag, Berlin, Germany.

Beer, R. (1995). A dynamical systems perspective on agent-environment interaction. *Artificial Intelligence*, 72, pp. 173–215.

Bittanti, S., P. Colaneri, and G. Guardabassi (1984). H-Controllability and observability of linear periodic systems. *SIAM Journal on Control and Optimization*, 22, pp. 889–893.

Bressler, S., R. Coppola, and R. Nakamura (1993). Episodic multiregional cortical coherence at multiple frequencies during visual task performance. *Nature*, 366, pp. 153–156.

Brooks, R. (1991). Intelligence without representation. *Artificial Intelligence*, 47, pp. 139–159.

Brooks, R. and A. Rodney (1991). *Intelligence without reason*. MIT Press, Cambridge, MA.

Browman, C. and L. Goldstein (1995). *Dynamics and articulatory phonology*, pp. 175–193. MIT Press, Cambridge, MA.

Bruls, J., C. Chou, B. Haverkamp, and M. Verhaegen (1999). Linear and non-linear system identification using separable least-squares. *European Journal of Control*, 5, pp. 116–128.

Casey, M. (1996). The dynamics of discrete-time computation, with application to recurrent neural networks and finite state machine extraction. *Neural Computation*, 8, pp. 1135–1178.

Chomsky, N. (1998). *On Language: Chomsky's Classic Works Language and Responsibility and Reflections on Language in One Volume*. The New Press, New York, NY.

Crutchfield, J. (1989). Inferring statistical complexity. *Physical Review Letters*, 63, pp. 105–108.

Degen, H., A. Holden, and L. Olsen, editors (1986). *Chaos in Biological Systems*. Plenum Press, New York, NY.

Di, X., Y. Hao, and Z. Shouchang (1997). Extraction of 40 Hz EEG bursts for chaos analysis of brain function. *IEEE Engineering in Medicine and Biology Magazine*, 16, pp. 27–32.

Ferri, R., S. Pettinato, F. Alicata, S. Del Gracco, M. Elia, and S. Musumeci (1997). Chaotic behaviour of EEG slow-wave activity during sleep in children and young adults. *Electroencephalography and Clinical Neurophysiology*, 103, p. 176.

Franco, S. (1988). *Operational Amplifiers and Analog Integrated Circuits*. McGraw-Hill, New York, NY.

Freeman, W. (1988). Strange attractors that govern mammalian brain dynamics shown by trajectories of electroencephalographic *eeg* potential. *IEEE Transactions on Circuits and Systems*, 35, pp. 781 –783.

Giles, C., C. Miller, D. Chen, H. Chen, G. Sun, and Y. Lee (1992). Learning and extracting finite state automata with second-order recurrent neural networks. *Neural Computation*, 4, pp. 393–405.

Gonchenko, S., D. Turaev, P. Gaspard, and G. Nicolis (1997). Complexity in the bifurcation structure of homoclinic loops to a saddle-focus. *Nonlinearity*, 10, pp. 409–423.

Gray, G., D. Murray-Smith, Y. Li, and K. Sharman (1996). *Nonlinear model structure identification using genetic programming*, pp. 32–37. Standford University Press, Stanford, CA.

Hokkanen, J. (2000). Chaotic or periodic variation? Looking at crustacea hearts. *Journal of Theoretical Biology*, 203, pp. 451–454.

Kuznetsov, Y. and C. Piccardi (1994). Bifurcation analysis of periodic SEIR and SIR epidemic models. *Journal of Mathematical Biology*, 32, pp. 109–121.

Marzollo, A. (1972). *Periodic Optimization*. Springer-Verlag, Berlin, Germany.

Meade, A. and A. Fernandez (1994). Solution of nonlinear ordinary differential equations by feedforward neural networks. *Mathematical and Computer Modelling*. To appear.

Mira, C. (1996). About two-dimensional piecewise continuous noninvertible maps. *International Journal of Bifurcation and Chaos*, 6, pp. 893–918.

Morgul, O. (1999). Theoretical and experimental results for the control of some chaotic systems by using dither. In *European Conference on Circuit Theory and Design ECCTD*. Stresa, Italy.

Newell, A. (1990). *Unified Theories of Cognition*. Harvard University Press, Cambridge, MA.

Omlin, C. and C. Giles (1996a). Constructing deterministic finite-state automata in recurrent neural networks. *Journal of the ACM*, 43, pp. 937–972.

Omlin, C. and C. Giles (1996b). Extraction of rules from discrete-time recurrent neural networks. *Neural Networks*, 9, pp. 41–52.

Omlin, C. and C. Giles (1996c). Rule revision with recurrent neural networks. *IEEE Transactions on Knowledge and Data Engineering*, 8, pp. 183–188.

Omlin, C. and C. Giles (1996d). Stable encoding of large finite-state automata in recurrent neural networks with sigmoid discriminants. *Neural Computation*, 8, pp. 675–696.

Omlin, C., K. Thornber, and C. Giles (1998). Fuzzy finite-state automata can be deterministically encoded into recurrent neural networks. *IEEE Transactions on Fuzzy Systems*, 6, pp. 76–89.

Pearson, R. and M. Pottmann (2000). Gray-box identification of block-oriented nonlinear models. *Journal of Process Control*, 10, pp. 301–315.

Port, R., F. Cummins, and J. McAuley (1995). *Naive time, temporal patterns and human audition*, pp. 339–371. MIT Press, Cambridge, MA.

Preissl, H., W. Lutzenberger, F. Pulvermüller, and N. Birbaumer (1997). Fractal dimensions of short EEG time series in humans. *Neuroscience Letters*, 225, pp. 77–80.

Rabinovich, M. and H. Abarbanel (1998). The role of chaos on neural systems. *Neuroscience*, 87, pp. 5–14.

Rouabhi, S. and C. Mira (1998). How to store information as cycles of a discontinuous piecewise linear map. In *Proceedings of the CESA'98 Multiconfenrence*, pp. 750–753. Hammamet, Tunisia.

Shaked, U. and C. de Souza (1995). Continuous-time tracking problems in an H_∞ setting: A game theory approach. *IEEE Transactions on Automatic Control*, 40, pp. 841 –852.

Svobodny, T. and D. Russell (1989). Phase identification in linear time-periodic systems. *IEEE Transactions on Automatic Control*, 34, pp. 218 –220.

Thakor, N. (1998). Chaos in the heart: signals and models. In *Proceedings of the 2nd International Conference on Biomedical Engineering*, pp. 11–18.

Tsuda, I., E. Koerner, and H. Shimizu (1987). Memory dynamics in asynchronous neural networks. *Progress of Theoretical Physics*, 78, pp. 51–71.

Wang, F., Y. Sun, and H. Wu (1995). Forward-genetic learning and its application to system identification. *Electronics Letters*, 31, pp. 1806–1807.

Zwiener, U., D. Hoyer, R. Bauer, B. Lüthke, B. Walter, K. Schmidt, S. Hallmeyer, B. Kratzsch, and M. Eiselt (1996). Deterministic-chaotic and periodic properties of heart rate and arterial pressure fluctuations and their mediation in piglets. *Cardiovascular Research*, 31, pp. 455–465.

AUTHOR'S CURRICULUM VITÆ

Oscar De Feo received his Bachelor *Summa cum Laude* in Industrial Electronics in the 1990 from the Maxwell High School (Milan, Italy) and a five-year degree (equivalent to an M.Sc.) *Summa cum Laude* in Computer Science Engineering in 1995, from the Politecnico di Milano (Milan, Italy). Next, he collaborated with the Fondazione Eni Enrico Mattei (FEEM, Milan, Italy) as a postgraduate fellow, working on problems of ecologically sustainable development and environmental impact. He continued his research studies in nonlinear dynamics participating in the Young Scientists' Summer Program (YSSP) at the International Institute for Applied Systems Analysis (IIASA, Laxenburg, Austria) where he received the Mikhalevich Award for the results obtained during his research activities there. In January 1997 he joined the Laboratory of Nonlinear System at the Swiss Federal Institute of Technology Lausanne (EPFL), Lausanne, Switzerland, where he has worked until now (January, 2001) towards a Ph.D under the supervision of Professor Martin Hasler. During 1997 and 1998 he held visiting research positions at the IIASA, at the Research Institute for Mathematics and Computer Science (CWI, Amsterdam, The Netherlands) and at the Department of Electronic and Electrical Engineering of the University College Dublin in Ireland. Oscar, together with Gian Mario Maggio and Michal Peter Kennedy, has been awarded with the best paper award at the European Conference on Circuit Theory and Design (ECCTD99) held in September 1999 in Stresa, Italy. Title of the paper: "An Explicit Expression for the Output Amplitude of the Colpitts Oscillator". Oscar's research interest are in the fields of bifurcation and nonlinear systems theory, numerical methods for nonlinear system analysis, bioengineering, ecology, biology, and systematic methods for the design of nonlinear systems in engineering applications.

PUBLICATIONS

Baier, N. U., T. Schimming, and O. De Feo (2000). Nonlinear structures in voiced speech signals. In *International Conference on Nonlinear Theory and its Applications NOLTA*. Dresden, Germany.

De Feo, O. (1995). *Enrichment of Food Chains: relationship between mean production and bifurcations*. Master's thesis, Politecnico di Milano, Milano, Italy. In Italian.

De Feo, O. (2000). Qualitative resonance of periodically perturbed shil'nikov's strange attractors. In *International Conference on Nonlinear Theory and its Applications NOLTA*. Dresden, Germany.

De Feo, O. and R. Ferriere (2000). Bifurcation analysis of population invasion: on-off intermittency and basin riddling. *International Journal of Bifurcation and Chaos*, 10(2), pp. 443–452.

De Feo, O. and G. M. Maggio (2000). Bifurcation phenomena in the colpitts oscillator: A robustness analysis. In *International Symposium on Circuits and Systems ISCAS*. Geneva, Switzerland.

De Feo, O. and G. M. Maggio (2001). Bifurcations in the colpitts oscillator: Theory versus experiments. *IEEE Transaction on Circuit and Systems—I*. Submitted.

De Feo, O., G. M. Maggio, and M. P. Kennedy (2000). The colpitts oscillator: Families of periodic solutions and their bifurcations. *International Journal of Bifurcation and Chaos*, 10(5), pp. 935–958.

De Feo, O. and S. Rinaldi (1997). Yield and dynamics in tritrophic food chains. *The American Naturalist*, 150(3), pp. 328–345.

De Feo, O. and S. Rinaldi (1998). Singular homoclinic bifurcations in tri-trophic food chains. *Mathematical Biosciences*, 148(1), pp. 7–20.

De Feo, O. and T. Schimming (2000). Kalman filtering of strange attractors. In *IEEE Workshop on Nonlinear Dynamics of Electronic Systems NDES*. Catania, Italy.

Ferriere, R. and O. De Feo (1998). How should we define invasibility and fitness in populations with multiple attractors ? In *VII International Congress of Ecology INTECOL*. Florence, Italy.

Ferriere, R. and O. De Feo (2001). Adaptive dynamics: two routes to dimorphism. *Nature*. To submit.

Gragnani, A., O. De Feo, and S. Rinaldi (1998). Food chains in the chemostat: relationships between mean yield and complex dynamics. *Bulletin of Mathematical Biology*, 60(4), pp. 703–719.

Kuznetsov, Y., O. De Feo, and S. Rinaldi (2001). Belyakov homoclinic bifurcations in a tritrophic food chain model. *SIAM Journal of Applied Mathematics*. Submitted.

Maggio, G. M. and O. De Feo (2000). T-csk: A robust approach to chaos-based communications. In *IEEE Workshop on Nonlinear Dynamics of Electronic Systems NDES*. Catania, Italy.

Maggio, G. M., O. De Feo, and M. P. Kennedy (1998). Applications of bifurcation analysis to the design of a chaotic colpitts oscillator. In *International Conference on Nonlinear Theory and its Applications NOLTA*. Crans-Montana, Switzerland.

Maggio, G. M., O. De Feo, and M. P. Kennedy (1999a). An explicit expression for the output amplitude of the colpitts oscillator. In *European Conference on Circuit Theory and Design ECCTD*. Stresa, Italy. Best paper award.

Maggio, G. M., O. De Feo, and M. P. Kennedy (1999b). Nonlinear analysis of the colpitts oscillator and applications to design. *IEEE Transaction on Circuit and Systems—I*, 46(9), pp. 1118–1130.

Rinaldi, S. and O. De Feo (1999). Top-predator abundance and chaos in tritrophic food chains. *Ecology Letters*, 2(1), pp. 6–10.

Rinaldi, S., O. De Feo, and A. Gragnani (1998). Optimality and chaos of tri-trophic food chains. In *VII International Congress of Ecology INTECOL*. Florence, Italy.